

**A Process-Based Landscape Approach to
Landform Architecture**

by

Iryna Volynets

A dissertation accepted and approved in partial fulfillment of the
requirements for the degree of
Doctor of Philosophy
in Landscape Architecture

Dissertation Committee:

Mark Eischeid, Chair, Advisor

Ignacio López Busón, Core Member

Justin Fowler, Core Member

Erin Moore, Institutional Representative

University of Oregon

Spring 2025

© 2025 Iryna Volynets

This work is openly licensed via CC BY 4.0



DISSERTATION ABSTRACT

Iryna Volynets

Doctor of Philosophy in Landscape Architecture

Title: A Process-Based Landscape Approach to Landform Architecture

Landform architecture treats buildings as topographically continuous with their sites. Despite the growing interest in landform architecture among practitioners and scholars in the last few decades, a large gap between the broad concept and its application in design still exists. The current theory focuses on building aesthetics and uses natural landforms as a source of architectural metaphor. Design solutions are influenced by intuitive attempts to reconnect landscape and architecture and are focused on a form-based approach that ignores or fails to address landscape processes. This research proposes to expand the existing theory and practice by acknowledging landscape as a dynamic system to design buildings that not only look like landscapes, but function as landscapes. The purpose of this research is to develop a strategy that identifies site-specific landscape processes to design landform buildings. By engaging the potential agency of landforms to impact natural systems, landform architecture can play a significant role in addressing climate-related issues and urban growth challenges.

To address gaps in research and practice, as well as expand existing theory, the dissertation will critique existing landform architecture theory, offer a landscape approach to landform architecture, and propose a process for designing resilient buildings. The project is divided into three stages: (1) review of the existing state of theory and practice through literature review and case study analysis; (2) development of a theoretical approach to design landform architecture through comparative analysis, classification, 3D modeling, and simulations; and (3) tests of the theoretical approach through design experimentation.

ACKNOWLEDGMENTS

Never, never, never give up on your dreams.

It was my dream to earn a PhD in the United States. But I cannot say how many times I wanted to give up. I truly believe that I came to this moment because of the unwavering support of people to whom I am deeply grateful.

I want to say thank you to people who believed in me more than I believed in myself, especially in moments of self-doubt and difficulties.

To my advisor Mark Eischeid: Thank you for your guidance, support, and care. I cannot imagine anyone else in this role.

To my comprehensive exam committee, Roxi Thoren and Chris Enright: Thank you for your guidance and for helping to shape the research.

To my dissertation committee, Justin Fowler, Erin Moore, and Ignacio Lopez Buson: Thank you for support, encouragement, and advice.

To my sister and father: Thank you for supporting me to finish what I have started in times of complete uncertainty, when the war has started in our home country and we were ready to go back to Ukraine.

To my husband: Thank you for letting me follow my dream and for following me wherever my dreams are taking me. Thank you for your love, care, and for helping to raise our son Levko.

PREFACE

This dissertation is the culmination of a long personal and professional journey that explores the relationship between built form and landscape. I have not followed a typical academic path. I have been shifting back and forth between practice and research, as well as teaching. Each experience became a solid ground for further development, eventually leading me to the decision to pursue a PhD in Landscape Architecture.

Over the past decade, my interest in research and practice was at the intersection of building and landscape, with a focus on the potential of landform architecture to engage topography, territory, and urban ecosystems. My early professional experience in architecture—winning international competitions, collaborating internationally, and building landform projects in Ukraine and Norway—were intuitive attempts to landform design.

A major shift from practice to research happened when I received a Fulbright Faculty Development grant to begin a study of landform architecture. The Fulbright Program allowed me to initiate a theoretical exploration of my previous intuitive attempts in practice. As a Visiting Fulbright Scholar in the Department of Architecture at the University of Oregon, USA (2015–2016), my research focused on the exploration of natural landforms, the way they form, and the way they change over time. One of my conclusions was that we can understand and design landform architecture by referring to the original source—the land and its forms.

My doctoral work has expanded the investigation of landform architecture to how environmental processes can inform architectural form. Through simulation-based research, I have examined how architectural form, shaped by site-specific processes, changes local microclimate and addresses climate-related challenges.

As I complete this dissertation, I recognize how the diverse paths of my career, across countries, disciplines, and scales, have come together in this work. I am deeply grateful to the University of Oregon for its support and the opportunity for critical inquiry and creative experimentation.

I hope this work serves as a solid foundation for what comes next: a continuous exploration of the intersection of research and practice as well as architecture and landscape architecture. And I also hope to have a chance to share what I have learned with my colleagues and students.

TABLE OF CONTENTS

Chapter	Page
I. INTRODUCTION.....	28
1.1 Statement of the Problem	28
1.2 Purpose of the Study.....	29
1.3 Objectives of the Study.....	29
1.4 Definition of Terms	30
1.5 Research Through Design	31
1.6 Methods	37
1.6.1 Stage 1	38
1.6.1.1 Literature Review	39
1.6.1.2 Precedent Study	39
1.6.2 Stage 2	42
1.6.2.1 Comparative Analysis.....	44
1.6.2.2 Case Studies.....	44
1.6.3 Stage 3	47
1.6.3.1 Development of Site Selection Criteria	49
1.6.3.2 Site Visits.....	50
1.6.3.3 Site Selection	50
1.6.3.4 Data Collection for Site	53
1.6.3.5 Site Analysis.....	54
1.6.3.6 3D Simulations	55
1.6.3.7 Conceptual Design.....	58
1.6.4 Stage 4	58
1.6.4.1 Environmental Performance Evaluation.....	59
1.7 Significance of the Study.....	61
1.8 Assumptions, Hypotheses, and Researchable Questions.....	61
1.9 Summary.....	62
II. LANDFORM ACROSS TIME, CULTURE, AND DISCIPLINE.....	65
2.1 Ancient Landforms	65
2.1.1 Settlement	65
2.1.2 Defense	70
2.1.3 Rituals.....	72
2.2 Art.....	76
2.3 Design.....	83
2.3.1 Cosmomorphism.....	84
2.3.2 Hydromorphism.....	89
2.3.3 Biomorphism	101
2.3.4 Geomorphism	108

2.3.4.1 Topographical Integration	113
2.3.4.2 Geomorphological Form.....	116
2.3.4.3 Crystallographic Form.....	119
2.3.4.4 Landscape Integration.....	121
2.4 Discussion.....	122
2.5 Revised Definition of Landform Architecture.....	124
2.6 Summary.....	125
III. PROCESS AND LANDFORM ARCHITECTURE	128
3.1 Landscape as Process.....	128
3.1.1 Ecological Process-Based Design	129
3.1.2 Systems Process-Based Design	133
3.1.3 Phasing Process-Based Design.....	137
3.2 3D Simulations	140
3.3 Modeling of Natural Processes (Case Studies).....	146
3.3.1 Landform Simulation.....	147
3.3.2 Atmosphere Simulation	152
3.3.3 Fluvial Simulation	160
3.3.4 Vegetation Simulation	165
3.4 A Process-Based Landscape Approach to Landform Architecture	171
3.5 Summary.....	172
IV. SITE CONTEXT	174
4.1 Site-Specific Process-Based Approach to Landform Architecture	174
4.1.1 Site Selection	175
4.1.2 Context: Natural and Cultural History.....	183
4.1.3 Site Analysis	193
4.1.3.1 City Scale.....	193
4.1.3.1.1 Geomorphological Processes.....	195
4.1.3.1.2 Hydrological Processes.....	198
4.1.3.1.3. Vegetation Processes	212
4.1.3.2 Neighborhood Scale	218
4.1.3.3 Site Scale	227
4.2 Summary.....	233
V. SIMULATION OF SITE-SPECIFIC PROCESSES	236
5.1 A Process-Based Landscape Approach to Landform Architecture	236
5.2 Current Processes on Site	237
5.3 Simulations	248
5.3.1 Geomorphological Simulation.....	250
5.3.2 Hydrological Simulation.....	252
5.3.3 Wind Simulation.....	258
5.3.3.1 Building-Focused Wind Simulations on a Larger Scale	259

5.3.3.2 Building-Focused Wind Simulations on a Smaller Scale.....	263
5.3.3.3 Landform Wind Simulations	273
5.3.3.4 Vegetation Wind Simulation	277
5.3.4 Vegetation Simulation	279
5.4 Integrated Simulation Framework	281
5.5 Summary.....	289
VI. DESIGN EXPERIMENT	290
6.1 Introduction to the Design Experiment	290
6.2 Design Experiment	291
6.2.1 Simulations	291
6.2.2 Building Design.....	312
6.2.3 Landscape Design.....	318
6.3 Environmental Performance of Landform Building.....	319
6.4 Summary.....	324
VII. CONCLUSIONS.....	325
7.1. Contribution to Knowledge	326
7.1.1 Theoretical Contribution.....	326
7.1.2 Methodological Contribution	327
7.1.3 Evaluative Contribution.....	329
7.2. Limitations of the Research.....	331
7.3. Recommendations for Future Research.....	332
APPENDICES	334
APPENDIX A. LANDFORMS SHAPED BY DIFFERENT PROCESSES	334
APPENDIX B. HISTORICAL ANALYSIS OF PORTLAND.....	335
APPENDIX C. WIND SIMULATIONS.....	421
APPENDIX D. GRASSHOPPER 3D SIMULATION DEFINITIONS.....	446
REFERENCES CITED	453

LIST OF FIGURES

Figure	Page
Figure 1. Stages of the research.....	37
Figure 2. Stage 1.....	38
Figure 3. Stage 2.....	43
Figure 4. Stage 3.....	48
Figure 5. Site selection process for design experiment.	52
Figure 6. Stage 4.....	59
Figure 7. Typology of landform architecture.	67
Figure 8. Early settlement in Petra, Jordan. From Encyclopædia Britannica, n.d-a.....	67
Figure 9. Mesa Verde in Colorado, USA. From BBC, n.d.....	68
Figure 10. Machu Picchu in Peru, Mexico. From National Geographic, 2025.....	69
Figure 11. Dun Aengus in Ireland. From Heritage Ireland, n.d.	70
Figure 12. Maiden Castle in Dorset, England. From Ancient Origins, n.d.	71
Figure 13. Hambledon Hill in England. From National Trust, n.d.....	72
Figure 14. Stonehenge in Wiltshire, England. From Encyclopædia Britannica, n.d.-b. ..	73
Figure 15. Top: The Tovsta Mohyla kurgan in Ukraine. Bottom: The Golden Pectoral of the Scythians from Tovsta Mohyla. From Google Arts and Culture, n.d.....	75
Figure 16. <i>Asphalt Rundown</i> in Rome, Italy by Robert Smithson (1969). Left: Site map. Right: Picture of the site with the sculpture. From Holt/Smithson Foundation, n.d.-b.	79
Figure 17. <i>Spiral Jetty</i> in Great Salt Lake, Utah, by Robert Smithson (1970). From Holt/Smithson Foundation, n.d.....	80
Figure 18. <i>Broken Circle/Spiral Hill</i> in Emmen, the Netherlands, by Robert Smithson (1971). From Holt/Smithson Foundation, n.d.-d.	81
Figure 19. <i>Amarillo Ramp</i> in Lake Tecovas, Amarillo, Texas, by Robert Smithson (1973). From Holt/Smithson Foundation, n.d.-a.	82
Figure 20. <i>Landform Ueda</i> in Edinburg, Scotland, by Charles Jencks (1999–2002). From www.charlesjencks.com.	85
Figure 21. <i>The Scottish World</i> in Kelty, Scotland, by Charles Jencks (2003–2010). From Jencks, n.d.	87

Figure 22. <i>Land War Garden</i> in Salford, Manchester, by Charles Jencks (1998–2001). From Jencks, 2011.....	88
Figure 23. Left: The <i>Wave Field</i> in Ann Arbor, MI, by Maya Lin (1995). From Maya Lin Studio, n.d.-b. Right: Models for the <i>Wave Field</i> . From Lin et al., 2015.....	90
Figure 24. Left: <i>Flutter</i> in Miami, FL, by Maya Lin. From Maya Lin Studio, n.d.-a. Right: Sketch by Maya Lin. From Lin et al., 2015.....	91
Figure 25. Left: <i>Storm King Wavefield</i> in Windsor, NY by Maya Lin (2009). From Maya Lin Studio, n.d.-c. Right: Site plan sketch by Maya Lin. From Lin et al., 2015.	92
Figure 26. Left: Shell Petroleum Headquarters by Kathryn Gustafson in Rueil- Malmaison, France (1992). Right: Site image and sections of the building and adjacent landforms. From Levy & Gustafson, 1998.....	95
Figure 27. Left: Diana, Princess of Wales Memorial Fountain in London, United Kingdom (2004), birds-eye view. Right: Water running over textured stone. From Gustafson Porter + Bowman, n.d.-b.	96
Figure 28. Left: View of Cultuurpark Westergasfabriek in Amsterdam (2004). Right: master plan. From Gustafson Porter + Bowman, n.d.-a.	97
Figure 29. Parque do Tejo e do Trancão (1994) by Hargreaves Associates in Lisbon, Portugal, aerial view of the site and landforms. From Hargreaves et al., 2009.....	99
Figure 30. Left: Crissy Field (2001) by Hargreaves Associates in San Francisco, CA. Right: Aerial view of the site and landforms. From M’Closkey, 2013.....	101
Figure 31. The Möbius House in the Netherlands by UNStudio. From UNStudio, n.d..	103
Figure 32. HtwoOexpo pavilion in the Netherlands by NOX (1997). From Hidden Architecture, n.d.	104
Figure 33. Library Delft University of Technology in the Netherlands by Mecanoo. From Mecanoo, n.d.	105
Figure 34. Stranded Sears Towers in Chicago by Greg Lynn (1992). From Greg Lynn Form, n.d.	106
Figure 35. Yokohama International Port Terminal by FOA (1995). From Langdon, n.d....	107
Figure 36. Fort L’Empereur in Algiers by Le Corbusier (1931), conceptual rendering. From Foundation Le Corbusier, n.d.	110

Figure 37. NTR Headquarters in the Netherlands by MVRDV (1997). From MVRDV, n.d.-a.	114
Figure 38. Villa VPRO in the Netherlands by MVRDV (1997). From MVRDV, n.d.-b. ...	115
Figure 39. Olympic Sculpture Park in Seattle by Weiss/Manfredi (2013).....	116
Figure 40. City of Culture of Galicia in Spain by Peter Eisenman (1999–ongoing). From Eisenman Architects, n.d.	118
Figure 41. Mountain in Spain by Vicente Guallart (2002). From Guallart, n.d.	119
Figure 42. New Maribor Art Gallery project in Slovenia by Stan Allen (2010). From Stan Allen Architect, n.d.	120
Figure 43. Chulalongkorn University Centenary Park in Bangkok by LANDPROCESS (2017). From Landezine, n.d.	121
Figure 44. Underground Parking Garage in the Netherlands by Royal HaskoningDHV and OKRA Landschapsarchitecten (2016). From ArchDaily, n.d.	122
Figure 45. Byxbee Park by George Hargreaves, Palo Alto, CA (1989). Left: Photo from the site. Right: Phase-one master plan. From Hargreaves Jones, n.d.	130
Figure 46. Jardin élémentaires by Michel Desvigne (1987), hand drawings. From MDP Michel Desvigne Paysagiste, n.d.	131
Figure 47. Mill Race Park by Michael Van Valkenburgh, Columbus, Indiana (1993)..	132
Figure 48. Valley of energy: exploratory combination of surface and subsurface: Top: Flows of waste and water. Bottom: Mobility, and forestry by OPSYS. From Belanger, 2016.	133
Figure 49. Freshkills Park by James Corner/Field Operations, Staten Island, New York (2001–2036), field diagram. From ArchDaily, 2013.....	135
Figure 50. Parc de la Villette by Rem Koolhaas / OMA, France (1982), diagrams. From OMA, n.d.-b.	137
Figure 51. Downsvie Park by Rem Koolhaas/OMA, Toronto, Canada (2000), masterplan. From OMA, n.d.-a.....	139
Figure 52. Layering approach by Ian McHarg. From McHarg, 1992.	141
Figure 53. The Mississippi River Basin Model by the U.S. Army Corp of Engineers, physical model. From ElMalvaney, 2010.....	142

Figure 54. Heliomorphism. The study of sun process by Ralph Knowles. The diagram shows the arrangement of multifamily units on a site. From Knowles, 1980.	143
Figure 55. Guadalupe River Park by George Hargreaves, San Jose, California (1989–1990), physical model. From Hargreaves Associates, n.d.-b.	144
Figure 56. City of Culture of Galicia Santiago de Compostela, Spain by Peter Eisenman (1999–2011). Left: Overlay layers. Right: The building. From Eisenman Architects, n.d.	145
Figure 57. MAX IV Laboratory by Snøhetta, Lund, Sweden (2016), aerial view of the building and landscape. From Snøhetta, n.d.	147
Figure 58. Before and after the construction of the MAX IV Laboratory. Left: 2020 aerial view before the construction. Right: 2024 aerial view after the construction. From Google Earth Pro.	148
Figure 59. MAX IV Laboratory. Left: Building shape and the direction of the landscape. Right: The shape and location of landforms hills. From Snøhetta, n.d.	149
Figure 60. MAX IV Laboratory 3D model. Top: In Rhino. Bottom: Grasshopper definition.	150
Figure 61. Jade Eco Park by Philippe Rahm, Taichung, Taiwan, competition visualization. From Philippe Rahm architectes, n.d.	153
Figure 62. Before and after the construction of Jade Eco Park.	154
Figure 63. Human body reaction to heat, humidity, and pollution by Philippe Rahm, competition diagram. From Philippe Rahm architectes, n.d.	155
Figure 64. Anticyclone device, section. From Philippe Rahm architectes, n.d.	156
Figure 65. Dry Cloud device. From Philippe Rahm architectes, n.d.	156
Figure 66. Ozone Eclipse device, section. From Philippe Rahm architectes, n.d.	157
Figure 67. North Wind Speed simulation map. From Philippe Rahm architectes, n.d. .	157
Figure 68. Southwest Wind Velocity and Vector simulation map. From Philippe Rahm architectes, n.d.	158
Figure 69. North Wind Velocity and Vector simulation map. From Philippe Rahm architectes, n.d.	158
Figure 70. Yanghwa Riverfront: Mud-Infrastructure by PARKKIM in Seoul, Korea (2011), aerial view. From PARKKIM, n.d.	161

Figure 71. Before and after the construction of the Mud-Infrastructure. Left: 2006 aerial view before the construction. Right: 2023 aerial view after the construction. From Google Earth Pro.	161
Figure 72. Transformation of the Mud-Infrastructure park, initial concept drawing. From PARKKIM, n.d.....	163
Figure 73. Mud-Infrastructure Park. Left: Aerial view during its normal operational time. Right: Aerial view during flooding. From PARKKIM, n.d.	164
Figure 74. Sony City Ōsaki by AnS Studio in Tokyo, Japan (2011), view from the path. From AnS Studio.....	166
Figure 75. Before and after the construction of the Sony Forest. Left: 2010 aerial view before the construction. Right: 2012 aerial view after the construction. From Google Earth Pro. ...	166
Figure 76. The final composition of the Sony Forest. From Takenaka & Okabe, 2011.	168
Figure 77. Seed scattering process, various layouts. From Takenaka & Okabe, 2011. .	168
Figure 78. Sony Forest 3D model. Top: In Rhino. Bottom: Grasshopper definition.	170
Figure 79. A process-based approach to landform architecture.	171
Figure 80. Process-based approach and analysis of the site’s history.	174
Figure 81. Temperature map and tree canopy cover across Portland, Oregon.....	177
Figure 82. Site 1: Vanport (Northeast Portland along the Columbia River).	180
Figure 83. Site 2: Albina neighborhood (Interstate 5 area).	181
Figure 84. Site 3: Northwest of the Willamette River (historical Guild’s Lake area)....	181
Figure 85. Selected site for design experiment, marked by a dashed line.....	182
Figure 86. Portland historic maps of 1897, 1940, 1954, 1961, 1975, and 1990 (left to right). From Harvard Old Maps online.....	183
Figure 87. Cadastral map of Portland, 1852. From Public Land Survey System.....	185
Figure 88. Albina area plat map of 1873. From Roos, 1997.	186
Figure 89. The early development of the Albina neighborhood. From Glover, 1879....	187
Figure 90. Oregon Railway and Navigation Dock, 1882. The Albina community is shown in the background. From Wikimedia Commons.	188
Figure 91. The first Steel Bridge, connecting Portland across the river and Albina in the foreground, 1887 (before the bridge went into service). From Volga Germans, n.d.	189

Figure 92. Map of Portland, East Portland, and Albina. From Volga Germans, n.d.....	189
Figure 93. Albina neighborhoods. From Volga Germans, n.d.	190
Figure 94. Albina Vision Trust community investment plan by El Dorado Architects. From El Dorado, n.d.	192
Figure 95. Analysis of processes on the city scale.	194
Figure 96. Geomorphological processes influenced by environmental and human agents..	195
Figure 97. Workflow process.	196
Figure 98. Left: Geologic map of Portland. From USGS. Right: 2D AutoCAD drawing of the map.	196
Figure 99. Portland surficial geologic simulation map.....	197
Figure 100. Left: Missoula Floods inundation extent and primary flood features in the Portland metropolitan Area, 2012. From DOGAMI, 2012. Right: AutoCAD 2D drawing of the flood area.	198
Figure 101. Missoula Flood simulation map.....	199
Figure 102. Hydrological processes influenced by environmental and human agents. .	200
Figure 103. Willamette River flood crests simulation.....	203
Figure 104. USGS topographic maps of 1897, 1940, 1954, 1961, 1975, 1990, 2011, 2014, 2017, and 2020. From USGS.....	206
Figure 105. AutoCAD 2D drawings of the city.....	206
Figure 106. Willamette River simulation.	207
Figure 107. Willamette River bathymetry data, 1888 and 2005. From GIS.	211
Figure 108. Willamette River bathymetry simulation.	211
Figure 109. Vegetation processes influenced by environmental and human agents.	213
Figure 110. Workflow process.	214
Figure 111. Satellite maps for 1951, 1970, 1975, 1990, 1994, 2000, 2011, 2014, 2017, and 2020. From Google Earth, Oregon State Aerial Imagery, and Portland Maps Advanced...	214
Figure 112. Analyzed data in Photoshop.....	215
Figure 113. Vegetation simulation.	216
Figure 114. Analysis of processes on the neighborhood scale.	219
Figure 115. Workflow process.	220

Figure 116. Aerial photos from 1948, 1960, 1975, 1990, 2011, 2014, 2017, 2020, and 2023. From Google Earth satellite images and University of Oregon Knight Library aerial maps reserves.	221
Figure 117. AutoCAD 2D drawings of the neighborhood.	221
Figure 118. Albina neighborhood simulation.	222
Figure 119. Albina neighborhood gauge historic crests simulation.	226
Figure 120. Analysis of processes on the site scale.	227
Figure 121. Workflow process.	228
Figure 122. Aerial photos from 1948, 1960, 1975, 1990, 2011, 2014, 2017, 2020, and 2023. From Google Earth satellite images and University of Oregon Knight Library aerial maps reserves.	228
Figure 123. AutoCAD 2D drawings of the site.	229
Figure 124. Site scale simulation.	230
Figure 125. Lower Albina gauge historic crests simulation.	232
Figure 126. A process-based approach to landform architecture and analysis of a site’s current processes.	237
Figure 127. Top: Delaunay mesh definition in Grasshopper. Bottom: Site model with contour lines.	239
Figure 128. Simulation of FEMA’s 100-year flood plain.	240
Figure 129. Top: Groundhog Grasshopper definition for surface water flow. Bottom: Surface water flow simulation (larger view in Appendix D, Figure 351).	241
Figure 130. Ladybug + Grasshopper definition for wind rose analysis (larger view in Appendix D, Figure 352).	242
Figure 131. Wind rose analysis for prevailing wind and monthly wind patterns from January to February.	243
Figure 132. Wind rose analysis for prevailing wind and monthly wind patterns from March to August.	244
Figure 133. Wind rose analysis for monthly wind patterns from September to December.	245
Figure 134. Current wind conditions for northwest and southeast winds.	246
Figure 135. Simulation of vegetation process.	248

Figure 136. Computational workflow.	249
Figure 137. Geomorphological simulation. Definition in Grasshopper (larger view in Appendix D, Figure 353).....	251
Figure 138. Geomorphological simulation.....	251
Figure 139. Hydrological simulation. Definition in Grasshopper (larger view in Appendix D, Figure 354).....	253
Figure 140. Hydrological simulation. Options 1–4.....	255
Figure 141. Hydrological simulation. Options 5–10.....	256
Figure 142. Diagram of wind speed in urban and non-urban environments. From Krautheim et al., 2014.	259
Figure 143. Wind simulation. Definition in Grasshopper (larger view in Appendix D, Figure 355).	260
Figure 144. Wind simulation for prevailing wind 10 m/s for Option 1. Plan, perspective, side, and front views.....	261
Figure 145. Wind simulation for prevailing wind 10 m/s for Options 2–7. Perspective views.	262
Figure 146. Wind simulation for prevailing wind 10 m/s for Options 8–10. Perspective views.	263
Figure 147. Left: Wind simulation for cuboid shape. Right: Wind simulation for two cuboids.	264
Figure 148. Wind simulation for two cuboid shapes rotated 10 degrees.	265
Figure 149. Wind simulation for one, two, and three cuboid shapes rotated 30 degrees.....	266
Figure 150. Wind simulation for one, two, and three cuboid shapes.	267
Figure 151. Wind simulation for one-sloped shapes.	267
Figure 152. Wind simulation for convex-like shapes.....	268
Figure 153. Wind simulation for a concave-like shapes.	269
Figure 154. Wind simulation for u-shapes with right and fillet edges.	270
Figure 155. Wind simulation for u-shapes with fillet edges rotated every 45 degrees. .	271
Figure 156. Wind simulation for one-sloped u-shapes with fillet edges.....	272
Figure 157. Wind simulations for single landforms.....	274

Figure 158. Wind simulations for two landforms.....	275
Figure 159. Wind simulations for two landforms rotated 45 degrees.	275
Figure 160. Wind simulations for three landforms.....	276
Figure 161. Wind simulation for single tree with 6 m/s and 10 m/s wind speed.	277
Figure 162. Wind simulation for two trees.....	278
Figure 163. Wind simulation for three trees rotated 15, 30, and 45 degrees.....	279
Figure 164. Vegetation simulation. Definition in Grasshopper (larger view in Appendix D, Figure 356).....	280
Figure 165. Vegetation simulation.	281
Figure 166. Visual summary of the simulation process.	282
Figure 167. Visual summary of the geomorphological simulations.....	283
Figure 168. Visual summary of the hydrological simulations.....	284
Figure 169. Visual summary of the large scale wind simulations.....	285
Figure 170. Visual summary of the building-scale wind simulations.	286
Figure 171. Visual summary of basic forms wind simulations.	287
Figure 172. Visual summary of landform wind simulations.....	288
Figure 173. Visual summary of vegetation and wind simulation.....	288
Figure 174. A process-based approach to landform architecture and an envisioned future.	290
Figure 175. Simulation workflow diagram for building design.....	292
Figure 176. Visual summary of simulation process (building design).....	293
Figure 177. Visual summary of simulation process (building design, landforms, vegetation).	294
Figure 178. Wind simulation for cuboid building.....	295
Figure 179. Wind simulation for cuboid building with three pockets.....	296
Figure 180. Wind simulation for cuboid building with fillet pockets.	297
Figure 181. 1897 USGS map of Portland, fragment. From USGS, 2017.	298
Figure 182. Geomorphological simulation.....	299
Figure 183. Wind simulation for cuboid building with wave-like facade.....	300
Figure 184. Hydrological simulation.....	301
Figure 185. Wind simulation for building form.	301

Figure 186. Wind simulation for a landform building, with wind speed of 6 m/s.	303
Figure 187. Wind simulation for a landform building, with wind speed of 10 m/s.	303
Figure 188. Wind simulation for north landform.	304
Figure 189. Wind simulation for enlarged north landform.	305
Figure 190. Wind simulation for two north landforms.....	305
Figure 191. Wind simulation for south landform: Option 1.....	306
Figure 192. Wind simulation for south landform: Option 2.....	307
Figure 193. Wind simulation for two south landforms.	307
Figure 194. South wind simulation.....	308
Figure 195. Hydrological simulation for the landform building and adjacent landforms....	309
Figure 196. Vegetation simulation.	310
Figure 197. Seasonal vegetation simulation. Left: Fall months. Right: Spring months.	310
Figure 198. North wind simulation for building, landforms, and vegetation.	311
Figure 199. South wind simulation for building, landforms, and vegetation.....	312
Figure 200. Bird’s-eye view of the landform building from the Steel Bridge.	313
Figure 201. Zoning requirements for the site (outlined in white).	314
Figure 202. Bird’s-eye view of the landform building from above the Broadway Bridge.	315
Figure 203. Pedestrian bridge from N. Broadway green plaza. Building glass sections.	316
Figure 204. Historic 1948 streets and the project site.	316
Figure 205. North side of the building.	317
Figure 206. Building form and site program.	318
Figure 207. South side of the building.	318
Figure 208. UTCI definition in Grasshopper (larger view in Appendix D, Figure 357).	320
Figure 209. UTCI simulation for current site conditions.	321
Figure 210. UTCI simulation for cuboid shape.....	322
Figure 211. UTCI simulation for a community center building, developed by El Dorado Architects.	323
Figure 212. UTCI simulation for the landform building.....	323
Figure 213. UTCI simulation for the landform building and green roof.....	324

Figure 214. Different types of landforms and processes that shaped them.....	334
Figure 215. Willamette River gauge historic crest simulation on June 24, 1876.....	335
Figure 216. Willamette River gauge historic crest simulation on July 1, 1880.	336
Figure 217. Willamette River gauge historic crest simulation on June 14, 1882.....	337
Figure 218. Willamette River gauge historic crest simulation on June 21, 1887.....	338
Figure 219. Willamette River gauge historic crest simulation on February 6, 1890.....	339
Figure 220. Willamette River gauge historic crest simulation on June 7, 1894.....	340
Figure 221. Willamette River gauge historic crest simulation on June 23, 1899.....	341
Figure 222. Willamette River gauge historic crest simulation on June 18, 1903.....	342
Figure 223. Willamette River gauge historic crest simulation on June 13, 1913.....	343
Figure 224. Willamette River gauge historic crest simulation on June 12, 1921.....	344
Figure 225. Willamette River gauge historic crest simulation on January 8, 1923.....	345
Figure 226. Willamette River gauge historic crest simulation on May 31, 1928.....	346
Figure 227. Willamette River gauge historic crest simulation on June 13, 1933.....	347
Figure 228. Willamette River gauge historic crest simulation on June 14, 1948.....	348
Figure 229. Willamette River gauge historic crest simulation on June 1, 1948.....	349
Figure 230. Willamette River gauge historic crest simulation on June 26, 1950.....	350
Figure 231. Willamette River gauge historic crest simulation on June 4, 1956.....	351
Figure 232. Willamette River gauge historic crest simulation on December 25, 1964..	352
Figure 233. Willamette River gauge historic crest simulation on January 18, 1976.....	353
Figure 234. Willamette River gauge historic crest simulation on December 16, 1977..	354
Figure 235. Willamette River gauge historic crest simulation on February 21, 1982....	355
Figure 236. Willamette River gauge historic crest simulation on June 9, 1996.....	356
Figure 237. Simulation of the Willamette River in 1897.	357
Figure 238. Simulation of the Willamette River in 1940.	358
Figure 239. Simulation of the Willamette River in 1954.	359
Figure 240. Simulation of the Willamette River in 1975.	360
Figure 241. Simulation of the Willamette River in 1979.	361
Figure 242. Simulation of the Willamette River in 1990.	362
Figure 243. Simulation of the Willamette River in 2011.	363
Figure 244. Simulation of the Willamette River in 2014.	364

Figure 245. Simulation of the Willamette River in 2017.	365
Figure 246. Simulation of the Willamette River in 2020.	366
Figure 247. Willamette River bathymetry in 1888.....	367
Figure 248. Willamette River bathymetry in 2005.....	368
Figure 249. Portland vegetation simulation in 1951.....	369
Figure 250. Portland vegetation simulation in 1970.....	370
Figure 251. Portland vegetation simulation in 1975.....	371
Figure 252. Portland vegetation simulation in 1990.....	372
Figure 253. Portland vegetation simulation in 1994.....	373
Figure 254. Portland vegetation simulation in 2000.....	374
Figure 255. Portland vegetation simulation in 2011.....	375
Figure 256. Portland vegetation simulation in 2014.....	376
Figure 257. Portland vegetation simulation in 2017.....	377
Figure 258. Portland vegetation simulation in 2020.....	378
Figure 259. Lower Albina neighborhood simulation in 1948.	379
Figure 260. Lower Albina neighborhood simulation in 1960.	380
Figure 261. Lower Albina neighborhood simulation in 1975.	381
Figure 262. Lower Albina neighborhood simulation in 1990.	382
Figure 263. Lower Albina neighborhood simulation in 2011.	383
Figure 264. Lower Albina neighborhood simulation in 2014.	384
Figure 265. Lower Albina neighborhood simulation in 2017.	385
Figure 266. Lower Albina neighborhood simulation in 2020.	386
Figure 267. Lower Albina neighborhood simulation in 2023.	387
Figure 268. Lower Albina neighborhood gauge historic crest simulation on June 14, 1948.	388
Figure 269. Lower Albina neighborhood gauge historic crest simulation on June 26, 1950.	389
Figure 270. Lower Albina neighborhood gauge historic crest simulation on June 4, 1956.	390
Figure 271. Lower Albina neighborhood gauge historic crest simulation on December 25, 1964.	391

Figure 272. Lower Albina neighborhood gauge historic crest simulation on January 18, 1974.	392
Figure 273. Lower Albina neighborhood gauge historic crest simulation on December 16, 1977.	393
Figure 274. Lower Albina neighborhood gauge historic crest simulation on February 21, 1982.	394
Figure 275. Lower Albina neighborhood gauge historic crest simulation on February 24, 1986.	395
Figure 276. Lower Albina neighborhood gauge historic crest simulation on February 9, 1996.	396
Figure 277. Lower Albina neighborhood gauge historic crest simulation on June 2, 2011.	397
Figure 278. Lower Albina neighborhood gauge historic crest simulation on March 30, 2017.	398
Figure 279. Lower Albina neighborhood gauge historic crest simulation on April 4, 2019.	399
Figure 280. Lower Albina in 1948, site scale simulation.	400
Figure 281. Lower Albina in 1960, site scale simulation.	401
Figure 282. Lower Albina in 1975, site scale simulation.	402
Figure 283. Lower Albina in 1990, site scale simulation.	403
Figure 284. Lower Albina in 2011, site scale simulation.	404
Figure 285. Lower Albina in 2014, site scale simulation.	405
Figure 286. Lower Albina in 2017, site scale simulation.	406
Figure 287. Lower Albina in 2020, site scale simulation.	407
Figure 288. Lower Albina in 2023, site scale simulation.	408
Figure 289. Lower Albina gauge historic crest simulation on June 6, 1948.	409
Figure 290. Lower Albina gauge historic crest simulation on June 26, 1950.	410
Figure 291. Lower Albina gauge historic crest simulation on June 4, 1956.	411
Figure 292. Lower Albina gauge historic crest simulation on December 25, 1964.	412
Figure 293. Lower Albina gauge historic crest simulation on January 18, 1974.	413
Figure 294. Lower Albina gauge historic crest simulation on December 16, 1977.	414

Figure 295. Lower Albina gauge historic crest simulation on February 21, 1982.	415
Figure 296. Lower Albina gauge historic crest simulation on February 24, 1986.	416
Figure 297. Lower Albina gauge historic crest simulation on February 9, 1996.	417
Figure 298. Lower Albina gauge historic crest simulation on June 2, 2011.	418
Figure 299. Lower Albina gauge historic crest simulation on March 30, 2017.	419
Figure 300. Lower Albina gauge historic crest simulation on April 12, 2019.	420
Figure 301. Wind simulation Scenario 1.	421
Figure 302. Wind simulation for Option 1. Plan view, perspective, side view, and front view.	421
Figure 303. Wind simulation for Option 2. Plan view, perspective, side view, and front view.	422
Figure 304. Wind simulation for Option 3. Plan view, perspective, side view, and front view.	422
Figure 305. Wind simulation for Option 4. Plan view, perspective, side view, and front view.	423
Figure 306. Wind simulation for Option 5. Plan view, perspective, side view, and front view.	423
Figure 307. Wind simulation for Option 6. Plan view, perspective, side view, and front view.	424
Figure 308. Wind simulation for Option 7. Plan view, perspective, side view, and front view.	424
Figure 309. Wind simulation for Option 8. Plan view, perspective, side view, and front view.	425
Figure 310. Wind simulation for Option 9. Plan view, perspective, side view, and front view.	425
Figure 311. Wind simulation for Option 10. Plan view, perspective, side view, and front view.	426
Figure 312. Wind simulation for Option 11. Plan view, perspective, side view, and front view.	426
Figure 313. Wind simulation for Option 12. Plan view, perspective, side view, and front view.	427

Figure 314. Wind simulation for Option 13. Plan view, perspective, side view, and front view.	427
Figure 315. Wind simulation Scenario 2.	428
Figure 316. Wind simulation for Option 1. Plan view, perspective, side view, and front view.	428
Figure 317. Wind simulation for Option 2. Plan view, perspective, side view, and front view.	429
Figure 318. Wind simulation for Option 3. Plan view, perspective, side view, and front view.	429
Figure 319. Wind simulation for Option 4. Plan view, perspective, side view, and front view.	430
Figure 320. Wind simulation for Option 5. Plan view, perspective, side view, and front view.	430
Figure 321. Wind simulation for Option 6. Plan view, perspective, side view, and front view.	431
Figure 322. Wind simulation for Option 7. Plan view, perspective, side view, and front view.	431
Figure 323. Wind simulation for Option 8. Plan view, perspective, side view, and front view.	432
Figure 324. Wind simulation for Option 9. Plan view, perspective, side view, and front view.	432
Figure 325. Wind simulation for Option 10. Plan view, perspective, side view, and front view.	433
Figure 326. Wind simulation for Option 11. Plan view, perspective, side view, and front view.	433
Figure 327. Wind simulation for Option 12. Plan view, perspective, side view, and front view.	434
Figure 328. Wind simulation for Option 13. Plan view, perspective, side view, and front view.	434
Figure 329. Wind simulation Scenario 3.	435

Figure 330. Wind simulation for Option 1. Plan view, perspective, side view, and front view.	435
Figure 331. Wind simulation for Option 2. Plan view, perspective, side view, and front view.	436
Figure 332. Wind simulation for Option 3. Plan view, perspective, side view, and front view.	436
Figure 333. Wind simulation for Option 4. Plan view, perspective, side view, and front view.	437
Figure 334. Wind simulation for Option 5. Plan view, perspective, side view, and front view.	437
Figure 335. Wind simulation for Option 6. Plan view, perspective, side view, and front view.	438
Figure 336. Wind simulation for Option 7. Plan view, perspective, side view, and front view.	438
Figure 337. Wind simulation for Option 8. Plan view, perspective, side view, and front view.	439
Figure 338. Wind simulation for Option 9. Plan view, perspective, side view, and front view.	439
Figure 339. Wind simulation for Option 10. Plan view, perspective, side view, and front view.	440
Figure 340. Wind simulation for Option 11. Plan view, perspective, side view, and front view.	440
Figure 341. Wind simulation for Option 12. Plan view, perspective, side view, and front view.	441
Figure 342. Wind simulation for Option 13. Plan view, perspective, side view, and front view.	441
Figure 343. Wind simulation Scenario 4.	442
Figure 344. Wind simulation for Option 1 and 2. Perspective view with horizontal wind vectors and vertical wind vectors.	442
Figure 345. Wind simulation for Option 3 and 4. Perspective view with horizontal wind vectors and vertical wind vectors.	443

Figure 346. Wind simulation for Option 5 and 6. Perspective view with horizontal wind vectors and vertical wind vectors.	443
Figure 347. Wind simulation for Option 7 and 8. Perspective view with horizontal wind vectors and vertical wind vectors.	444
Figure 348. Wind simulation for Option 8 and 9. Perspective view with horizontal wind vectors and vertical wind vectors.	444
Figure 349. Wind simulation for Option 11 and 12. Perspective view with horizontal wind vectors and vertical wind vectors.	445
Figure 350. Wind simulation for Option 13. Perspective view with horizontal wind vectors and vertical wind vectors.	445
Figure 351. Groundhog Grasshopper definition for surface water flow.	446
Figure 352. Ladybug Grasshopper definition for wind rose analysis.....	447
Figure 353. Definition for geomorphological simulation in Grasshopper.	448
Figure 354. Definition for hydrological simulation in Grasshopper.	449
Figure 355. Definition for wind simulation in Grasshopper.	450
Figure 356. Definition for vegetation simulation in Grasshopper.....	451
Figure 357. Definition for UTCI simulation in Grasshopper.	452

LIST OF TABLES

Table	Page
Table 1. Differences Between Research and Design.....	32
Table 2. Suitability analysis of potential sites for design experiment.....	179
Table 3. Willamette River gauge data (Morrison Bridge gauge).....	201

LIST OF SCHEMES

Scheme	Page
Scheme 1. Albina neighborhood building footprint areas vs. vegetation area.	223

I. INTRODUCTION

1.1 Statement of the Problem

The growing urgency of climate-related issues and their compounding negative effects require innovative design strategies. While landform architecture has a significant potential to address such challenges, the current approach in research and practice remains predominantly form-oriented. The form-oriented approach neglects the site, its history, and landscape processes that have the potential to shape the building. Such an approach fails to fully address critical challenges, such as urban heat growth, flooding, and habitat loss.

These issues are especially evident in urban areas like Portland, Oregon, where postindustrial land, hydrological shifts, and disrupted ecology lead to environmental problems. The Lower Albina neighborhood offers an opportunity to critically rethink infrastructural violence and erasure via the lens of landform architecture.

The lack of theoretical, methodological, and evaluative frameworks for landform architecture diminishes its potential to respond to climate-related challenges. There is a need to develop a process-based approach to landform architecture that:

- Establishes a theoretical framework that repositions landform architecture within a broader historical context by embracing site history and unique characteristics.
- Proposes a methodological framework that integrates site-specific landscape processes into the design process.
- Illustrates an evaluative framework that incorporates digital modeling and 3D simulation tools to visualize time, change, and history, along with site-specific processes to design a landform building and adjacent landscape within the selected site in the Lower Albina neighborhood.

The gap in knowledge and practice limits the potential of landform architecture. This study proposes a paradigm shift of landform architecture to process-oriented design that embraces the concept of time and change to seamlessly merge with context while mitigating site-specific problems. By focusing on the selected site for a design experiment, this study illustrates how process-based landform architecture engages with the site, its history, and environmental processes. Such an approach has the potential to develop a design that creates comfortable outdoor conditions and responds to climate-related issues.

1.2 Purpose of the Study

The history of landform design dates to prehistoric times, where landform hills and mounds were used for settlements, military defense structures, religious purposes, and protection from natural forces. More recently, landforms have been a source of inspiration for architects, landscape architects, and artists. With the development of digital technologies and construction practices, architects have been able to design landform buildings that use landscape as a generative metaphor to imitate natural forms. Landscape architects have designed landforms for a range of expressive and functional purposes, such as directing movement, providing visual frames and foci, dividing space, and fostering stormwater management. Land artists have used earth as a material to create site-specific earthworks and landforms in the landscape.

While landforms are understood by geomorphologists in terms of their form and the processes that shape them, current theory and practice of landform architecture focuses on a form-based approach based on the metaphoric interpretation of nature, rather than landscape processes and their potential to address large-scale problems. Landscape processes create a dynamic system that is constantly changing over time. In this research, landscape processes that shape the resultant form are a key research interest for design theory and practice. Understanding these processes is essential for designers to move beyond the static representation of the relationship between nature and architecture toward the living and changing qualities of the environment. Such a shift enables more responsive and integrated design solutions that can address climate change issues.

The purpose of the study is to develop a process-based approach to landform architecture that integrates landscape history, natural processes, and a site's challenges into design. Such an approach moves beyond form-based design solutions to process-oriented architecture that is responsive to climate-related challenges.

1.3 Objectives of the Study

The objective of this study is to develop a process-based landscape approach to landform architecture that addresses climate-related challenges and integrates site-specific processes into design. The research objectives are:

- Theoretical: Critique existing landform architecture theory and practice to identify gaps in knowledge and a process-based landscape approach to landform architecture, where landforms are understood as a process rather than a fixed form.
- Methodological: Establish a design method that integrates landscape processes into landform architecture.
- Evaluative: Test and refine the proposed approach through design experimentation by using digital modeling and simulation tools.

By structuring the research around these interconnected objectives, this study provides a framework for advancing landform architecture as a process-oriented design practice.

1.4 Definition of Terms

Research through design (RTD): An approach to scientific inquiry that takes advantage of the unique insights gained through design practice to provide a better understanding of complex and future-oriented issues in the design field (Frayling, 1993).

Simulation: The action or practice of simulating, the technique of imitating the behavior of some situation or process by means of a suitable analogous situation, especially for the purpose of study (Oxford University Press, n.d.-b).

Case study: A well-documented and systematic examination of the process, decision-making, and outcomes of a project that is undertaken for the purpose of informing future practice, policy, theory, and/or education (Francis, 1999).

Landform: A content-driven art form that operates between different categories of urbanism, landscape, architecture, and sculpture, and that brings together different levels of nature (Jencks, 2002).

Microclimate: The climate of a very small or restricted area, especially when this differs from the climate of the surrounding area (Oxford University Press, n.d.-a).

Urban Heat Island (UHI): A effect that occurs when a developed area experiences higher temperature than nearby rural areas, or when areas experience hotter temperatures within a city (U.S. EPA, 2022).

Universal Thermal Climate Index (UTCI): A measure of the human physiological response to the thermal environment. The UTCI describes the synergistic heat exchanges between the thermal environment and the human body (Climate-ADAPT, n.d.-b).

Mean Radiant Temperature (MRT) : The average temperature of all surfaces that surround a person, which represents the combined radiant heat exchange between a human body and the environment (Climate-ADAPT, n.d.-a).

*Other terms developed in this dissertation are introduced later in the body of the text.

1.5 Research Through Design

Research through Design (RTD) is a practice-based approach that positions design as a process and a mode of inquiry. It generates new knowledge through an iterative design process, where practice and theory inform each other. In this research, RTD is a general methodological approach that informs subsequent methods.

Multiple publications on RTD claim that connection between research and design creates a fertile ground and produces a new type of knowledge. Furthermore, RTD considers design as a method of inquiry to solve complex spatial questions. While RTD became one of the most-used methods in design disciplines over the last few decades, this method is still discussed and debated because there is no agreed-upon model that allows its practical use. The present study argues that the RTD method still lacks practical guidelines to use appropriately and thus creates confusion for practitioners and researchers to thoroughly understand and apply the method.

To understand the RTD method from academic and practice perspectives, it is necessary to define the terms “research” and “design” separately. Despite many definitions of both terms, I propose to use the one that is cited in design publications (Lenzholzer et al., 2018). In general discourse, research is understood to be a process of searching and researching again. Glanville defines research as an act of seeking deeply, with intensity, where the result of the search is a “new knowledge” (Glanville, 2014). The misunderstanding of the term “research” creates confusion, especially for practitioners, who are stating that they produce new knowledge through their practice. In contrast, the misunderstanding of the term “design” in the academic environment is mostly rooted in the design process. In creative disciplines, design is understood as a way of giving form and function. Carl Steinitz proposed a dual framework for thinking about design as a “verb” and design as a “noun” (Steinitz, 1995): Design as a verb is used for asking questions, and design as a noun is used for choosing among answers. In other words, design is an activity and process, as well as the result of activity in which a product has been given a shape.

There are many studies that support the idea that academics and practitioners learn and produce knowledge differently (Table 1). While there is a general consensus that research is more objective and design is more subjective (Simon, 1974; Schön, 1983; Lawson, 2010), there are other differences. Good research is characterized by a systematic process, which includes validity, transparency, communicability, and originality (Archer, 1995), and, as a result, produces fact-based knowledge. On the other hand, design is defined by project goals and requirements and produces practical knowledge (Schön, 1983; Lawson, 2010; Cross, 2006). Research questions can be identified as “puzzles” that scientists set for themselves, whereas design questions are “wicked” (Cross, 2006), typically not well defined and lacking all necessary information (Lawson, 2010). Researchers solve problems by analysis, while designers solve problems by synthesis (Cross, 2006). In other words, practitioners learn about the problem through the process of finding the solution, whereas academics are focused on studying the problem. The final outcome of research is new knowledge that is oriented toward theory development. On the contrary, in practice, design is the final product that offers specific solutions to a problem.

Table 1

Differences between research and design

	Research	Design
Type of perception	Objective	Subjective
Type of knowledge (Simon, 1974; Darke, 1979; Schön, 1983; Lawson, 2010)	Explicit knowledge Rational Fact-based How things are	Tacit knowledge Practical Appropriate How things ought to be
Type of questions (Cross, 2006; Lawson, 2010)	“Puzzle” questions	“Wicked” questions
Methods of developing knowledge (Cross, 2006)	Controlled experiment, classification, analysis	Modeling, pattern, synthesis

	Research	Design
Type of perception	Objective	Subjective
Process (Lawson, 2010)	Problem-defining Analysis Problem-focused strategy Systematic process	Problem-solving Synthesis Solution-focused strategy Process is based on project requirements
Final outcome (Cross, 2006)	Knowledge General concept or theory	Design Specific solution

The essential difference between research and design is that academics use a problem-focused strategy, while practitioners use a problem-solving strategy. In other words, academics and practitioners understand solutions to a specific problem differently and produce different types of knowledge.

In academic discourse, the combination of research and design, especially in creative disciplines, was understood as an approach that can answer complex questions (Archer, 1995; Zimmerman et al., 2007) and incorporate design activity into the research process.

The discussion about the relationship between research and design started with the urge to find new research methods to answer spatial questions. In 1993, design theorist Christopher Frayling described such a relationship in his seminal paper “Research in Art and Design,” where he pointed out that while research has historically been associated with words, not actions, that type of activity is far from the typical designers’ actions. Thus, Frayling developed a framework, which is used today as well, to describe relationships between research and design. He identified three groups of “research and design interaction[s]” based on relationships between academia and practice: (1) research for art and design, (2) research into art and design, and (3) research through art and design (Frayling, 1993).

Research for art and design includes the production of an artifact and gathering of research materials. The study in this category is focused on the design product and design process, and on what designers do when they collect information for the purpose of designing. Here, research outcomes inform the design process, so both design product and design process

benefit. In landscape architecture, this may include material studies or soil testing for green roofs (Simon & Steinemann, 2000) and produce design guidelines.

Research into art and design includes historical, aesthetic, and perceptual research into theoretical perspectives of art and design. The study in this category is focused on the design product. In landscape architecture, this may include a critical study of landscape, urban design, and their interpretation from different points of view (Nijhuis & Bobbink, 2012), as well as comparative case study analysis (Brinkhuijsen, 2008) and evaluation of design after realization (Meir et al., 2009; Sherman et al., 2005).

Research through art and design includes research processes that use design. Here, the act of design(ing) is considered as a research method. In order to consider it as research, however, the study in this category requires careful step-by-step documentation of the process. The result of such research cannot be just design itself: it should produce a new knowledge (Frayling, 1993). In landscape architecture, RTD is focused on the design process as a research instrument (van den Brink, 2017).

Frayling's categories were a stepping stone in the development of the RTD method, as they prompted a discussion that design can be considered as a research method. And in order to become a research strategy that produces a new type of knowledge, RTD would require a theoretical framework.

In the landscape architecture academic environment, Frayling's categories fostered a discussion about whether design has a potential to be accepted as a research method, and if so, how. This period was signified by the use of different terms that were supposed to describe the role of design and the application of its insights in research. Steenbergen et al. (2008) used "design experiment" and "experimental design" to describe design research in landscape architecture. A design experiment, in their understanding, is developed within the specific context, while investigation requires different design-based strategies. Experimental design, on the contrary, is developed when context and design strategies are changeable. Deming and Swaffield (2011) introduced "projective design," which represents a unique design process for research outcome. Projective design, in their definition, helps to incorporate a design framework and evaluation of design projects by testing them through design processes (Deming & Swaffield, 2011). The above-mentioned literature also emphasized that design needs to be guided by a clear research question, appropriate method, and valuable research outcome.

Nevertheless, it was not obvious how to apply these requirements into a research process. In my opinion, the design strategy during that period still remains poorly understood, even though it was frequently discussed.

In contrast to academia, the application of Frayling's framework in practice was signified by a shift to the idea that design can produce recognizable knowledge (Davis, 2008; Rodgers & Yee, 2015; Zeisel, 2006). In practice, such research was described as "practice-based" (Candy & Edmonds, 2018) or "practice-led" (Smith, 2009). Practice-based design research, contrary to academic understanding, was focused on the role of the practitioner, who had the skills and expertise in the field to undertake such research. Vaughan (2017) claimed in her book *Practice-based Design Research* that design-specific skills are the foundation needed to carry out practice-based research. The result of practice-based research was understood as one that advances knowledge and provides valuable application for practice.

During this period, design as research was described with the use of different, yet similar, terms. Different publications (Archer, 1995; Downton, 2005; Zimmerman et al., 2010; Collins, 2019; Glanville, 2014; Vaughan, 2017) also supported the idea that RTD is associated with learning through the process of designing. The huge development during this period was an alignment of RTD with research criteria, such as a research question, appropriate methodology, and a clear outcome. However, the process of designing was still underrepresented.

As the RTD method continues to develop in the landscape architecture field, some scholars have begun to investigate practical guidelines to use the RTD method. Multiple publications and studies have explored research as a part of the design process (Lenzholzer et al., 2013; RTD Conference Series, 2015). One publication described a three-staged study, where the major part of the research was focused on in-depth interviews and surveys with university faculty.

Following the interviews, Milburn and Brown (2003) developed a survey, where landscape architecture educators discovered that there are three design stages where research is incorporated into design: before design, during design, and after design. Before design includes library research, precedent study, case study analysis, and site analysis. During design, research influences the concept development. Finally, after design research allows the evaluation of the design itself (Milburn & Brown, 2003).

The most recent publication by Nijhuis and de Vries (2019) describes the RTD process as a sequence of design problem, design process, and design solution. The authors distinguish three interconnected phases of the design process: analysis, synthesis, and evaluation. The analysis phase includes data collection and understanding the context. The synthesis phase introduces different form-based solutions to the problem. The evaluation phase is focused on solution assessment (Nijhuis, & de Vries, 2019). At the same time, there is no data in the publications cited above that prove that practitioners incorporate research into the design process as the authors described. While the general framework for the design process proposed by Nijhuis and de Vries is valuable, the design itself is a more iterative and complex process. Additionally, there is a lack of literature that describes how RTD should be carried out in a practical sense.

Though scholars identified what the RTD approach means and explored the potential influences on knowledge, there is little information on how practitioners understand this research approach and design processes. Practitioners rarely communicate about their design processes; it is rather something more mystical than well documented and well explained. Currently, the number of practitioners who communicate their work as research-influenced is growing. However, they misuse the term “research” in the design process and do not have a complete understanding of what RTD actually means.

RTD is a relatively new method in design disciplines, which is considered to be a link between academia and practice, as well as research and design. Despite scholars’ and practitioners’ rising interest in this research method, that link is still not well established. The main difference between academic and practice approaches to RTD is that researchers and designers think differently. This explains why academics focus on discovering the theory, while designers focus on the solution and final result. In academia, the strategy to address the research question is problem-focused, while in practice it is problem-solving.

Researchers solve problem by analysis, while practitioners solve by synthesis. In other words, researchers study the problem, while designers discover something through the process of making and trying out multiple solutions. While RTD might look very similar to the actual design process, its goal, however, is new knowledge, not the design itself. Contrary to the typical design process, it requires careful documentation of the entire research process, so someone else could recreate that process too.

1.6 Methods

This research aims to contribute to existing theory and design knowledge in landform architecture and uses a combination of research methods to answer research questions. This study consisted of four stages (Figure 1):

Stage 1. Review of the existing state of theory and practice.

Stage 2. Development of a methodological framework for a process-based approach to landform architecture.

Stage 3. Design experimentation.

Stage 4. Environmental performance evaluation.

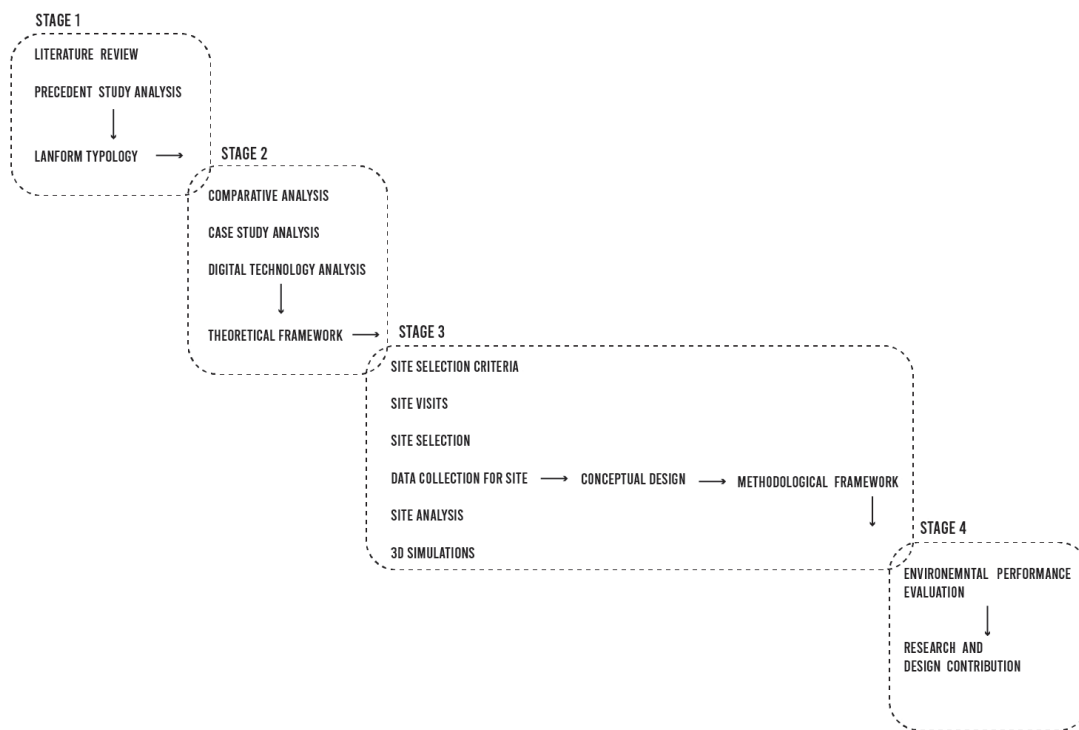


Figure 1. Stages of the research.

By structuring research in stages, where each stage builds on findings from the previous one, the study aimed to create a systematic approach to develop and test a process-based framework to landform architecture.

1.6.1 Stage 1

Stage 1 examines the existing state of knowledge both in research and practice in order to identify a knowledge gap and critique existing landform architecture theory. This stage (Figure 2) examines how landforms have been utilized in various fields and combines the knowledge and insights gathered from different disciplines to shape a comprehensive approach toward landform architecture. This stage enables a deep understanding of how the concept of landform architecture has developed over time, how it has been employed in other areas, and how insights from other fields could be incorporated to develop an approach to landform architecture design.

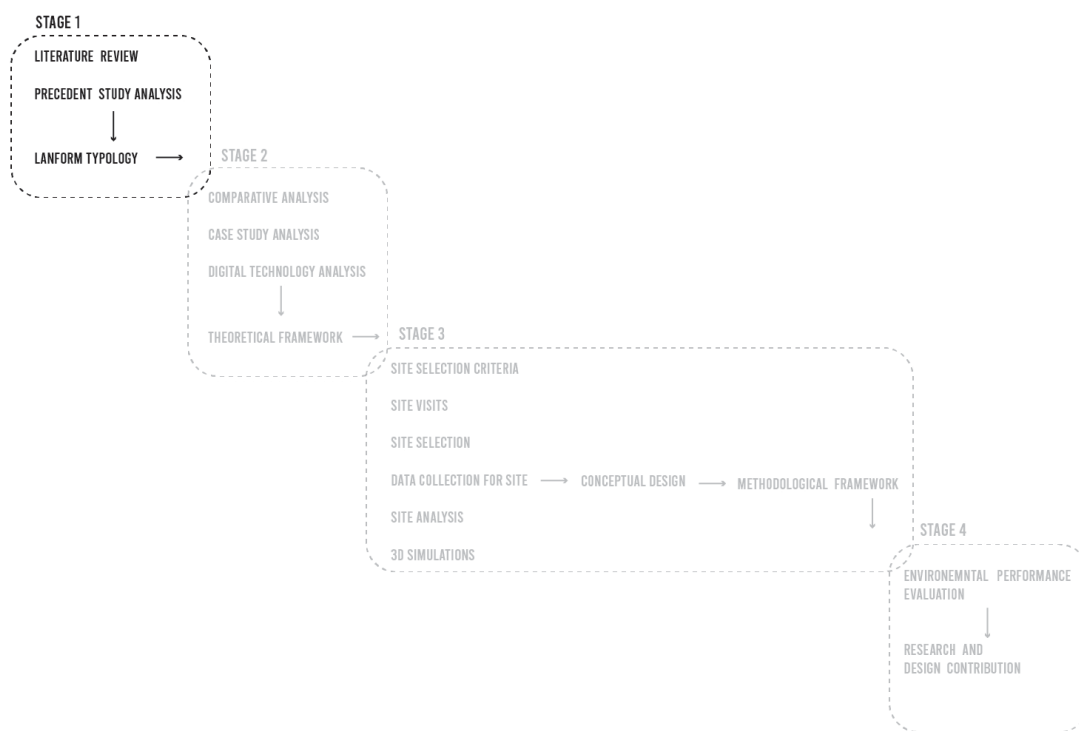


Figure 2. Stage 1.

The objectives of Stage 1 were to:

- trace the evolutionary development of landform architecture,
- understand how landforms have been used in other disciplines, and
- synthesize how knowledge from other disciplines could inform an approach to landform architecture.

This stage of research consisted of the literature review and precedent study analysis. Qualitative data, such as text and images, were employed for analysis. The sources for analysis included peer-reviewed articles, books, architects' and artists' websites, and site visits to some precedent study projects.

1.6.1.1 Literature Review

The literature review addressed the following categories of landform expression:

- landform in ancient cultures,
- landform in art,
- landform in landscape architecture, and
- landform in architecture.

These categories were selected to provide a comprehensive understanding of how landforms have been represented, utilized, and conceptualized across different disciplines and historical contexts.

The literature review informed theory and helped to:

- explore the use of landforms throughout history across cultures and disciplines,
- explore the development of landform architecture theory,
- critique landform architecture theory, and
- identify the theoretical potential of landform architecture.

1.6.1.2 Precedent Study

The precedent study analysis examined selected projects that integrated landforms into art, landscape architecture, and architecture. Such analysis helped to connect theoretical research with design practice.

The list of precedent study projects was derived from the literature review and analysis of key themes and trends in the field. The precedent study included the following selection criteria:

- The project resembled a landform (vegetated hills, grass mounds, earthworks).
- The project description included words such as “earthwork” or “landform.”
- The project was integrated into the context in a way that asserted the continuity of the context.

The literature review identified the following precedents:

1. Architecture

- The Möbius House in the Netherlands by UNStudio
- HtwoOexpo pavilion in the Netherlands by NOX
- Library Delft University of Technology in the Netherlands by Mecanoo
- Stranded Sears Towers in Chicago by Greg Lynn
- Yokohama International Port Terminal by FOA
- Fort L'Empereur in Algiers by Le Corbusier
- NTR Headquarters in the Netherlands by MVRDV
- Villa VPRO in the Netherlands by MVRDV
- Olympic Sculpture Park in Seattle by Weiss/Manfredi
- City of Culture of Galicia in Spain by Peter Eisenman
- Mountain in Spain by Vicente Guallart
- New Maribor Art Gallery in Slovenia by Stan Allen
- Chulalongkorn University Centenary Park in Bangkok by LANDPROCESS
- Underground Parking Garage in the Netherlands by Royal HaskoningDHV and OKRA Landschapsarchitecten

2. Ancient cultures

2.1. Settlements

- Early settlement in Petra, Jordan
- Mesa Verde in Colorado, USA
- Machu Picchu in Urubamba Province, Peru

2.2. Defense

- Dun Aengus in Ireland
- Maiden Castle in Dorset, England
- Hambledon Hill in England

2.3. Death and life

- Stonehenge in Wiltshire, England
- Kurgan Tovsta Mohyla in Ukraine

3. Art

- 3.1. Robert Smithson
 - *Asphalt Rundown* in Rome, Italy
 - *Spiral Jetty* in Great Salt Lake, Utah
 - *Broken Circle/Spiral Hill* in Emmen, the Netherlands
 - *Amarillo Ramp* in Amarillo, Texas
4. Landscape architecture
 - 4.1. Charles Jencks
 - *The Landform Ueda* in Edinburg, Scotland
 - *The Scottish World* in Kelty, Scotland
 - *Land War Garden* in Salford, Manchester
 - 4.2. Maya Lin
 - *The Wave Field* in Ann Arbor, Michigan
 - *The Wave Field Flutter* in Miami, Florida
 - *The Storm King Wavefield* in New Windsor, New York
 - 4.3. Kathryn Gustafson
 - The Shell Petroleum Gardens in Rueil-Malmaison, France
 - Diana, Princess of Wales Memorial Fountain in London, United Kingdom
 - Cultuurpark Westergasfabriek in Amsterdam, the Netherlands
 - 4.4. George Hargreaves
 - Parque do Tejo e do Trancão in Lisbon, Portugal
 - Crissy Field in San Francisco, California

Each precedent study project was reviewed based on the following template:

- The name, year, and location of the project.
- The main idea, design intentions, and role of landforms in the design.
- The site history and challenges with the site.
- Design transformations.
- The way different designers approached the integration of landform into their designs.

- A summary of the design and how the particular project shapes landform understanding.

Precedent study analysis informed practice and helped to:

- identify the gap in practice,
- critique the form-based approach in design,
- identify the potential development of landform architecture, and
- develop a typology of landform architecture.

The final part of Stage 1 was a synthesis of the literature review and precedent analysis into a landform typology, which aimed to categorize landform buildings according to the dominant metaphor used, including biological, geological, or ecological metaphors. Such typology helped to identify an approach to design landform architecture in different contexts, whether it is an integration with an existing landform, an extension of an existing landform, or a completely new landform.

1.6.2 Stage 2

Stage 2 (Figure 3) aimed to develop a methodological framework for a landscape approach to landform architecture and included theoretical and practical explorations. The theoretical exploration consisted of the analysis of a process-based approach in landscape architecture. The practical exploration included case study analyses of projects that used 3D simulations of natural processes.

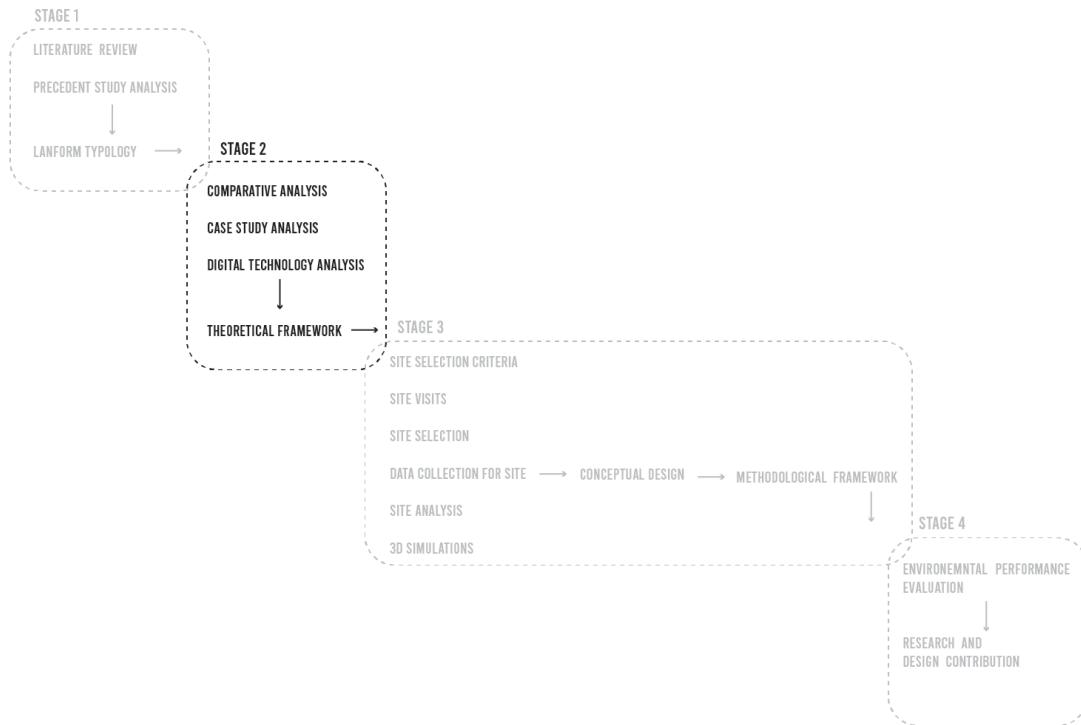


Figure 3. Stage 2.

The objectives of Stage 2 were to:

- develop a theoretical framework for a process-based landscape approach to landform architecture,
- analyze the application of process-based design in landscape architecture,
- explore the potential of 3D simulation to model natural processes,
- conduct detailed case study analyses of selected projects, and
- synthesize findings into a theoretical framework.

This stage of research consisted of the comparative analysis and case study analysis of selected projects. Qualitative data, such as text and images, were employed for analysis. The sources for analysis included peer-reviewed articles, books, architects' websites, and informal interviews.

1.6.2.1 Comparative Analysis

The theoretical exploration of a process-based approach in landscape architecture included a review of landscape architects and architects who used this approach in their design work. This analysis was divided into three categories:

1. Ecological process-based design
 - 1.1 George Hargreaves
 - 1.2 Michel Desvigne
 - 1.3 Michael Van Valkenburgh
2. Systems process-based design
 - 2.1 James Corner/Field Operations
 - 2.2 Rem Koolhaas/OMA
3. Phasing process-based design
 - 3.1 Rem Koolhaas/OMA

Based on such analysis, this dissertation presented a process-based landscape approach to landform architecture that considers the dynamic nature of natural processes that can shape the form of a building.

The next section of Stage 2 research analyzed digital technologies and software that can simulate time, possible changes, and natural processes. Computational Fluid Dynamics (CFD) simulations of natural processes were conducted using Ansys, SimScale, and Rhinoceros (Rhino) + Grasshopper programs. In this research, Rhino and Grasshopper software were used for 3D modeling and 3D simulations, as these programs are more commonly used by architects and landscape architects. Rhino provided a platform for creating and modifying 3D models, while Grasshopper allowed for the creation of complex algorithms, such as CFD simulations of fluid flow, heat island analysis, and outdoor comfort analysis. Together, these tools created and tested various simulations that helped in understanding natural systems, such as wind and water flow, and heat transfer.

1.6.2.2 Case Studies

To understand 3D simulations of natural processes, the next step of Stage 2 research was a case study analysis of selected projects that used 3D simulations as a research method.

Case study analysis consisted of the following steps:

1. Identify specific processes for case studies analysis. The selected processes are based on those typical for the development of natural landforms: geomorphological, fluvial, wind, and vegetation processes.
2. Identify case study projects that use 3D simulation of specific processes, such as landform simulation, fluvial simulation, wind simulation, and vegetation simulation. This stage involved a review of published literature and online sources to find examples of relevant projects. The following projects were selected based on their relevance to landform architecture and this research, their use of a specific type of simulation as a generative tool, and the accessibility of information about the project:
 - MAX IV Laboratory by Snøhetta
 - Jade Eco Park by Philippe Rahm Architectes
 - Yanghwa Riverfront by PARKKIM
 - Sony Forest by Tsukasa Takenaka and Aya Okabe

While there were limited case study projects for specific processes, such as vegetation and landform simulations, one case study was selected for each simulation category based on the relevance to the research.

1. Data analysis. Once the case studies were identified, the next step was to gather data about each project, which involved interviews and a review of published peer-reviewed papers, books, and project descriptions from websites to understand the scope, objectives, and outcomes of each project. The data was organized in a chart for comparison and analysis.
2. Project analysis using a case study method for landscape architecture. A case study analysis method for landscape architecture, developed by Mark Francis, included analysis of three levels of information for each project: (1) a project introduction, (2) a full case study, and (3) more in-depth information of a more contextual or specialized nature unique to the case study. Each level included specific data relevant to the research.

The first level included:

- photos,
- project background,
- project significance and impact, and

- lessons learned.

The second level included:

- project name;
- location;
- date designed/planned;
- construction completed;
- cost;
- size;
- landscape architect(s);
- client;
- consultants;
- management;
- context;
- site analysis;
- project background and history;
- genesis of project;
- design, development, and decision-making process;
- role of landscape architect(s);
- program elements;
- maintenance and management;
- photograph(s);
- site plan(s);
- user/use analysis;
- peer reviews;
- criticism;
- significance and uniqueness of project;
- limitations; and
- generalizable features and lessons.

The third level included unique case study information:

- 3D simulations.

3. Conclusions. Based on the case study analysis, the effectiveness of 3D simulations, project results, and limitations were identified. This information informed the development of a theoretical framework for a process-based landscape approach to landform architecture.

The synthesis of comparative analysis of the process-based landscape approach and case study analysis formed a theoretical framework for a process-based landscape approach to landform architecture. This theoretical framework treated buildings as a continuation of the site. In this context, site research, its history, and analysis of site-specific processes that shaped the site to its current state, and, more importantly, anticipated future changes were an important part of the design process.

1.6.3 Stage 3

To test the theoretical framework developed in Stage 2, Stage 3 (Figure 4) consisted of a practical design exploration. This stage employed the RTD method, along with other methods related to site analysis and data collection. The intention was to examine a new approach to landform architecture and to use 3D simulations of natural processes to develop a 3D model of a landform building and adjacent landscape. The modeling and simulation were performed with the use of Rhino and Grasshopper programs. Based on the design experiment, the framework for landform architecture was revised and updated.

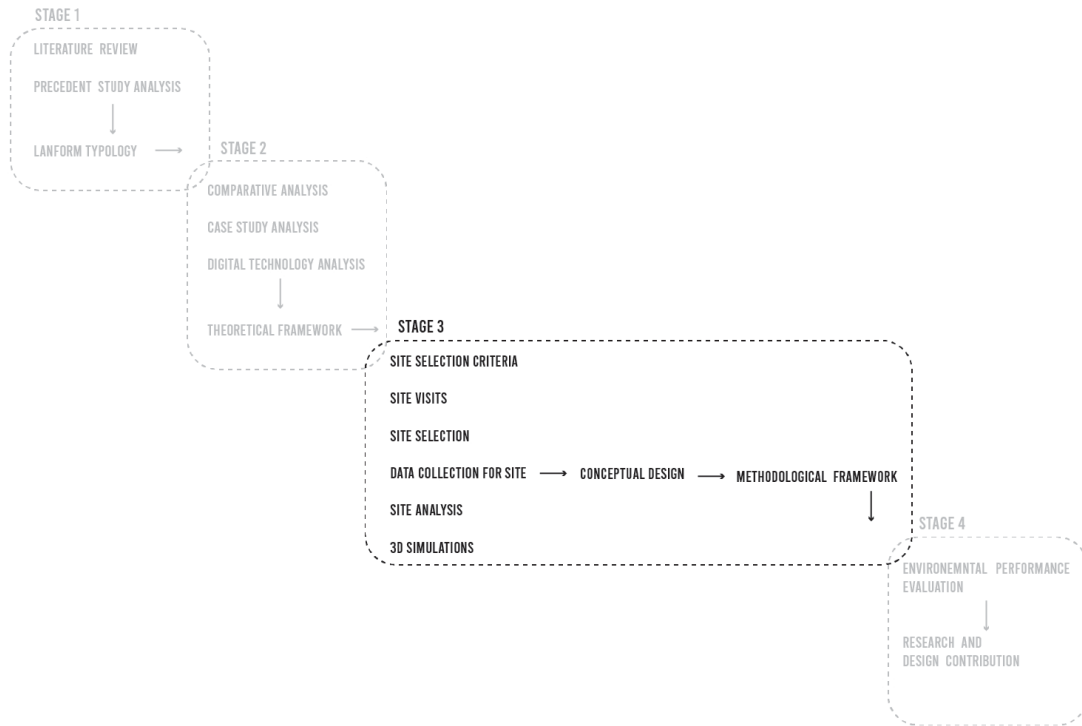


Figure 4. Stage 3.

The objectives of Stage 3 were to:

- illustrate the role of design as a tool for inquiry,
- establish site selection criteria,
- conduct site visits and site analysis,
- collect and analyze site data,
- develop 3D simulations of natural processes,
- test the design framework,
- identify how the history of the site and site-specific processes shape landform architecture,
- develop a landform building design with the use of a process-based approach, and
- develop a methodological process-based framework to landform architecture.

In this study, the RTD method was an iterative process that constantly shifted between theoretical and practical perspectives. The combination of experiments from the design process, as well as reflections from research processes, enabled the development of more valuable results. These results were problem-solving oriented, which is natural for the design process. However,

they generated new knowledge rather than the design solution itself. Thus, the aim of this study was to contribute to the RTD discourse by developing theoretical and practical design frameworks and illustrating how such a framework worked with a design project.

This stage consisted of the development of site selection criteria, site visits, site selection, data collection for the site, site analysis, 3D simulations, and conceptual design. Qualitative data, such as text and images, were employed for analysis. The sources for analysis were archival records, topographic maps, satellite and aerial imagery, hydrological data, Geographic Information System (GIS) and land-use data, and climate data.

1.6.3.1 Development of Site Selection Criteria

The development of site selection criteria can occur in two ways: (1) the client has a site and chooses a program for the specific site, or (2) the client has a program and needs to select a site for those uses (LaGro, 2009). While this is applicable for client-initiated projects, it required adaptations for a research-initiated project.

In this research, the site selection process was based on two possible approaches:

1. Explore a region's environmental problems that landform architecture can address and then search for a site that exemplifies that problem.
2. Choose the site and, after the inventory of the site's physical, biological, and cultural attributes, decide what attributes a landform building(s) can address.

In this research there was no specific site for design, so the site selection process followed the first approach that started with the analysis of environmental problems and their effects on specific regions.

The development of site selection criteria started with the selection of the region. The city of Portland, Oregon, was selected as the geographic context due to its significant urban climate challenges that provide a relevant context for exploring the potential of landform architecture to influence the local microclimate. Portland also offered extensive and available data, and travel suitability for research and the design experiment.

The following site selection criteria were used to identify potential sites within the Portland area:

- UHI intensity for the site at 30–35 °C
- Tree canopy cover at 0–25%

- Vacant or underutilized land
- Presence of site-specific landforms
- Historical significance
- Dynamic environmental changes (e.g., flooding)
- Integration with an urban renewal plan

These criteria were developed to identify a location where landform architecture could have a significant impact while aligning with the research objectives.

The UHI effect criteria focused on areas with high temperatures due to urbanization, which helped to identify locations where a design intervention could help to mitigate extreme heat. The tree canopy cover was a critical parameter, as vegetation plays a central role in cooling and providing shade. Sites with lower canopy areas were prioritized, since they could benefit from landform architecture integration.

The study prioritized vacant areas because they proposed opportunities for transformation. The selection process included site-specific characteristics that reflect the uniqueness of the site, such as site-specific landforms. Sites with historical significance were considered in the selection process as they make it possible to integrate cultural and urban history into the design process. The alignment with an urban renewal plan criteria positioned the selected site within broader city planning strategies.

To narrow down the site selection further, a site suitability analysis was conducted. This process helped to identify a site that supports the objectives of the research and allowed for design intervention.

1.6.3.2 Site Visits

A series of site visits to potential sites in Portland were conducted to assess their urban context, environmental conditions, and suitability for implementing landform architecture interventions. The first site visit focused on observation and visual analysis of each site's context. The subsequent site visits included photographic documentation for further analysis. The last site visit incorporated drone imagery for the final site consideration.

1.6.3.3 Site Selection

The final site selection process consisted of the following steps (Figure 5):

- Identify project objectives. The process begins with defining the objectives of the project or issues that landform architecture can address.
- Identify potential sites and develop site selection criteria. Using the established criteria, multiple sites were identified for further analysis. These sites were later evaluated based on their alignment with the project's objectives and suitability parameters.
- Data analysis. Data was analyzed to identify which site has the potential for design intervention.
- Identify modeling processes for the specific site.
- Identify data necessary for 3D simulations and modeling.

In this research, project objectives were divided into:

- Urban objectives: urban growth, urban heat island, urban noise, and urban deforestation.
- Environmental objectives: climate change, global warming, brownfield restoration, wetland restoration, riparian restoration, ecological conservation, greater rainfall, sea-level rise, flooding, high-tide flooding, wetland flooding, erosion, and environmental hazards.

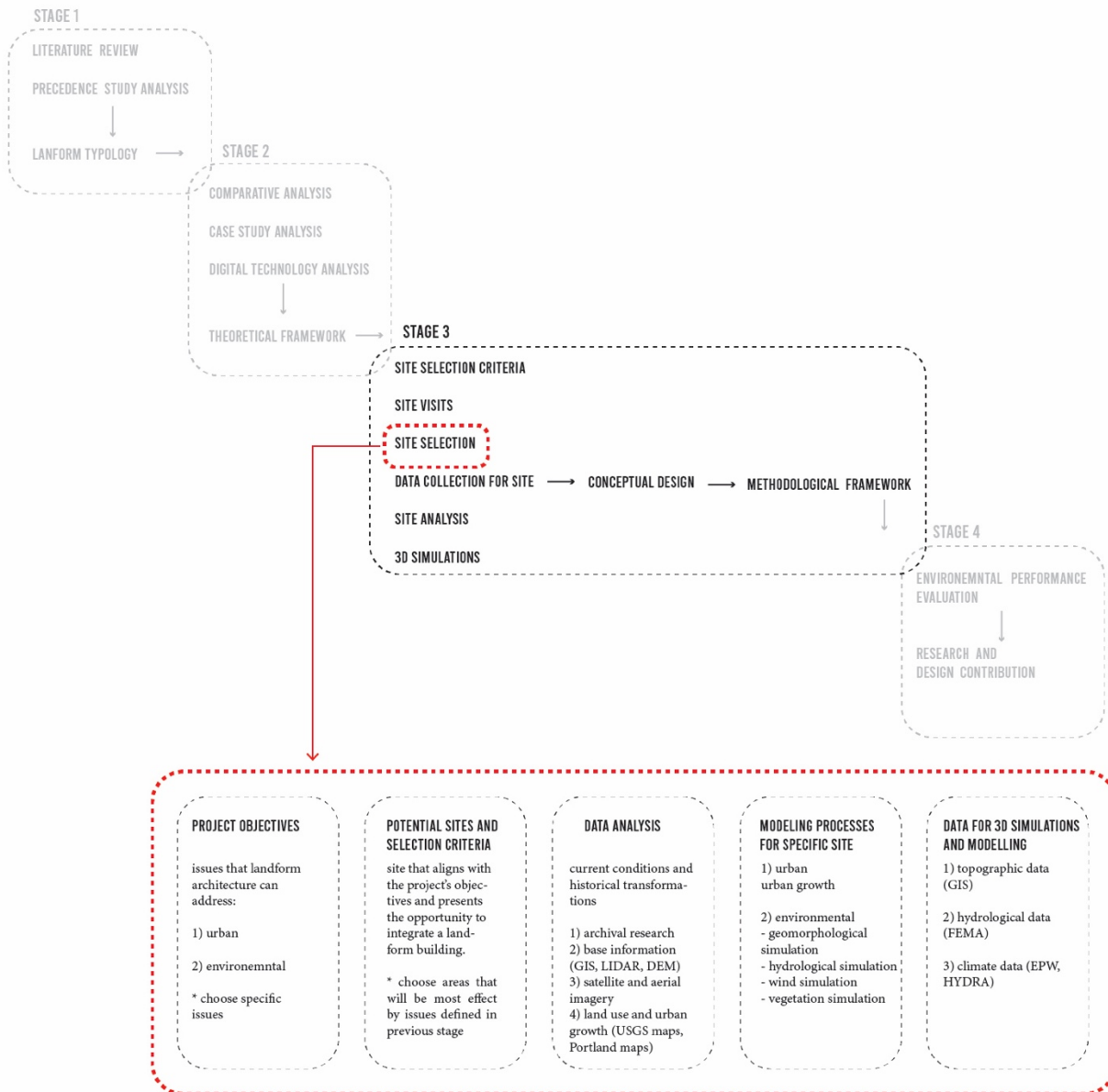


Figure 5. Site selection process for design experiment.

Based on the site analysis, a site was selected that aligned with the project's objectives and presented the opportunity to integrate a landform building.

1.6.3.4 Data Collection for Site

The data collected included information about the selected site to understand its current conditions and historical transformations. This was achieved through archival research, base information analysis, aerial images, maps, site visits, and interviews with professionals.

Data from archival research came from historical records, reports, and documents, such as:

- Historic maps: Harvard Old Maps Online.
- Governmental records: documents from city planning departments, historical societies, federal agencies such as the Federal Emergency Management Association (FEMA), and the Portland Bureau of Planning and Sustainability.

The base information data was collected from geospatial platforms and governmental databases:

- GIS: data on land use and site boundaries.
- LIDAR and DEM (Digital Elevation Models): detailed topographic information.

The high-resolution satellite and aerial imagery were collected to analyze the physical attributes of the site, vegetation cover, and urban morphology. Such data was collected from:

- U.S. Geological Survey (USGS).
- City of Portland Aerial Imagery Database.
- University of Oregon Knight Library aerial maps reserve.
- Google Earth Pro.

The selection of historical and contemporary maps helped to collect information related to the transformation of the site over time, such as land-use patterns, urban growth, and tree canopy cover. The data was collected from the following sources:

- USGS topographic maps.
- Portland Parks and Recreation Urban Forestry maps to collect tree canopy covers.
- Portland State University's Sustaining Urban Places Research Lab temperature maps.

The series of informal discussions with landscape architects, urban planners, architects, and other experts contributed to this study by offering insights into historical, cultural, and environmental contexts.

1.6.3.5 Site Analysis

Site analysis was a comprehensive analysis of the selected site's history and changes over time. This analysis provided a deeper understanding of the site as a dynamic system and its environmental conditions and focused on historical, cultural, and environmental contexts and their transformations across various scales. The analysis aimed to understand processes that have shaped the site and considered both environmental and human influences.

The site analysis was structured into three scales: city scale, neighborhood scale, and site scale. The city-scale analysis focused on the larger urban framework to understand the site's position within the city of Portland. The neighborhood-scale analysis focused on the immediate context and historical development, cultural changes, and urban dynamics. The site-scale analysis focused on specific characteristics of the site, including topography, hydrology, vegetation, and urban changes.

For each scale, an analysis of geomorphological, hydrological, wind, and vegetation processes were conducted, considering environmental and human agents that have shaped the site. Analysis of geomorphological processes included changes of geomorphological formations over time and physical terrain. Analysis of fluvial processes focused on transformations of the Willamette River over time. Analysis of vegetation processes illustrated the change in land cover and the influence of human-induced processes of urbanization on such changes.

The historical transformation of the site was studied with the use of various data types and sources, including:

- Archival records: University of Oregon Knight Library aerial maps reserve; Portland Maps Advanced.
- Topographic maps: USGS topographic maps of 1897, 1940, 1954, 1961, 1975, 1990, 2011, 2014, 2017, and 2020, and Portland Geologic Quadrangle maps.
- Flood and bathymetry data: USGS Missoula Floods Inundation map and GIS bathymetry data.
- Satellite and aerial imagery: Google Earth satellite images and Oregon State University Aerial imagery.
- Hydrological data: Willamette River gauge data and annual rainfall data from the City of Portland HYDRA Rainfall Network.

Additional data gathering related to 3D modeling in Rhino included:

- Topographic data: LIDAR, DEM topographic data, and contour maps.
- GIS and land-use data: GIS data on location, boundaries, land use, vegetation, and hydrology.
- Hydrological data: water flow patterns, gauge data, and water features.
- Climate data: temperature, rainfall, and wind speed data that can be used to simulate weather patterns and existing environmental conditions.

This analysis was performed by using and tracing 2D data from different sources in AutoCAD. Such data was later transferred into 3D models and simulations of historic transformation in Rhino. The site analysis revealed how environmental and human processes have shaped the complex history of the site and represent the site's evolution at multiple scales.

1.6.3.6 3D Simulations

The next step of Stage 3 research was a series of 3D simulations of site-specific processes within a process-based landscape approach to landform architecture. These simulations aimed to understand the current state of the project site and how natural processes have influenced the site. The proposed design framework consisted of 3D simulations of geomorphological, hydrological, wind, and vegetation processes. Once the current state of the site was analyzed, the study focused on testing the basic architectural forms within the site and their interaction with natural processes.

The simulations were used to study stormwater drainage, flooding from the Willamette River, wind patterns, and vegetation changes over time. By conducting simulations, it was possible to gain insights into how the site's microclimate functioned, which was essential for designing landform buildings and addressing climate issues, such as the urban heat island effect and flooding.

These simulations used the following data:

- Topographic data: GIS data with 2-foot contour lines served as a base for precise 3D models.
- Hydrological data: FEMA 100-year floodplain map.

- Climate data: EPW (Energy plus weather) files from the Portland International Airport, and annual rainfall data from the City of Portland HYDRA Rainfall Network.

The first step in a series of simulations was a topographic 3D model. The model was developed in Rhino using the Delaunay mesh triangulation method, and input data was from the GIS. The model also included urban features and structures, adjacent infrastructures of highways and roads, and existing vegetation. After the base model was developed, the next step was a series of 3D simulations to analyze current processes on site.

Analysis of the current geomorphological process was performed in Grasshopper, a visual programming tool for Rhino. The objective of landform simulation was an analysis of existing landforms and their potential to inform landform buildings and adjacent landscapes. In this process, the 3D mesh was developed to represent geological terraces.

Analysis of the current hydrological process was performed in Grasshopper. The objective of hydrological simulation was to understand the water flow, rainfall impact, and floodplain interaction on the site. FEMA's 100-year floodplain data was translated into the 3D model to evaluate the flood impact on the site. Additionally, the surface water flow was simulated with the Groundhog plug-in with the input of site mesh and topographic data. The rainfall data was used for analysis of the seasonal patterns and water interactions with the terrain.

The initial analysis of the wind process to test current conditions was performed in Eddy 3D, a Grasshopper plug-in for Rhino. However, during the final calculation step, where wind data is converted into vectors, the plug-in consistently showed an error. Because of this, simulations were done in the Ladybug suite for Grasshopper instead.

Analysis of the current wind process was performed in Grasshopper with the use of the Butterfly plug-in from the Ladybug suite and the OpenFOAM platform. Before running the wind simulation in Butterfly, it was necessary to make a wind rose analysis for each month to identify wind patterns by using the Ladybug plug-in. The objective of wind simulation was to evaluate wind speed and wind direction, and visually represent wind patterns and the influence of the wind process on the site. The input data for wind analysis was EPW data, neighboring existing structures, and site topography.

Analysis of the current vegetation process was performed in Rhino. The aim of the simulation was to show the current vegetation and identify the role of vegetation in shaping the

site's ecological and microclimate conditions. The 3D model represented the current distribution of trees on site.

After the analysis of current processes, a framework for a process-based approach to landform architecture was developed. The framework consisted of geomorphological, hydrological, wind, and vegetation simulations. The next set of 3D simulations followed an iterative process that aimed to test how site-specific processes interacted with basic architectural forms. This framework integrated dynamic 3D simulations into the design process. The simulations helped to represent the relationship between architecture and landforms, water flow, wind flow, and vegetation.

The geomorphological simulation was performed in Grasshopper with the use of the Anemone plug-in to create iterative loops that generate a 3D polysurface. Landform simulation aimed to analyze how landform interacts with natural forces. The input for this simulation was a closed curve. The iterative process created an optimal landform shape. The resulting landform simulation shape was the base for hydrological, wind, and vegetation simulations.

The hydrological simulation was performed in Grasshopper with the use of the Anemone plug-in to simulate stormwater flow to evaluate runoff patterns. The input for the simulation was site topography, variations of building forms, sloped roofs, and wave-like structures. Additional input parameters were a number of points that served as starting points for water runoff, and a number of iterations—continuous loops that simulate the water flow. The simulation illustrated the interaction between form and fluvial process; geometry can be modified based on the simulation results right in the program.

The wind simulation was performed in Grasshopper with the use of the Butterfly plug-in. The simulation indicated how a landform building influenced wind behavior and local microclimate. The input parameters were building geometry, wind speed, wind direction, EPW data, and bounding box for wind vectors. The simulation explored various shapes, orientations, and configurations. In addition, the simulation explored not only building shapes, but also landscape features, such as landforms and trees. The output results were a series of vectors that represent wind conditions around the designed object. The iterative testing approach tested various parameters of the building along with adjustments in building and landscape placement and orientation.

The vegetation simulation was the final simulation in the process-based approach. The simulation was performed in Grasshopper with the use of the Anemone plug-in to simulate an iterative tree growth cycle. These simulations visualized vegetation growth and change over time to understand how vegetation evolves with design intervention, interacts with wind patterns, and changes the local microclimate. The input parameters were a group of points that marked the location of a tree, and tree parameters, such as height, amplitude, radius, number of segments, and number of simulation iterations. The output parameters were a group of trees. After the tree geometry was generated, the tree placement was tested on wind conditions and whether they created a comfortable microclimate.

The set of 3D simulations modeled how local processes interact with the site and architectural form. Each simulation focused on a specific process and interaction between the geometry and local microclimate. The iterative approach integrated natural processes into the design process and incorporated design adjustments based on simulation results. The simulation results informed the design decisions in the following design experiment.

1.6.3.7 Conceptual Design

The last step of Stage 3 research was to test a process-based methodological framework for landform architectural design. In this process, the set of 3D simulations were integrated into the early stages of the design process. This stage explored how site-specific processes, such as geomorphological, hydrological, wind, and vegetation, can inform the design of a cultural center and waterfront park along the Lower Albina area in Portland, Oregon.

This stage applied the process-based framework to create a conceptual design of a landform building in Rhino. This stage used information obtained in the previous stages to develop a building design and adjacent landscape. The results of this stage demonstrated how computational tools and a process-oriented approach can inform a landform building. The findings from the simulations were integrated into a cohesive design that illustrated the use of computational tools and a process-oriented method.

1.6.4 Stage 4

Stage 4 (Figure 6) aimed to evaluate the environmental performance of a landform building. The objective of this stage was to analyze how the proposed design influences the local

microclimate. This stage used Grasshopper plug-ins to generate and analyze the outdoor comfort level. In this simulation, a series of microclimate maps were developed.

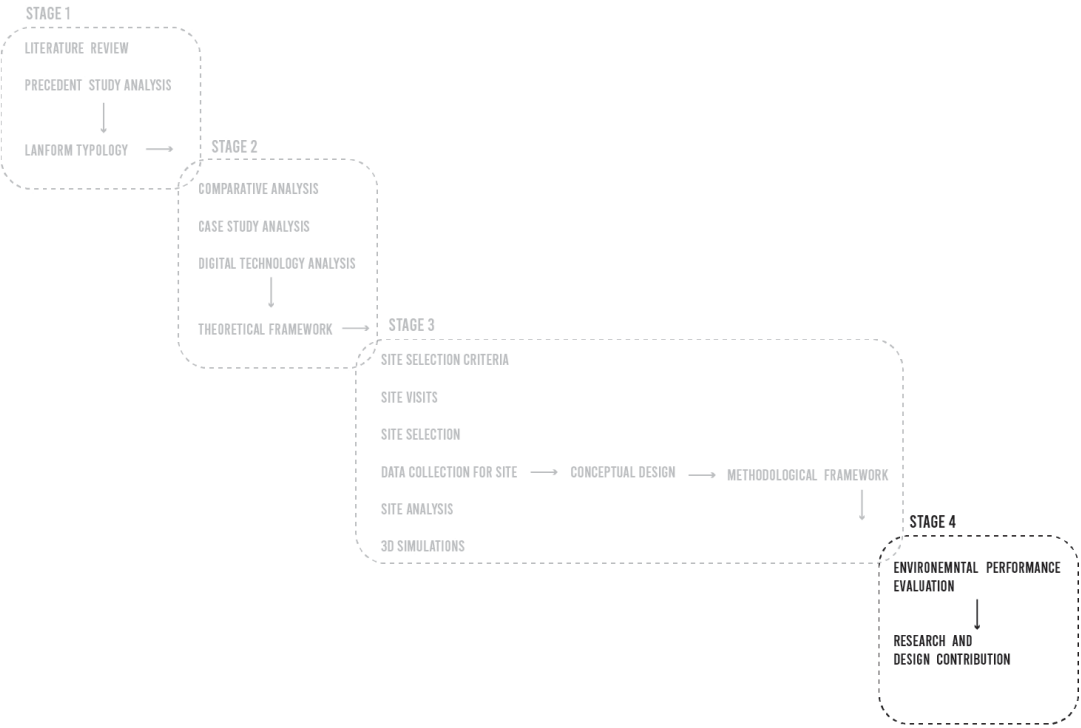


Figure 6. Stage 4.

The objectives of Stage 4 were to:

- test the environmental performance of the developed design,
- identify the influence of a landform building on the local microclimate,
- identify the influence of a landform building on a local microclimate, and
- refine design strategies and theory developed in Stages 2 and 3.

This stage consisted of data collection for environmental performance evaluation, Grasshopper analysis, and interpretation and comparison of results. The sources for analysis included climatic data and the 3D model that was developed in Rhino in the previous stage.

1.6.4.1 Environmental Performance Evaluation

To test the landform building designed in Stage 3, Stage 4 focused on gathering data for Grasshopper simulations on existing microclimate and urban conditions in the project area. This data included:

- building geometry and adjacent landscape,
- EPW climate and weather data,
- solar radiation and MRT, and
- wind speed.

The EPW data and solar radiation with MRT were collected using the Ladybug simulation. The wind speed data was collected from the Grasshopper simulations with the use of the Butterfly plug-in.

This simulation tested 3D models that represent different design conditions:

- predevelopment or existing state,
- simple architectural shape,
- current proposed building design for a cultural center,
- landform building with adjacent landscape, and
- landform building with adjacent landscape and green roof.

The Grasshopper analysis used plug-ins from the Ladybug suite, such as Honeybee, Butterfly, and Ladybug, to simulate the potential effects of a landform building on the local microclimate. The Grasshopper Ladybug plug-in used accessible EPW data into a site model to simulate the environmental impact of the building and its surroundings. The Ladybug tool simulated and analyzed the solar radiation impact on the model, identified shadow masks, and characterized outdoor comfort. The output in the form of microclimate maps evaluated building performance for various options of the building, based on its shape, orientation, and surfaces.

The base simulation of the existing state tested the current condition of existing asphalt parking. The next simulation focused on a basic architectural shape and concrete material. Another scenario tested a building design for a cultural center by El Dorado Architects with concrete as a ground material. To compare the results, the next simulation tested a landform building with an adjacent landscape and a grassy lawn as a ground material. The final simulation tested a landform building with an adjacent landscape, green roof, and a grassy lawn as a ground material.

This study conducted several simulations using different inputs to evaluate the environmental performance of the selected design. The results of these simulations were compared to determine whether landform design was effective in reducing the outdoor temperature and improving local microclimate conditions.

1.7 Significance of the Study

Over the last decade, global climate change and its compounding effects has become one of the most important and urgent issues in design. Designers and researchers have been trying to find different solutions to mitigate the negative effects of climate change on the environment and to address future uncertainties. Landform architecture has the potential to address climate-related issues, such as the urban heat island effect, sea-level rise, flooding, stormwater management, and loss of habitat, by integrating landscape processes and architectural form.

The significance of this study lies in its exploration of landform architectural design as a process-oriented, rather than form-oriented, approach in architecture. By engaging with topography, history, and site-specific processes, this approach not only rethinks the relationships between the built environment and nature but also addresses environmental problems. This research builds on landform-related knowledge while leveraging 3D modeling and simulation techniques.

Recent advancements in digital techniques of modeling, simulation, and analysis open up new opportunities for designing landform buildings and structures to both address climate change and serve human needs. These tools make it possible to simulate fluvial and wind patterns, analyze microclimate conditions, and predict the long-term development of design interventions. This research proposes a new process-based approach to designing landform architecture that engages landscape processes into the design process.

1.8 Assumptions, Hypotheses, and Researchable Questions

Assumptions:

1. Process-oriented landform architecture can address climate-related challenges.
2. The integration of digital techniques, such as 3D simulations, enhances the ability of landform architecture to respond to time, change, and history.
3. Site-specific processes provide valuable insight for developing a process-based landform architecture.

Hypotheses:

1. Interdisciplinary practices of landscape architecture can enhance the theoretical and practical framework of landform architecture.

2. A process-based landform architecture can mitigate climate challenges.
3. Architectural forms that are shaped by local processes can improve local microclimate.

Researchable questions:

1. How has landform architecture been practiced to date?
 - 1.1 How does this relate, or not, to the understanding and integration of landform in other disciplines?
 - 1.2 How might these other disciplines inform a new practice of landform architecture?
2. What is a process-based approach to landform architecture?
 - 2.1 How might landscape processes shape landform architecture?
 - 2.2 What methods are available or applicable for a process-based approach to landform architecture?
 - 2.3 How can the history and processes of a site inform a process-based landscape approach for landform architecture?
3. How can landform architecture address climate challenges?
 - 3.1 What is the potential benefit of landform buildings in urban areas?
 - 3.2 What is the impact of landform buildings on a local microclimate?
 - 3.3 What is the role of landform buildings in minimizing outdoor temperature?

1.9 Summary

The current form-oriented approach in landform architecture ignores landscape processes, which limits the ability of landform architecture to address climate-related challenges. A gap in theory and practice requires a shift to a process-based approach that integrates site-specific processes and site history to design landform architecture. Such a shift makes landform buildings more responsive to environmental issues.

This research utilizes a multistage approach, consisting of four stages: (1) literature review, (2) comparative analysis and case study analysis, (3) design experiment, and (4) performance evaluation. Each stage consists of substages and different steps to develop a theoretical and design framework to landform architecture.

Stage 1, covered in Chapter 2, consists of a literature review that presents the evolution of landform architecture, natural landforms, land art, and landscape architecture. Precedent studies that were part of the literature review were selected based on their integration of landforms into the context. This stage highlights the limitation of the current form-oriented approach and identifies the potential for a process-oriented approach to address climate-related challenges.

Stage 2, covered in Chapter 3, focuses on comparative analysis of a process-based approach in landscape architecture. The current process-based approach in architecture focuses on simulations of natural processes, time, and change. This becomes possible with the use of digital tools, such as Rhino and Grasshopper. Another step of this stage is a case study analysis of selected projects that used early forms of simulations and incorporated natural processes to develop their design. The insights from this stage form a base for a theoretical framework of a process-based approach to landform architecture that emphasizes dynamic connections between the site, its history, its processes, and future changes, and positions buildings as a continuation of their site.

Stage 3, covered in Chapters 4, 5, and 6, tests the theoretical framework developed in Stage 2. This stage is a practical design exploration that uses the RTD method. The study focuses on Portland, Oregon, a city that faces significant climate-related issues, such as high temperature and flooding risks. The Lower Albina neighborhood was selected for the design experiment because of its historical significance and alignment with the research objectives. The comprehensive analysis of Lower Albina was conducted on three scales: city scale, neighborhood scale, and site scale, where attention to site processes moved from larger to smaller scale. After the site analysis, a series of 3D simulations were performed to analyze current conditions on site. Such analysis helped to shape a framework that includes the process to design a landform building. To test such a framework, the next step of this stage was a conceptual design of a cultural center and waterfront park in Lower Albina. The iterative design process helped to refine the process-oriented design framework based on simulation results.

Stage 4, presented in Chapter 6, evaluates the environmental performance of the proposed design developed in Stage 3 and analyzes the influence of the design on the local microclimate. This stage generates microclimate maps to assess outdoor comfort and environmental impact. The series of simulations tested different design options, including the

predevelopment state up to a landform building and adjacent landscape design. The results of these stages determine whether landform architecture reduces outdoor temperature and mitigates climate-related issues.

II. LANDFORM ACROSS TIME, CULTURE, AND DISCIPLINE

This chapter presents a history of the manifestation of landform across time, culture, and discipline through selected projects that illustrate key theories and practices. This history provides the basis for a more extensive typology of landform architecture (Figure 7) in the built environment than has been previously presented, reflecting a changing relationship between nature and design.

The chapter traces the evolution of landform use from ancient settlements, defense structures, and ritual sites to architectural approaches that integrate digital modeling. It examines how landforms were historically used for protection and cultural expression and how these early interventions influenced art, landscape architecture, and architecture. The typology of landform architecture presents the Land Art movement along with cosmomorphism, hydromorphism, biomorphism, and geomorphism design approaches. The analysis reveals a shift from form-oriented approaches that emphasize aesthetics and metaphor to process-based strategies that integrate natural processes to design dynamic built environments.

2.1 Ancient Landforms

Landforms are shaped by geological processes over time. Tectonic activity uplifts mountains and forms valleys; erosion carves canyons and shapes landscapes through wind and water; deposition creates deltas and dunes landforms. While mountains, hills, and canyons are landforms visually recognizable by their geological composition, slopes, and distinct elevations, other historically significant landforms, such as cave homes, defensive earthworks, and ceremonial mounds, were shaped by humans and used for different purposes. The following sections present an overview of ancient landforms for settlement, defense, and ritual purposes.

2.1.1 Settlement

Many historic settlements around the world were integrated into landforms. The earliest settlements were built into natural features, such as caves, cliffs, hills, and mountains, which provided natural protection. Caves were among the earliest shelters for humans because they offered protection from weather conditions and animals. Hills and mountains played a

LANDFORM ARCHITECTURE

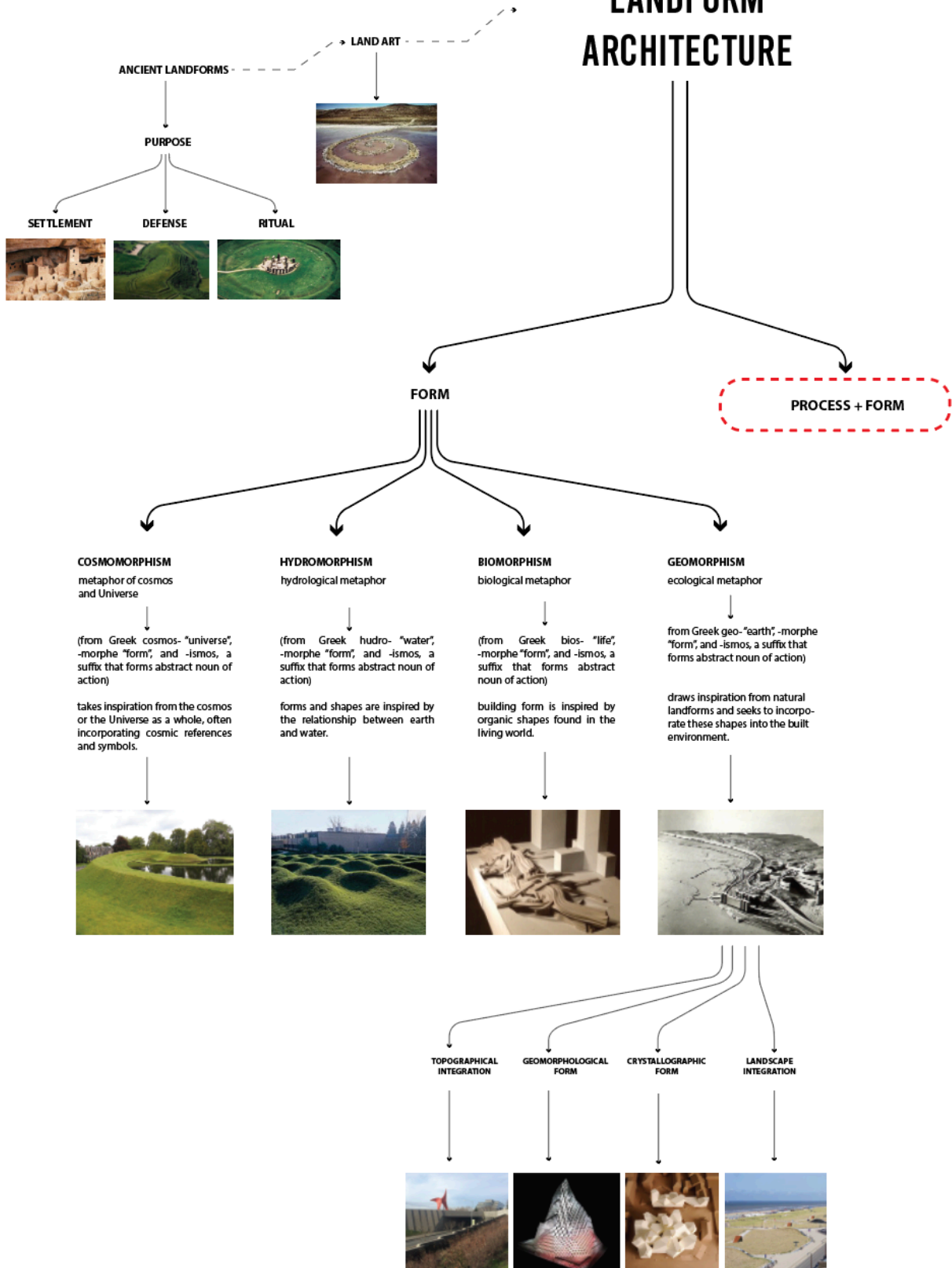


Figure 7. Typology of landform architecture.

critical role in settlement design, as elevated terrains provided advantages for defense and protection from invaders. These natural landscapes not only provided physical protection but also contributed to the development of adaptive approaches to settlement design. The challenging terrains forced the development of terraced settlements, agriculture, and pathways to trade routes. The following examples illustrate how humans used landforms to create early settlements.

Among the settlements that were integrated into natural cliffs is Petra, Jordan, a UNESCO World Heritage Site. The city, carved into the red sandstone cliffs between the 4th century BCE and the 2nd century CE (Bourbon, 2007), was a place where people lived in cave dwellings. The Nabataeans, an Arab people, created Petra as a critical city along ancient trade routes connecting Arabia, Egypt, and the Mediterranean. The homes were cut into the natural rock that not only served as a stable material for the settlement, but also provided thermal insulation, protection, and privacy. Such integration offered protection from a harsh desert climate: The rock stayed cooler during daytime and provided insulating warmth at night. Petra's development also incorporated other carved spaces, such as tombs, temples, and public gathering areas (Figure 8). The structures are examples of adaptation to challenging environmental conditions, where buildings are integrated into the natural landform and are designed to respond to climatic conditions.



Figure 8. Early settlement in Petra, Jordan. From Encyclopædia Britannica, n.d-a.

Mesa Verde (Figure 9) is a complex of historic cliff dwellings built by Ancestral Puebloans between approximately 450 CE and 1300 CE in southwestern Colorado (Kilroy-Ewbank, n.d.). The complex consists of over 600 cliff dwellings and other structures, including pit houses, kivas, and towers. The cliff dwellings were built into natural alcoves in the sandstone cliffs and were accessed by ladders or stairways. The structures were constructed from stone, adobe, and timber and were originally covered with plaster and mud. The construction of many of the houses built in alcoves or rock overhangs along the canyon were similar in terms of material and structural organization; however, some houses were unique due to variations in alcove size, shape, and orientation. Differences in natural rock formations led to variations in layout; some dwellings were more expansive or multileveled, while others were compact or irregularly shaped within the available space. Along the canyon walls, alcoves were different due to topography (O'Donnell, 2022). The buildings were built in U, E, and L stone shapes facing south. Many of the dwellings contained multiple rooms and were designed to accommodate large groups of people. Mesa Verde dwellings are an example of ancient housing integrated into a cliff, which illustrates a connection between nature and built form. It also shows how the topography and geological features shape the form of the houses by defining their placement, orientation, and structural organization. The natural alcoves provided a shelter, while canyon walls required ladders for access (Gothein, 2014).



Figure 9. Mesa Verde in Colorado, USA. From BBC, n.d.

Another example of a historical settlement is Machu Picchu in Peru, located on a mountain ridge in the Andes Mountains (Figure 10). The name of the site is translated from the

Quechua language as “old mountain” or “old peak.” The site is on a narrow saddle between two mountain peaks, Machu Picchu and Huayna Picchu. The Machu Picchu settlement is a citadel built by the Inca in the 15th century with dry-stone walls. The blocks of stone were cut to fit together tightly without mortar. The three primary structures on site are the Temple of the Sun, the Temple of the Three Windows, and the Intihuatana. The Inca at Machu Picchu farmed on man-made terraces called andéns. These terraces were built to provide good drainage and fertile soils, while also protecting the mountain from erosion. In 2007, Machu Picchu was voted as one of the New Seven Wonders of the World. Machu Picchu is an example of how architecture can be shaped by topography and environmental conditions, where settlement patterns conformed to a mountainous context.



Figure 10. Machu Picchu in Peru, Mexico. From National Geographic, 2025.

Ancient settlements were often integrated into natural landforms such as caves, cliffs, and mountains. The integration of dwellings and nature provided protection, shelter from harsh weather conditions, and strategic safety. Sometimes the settlements also served spiritual, economic, and social functions. The examples above demonstrate how early human societies adapted to and used their natural surroundings.

2.1.2 Defense

Landforms such as hills served as defense structures that were sometimes combined with settlements. Hillforts are examples of landforms that served a variety of functions, including protection against enemies and wild animals. Hillforts are fortified settlements that were constructed during the Iron Age period in Europe, between approximately 1100 BCE and 100 CE. These settlements were usually built on elevated land, such as hills or ridges, and were often surrounded by ditches, ramparts, and walls made of earth or stone. Hillforts varied in size; some were small and designed for a single family or clan, while others were much larger and could accommodate hundreds or people. The following examples are presented in chronological order to show the evolution of hillfort design and construction techniques.

Dun Aengus, dated to around 1100 BCE, is a hillfort located on the Aran Islands in Ireland (Figure 11). It is situated on the edge of a cliff and consists of four concentric walls that enclose an area of approximately 14 acres. The stone walls that hug the cliff create a boundary on three sides, leaving an extremely steep side of defense toward the ocean. The structure shows an understanding of nature's protective power. The hillfort illustrates how natural landscape was used for functional and environmental purposes. The placement of the hillfort on the edge of a cliff shapes spatial organization and highlights the defense potential of natural landforms.



Figure 11. Dun Aengus in Ireland. From Heritage Ireland, n.d.

Maiden Castle (Figure 12), located in Dorset, England, was built around 600 BCE. It is one of the largest and most complex hillforts in Europe. It covers an area of over 47 acres and contains multiple ditches, ramparts, and entrances. The elevated position of the castle offers protection from invaders. The site's layout illustrates that the planning included advanced safety measures, such as narrow entrances and overlapping defense ditches. This was made to control access and maximize security. The castle is an example of how an elevated terrain is used as environmental protection and also structural buffer. The complexity of the ditches and ramparts illustrates an early form of terrain modifications that preserve the overall landform structure rather than destroying it.



Figure 12. Maiden Castle in Dorset, England. From Ancient Origins, n.d.

Hambledon Hill is an Iron Age hillfort located in Dorset, England, on a hilltop overlooking the town of Child Okeford and the River Stour (Figure 13). Hambledon Hill included multiple features, such as a central enclosure, several smaller enclosures, and a number of pits and ditches. The hillfort covered an area of approximately 35 acres and is surrounded by huge mounds of soil and ditches that protected people living on the top (Giroto, 2016). The hill was also protected by dense forest, while the clear-cut on the hill symbolized an open sky that brings light. The site's elevated position influenced spatial organization and provided natural protection, which shows that landforms can be used for strategic purposes. It also serves as an early example of how landforms can be modified for human purposes.



Figure 13. Hambledon Hill in England. From National Trust, n.d.

The above examples focus on Britain and Ireland, where hillforts are well documented and played a significant role as defense structures. While hillforts exist in other parts of Europe, this selection highlights variations within a geographic region. These examples illustrate how ancient societies used the potential of terrain and landscape to create fortified settlements and mark boundaries. The concentric ramparts or steep ditches on top of the hill illustrate planning for protection. However, the human interventions did not dominate over the landscape and were mostly carefully integrated into natural landforms and landscapes.

2.1.3 Rituals

Landforms were also adopted or created for ritualistic purposes. Henges are circular or oval landform enclosures with a ring-shaped bank on the outside and a ring-shaped ditch inside, typically built during the Neolithic and Bronze Ages in the British Isles. For different cultures, the central space of the henge was sacred. It often contained one or more entryways and included standing stones. The causeways to the central space often faced one another across the circle.

Stonehenge, one of the most well-known henges, is located in Wiltshire, England (Figure 14). The stones were erected around 2500 BCE, during the Neolithic period. Stonehenge consists of a ring of standing stones, each weighing up to 25 tons, arranged in a circular pattern. The

monument is surrounded by a circular ditch and bank. The alignment of stones with the summer and winter solstices suggests its use as a prehistoric calendar that marks the longest and shortest days of the year. The site's orientation and alignment of the central axis with the rising sun on the summer solstice and the setting sun on the winter solstice shows an understanding of astronomical cycles.

Stonehenge was not only a place for keeping track of seasonal changes, but also a place for ritual occasions (Hobhouse & Edwards, 2020). Archaeological findings suggest that people gathered for ceremonies, feasting, and other rituals at the site. The findings of human remains dating to around 3000 BC suggests that Stonehenge may have also served as a burial site. The evidence of processional routes leading to and from the site indicate that Stonehenge may have been used for seasonal festivals or gatherings. The landform itself—the ditch and bank around the stone circle—may have functioned as a boundary between the surrounding landscape and the sacred interior, reinforcing the idea of the space for rituals.

The ring-shaped bank and ditch are early examples of land movement and manipulation that is done intentionally to shape the terrain to enhance the ceremonial function. The circular form of the bank mimics the arrangement of stones and reinforces the sense of spatial unity and continuity with the environment. Stonehenge's connection to the seasonal cycles highlights the relationship between built form and environmental forces.



Figure 14. Stonehenge in Wiltshire, England. From Encyclopædia Britannica, n.d.-b.

Other examples of henges include Avebury in Wiltshire, Durrington Walls in Wiltshire, and the Ring of Brodgar in Orkney. Some henges also contain evidence of burials, suggesting that they may have served as funerary sites.

Burial mounds containing human remains and artifacts, called kurgan (“fortress,” “embarkment,” or “high grave” in the Polovtsian language), are ancient burial sites found in the southern Ukraine steppe. The burial mounds date to 3000 BCE and are often associated with the Bronze and Iron Ages cultures, such as the Scythians. The complex structures of kurgans were made of mounds of earth and stones raised over internal chambers. Within the chamber, elite individuals were buried with grave goods, and sometimes even horses and chariots for the afterlife. Kurgans were built gradually as new burials were added. The soil for these additions was excavated nearby, resulting in a circular depression around the burial mound. In addition to their burial function, kurgans also served as prominent landmarks in the Ukrainian landscape, measuring up to 65 feet tall.

The Tovsta Mohyla (“fat barrow” in Ukrainian) kurgan, an ancient Scythian burial mound dating back to 4000 BCE, is located in southern Ukraine, near the city of Pokrov in Dnipropetrovsk Oblast (Figure 15). The kurgan is 25 feet high and 230 feet in diameter. The excavation of the kurgan in 1971, by the Ukrainian archaeologist Borys Mozolevski, uncovered the “Golden Pectoral,” a piece of gold jewelry depicting scenes of Scythian life and mythology.

The Tovsta Mohyla kurgan consisted of two burial spaces: the central and the side. An adult male skeleton with fragments of gold plaques, pieces of metal armor, a bronze war belt, a golden whip, two knives and forks, part of a mace, fragments of iron spear tips, four quivers with arrows, bronze cauldrons, and a clay amphora were found inside the central burial space. A golden pectoral and iron sword in a golden scabbard were found in a short corridor connecting the entrance and the central burial space. The burial also contained the remnants of six horses with their caretakers. The side burial was built later with two corridors for access, where an adult female skeleton, a child’s skeleton, and three skeletons that likely belonged to servants were found.



Figure 15. Top: The Tovsta Mohyla kurgan in Ukraine. Bottom: The Golden Pectoral of the Scythians from Tovsta Mohyla. From Google Arts and Culture, n.d.

Kurgans in Ukraine are not only burial sites. They are culturally and historically important places that reflect spiritual beliefs, reveal ideas about social hierarchies, and preserve artistic treasures of the ancient people of the steppe. The presence of grave goods, such as a gold pectoral, weapons, and armor, indicates belief in an afterlife where material possessions and status were significant. The presence of horses and human attendants suggests ritual practices tied to the deceased's journey and the concept of an elite class that extends after death. Such burials are an example of hierarchical culture, where people with higher status had individual burials, while servants often accompanied them.

Tovsta Mohyla is an example of an early engagement between humans and landscape for cultural, functional, and symbolic purposes. The construction techniques also illustrate adaptation techniques to climate and natural processes, such as wind and erosion. The elevated mound provided visibility across the steppe, serving as a landmark. The compacted earth layers stabilized the kurgan against wind-driven erosion.

2.2 Art

Inspired by prehistoric ancient monuments and landforms, land artists created site-specific structures, sculptures, and art forms by using earth, stone, sand, and other natural materials in the landscape (Tiberghien, 1995, 2018). Land Art, also known as Earthworks, is an art movement that emerged in the 1960s–1970s in the United States. It envisions a link between art and landscape (Howett, 1977; Weilacher, 1996) that brings metaphorical meaning of time (Kaiser et al., 2012; Jacob, 2013).

The emergence of Land Art was influenced by multiple processes that have changed the way art and landscape have been understood: rejection of existing art practices, changes in how people experience art, the development of industrial technology that can move large volumes of earth material, and changing social context along with rising awareness of environmentalism around the world.

The period of the 1960–1970s in the U.S. was signified by rapid economic growth after WWII (Marwick, 1998). President John F. Kennedy’s economic policies resulted in the end of recession and the start of economic recovery. One of Kennedy’s important accomplishments was decreasing unemployment in the United States. During his presidency, the gross national product value also significantly increased (Amadeo, 2020). The percentage of Americans who lived in poverty dropped, which resulted in the continued development of the middle class (O’Doherty, 1974).

During this economic uplift in the early 1960s, the federal government supported a range of programs for education, urban renewal, and social welfare (Beardsley, 2006). Art was also well funded by government and corporate businesses. In 1966, the *New York Times* reported that the amount of original artwork in business offices was increasing. Following a national interest in art, David Rockefeller, the president of Chase Manhattan Bank, started the nonprofit Business

Committee for the Arts (Rockefeller Foundation, 1967; Museum of Modern Art, 1999). The committee provided expert consultations to corporations that were interested in art purchases.

Artists' responses to "ruthless art commercialization" (Boettger, 2002) were conflicting. While some were satisfied with greater income, others opposed corporate commodification of art by business. Some artists rejected the idea of their work as entertainment, arguing that their work has been consumed rather than understood (Lintott, 2007; O'Doherty, 1974). Such context gave rise to multiple movements, including Minimalism and Land Art.

While Minimalism focused on simplified shapes, sizes, and minimalistic expression (Strickland, 1993), Land Art creators expanded this idea by making minimalistic forms and shapes in remote landscapes (Prigann et al., 2004). Minimalist art inside the gallery was scaled to human dimensions, while Land Art was scaled to landscape dimensions, necessarily creating different experiences between the visitor and their environment.

Artists such as Robert Smithson, Nancy Holt, and Michael Heizer wanted to bring people out of the museum into the landscape, which they modified with their artworks (Boettger, 2002). They were determined to make work that could reject traditional approaches while simultaneously offering a space for cultural critique, along with a rejection of traditional art museums. Traditional art works were typically two-dimensional, presented on vertical surfaces of art galleries, and offered a limited experience for a visitor. Land Art offered a three-dimensional experience of the sculptural object. The visual qualities of art were expanded to additional aesthetic characteristics of an object: mass and volume, and rough materials (Brunt, 2023).

In 1967, the Los Angeles County Museum of Art (LACMA) presented an exhibition titled "American Sculpture of the Sixties" that marked the development of large-scale sculptures (Lailach, 2007). The exhibition celebrated the emergence of American sculpture by presenting over 166 works, including Land Art, that were challenging traditional forms and approaches to art. One aspect of sculpture emphasized by critics was the large scale. Maurice Tuchman argued in the exhibition catalog that "scale" became the synonym for "large" (Tuchman, 1967).

The large-scale Land Art works were typically located outside the cities in remote terrains. The construction of such large works became possible with the development of industrial technology and machines that could manipulate earth easily (Rogers, 2001). Many of the monumental earth works were expensive to create, and so required financial support from

individuals and agencies. Some funding came from major patrons like the Dia Art Foundation in New York, the Lannan Foundation, and collectors like Robert Scull of New York, who supported projects by Robert Smithson and Michael Heizer.

The rise of the Land Art movement overlaps with a period of environmental awareness in 1965–1972. During this time, the idea of protecting the environment from natural disruptions became more widespread (Carson et al., 2018). The spark of the movement was initiated by Rachel Carson’s book *Silent Spring* (Carson, 1962); however, Land Art was not an environmentalist movement. Land Art works required a lot of heavy machinery to move massive amounts of earth to build large-scale land sculptures.

Some of the Land Art projects were built as a critique of traditional art and forced it to move outside to the landscape; other projects were developed as a critique of environmental concerns and degradation during the Industrial period (Rogers, 2001). One of the major changes that Land Art brought to the discipline was the spatial experience of visitors who move through the landscape.

In the late 20th century, the vision of human relationships with the environment became increasingly important. During the Land Art period, the landscape was often represented as a place with scars of disruption (Beardsley, 2006). Robert Smithson, known as a pioneer of Land Art movement, was one of the first artists who started representing landscape as a place that is changing.

Robert Smithson (1938–1973) was an American artist, writer, and theorist. In his early career, he created expressionistic paintings and collages. From the 1960s, Smithson’s art and writing were inspired by crystalline structures and geological sciences. He created large-scale artworks that were placed not in museums, but in open landscapes. Smithson expanded the understanding of what art is and where it can be located by creating large-scale land art works in remote landscapes. He brought art to the natural environment and started to use heavy machinery to shape his land art. The earth was not only the place where his sculptures were located, but also the material. Smithson’s early earthworks include *Asphalt Rundown* in Rome, Italy (1969), *Glue Pour* in Vancouver, Canada (1969), *Concrete Pour* in Chicago (1969), and *Partially Buried Woodshed* on the Kent State campus in Ohio (1970). He is known for his earthworks trilogy *Spiral Jetty* in Great Salt Lake, Utah (1970), *Broken Circle/Spiral Hill* in Emmen, the Netherlands (1971), and *Amarillo Ramp* in Amarillo, Texas (1973).

Asphalt Rundown (1969) in Cava dei Selce, Rome, Italy, was Smithson's first outdoor project. The earthwork (Figure 16) was a demonstration of Smithson's idea of the "crystalline structure of time." He coined the term in 1967 to describe how time does not pass but rather builds upon itself (Smithson et al., 2004). Smithson poured a truckload of hot asphalt on a quarry hill. He used natural terrain as a medium and asphalt as an active participant in a process that illustrates how topography, gravity, and other materials function together. The project illustrates how gravity shapes an earthwork and engages with environmental forces.

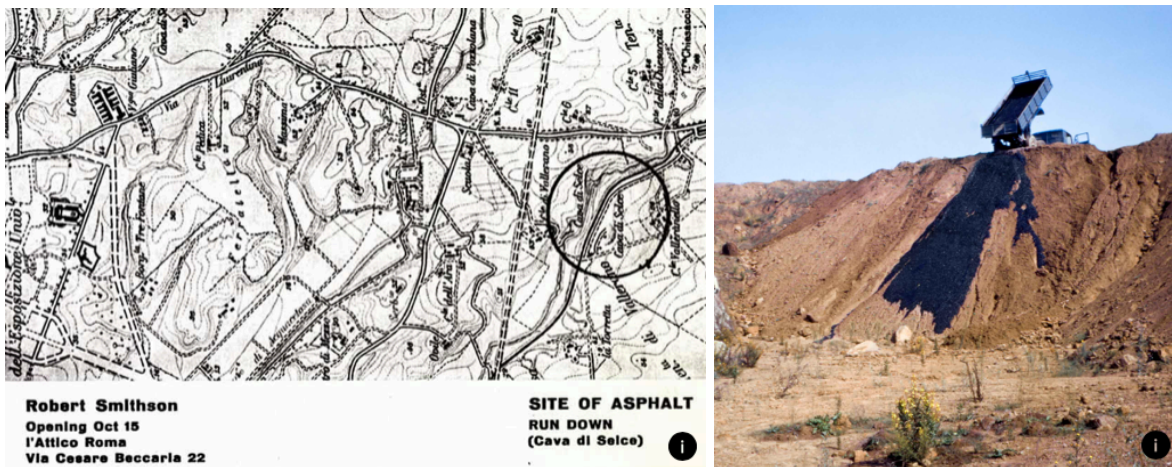


Figure 16. *Asphalt Rundown* in Rome, Italy by Robert Smithson (1969). Left: Site map. Right: Picture of the site with the sculpture. From Holt/Smithson Foundation, n.d.-b.

Spiral Jetty (1970) (Figure 17) was built on the northeastern shore of the Rozel Point peninsula at the edge of the Great Salt Lake in Utah. Smithson chose the site for the red-colored water caused by salt-tolerant bacteria and algae that thrive in the lake. Rozel Point is also one of the oldest oil fields in Utah. When the water level at Rozel Point drops below 4,200 feet elevation, the oil seeps appear and *Spiral Jetty* becomes visible (Holt/Smithson, n.d.-c.).

The earthwork is 1,500 feet long and 15 feet wide and spirals counterclockwise from the shore into the water. The earthwork was formed by over 6,000 tons of black basalt rocks and soil from the site. The visibility of the sculpture varies based on the water level; sometimes it is visible and sometimes it is submerged. *Spiral Jetty* is an example of how an earthwork interacts with topography and climate across seasons and years.

Smithson documented *Spiral Jetty*'s construction in a 32-minute color movie titled *Spiral Jetty* (1970). In 1999, the earthwork was donated to the Dia Art Foundation by Smithson's wife,

Nancy Holt. At the time the Dia Foundation acquired the sculpture, it was completely submerged.



Figure 17. *Spiral Jetty* in Great Salt Lake, Utah, by Robert Smithson (1970). From Holt/Smithson Foundation, n.d.

Broken Circle/Spiral Hill (1971) was built by Smithson in a sand quarry in Emmen, the Netherlands (Figure 18). The quarry is located on the edge of a terminal moraine, constituted of sand and gravel left behind by a glacier. The sediment layers vary from red and yellow to brown and black, while the water of the lake has a bright green color.

The earthwork is embedded into the shore of the quarry lake; one half is made of sand and the other becomes part of the lake with a circular path. The shape of the earthwork is similar to the quarry's circular shape. *Broken Circle* is a manifestation of Smithson's manipulations with spirals and their meaning of a final destination (Shapiro, 1995). The hillside incorporates a circular path; however, the circle is broken and ends up in the water. At the center of the broken circle is a glacial boulder, a placement Smithson called accidental.

Smithson was fascinated by Dutch water management systems and land construction approaches to reclaim land from the sea. *Broken Circle* illustrates how landform, an earthwork, and time interact. The project manipulates existing topography to introduce a new form, which highlights the gentle integration of a designed form into the context.



Figure 18. *Broken Circle/Spiral Hill* in Emmen, the Netherlands, by Robert Smithson (1971).
From Holt/Smithson Foundation, n.d.-d.

Amarillo Ramp (1973) is located on the artificial Tecovas Lake outside Amarillo, Texas (Figure 19). Like *Broken Circle*, *Amarillo Ramp* has a circular shape; a nearly complete circle rises from the lake bed to a height of 15 feet.

For the construction, Smithson used similar techniques of excavation and controlled flooding as he used for *Spiral Jetty* (Commandeur & Riemsdijk-Zandee, 2020). In his film about *Broken Circle/Spiral Hill*, he included historical footage of the devastating flood in the Netherlands in 1953 (Holt/Smithson, n.d.-c).

This earthwork is Smithson's final work. While surveying the site, Smithson died in a small plane crash with the pilot Gale Ray Rogers and photographer Robert Curtin. The sculpture was built one month after his death by Nancy Holt, Tony Shafrazi, and Richard Serra. Currently, the lake is dried up and *Amarillo Ramp* is partially eroded and covered with vegetation. The impact of natural processes and time illustrate the temporal dimension of earthworks.

Smithson's work and writing have influenced generations of artists and creative thinkers. Contemporary artists, such as Sam Durant, Renée Green, and Mike Nelson, have been inspired by Smithson's ideas. He played a critical role in redefining contemporary art by introducing earthworks. Jack Flam argues that Smithson reshaped the nature of art and its role in society.

Smithson constantly questioned common attitudes toward art and culture, which he expressed not only in his earthwork, but also in writing. The act of writing was understood as drawing, mapping, photographing, and diagramming (Smithson & Flam, 1996). Smithson's approach to disrupted landscape is innovative even from today's perspective. His ambition to create monumental art was critical and visionary. His sudden death interrupted his artistic potential and further influence on art (Commandeur & Riemsdijk-Zandee, 2012).



Figure 19. *Amarillo Ramp* in Lake Tecovas, Amarillo, Texas, by Robert Smithson (1973). From Holt/Smithson Foundation, n.d.-a.

Robert Smithson saw his work as mediating between the environment and 20th century industry. His earthwork sculptures are located in landscapes that have been disrupted by human actions. Most of his earth sculptures are constructed at the intersection of land and water. Each of his artworks has a special meaning and drives attention to the site. For most of his work the site is located far from popular destinations, which reinforces Smithson's critique of industrialization and human intervention in nature. By situating earthworks in isolated settings, he compels visitors to make an effort to get to a remote place and engage with the site. By doing so, Smithson raises their awareness about the altered state of the landscape and the environmental impact of human activity on nature.

The Land Art movement changed the traditional understanding of art as an object into art as a sculptural object located in an open field. Traditional two-dimensional art objects that were

typically represented on vertical planes in galleries were replaced with three-dimensional sculptures located in remote landscapes. Contrary to the traditional interaction between art and visitor that was limited by observation from a specific angle, Land Art proposed physical interaction between a sculptural land work and a person, which involved more senses and different activity. Such change creates a transition from two- to three-dimensional object. Landform architecture can extend the notion of spatial relationships between object and landscape by proposing four-dimensional works, where landscape changes over time, and such changes are reflected in its form. Land artists used natural materials for their projects. More often earth was the main material, but sometimes they used materials from the site, such as stone and sand. At the end of the Land Art movement, artists were using mostly soil and grass to create landform-like shapes.

Land Art projects bring metaphorical meaning to the place where they were located, as artists expressed different messages through sculptural shapes. Land Art artists used natural shapes to express metaphors of time to tell the story of the site that highlights its history or identity.

With the Land Art movement, the role of a person in the landscape and in experiencing art becomes important. Land Art projects are created for people to interact with, walk on top of, and touch. The direct human interaction with the art object might explain the phenomenon of Land Art. People are willing to travel to remote locations to see land art objects and interact with them.

2.3 Design

The evolution of landform use in landscape architecture and architecture has led to the development of different conceptual approaches. This section explores cosmomorphism, hydromorphism, biomorphism, and geomorphism approaches, as well as their subcategories. These approaches emerged from theoretical shifts that were influenced by a metaphorical view of nature, politics, economics, environmental changes, and urban growth. Each approach reflects a different way of integrating landform into the landscape or built environment, which is illustrated by a series of precedent study projects.

Cosmomorphism envisions landforms as sculptures embedded with cosmic and historical symbolism. Hydromorphism explores the relationship between water and earth, by using the

hydrological metaphor to create site-specific designs. Biomorphism explores fluid and lifelike forms in architecture to create nonlinear buildings. Geomorphism explores the use of digital techniques to imitate natural forms. Geomorphism includes several subcategories: topographical integration, geomorphological form, crystallographic form, and landscape integration.

These approaches illustrate the transition from form-driven landform architecture to process-based strategies that engage with natural processes. The following sections examine how these design paradigms shaped design projects.

2.3.1 Cosmomorphism

In this dissertation, the term cosmomorphism (from the Greek *cosmos* for “universe,” *morphe* for “form,” and *-ismos*, a suffix that forms abstract nouns denoting a practice or system) is used to describe the design approach that takes inspiration from the cosmos or the Universe as a whole, often incorporating cosmic references and symbols. Cosmomorphism seeks to express the interconnectedness of all things in the Universe with abstract forms.

In the mid-1990s, the Land Art traditions of symbolism and a hybrid combination of landscape and sculpture continued (Jencks, 2002). Charles Jencks extended the idea of Land Art to landforms, which he explained as an art of manipulating nature and natural forms for aesthetic and utilitarian purposes. Jencks (1939–2019) was an American cultural theorist, architectural historian, and landscape designer. He became known in the 1980s as a Postmodernism theorist and architectural critic; however, in practice he devoted his life to landscape design. Jencks created numerous landform projects, such as *Landform Ueda* (1999–2002), *Cells of Life* (2003–2010), and *Northumberlandia* (2004). His design projects and associated writings were intended as a critique of the current economically driven art practices. Jencks used landforms to study laws of nature and natural forms. His metaphorical understanding of landforms explored gravity, DNA, black holes, and galaxies as systems that can be brought to life and become content-driven aesthetic forms.

Jencks used landforms in his design projects as a metaphor. He told the history of contemporary science and identity of place with artificial landscape. He often used landforms to heal an industrial site or develop strategies that are forward-looking and can heal visitors (Haddad, 2009). While his projects were still metaphorical, they were also a transition to the period of digital modeling of landforms in architecture (Jencks, 1973). Jencks refers to 3D

modeling and simulation as a powerful tool that helps designers understand relationships between existing landscape and proposed design.

While cosmomorphism draws inspiration from the Universe and expresses interconnectedness through abstract shapes, the evolution of landscape architecture has moved from a focus on abstract shapes to a more thoughtful connection between landform, earth, and water.

Landform Ueda (1999–2002), located outside the National Gallery of Modern Art in Edinburgh, Scotland, was designed by Charles Jencks (Figure 20). The landform protects buildings and landscape from road traffic, provides views of sculptures, and acts as a gateway to two museums. The main concept behind the design of the landform was to communicate self-organizing principles of nature, cosmic orientation, and scientific insights to “chaotic attractors” (Sprott et al., 2013).



Figure 20. *Landform Ueda* in Edinburg, Scotland, by Charles Jencks (1999–2002). From www.charlesjencks.com.

The project was developed after the analysis of forms that occur in nature, specifically related to chaos theory and nonlinear dynamics. Chaos theory, in mathematics and physics, is the study of unpredictable behavior in systems that are defined by deterministic laws—any event is determined by an event that happened in the past (Encyclopædia Britannica, 2025). Jencks identifies that most of his projects, including *Landform Ueda*, were inspired by “strange

attractors” or “chaotic attractors.” In fluid dynamics, attractors are a set of states toward which a system tends to evolve. Fractals, a never-ending pattern, are an example of a chaotic attractor (Grebogi et al., 1987). In nature, trees, mountains, coastlines, rivers, and clouds can be qualified as fractals (Fractal Foundation, n.d.).

Landform Ueda was inspired by the Ueda Attractor, named after the Japanese scientist Yoshisuke Ueda. The Ueda Attractor is generated by a series of simple transformations that happen in strange attractors. Jencks argued that most living systems have periodic attractors, which means that the evolution of the system results in moving cyclically through each state (Prominski & Koutroufinis, 2009). The Ueda Attractor has a complex, ever-changing pattern of S-curves that became an inspiration for this landform design. For Jencks, it symbolized the growth of cells, the spiral of galaxies, and the process of thinking and feeling (Jencks, 2011).

For this project, Jencks developed a 3D computer study of the landform to explore the volumes and their potential impact on the adjacent landscape of the National Gallery of Modern Art. This study helped him see the underlying spatial and structural dynamics; however, this was more than a supplemental system. Jencks states that re-drawing, re-laying, and re-modeling with tape are still important tools in landform design (Jencks, 2011). Computer-aided design is necessary to rationalize the process of shaping the earth, since it requires the movement of a large amount of material, and such movement is typically expensive.

The Scottish World (2003–2010) in Kelty, Scotland, (Figure 21) is an example of an identity project designed by Charles Jencks. The project consists of a series of landforms, an artificial lake, and boulders located on a previously open-cast coal mine site. Jencks considered this site as an opportunity to restore the land with four landforms, rather than as a flat, pastoral landscape.

Jencks argued that his landform design explores the identity of Scotland, which is informed by the land. The site becomes a map that represents the Scottish people who were dispersed around the world. The lake is in the shape of Scotland, while pathways around it connect major cities. In this project, landforms are a means for Jencks to communicate Scottish history to the visitor.

Jencks viewed the project as a microcosm of Scottish history, where the site history was represented onto the transformed terrain. The large and heavy equipment used for coal mining inspired simple landforms. The so-called “grammar of pyramidal landforms” that Jencks used in

this project reminds one of the geometry of the pyramid. His idea was to create a landscape that is of the scale of the Grand Canyon, but emphasizes horizontal openness (Jencks, 2007).



Figure 21. *The Scottish World* in Kelty, Scotland, by Charles Jencks (2003–2010). From Jencks, n.d.

Jencks's *Land War Garden* (1998–2001) is located in Salford, Manchester, near the Imperial War Museum designed by Daniel Libeskind (Figure 22). The project is a representation of the metaphor of death and war. Jencks turned the misery of the destruction of nature into the landscape, such as representing missiles as trees. Transformation was the basic strategy in this design project.

The idea of the garden was to create a space of reflection, tranquility, and pleasure. Moreover, Jencks wanted to highlight that nature regenerates after conflict to show its healing power, expressed through a combination of natural grass and industrial concrete and asphalt.

The site plan presents a timeline of conflict in nature, expressed through the colors of black, red, and green. This history starts from the entrance on the right side of the plan representing the period of 700 million years ago. Mass extinctions are indicated in red as they leave their trace in geological strata. After each red period follows green, which symbolizes

regeneration. The symbolic end of the garden is the bridge, which represents the present moment in this history.

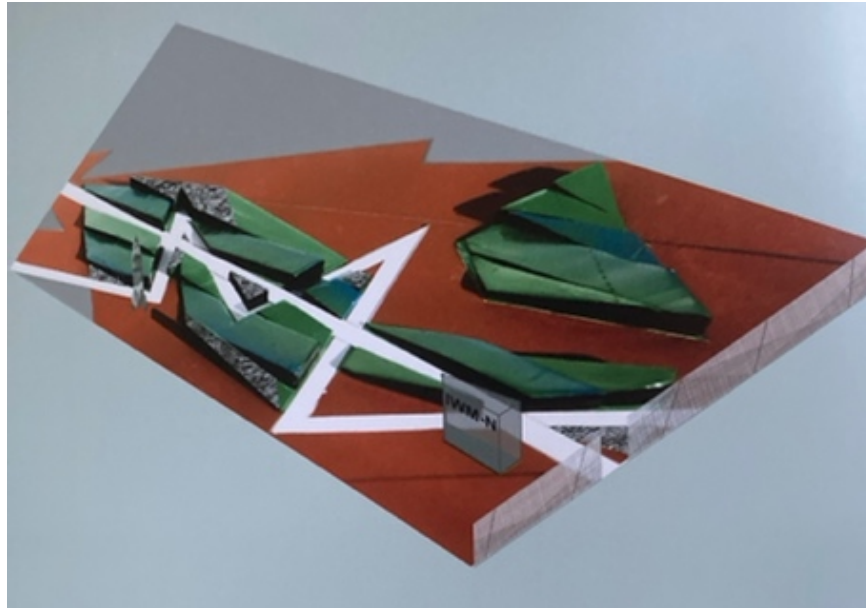


Figure 22. *Land War Garden* in Salford, Manchester, by Charles Jencks (1998–2001). From Jencks, 2011.

Jencks argued that the garden is an example of “linearism” (Jencks, 2011), a linear historical continuity without significant deviation. The lines break and weave together. While the plan shows parallel lines, grass surfaces arch and culminate with edgy surfaces. Unfortunately, the project was only partially completed due to the budget limitation from the museum.

Jencks understands landforms as large-scale sculptures made out of earth, stone, and turf, and he uses nature to speculate about the Universe and its systems and laws. His landform designs are more than just sculptures, as they stimulate thoughts about our relationship to place and ourselves (our own body and cells) to the world. His design must be physically experienced to be fully understood. However, his projects are multidimensional and complex—even one’s presence on site does not give the full story. Garry MacKenzie argues that reading Jencks’ books and explanations is required to fully understand the aesthetics and science behind each project (MacKenzie, 2013).

2.3.2 Hydromorphism

In this dissertation, the term hydromorphism (from the Greek *hydro* for “water,” *morphe* for “form,” and *-ismos*, a suffix that forms abstract nouns denoting a practice or system) is used to describe the design approach in which the forms and shapes are inspired by the relationship between earth and water. Hydromorphism involves the representation of water and related processes in the natural landscape.

In the 1980s, ideas from the Land Art movement had a significant influence on the development of hydrological metaphor in landscape architecture, related to fluvial shapes and processes, where landscapes mimic the patterns of rivers or water features. The Land Art movement encouraged the use of natural materials, such as stone, sand, and water, to create designs that seamlessly blend with the surroundings. It also reinforced a site-specific approach, where landscape interventions respond to existing topography, hydrology, and ecological conditions rather than introducing predefined design. In addition to metaphorical representations of nature, landforms play a significant role in landscape architecture as a tool to functionally organize the space, create the aesthetic character of the landscape, and influence human perception of the space.

Maya Lin (1959–) is American architect and artist known for her environmental art work, memorial designs, and architectural projects. Lin’s art work is exhibited at the National Gallery of Art and the Smithsonian Institution in Washington, DC; the Metropolitan Museum of Art in New York; and the California Academy of Sciences in San Francisco. In her architectural projects, Lin creates a conversation between the landscape and built environment, with a focus on sustainable solutions. Her architectural projects are mainly designed for nonprofit institutions and include the recently completed Neilson Library (2021) at Smith College in Massachusetts, the Novartis Institute for Biomedical Research (2015) in Massachusetts, and the Riggio-Lynch Interfaith Chapel (2004) in Tennessee.

Natural environment has been one of the central elements in Lin’s design, as she was interested in integrating buildings into the landscape. She seeks to establish a harmonious connection between the site and new construction (Harvey & Phumiruk, 2017). For Lin, landforms are an interface between landscape and art; she represents artificial and natural by proposing her way of seeing the world.

The *Wave Field* is a series of three earthworks that represent water waves in the landscape. Each field has a different view and representation of the wave itself. Through each iteration, Lin studied different formal qualities and the process of wave formation.

The first *Wave Field* (1995) is located at the Francois Xavier Bagnoud Aerospace Engineering Building at the University of Michigan in Ann Arbor (Figure 23). The Engineering Building was named after a graduate of the aerospace engineering department who died in a helicopter accident at an early age (Lin et al., 2015). Lin was commissioned to design the memorial. The earthwork is 105 feet by 80 feet and up to 3 feet tall. A 10,000 square-foot memorial is made out of earth and grass (Figure 23) and consists of eight rows of 50 waves. The first and last rows have only three waves; others have from six to eight.

The *Wave Field* was based on the exploration of the Stokes wave. In fluid dynamics, the Stokes wave is defined as a nonlinear and periodic surface wave that occurs on water with a constant depth (Glossary of Meteorology, n.d.). It is the smallest wave in a series. The earthwork serves different purposes. For students, waves are like armchairs where they can sit and read; for children, they are a playground; and for engineering students, a place for experiments.



Figure 23. Left: The *Wave Field* in Ann Arbor, MI, by Maya Lin (1995). From Maya Lin Studio, n.d.-b. Right: Models for the *Wave Field*. From Lin et al., 2015.

The second *Wave Field*, called *Flutter* (2005), sits at the Wilkie D. Ferguson, Jr. United States Federal Courthouse in Miami, Florida (Figure 24). The artwork is a site-specific response to the boat-like shape of the building, which makes the building appear to float in the grassy waves. The earthwork is 459 feet by 105 feet, and 3 feet tall, covering 30,000 square feet, with a walkway that intersects the sculpture in front of the building.

Flutter was based on the study of shallow ripple formations that are created in sand by wave actions. As the waves shift through the landscape, they shift the ground plane diagonally. Each row shapes a continuous pattern that changes in height from two to three feet. According to Lin, the waves remind us of how water travels over the sand (Lin, 2005). The earthwork offers different relationship when you walk through it.



Figure 24. Left: *Flutter* in Miami, FL, by Maya Lin. From Maya Lin Studio, n.d.-a. Right: Sketch by Maya Lin. From Lin et al., 2015.

Storm King Wavefield (2009), located at the Storm King Art Center in New Windsor, New York, is an environmental reclamation project and a study of waves (Figure 25). It is the largest of Maya Lin's earthworks: 410 feet by 490 feet, ranging from 12 to 18 feet above a person's head, with an area of 240,000 square feet.



Figure 25. Left: *Storm King Wavefield* in Windsor, NY by Maya Lin (2009). From Maya Lin Studio, n.d-c. Right: Site plan sketch by Maya Lin. From Lin et al., 2015.

The last in the series, this work represents the culmination of Lin's wave studies. When you walk in the large field, you become lost inside the waves. Whether you walk through a row of waves or from higher to lower points, the experience changes.

Storm King Wavefield consists of seven rows of undulating hills of earth and grass that are shaped like ocean waves in a gently sloping valley (Lin et al., 2015). The wave movement is typically described as an undulating up-and-down movement. The project was a culmination of Lin's wave study that found its form in a large-scale earthwork. The site is 90,000 square feet, while the size of the wave is at a true-to-life scale. Because of such scale, people experience it as real sea waves—however, the waves are made of earth and grass. The scale of each *Wave Field* site changes from 10,000 to 30,000 and to 90,000 square feet, thus introducing three different scales of wave formation. The smallest wave is only two to three feet high, while the middle is closer to human scale, in a range from four to five feet. The largest wave is up to eighteen feet and exceeds human scale; however, it was Lin's intention to create different three-dimensional experiences for people.

Lin's *Wave Field* can also be interpreted as sand dunes or mounds that are covered by grass (Phillips, 2015). Lin created her own wave fields that merge water and earth in landscape, inspired by naturally occurring formations. Phillips states that Lin pulls water features, like rivers and oceans, as a complete form and represents them in her designs. The resulting shapes represent water bodies in a condition never seen before.

Kathryn Gustafson's landscape design style can be described as a combination of fluid landforms that are accompanied by water and light. Gustafson (1951–) is an American landscape architect and environmental artist known for creating sculptural landscapes. Her early career started in France, after she graduated in 1977 from the *École Nationale Supérieure du Paysage* landscape school in Versailles. In 1980, she opened her own office in Paris and was a lead designer for the headquarters of Shell (1990) and Esso (1992), and the L'Oreal model factory (1993). In 1997, Gustafson opened a London office, Gustafson Porter + Bowman (GP+B), with architect Neil Porter (Mary Bowman joined the office later, in 2002). Her second office, Gustafson Guthrie Nichol (GGN), is located in Seattle. Both offices have projects that range in scale and are located in Europe, North America, Southeast Asia, the Middle East, and Africa. They include the Diana, Princess of Wales Memorial Fountain in London (2004), Old Market Square in Nottingham (2005–2007), Cultuurpark Westergasfabriek in Amsterdam (2006), Seattle City Hall Plaza (2014), landscape design for the Natural Museum of African American History and Culture in Washington, DC, (2016), and others. Currently, Gustafson has over 35 years of distinguished practice in landscape architecture. She is also an international lecturer and an Honorary Fellow of the Royal Institute of British Architecture. Her team, and she individually, are recipients of numerous awards and prizes.

Gustafson also follows a site-specific approach in her design projects that takes into account the main characteristics of a specific site; its culture, history, and environment; and the programmatic functions (Levy & Gustafson, 1998). These projects are integrated into the context such that it looks like it was there before. Gustafson's designs are based on the principles of Picturesque, where the landscape is a sequence of experiential spaces leading to a specific object or destination. She thinks about middle ground, foreground, and far ground as she creates views and a journey for the person using the space. In the contemporary context, she interprets Picturesque as a method to clean up pollution, restore and preserve historical landscapes, use nature as a program, design landscape that has a function, and create designated spaces for a group of people and quiet spaces for one person.

When sculpting the land, Gustafson creates a relationship between the human body and landform. She combines visible natural elements, such as water, earth, and stone, and not visible, such as light, sound, and atmosphere. By combining these elements, Gustafson designs a movement of different materials in the landscape, which for visitors creates an experience that

involves all senses. The human body that moves through the site is an important driver for Gustafson's landform design. The dynamic shift of form and movement allows visitors to perceive landscape from different points of view and open new parts of the landscape.

Gustafson defines landforms as work that changes in depth, level, and scale, and, as a result, creates changes in human perception while moving through such space (Gustafson Porter + Bowman, n.d.-c). Landforms highlight the movement of light and shade across the surface. When light passes over the surface, it reveals slopes, as well as convex and concave forms that change in space and time.

Gustafson has a unique method to design landform landscapes. She creates a clay model, which, contrary to drawings, links a sequence of objects and forms of different heights and scales into one seamless fluid form. In this case, clay creates a material connectivity that represents the connectivity of a landform and resembles work with land. The process of layering clay follows the process of sketching and thinking, while also helping her understand human movement and interaction with the site.

The Shell Petroleum Gardens project (1992), located at Shell's Petroleum Headquarters in Rueil-Malmaison, outside of Paris, explores the dynamic interaction between land and fluid movement (Figure 26). The design for the factory's 2.5-hectare suburban complex near the Seine originated from the natural forms that rise from beneath the ground. The first sketches Gustafson developed expressed forces that move up and out from the earth in wave-like movements. Such sketches echoed the work of Shell Petroleum, as the company extracts fossil fuels from the ground. While the garden design does not directly represent political issues, it metaphorically reflects climate change issues that the company faces.

The programmatic functions of the landscape are divided into three main areas: the entry (international area), aquatic garden (community area), and pocket gardens (private area). The entry court represents landforms that look like grass waves.

One may also see the connection between the metaphor of the ribbon, which is used by Gustafson in multiple projects, and the wavy grass lawn. As grass mounds rise from beneath the ground at different heights, the concrete walls that appear from the earth further reinforce the idea of water shaping terrain over time. The walls also function as fire escape, service entry, and ventilation for underground parking. Service facility rooms are under the hills, and the landscape marks the beginning of an office building. The scale of the grass waves dominates over the

human scale as the lawn moves above eye level. With such dramatic differences in scale, a visitor’s experience of the place is exaggerated.

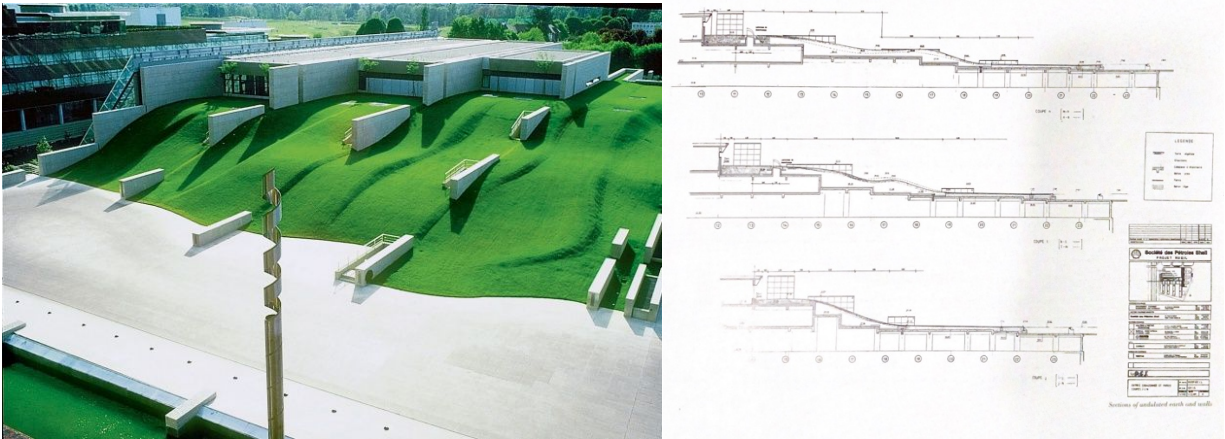


Figure 26. Left: Shell Petroleum Headquarters by Kathryn Gustafson in Rueil-Malmaison, France (1992). Right: Site image and sections of the building and adjacent landforms. From Levy & Gustafson, 1998.

The Diana, Princess of Wales Memorial Fountain (2004), located in London in Hyde Park (Figure 27), is one example of hydromorphic design, where water movement and sculptured form merge into a cohesive experience. In the design of the memorial, Gustafson wanted to express the concept of “reaching out—letting in,” which is how one can describe Princess Diana’s main qualities.

The main element of the memorial is a fountain—a continuous flowing water feature—interpreted as a necklace made of water. The ribbon-like structure of the fountain integrates with the topography and reinforces the seamless relationship between earth and water, as the fountain form is integrated into the hill of Hyde Park. Its horizontal profile flows down and hugs the landform. The fountain has detailed grooves and channels combined with air jets that create different effects—gliding, rippling, and churning as the water flows around the oval elongated shape. At the top of the fountain, the water is divided into two streams that flow down into a still basin.

In recent years, the Gustafson Porter + Bowman team has transformed their clay model-making to another level. They still continue to use clay models to develop basic forms, but now they scan such models and transform them into 3D models. In this project, they used 3D imaging and modeling software, such as Rhino and Grasshopper, for making clay models digital and

continuing to develop the design. The Gustafson team also used complex computer numerical code (CNC) stone-cutting technology to achieve all of the complex details of stonework that represent different movements of water. While design for the memorial at first sight might seem overly simplistic, the beauty of the water necklace draws visitors' attention because of its complex combinations of the form of the fountain with the landscape, water, and stone.



Figure 27. Left: Diana, Princess of Wales Memorial Fountain in London, United Kingdom (2004), birds-eye view. Right: Water running over textured stone. From Gustafson Porter + Bowman, n.d.-b.

Cultuurpark Westergasfabriek (2006) located in Amsterdam (Figure 28) is one of Gustafson Porter + Bowman's defining projects of brownfield reclamation that is transformed into dynamic hydromorphic landscape, where water and landforms shape visitors' experiences. The site area is almost 13 acres of a former coal-gas plant on the edge of the city. In 1981, the territory of the plant was rezoned as a recreation space because of the potential to reuse gas-holding structures that have commercial and cultural values and the close proximity to historic Westpark.

At the heart of the park is the Field of Events that includes a grass-sloped amphitheater and artificial lake. The lake can be drained to accommodate large events. Landforms in this project function as a stormwater management system and help to filter and direct water across the site. By sculpting the site with fluid forms, the project reconnects the site with natural hydrology and restores water circulation in a previously industrial site.



Figure 28. Left: View of Cultuurpark Westergasfabriek in Amsterdam (2004). Right: master plan. From Gustafson Porter + Bowman, n.d-a.

Gustafson argues that sculpting the land and earthwork is based not only on aesthetic purposes. On a large scale, land sculpting is also based on economic or environmental purposes. Her design team considers where they place the soil taken from the ground for the infrastructure construction, how to clean polluted soil on the site, and where to place reservoirs for water catchment in hardscapes. Landforms in that case can be an engineering solution that creates a seamless environment between natural and urban context.

Gustafson Porter + Bowman made great progress over the last two decades and adopted computer software to create fluid landforms. The team extended the understanding of fluid landforms by introducing dirt, stone, concrete, and water to create fluid shapes. In their Diana, Princess of Wales Memorial Fountain, the flow is represented through the stone shape and continuous water movement. For the Cultuurpark Westergasfabriek, the team used their molding technique to combine different environments and bring different groups of users. Landforms by Gustafson make places previously disconnected from nature back to life and suitable for social use (Betsky, 2005). Gustafson is shaping the land and topography in her design projects. Her landforms echo the nature, architecture, or elements from the site history. Land, water, and sky are the main medium of her landscape architecture work. Such a combination creates a connection to the ground for people that use the designed landscapes (Way, 2018).

Gustafson approaches landscapes as a sculptor. She begins a design with a clay model that encompasses a smooth form well integrated into the context. For Gustafson, landforms are fluid landscapes that change form, scale, and depth and create different places for interactions with visitors along that form. The dynamic form of the landscape and different scenarios for interaction between landforms and human bodies make such landscapes more livable. With her landscape projects, Gustafson shows that landforms can also address environmental concerns and create spaces for social interactions.

George Hargreaves designs complex and articulated topography in his projects. Hargreaves (1952–) is an American landscape architect and educator. He received a Bachelor of Landscape Architecture degree in 1977 from the University of Georgia and a Master of Landscape Architecture degree in 1979 from Harvard University. He worked for several years at architectural firm SWA before starting his own practice, Hargreaves, Allen, Sinkosky & Loomis (HASL) in 1983. A few years later the company became Hargreaves Associates in San Francisco. Parallel to his practice, Hargreaves started his teaching career at the California Polytechnic State University (Cal Poly), and later taught at the University of Illinois Urbana-Champaign, and the University of Virginia. In 1996, after Hargreaves became a chair of the department of landscape architecture at Harvard University, his firm also opened an office in Cambridge, Massachusetts. After Hargreaves left his position at Harvard, they also opened offices in New York and London. Hargreaves Associates designed numerous large-scale projects around the world, including the masterplan for the Sydney 2000 Olympics (2000) in Sydney, Australia; Crissy Field (2001) in San Francisco; and Jamaica Bay Vision Plan (2013) in Brooklyn, New York.

Hargreaves uses landforms to organize movement, orientation, different zones, and functions. Some landforms, called “cones” and “spirals,” have geometrical shapes; others have forms that derive from natural formations; and others have forms from past uses on the site. Hargreaves works with earth, water, and vegetation as media for landform design, including physical support elements, such as retaining walls and geotextiles to support the form.

When Hargreaves Associates first opened their practice in 1983, the art and architecture world were in transition from Modernism to Postmodernism. However, Postmodernism was still trying to find its own design language that referenced history, but without using Modernism’s formal strategies (Hargreaves et al., 2009). Hargreaves was inspired by the Land Art movement,

especially by Robert Smithson, Michael Heizer, and Walter De Maria, who created site-specific earthworks and shifted the understanding of materials toward earth, sky, and water (Hargreaves et al., 2009). Robert Irwin's site-specific approach to sculpture inspired Hargreaves Associates to look for conditions and forms that derive from the site, rather than unrelated forms (Czerniak et al., 2007). Later, the site-generated approach became the main idea for most of the company's projects. In addition to this approach, the company also referred to the site history and ecological processes to create a new formal expression.

Parque do Tejo e do Trancão (1994) in Lisbon, Portugal (Figure 29) was inspired by the Land Art movement, especially by Robert Smithson (Hargreaves et al., 2009). This project illustrates how hydromorphic principles can inform large-scale landform interventions. Hargreaves uses landforms to organize movement, orientation, different zones, and functions. The park is located in Lisbon, Portugal, at the confluence of the Tejo River and the Trancão River, landfills polluted by industrial use. The design was based on a site-generated approach that addressed the area's environmental issues and created the identity of the new park. The idea of the design was to create earthworks that respond to the landfill processes below the ground and wind processes above it. The landforms were built with 500,000 cubic yards of sediment that was dredged from the harbor. The overall landform covered the landfill and sculpted the site to create areas protected from the wind. The earthen landforms masked landfill, and dendritic landforms imitated the wind and water action on the site (Hargreaves et al., 2009).



Figure 29. Parque do Tejo e do Trancão (1994) by Hargreaves Associates in Lisbon, Portugal, aerial view of the site and landforms. From Hargreaves et al., 2009.

The later projects from Hargreaves Associates include a series of parks on brownfield sites along waterfronts, such as Crissy Field, Louisville Waterfront Park in Kentucky, the New Orleans Waterfront, and the Chattanooga 21st Century Waterfront in Tennessee. The emergence of waterfront redevelopment parks was a result of the postindustrial decline of waterfronts, and the desire to bring people from rural to urban areas and stimulate urban renewal (Hargreaves et al., 2009). In waterfront redevelopment projects, Hargreaves Associates integrated natural systems of the site with strategies for better access for people and programmatic functions that create more diverse park experiences. The landscape design of such projects was a result of manipulations with earthforms, water, and vegetation.

Crissy Field (completed in 2001) is a national park located within the Golden Gate National Recreation Area in San Francisco (Figure 30). The 100-acre park, one of the first large-scale projects that transformed a U.S. military aviation site, integrates ecological habitat and recreates a marsh ecosystem. The design creates a balance between environmental needs and active use, while also balancing ecology, program, and the history of the site.

Crissy Field was first used as a military site. Since 1776 when the Spanish built the Presidio, the site was occupied by Spanish, Mexican, and American military forces. In 1915, the existing tidal marsh was completely destroyed, and a racetrack for the Panama-Pacific International Exposition was built. After the exposition, the site was converted to become the first grass airfield on the West Coast. In later years, the military base became available for public use, mostly for beach access and dog walking (Landscape Architecture Foundation, 2019). The informal use of the site continued when it was transferred to the Golden Gate National Recreation Area. However, due to the past military use, pollution of the soil and groundwater was significant and required cleanup actions to transform the area into a national park.



Figure 30. Left: Crissy Field (2001) by Hargreaves Associates in San Francisco, CA. Right: Aerial view of the site and landforms. From M'Closkey, 2013.

The design accommodates a variety of functions, such as a beach area, tidal marsh restoration area, recreated airfield, and picnic area, that are hidden from each other by grade change and plants. The fill from the construction of the tidal marsh was used to form an airfield, a landform that shapes the site, creates a park experience, and protects from strong winds. The grade of the airfield increases up to eight feet to the tidal marsh, creating a slowly rising landform that enhances wind protection and directs water flow across the site. Hargreaves Associates was able to achieve the space's visual connectivity while at the same time limiting physical access to different parts of the site. The design layers the site's history and dynamic ecology with contemporary recreational use.

The exploration of hydromorphism in landscape architecture illustrates the relationship between water and earth as the main material to shape landforms. Ideas and metaphors from the hydromorphism period highlight the use of natural materials and site-specific approaches. Landforms in natural landscapes create general site organization as well as different uses and spaces, but are also a base for other design elements, such as buildings. Landscape architects and their landform design projects had a significant influence on the development of the formal connection between landscape and buildings in architecture.

2.3.3 Biomorphism

In this dissertation, the term biomorphism (from the Greek *bios* for “life,” *morphe* for “form,” and *-ismos*, a suffix that forms abstract nouns denoting a practice or system) is used to describe the design approach in which a building form is inspired by curvilinear shapes found in

the living world. Biomorphism involves the use of curves, flowing lines, and shapes that resemble nonlinear forms.

In the 1990s, the dominant metaphor in architecture was biological (Allen & McQuade, 2011), which was an attempt to imitate nature and create more fluid and lifelike buildings. The emergence of the biological metaphor was a result of three key processes that have happened simultaneously during the last few decades: (1) the development of theory describing these processes as a new way of thinking about architecture and landscape, (2) technological advancements, and (3) the desire to recreate natural forms and manipulate topography at a larger scale.

The use of biomorphic metaphor at the beginning of the 1990s was influenced by the desire to make architectural forms more fluid and lifelike. While Stan Allen noted that the biomorphic metaphor was developed from D'Arcy Wentworth Thompson's description of natural form as a "diagram of forces" (Allen & McQuade, 2011), Jencks argues that the shift in design thinking in the 1990s was influenced by a nonlinear paradigm (Jencks, 1997). The term "nonlinear" derives from mathematics and refers to a nonlinear function, where the relationship between two variables cannot be expressed as a straight line. The term is used to describe complex systems that are not linked by cause-and-effect relations (Carpo, 2013). The nonlinearity in design manifests as curvilinear architectural forms. Frank Gehry was primarily interested in the sculptural qualities of curvilinear buildings. Enric Miralles and his *Biblioteca* building in Spain (2007) manifested complex curvilinear surfaces. Such architecture was characterized by the complexity of form, variations, and visual qualities (Jencks & Kropf, 2006). The concept of nonlinearity expanded into new architecture languages with a main focus on curvilinear forms.

The concept of nonlinearity in architecture expanded into the use of biological metaphor that can be described by a complexity of form and visual characteristics that brings buildings closer to our understanding of nature (Jencks, 1997). Examples of such projects include UNStudio's Möbius House (1998), NOX's hypersurfaces in the HtwoOexpo pavilion (1997), and Mecanoo's landform Library Delft University of Technology (1993–1995).

The Möbius House (Figure 31) is a private residence designed in 1998 by UNStudio's Ben van Berkel and Caroline Bos in Het Gooi, the Netherlands. The house is an example of biomorphic principles through its continuous spatial organization. The design is inspired by the

continuous loop of a Möbius strip and symbolizes the combination of work and family lifestyles into a single fluid spatial arrangement. The layout of the house is organized as a seamless flow between spaces, where the circulation has no clear beginning or end. The fluidity of the space is achieved through interconnected spaces. The living and workspace areas are connected and reflect the overlapping functions of the house. Large windows create a connection between the inside of the building and the landscape. The house geometry, with its nonlinear forms, changes traditional ideas about residential design and spatial organization.



Figure 31. The Möbius House in the Netherlands by UNStudio. From UNStudio, n.d.

The HtwoOexpo pavilion (Figure 32) was designed by Lars Spuybroek at NOX in 1997 as part of a water exhibition in the Netherlands. The fluid pavilion geometry is designed as a living structure that reacts to the environment and visitors. The pavilion is an example of hypersurface, where fluid forms create interactive and dynamic spatial experiences. The fluid form mimics the movement of water and creates the curvilinear geometry of the building. By doing so, Spuybroek changes traditional perceptions about walls, floors, and ceilings and creates a continuous space. The building was also designed with a wide range of sensory interactions between visitors and interior. The visitors can alter the atmosphere of the interior by altering the sound, light, and projections.



Figure 32. HtwoOexpo pavilion in the Netherlands by NOX (1997). From Hidden Architecture, n.d.

Library Delft University of Technology (Figure 33), designed by Mecanoo in 1993–1995 in Delft, the Netherlands, is an example of how a sloping green roof of the building seamlessly integrates into the landscape. The library is set into an artificial hill with the structure underneath the landscape surface. The green roof forms a sloping hill that merges with the campus landscape. At the center of the library, a cone structure rises through the green roof, which helps to bring natural light inside the building and symbolizes knowledge and innovation. Inside the library, flexible spaces are organized around the cone, which helps to maximize the daylight and create an openness and connectivity. The sloping green roof is also a public space and an extension of the campus landscape. It is a space for faculty and students to relax, study, or socialize. The building symbolizes a connection between nature and education.



Figure 33. Library Delft University of Technology in the Netherlands by Mecanoo. From Mecanoo, n.d.

In the biomorphism period, architects used different terms to describe curvilinear architectural forms, such as biomorphic, fractal, folding, and landform architecture. Jencks defined “landform architecture as articulated landscape,” a new direction based on the complexity sciences emerging at the intersection of urban design and land art (Jencks, 2002). Such an approach allows one to design a building that encompasses a large volume of the city without making it too monumental (Jencks, 1997). While introducing a landform, Jencks explains opposing forces that create landform structure. One force is the real estate pressure to accommodate as much activity as possible into the smaller space. On the other hand, Jencks emphasizes the idea of environmental forces, such as wind, gravity, and landscape, that inspires a new way of thinking (Jencks, 2002). Jencks identifies Greg Lynn and Foreign Office Architects (FOA) as firms who design landform buildings.

The Stranded Sears Towers (1992) is a conceptual project designed by Greg Lynn in Chicago (Figure 34). The project reimagines the transformation of the rigid, rectilinear architecture of the Sears Tower into fluid, intertwining building strands connected to the topography. The project is a part of Lynn’s exploration of biomorphic form in architecture and digital technologies. With the help of digital technologies, Lynn deconstructs the rectilinear form of the Sears Tower to fluid, curvilinear shapes that change the original geometry into

intertwining strands. The transformation symbolizes the shift from a static to a dynamic approach in architecture and challenges conventional norms by suggesting that a cityscape can move away from rigid geometries.



Figure 34. Stranded Sears Towers in Chicago by Greg Lynn (1992). From Greg Lynn Form, n.d.

The Yokohama International Port Terminal (1995), a transportation hub designed by FOA in Yokohama, Japan (Figure 35), redefines the relationship between architecture and landscape through space fluidity. The terminal changes the traditional understanding of architectural elements, and instead introduces a continuous folded surface that integrates roof, walls, and floors into a single fluid form. FOA created a new topography with their design and prioritized public spaces, such as a roof deck. The nonlinear, uninterrupted circulation for passengers and vehicles consists of a series of ramps and open pathways through the building. Such fluid forms were achievable because of advancements in structural design. The steel-plate construction and long-span beams made it possible to create a fluid interior space. The fluid form of the inside and outside spaces highlights the connection with the waterfront context.



Figure 35. Yokohama International Port Terminal by FOA (1995). From Langdon, n.d.

The ability to create more fluid and curvilinear forms was associated with the rapid development of computer technology. Computer programs such as Computer-Aided Three-Dimensional Interactive application (CATIA), computer-aided design (CAD), and 3Ds Studio Max were widely used as tools to develop complex surfaces. Computer-aided design made modeling and calculating complex curvilinear forms possible. Such complex manipulations with topography were also possible with the development of building technologies that were able to sustain the complexity of form through computerization. The idea of fluid grassy landscapes had an influence on the architectural understanding of fluid form. In architecture, it forced the development of new field-like buildings that look like an open-ended landscape.

The biological metaphor represented a shift from the single-standing building toward one more integrated with the context. The integration of building and landscape and the emergence of landform architecture also demonstrated the growing role of digital tools in shaping architectural form and metaphorical expression.

On the other hand, landscapes are also shaped by different forces and “evolve” over time. A parallel trend that was dominant in landscape architecture focuses not on the biological organization of individual species, but on a systems-based process that shapes landscapes and cities. Allen indicates that through the 1990s, architects were inspired by landscape architecture,

and later by landscape urbanism as a model that fosters extended and continuous form while accommodating a complex program. The combination of folded and warped surfaces that are extended horizontally promised more consistent form and smoothness in combination with various programmatic functions (Allen & McQuade, 2011).

2.3.4 Geomorphism

In this dissertation, the term geomorphism (from the Greek *geo* for “earth,” *morphe* for “form,” and *-ismos*, a suffix that forms abstract nouns denoting a practice or system) is used to describe the design approach that draws inspiration from natural landforms and seeks to incorporate these shapes into the built environment. Geomorphism involves the use of digital tools to create forms that mimic natural landscapes and forms, as well as the use of materials and construction techniques that reflect the qualities of natural forms. Geomorphism also includes subcategories such as topographical integration, geomorphological form, crystallographic form, and landscape integration.

In the early 2000s, the biological metaphor in architecture shifted to geological metaphor, where buildings were like the ground—more stable rather than fluid (Allen & McQuade, 2011). The idea of the building as a complex geological structure with dynamic form emerges as a result of the development of new technologies, design techniques, and the need for enhanced environmental performance.

The geological metaphor in architecture builds on Kenneth Frampton’s concept of megaform. The concept of megaform emerged after the decline of the megastructure concept. It has been influenced by intertwined and interconnected issues of politics, economics, environmental crisis, and urban growth (Arquitectura Viva, 2022). The neoliberal ideology has played a crucial role in urban development. While that period was characterized by a decentralization of power, less government control, and the rise of the private sector development, one of its major causes was urban sprawl. Neoliberal development was identified as chaotic suburban growth and freestanding objects, which required large-scale infrastructures to reach distant areas. Architects critiqued rapidly growing megalopolises, which were developing as a result of standard planning regulations and which lacked engagement with the environment. The architectural objects were spontaneously developing in urban and suburban

areas with no culturally significant landmarks. Frampton's idea of "megaform" reflected this tension.

Kenneth Frampton (1930–) is an architectural critic, historian, and architect. In "Megaform as Urban Landscape" (Frampton, 1999), Frampton proposes the concept of "megaform" to address issues of placelessness and monotonous urban growth. The "megaform" is defined as a large, horizontally extended form that is topographically integrated into the site and has place-making potential.

The concept of megaform was a form-oriented solution to complex problems, such as the uncontrolled urban growth of megalopolises and issues of placelessness. Megaform, as defined by Frampton, is a large-scale horizontally extended architectural intervention that integrates with topography and has a place-making potential. While in early writings Frampton focuses on urban contexts, in his later lecture, Frampton argues that the concept of megaform is still relevant. He expands the potential of megaform to address environmental degradation and restore connection with nature. Frampton suggests that megaform can serve as a catalyst for regional development by also sustaining a sense of place through connection to the landscape (Frampton, 2021). This opens up the possibility of applying the concept to suburban areas and allowing megaform to interact with unique landscape conditions.

Frampton argues that "megaform" can be identified by the following characteristics:

- Horizontal, rather than vertical, integration with the site, where topographic character may be so dominant that it almost becomes a landscape.
- Hybrid program as an accumulation of required building program and further future activities that develop as a result of connection with the site.
- Public use, which provides a public domain in highly urbanized cities and suburban areas.
- Landmark in a unique form.
- Large scale, which allows buildings to have a different place-creating potential, and which is based on the program and form in the specific context.

Frampton provides a series of projects that illustrate his understanding of "megaform." The Fort L'Empereur for Algiers (1931) by Le Corbusier (Figure 36) is an early example of megaform. For Frampton, this project shows an integration of form and natural contours, which transforms megaform from a horizontally extended landmark to the vast scale landform.

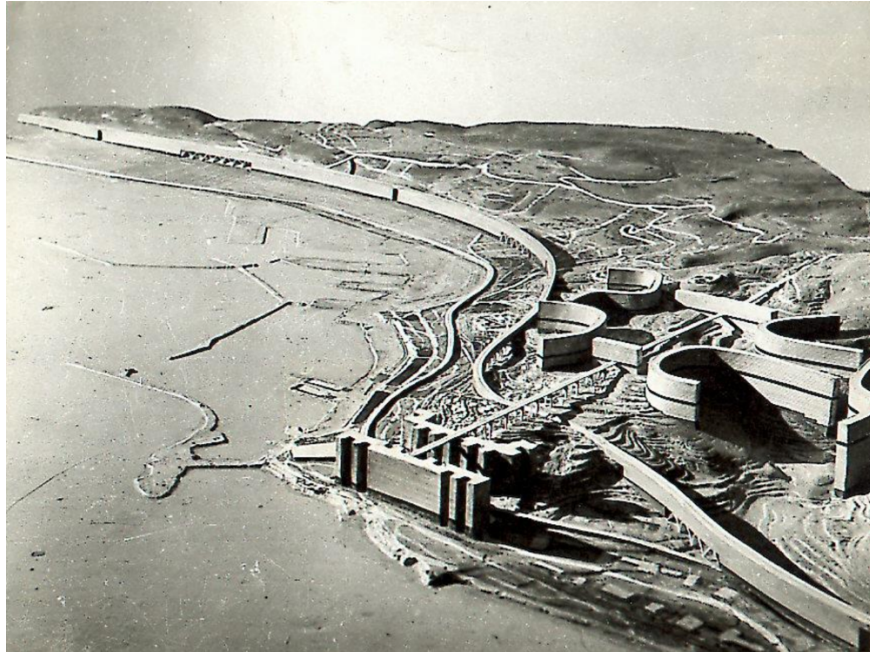


Figure 36. Fort L'Empereur in Algiers by Le Corbusier (1931), conceptual rendering. From Foundation Le Corbusier, n.d.

At the end of “Megaform as Urban Landscape,” Frampton provides a historical manifesto, where he traces the appearance of megaform in 20th century architecture. He argues that within megalopolises, architects can intervene in urban landscapes by developing a large-scale form—megaform—which can incorporate existing topography and give a building a specific identity. Such large-scale form changes the understanding of the building from a single-standing structure to a form that is connected to the landscape.

Over two decades after the first publication of his essay on megaform, Frampton continues to revisit this idea. In the Raoul Wallenberg Memorial Lecture at University of Michigan’s A. Alfred Taubman College of Architecture + Urban Planning in 1999, Frampton stated that he developed “megaform” as a unifying environmental concept that might be the only realistic formal approach left for urban interventions. He critiques himself by saying that not all of the selected examples presented in his essay are of the same scale or the same level of abstraction. However, they blur in different ways the distinction between architecture and landscape. Similarly to artificial dikes and canals that merge with the landscape and become almost invisible, megaform, due to its horizontal form, is also capable of becoming a new artificial landscape (Frampton, 2021).

The megaform concept was introduced to the architectural discourse, where the solution for urbanized regions was to build a topographically integrated “mega” project. While the idea has largely been well-accepted among architects and scholars, “megaform” has also been criticized for its complexity and large scale. Paul Lewis says that it is impossible to design a megaform without being optimistically naïve (Manfredi & Weiss, 2015). The complexity of the form and program requires a huge time investment to design it. Moreover, such a large urban form typically requires an empty site and entails expensive construction. He sums up that megaform projects are examples of ambitious design; however, some of them were not as successful due to the implication of size.

While explaining landform architecture that focuses on the use of geological form as a metaphorical response to potential social, environmental, and urban changes, Allen refers to Frampton’s idea of the “megaform.” The further extension of landform architecture was the idea of “landform building” that establishes a relationship between building and landscape. Allen described this idea in his book *Landform Building: Architecture’s New Terrain* (Allen & McQuade, 2011). It opened up new possibilities for manipulations of territory that signified a shift to the geological metaphor.

Allen describes the evolution of landform architecture as an artificial landscape with a focus on geological large-scale structures. Landform buildings, as defined by Allen, are “green roofs, artificial mountains and geological forms; buildings to walk on or over; networks of ramps and warped surfaces; buildings that carve into the ground or landscapes lifted high into the air” (Allen & McQuade, 2011, p. 40). The understanding of “landform architecture” was based on the process of rethinking a traditional relationship to the ground that is possible because of new technologies, design techniques, and a need for enhanced environmental performance.

Landform building was the topic at the working conference “Landform Building: Architecture’s New Terrain” at the Princeton University School of Architecture in April 2009. The conference examined different ways landscape influences architecture. The participants were practitioners that used new technologies and design techniques in their design. Among them were Iñaki Ábalos, Stan Allen, Vicente Guallart, Michael Jakob, Michael Maltzan, Michael Manfredi, Mónica Ponce de León, Jesse Reiser, Fabian Scheurer, Nader Tehrani, Nanako Umemoto, Marion Weiss, and Mirko Zardini. The conference was a theoretical ground for further manipulations with the landscape and settled its conceptual framework for further

development in landform direction, later published in Allan's *Landform Building*. In this framework, the architect's work was considered not only as a cross-disciplinary phenomenon, but as a new design strategy that solves problems.

Allen begins the book's introduction to landform architecture with an essay that describes the shift from the biological to the geological metaphor. He states that the biological metaphor over the previous two decades was influenced by the desire to make buildings more fluid and adaptable. This desire was influenced by the development of computer technology that models new forms in response to climatic, structural, and programmatic forces.

As *Landform Building* attempts to trace an alternative history of architecture as an artificial landscape, Allen introduces seven working concepts in order to find a system that unifies design strategies:

- Landform building creates a field-like effect at the building scale by reconsidering the tension between two different scales of a landscape field and building object.
- Landform building is less about the form imitation, but more about programmatic potential from the artificial terrain.
- Landform building is developing in horizontal and vertical directions, which offers new connectivity and represents the iconic power of an architectural object.
- The city is constantly evolving, so it is necessary to develop an adaptive model.
- Landform building can suggest a new approach to sustainability and improve environmental performance.
- Landform building blurs the boundary between inside and outside, and extends the notion of interior.
- Even though landform building uses fabrication and envelope technologies to construct an artificial environment, it is still conceived as a "technical problem within architecture" (Allen & McQuade, 2011).

While on a form level it was possible to generate more dynamic shapes, on a performative level a structure needs to be adaptive and lifelike. Allen emphasizes that the old metaphor of buildings as "evolving bodies" with the potential to change is still limited in that buildings cannot evolve and adapt as rapidly as their context (Kubo, 2012). In addition, there is still a gap between computer-generated form and what the construction industry can provide as

available building materials. Thus, he argues that buildings are “hard and slow” (Allen & McQuade, 2011) and indicates a shift to the geological metaphor.

The following sections present the geomorphism approach’s related subcategories: topographical interaction, geomorphological form, crystallographic form, and landscape integration.

2.3.4.1 Topographical Integration

In this dissertation, the term “topographical integration” refers to the way a building or structure is integrated into the natural topography of a site. The main goal of topographical integration is to create a seamless transition between the built environment and the natural environment. This approach builds on ideas from landscape architecture and results in the development of new field-like buildings that look like an open-ended landscape.

One example of a horizontally extended building that connects to the landscape is the NTR Headquarters (1997) by MVRDV (Figure 37). The single-story building is connected to the topography in a way that it becomes invisible from the city. The roof of the building is treated as an extension of the landscape and becomes a public space for office workers. The building challenges traditional approaches to the workplace by offering a space with a connection to the outdoors. The rooftop becomes a space for social and recreation activities.

From the park side, the building is elevated on columns above the ground, which creates a sheltered space beneath it. The space beneath the building structure becomes a shaded and protected part of the park. The project is an example of building integration with the site.



Figure 37. NTR Headquarters in the Netherlands by MVRDV (1997). From MVRDV, n.d.-a.

Another building that is a part of an office complex is Villa VPRO (1997), a transparent envelop of stacked surfaces that fold into each other (Figure 38). The folding geometry changes the traditional approach to rigid office design and introduces a new way of creating office space. The design consists of folding and fluid surfaces that blur the boundary between interior and exterior.

The seamless transition between floors shifts the conventional circulation form of elevators and stairs to fluid movement throughout the building. Such changes promote collaboration and interaction between workers, as there are no visual barriers; instead, architects propose an open and interconnected space.

The office does not occupy the existing landscape, but constructs the site itself. The building rises from the ground as an extension of the earth and rethinks the relationship between architecture and landscape. The transparency of the envelop further enhances this connection by allowing natural light to flow to interior spaces. From the inside, this transparency makes views of the surrounding landscape an integral part of the building experience. Villa VPRO challenges traditional architectural paradigms by merging spaces and structural elements into a cohesive design.



Figure 38. Villa VPRO in the Netherlands by MVRDV (1997). From MVRDV, n.d.-b.

The Olympic Sculpture Park (Figure 39) in Seattle, WA, designed by Weiss/Manfredi and completed in 2007, is a public space that integrates urban infrastructure and art into the landscape. Located in the heart of Seattle, the park transforms the formerly industrial waterfront site into cultural space. The Olympic Sculpture Park is embedded into the existing railway and road infrastructure, and the design of the park transforms the surface and incorporates a z-shape path that rises and falls to create a “moving topography” (Manfredi & Weiss, 2008, 2015). This artificial landform moves over the existing infrastructure of a four-lane roadway and railway, connecting downtown Seattle to the waterfront, and provides ecological and social performance. The Olympic Sculpture Park introduces green spaces that filter runoff and increase biodiversity, restores native shoreline habitat, and creates intertidal zones that support fish spawning. Socially, the z-shape of the park provides public access to the waterfront and creates a space for recreation and cultural use.

For Frampton, this project is an example of landscape megaform that is integrated into an existing context. He further explains it as an artificial topography that transforms the surface and serves as a public domain and a landmark (Frampton, 2021).



Figure 39. Olympic Sculpture Park in Seattle by Weiss/Manfredi (2013).

Topographical integration challenges the traditional architectural paradigm, where a building dominates the site, and instead proposes an approach where buildings and landscape create a cohesive form or seamlessly blend into the natural surroundings. The projects presented above illustrate how design can not only reshape the relationships between building and landscape, but also foster connection between users and public spaces.

2.3.4.2 Geomorphological Form

In this dissertation, the term “geomorphological form” refers to a design approach that uses or mimics natural forms as inspiration for architectural forms. This approach focuses on the use of the geological form as a metaphorical response to potential social, environmental, and urban changes.

The idea of the building as a complex geological structure with dynamic form that has an intricate message for the observer lies in the concept of “vital materialism” that was developed by political theorist Jane Bennett (Bennet, 2010). This concept focuses on the shift from the human experience of things to the things themselves, along with a recognition of nonhuman forces. In architecture, Bennet’s concept might suggest the shift to the life of things and the reconsideration of materiality as a dynamic exchange of information. If there is no differentiation between environmental and human objects, but a continuous sequence that is

based on a speed, then buildings are as “hard and slow” as the ground is (Allen & McQuade, 2011).

Stan Allen introduces geomorphological form by using different landform terms that become a metaphor. He describes densely populated American cities through the lens of the vast landscapes by calling streets “chasms,” skyscrapers “cliffs,” and landform buildings “artificial mountains.” By making a turn toward geological form, landform architecture has created an opportunity to design buildings in response to natural vulnerabilities and the disruption of geological surfaces, which Allen explains as a metaphor of canyons between skyscrapers.

The appeal of hard surfaces can be explained as a desire to create a landmark that is capable of resisting urban changes. The geological form of the building emphasizes the relationship to the ground and connection to the context. Allen provides examples of buildings that reflect the idea of geological form. Among them are City of Culture of Galicia by Peter Eisenman and Mountain by Vicente Guallart.

The City of Culture of Galicia (1999–) by Peter Eisenman is located in Santiago de Compostela in Spain (Figure 40). The shape of the cultural complex derives from a series of overlay computations that results in a form of artificial mountain. This computational approach is identified by the architect as the “principle of superposition” and consists of three sets of information. The first is the medieval street plan of Santiago superimposed upon topography. The second is a modern grid superimposed upon medieval routes. And the third is a combination of the first two, which results in the final form. The shape of the roof is reminiscent of the shape of flowing topography—similar to the shape of the site, along with cracks and openings for the buildings. The complex consists of large libraries, museums, and a performance space. While the project represents a unique approach to designing large-scale buildings, its construction was not completed.



Figure 40. City of Culture of Galicia in Spain by Peter Eisenman (1999–ongoing). From Eisenman Architects, n.d.

The Mountain (2002) is a conceptual project designed by Vicente Guallart in Spain (Figure 41). The project reimagines architecture as a relationship between building and environment and portrays the building as a mountain. In this project, Guallart searched for the logical guidelines to develop an architectural response to the specific environmental conditions. Such geological form manipulations arise as an attempt to create a topography that critically responds to the social and economic issues of the city (Guallart, 2009). Guallart envisioned the building as a self-sufficient mountain structure that incorporates ecological principles. The form of the building mimics a natural shape while also combining green roofs, terraced spaces, and public zones for visitors. Guallart challenges the conventional approach of building isolated buildings and proposes a model where architecture becomes an extension of the landscape and redefines the relationship between nature and architecture.

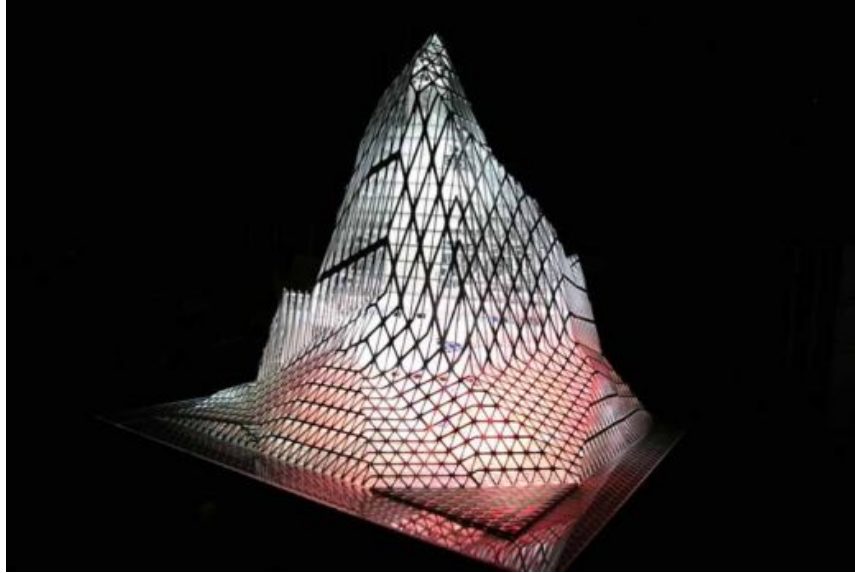


Figure 41. Mountain in Spain by Vicente Guallart (2002). From Guallart, n.d.

The geological metaphor was dominant for nearly a decade. The wide range of design projects developed during this period were focused on formal expression and topographical transformations. Architects were drawn to the idea of recreating mountains and other types of landforms with the building silhouette. However, the geological metaphor was transformed by the idea of a hybrid combination of landscape and architecture.

2.3.4.3 Crystallographic Form

In this dissertation, the term “crystallographic form” refers to a design approach that draws inspiration from the geometric structures of minerals and crystals. This approach emphasizes sharp edges and faceted surfaces to create a structured dynamism that explores how such a form can illustrate the identity and interact with the site.

One project that uses crystallographic form is the New Maribor Art Gallery (2010) in Slovenia, designed by Stan Allen (Figure 42). The strong figural presence of the building establishes a clear identity in the historical area of Maribor. The project manifests the idea of open, in-between spaces that behave like landscapes and are capable of responding to changing circumstances of use and building program. The logic of the five-sided plan transformation is explained via form generation diagrams, plans of extrusion, and unfolded schemes of a building structure. Although the project has a mountain-like folding form, it says very little about how

such form responds to social, environmental, and urban challenges. With an emphasis only on form, the architecture loses its connection to nature.

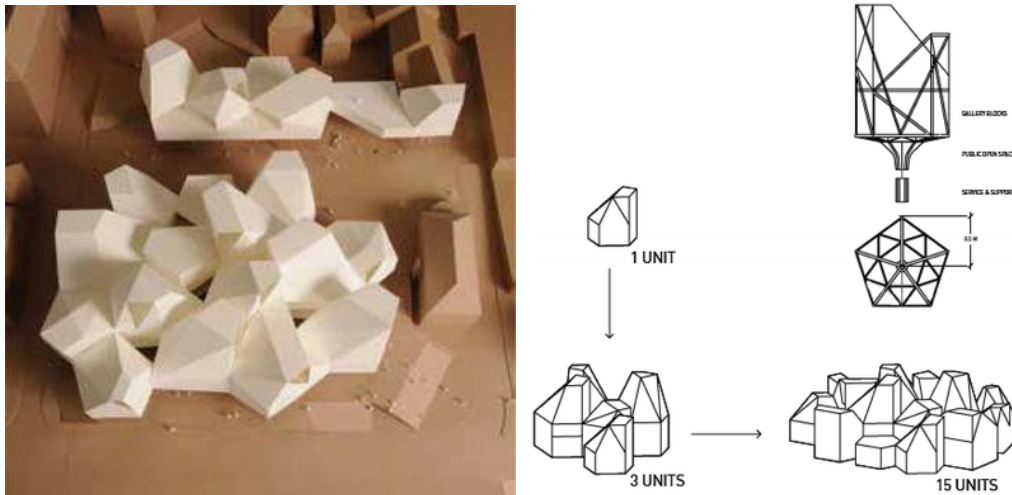


Figure 42. New Maribor Art Gallery project in Slovenia by Stan Allen (2010). From Stan Allen Architect, n.d.

Allen argues that for Frampton, the transformation from metropolis to megalopolis provoked a reevaluation of architectural scale. The key argument was that large-scale horizontal structures can change the urban landscape (Frampton, 1999). However, Allen proposes that a “landform building” creates the site itself, instead of merely “occupying” a landscape. While in general architecture has some level of interaction with the site, landform buildings change traditional architectural techniques by also combining a landscape with a building, which extends the scale of the building to the site size (Allen & McQuade, 2011). Such design techniques produce more diverse, large-scale structures that establish a relationship between building and landscape.

Architects that are working in a hybrid landscape—a place that has multiple layers of human inhabitation that is adjusted to the building envelop—rarely transform uninhabitable wilderness, but add new layers to the existing environment (Allen & McQuade, 2011). On a large scale, this approach suggests that the city becomes a complex organizational form, where even a single architectural intervention can have a positive effect on urban development by recognizing the complexity of the city.

2.3.4.4 Landscape Integration

In this dissertation, the term “landscape integration” refers to a design approach that emphasizes the seamless connection between built environment and landscape. The landscape integration subcategory responds to global climate change and rapid urbanization challenges. This approach focuses on connecting design to larger systems by using more sustainable materials and solutions.

The Chulalongkorn University Centenary Park (2017) in Bangkok (Figure 43) was designed by N7A in collaboration with the landscape firm LANDPROCESS as a reconnection between the city’s history and adaptation to climate challenges (Arifwidodo & Tanaka, 2015). The value of Chulalongkorn University Centenary Park is not in its programmatic functions, but in its resilient design. The park is designed to respond to climate change and an unstable future. The entire park is viewed as a water storage, which could hold one million gallons of water during a flood. The runoff water flows from elevated green roofs of the large-scale building that is integrated into the landscape through rain gardens into a constructed wetland, and further to a retention pond. The middle part of the park is designed to collect floodwater and retention pond overflow. The park also collects water from neighboring areas by treating it with a filtration system. The other important function of the park is reducing urban heat. The park spreads out through adjacent neighborhood blocks with green pathways. Landscape architect Kotchakorn Voraakhom changed the design of neighboring streets by replacing car lanes with bike lanes and street trees. The attempt was to make Bangkok accessible for people, for walking, and for biking more than for driving.



Figure 43. Chulalongkorn University Centenary Park in Bangkok by LANDPROCESS (2017).

From Landezine, n.d.

The Underground Parking Garage (2016) in Katwijk, South Holland, the Netherlands (Figure 44), was designed by architects from Royal HaskoningDHV and landscape architects

from OKRA Landschapsarchitecten. The structure is part of a project focused on the protection of the Katwijk Netherland coastline for the next 50 years. The building, located between the shoreline and the sea, was a part of the Kustwerk Katwijk flood management initiative that aimed to keep the city as a tourist destination and improve the local economy.



Figure 44. Underground Parking Garage in the Netherlands by Royal HaskoningDHV and OKRA Landschapsarchitecten (2016). From ArchDaily, n.d.

The multidisciplinary team developed a building that serves as a coastal defense structure, parking, and landscape that is carefully integrated into the coastal environment. As a part of the initial analysis, the landscape team identified that the connection between the city and the beach is valuable for Katwijk. The dike and parking, completely covered by the dune, creates minimal disruption for the city and beach. The structure is covered with green grasses that recreate the dune landscape. The car park is not only the architect's appreciation of the existing environment, but also a building that preserves the public space and provides universal access to the beach.

The majority of projects described here can be interpreted as megaform buildings, as advocated by Frampton, that change the meaning of the concept by adding a new function or possibility to address climate-related issues, such as the urban heat island effect and flooding. The selected precedent analysis shows that in the current context, landform buildings can also address climate issues. One of the important advances in landform buildings with the ecological metaphor is the use of natural materials.

2.4 Discussion

While landforms are understood by the form and processes that shape them, current theory and practice of landform architecture focuses on a form-based approach and metaphoric interpretation of nature, rather than landscape processes and their potential to shape landform buildings.

Landform architecture theory was focused on building aesthetics and used landforms as a source of architectural metaphor and inspiration. The generated forms looked like natural landforms, but they did not function as landscapes. Landform buildings, even when they were incorporated into existing landscape, were still stable structures. The landscape itself, on the contrary, is an open-ended field that functions as a living system.

The current theory and practice focus on architectural form, while the landscape potential of landform buildings remains underexplored. Landform buildings are more than just a green roof and a form that recreates nature. Landform buildings can address the current climate crisis by solving the problems of the urban heat island effect, sea-level rise, and flooding; play an important role in storm water management; and provide a space for habitat. The design approach of such buildings can also change from form-based to process-based.

The idea of a process-based approach is not new in landscape architecture, where landscape is considered as a dynamic system of processes. A process-based approach that reflects shifts in cultural and disciplinary contexts was described as open-ended, dynamic, fluid, adaptive, and engaging with time and change. The emergence of a process-based landscape approach in the late 1980s in landscape architecture was influenced by the critique against a form-based approach, a cultural shift toward a new ecological paradigm, and the emergence of digital technology that can model process and time. The discussion of a process-based approach involves the theory of landscape and ecological urbanism, a theory that supports the idea that the designer sets the initial condition of a landscape and allows ecological processes to unfold.

Landscape is considered as a dynamic and interconnected system that encompasses ecological, social, and economic processes. Rather than being a static result, it is viewed as an ongoing process that is shaped by natural processes and social interactions. Design in this context is seen as an open-ended strategy that aims to guide and shape the landscape development, rather than proposing a fixed form. Projects, in this case, are approached as opportunities to embrace future conditions; for example, manipulating erosion and sedimentation processes makes it possible to create a new topography (Nijhuis, 2013). The goal of a process-

based approach is to promote relationships between natural systems and humans that are both aesthetic and functional, but also to promote social and ecological comfort. This is a layer approach that helps designers understand landscape as a complex system.

In this research, the process-based approach is applied to design landform buildings that are shaped by natural processes. Rather than proposing a fixed form, this approach will focus on the interaction with the natural processes that are already present within the site. This process will also consider a landform building as one situated in a landscape that is constantly changing, which means that the building design will consider the history of the specific site and its potential future.

2.5 Revised Definition of Landform Architecture

Contemporary landform architecture establishes relationships between natural processes and built form, landscape and architecture. It has a potential to blur boundaries between natural and artificial, ground and underground, interior and exterior, past and present. On a larger scale, landform architecture can address environmental issues and be a remedial operation for urbanized areas or previously damaged sites. It makes it possible to create structures and systems that evolve over time.

Landform buildings are those that become part of the existing environment or new nature-like forms that are blended into the landscape. Landform buildings are designed to respond to territory, topography, and urban conditions.

One can identify a landform building by specific characteristics. A landform building is a large-scale form that comes from the idea of megaform. The large scale of the building can respond to global issues. Typically, such issues are complicated and require large-scale solutions. A horizontally extended profile of the building, which was also one of the megaform characteristics, connects the structure with the landscape. The connection between building and landscape makes it possible to integrate the structure to the specific topography. Another characteristic of a landform building, similar to megaform, is a landmark that makes such structures visible for people. This characteristic also plays an educational role—people can see different processes that are happening with the landform building and observe changes over time through its visual presence. A landform building also can highlight the identity of the place. This characteristic acknowledges the fact that large-scale processes are not exactly the same in

different locations. The cultural identity of a landform building can be supported by users' participation in the design process. Large-scale buildings are costly and time-consuming; thus, it is important to have local support for its construction. Such public involvements foster the identity of the place. The last characteristic of a landform building is that it combines multiple functions. The combination of multiple functions makes this building efficient and resilient to future changes.

2.6 Summary

The evolutionary development of landforms presented in this chapter illustrates transformations of ideas, concepts, and paradigms over time that have shaped the current understanding of landform architecture.

The ancient landforms were used as settlements, defense structures, and places for rituals. The examples of ancient settlements around the world show how humans used existing environmental conditions for protection, survival, and social needs. Settlements were often built into caves, cliffs, hills, and mountains for the purpose of shelter, defense, or protection from harsh weather conditions. Elevated landforms, such as hills, served as defensive structures. During the Iron Age, hillforts were surrounded by ditches, walls, and ramparts to provide protection from enemies and wild animals. Henges and kurgans are ancient landforms that reflect spiritual, cultural, and societal traditions of ancient civilizations. Henges were circular enclosures with ditches, while kurgans were circular-shaped burial mounds. Ancient landforms show a deep connection of any type of human-built structure to the environment.

Ancient landforms had a significant influence on Land Art. In Land Art, the dominant idea was to use natural materials, such as rocks, earth, and stone, and processes that have shaped these materials over extensive periods of time to create large-scale, site-specific works in remote landscapes. The movement arose as a critique of traditional art presented in galleries and offered art sculptures in open landscapes, where visitors could physically interact with the work. Land Art also transformed art from two-dimensional static art to three-dimensional experiences that engaged visitors' senses and encouraged exploration. The Land Art works usually highlighted specific information about the history of their site and metaphorically represented the time and change.

In landscape architecture, the ideas from Land Art had a significant influence on the development of the cosmomorphism design approach, where landforms were envisioned as multidimensional sculptures that connect visitors to the surrounding environment, history, and the universe. This design approach focused on integrating symbols and cosmic references into landscape architecture. This approach advanced the understanding of landforms by introducing metaphorical design and digital modeling.

The ideas from the Land Art movement and the cosmomorphism approach had a significant influence on the development of the hydromorphism design approach in landscape architecture. This approach focused on the use of the hydrological metaphor in the development of site-specific design projects. The precedent studies show how landscape architects understood the relationships between water and earth as the main material to shape the landforms. Landforms in landscape architecture were key compositional elements for the site organization, navigation, and different uses of space. Sometimes landforms served as a base for other design elements, such as buildings. This approach had a significant influence on the future development of the relationships between architecture and landscape.

The ideas from landscape architecture influenced the development of the biomorphism approach in architecture, where the buildings were treated as fluid and lifelike forms, with the desire to imitate nature. This design approach was inspired by organic shapes and was driven by the advancement in digital technologies, such as computer programs like CAD and CATIA, alongside the theoretical shift in architecture and development of the nonlinear paradigm. The biomorphic projects and landform designs marked a shift from static, standalone structures to forms integrated into the context, which also forced the development of structural engineering and digital modeling. This period emphasized a synthesis between architecture and landscape, reflecting the fluidity and adaptability as a new way of thinking about the built environment.

The shift from biological metaphor to geological marks the development of the geomorphism approach. Geomorphism integrates digital tools, materials, and construction techniques to mimic natural forms and merge with the landscape. The concept is based on the idea of megaform, where buildings are large-scale horizontal structures that respond to the issues of placelessness; however, landform architecture adjusts the concept by reimagining buildings as artificial landscape. The geologically inspired design highlights the potential of landform architecture to combine landscape and architecture through innovative design strategies. The

geomorphism approach includes the subcategories of topographical integration, geomorphological form, crystallographic form, and landscape integration. The topographical subcategory focuses on buildings that are topographically integrated into the context and look like an open-ended landscape. Geomorphological architecture draws inspiration from geological forms, while crystallographic uses geometric forms found in minerals and crystals as inspiration for architectural form. The landscape integration category highlights the need to connect design to larger systems, and to use more sustainable approaches and materials. The selected precedent study projects demonstrate a move from formal expressions to more resilient structures that respond to climate needs. This evolution reflects deeper engagement with ecological metaphor and the attempt to harmonize architecture with its environment.

The analysis of the evolutionary development of landform architecture shows that the dominant approach in landform design was form-oriented, emphasizing aesthetics and metaphor rather than engaging with dynamic processes. This research proposes a shift to a process-based approach, which views landscape, and, as a result, a landform building as a living system. Process-based landform architecture combines natural processes and built form by blending landscape and architecture while also addressing environmental changes.

III. PROCESS AND LANDFORM ARCHITECTURE

3.1 Landscape as Process

The idea of a process-based approach is not new in landscape architecture. Over the last four decades, process-based design, also associated with terms such as open-ended, indeterminate, and dynamic, was one of the dominant concepts in landscape architecture that understood landscape as a complex and dynamic system. Landscape, as a dynamic and interconnected system, encompasses ecological, social, and economic processes. Rather than a static result, it is viewed as an ongoing process that is shaped by natural processes and social interactions (Nijhuis, 2013).

Design in this context is understood as an open-ended strategy that aims to guide and shape the landscape development, rather than proposing a fixed form. Design projects are approached as opportunities to anticipate future conditions; for example, manipulating erosion and sedimentation processes makes it possible to create a new topography.

In this chapter, the evolution of a process-based approach is traced via precedent study projects by highlighting the key shifts that have shaped this approach. The evolution of a process-based design in landscape architecture and the transition from form-based to process-based thinking is divided into several stages. First, the ecological stage focuses on the dynamic conditions of the landscape and considers seasonal changes and changes over time. Second, the systems-derived stage considers ecological conditions and relationships between different species, and acknowledges that these relationships are sometimes unpredictable. This stage also focuses on diagrams and maps to represent complex interactions. However, over time it becomes clear that diagrams and maps have limited ability to engage dynamic systems within the design process. Third, the phasing stage focuses on large-scale designs and introduces a framework that sustains the development of the landscape over a longer time period.

To understand the current trends of process-based design, another part of the chapter is focused on analysis of simulation techniques and case study projects that apply simulations in different contexts and for a variety of purposes. As a result of such analysis, a process-based landscape approach to landform architecture is presented at the end of this chapter.

3.1.1 Ecological Process-Based Design

The emergence of a process-based approach in landscape architecture in the late 1980s was influenced by the critique of a form-based approach. The shift was driven by a move toward an ecological paradigm. During this period, process-based design moved from a static and compositional framework toward strategies that embrace the evolving nature of landscape. This approach acknowledges landscape as a dynamic system influenced by seasonal changes and long-term processes. Rather than focusing on fixed static outcomes, landscape architects engage with these processes, allowing landscapes to develop over time.

The ecological stage of a process-based design describes the landscape's continual state of transformation. This includes seasonal changes in materials and colors, vegetation growth, hydrological cycles, and changing urban conditions (Berrizbeitia, 2016; Ruthen, 2019). Early projects of George Hargreaves, Michel Desvigne, and Michael Van Valkenburgh are examples of critique against the formal approach and use of a process-based approach that embraces ideas of change and time.

George Hargreaves' early projects were inspired by the notion of process from art, especially by artists Robert Smithson and Richard Serra. Hargreaves's designs used to refer to natural processes. He was approaching landscape design with geometric landforms that responded to ecological dynamics while remaining static themselves. The notion of the fixed form changes with the fact that the site and natural processes are continuously changing and evolving (Hargreaves et al., 2009). His projects incorporated the change over time in a form of seasonal variations and planting strategies.

Byxbee Park (1989), designed by George Hargreaves, is in Palo Alto, California (Figure 45). Hargreaves created a master plan for a 150-acre public waterfront park, located on a sanitary landfill on the San Francisco Bay, and designed the 30-acre phase-one plan (Figure 45). The park is an example of a process-based project that integrates ecological processes, such as seasonal changes, water collection, and plant selection. Byxbee Park, planted with native grasses that cover the sanitary landfill, experiences seasonal changes to the marsh below. Seasonal color flips: when the marsh is green in the winter and spring, the field is golden; in the summer, the reverse is true (M'Closkey, 2013). The planting selection was made based not only on visual effect, but also on plants' survivability without irrigation. The concrete curbs placed parallel to contour lines were designed to collect rainwater and encourage the growth of water-loving plants

and reinforce the park’s responsiveness to hydrological processes. These strategies demonstrate how landscape can engage with ecological processes rather than introducing a static form.



Figure 45. Byxbee Park by George Hargreaves, Palo Alto, CA (1989). Left: Photo from the site. Right: Phase-one master plan. From Hargreaves Jones, n.d.

Michel Desvigne (1958–), a French landscape architect, artist, and educator, is known for using a process-based approach in his projects. His approach to landscape design recognizes the history of the site and acknowledges future uses rather than transforming the site to a purely scenic landscape. In his projects, Desvigne gives priority to processes that shape landscape rather than fixed design. He anticipates the long and uncertain effect of time along with ongoing changes by designing his projects in a way that they can evolve and transform over time.

Jardin élémentaires (1987) is a theoretical experiment of physical dialogue between natural phenomena and infrastructure (Figure 46). Desvigne developed hand drawings of the territory based on satellite photographs. He imagined the transformation of selected sites by natural processes of erosion, sedimentation, and rising water, and by dams. Environmental and human processes in his drawings create changing patterns of streams and sedimentary islands in a valley landscape (Desvigne & Imbert, 2019). Such drawings through observation allowed him to physically experience the mechanism at work. Later he developed a series of models to test his observations physically.

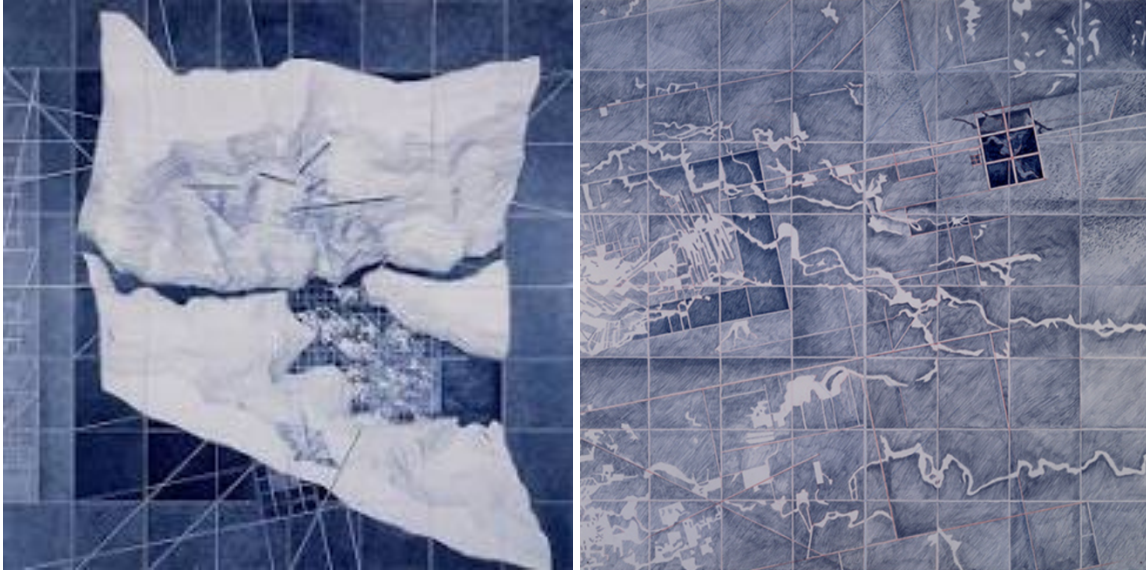


Figure 46. Jardin élémentaires by Michel Desvigne (1987), hand drawings. From MDP Michel Desvigne Paysagiste, n.d.

Michael Van Valkenburgh (1951–), an American landscape architect and educator, also used a process-based approach in his early projects by designing landscapes that evolve with ecological processes. Rather than proposing a fixed form, his work engages with site-specific processes, such as hydrological fluctuations, plant succession, and seasonal transformations. His understanding of place derives from experiences of events, materials, plants, and time that bring a fuller experience to the landscape (Corner, 1999). The resulting landscapes are not only site-responsive but also adapting and transforming over time.

Mill Race Park (1993), designed by Michael Van Valkenburgh, is in Columbus, Indiana (Figure 47), at the confluence of two rivers. Before the construction of the park, the area was prone to annual flooding, sometimes reaching up to 10 feet. The area was cut off from residential neighborhoods and adjacent businesses by railroad tracks. In this design, Van Valkenburgh integrated annual flooding events into the design rather than preventing high water. The fill from excavating Round Lake was reused to create berms and an earthen amphitheater. The playground is also elevated on an earth landform. The selection of plants was based on hardy native species, such as grasses that withstand drought and trees that withstand saturated soil. In terms of materials, most of the paved surfaces were made from reinforced concrete, which does not deteriorate during flooding.



Figure 47. Mill Race Park by Michael Van Valkenburgh, Columbus, Indiana (1993). Left: Aerial view of the park in regular time. Right: Aerial view of the park during flooding. From Michael Van Valkenburgh Associates, n.d.

Ecological process-based design emphasizes a continual transformation of the landscape through seasonal and natural changes. It acknowledges changes in materials, colors, vegetation growth, and hydrological cycles. Building on this foundation, the understanding of a process-based design shifted toward an ecological perspective and designs of landscapes of a larger scale.

3.1.2 Systems Process-Based Design

In the late 1990s–2000s, the understanding of a process-based approach shifted toward a system-based thinking. A system framework of process-based design addresses landscapes of larger scales with more complex relationships between habitat, species, and culture (Cantrell & Holzman, 2016). The evolution of a systems process-based design is related to understanding landscape not as natural phenomena, but as a dynamic system that evolves over time. Landscape operates as infrastructural space shaped by humans, where time plays a critical role in multilayered and connected ecological processes (Figure 48). This perspective supports the idea that a designer sets the initial condition of a landscape and allows ecological processes to unfold.

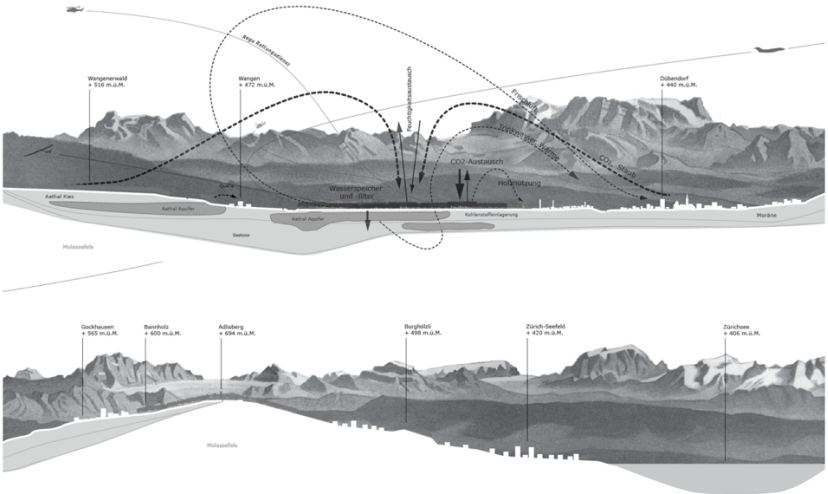


Figure 48. Valley of energy: exploratory combination of surface and subsurface: Top: Flows of waste and water. Bottom: Mobility, and forestry by OPSYS. From Belanger, 2016.

The foundation of landscape urbanism can be traced back to the 1960s. The concept, however, gained prominence in the late 1990s because of a growing awareness of ecological issues, such as climate change, habitat loss, and pollution; shifts in urbanization resulting in large-scale infrastructural projects that led to spatial segregation; but also advances in landscape

architecture allowing the discipline to move toward a holistic approach that includes ecological and social concerns (Waldheim, 2006). During the mid-20th century, the construction of highways, development of industrial zones, and large-scale redevelopment projects prioritized the efficiency and economic growth over environmental concerns. This led to fragmented urban spaces, disconnected communities, and disturbed ecosystems. The concept of landscape urbanism appeared as a critique of architecture's and urban design's inability to offer comfortable urban conditions and address pressing questions.

Landscape urbanism emphasized the shift from form-oriented thinking to a systems-based approach. Landscape urbanism is less focused on form, composition, or result; instead, it suggests open-endedness and change over time (Waldheim, 2016). The future that landscape urbanism envisioned was based on the understanding of processes and how they work in space and time. Landscape urbanism design interventions were focused on recovering landscapes and reclaiming postindustrial sites by integrating engineering systems into complex ecological processes.

In his seminal essay "Terra Fluxus," James Corner identified four themes that formulated the theory of landscape urbanism: (1) processes over time, (2) the staging of surfaces, (3) the operational or working method, and (4) the imaginary (Corner, 2006). The first theme addresses the importance of processes. For example, the process of urbanization consists of other small processes of deregulation, globalization, and environmental protection that are more significant than spatial form. The emphasis on the process does not exclude the form but rather shifts attention to systems that shape the urban environment. In this case, it is helpful to understand the relationships between different processes through the lens of ecology by using graphic techniques, such as field diagrams and maps, which help to analyze and project alternative futures. The second theme addresses horizontal surfaces and their realignment with the landscape. This phenomenon ranges between different scales, from sidewalks to urban structures. Horizontal continuity also suggests a connection between the building and the landscape when the roof of the building connects to the ground. While architecture occupies the site, urban infrastructure connects and creates future possibilities. Landscape urbanism in this case attempts to create an environment that is not designed, but is more an interaction between different elements and systems. The third theme of landscape urbanism seeks to find techniques that work between different scales and time. This opens opportunities for computer software but

also considers traditional forms of model-making and drawing. The fourth theme, the imaginary, plays an important role in connecting all themes and brings up new relationships and possibilities. This theme also emphasizes the importance of storytelling, symbolism, and metaphor and encourages designers to use the power of imagination to create landscapes.

Freshkills Park (2001–2036), designed by James Corner/Field Operations and located on Staten Island, New York (Figure 49), is one of the largest renewal initiatives in the city and an example of landscape urbanism. The winning proposal envisioned the transformation of 1,000 acres of closed landfill and 450 acres of wetland to parkland over time. The park’s design combines ecological restoration and an engineered system to collect landfill byproducts underground.

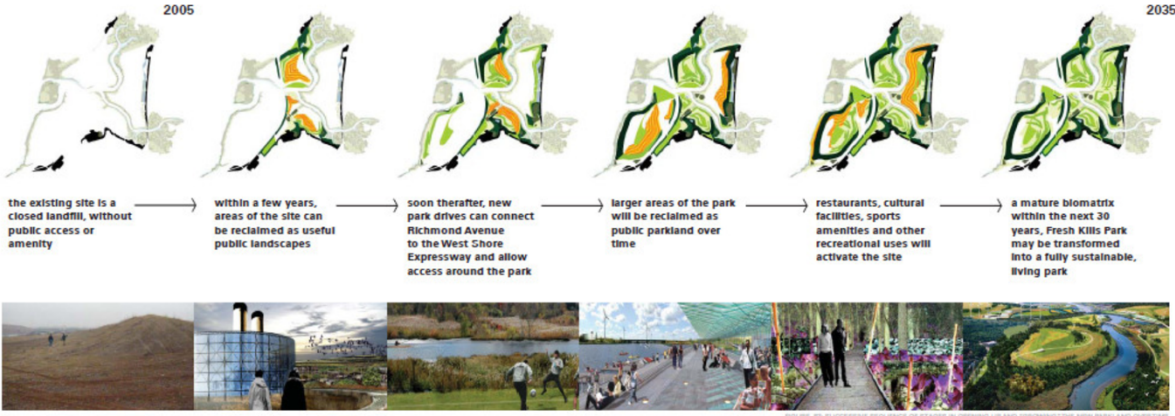


Figure 49. Freshkills Park by James Corner/Field Operations, Staten Island, New York (2001–2036), field diagram. From ArchDaily, 2013.

Corner’s project responds to the natural and human-created topography of the site and demonstrates a different view of the significance of the place. Four large mounds of garbage were sealed and transformed into a reclamation park. The field diagram (Figure 49) represents the site’s transformation for over 30 years, which includes the development of new habitat, planting succession, and changes to the hydrological system. The diagram also shows programmatic phases that include passive and active recreation. Currently under construction, the main public access is focused on the interior part of the site with access to creeks, wetlands, expansive meadows, and a view to New York City.

The transformation of one of the largest landfills is a symbol of urban renewal and reclaimed landscape. Corner’s proposal illustrates the complexities of the project of such a scale,

which includes an understanding of ecological processes along with social, cultural, and infrastructural layers of the city. The project is an example of “precise openness” that offers the potential to change (Pollak, 2007).

By a decade later, in the 2010s, ecological urbanism emerged as a critique of landscape urbanism in response to global population growth, rapid urbanization, and limited global resources. Acupuncture architectural projects were no longer able to address the rising issues on a larger scale. Ecological urbanism was an opportunity to develop a speculative design instead of promoting technical solutions by also viewing the city as a dynamic field of forces (Mostafavi et al., 2013).

Ecological urbanism considered the city not as a physical object but envisioned it as a dynamic field of forces. The strategies where ecological processes are dominant became a guiding paradigm for ecological urbanism. Ecological processes helped to analyze and project alternative urban futures. The city was understood as an ecological system, and the main attempt was to design parts of the city as an artificial ecological system.

By emphasizing the role of the city as an artificial ecological system, ecological urbanism suggests an open-ended result. An open-ended design in ecological urbanism overlaps with the concept of self-organizing systems in architecture, described in the previous chapter of this dissertation. However, in landscape architecture, ecological urbanism recognizes the interconnectedness of urban elements and suggests that ecological processes will guide the city development toward a complex and diverse one by avoiding strict compositional design and planting, and, as a result, responding to future changes.

Parc de la Villette (1982), designed by OMA, was a competition entry for a park in Paris, France (Figure 50). La Villette is a neighborhood in Paris that transformed from a small suburban town to an urban zone of Paris. The design aims to solve urban problems that were the result of such transformation.

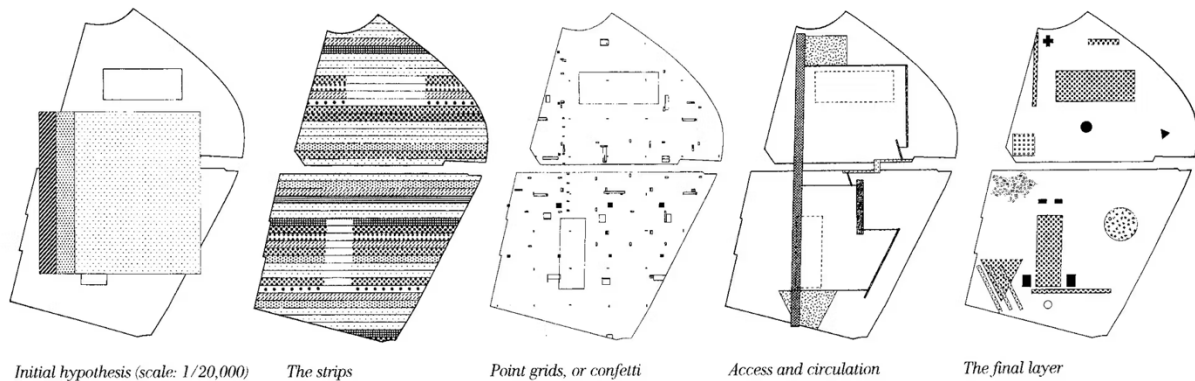


Figure 50. Parc de la Villette by Rem Koolhaas / OMA, France (1982), diagrams. From OMA, n.d.-b.

The proposed competition entry was not a design solution but rather a method that aims to generate a park. The concept of the park, developed by Rem Koolhaas, consists of different layers. Parallel strips contain different programmatic elements, such as playgrounds and gardens, distributed horizontally across the site. Point grids or confetti are small programmatic elements placed on site. Two major roads, one of which is runs in a north-south direction, create an access and circulation layer. And, finally, the large units layer consists of big or unique objects that fit into the system.

The proposal incorporated nature in the form of a series of “wings” that create the illusion of a park without consuming the territory. While all programmatic elements were considered unstable, the only stable part of the design was a round-shaped forest and the rows of trees. However, the trees also suggested some sort of instability due to their growth and change.

The ecological process-based approach changed the focus from form-oriented design to performance-oriented. Landscape urbanism focuses on the reclamation of large industrial sites by integrating ecological processes into the design. Ecological urbanism evolved even further by viewing the city as a dynamic field of forces. Ecological process-based design is focused on the design of parts of the city as artificial ecological systems by emphasizing interconnectedness and future changes.

3.1.3 Phasing Process-Based Design

Over the past two decades, the ongoing discussion of process-based design has expanded to the phasing stage. The evolution of the phasing stage is related to the design of large parks

that emerged from the transition from an industrial- to a service-based economy (Corner, 2007). This transition left behind a huge number of large, abandoned sites, such as old factories, landfills, former ports, and waterfronts. These large-scale sites around the world are now being transformed into a new form of public parks.

Large-scale parks not only required the insertion of a program for different activities but also the management of multiple forms of organization. Because of the size, large-scale parks are constructed over longer periods. The phasing process-based approach is an open-ended approach that includes the understanding of multiple layers of organization and the recognition that within one space, multiple scales work simultaneously.

The Downsview Park International Competition, organized in 2000, aimed to transform a former military base into an urban park in the northern part of Toronto. The site, previously located on the outskirts of the city, became an urban center due to urban growth. The key theme that emerged in the top five competition entries was the idea of a programmatic framework that structures the site and allows its growth over time. The entries consisted of guidelines for park design, a flexible program, and a long-term implementation process that considers the changing political and economic conditions.

Downsview Park (2000), designed by Rem Koolhaas and Bruce Mau/OMA, was a winning competition entry (Figure 51). Among other competition entries from James Corner and Stan Allen, Bernard Tschumi, and Nina-Marie Lister, the winning “Tree City” proposal from Koolhaas and Mau expressed the emerging process-driven design in contrast to the stable formal expression (Walliss & Rahmann, 2016).

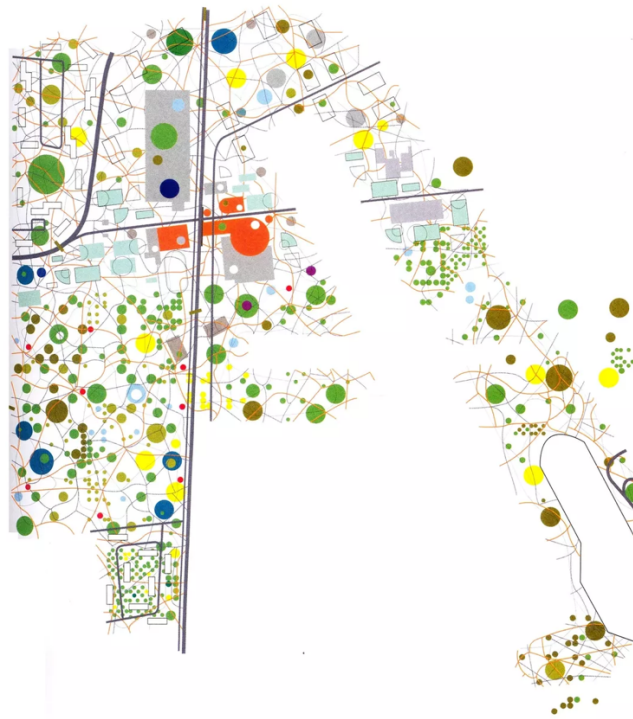


Figure 51. Downsview Park by Rem Koolhaas/OMA, Toronto, Canada (2000), masterplan.
From OMA, n.d.-a.

The competition proposal was developed around the idea of planted tree clusters and flexible design that develops around the tree clusters. Tree clusters, as the most distinguished feature of the park, catalyze urbanization and provide site identity. While the design process was extremely open-ended, nevertheless architects proposed a formula for the park's evolution: Grow the park + manufacture nature + curate culture + 1,000 pathways + destination and dispersal + sacrifice and save = low-density metropolitan life (Carpo, 2013). This process was planned in three phases: (1) site and soil preparation, (2) pathway construction, and (3) cluster landscaping. The speed of expansion and growth is determined by the available budget.

While the project was criticized for its theoretical strategy and the difficult implementation of such an open concept, it influenced how large parks were perceived and designed over the next decade (Czerniak, 2001).

The recent focus of process-based design was on performance, flow, natural processes, and constant changes. The process-based design in the present sets up conditions for future unknown events (Berrizbeitia, 2007). In the case of designing for the future by considering

unstable events, digital technologies play a key role in 3D modeling of natural processes by making it possible to simulate dynamic changes over time.

3.2 3D Simulations

Before the development of digital technologies and 3D modeling software, landscape architects and architects used different approaches to represent the landscape as a complex system. These approaches were less precise and dynamic compared to modern modeling software; however, they laid the foundation for spatial analysis (Booth, 1990) and were early forms of simulation.

One of the early methods in landscape architecture to explore spatial information was developed by Ian McHarg, an American landscape architect and planner. In his seminal book *Design with Nature*, McHarg proposed an overlay method that involves layering environmental and social data to identify suitable land use. The layers included the representation of regions (Figure 52) with geology as the base information, followed by meteorology, groundwater hydrology, physiography, surficial hydrology, vegetation, and wildlife, culminating with land use (McHarg, 1992). The investigation began with the oldest information to the present time, which suggests that McHarg's method was also a process-based approach. The method enables visualizing the relationships between different landscape elements and informs planning decisions.

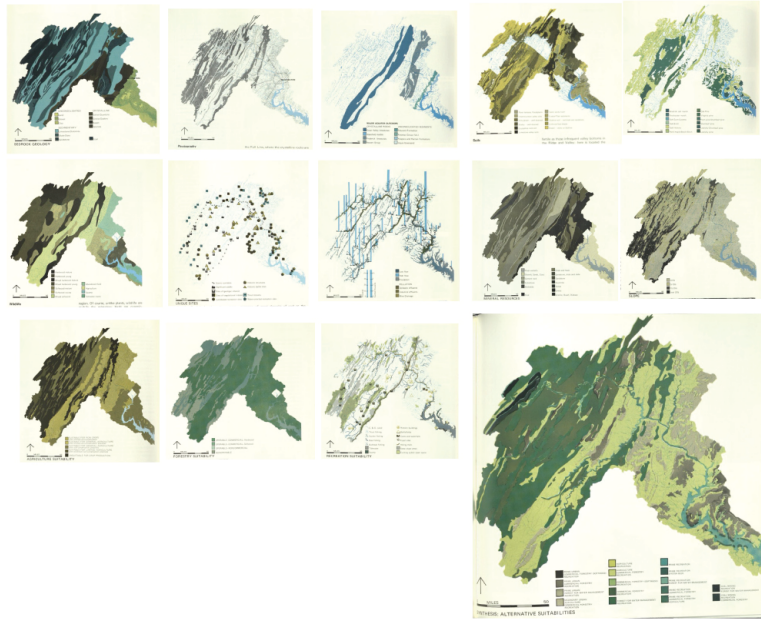


Figure 52. Layering approach by Ian McHarg. From McHarg, 1992.

McHarg's overlay method laid a conceptual foundation for the development of Geographic Information Systems (GIS). In 1963, the first GIS software, called CGIS (Canada Geographic Information Systems) was developed by Roger Tomlinson. The software was designed to store, analyze, and manage data for the Canadian land inventory (Anderson & Ortega, 2016). The GIS technology has continued to evolve since then, incorporating spatial analysis and data management.

Another way to study complex systems before the development of computer software was physical scale models. One of the largest physical models ever built was the Mississippi River Basin Model (Figure 53) constructed from 1949 until 1973 by the U.S. Army Corps of Engineers near Clinton, Mississippi. The large-scale hydraulic model represented the entire Mississippi River on a three-dimensional map on a scale of 1:2,000 horizontally and 1:100 vertically. The 200-acre model was built to study and simulate floods, drought, and other weather events. Over the period of model operation, the main goal was to evaluate the effect of flood control measures, such as levees and dams, on the entire river system over time.



Figure 53. The Mississippi River Basin Model by the U.S. Army Corp of Engineers, physical model. From ElMalvaney, 2010.

Parallel to the use of physical models for early simulations, the architecture and engineering professions were facing the technological advancement and early developments of computer software. The main catalyst for computer-aided design (CAD) is considered the work of Ivan Sutherland, a PhD student from the Massachusetts Institute of Technology. He developed a Sketchpad program that allowed users to manipulate graphical images on a computer screen (Davis, 2013). In the early 1970s, CAD started to develop into 2D early systems that set the stage for complex 3D systems.

While this period was marked as an early development of CAD, a lot of theoretical discoveries were still made with the use of physical models. In 1974, Ralph Knowles, an American professor and theorist, developed a concept of heliomorphism (derived from the Greek *helios* for “sun” and *morph* for “form”). The concept focuses on the development of buildings and urban spaces that respond to the movement of the sun in areas where solar positioning is one of several spatial-orientation problems. Knowles developed a conceptual technique at the Natural Forces Laboratory and tested hypotheses with his students in the design studio. The result of testing was a volumetric model—a solar envelope—that helps design buildings that receive optimal sunlight but also minimize the impact of shadows on adjacent buildings (Knowles, 1980). The solar envelope is also used to design a network of buildings in an urban environment (Figure 54). Knowles’s concept of heliomorphism aimed to create environmentally responsive architecture that improves the quality of design with respect to the surrounding context.

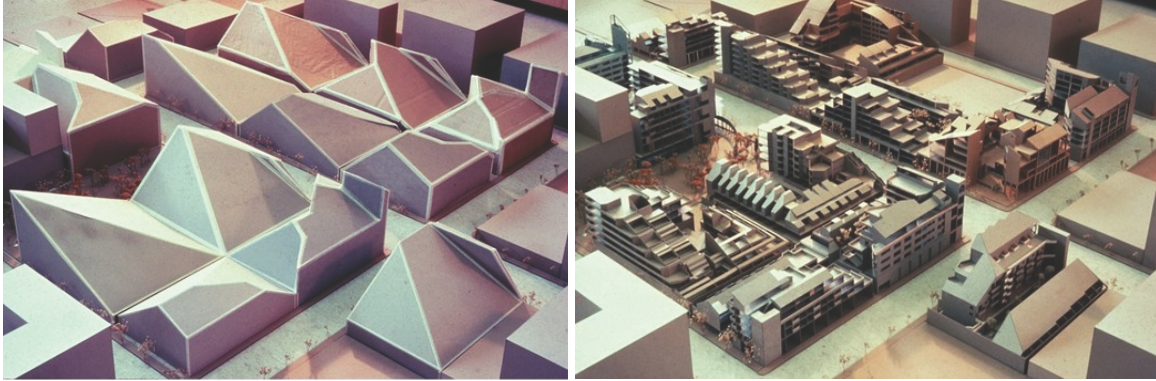


Figure 54. Heliomorphism. The study of sun process by Ralph Knowles. The diagram shows the arrangement of multifamily units on a site. From Knowles, 1980.

The ambition to explore the potential of computers to inform design continued to grow. In the early 1980s, two programs were released into the industry. In 1982, Archicad and AutoCAD became available for 2D and 3D drawings for architects, engineers, and landscape architects. However, most professionals used software for traditional 2D plans, elevation, and section drawings.

Landscape architects slowly started to incorporate computer models into their practice. In 1989–1990, George Hargreaves designed the Guadalupe River Park in San Jose, California. The City of San Jose’s design requirements related to the transformation of the river into an amenity and the creation of habitat for people and wildlife; the city also requested improvements in flood control for the Guadalupe River. Flooding on the Guadalupe River happens rapidly with great destruction. To address challenges within the site, the entire park was digitally modeled to find the best design scenario; however, a physical model remained important to test hydraulic performance. In collaboration with the U.S. Army Corps of Engineers, Hargreaves built an 80-foot-long physical simulation model (Figure 55) to study the impacts of potential flood flows and sedimentation. Over 10 years, the team of environmental and ecological consultants, along with hydraulic, civil, structural, and geotechnical engineers, tested various design alternatives. The resulting design incorporated unique landscape and engineering solutions that make the park resilient to flood and promote habitat and vegetation growth.



Figure 55. Guadalupe River Park by George Hargreaves, San Jose, California (1989–1990), physical model. From Hargreaves Associates, n.d.-b.

The major shift in computer software happened in the 1990s, when object-driven design drawing was shifted toward more sophisticated computer modeling. The shift was influenced by architects' desire to explore the potential of nonlinear geometry and modeling of continuous surfaces (Walliss & Rahmann, 2016).

The desire to model complex surfaces made architects use software that was initially developed for other purposes. The design for the City of Culture of Galicia (1999–2011) in Santiago de Compostela, Spain (Figure 56) was developed by Peter Eisenman, an American architect and theorist, by using the computer modeling software CATIA. CATIA was initially developed to model and manufacture aircrafts. Eisenman's project also challenged the traditional approach to form and space creation by introducing the principle of superposition, which allowed designers to layer multiple systems in the design process (Corbo, 2020). The design was developed by using three layers of information (Figure 56). The first layer was the medieval street plan of Santiago superimposed upon topography. The second layer was a modern grid superimposed upon medieval routes. The third layer was developed by using 3D modeling, where the topography of the hillside was distorted. The generated topological surface was a result of a combination of two layers in a form not seen before. The principle of superposition resulted in a complex, multilayered building.

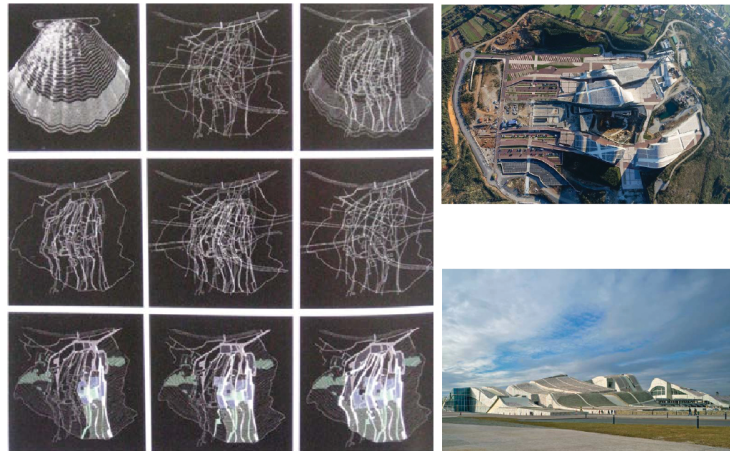


Figure 56. City of Culture of Galicia Santiago de Compostela, Spain by Peter Eisenman (1999–2011). Left: Overlay layers. Right: The building. From Eisenman Architects, n.d.

The need for design-friendly software for complex 3D modeling spurred the development of new programs. In 1996, Autodesk released a 3D Studio (3ds Max) program that became a leading software for 3D modeling and animation and was used in architecture, engineering, and entertainment. 3ds Max uses polygonal modeling, an approach that uses polygon meshes to represent modeling surfaces that allow the creation of complex shapes.

The mid-1990s was also marked by the development of simulation software, such as Ansys and SolidWorks. These programs were used by engineers for detailed simulation of physical processes, structural analysis, and fluid dynamics.

The later development of 3D simulation software is related to the development of 3D modeling programs. The first version of Rhinoceros (also known as Rhino), 3D modeling, and CAD software was developed by Robert McNeel & Associates and released in 1998. What made Rhino different from 3ds Max was a geometry that is based on the non-uniform rational b-spline (NURBS) mathematical model. As opposed to polygonal modeling, NURBS allows for the creation of highly accurate and smooth curved surfaces. Rhino, with its robust modeling tools, became an attractive program for modeling by engineers, architects, product designers, and industrial designers.

The recent focus on performance and representation of dynamic systems required new approaches. Simulation has evolved over the last decade, from physical models to computer 3D modeling. Currently, computer software can simulate complex systems and influence design

decision within the 3D model, allowing quick adjustments to the design based on simulation results. With the development of digital technologies and software, it became possible to simulate time, possible changes, and environmental processes (Anderson & Ortega, 2016). CFD simulations of natural processes can be conducted using Ansys, SimScale, and Rhino + Grasshopper programs. In the mid-2000s, the early CFD tools for Rhino were focused on model compatibility with engineering software, allowing users to export a Rhino model for analysis in external applications. One of the early attempts to bring CFD to Rhino was the RhinoCFD plug-in developed by Concentration, Heat, and Momentum Limited (CHAM). This plug-in was used to investigate the interaction of the model with fluid flow.

In 2008 Rhino released a parametric modeling plug-in, called Grasshopper. The plug-in became famous for its ability to create complex algorithmic structures. Later, the development of Grasshopper revolutionized the integration of CFD plug-ins. Programs such as Rhino and Grasshopper can address multiple processes within one site. Nowadays, parametric modeling tools, such as Ladybug, allow for advanced CFD simulation of natural processes as one of the steps in the design process. The Ladybug plug-in for Grasshopper, released in 2013, allows for integration of CFD analysis with parametric design workflow in Grasshopper. The first version of Ladybug allowed for weather data visualization, solar radiation studies, and sunlight analysis. Later, plug-ins like Butterfly, Honeybee, and Dragonfly were added to the Ladybug suite. The Butterfly plug-in runs several types of airflow CFD simulations, such as urban wind patterns and ventilation, that are useful for building design. The Honeybee plug-in runs detailed daylight and thermodynamic modeling simulations. Dragonfly runs energy simulations and allows modeling of urban heat islands.

Today, simulations are run on computer models because they can handle much higher levels of complexity and flexibility to test various parameters and scenarios. Computer simulation also allows users to change the design according to simulation results much faster than physical models do. Also, the main limitation related to physical models is that they cannot represent complex systems, such as climate.

3.3 Modeling of Natural Processes (Case Studies)

The following case study analysis focuses on 3D modeling and simulation of natural processes that shaped specific design projects. By analyzing selected projects, it is possible to

understand how advanced modeling and simulation tools were used in response to specific natural processes. These projects highlight specific aspects of simulation and modeling related to landform, atmosphere, fluvial, and vegetation processes. They also reveal the outcomes of the simulation on the design process and implementation. Each case study project highlights different aspects of modeling or simulation. Selected case study projects represent landform, atmosphere, fluvial, and vegetation processes, and are related to the process simulation. While some projects are an early example of simulation, such detailed analysis helps to explore the methodologies, challenges, and outcomes of using simulation in design, and inform a process-based design to landform architecture.

3.3.1 Landform Simulation

The MAX IV Laboratory Landscape (Figure 57), located in Lund, Sweden, is a 19-hectare public space project designed by Snøhetta in 2016 and built in the same year. The client for the project was Fastighets AB ML 4, with FOJAB architects as consultants for the laboratory facility. The project is the first phase of the larger transformation of agricultural land into a “Science Village.” The location of the laboratory fosters engagement between the research center and the surrounding community. Even though the project is located on the outskirts of Lund, it is carefully integrated into the neighboring area.



Figure 57. MAX IV Laboratory by Snøhetta, Lund, Sweden (2016), aerial view of the building and landscape. From Snøhetta, n.d.

Site analysis reveals that before the construction of the Science Village and the laboratory facilities, the area was agricultural land (Figure 58). Currently, the MAX IV

Laboratory is bounded by the Oatly Global Science and Innovation Center to the northeast; Kunskapsparken to the east; and Sony Mobile and Ericson facilities to the south. The residential area with agricultural land to the west and north is cut off from the project site by the E22 highway.



Figure 58. Before and after the construction of the MAX IV Laboratory. Left: 2020 aerial view before the construction. Right: 2024 aerial view after the construction. From Google Earth Pro.

The project background and history are related to the construction of the neighboring highway. The traffic from the highway posed a significant concern for ground vibrations. The engineers and researchers revealed that such vibrations could interrupt the experiments in the laboratory. The main purpose of the landscape was to reduce the ground vibrations from the highway for the function of the synchrotron radiation MAX IV Laboratory.

The genesis of the landscape project builds upon the development of the building design. The placement and form of the landscape work in conjunction with the shape of the main research laboratory. The laboratory complex consists of two storage rings, a linear accelerator, office buildings, and the surrounding landscape. The building form (Figure 59) is generated from the ring shape that is twisted and creates a dynamic shape based on a Möbius strip. The landscape hills develop around the building shape.

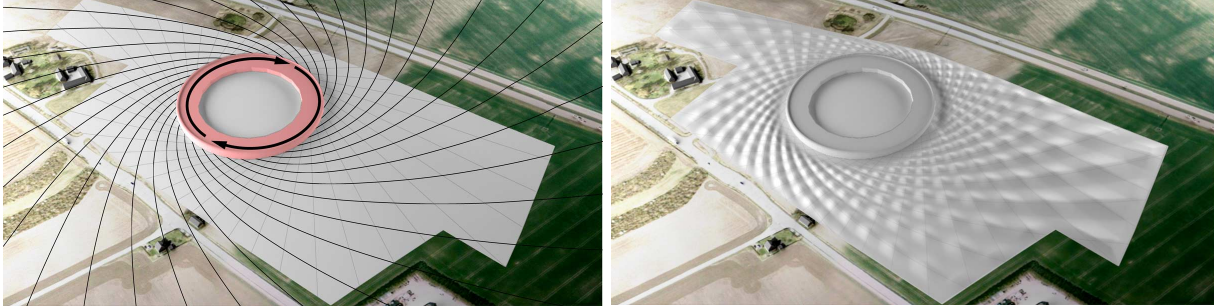


Figure 59. MAX IV Laboratory. Left: Building shape and the direction of the landscape. Right: The shape and location of landforms hills. From Snøhetta, n.d.

Design, development, and decision-making processes of the landscape design were based on four important criteria: (1) mitigating ground vibrations, (2) mass balance, (3) stormwater management, and (4) plant selection.

The ground vibrations on the site are created by the wavelengths from the highway, between 32 feet to 130 feet high. The vibration wave follows the ground surface and is likely to interfere with the research facility. The flatter the ground surface, the stronger the influence of the wave on the research experiments. Snøhetta addressed the challenge of ground vibrations by designing landform hills (Figure 59). By going through multiple design iterations and testing, the architects identified that chaotic and uneven topography protects the laboratory from the ground vibrations. Later, the landforms were organized in a circular pattern and distributed around the site.

In this project, Snøhetta also focused on optimizing the mass balance. The architects used a cut-and-fill strategy to reuse excavated land for the earthen mounds. They were able to keep the mass balance by developing the 3D model. The model was later uploaded to GPS-controlled bulldozers that relocated the masses to their final position. This strategy helped keep the soil onsite.

The city of Lund restricts the amount of water that runs into the city's pipeline. To address the water management restrictions within the site and meet the city's sustainability goals, the architects designed 1-year and 100-year stormwater wet and dry ponds. The vegetated mounds also help manage the water runoff. For the planting, Snøhetta used a selection of natural species. They harvested the hay from the nearby natural reserve area and spread it on the hilly landscape.

The 3D simulation and design process involved using Rhino software and Grasshopper definitions to create a 3D model. The 3D model (Figure 60) was created using numerical data extracted from the vibration process. Vibration properties defined parameters such as length, location, orientation, and direction for form-making. The layout of the landforms was based on intersecting tangents starting from the main building and forming the wave pattern. The first set of waves was defined at the starting point by 30-foot and 40-foot vibration wavelengths and 15-foot amplitude. The more chaotic the combination of waves was at this stage, the better it was for absorbing the ground vibrations. The second set of waves started from the storage ring and merged with the site boundary by creating a spiral movement. The environmental performance of the design was tested using a Kangaroo plug-in in Grasshopper that visualizes physical behavior through simulation flow.

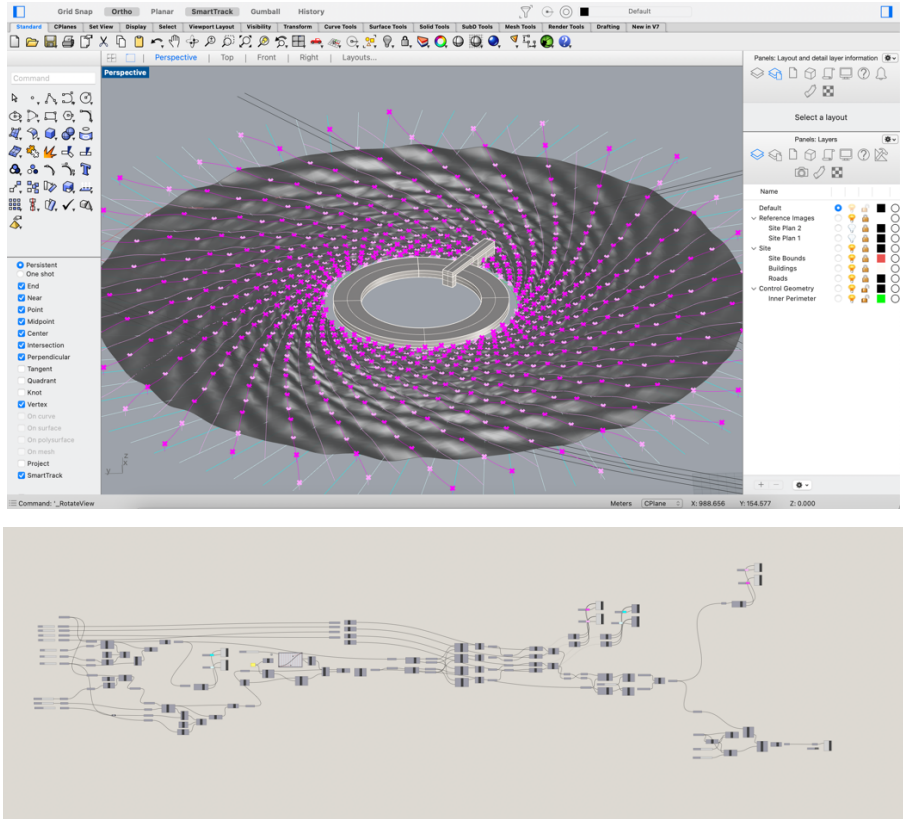


Figure 60. MAX IV Laboratory 3D model. Top: In Rhino. Bottom: Grasshopper definition.

The MAX IV Laboratory illustrates how parametric modeling can be integrated into a process-based approach. The project used iterative 3D simulations to refine the topography in response to environmental forces. This approach aligns with a process-based landscape strategy

that focuses on site-responsive design. While earlier ecological process-based strategies, such as McHarg's approach, used overlay strategies to determine site suitability based on environmental conditions, Snøhetta's approach uses parametric modeling and 3D simulations to optimize landform responses. The project shows that using Rhino and Grasshopper helps to determine how the changes in the landform's height influence the ground vibration.

Snøhetta's role was central in shaping the outdoor environment for the MAX IV Laboratory. Their expertise informed the development of an outdoor space that not only addresses the key concern of the ground vibration, but also solves stormwater issues, enhances biodiversity, and improves public access to the site.

Program elements of the landscape were connected with the program of the building. While the main building encompasses a range of program elements, such as a research laboratory and experimental facility, the landscape includes public space and a recreational area.

The maintenance and management strategy includes a combination of conventional approaches for meadow mowing, but also introduces ecological maintenance, such as grazing sheep from the nearby natural reserve area.

User analysis of the MAX IV Laboratory includes analysis of the research facility and outdoor landscape. The MAX IV Laboratory not only functions as a research facility but also creates an outdoor recreational area that has open public access. The local habitat also utilizes the site for grazing.

Peer reviews note that Snøhetta's project inspired a fundamental shift in design culture by exploring the potential of digital technologies and encouraging designers to explore the opportunities created by 3D modeling and simulation software. The project also highlights the new role the designer plays in moving from a linear to nonlinear workflow (Walliss & Rahmann, 2016). The designer becomes an editor of the generative potential of computational software, while the choice of the form is driven by the designer's aesthetic preferences (Kolarevic, 2009).

The criticism of the project is that, while the landscape serves its main purpose of mitigating the ground vibrations, the shape of the landforms does not derive from the site, its geology, or its history. The architects did not consider the site history or a deeper analysis of the context.

The significance and uniqueness of the project lies in its combination of research facility and publicly accessible outdoor space. The project sets a new standard for the research

laboratory. Instead of designing the introverted and fenced-off research center, Snøhetta created a new park open for public use. In the MAX IV Laboratory project, 3D simulation played a key role in the design process and in optimizing existing conditions. By using Rhino and Grasshopper definitions, Snøhetta created a detailed 3D model based on data from vibration processes. To address the underground vibration from the nearby highway, the architects developed landform hills to protect the research facility. The simulation process allows for testing multiple layouts and size options to find an optimal solution. The simulation and advanced 3D model also enabled a precise cut-and-fill strategy to maintain mass balance on the site. For the 3D simulation process, knowing if different site-specific landforms can also address vibration issues would be helpful.

Limitations are focused on the accessibility of the landscape to the public. The location of the project on the outskirts of Lund and the placement between other science buildings limits easy public access. Moreover, the residential area across the highway has only one underground pedestrian crossway.

Generalizable features and lessons are focused on the benefits of the 3D model. The model was developed in Rhino, which allowed designers to visualize and create complex surfaces, but also to do continuous testing of the pattern's effect on mitigating the ground vibrations. Additionally, the model was plugged into bulldozers that functioned as a giant 3D printer developing a 1:1 model on site. This combination of advanced geometry and fabrication helped to minimize mass movement on the site and made this process more efficient. Snøhetta's parametric modeling demonstrates how to generate a topographic form through prescribed parameters of slope, vibrations, and drainage.

3.3.2 Atmosphere Simulation

The Jade Eco Park (Figure 61) project is a 70-hectare park and visitor center, designed by Philippe Rahm Architects and Catherine Mosbach, located on the site of the former Sui-Nan Airport in Taichung, Taiwan. The project was designed in 2012 and completed in 2016. The Taichung City Government was the client for the project. The project combines outdoor and indoor activities for leisure and sport and addresses climatic challenges through innovative design. In this project, Philippe Rahm aimed to create an outdoor space that is comfortable to spend time in Taichung's warm and humid climate and offers relief from noise, pollution, heat, and humidity.



Figure 61. Jade Eco Park by Philippe Rahm, Taichung, Taiwan, competition visualization. From Philippe Rahm architectes, n.d.

The site for Jade Eco Park is centered within the new district on the foothill of the mountain. Before the construction of the park (Figure 62), the site was a former airport. On a smaller scale, the former airport site left many challenges for a park, such as deforestation, high pollution, compacted soils, and steep slopes. On a larger scale, the island of Taiwan is located within an environmentally sensitive area. Taiwan is shaped by a continuously moving seismic zone and one of the largest ocean currents: Kuroshio. Currently, the site is bounded on each side with roads of different intensity, but also with Xitun Tai An Elementary School to the north; China Medical University Campus and other development to the east; residential development to the south; and Xitun District to the west.



Figure 62. Before and after the construction of Jade Eco Park. Left: 2010 aerial view of before the construction. Right: 2024 aerial view of after the construction. From Google Earth Pro.

The project background and history are based on the urban growth of Taichung. As the city grew due to the development of light industry and manufacturing of electrical vehicle parts, the land previously occupied by the airport became the center of an urban area. In 2008, Stan Allen developed a masterplan that envisioned residential, commercial, educational, and recreational areas. Among them were a cultural center designed by SANAA and a new park. In 2011, Taichung City Government announced an international design competition to transform the former airport site into the central park. The winning team led, by Philippe Rahm, proposed a unique solution that explores climatic issues (Figure 63).

The genesis of the project lies in Philippe Rahm's long interest in atmosphere and its performative potential. The Jade Eco Park project was an exploration of Rahm's ideas at an urban scale, but with a focus on the human experience. For the competition proposal, Rahm presented an image of the human body's physiological reaction to environmental conditions such as heat, humidity, and pollution (Figure 63).

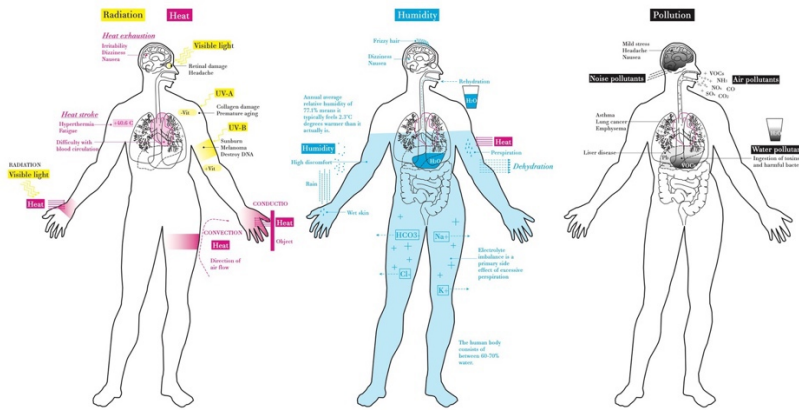


Figure 63. Human body reaction to heat, humidity, and pollution by Philippe Rahm, competition diagram. From Philippe Rahm architectes, n.d.

The design, development, and decision-making process started with the use of CFD analysis and the development of maps that show heat, humidity, and pollution on the site. By overlaying the maps and highlighting intersecting areas, Rahm created a variety of conditions and experiences. To address different climate conditions within the park, he designed natural and artificial climatic devices that create more comfortable environments. These devices are divided into three categories: cooling, drying, and depolluting devices that create spaces with different experiences and levels of comfort.

The first set of devices consists of natural and artificial cooling devices that have specific qualities to cool the atmosphere. The natural cooling devices are trees with large leaves or many leaves to create shadows; trees with waxy leaves to reflect the sun's rays; and trees that produce strong evaporation to cool the air around them. Artificial cooling devices work by using convection, conduction, evaporation, or reflection strategies to cool the air or the human body directly. The Anticyclone (Figure 64) is a convective cooling device that blows the air cooled by underground heat exchange. The Night Light is a conductive cooling device that has a cold surface chilled by the water; the human skin can be cooled by touching this device. The Stratus Cloud is an evaporating device that sprays mist or rain and refreshes the surrounding area. The Moon Light is a reflective cooling device that reflects the sun's rays and heat.

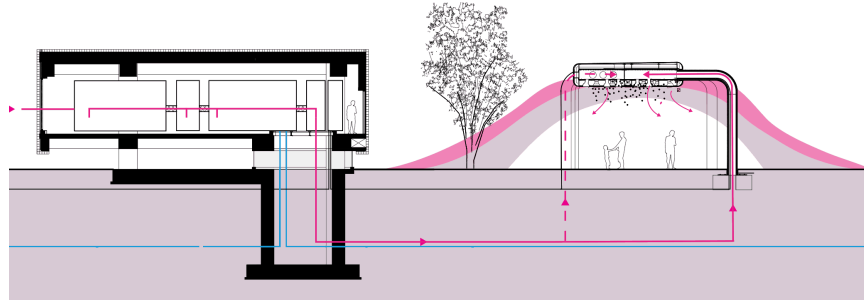


Figure 64. Anticyclone device, section. From Philippe Rahm architectes, n.d.

The second set of devices consists of natural and artificial drying devices that protect visitors from rain and excess humidity. The natural protectors from the rain are trees with dense crowns, while the artificial devices that protect from the rain are shelters. The excess humidity is absorbed by natural vegetation with floating roots and an artificial drying device, called Dry Cloud (Figure 65), which dries the air with a silicate gel.

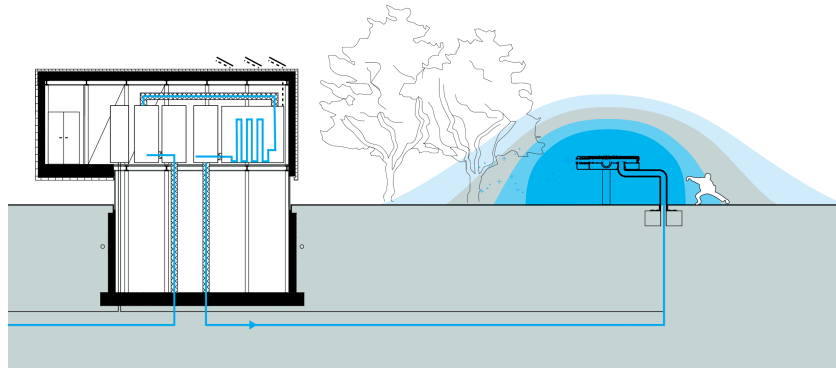


Figure 65. Dry Cloud device. From Philippe Rahm architectes, n.d.

The third set are natural and artificial depolluting climatic devices that reduce air pollution, noise, and mosquitos. The natural depolluting devices are trees that absorb dirty air and soundproof the area. The artificial device Ozone Eclipse (Figure 66) blows filtered air in the park, and the Preindustrial Draught device blows in the air without particles emitted by cars. The Ultrasound Repellant device fights back mosquitos with sound waves at the same frequency as dragonflies, their predators.

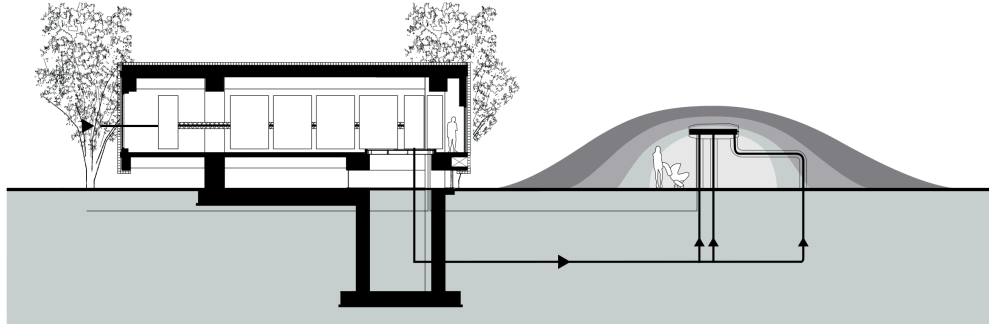


Figure 66. Ozone Eclipse device, section. From Philippe Rahm architectes, n.d.

3D simulations represent the existing climatic conditions in the form of maps that depict areas that are: (1) warmer or colder, because of the cold wind coming from the north (Figure 67); (2) humid or dry, because of the southwest wind carrying humidity from the sea (Figure 68); or (3) polluted or clean, based on the proximity to the road (Figure 69). The maps were developed by the German firm Transsolar by using Ansys Fluent software and weather data from a Taiwan Central Weather Bureau measuring device near the site. Each map represents the intensity of climatic conditions on the site.

By integrating climatic analysis and 3D simulations into the design process (Figure 67–Figure 69), the project aligns with the process-based approach, where the solution is not fixed but responds to dynamic conditions of the site. While earlier analysis of climate conditions was performed manually, the project represents a transition to digital tools that allow designers to make adjustments to design faster.



Figure 67. North Wind Speed simulation map. From Philippe Rahm architectes, n.d.

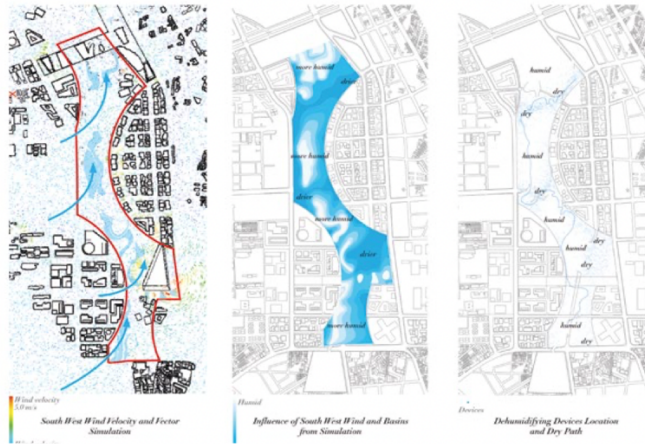


Figure 68. Southwest Wind Velocity and Vector simulation map. From Philippe Rahm architectes, n.d.



Figure 69. North Wind Velocity and Vector simulation map. From Philippe Rahm architectes, n.d.

The role of the landscape architect in the design is based on the collaboration between Swiss architect Philippe Rahm and French landscape architect Catherine Mosbach. Later, the local Taiwanese architect Ricky Liu & Associates joined the team. Philippe Rahm played a key role in this project because of his unique design approach.

Program elements of Jade Eco Park consist of a 70-hectare park, a 3,000-square meter visitor center, a maintenance center, and the Taiwan Tower. The three climatic interventions create different microclimate conditions and sensory experiences at different times of the day

within one site. Within each climatic intervention is a specific program. Cold climatic areas contain a rest program; dry climatic areas contain a sport program; and clean climatic areas contain a family program. The same type of areas are linked along the park with three paths.

The North Wind Speed simulation map (Figure 67) shows the intensity of the wind, depicts areas that are warmer or cooler, and proposes the placement for cooling devices and a location for the cool path. The North Wind Velocity and Vector simulation map (Figure 69) shows wind velocity, the influence of the north wind and surrounding roads on the pollution level, and placement for depolluting devices. The Southwest Wind Velocity and Vector simulation map shows wind velocity (Figure 68), the influence of the southwest wind on the level of humidity or dryness of the area, and placement for dehumidifying devices and a location for the dry path.

The park is maintained and managed by Taichung City. At the same time, visitors can manage their experience by modifying the intensity of climatic devices with their smartphone, which creates individualized experiences for each user.

The park creates a variety of user experiences that overlap, separate, or densify in some places. For example, the air will be less humid and less polluted in certain places, but still hot. The visitors can also access real-time climatic data and suggested activities for current conditions.

Peer reviews summarize that the winning proposal for Jade Eco Park demonstrates the use of computational techniques in the design of a large-scale park and is an example of successful manipulation of external conditions with the use of technological devices (Walliss & Rahmann, 2016). The jury highlighted the project as a visionary proposal that combines microclimatic studies of the area and a new innovative approach to landscape design (King, 2017).

The criticism of the project is in the use of different design devices. While the architect used climatic maps and 3D simulation to address uncomfortable conditions, most of the design decisions were artificial devices, except for trees, for different purposes. Some view the devices as unwelcome technological insertions into the park (Walliss & Rahmann, 2016).

The significance and uniqueness of the project is in its design solutions to mitigate climate conditions. Contemporary climate challenges and especially climate issues with the project site demand changes in landscape design. This project differs from other design

responses as it proposes the management and manipulation of external conditions, such as wind, heat, and humidity, to achieve the desirable performance. It also sets a precedent of the human ability to influence environmental conditions. For Jade Eco Park, 3D simulation played a crucial role in understanding and visualizing climatic processes within the site. The CFD analysis performed by Ansys Fluent software resulted in detailed maps that show areas prone to heat, humidity, and pollution. While some parts of the site were warmer, others were colder; some areas were more humid or dry; and some more polluted or cleaner. The comprehensive CFD analysis informed the placement of climatic devices that aimed to enhance comfort levels within the park. By overlaying maps, Rahm and his team were able to place cooling, drying, and depolluting devices at the right location and influence the site's microclimate. Even though Rahm ran climatic simulations before the design process, the architect created infrastructural devices to address climate issues. It would be interesting to know if nature-like solutions can have the same beneficial effect.

The limitation of the project is its strictly focused design solution. Rahm addressed the challenges within the park by designing climatic devices; however, it would be beneficial to test whether the insertion of landforms can minimize heat, humidity, or pollution within the park.

Generalizable features and lessons of the Jade Eco Park project are that it explores a process-driven design through computational techniques. The design engages with dynamic systems and aims to address climate challenges. Design decisions and program follow an initial CFD analysis. The project introduces different devices into the park design and sets a precedent of merging the natural and artificial.

3.3.3 Fluvial Simulation

The Mud-Infrastructure project (Figure 70) is a 20-hectare park, designed by PARKKIM landscape architects, located along the Yanghwa riverfront in Seoul, Korea. The design was completed in 2011. The Seoul Metropolitan Government was the client of the project. The project transforms the riverfront from concrete terraces to landforms for visitors' physical access to the river and easier maintenance. The project incorporates hydrological processes that make it possible for the park to function the entire year, even during flooding season. In addition, the project addresses the massive amount of sediment that deposits during floods.



Figure 70. Yanghwa Riverfront: Mud-Infrastructure by PARKKIM in Seoul, Korea (2011), aerial view. From PARKKIM, n.d.

Site analysis includes the analysis of current conditions. The Han River flows approximately 30 miles within the boundaries of Seoul and reaches a width of 0.6 miles. The project site is located at the western end of Seoul along the Yanghwa riverfront, which is part of the Han River system. The site is approximately 1.3 miles long and 330 feet wide. Before the construction of the Mud-Infrastructure (Figure 71), the area was a triple-terrace concrete shoreline with a basic park area. Currently, the site is bounded by the Yanghwa River and Seonuydo Island across the river to the north; Yanghwa Bridge to the east; Olympic-daero and Nodeul-ro highways to the south; and Seongsan Bridge to the west.

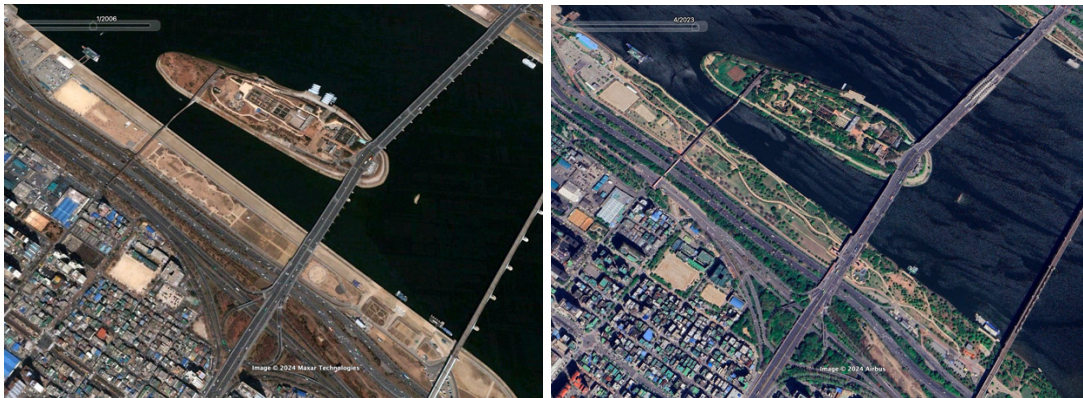


Figure 71. Before and after the construction of the Mud-Infrastructure. Left: 2006 aerial view before the construction. Right: 2023 aerial view after the construction. From Google Earth Pro.

The project background and history include an overview of the government solutions regarding the riverfront. In 2006, the Seoul Metropolitan Government started the Han River Renaissance Project with a budget of \$600 million, which included the redevelopment of six riverfronts, including the Yanghwa riverfront. In 2009, the former mayor Oh Se-hoon initiated a second phase of the Han River Renaissance competition to revitalize the river's embarkment into a public park. The goal of the competition was to find conceptual ideas to transform engineer-focused existing conditions of the riverfront. In contrast to other competition entries that only proposed new routes, PARKKIM proposed the Mud-Infrastructure design. The competition proposal focused on the development of a responsive park. By incorporating hydrological processes, the park functions during the flooding season.

Before the modernization of the Han River in the 1970s and the transformation of river riparian edges to concrete shorelines, the river was the main source of transportation and leisure. Today, the river is the main infrastructure to prevent flooding. During the summer rain seasons, mud is carried from the mountains and deposited along the concrete edges of the river. Every year, the mud deposits create a huge challenge for maintenance and a high cost for the city budget. The economic growth and development of Seoul after the 1990s created a demand for a better quality of life. After the successful development of the Chenggyecheon River public space in downtown Seoul, the city government started redeveloping the Han River waterfront.

The design, development, and decision-making process lies in the attempt to transform the concrete riverfront that created physical and visual barriers for visitors. The design was driven by the process of sedimentation, program, and circulation. Landscape architects reshaped the topography to improve the spatial experience, make it possible to use the park at different times of the year and different water levels (Figure 72), and address maintenance issues. The concrete terraces were transformed into landforms that sloped down to the water. The landforms connect both ends of the park and enable universal access to the water. The slopes range 4%–13%, and a pathway system was graded less than 5%. The landforms were designed not only for better access but also for the removal of sedimentation buildup after flooding. PARKKIM also tested different iterations of landforms to make them a scenic component of the design, which will be visible from the pedestrian bridge that connects the riverfront with Seonuydo Island. The designed topography functions as mud-removal infrastructure, and the park program matches landforms with minimal integration of facilities.

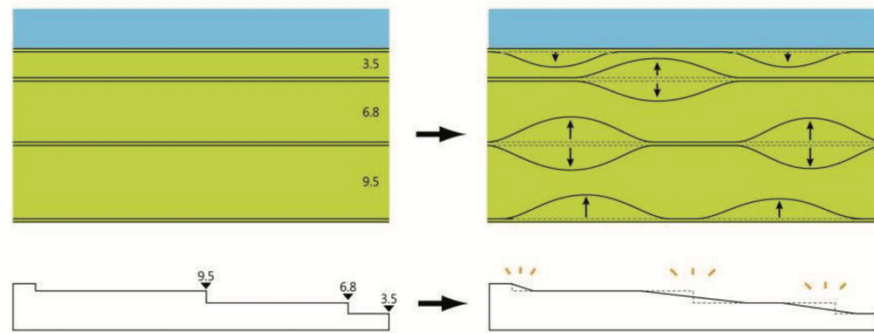


Figure 72. Transformation of the Mud-Infrastructure park, initial concept drawing. From PARKKIM, n.d.

3D simulations were not the starting point of the project; however, the resulting design represents the process-driven approach that responds to environmental processes. The initial idea of the park was developed first in the plan (Figure 72). Later, the drawing was transferred into a Rhino 3D model to construct and test landforms. 3D modeling played a crucial role in creating continuous geometry. 3D models also allowed the landscape architects to design multiple iterations of landforms and test different edge conditions based on water levels. A series of landforms were designed to improve water circulation and prevent mud buildup. While landscape architects did not use 3D simulation to revise the design, the multiple iterations within the 3D model helped to refine their solutions in response to dynamic conditions, such as fluctuating water levels that require changes in circulation and reduction of the mud buildup.

The role of landscape architect PARKKIM was key in the design process. The landscape architects did an extensive landform study. Later in the process, they collaborated with a hydro engineer to design a topography that drains water sediment back to the river. The engineer advised them to exaggerate the landforms, which increased the irregularity of the shoreline. He also tested the placement of trees during the documentation phase to confirm that trees will not have an adverse effect on the water flow.

The program elements of the park consist of three main components: an open field, wild hills, and riverine theater. The western part of the park, close to the parking lot, is considered the most active part program-wise. To fulfill this program, landscape architects kept an open field in this area. On the other side of the park, they designed wild hills that are suitable for wildlife

habitat due to the topography and the smaller number of pathways. In the middle of the site, where the slope reaches its peak, is the riverine theater that overlooks the island.

The maintenance and management of the site after the completion is the responsibility of the river authority. Since the construction of the Yanghwa riverfront, the site was inundated multiple times (Figure 73), and the design proved to be successful in decreasing maintenance expenses associated with the removal of seasonal mud. The maintenance cost of the Mud-Infrastructure project is 17% less than that of the nearby riverfront.



Figure 73. Mud-Infrastructure Park. Left: Aerial view during its normal operational time. Right: Aerial view during flooding. From PARKKIM, n.d.

User analysis reveals how the park functions in various seasonal scenarios. Based on the park usage in Seoul, the landscape architects wanted to make the park as open as possible. However, it was important for landscape architects to give universal access to the river.

Peer reviews argue that the Han River Renaissance initiative was unprecedented in the Asian context. The PARKKIM proposal changes the existing layout of the riverfront by proposing a new topographical surface. The project incorporated hydrological principles and made it possible for the park to function at any time of the year. The design also addresses park management and the massive amount of sediment deposited after the flood (Walliss & Rahmann, 2016).

Criticism of the project is that more advanced digital techniques and 3D simulation would allow the designers to better engage with dynamic environmental systems. Even though PARKKIM did not engage the simulation process in their design, the project could be considered an early precedent of how to address fluvial processes with riverfront design.

The significance and uniqueness of the project is that it changes visitors' relationships with the river by integrating landforms that provide easier access to the river's edge. Mud-Infrastructure sets a precedent for living shorelines in Seoul. While PARKKIM did not perform a

3D simulation for the Mud-Infrastructure project, the project sets the case for the design of a flood-prone park that functions at different times of the year. The advanced 3D model in Rhino was essential to transforming the concrete riverfront into an accessible park and testing different landforms. The 3D modeling allowed the landscape architects to create continuous geometry and test multiple landform iterations for different water levels and seasonal conditions. By changing the existing concrete conditions to landforms, the landscape architects not only enabled year-round use but also prevented buildup from sedimentation and fluvial processes. The 3D model also helped to design slopes for universal access and floodwater circulation. While the project is the perfect case to analyze how fluvial and sedimentation processes were addressed in the design, the 3D simulation of seasonal river changes would help landscape architects shape the project more efficiently.

The limitation of the project is that the Mud-Infrastructure was not designed by using 3D simulations to reflect dynamic flow conditions. The main limitation related to dynamic simulations is that the yearly water and velocity levels in Seoul are considered too unpredictable. Because of that, there is no reliable data to develop a simulation.

Generalizable features and lessons are that the Mud-Infrastructure project engages with fluvial and sedimentation processes. The design contributed not only to better public space but also to the development of habitat. The riprap edge increased biodiversity and created sheltering spaces for fish and other species. Over time, the deposition of mud in between ripples contributes to native plant growth. The waterfront also attracts a large variety of birds.

3.3.4 Vegetation Simulation

The Sony City Ōsaki project (Figure 74) is a 0.6-hectare urban park, designed by AnS Studio landscape architects with consultancy and architectural support from Nikken Sekkei. It is located around the Sony office building in Tokyo, Japan. The project was designed and completed in 2011. The design aims to transform the urban environment into a so-called natural forest. The project is driven by the existing and future environmental processes and plant growth processes. The design is guided by the idea of continuous change in the urban environment and the way the landscape responds to it.



Figure 74. Sony City Ōsaki by AnS Studio in Tokyo, Japan (2011), view from the path. From AnS Studio.

Site analysis of the design includes analysis of the existing context. The Sony Forest landscape surrounds the newly redeveloped area near the Ōsaki Train Station. Before the construction of the Sony Forest, the area was part of the urban surroundings (Figure 75). Currently, the site is bounded by Think Park Tower to the north, Ōsaki Train Station to the east, residential development to the south, and high-rise office buildings to the west.



Figure 75. Before and after the construction of the Sony Forest. Left: 2010 aerial view before the construction. Right: 2012 aerial view after the construction. From Google Earth Pro.

The Project background and history includes an overview of building design. The Sony Forest building was designed by the Nikken Sekkei architecture office. The building is a unique example of the BioSkin facade system, the first of such a cooling system in the world. The idea of the bioskin facade derives from the ancient Japanese tradition of uchimizu: cooling streets by

sprinkling water. A similar approach is used to cool the Sony Forest building and the surrounding air by using vaporization. The main element of the facade is a system of ceramic pipes that collect rainwater. The water circulates and reduces the building's internal cooling load.

The genesis of the project derives from the idea of a natural forest. While the conventional design approach would try to imitate the trees' location and atmosphere like a natural forest, the landscape architects proposed their method to design a so-called natural forest in the urban environment.

The design, development, and decision-making process starts with the analysis of environmental conditions around the site. This included analysis of initial conditions, such as wind direction, wind speed, thermal conditions, and soil conditions. The input data for this analysis included satellite images, digital elevation model (DEM) data, traffic, and geographical data. In addition to the urban analysis, landscape architects analyzed the biological characteristics of each plant, focusing on acceptable environmental conditions for selected species. The second step of the design process included the development of design rules by using the plant growth algorithm to generate the form of the forest. The third step was a 3D simulation of the growth process under the given environmental conditions.

The 3D simulation started with the Seed Scattering process that contained the environmental data, such as wind and lighting. By scattering seeds, landscape architects generated various layouts (Figure 76). By using Delaunay triangulation, landscape architects analyzed the seed distribution and neighboring seeds. This helped to find optimal distances between seeds and generate plant communities. Pedestrian paths were planned in empty areas between plant communities, which helps to protect plant roots from visitors' activities. After the seed layout and plant communities were determined, the next step was to optimize plant composition. The final step was the simulation of the forest's growth and appearance at 10, 15, and 30 years (Figure 77). While earlier approaches to process-based design that included ecological succession models relied on field studies and theoretical phasing strategies, this project illustrates that the use of simulation techniques enhances the precision of design solutions.

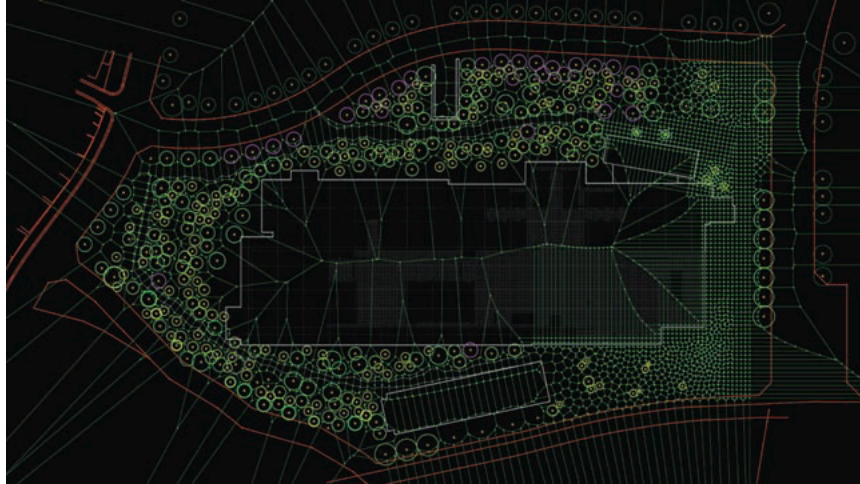


Figure 76. The final composition of the Sony Forest. From Takenaka & Okabe, 2011.

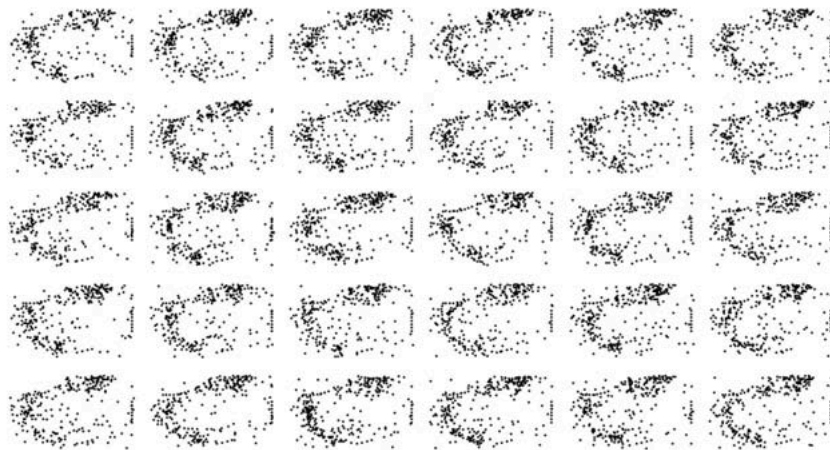


Figure 77. Seed scattering process, various layouts. From Takenaka & Okabe, 2011.

The role of landscape architect AnS Studio was key in the development of the Seed Scattering method. The AnS Studio also highlights that in this project their role was not to manipulate the geometry and composition of trees, but to design a landscape that belongs to a specific site and responds to changing conditions.

Program elements consist of the main path and outdoor landscape. The initial design focused on simple arrangements of trees around the building to imitate the natural forest and a path. Later, the path was modified based on visitors' traffic and entrances to the building. Later, LCD monitors were installed in front of the building.

The project is maintained and managed by Sony Corporate Services. User analysis was performed after the completion of the project. According to this analysis, pedestrians noted the difference between Sony Forest and the nearby landscape designed in a conventional way. The users noted that Sony Forest's design reflects meaningfully random placement of trees that resemble those in a natural forest.

Peer review of the Sony Forest project is that it differs from other modeling and simulation approaches by the process-driven approach to design a natural forest. The focus of the project was not a landscape form followed by an analysis of changes, but the development of form from environmental analysis and biological characteristics of plants (Belesky, 2018).

Criticism of the project is that a single 3D model was used from the early stages of site analysis to design documentation. Rather than using one model, it might be useful to separate models for different purposes, such as formal representation and analysis (Belesky, 2018).

The significance and uniqueness of the project is in its proposed method. The Seed Scattering method considers not only the environmental conditions of Tokyo, but also plant attributes, such as species, size, height, and growth over time. For this project, the trees were planted with an average height of 16–20 feet. Over 30 years, they will double in size, and it is necessary to understand how such changes will fit into the existing environment. The main idea behind the Seed Scattering method is to consider not only the current conditions but growth changes associated with each plant.

For the Sony Forest, the 3D simulation (Figure 78) was essential for the optimal design and layout of trees. The simulation process started with comprehensive data collection of the site's environmental conditions, such as wind speed, DEM data, and soil characteristics. The simulation, performed in Rhino and Grasshopper, involved scattering seeds that contained environmental data, followed by analysis of seed distribution and conditions between neighboring trees. The 3D simulation helped landscape architects to determine the optimal distance between trees but also refine the placement based on the timely development of plants.

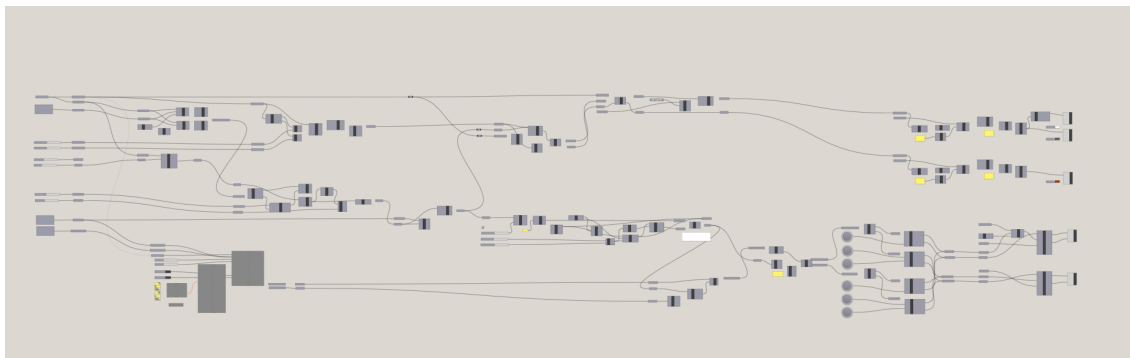
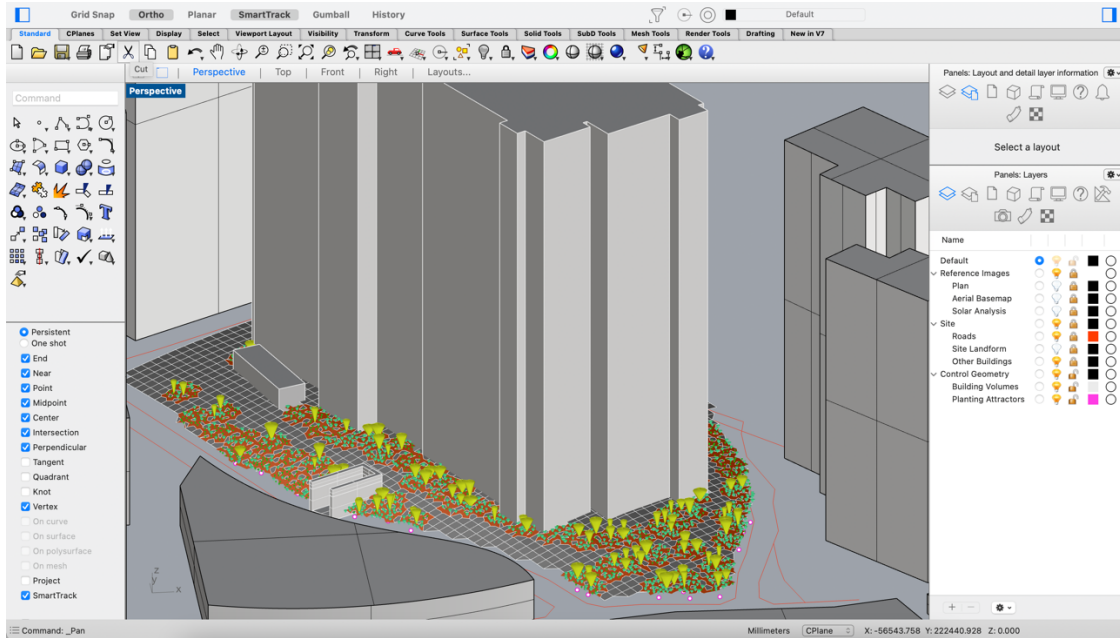


Figure 78. Sony Forest 3D model. Top: In Rhino. Bottom: Grasshopper definition.

The analysis of the evolution of process-based design and the case study analysis of selected projects informed a process-based approach to landform architecture. This approach to landform architecture helps to develop a more intuitive understanding of the relationship between process and form and addresses site-specific conditions.

The limitation of the Seed Scattering method is that it is developed for a relatively flat urban site. Once topography is more complex, the result of the simulation might not be as successful as in the Sony Forest. The method might require some adjustments for the simulation to run in different conditions.

Generalizable features and lessons are that the Seed Scattering method proposes a system that can manage environmental conditions and biological characteristics of plants in design

decisions. The development of the Seed Scattering system was driven by two processes: environmental conditions on the site and biological characteristics. In the Sony Forest project, these processes helped designers understand the conditions around the building and select appropriate plants that grow under such circumstances.

3.4 A Process-Based Landscape Approach to Landform Architecture

A process-based approach to landform architecture (Figure 79) is based on the understanding of dynamic processes that have shaped the site over time and will continue to shape it in the future. This method considers environmental and human-induced processes as a fundamental part of the design process and includes a series of steps.

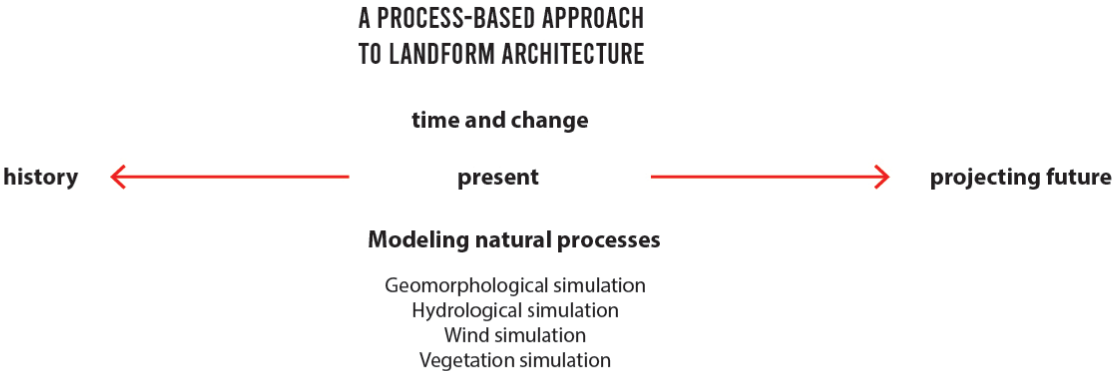


Figure 79. A process-based approach to landform architecture.

A process-based approach starts with a comprehensive analysis of environmental dynamic processes that have shaped the site. The foundation of this analysis is a site’s geological history. By studying the transformation of the site from its geological time to the present moment, an architect gains a knowledge of historical geological events and processes that created a landscape. Analysis of environmental processes also includes the study of hydrological processes and sedimentation patterns that have contributed to the current topography. Also, environmental processes analysis includes studying vegetation changes over time. Such analysis reveals the history of the site from a multilayered perspective.

In addition to the analysis of environmental processes and the history of the site, it is also crucial to analyze the impact of human processes. This analysis includes the study of urbanization, economic processes, and the resulting environmental changes. This may involve

archival research, oral histories, mapping historical land divisions, or tracing changes over time. These human processes not only shape site identity, collective memory, and shifting relationships between people, but also contribute not only to physical changes of the site and its context but also to invisible changes, such as climate. Understanding these factors helps to create a design that responds to artificial factors that have shaped the site.

While analysis of environmental and human processes contributes to the analysis of the history of the site from its geological origins to the present time, it is also essential to address current and future conditions, as process-based design anticipates change and growth. By analyzing current climate conditions, urban dynamics, and potential natural changes, it is possible to create a design that responds or adapts to future changes.

The use of digital technology is an integral part of a process-based landscape approach to landform architecture. Advanced modeling software helps to simulate natural processes and future changes. 3D modeling programs, such as Rhino and Grasshopper, help designers understand the site's dynamics and inform the design process. Digital 3D models play a key role in the iterative design process and allow designers to test and refine ideas throughout the design process. The design process is controlled by an architect and not dictated by the software. The digital tools only contribute to the overall process.

Finally, this approach represents a shift from form-oriented to process-oriented thinking. As a result, a form of a building and the adjacent landscape derive from the site and its history. The design also anticipates change and growth.

3.5 Summary

This chapter presented the evolution of process-based design in landscape architecture and the transition from form-based to process-based thinking. The shift can be understood through the key stages of ecological process-based design, systems-derived process-based design, and phasing process-based design. The ecological stage considered seasonal and temporal changes, the systems-derived stage focused on complex interactions, and the phasing stage focused on a framework for large-scale designs that sustain the development of the landscape over time.

With advancement in digital technologies, process-based design has incorporated 3D simulations to model and visualize site conditions. The early examples of simulations with

physical models are now changed by parametric design and CFD simulations. With the use of software such as Rhino and Grasshopper, it is possible to integrate environmental data into the design process. These tools allow for quick iterations and testing of site-specific interventions.

The analysis of case study projects in this chapter reveals how 3D modeling and simulations were used to address different conditions within various sites. These projects highlight specific aspects of simulations and modeling related to landform adaptation, atmospheric conditions, fluvial dynamics, and vegetation growth. In the MAX IV Laboratory project, 3D simulation played a key role in the design process and optimization of existing conditions. For Jade Eco Park, 3D simulation played a crucial role in understanding and visualizing climatic processes within the site. While PARKKIM did not perform a 3D simulation for the Mud-Infrastructure project, the project sets the case for the design of a flood-prone park that functions at different times of the year. For the Sony City Ōsaki Forest, the 3D simulation was essential for the optimal design and layout of trees. These case study projects illustrate how advances in digital technologies and computational modeling can respond to site conditions.

The analysis of the evolution of a process-based design and the case study analysis of selected projects informed the development of a process-based approach to landform architecture. The process-based approach to landform architecture focuses on environmental and human processes that have shaped the site over time and will continue to influence it in the future. This approach starts with a comprehensive analysis of geological history, hydrological processes, sedimentation patterns, and vegetation changes to understand the site's development. In addition, this approach considers visible and invisible forces, such as processes of urbanization, that result in economic changes and environmental shifts. While historical analysis plays a major role in this approach, it also anticipates future changes by considering climate conditions. To help simulate and visualize natural processes, digital tools like Rhino and Grasshopper play a critical role in the design experiment discussed in the next chapters. The method shifts from form-oriented to process-oriented design, where landscape and architecture merge together.

IV. SITE CONTEXT

4.1 Site-Specific Process-Based Approach to Landform Architecture

A process-based approach to landform architecture involves designing buildings that are shaped by, and are responsive to, environmental processes within a specific site. Instead of introducing a predetermined form into the existing context, this approach emphasizes a dynamic interaction with existing environmental processes. In this case, the design process focuses on understanding and engaging with environmental processes already present on the site. Such an approach recognizes the uniqueness of a specific site and takes into account geomorphological, hydrological, and climatic conditions.

In this chapter, the process-based approach to landform architecture is focused on the detailed analysis of the history of the selected site (Figure 80). This analysis embraces time and change, aiming to identify how environmental and human processes have shaped the site into its current state. The site's history provides insight into the site's evolution, which influences the connection of context with future design.



Figure 80. Process-based approach and analysis of the site's history.

By understanding the history of the site, site-specific processes, and transformations over time, it is possible to consider potential future changes. A process-based approach that involves a deep understanding of natural processes helps to design buildings that respond to their dynamic context.

4.1.1 Site Selection

The city of Portland, Oregon, is the second largest city in the Pacific Northwest, after Seattle. Portland was selected as the study site due to its unique geographic location and rising climate-related challenges of the urban heat island (UHI) effect and flooding. The city's diverse topographical and hydrological conditions make it a perfect case to explore how landform architecture can mitigate climate-related issues.

The city is located along two major rivers: The Willamette River flows through downtown Portland, while the Columbia River forms the northern edge of the city. As of 2024, the population of Portland was estimated at around 630,000 people, and approximately 2.5 million people live in the larger metropolitan area (U.S. Census Bureau, n.d.). Like many urban areas, Portland faces a number of climate-related challenges (Goldman Sachs, 2022), including UHI, and more extreme weather and events like heat waves, wildfires, and flooding.

While the flood-prone areas include neighborhoods near the Columbia River and the Willamette River, other climate-related issues distribute more evenly across the city. In recent years, Portland has experienced several heat waves, with a record high temperature of 118 °F recorded in 2021. The risk of heat waves is increased by UHI (Voelkel et al., 2018; Fahy et al., 2019). UHI occurs when urban areas trap and absorb more heat than the surrounding rural areas, leading to higher temperatures and negative impacts on air quality and human health (Hart & Sailor, 2009).

The city of Portland has implemented a number of initiatives aimed at mitigating UHI (UHI Mitigation Plan, 2022; U.S. Environmental Protection Agency, 2022) and reducing flood risk (FEMA, 2013). These include increasing the amount of green infrastructure such as parks and trees to provide shade and cool urban areas, implementing stormwater management strategies, and improving building design to increase energy efficiency (UHI Mitigation Plan, 2022; Sailor, 2007; Voelkel et al., 2016; Makido et al., 2019). The Urban Heat Mitigation Plan focused on vegetation cover, pavement materials, green roofs, electrical vehicles, and smart growth (UHI Mitigation Plan, 2022; Columbia Slough Watershed Council, 2020). Another research study focused on the potential of vegetation and shaded areas to mitigate UHI and microclimate in the Portland area (Voelkel et al., 2016; Sailor, 2007). Nature-based design solutions to mitigate urban heat by Yasuyo Makido focused on six green infrastructure interventions across different land-use types (Makido et al., 2019). However, there is no

information related to the potential benefit of landform buildings in urban areas and their influence on local microclimate. Thus, this research will focus on landform design solutions that can lower the temperature and improve outdoor thermal comfort by integrating a building form into topography. The strategy aims to create comfortable outdoor public spaces and improve temperature conditions of the selected site.

The initial process of site selection was based on analysis of urban heat island and climate change issues in different areas in Portland. The preliminary analysis of temperature and urban heat islands across Portland, developed by researchers from Portland State University (Voelkel & Shandas, 2017), shows that the temperature is significantly higher in Northeast Portland along the Columbia River, Interstate 5, and northwest of the Willamette River (Figure 81). After an analysis of the tree canopy cover map, it became clear that the areas that have the highest temperatures have the smallest percentage of tree canopy cover. One of the most important characteristics in urban heat island studies is the canopy cover that separates warmer regions from cooler (Makido et al., 2019; Loughner et al., 2012; Hart & Sailor, 2009). Thus, the areas with tree canopy cover smaller than 25% and temperatures higher than 30 °C, represented as dashed areas on the map in Figure 81, were selected as three potential areas for the design experiment.

In site-scale exploration, special attention was dedicated to vacant land and sites with historical significance. Site boundaries were defined based on land-use patterns, the intensity of the urban heat island, and unique characteristics that provide opportunities for a landform design. The selection process included areas with high outdoor temperatures. Specific attention was dedicated to empty lots with minimum to no vegetation.

Site history played a crucial role in site-scale explorations, as understanding the site's past transformations helps to understand potential future transformations. Northeast Portland along the Columbia River is the historical site of Vanport (Site 1), a large housing project built during WWII. It was a diverse community of African Americans and Japanese Americans; however, the city was destroyed in 1948 by a severe flood (Skovgaard, 2007). The Albina neighborhood (Site 2), named after a railroad depot, is historically significant as the center of Portland's African American community, who were excluded from other parts of the city due to segregation. The construction of Interstate 5 in the 1950s–1960s and other urban renewal projects destroyed much of the area and displaced residents (Gibson, 2009; Norwood, n.d.).

Northwest of the Willamette River was once a riparian marsh, Guild’s Lake, which was the setting for the 1905 Lewis and Clark Exposition (Site 3). Once the fair was over, the Olmsted Brothers’ firm proposed transforming the site into a public open space; however, despite an effort to save it as a park, the lake was filled in for industrial use by 1913 (March, 2000).

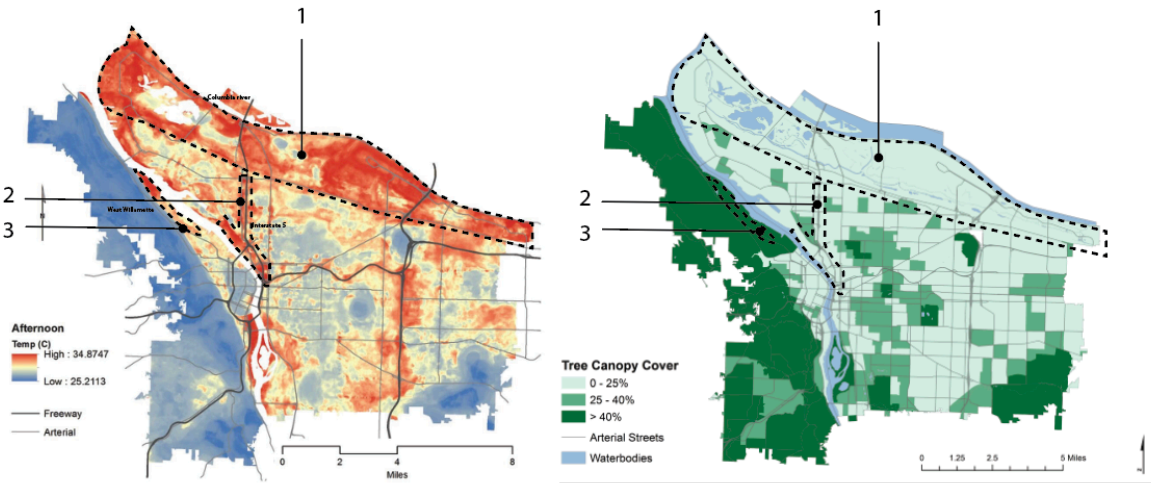


Figure 81. Temperature map and tree canopy cover across Portland, Oregon. Left: Temperature map. Site 1: Vanport (Northeast Portland along Columbia River); Site 2: Albina neighborhood (Interstate 5 area); Site 3: Northwest of the Willamette River (historical Guild’s Lake area).

From Sustaining Urban Places Research Lab, Portland State University, 2018.

Right: Tree canopy cover, grouped by census block. Site 1: Vanport (Northeast Portland along Columbia River); Site 2: Albina neighborhood (Interstate 5 area); Site 3: Northwest of the Willamette River (historical Guild’s Lake area). From Portland Parks and Recreation Urban Forestry, 2014.

In order to identify a potential site out of the three possible sites, the following parameters for site suitability were developed:

- Area affected by urban heat island 30–35 °C. This parameter helps identify areas with elevated temperatures due to urbanization.
- Tree canopy cover percentage 0%–25%. This measures the density of the vegetation essential for cooling, shade, and biodiversity. It also influences the above parameter of a site’s temperature.
- Vacant area with no development. This helps to identify spaces that have the potential for future transformations into public areas.

- Underused site. This identifies sites that have potential to be a public space due to their location and views, but have limited activity or inefficient land use.
- Site-specific landforms. This helps identify geologically distinct features that influence the topographic profile of the site and make it a unique area.
- Site with historical significance (urban history). This parameter helps to identify locations of cultural importance that inform design decisions.
- Site with dynamic changes over time (flooding history). This identifies areas vulnerable to historical and future hydrological changes. This parameter also helps to identify areas that require resilient solutions.
- Urban renewal plan. This parameter outlines redevelopment efforts and keeps design efforts aligned with the city's strategies.




The site suitability analysis (Table 2) involved quantitative and qualitative data evaluation in order to select the most suitable site. Site suitability is defined as a function of the site's capacity to provide conditions necessary for the proposed uses (LaGro, 2009). Each site was screened according to site suitability parameters.

- Site 1: Vanport meets all but one requirement.
- Site 2: Albina has site-specific landforms and dynamic changes over time that are influenced by natural processes.
- Site 3: Willamette River does not have a vacant area for development, as this area, according to the Urban Renewal Plan, is suitable only for industrial use (Norwood, 2023).

Based on the suitability analysis, the Northeast Portland site along the Columbia River is the most suitable for design, as it meets all selection criteria. Within the historical Vanport area, a vacant site was selected that was once the Japanese American Portland Assembly Center, which was a temporary detention center established by the U.S. government during WWII (before that, it was the North Portland Livestock and Exposition Center) (Gayne, 2003).

Table 2

Suitability analysis of potential sites for design experiment

Parameters	Site 1	Site 2	Site 3
	Vanport	Albina neighborhood	Northwest of the Willamette River
			
Urban heat island 30–35°C	+	+	+
Tree canopy cover percentage 0%–25%	+	+	+
Vacant area with no development	+	+	-
Underused site	+	+	+
Site-specific landforms	+	+	+
Site with historical significance	+	+	+
Site with dynamic changes over time	+	+	+
Urban renewal plan	+	+	-
Urban connection with the city	-	+	-

The site suitability analysis was followed by site visits and visual analysis of a preselected Northeast Portland site along the Columbia River, along with two other alternative sites. The visual analysis was supplemented by drone images (Figure 82–Figure 84) to confirm

that the selected site is the most suitable area for the design experiment. This process revealed that the initial suitability analysis did not consider the urban connection of the selected site with the city. After including this parameter in the suitability analysis (Table 2), it became clear that Vanport and Northwest Willamette River site locations were disconnected from the city. Based on the analysis, the most suitable site for the design experiment is the Albina neighborhood (Figure 85).



Figure 82. Site 1: Vanport (Northeast Portland along the Columbia River).



Figure 83. Site 2: Albina neighborhood (Interstate 5 area).



Figure 84. Site 3: Northwest of the Willamette River (historical Guild's Lake area).

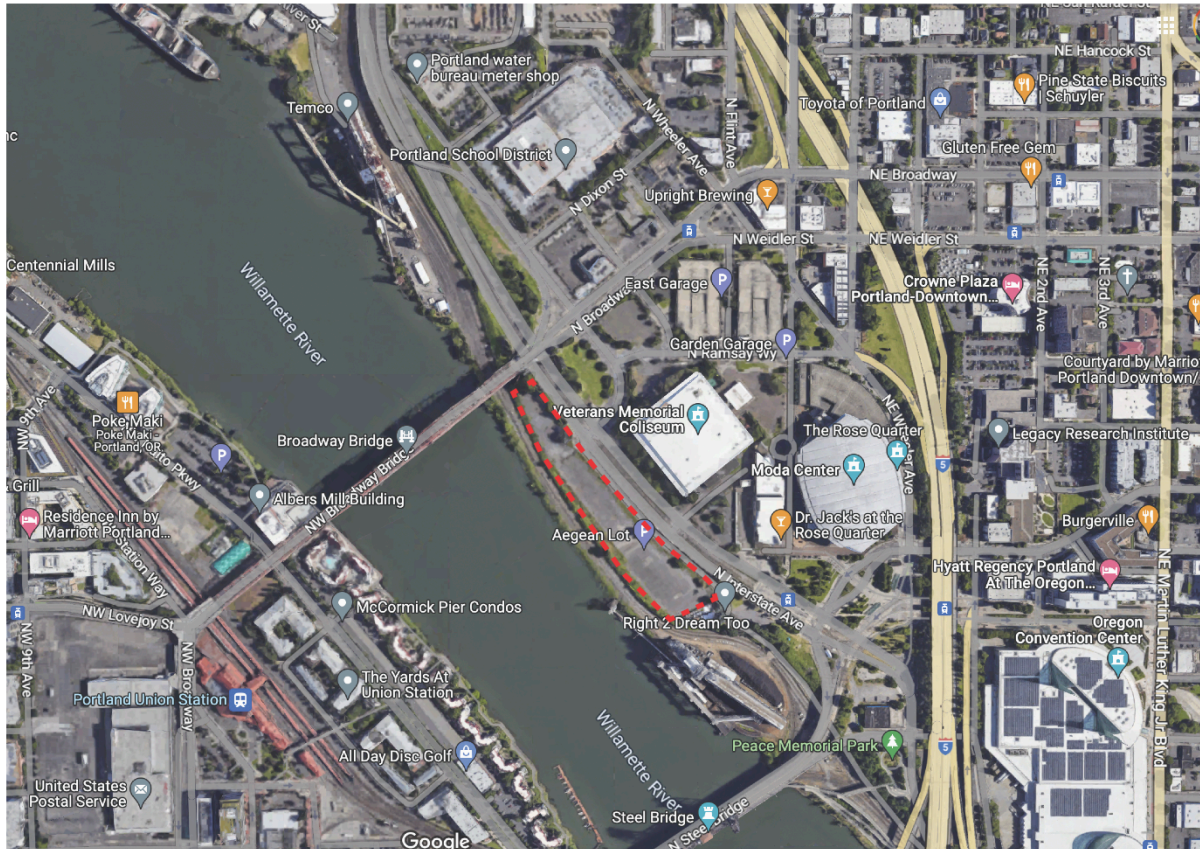


Figure 85. Selected site for design experiment, marked by a dashed line.

The site was selected due to its historical significance, dynamic environmental conditions, and potential for landform design intervention that addresses climate-related and urban challenges. Data collection included collecting information about the selected site to understand its history and current state by using archival research, base information, aerial images, maps, site visits, and interviews with professionals. The comparative analysis of historic maps of the selected region shows the transformation of the area from 1897 to 1990 (Figure 86).

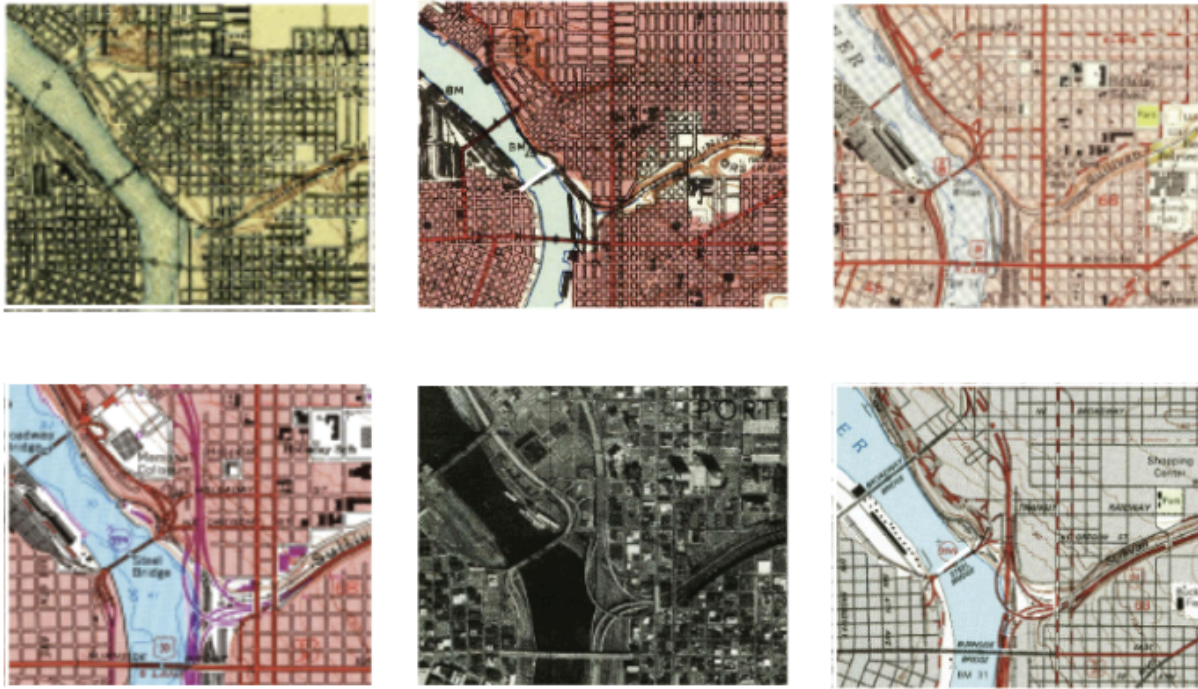


Figure 86. Portland historic maps of 1897, 1940, 1954, 1961, 1975, and 1990 (left to right).
From Harvard Old Maps online.

Site analysis involves analyzing the site and its history, and conducting 3D simulations of existing processes in Rhino and Grasshopper to identify opportunities for landform buildings. 3D simulations of existing processes on the site can provide a deeper understanding of the site as a dynamic system and its environmental conditions. The simulations can be used to study how water flows through the site, potential flood-prone areas from the Willamette River, how wind affects the area, and how vegetation changes over time. By conducting simulations, it will be possible to gain insights into how the site's microclimate functions, which is essential for designing landform buildings and addressing climate issues such as UHI and flooding.

4.1.2 Context: Natural and Cultural History

The natural and cultural history analysis provides a comprehensive overview of the historical development of the Albina neighborhood in Portland, Oregon. Situated at the confluence of social, economic, and environmental factors, Albina's evolution is marked by a complex interplay of cultural, environmental, and urban development dynamics. From its indigenous roots to the contemporary issues of spatial segregation, this study explores the

multifaceted history of Albina, by examining the forces that have shaped and continue to shape this neighborhood.

Before the arrival of European settlers, the area that would become Albina was inhabited by the Multnomah and Clackamas Native nations. A preliminary examination of Albina's natural history should acknowledge this indigenous presence and its impact on the region's ecology. Native nations inhabited various regions along the Willamette River and Willamette Valley, which was covered with grassy prairies, tall fir trees, and clusters of oaks (City of Portland, n.d.). During this time, their interactions with the river were characterized by relatively modest alterations. They used the river for salmon and steelhead fishing and utilized the waterways for transportation (Roos, 1997).

The arrival of the first European settlers in the 1800s marked a turning point in Portland's history. The settlers were farmers and merchants, who planted crops and built towns. They viewed the river as the main transportation corridor. New settlers started the transformation of the Willamette River by deepening the channel and using paddle-wheel boats to transport wheat and bring more people to the town.

The development of the west bank of Portland started in the 1840s with the construction of the first docks to service the port town. The 1852 Cadastral map of Portland (Figure 87) shows the grid that forms current downtown Portland. The east side of the river is shown on the map as a lowland marsh with streams. At that time, the area was heavily forested with cedar and hemlock trees to the east and north.

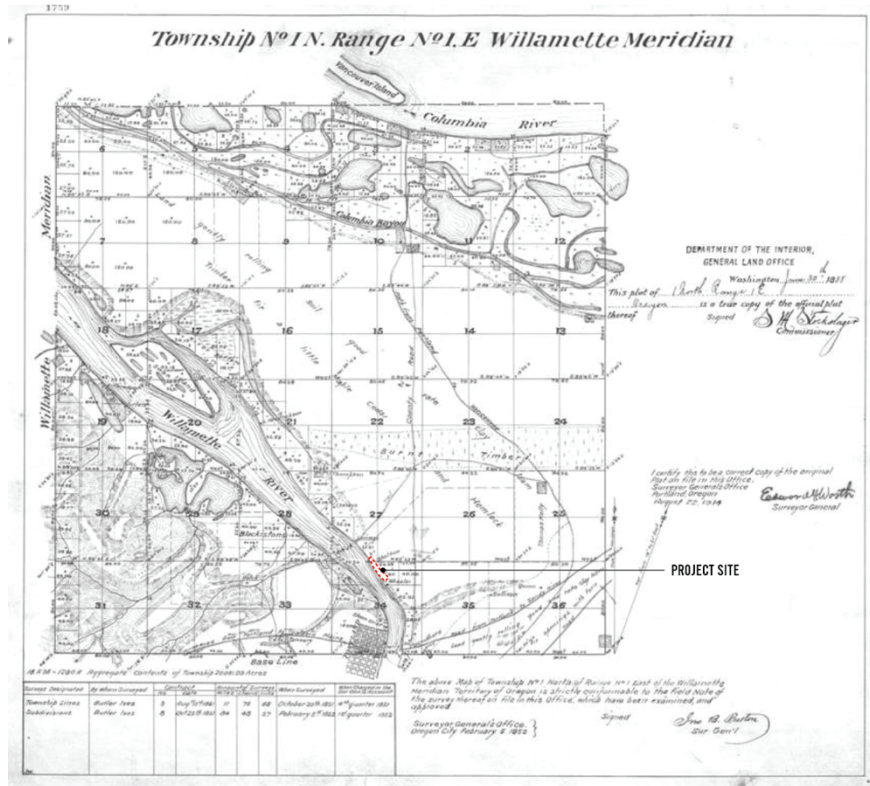


Figure 87. Cadastral map of Portland, 1852. From Public Land Survey System.

The history of the east side of the river, especially the development of the Albina neighborhood, reflects abundant economic opportunities for early settlers and businessmen. In the 1880s, Albina emerged as the fastest growing city in Oregon, located east of the Willamette River from Portland. The town of Albina was named after Albina V. Page, the wife of William W. Page, one of the townsite's landowners. In 1872, William Page sold the land to George H. Williams, former senator and future mayor of Portland, and Edwin Russell, manager of the Bank of British Columbia (Volga Germans, n.d.). In 1873, Williams and Russell undertook the platting and layout of the town, which was situated within the present Eliot neighborhood and bounded by the Willamette River (Figure 88). The area that became Albina overlaps with the current Eliot neighborhood; however, historical boundaries of Albina extended beyond Eliot neighborhood boundaries.

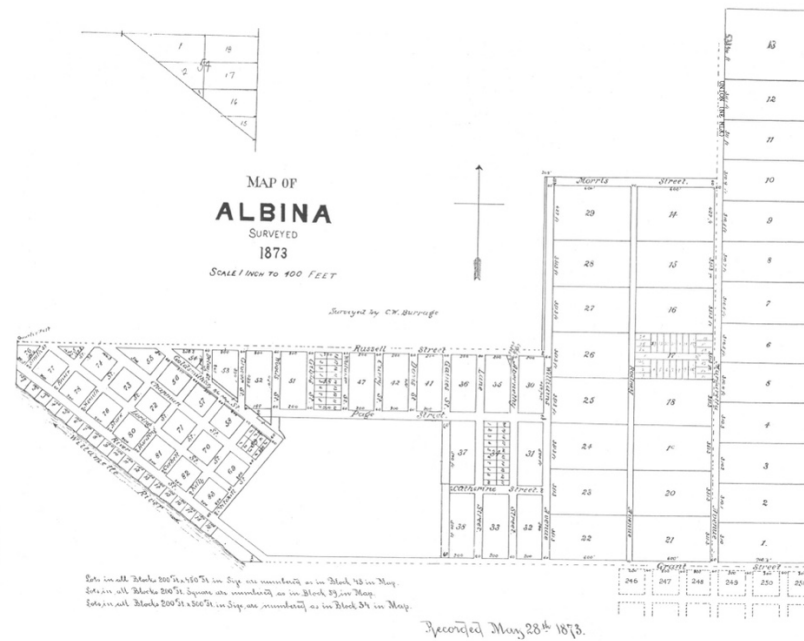


Figure 88. Albina area plat map of 1873. From Roos, 1997.

In the early 1870s, the railroad magnate Ben Holladay initiated the construction of a railroad from the east side of the Willamette River to California. The project included plans for the terminal next to Albina and extensive docks along the river with maintenance facilities. However, the recession of 1874 left Holladay bankrupt and the railroad unfinished.

In 1879, the developers William Reid and James Montgomery purchased a large part of Albina (Figure 89) and established a new industrial infrastructure, including railroad terminals and shipping docks. The expansion resulted in economic growth and the arrival of new residents who found employment opportunities in the railroad terminals and on the docks. This led to the development of small businesses and the construction of new homes to accommodate the growing workforce.



Figure 89. The early development of the Albina neighborhood. From Glover, 1879.

In 1882, the Oregon Railroad and Navigation Company started construction of the “Great Depot” in the marshland below Albina (Roos, 2008). The construction included car and machine shops, a rail yard (Figure 90), grain and coal terminals, and shipping docks (Volga Germans, n.d.). *The Oregonian* reported that around 300 men would be employed in car and machine shops, and around 4,000 men would be employed at passenger depots, shipping docks, and coal and grain terminals. Such economic development of the railroad was associated with not only the construction of new homes, but also the growth of hotels, grocery stores, and other small businesses (Butler, 2018).

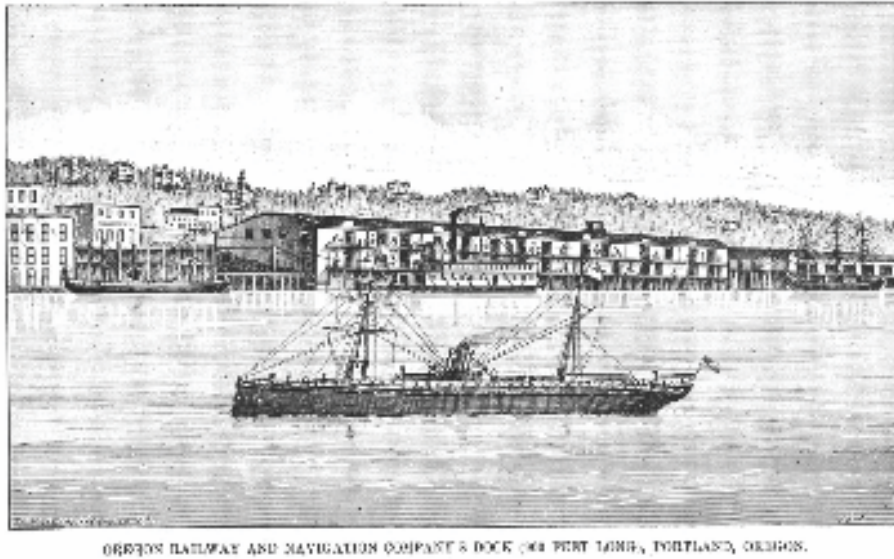


Figure 90. Oregon Railway and Navigation Dock, 1882. The Albina community is shown in the background. From Wikimedia Commons.

In the 1880s, Albina's growth attracted European immigrants, especially from Ireland, Germany, and Scandinavia. These immigrants not only found jobs but also shaped the cultural and architectural image of the town. Immigrants brought specific skills, such as carpentry, that were passed through generations. Some of the homes they built remain as historical artifacts within the Albina neighborhood. The growth of the city also influenced the gradual transformation of Albina from a rural landscape to an industrial center. Forests were cleared, wetlands were drained, and transportation infrastructure, including bridges and railways, were established, changing the landscape significantly.

Albina was officially incorporated as a town in 1887, including areas that were outside the original townsite. The city was connected to Portland by two ferries and small boats before the construction of the Morrison Bridge in 1887. In 1889, the Oregon Railroad and Navigation Company completed the first Steel Bridge to connect the east and west banks of the Willamette River (Figure 91). Trains crossed the Willamette River on the lower level, while the upper level was for pedestrians and carriages. As Albina's population grew and urban expansion increased travel demands, electric streetcar lines were introduced over the bridge to improve the connectivity between Albina and Portland.



Figure 91. The first Steel Bridge, connecting Portland across the river and Albina in the foreground, 1887 (before the bridge went into service). From Volga Germans, n.d.

In 1891, the city of Portland annexed the city of Albina, marking a transformative moment in the neighborhood's history. The annexation also included East Portland (Figure 92), an area situated south of Albina on the east side of the Willamette River. The expansion led to a significant migration of residents from the Portland's west side to the newly incorporated areas.

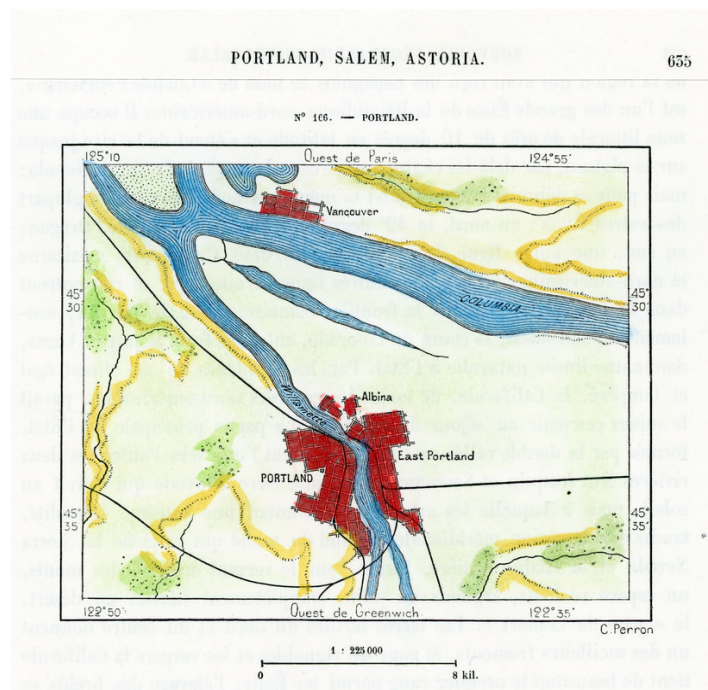


Figure 92. Map of Portland, East Portland, and Albina. From Volga Germans, n.d.

In the 1910s, African Americans started to migrate from Northwest Portland to the Lower Albina near today's Veterans Memorial Coliseum and Rose Quarter. They were driven to Albina by economic opportunities, affordable housing, and jobs in the railroad industry. The population of the African American community increased during WWII due to the increase in jobs in the shipbuilding industry. Many workers from the shipbuilding industry lived in Albina due to racial housing restrictions that limited their ability to rent or buy anywhere else. This migration not only reshaped the neighborhood's demographics but also created a housing shortage. In 1942, a large housing development, known as Vanport, was built in North Portland to house shipyard workers. After the war, the shipbuilding jobs declined and the majority of the African American population faced unemployment and displacement. Another migration wave was forced by the 1948 Columbia River flood, which completely destroyed the town of Vanport. African Americans were forced to move to North Portland and Albina.

The construction of Interstate 5 and the Veterans Memorial Coliseum in the 1960s displaced a substantial portion of residents and businesses in the Eliot, Boise, and Humboldt neighborhoods (Figure 93). The expansion of the Emanuel Hospital in the 1970s led to further economic challenges in the Eliot neighborhood. This phase was a pivotal moment in Albina's history, impacting both the sociocultural fabric and the physical environment.



Figure 93. Albina neighborhoods. From Volga Germans, n.d.

The late 20th century and early 21st century have seen Albina experience the effects of gentrification, with rising property values, demographic shifts, and the displacement of long-term residents (Courtright, 2021). Despite these challenges, efforts to preserve the cultural heritage of Albina have been ongoing. Community organizations and activists have sought to raise awareness of the neighborhood's history, advocate for affordable housing, and support businesses. The Vanport Mosaic project involved collecting oral stories of displaced communities and initiatives to restore African American community spaces and reverse the impacts of gentrification, reflecting the resilience of the community in the face of environmental and sociocultural changes.

The Albina Vision Trust aimed to restore the cultural significance of the Lower Albina neighborhood. This project is a collaboration between the city of Portland and the community organization Albina Vision Trust. The partnership focuses on strategies to reconnect the Lower Albina neighborhood to the city without displacing current residents and businesses. The redevelopment of a historically African American neighborhood is a large-scale initiative that addresses the displacement of the community due to urban renewal projects and highway construction.

The Albina Vision plan focuses on the restorative development of 94 acres along the Willamette River (Figure 94). This includes affordable mixed-use housing, infrastructure improvements to reconnect the neighborhood to surrounding areas, and cultural spaces. One of the efforts is focused on reconnecting Lower and Upper Albina and repairing the set of negative consequences after the construction of the I-5 highway. The solution proposed by the Albina Vision Trust in collaboration with the Oregon Department of Transportation (ODOT, n.d.) envisions that part of the highway by the Rose Quarter will be tunneled. The highway cover will support the development of multistory buildings and green spaces atop the cover.



Figure 94. Albina Vision Trust community investment plan by El Dorado Architects.

From El Dorado, n.d.

In 2023, the Albina Vision Trust received a grant from the Metro Regional Government and started a process of buying parcels of land to create a waterfront park between the Steel and Broadway Bridges. This project aims to restore not only economic and racial justice but also public access to the river. In this dissertation, this area becomes a site for a design experiment that explores how computational tools and simulations can inform a landform building with an adjacent landscape.

The building program for the Lower Albina cultural center includes cultural spaces, community spaces, and recreational spaces, with an area of 62,400 square feet. The cultural space can include a museum or exhibition area dedicated to the history of the African American community that was displaced due to urban renewal projects in the 1950s through the 1970s. Such space can also include an area for community events, live performances, and art from local artists. The community space can include multipurpose spaces for meetings, workshops, training, and other educational programs. The recreational space can be integrated with the building and offer recreational areas that promote a connection with the river. It also includes a waterfront park with a series of paths that connect the area to other parts of the neighborhood.

The history of the Albina neighborhood in Portland shows a complex interaction between urban development, cultural evolution, and economic and demographic factors. By considering these historical factors, this study contributes to a more comprehensive understanding of Albina

and its role in the larger context of urban development. Furthermore, it underscores the importance of addressing contemporary challenges such as spatial segregation in future design development projects.

The history of Albina is essential to understand current urban challenges and inform future design interventions. The history of displacement and redevelopment demands a critical reevaluation of the existing state and solutions for future changes. This research contributes to a broader conversation by examining how landform-based strategies can improve connectivity in the Lower Albina area with neighboring areas that were disconnected due to urban renewal projects. The following sections present a detailed history of the area on multiple scales in the form of 3D simulations.

4.1.3 Site Analysis

The site analysis aims to understand the processes that have shaped the selected Albina neighborhood site into its current state on various scales. For this analysis, I use 3D simulation based on historical records and selected data up to the present time. Collected data is transferred to 3D models, which is considered a way of learning and analyzing the information about the site in a spatial dimension. The final result of the collected data and resulting 3D models are represented in perspective images, which are later combined in a simulation .gif that allows for tracking changes over time.

The following sections present an analysis of a series of environmental processes, such as geomorphological processes, hydrological processes, and vegetation processes, but also human processes, such as urbanization, on three scales: (1) city scale, (2) neighborhood scale, and (3) site scale. For each type of process, environmental and human agents that have shaped the research area are considered.

4.1.3.1 City Scale

In order to understand environmental processes on a larger scale, this research begins with the area that is larger than the project site. The site analysis on the city scale consists of analysis of geomorphological, hydrological, and vegetation natural processes. These processes were chosen because they have played a key role in shaping the site over time. Environmental processes have shaped terrain and ecosystems, while urbanization reshaped the landscape by

changing physical and ecological characteristics of the area. Each process is considered to be influenced by environmental (nonhuman) and human agents (Figure 95). This analysis becomes a record of historical events and processes that have shaped Portland and the project site into its current state.

The hypothesis of the city scale analysis is that, because of the project sites' close proximity to the Willamette River's edge, large-scale fluvial processes have played a crucial role in shaping the site into its current state. Another hypothesis is that this analysis will help to identify characteristic landforms and will guide the landform architecture design experiment. And, finally, the hypothesis for vegetation processes is that vegetation patterns or specific types have shaped landforms on the city scale.

Contrary to traditional historical city-scale analysis that is based on 2D map and diagram analysis, this research proposes 3D simulation as the main tool to collect data, analyze information, and make assumptions about the site. The 3D simulation is based on 3D models, which helps to analyze information spatially and understand the relationships between geology, flooding, vegetation, and topography. In addition, 3D simulation compiles data from different sources using a common spatial framework, which allows for comparison of selected processes. Such a process makes it possible to quickly compare geomorphological, hydrological, and vegetation processes and find interdependence between them.

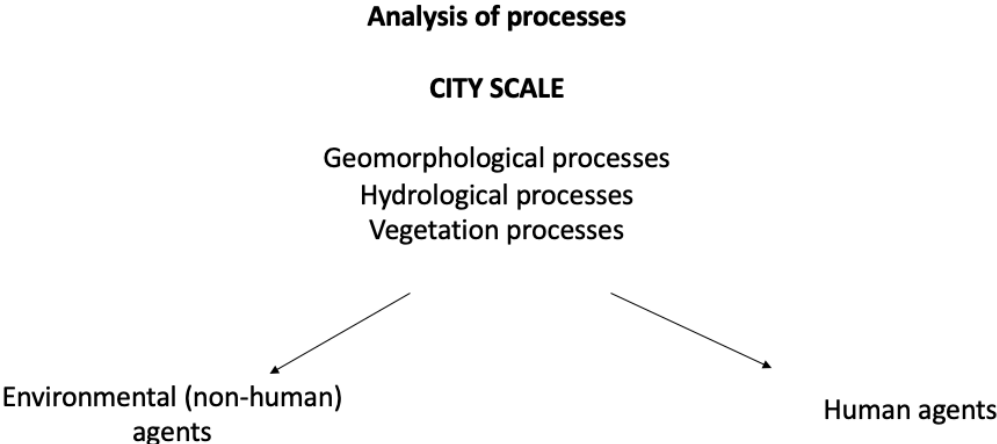


Figure 95. Analysis of processes on the city scale.

4.1.3.1.1 Geomorphological Processes

The landscape of Portland was shaped by a series of geologic events, including volcanic activity, and fluvial processes, which had a significant influence on the current state of the city. The focus of this analysis is geologic formations near the project site. The aim of this analysis is to identify the major geologic processes that shaped the city’s topography. Thus, this section presents an analysis of geologic processes, how they shaped the current topography, and the major changes over time.

Portland is situated in a broad valley at the confluence of two rivers and framed by hills. The area is situated within the Columbia River Basin, where geologic activities over millions of years played a role in shaping the landscape. The formation of the Cascade Range started over 40 million years ago from subduction volcanic activity. The volcanic activity created a mountain range that forms the Pacific Northwest topography. Sedimentary depositions from ancient seas and rivers contributed to underlying geologic layers (Trimble, 1963). The processes of erosion, deposition, and tectonic activity transformed the landscape of the city.

In this analysis, the two geologic processes are qualified as changes influenced by environmental agents (Figure 96). In contrast to environmental events, Portland was also shaped by human activity. Such changes are considered to be shaped by human agents, which are actions of human-induced filling, a process of adding debris to modify the topography of the site.

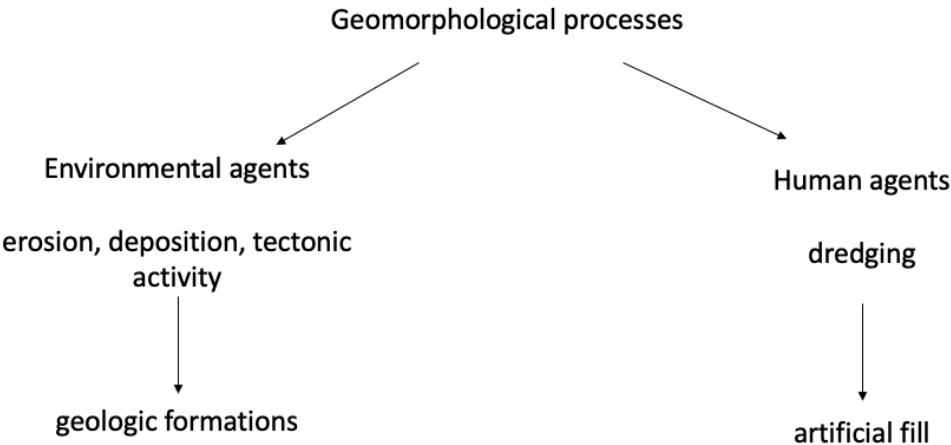


Figure 96. Geomorphological processes influenced by environmental and human agents.

The geologic simulation map (Figure 99) includes data from the *USGS Geologic Map of the Greater Portland Metropolitan Area and Surrounding Region* (Figure 98). The simulation

presents the relationship between geologic history and the city’s topography. The aim of this simulation is to identify geologic processes that shaped the current landscape of Portland and influenced the formation of landforms. As seen in the workflow process (Figure 97), the collected data from the USGS map was translated into a 2D AutoCAD drawing, which was used for the 3D Rhino model, and later converted into a 3D perspective image. The resulting 3D simulation helps identify the relationship between the city’s topography and layers of geologic history.



Figure 97. Workflow process.

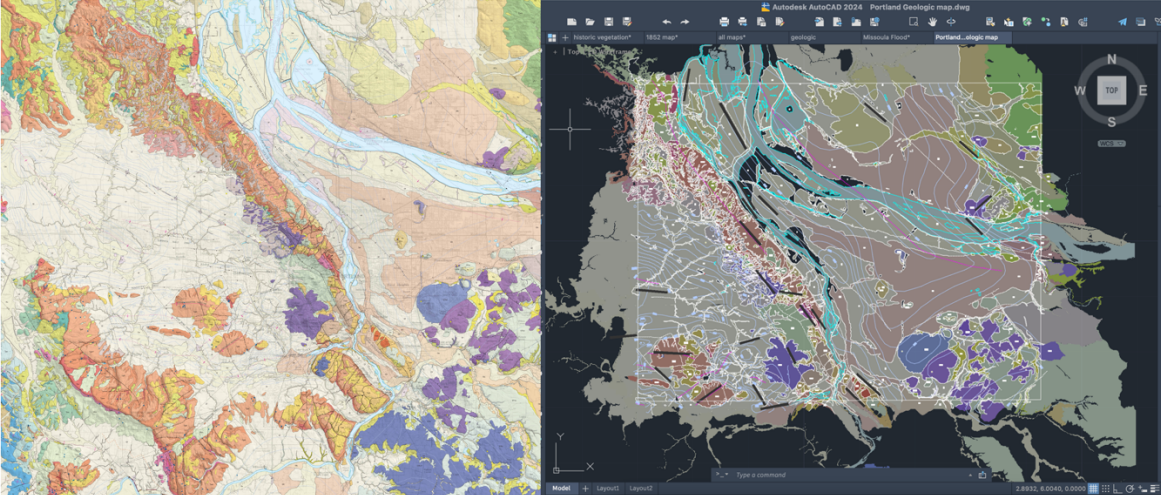


Figure 98. Left: Geologic map of Portland. From USGS. Right: 2D AutoCAD drawing of the map.

Portland was shaped by two catastrophic floods over the geologic time. The first was the lava flow that inundated the region from Eastern Oregon through the Columbia Gorge. Over time the lava flow was folded, faulted, eroded, and weathered. The second flood was a series of

floods that originated from the mountains in the east. The floods of water, rock debris, and ice surged through the Portland area.

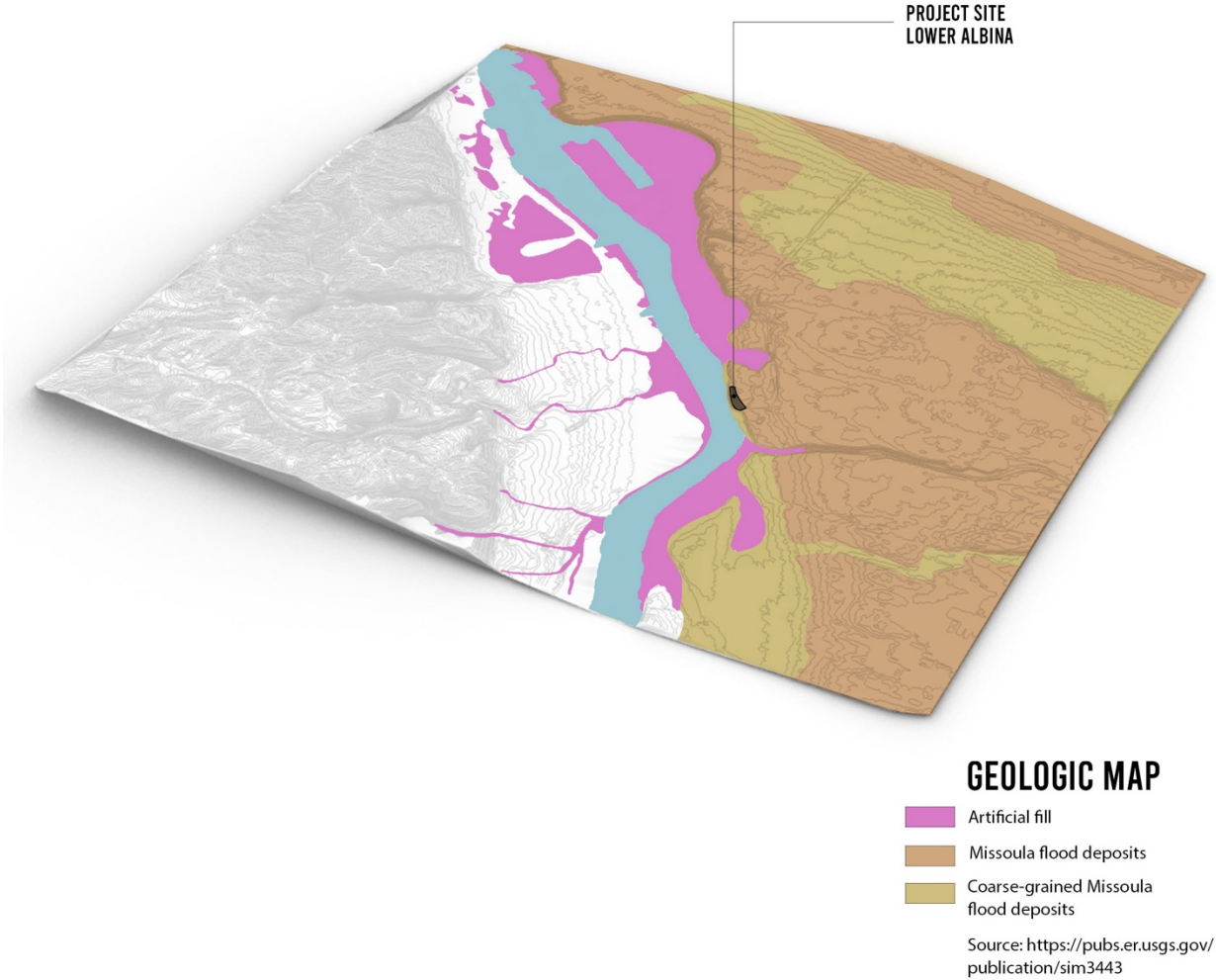


Figure 99. Portland surficial geologic simulation map.

The foundational basalt bedrock of Portland was shaped by multiple flows of volcanic lava. The Columbia River Basalts (17–14 million years ago) was a series of broad lava flows that started from Eastern Oregon to Washington, through the Cascades all the way to the ocean. The Columbia River Basalt Group has undergone the processes of folding, faulting, and erosion, resulting in folded and faulted structures (Trimble, 1963).

4.1.3.1.2 Hydrological Processes

One of the most profound effects on the city's geomorphology was the Missoula Floods, a series of catastrophic events triggered by the failure of Glacial Lake Missoula in Western Montana. The Missoula Floods (15,000–13,000 years ago) was the flow of ice and rock that started from Eastern Oregon through Washington and the Cascades, filling up the entire Willamette Valley, and finally reaching the ocean.

The Missoula Flood simulation map (Figure 101) includes data from *Missoula Floods Inundation Extent and Primary Flood Features in the Portland Metropolitan Area, 2012*, map from the State of Oregon Department of Geology and Mineral Industries (DOGAMI) (Figure 100). The simulation presents the relationship between the water inundation area and the city's topography. The aim of the simulation is to identify how the flood has shaped the city's current landforms and topography. The line defining the inundation area was interpreted using the GIS dataset. The maximum flood height for the Willamette Valley is suggested by the DOGAMI map as a 400-foot elevation above the sea-level contour line. The collected data from the DOGAMI map was translated into a 2D AutoCAD drawing (Figure 100) that was then used for the 3D Rhino model, and later converted to a 3D perspective image. The resulting 3D simulation helps identify the relationship between the Portland geologic surficial simulation map (Figure 99) and the influence of the Missoula Floods on the present landscape.

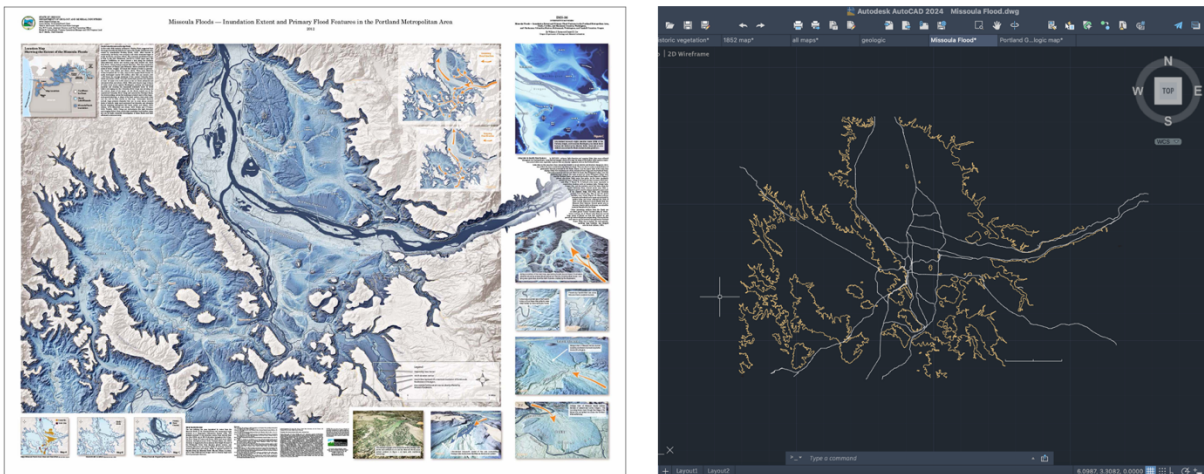


Figure 100. Left: Missoula Floods inundation extent and primary flood features in the Portland metropolitan Area, 2012. From DOGAMI, 2012. Right: AutoCAD 2D drawing of the flood area.

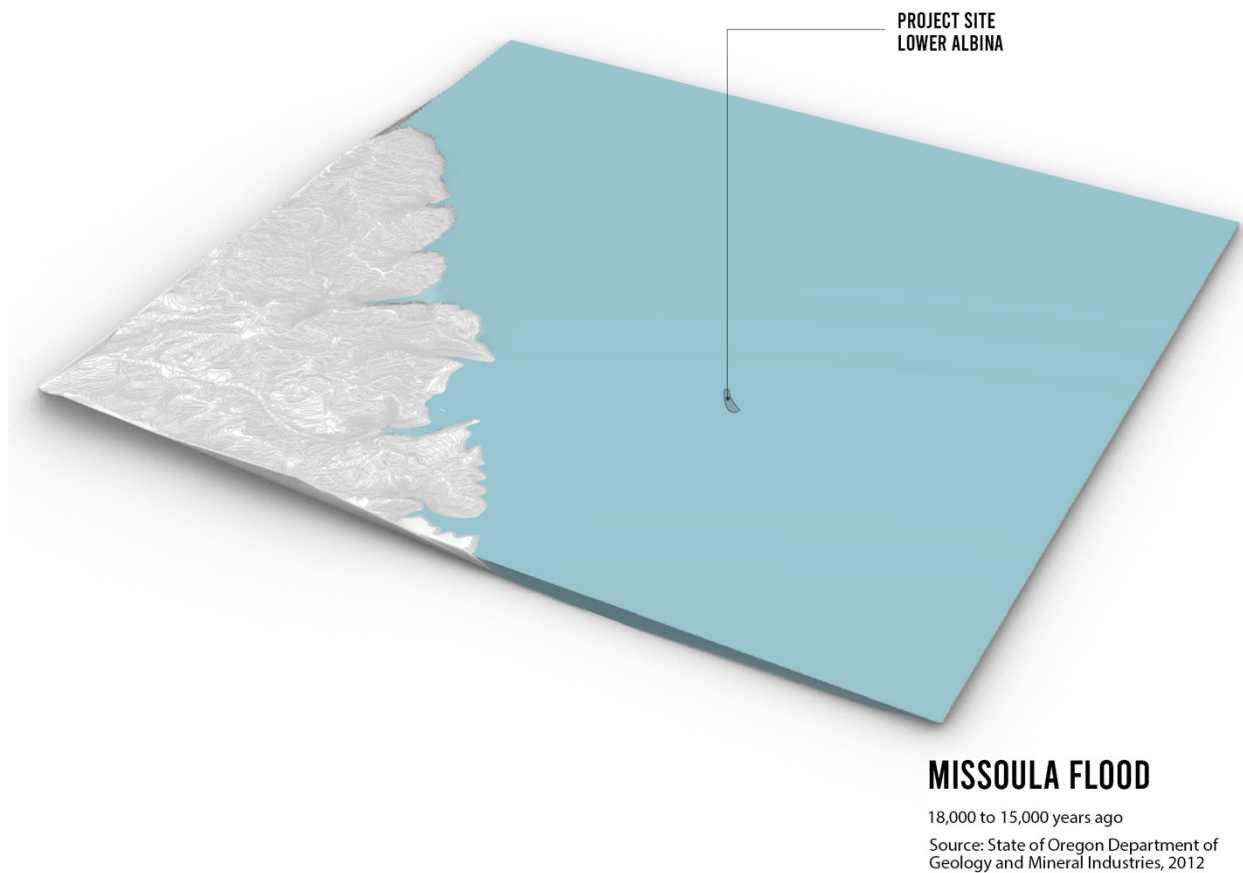


Figure 101. Missoula Flood simulation map.

As the Missoula Floods surged over the landscape, it created major geomorphological features that are present today. Such a powerful flow of water with rock materials had a significant erosional impact on dry canyons, potholes, and depressions, but also on large sand and gravel deposits, and on the formation of extensive fluvial landforms (Waitt et al., 2021). However, the flood also shaped depositional terraces made out of unconsolidated sand and gravel. These gently sloping-to-flat terraces are best seen in the eastern part of Portland, at the project site and around it at various elevations (Trimble, 1983).

The Portland geologic map (Figure 98) shows that Eastern Portland has two dominant geologic layers: Missoula Flood deposits and coarse-grained Missoula Flood deposits. The Albina neighborhood project site is located along the contact of two geological layers. The overlaid topography shows the terraces that reach up to 200 feet. The edge of each terrace, before it connects to the riverbed, is quite steep.

However, the Portland geologic simulation map also reveals human-induced processes along the Willamette River that led to significant changes to Portland’s landscape. As the city of Portland grew, wetlands and streams were filled in with sawdust, dredge material, gravel, and even garbage. The artificial fill is shown on the simulation map in pink.

Being situated amid the Willamette and Columbia Rivers, the landscape of Portland was shaped by fluvial processes. The focus in this analysis is on the Willamette River, as the project site is located along this river. The aim is to identify how and to what extent the city was shaped by fluvial processes of erosion and deposition, or whether such processes contributed to the formation of distinct landforms, such as floodplains or terraces. Thus, this section presents an analysis of fluvial processes of the Willamette River, how it changed over time, and what influenced such changes.

The Willamette River in Portland has undergone a range of natural and human-induced changes since the mid-19th century. Natural changes, such as flooding, have played a significant role in shaping the city’s landscape over time. Meanwhile, human changes, including dredging and shoreline extension, have had a profound impact on the physical and environmental characteristics of the area adjacent to the river. In the context of this analysis, hydrological processes are influenced by environmental and human agents (Figure 102). By environmental agents I consider a series of historic flooding and gauge data, while human agents are actions of extending the river shorelines and dredging.

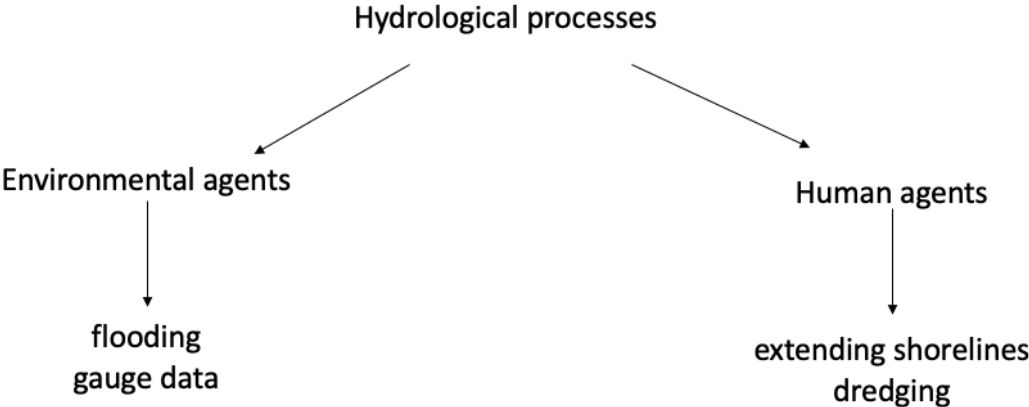


Figure 102. Hydrological processes influenced by environmental and human agents.

4.1.3.1.2.1. Flooding

Willamette River flooding had a profound influence on Portland over its history. The river is prone to seasonal flooding due to heavy rainfall and snowmelt, and these floods have caused significant damage and loss of life in the past, but have also had an impact on the natural environment and human infrastructure.

The Willamette River flooding and gauge simulation (Figure 103) includes NOAA weather data for historic and recent crests (Table 3), covering the period from 1876 to 2019. While the simulation presents the relationship between flooding and the city’s topography, the aim of this simulation is to identify whether the natural process of flooding has shaped the river and adjacent areas, and if so, how. The gauge data location was selected based on the proximity to the Albina neighborhood. The closest gauge data location was the Morrison Bridge. The collected data for each year was translated into 3D Rhino models and later to 3D perspective images, which resulted in a .gif simulation. The resulting 3D simulation helps to track historical river flooding in relation to topography and identify changes over time.

Table 3
Willamette River gauge data (Morrison Bridge gauge)

Historic Flood Crests	
Flood level, in ft	Date
28.20	06/24/1876
27.30	07/01/1880
26.20	06/14/1882
25.70	02/06/1890
33.00	06/07/1894
24.20	06/23/1899
24.00	06/18/1903
24.00	06/13/1913
25.30	01/08/1923
24.40	05/31/1928

Historic Flood Crests	
Flood level, in ft	Date
24.80	06/13/1933
30.00	06/14/1948
24.80	06/26/1950
26.40	06/04/1956
29.80	12/25/1964
23.84	01/18/1974
18.27	12/16/1977
20.10	02/21/1982
28.55	02/09/1996

Note: Major flood stage, 28 ft.; moderate flood stage, 24 ft.; flood stage, 18 ft.; action stage, 17 ft.; low stage, 1 ft. From NOAA, 2019.

The first recorded flood data available from NOAA is dated June 1876, with a Willamette River crest at 28.2 feet. According to the NOAA flood range, a river level higher than 28 feet is categorized as a major flood. Before the construction of upstream dams on the Willamette River and the sea wall in downtown Portland, spring floods were very common. The 1876 3D image shows that water level covers low-lying areas of northwest, downtown, and northeast Portland. Other major floods occurred in 1948, 1964, and 1996. (Willamette River gauge historic crest simulations for each year can be found in Appendix B, Figure 215–Figure 236236.)

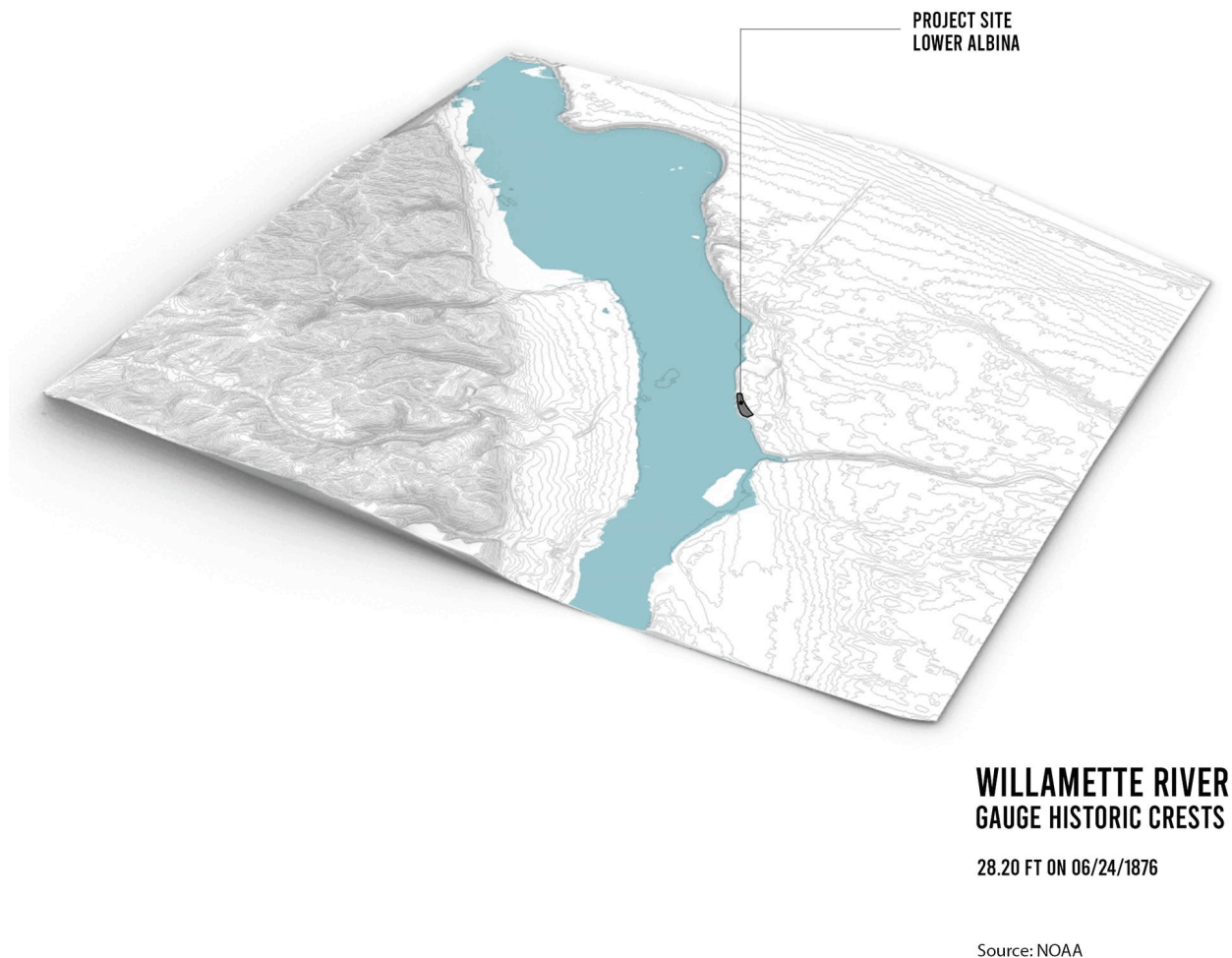


Figure 103. Willamette River flood crests simulation.

The next few historic flood crests fall into the moderate flood category, which is equal to or higher than 24 feet. The 3D images show the extent of Willamette River flooding smaller than the 1876 3D image, but still covering a major part of low-lying areas. Floods reaching 18 feet and higher were less extreme but still had some impact on low-lying areas.

The Great Flood of June 1894 is another historic crest that falls into the category of major flood, when the river crested at 33 feet, the highest stage recorded in the city. It was one of the worst flooding events, with water covering nearly 250 square blocks in Portland. It resulted in damage to public utilities, warehouses, and service docks. The Union Pacific Railroad suspended their service because over 100 miles of track were washed out. This flood affected various communities along the river, causing infrastructure damage and forcing discussion about the need for flood control.

After the 1894 major flood, the crest data shows smaller descents of flooding levels. The 3D images from 1899 shows the river crest at 24.2 feet, from 1903 and 1913 at 24 feet, from 1923 at 25.3 feet, from 1928 at 24.4 feet, and from 1933 at 24.8 feet.

One of the most dramatic transformations to prevent flooding in Portland was the construction of the Portland Harbor Wall in the 1920s. The wall was built in front of the docks and buildings, which shifted the west edge of the river 50 feet eastward. A series of dams and channels on the Willamette River were built from the 1940s to 1960s by the U.S. Army Corps of Engineers. The purpose of the dams was primarily flood control, water storage, and power generation (Kline & Bahus, 1999).

In May 1948, a major catastrophic flood, also known as the Vanport Flood, occurred due to heavy rainfall and snowmelt, leading to the collapse of a railroad berm that formed a dike holding back the Columbia River. The Vanport area, a low-lying housing development north of Portland, was devastated as the floodwater breached the dike, causing extensive damage, death, and displacement of those who survived. The Willamette River crested at 30 feet in June 1948 at the Morrison Bridge gauge. The 1948 3D images show that the water level covers topographically low-lying areas. The historic flood of 1948 was a catastrophic event that caused widespread damage and loss of life in the Portland area. Since then, there have been a number of efforts to improve flood control measures, including the construction of new levees and the implementation of early warning systems to alert residents and businesses in the event of a flood.

Although the Willamette River was controlled by a series of dams and barriers, it continues to experience flood events. The flooding events following the 1948 flood fall into the moderate flood category. The 1950 3D image shows the river crest at 24.8 feet, and the 1956 3D image at 26.4 feet. The water level extends along low-lying areas.

Another historic major flood occurred during the Christmas season of 1964, when the Willamette River crested at 29.8 feet. The flood was caused by a series of intense storms that brought heavy rains and warm temperatures, which led to snow melting in the Cascade Range. The 1964 3D image shows the extent of water almost identical to the one in the 1948 flood event. The floodwater overwhelmed other rivers in Oregon and led to deaths, destruction of homes, numerous landslides, and road collapses. After the 1964 flood, the U.S. Army Corps of Engineers added four more flood control dams to the Willamette River.

The historic crests after the 1964 Christmas flood show decreases in water levels. The 1974 3D image shows the river crested at 23.84 feet, the 1977 3D image at 18.27 feet, and the 1982 3D image at 20.10 feet. Such flood levels fall into the category of flood stage, which is equal to or higher than 18 feet.

The most recent major flood occurred in February 1996, with a river crest at 28.55 feet. The flood was a culmination of unusual weather events, such as abnormal precipitation in fall and winter, tremendous amounts of snow in late January, and strong subtropical warm temperature and heavy rain that caused rapid snowmelt. The 1996 3D image shows the extent of water almost similar to the 1964 flood, covering major parts of low-lying areas. The 1996 flood renewed the discussion about the existing flood control measurements and the need for further improvements.

While each flood had a lasting impact on the region's landscape and communities, the most devastating were the Willamette River floods of 1894, 1948, 1964, and 1996. Each major flood was followed by decisions that transformed the river to make adjacent neighborhoods less vulnerable to flooding. Over the years, Portland implemented different strategies, including the construction of dams, a harbor wall, flood management techniques, and improved forecasting systems, to mitigate the impacts of flooding along the river. River dredging (discussed in the following sections) also minimized the effect of flooding events, as the river became deeper over the time.

4.1.3.1.2.2. Shoreline Extension

Historically, the Willamette River consisted of shallow braided channels across a floodplain (Robbins, 2023). Native nations that inhabited the area did not significantly alter the river. The alteration of the river's banks began in the 1840s with the arrival of the first settlers, who over time transformed the city into the port town.

The Willamette River simulation (Figure 106) includes data from USGS topographic maps of 1897, 1940, 1954, 1961, 1975, 1990, 2011, 2014, 2017, and 2020 (Figure 104) and aims to track changes over 120 years up to the present time and identify what influenced such changes. The collected data was translated into 2D AutoCAD drawings (Figure 105), later into 3D Rhino models, and, finally, to 3D perspective images, which resulted in a .gif simulation. The simulation provides a record of the city's topography and historical configurations of the

Willamette River and adjacent water features. (Simulations of the Willamette River for each year can be found in Appendix B, Figure 237–Figure 246).

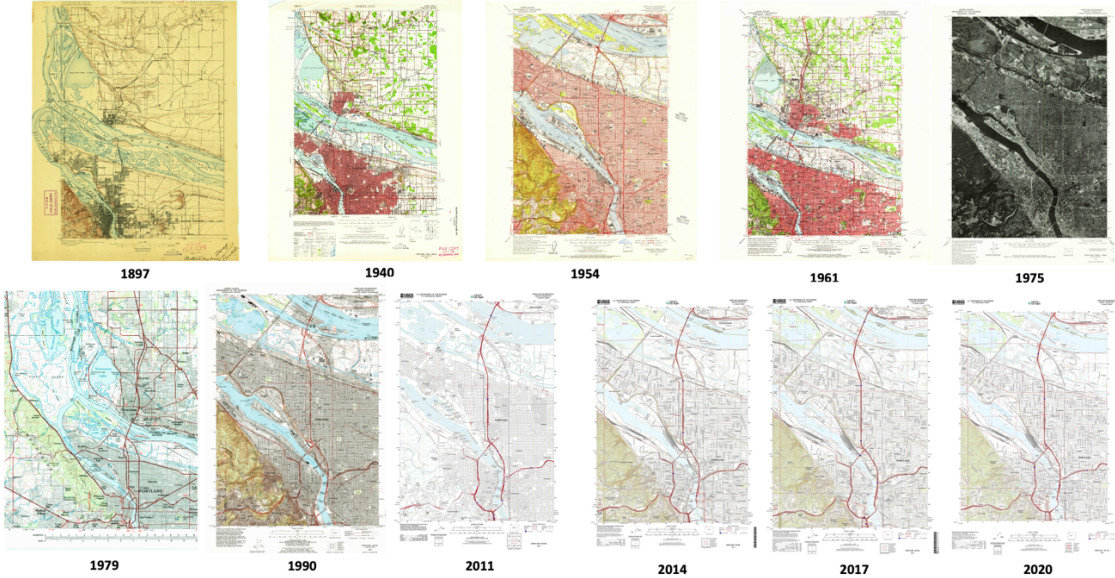


Figure 104. USGS topographic maps of 1897, 1940, 1954, 1961, 1975, 1990, 2011, 2014, 2017, and 2020. From USGS.

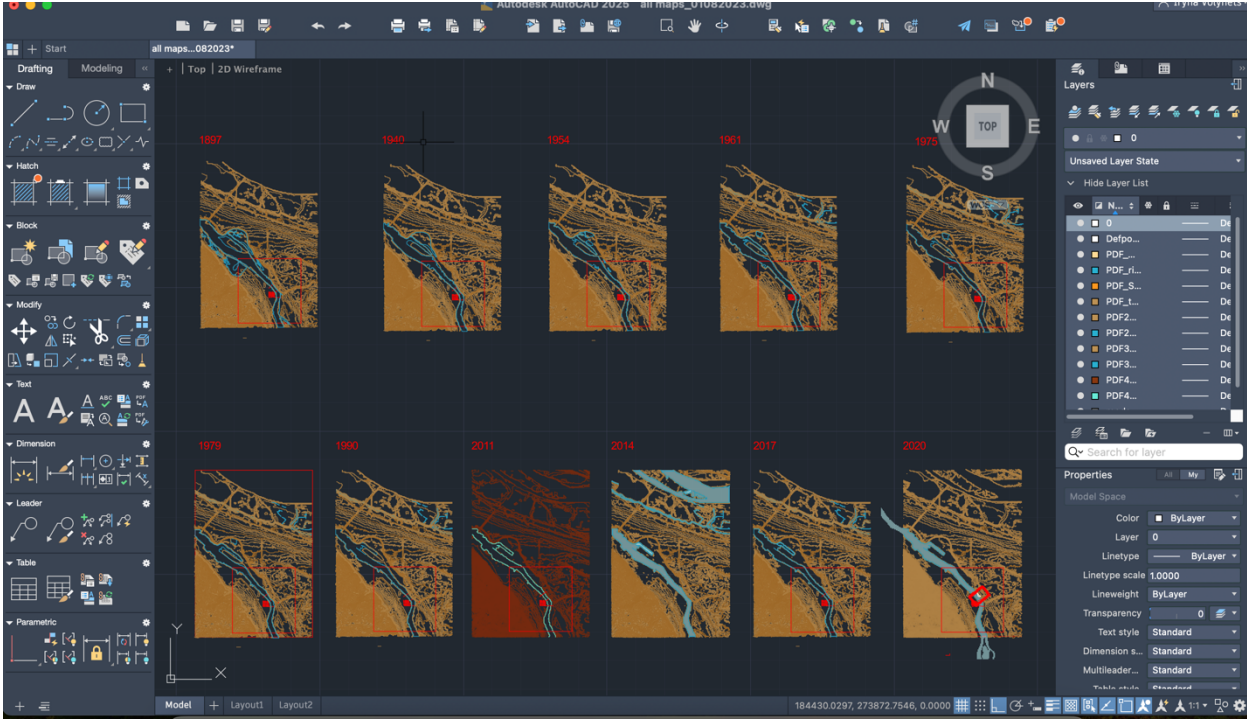


Figure 105. AutoCAD 2D drawings of the city.

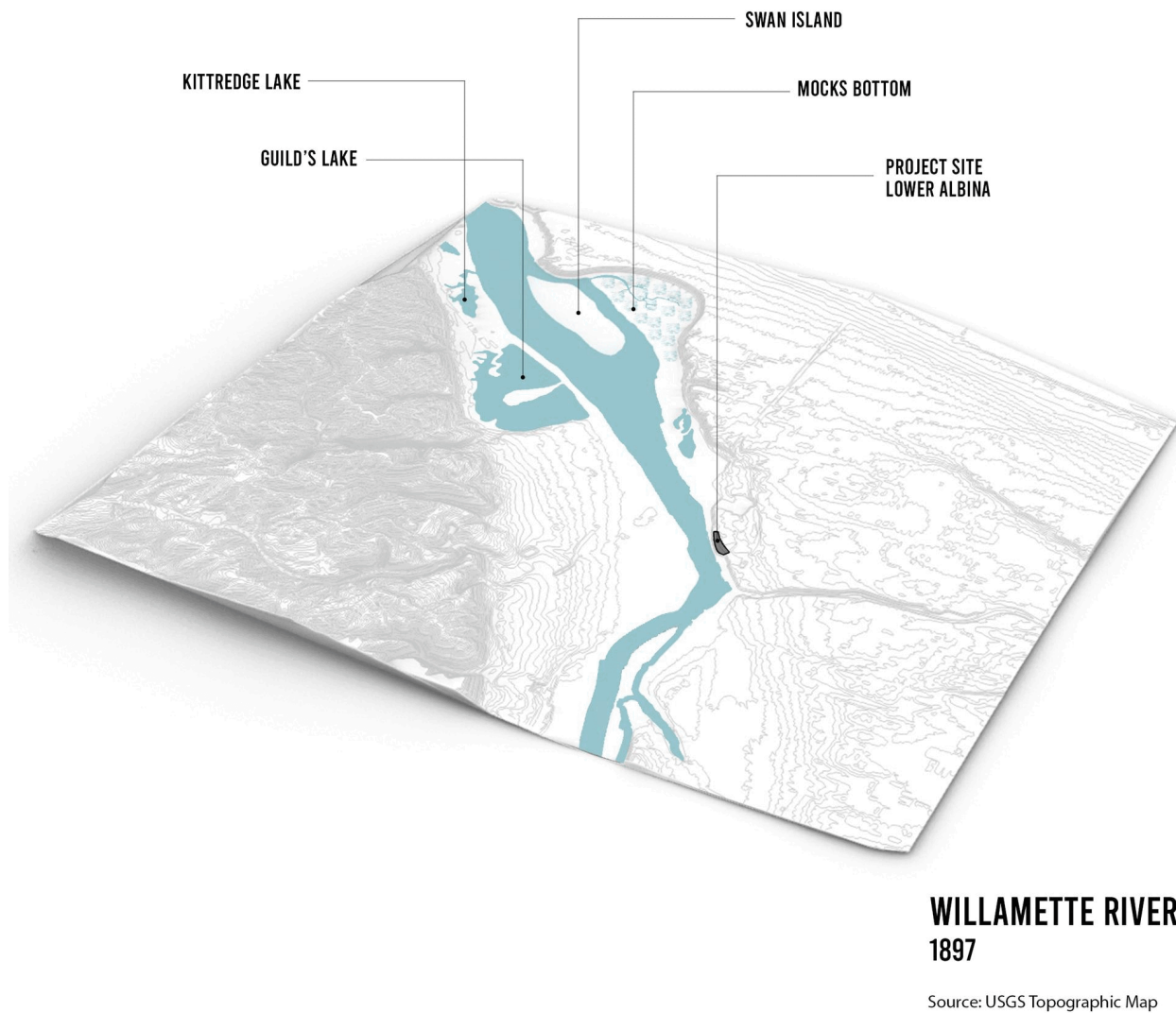


Figure 106. Willamette River simulation.

The 1897 3D image of Portland shows the Willamette River as a wide river with adjacent water features. The topography of the map, along with riparian zones, suggests that low-lying areas along the river were typically flooded over different times of the year. On the west side of the river's bank, in the northwest part of Portland, a series of small streams flow from the hills. However, the most significant water features in northwest Portland were Kittredge Lake and Guild's Lake, the crescent-shaped marsh (Dibling et al., 2006). In the middle of the Willamette River is Swan Island, an island that separates the Willamette River into two channels. The channel to the west side of the island was shallow and wide, while the channel to the east side

was the river's main connection. On the east side of the river's bank, in the northeast part of Portland, a tributary channel and other small water features are connected to the wetland area, called Mocks Bottom. Moving down the image, there is also a small stream in the Lower Albina neighborhood that connects to the Willamette River. Where the Willamette River makes a northwesterly turn, there is Sullivan's Gulch, a series of waterfalls, and a spring-fed pool. In the very bottom of the image, the river braids and creates an additional channel.

The 1940 3D image shows a significant transformation of water bodies along the Willamette River. As the city grew, the major wetlands and other water bodies along the river were filled with sawdust, dredge material, and even garbage, leading to significant changes in the river's landscape and its use for industrial purposes. Additionally, buried streams and lakes, such as Tanner Creek that once flowed across the downtown area, were diverted into the sewer system and filled for urban development.

Contrary to the 1897 3D image, this image no longer includes Kittredge Lake, Guild's Lake, and small streams in the northeast part of Portland. Guild's Lake, a cut-off meander of the Willamette River that was once an important water feature of the Lewis and Clark Exposition, was filled for industrial uses, which reflects the extensive artificial alterations of the river and adjacent low-lying areas. In the 1920s, the Port of Portland filled in the 250-acre Guild's Lake with silt from the Willamette River. Later, the Northern Pacific Terminal Company established a railway yard on filled land (Tucker, 2024). Another significant alteration to the west bank occurred in the 1920s with the construction of the Harbor Wall, which shifted the river's edge eastward by 50 feet and destroyed the city's historical waterfront. The further growth of the city, especially after the consolidation of Portland and Albina in 1891, led to the filling of low areas and sloughs.

However, the most significant transformation occurred to Swan Island. Some portions of the island were filled for industrial uses. In 1927, the Port of Portland received permission from Congress to connect Swan Island to the mainland, where the Port developed a large airport. This change shifted the historical location of Swan Island by connecting it to the east bank of the Willamette River.

Similar transformation also occurred in Northeast Portland, where parts of Mocks Bottom are no longer seen on the image. In 1920, the Portland City Council and city mayor recommended that Mocks Bottom be filled for industrial development (MacColl, 1979). In 1958,

the Port of Portland purchased Mocks Bottom for the development of an industrial park (McArthur & McArthur, 2003). In addition, the small stream in the Albina neighborhood is no longer present on the image; instead, the area is transformed into residential development. The location of the Willamette River in the Lower Albina area near the project site did not change compared to the previous 1897 image. The Sullivan's Gulch waterfalls and pool became significantly smaller compared to the previous image. The very south part of the image no longer shows the braided channel; instead, the area is used for development. However, in this specific part, the river channel is shown slightly bigger compared to the previous image.

The 1954 3D image shows more shoreline extensions on the west and east banks of the Willamette River. The transformation of the northwest shoreline was due to the development of the oil refinery and Portland Terminal No.1. During WWII, the military port facilities expanded by using dredged sand from the Willamette River, which shifted the shoreline eastward. The outline of Swan Island was altered as well, as during WWII it served as a shipyard. The channel between the island and the east side of the river was called Swan Island Basin. The northeast shoreline was also transformed due to the growing industrial needs. The Mocks Bottom area still shows some wetlands and a new water feature that was formed between railroad lines. The Albina neighborhood shoreline was transformed due to the development of the Albina railroad yard. However, the area near the project site did not change compared to the previous image.

The 1961 3D image shows more shoreline extension in the northwest industrial part of Portland. The south inland connection of Swan Island becomes bigger and wider, cutting out part of the river shoreline. In the northeast part of Portland, the Mocks Bottom area disappears completely.

The 1975 and 1979 3D images show little shoreline extension in the northwest part of Portland. The Lower Albina site did not change compared to the previous image. The south part of the image, after the river makes its turn, shows shoreline extension on both riverbanks.

The 1990 3D image shows some shoreline extension along the northwest part of Portland and south part of the river. In addition, the end part of the Swan Island Basin disappears, which suggests that it was filled in.

The 2011, 2014, 2017, and 2020 3D images show no significant transformation to the Willamette River, which suggests that there were no additional alterations to the river shorelines.

The 3D simulation reveals that the Willamette River narrowed down and changed its natural shape due to industrial growth of the city and intensive development of the shorelines. Even though the initial hypothesis was that natural processes of erosion and deposition influenced the shape of the river, it was not supported by this analysis. Instead, the simulation reveals that artificial alterations of the river were more transformative and consistent than natural alterations. Also, the Lower Albina area and the project site are located where the Willamette River makes a northwesterly turn. The initial hypothesis was that due to the turn of the river, this part of the shoreline eroded over time; however, it was not supported by the analysis. Instead, the river shoreline along the Lower Albina barely changed over 120 years of Willamette River history. This finding suggests that topographically higher sites, such as Lower Albina, were not influenced by fluvial processes, while low-lying areas that were prone to river flooding changed dramatically over time. The findings also suggest that the Lower Albina is less prone to erosion, possibly due to more consolidated flood deposits.

4.1.3.1.2.3. Dredging

One of the most significant human-induced changes along the Willamette River in Portland has been dredging, which involves removing sediment from the riverbed to deepen the channel for navigation purposes. The history of dredging in Portland is intertwined with the city's economic and infrastructural development. Dredging has been a key factor in the development of the river as a major transportation route, but it has also altered the river's natural flow and ecology.

The Willamette River bathymetry simulation (Figure 108) includes GIS data available only for 1888 and 2005 (Figure 107); however, even such a narrow data range shows the transformation of the river over time. The aim of this simulation is to identify what influenced such extensive changes of the river's bathymetry and whether it was only the result of artificial activity. The GIS data was downloaded to 2D AutoCAD drawings, later translated into 3D Rhino models, and, finally, to 3D perspective images, which resulted in a .gif simulation. The simulation provides a record of the river's bathymetry. The proposed 3D modeling and analysis method helps to track river changes in relation to topography and identify what influenced changes over the time.

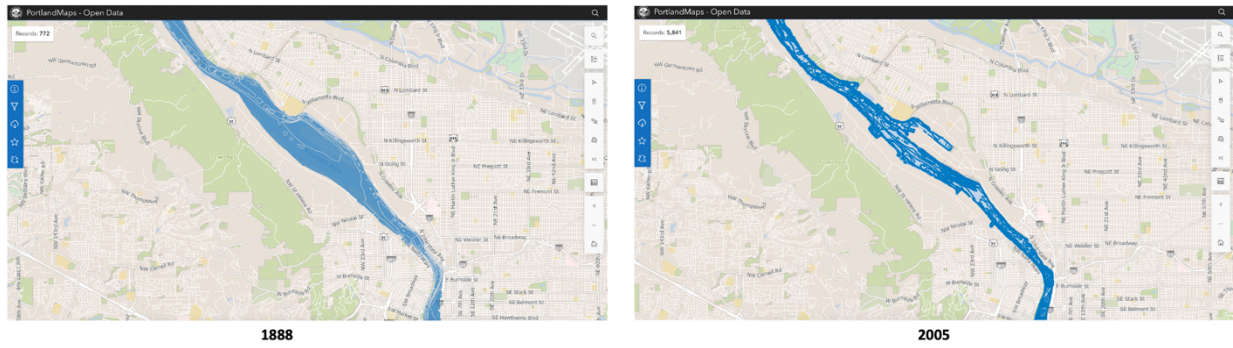


Figure 107. Willamette River bathymetry data, 1888 and 2005. From GIS.

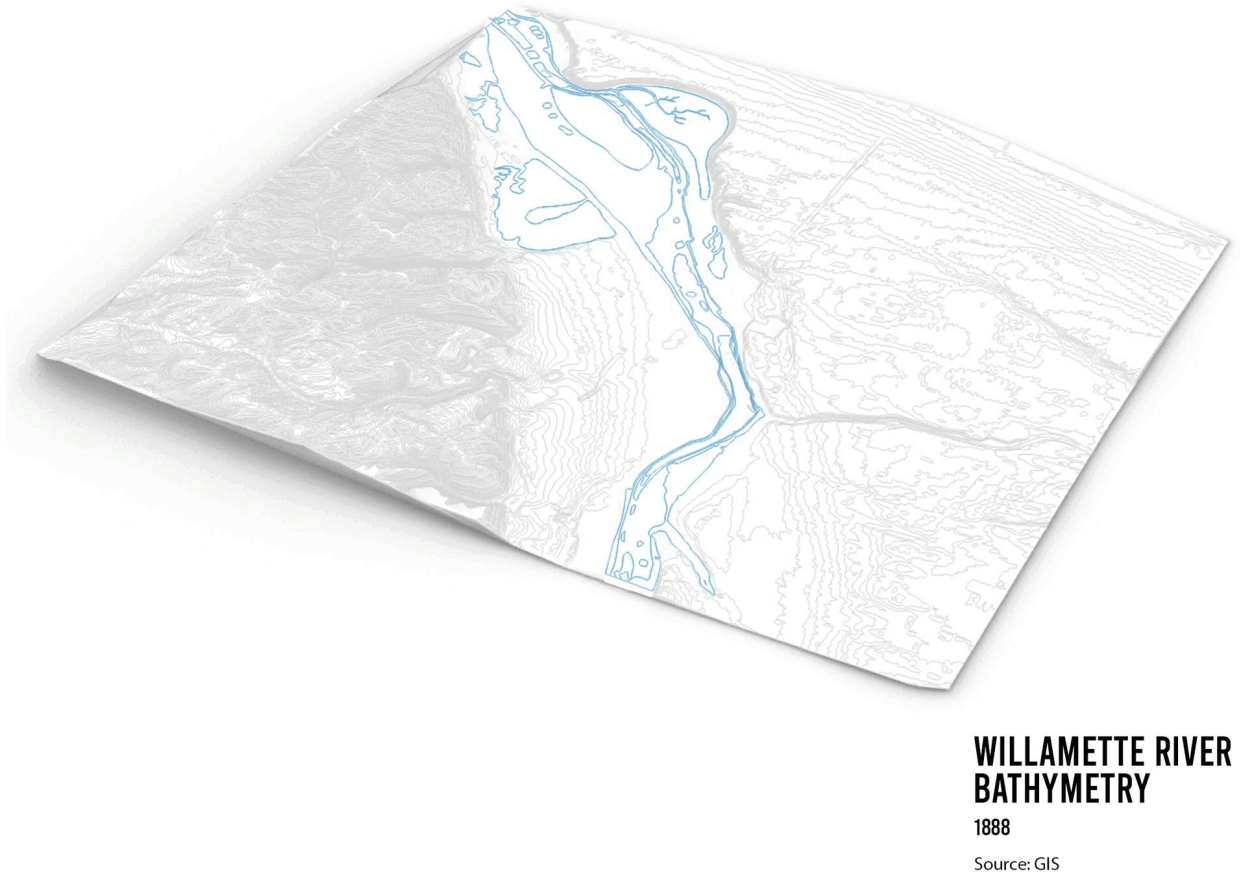


Figure 108. Willamette River bathymetry simulation.

The 1888 3D image (Figure 247 in Appendix B) shows the Willamette River at its historical shape and its adjacent streams, wetlands, and other water bodies, with a maximum river depth at 18 feet.

In 1891, the city recognized the crucial role of transportation infrastructure in facilitating trade through Portland. The Oregon Legislature established the Port of Portland with a goal to deepen the Willamette River to 25 feet, making Portland the second largest port on the West Coast after San Francisco (Port of Portland, n.d.).

In the early 1920s, dredging activities were not limited to improving the river as a navigation channel; the river bottom was shaped in a way to accommodate large ships. The massive dredging processes dramatically changed the river and shaped new areas. This process shifted the river channel, using dredge material to fill sections of the river. It also reshaped the surrounding landscape. Swan Island was connected to the inland area, Guild's Lake was transformed into an industrial area, and Mocks Bottom was repurposed as port facilities.

The 2005 3D image (Figure 248 in Appendix B) shows the current state of the Willamette River at a depth of 40 feet, with a channel suitable for port infrastructure. The river changed dramatically over time, and dredging was the main force in shaping the city's topography and bathymetry.

The process of dredging in Portland was a strategic planning approach to shape the river for navigation and infrastructural development; however, it had an influence not only on the city's economic growth, but also on the physical appearance of the river and adjacent water features. While significant parts of the river shorelines were transformed, the simulation also reveals that the area in close proximity to the project site in Lower Albina was not significantly altered by artificial dredging processes, either horizontally or vertically. This finding suggests that this area was left intact due to its higher elevation, while natural river dynamics, such as erosive force at the riverbend, may have maintained sufficient depth and reduced the need for dredging.

4.1.3.1.3. Vegetation Processes

Portland's climate and topography play a significant role in shaping the vegetation. The region experiences distinct seasons, including wet winters and dry summers. The topography, characterized by hills, valleys, and proximity to water bodies, creates a diverse microclimate that influences the types of vegetation that are dominant in the city. The focus in this analysis is on the city's vegetation. The aim is to identify what influences vegetation processes, and how these

processes shaped the city’s landscape. Thus, this section presents an analysis of vegetation processes, how it changed over time, and what influenced such changes.

Portland’s vegetation reflects a complex interplay between environmental factors and the consequences of human activity. The vegetation of Portland is influenced by environmental and human agents (Figure 109). This analysis considers that vegetation is tied to topography; thus, topography is the key natural agent that affects drainage and exposure to wind and sunlight. Key artificial agents are the removal of riparian areas and loss of vegetation due to urban development.

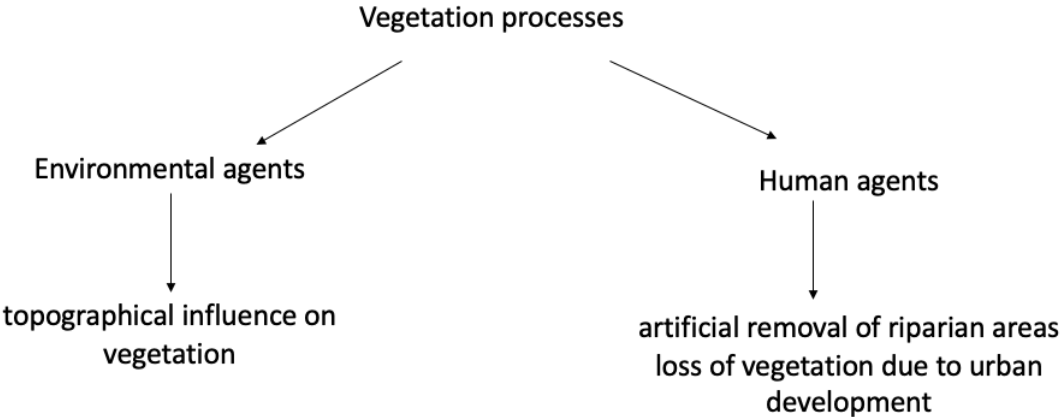


Figure 109. Vegetation processes influenced by environmental and human agents.

The vegetation simulation (Figure 113) includes satellite data from Google Earth, Oregon State Aerial Imagery, and Portland Maps Advanced available for 1951, 1970, 1975, 1990, 1994, 2000, 2011, 2014, 2017, and 2020 (Figure 111). The aim of this simulation is to identify what influenced vegetation changes over time. As shown in the workflow process in Figure 110, the satellite data was analyzed in Photoshop (Figure 112), later translated into regions to 3D Rhino models and, finally, to 3D perspective images, which resulted in a .gif simulation. The simulation provides the record of historical vegetation up to the present time. This 3D modeling and analysis method helps to track vegetation changes in relation to the city’s topography and identify what influenced changes over time. (Vegetation simulations for each year can be found in Appendix B, Figure 249–Figure 258).



Figure 110. Workflow process.

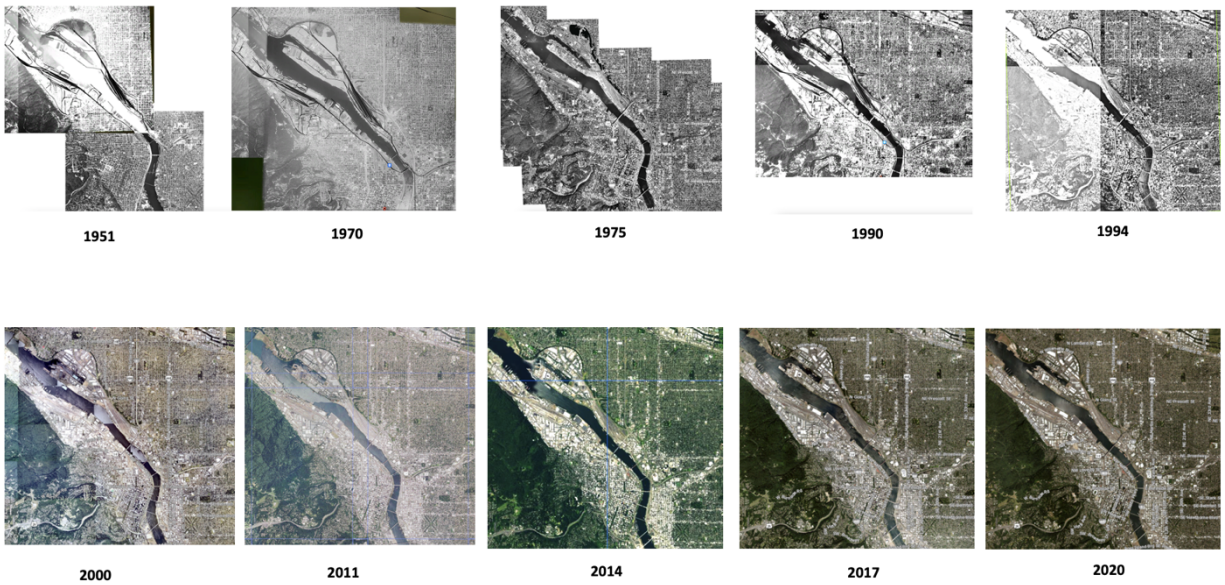


Figure 111. Satellite maps for 1951, 1970, 1975, 1990, 1994, 2000, 2011, 2014, 2017, and 2020.
From Google Earth, Oregon State Aerial Imagery, and Portland Maps Advanced.



Figure 112. Analyzed data in Photoshop.



Figure 113. Vegetation simulation.

The historic Portland vegetation managed by Native nations included a mix of riparian areas, prairies, and upland forest (Christy & Alverson, 2011). These ecosystems provided habitat stability, supported biodiversity, and regulated local microclimates. The arrival of the first settlers in the 1850s marked a significant turning point in vegetation patterns, as land was cleared for agriculture, industry, and urban expansion, leaving behind mud and stumps. Urbanization and the city's industrial growth led to the clearing of land, removal of prairie, and disruption of natural vegetation patterns and ecological connectivity. After the clearcutting, communities started to replant trees, but without comprehensive planning.

In 1903, the Olmsted firm proposed a comprehensive plan for tree planting and management of trees in public rights-of-way (*Report of the Park Board*, 1904). However, the

city failed to adopt the plan. In 1912, the city attorney placed the responsibility of maintaining street trees on property owners (Hedberg, 2020). This resulted in an unequal distribution of trees across the city: wealthier neighborhoods maintained large trees, while lower-income neighborhoods with smaller planting strips, such as Albina, struggled to maintain and keep trees.

The analysis of historical satellite images and the resulting 3D vegetation simulation illustrate the above transformations. The 1951 3D vegetation image reflects the processes that had been happening along the Willamette River at that time. The low-lying areas along the east side of the river were mostly riparian forests. However, due to industrial growth, riparian forests along the Willamette River were cleared. The simulation image shows remnants of riparian vegetation at Mocks Bottom. The removal of riparian areas had negative consequences, as it reduced the ability to slow floodwater. The 3D image also shows clustered vegetation along the edge of geomorphological terraces, indicating that higher elevations with well-drained soils had more stable conditions for tree growth. Moving eastward, the upland forest aligns with the residential pattern of streets and houses, as trees were preserved along property boundaries and roadways. The vegetation along the residential development formed linear vegetation corridors that follow the pattern of the built environment.

The 1970 and 1975 3D images show less riparian vegetation at the Mocks Bottom area. The clustered vegetation along terraces on the east side of the river is still present; however, the amount of vegetation in the Lower Albina area is less compared to the 1951 3D image. The amount of vegetation in residential areas further east is reduced. The changing pattern in vegetation illustrates a process of natural decline. As trees matured, they showed signs of decline and caused significant damage to sidewalks and curbs. Under city policy, the owner of the adjacent property was responsible for maintaining trees. Albina's residents prioritized repairing their houses and property rather than taking care of trees (Hedberg, 2020). Additional analysis of the 3D simulation suggests the influence of urbanization on vegetation. The white scars on images show how the construction of Interstate 5 resulted in clear-cut corridors and fragmented existing vegetation. Also, the empty white area near the project site shows how the construction of large-scale urban projects, such as the Veterans Memorial Coliseum, affected the vegetation loss. In the 1960s, a pioneering community-led initiative, the Albina Neighborhood Improvement Program (ANIP), was developed to address urban deforestation issues. In 1962, the program initiated a full inventory of trees in the Albina neighborhood and noted that 173

trees needed removal. From 1963 to 1968, nearly 500 trees were planted in parking strips, including 295 trees of the popular Kwanzan Flowering Cherry tree. The final report indicates that nearly 1,115 trees were planted in the Albina neighborhood.

The 1990 3D image shows almost no riparian vegetation left at the Mocks Bottom area. The clustered vegetation along the terraces in the Albina neighborhood is decreased compared to the 1970 3D image. The overall vegetation pattern from single dots of trees in residential areas changes to groups of trees with empty space around, which indicates the success of the ANIP urban reforestation initiative. The vegetation scar from Interstate 5 is more clear and distinct. The area near the project site has very little vegetation compared to all previous years.

The 1994 3D image shows similar vegetation patterns to the 1990 3D image; however, the density is slightly greater, which indicates that trees planted as a part of the ANIP initiative had matured. The 2000 3D image shows the growth of vegetation density. The 2011, 2014, 2017, and 2020 3D images do not show significant changes in vegetation patterns; however, they represent the growth of vegetation density over time. The change might be a result of urban greening and tree planting initiatives to restore green spaces.

The vegetation processes in Portland have been shaped by environmental and human agents. The historical and current vegetation processes in Portland influence the microclimate of the specific region. Even small microclimate changes and distribution of vegetation could impact the temperature and precipitation patterns, but also shift vegetation types. The removal of riparian forests reduced shading and moisture retention, leading to temperature fluctuations and issues contributing to the urban heat island effect. The loss of tree cover in residential areas changed wind patterns and increased the exposure of the neighborhood to strong winds. In contrast, the increase in tree density suggests the success of urban reforestation initiatives. Such efforts led to improvement in urban cooling and increased biodiversity of the area. Understanding historical trajectories of vegetation processes is crucial for future design interventions. The relationship between the topography, urban expansion, and ecological restoration efforts highlight the importance of vegetation in environmental resilience.

4.1.3.2 Neighborhood Scale

The neighborhood scale is the next level of analysis to understand how natural processes have shaped the area slightly bigger than the research site to its current conditions. The

neighborhood-scale site analysis also consists of modeling geomorphological, hydrological, and vegetation processes. While the city-scale processes involved analysis of processes on a larger scale and involved patterns of urbanization, regional infrastructure, and policy-driven development, the neighborhood scale focuses on localized changes, such as zoomed-in morphological changes, land-use shifts, and environmental impacts.

Each process in this analysis is influenced by natural (nonhuman) and artificial (human) agents (Figure 114). In this case, natural agents are topography, vegetation, and the local microclimate. The artificial agent, on the contrary, is the process of urbanization that is followed by additional transformations. This analysis becomes a record of historical events and processes with a zoomed-in view of the neighborhood area.

The hypothesis of the neighborhood-scale analysis is that the process of urbanization had the biggest influence on geomorphological, hydrological, and vegetation processes and influenced the changes in the area over time.

For neighborhood-scale analysis, 3D simulation is also the main tool to collect and analyze information, and make assumptions about the site. The major difference in 3D simulation on this scale is that collected data is from different sources, and the level of detail is more precise compared to the city scale. The neighborhood simulation helps to track historical changes of the area up to the present time.

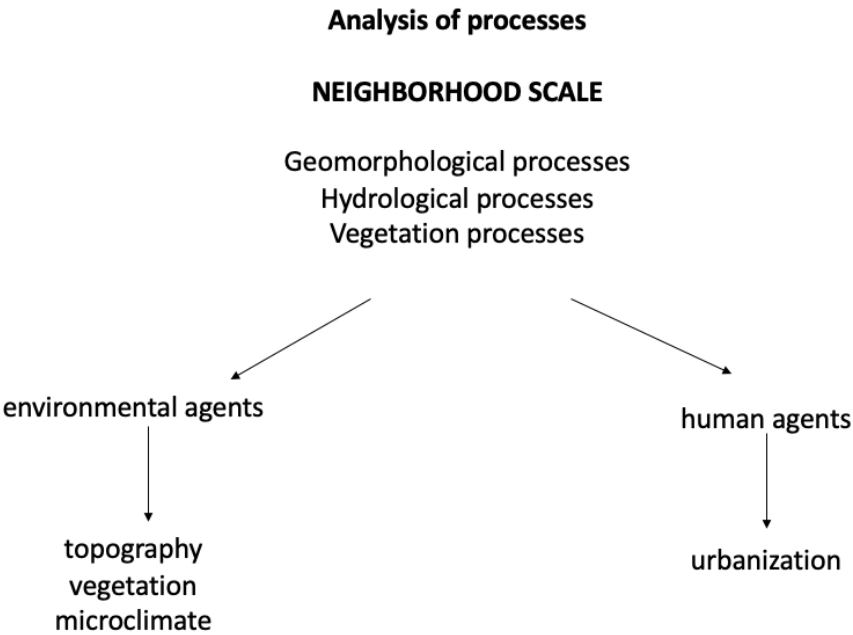


Figure 114. Analysis of processes on the neighborhood scale.

The Albina neighborhood went through significant transformations over its history. The construction of Interstate Avenue, the Veterans Memorial Coliseum, the Moda Center, and the development of Interstate 5 played a significant role in Albina’s transformation from a residential to a civic neighborhood in Portland. While these infrastructural projects were part of the urban renewal plan, they led to the destruction of housing, population decline, spatial disconnection between different parts of the neighborhood, and lost connection to the riverfront.

The Albina neighborhood simulation (Figure 118) includes data from Google Earth satellite images and aerial photos from 1948, 1960, 1975, 1990, 2011, 2014, 2017, 2020, and 2023 (Figure 116). The aim of this simulation was to identify how environmental processes and human activity have shaped the site. As shown in the workflow process in Figure 115, the collected data from aerial images were translated into 2D AutoCAD drawings (Figure 117), later into 3D Rhino models, and, finally, to 3D perspective images, which resulted in a .gif simulation. The simulation presents the historical record of the city’s topography, Willamette River changes, and vegetation changes. The simulation reveals how the process of urbanization changed the neighborhood. (Lower Albina neighborhood simulations for each year can be found in Appendix B, Figure 259–Figure 267).



Figure 115. Workflow process.

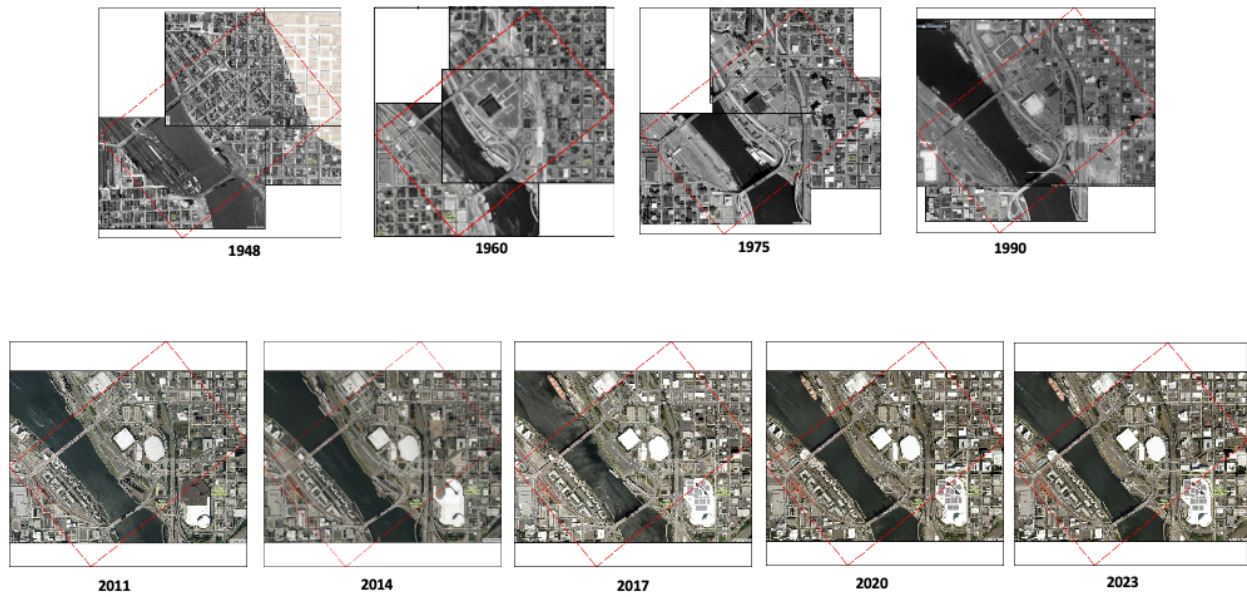


Figure 116. Aerial photos from 1948, 1960, 1975, 1990, 2011, 2014, 2017, 2020, and 2023. From Google Earth satellite images and University of Oregon Knight Library aerial maps reserves.

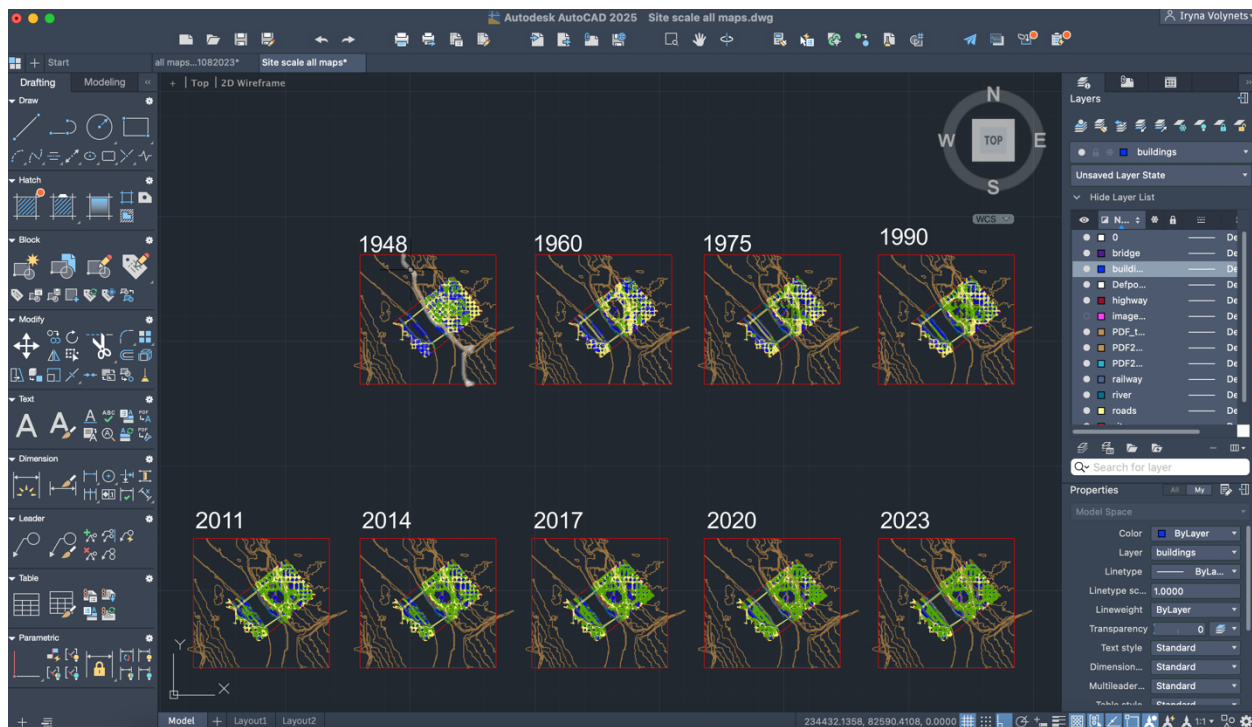


Figure 117. AutoCAD 2D drawings of the neighborhood.

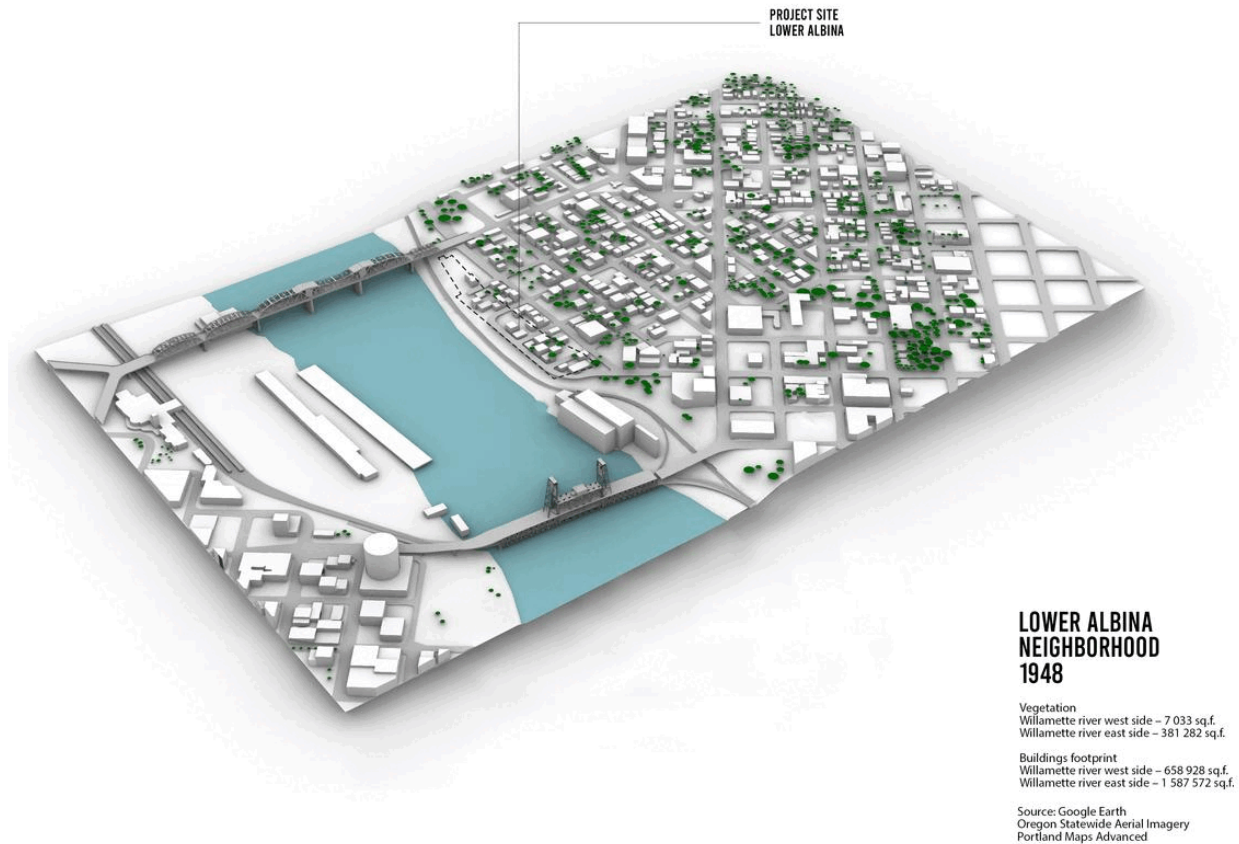
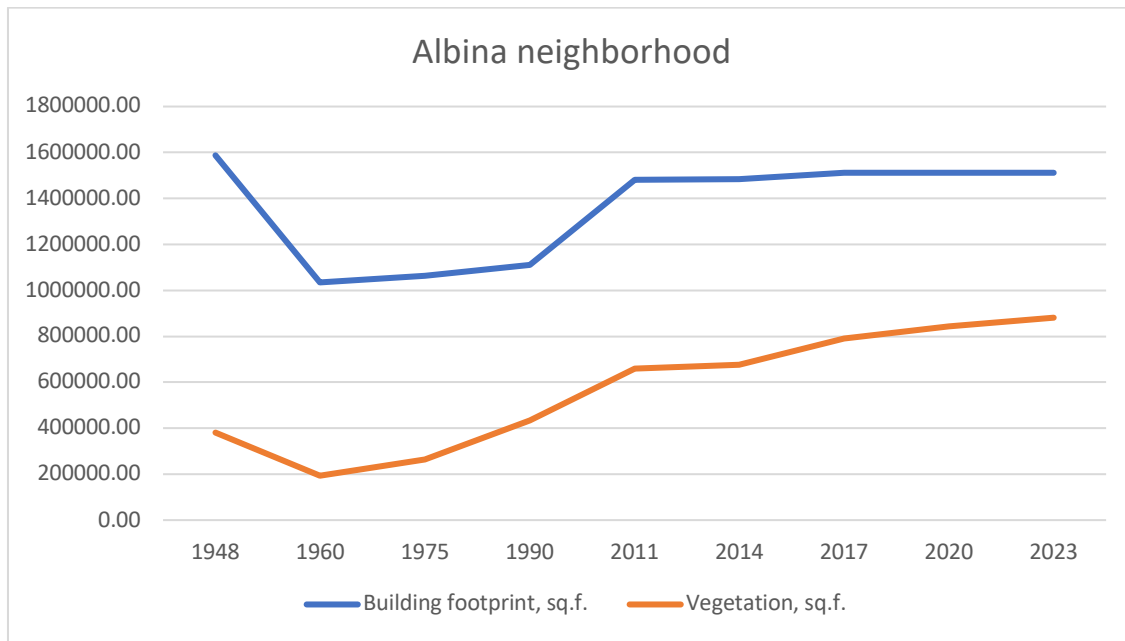


Figure 118. Albina neighborhood simulation.

In addition to the Albina neighborhood simulation, it was possible to quantitatively calculate building footprint area and vegetation area for different years. The calculation was based on AutoCAD 2D data. The quantitative building footprint and vegetation results are presented in Scheme 1. Such data results help to estimate what year the changes to the built and natural environments have happened and identify the reason for such transformations.



Scheme 1. Albina neighborhood building footprint areas vs. vegetation area.

The 1948 3D image shows Albina as a dense residential neighborhood with a gridded street network and railway line along the water’s edge. The streets follow terrain contours rather than altering the terrain. The vegetation occurs between residential buildings in a 1:4 proportion (vegetation area to building footprint area), based on the chart information. The neighborhood has access to the riverbank.

In 1950, the Oregon State Highway Department built Interstate Avenue along the Willamette River. Due to this construction, the line of houses along the river was demolished, along with adjacent streets.

The 1960 3D image shows significant transformation of the area from residential neighborhood to a large-scale sport and entertainment area. These transformations were the result of the construction of Interstate Avenue, demolition of a large area of residential buildings and roads, construction of the Veterans Memorial Coliseum, and start of the Interstate 5 highway construction. The grid of residential streets was destroyed by two highways and a parking lot for the Veterans Memorial Coliseum. As a result of such transformations, the Albina neighborhood was cut off from the riverfront. The construction of Interstate Avenue and Interstate 5 created physical barriers for vehicular and pedestrian access to the riverfront. The construction of large event spaces and parking lots further limited public access to the river. Such disconnection

limited recreational opportunities, changed the neighborhood's relationship with the landscape, and resulted in social and economic isolation. Due to extensive demolition and infrastructural construction, the building footprint area decreased by approximately 35%, and the vegetation area decreased by almost 50% due to changes in land use and the demolition process.

The construction of the Veterans Memorial Coliseum, completed in 1960, contributed to a major transformation of the area. The development of such a large-scale project led to another wave of clearance of existing structures and businesses, which led to the displacement of Albina residents. While the Coliseum brought cultural and entertainment opportunities to the city, it also represented a form of spatial disruption of the existing sociocultural fabric of the neighborhood. The impact was particularly devastating for the African American residents. Albina was historically home to the African American community that already faced housing discrimination and exclusion. The displacement not only forced families and businesses to relocate but also erased social connections and economic foundations of the neighborhood.

The construction of Interstate 5 in the 1960s required significant topographical changes, which made the highway one of the most dominant artificial landforms in the neighborhood. By cutting through the heart of the neighborhood, the highway physically divided Albina and cut off its connections with adjacent neighborhoods. Another wave of demolition also resulted in the displacement of African Americans, which led to the disruption of closely related communities and lasting social, cultural, and economic impacts.

The 1975 3D image shows the further transformation of the Albina neighborhood. Contrary to the 1960 3D image, the 1975 3D image shows a completed Interstate 5 highway with adjacent exits and streets. While the building footprint area increased by 3%, more residential buildings were demolished and replaced by public buildings. The vegetation area increased by approximately 37% due to urban greening initiatives around the newly built areas. The result of ODOT's highway construction was the isolation of remaining parts of the neighborhood and population decline.

The 1990 3D image shows less residential development; however, the simulation shows some new public buildings. Based on the analysis, the building footprint increased by 5% and vegetation increased by 64% due to natural growth.

The 2011 3D image shows another wave of Albina neighborhood transformation. The construction of the Moda Center, completed in 1995, was followed by the construction of

parking garages, changes in street layout, and construction of a MAX public transit line (Portland.gov, 2024). Based on the analysis, the building footprint increased by 33% and vegetation increased by 50% due to urban greening initiatives and natural growth. By 2011, the Albina neighborhood was completely transformed from a residential area to a site with two major sport facilities.

The 2014, 2017, 2020, and 2023 3D images show little to no transformation to the built environment and the Willamette River; however, the simulation shows the vegetation canopy grew by 33% over 10 years. Over time, the vegetation canopy increased due to urban greening efforts and natural growth. The growth of the vegetation cover contributed to improved air quality. While in theory such a change should also contribute to enhanced public areas, this was not the case for the Albina neighborhood, as the area was spatially segregated. Considering the transformation of Albina from residential into commercial and entertainment area, the change in the vegetation cover had a short-term influence on visitors rather than residents, whose numbers had already declined due to the series of displacements.

The Albina neighborhood gauge historic crests simulation (Figure 119) presents additional information about how the gauge historical crests affected the neighborhood and project site. The simulation creates an overlay of NOAA historic crests data (Table 3) and makes it possible to track changes over time. The simulation is a zoomed-in version of historic crest simulations presented above, with greater attention to details. (Lower Albina historic crest simulations for each year can be found in Appendix B, Figure 268–Figure 279).

The gauge simulation shows how seasonal and major flooding affected the area. Based on the analysis, the east side of the Willamette River was less flooded than the west side. The simulation shows that water levels did not reach buildings and other facilities. The major flood levels only covered the railway line, which is the lower part of the geomorphological terrace. This suggests that the topography of the area prevents floodwaters from reaching the buildings. The location of the railway made it more vulnerable to flooding, while higher elevations were protected.

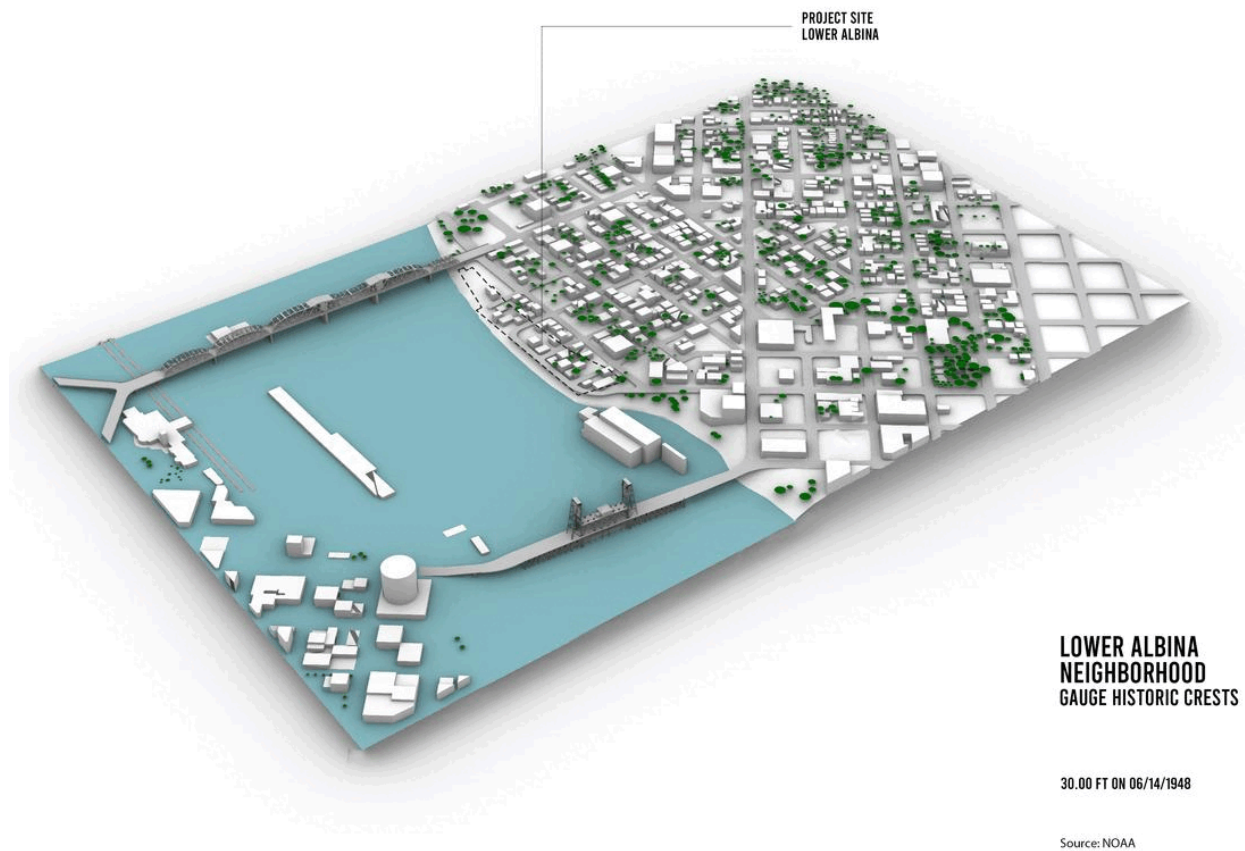


Figure 119. Albina neighborhood gauge historic crests simulation.

The initial hypothesis that the biggest influence on the neighborhood was the process of urbanization rather than any natural process was confirmed.

The result of the infrastructural and urban renewal projects in the Albina neighborhood was the spatial segregation of the area and disproportionate impact on the African American population. The destruction of residential buildings and businesses, followed by economic and cultural shifts brought by these developments, led to the displacement of residents. The physical barriers created by the highway system made it difficult to access other parts of the neighborhood. The series of infrastructural projects and sports facilities construction destroyed the connection to the river. The process of urbanization has shaped the local topography and vegetation, and thus influenced the local microclimate. As shown in the vegetation analysis, changes in canopy cover over time illustrate shifts in land use, which resulted in temperature rise, poor air quality, and a decrease of the thermal comfort in the neighborhood.

4.1.3.3 Site Scale

The site scale is the next level of analysis to understand how natural processes have shaped the project site to its current conditions. The site-scale site analysis consists of modeling geomorphological, hydrological, and vegetation processes. The analysis of the site on a smaller scale reveals patterns and relationships that were not visible at the city and neighborhood scales. Each process is considered to be influenced by natural (nonhuman) and artificial (human) agents (Figure 120). In this case, natural agents are topography, vegetation, and microclimate. The artificial agent, on the contrary, is the process of urbanization. Such analysis becomes a record of processes and the different uses of the site, with a greater level of detail in the project area.

The hypothesis of the site-scale analysis is that the process of urbanization, and, on a smaller scale, fluvial processes, have the biggest influence on the area.

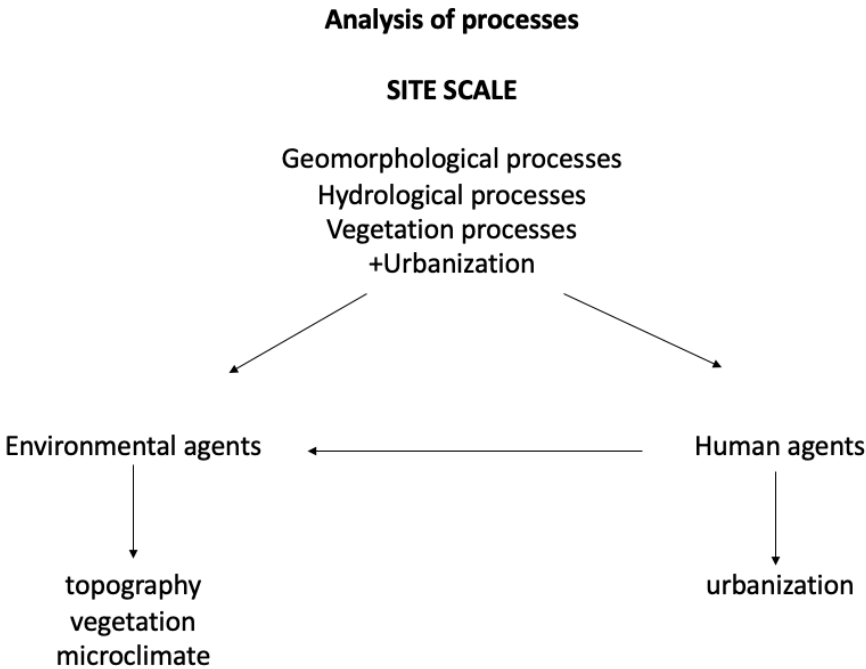


Figure 120. Analysis of processes on the site scale.

The project site went through urban development and changes over time. The historically residential area with a connection to the river was transformed into a site with motel buildings, and later into the Lower Albina industrial area.

The site-scale simulation (Figure 124) includes data from Google Earth satellite images and aerial photos from 1948, 1960, 1975, 1990, 2011, 2014, 2017, 2020, and 2023 (Figure 122). The aim of this simulation was to identify how natural processes along with artificial human activity have shaped the project site. As seen in the workflow process in Figure 121, the data collected from aerial images was translated into 2D AutoCAD drawings (Figure 123), later into 3D Rhino models, and, finally, to 3D perspective images, which resulted in a .gif simulation. The simulation presents the historical record of the city's topography, Willamette River changes, and vegetation changes, along with urbanization transformations.



Figure 121. Workflow process.

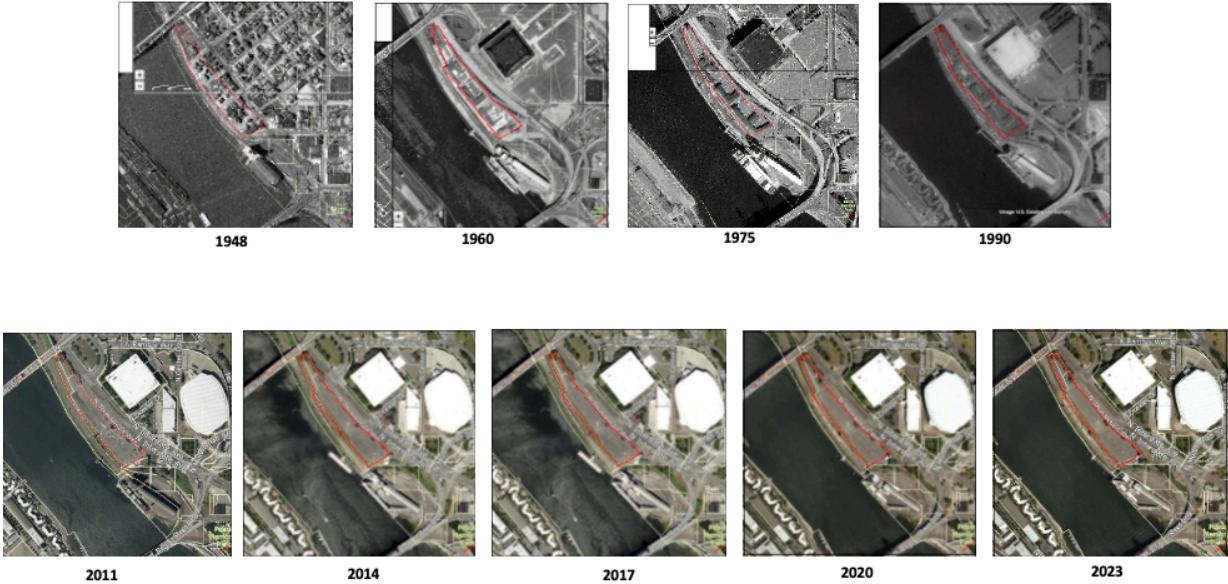


Figure 122. Aerial photos from 1948, 1960, 1975, 1990, 2011, 2014, 2017, 2020, and 2023. From Google Earth satellite images and University of Oregon Knight Library aerial maps reserves.

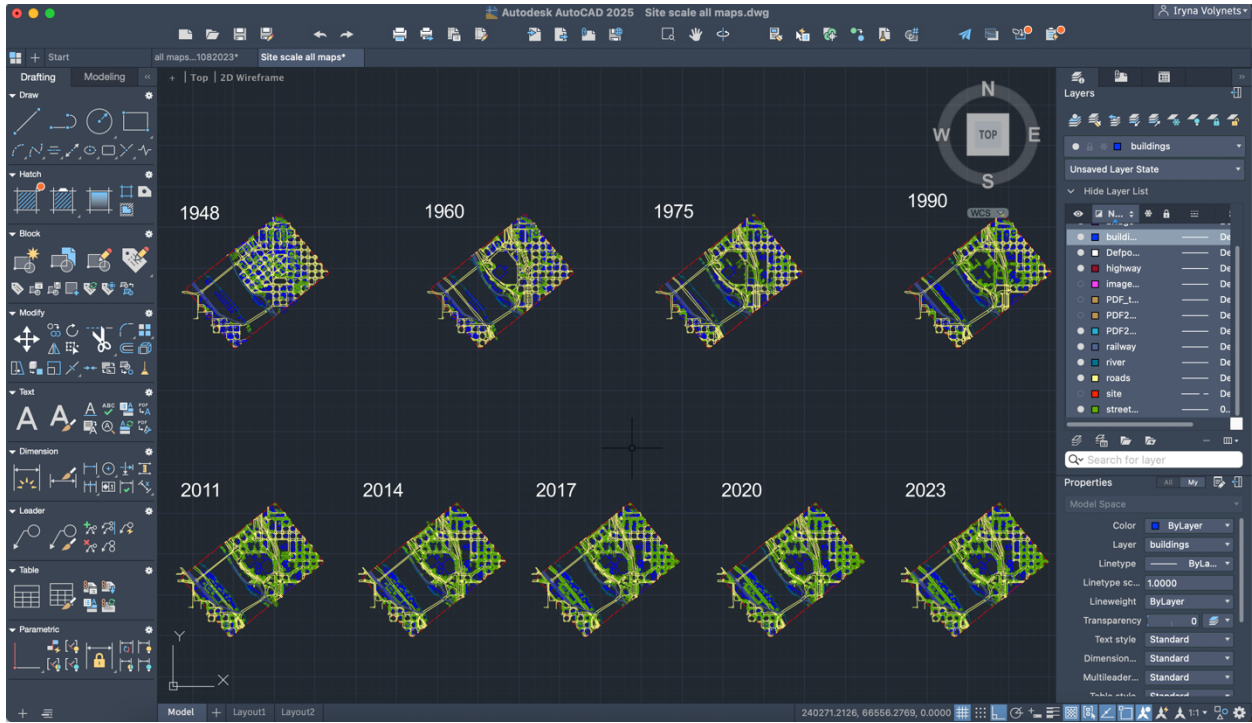


Figure 123. AutoCAD 2D drawings of the site.



Figure 124. Site scale simulation.

The 1948 3D image shows an orthogonal grid of streets with residential buildings and local businesses at the project site. The street grid terminates at a road along the edge of the river. On the lower level of the geomorphological terrace is a double railroad line. In the lower right corner of the image is an industrial building (also known as a grain elevator). Sparse vegetation is present between residential buildings, mainly in backyards and along street edges. (Lower Albina site simulations for each year can be found in Appendix B, Figure 280–Figure 288.)

The 1960 3D image shows dramatic changes since 1948: There are no residential buildings, as much of the neighborhood was cleared for the construction of Interstate Avenue and the Veterans Memorial Coliseum. The project site itself was transformed from single-family residential houses and redeveloped into a motel with associated parking lots. The Thunderbird Motel and Restaurant was built in 1960, featuring 90 units, two dining halls, a cocktail lounge, and a 40-foot-long swimming pool. The motel was designed to cater to travelers by taking

advantage of its close proximity to the Coliseum, a major sport and entertainment venue. The simulation shows a slightly elevated level of the Willamette River. Vegetation appears underneath the Broadway Bridge, and along the Interstate Avenue and railroad lines.

The 1975 3D image shows further expansion of the Thunderbird Motel. The motel doubled in size due to the growing demand for accommodation in the area. In 1961, the expansion included 100 more rooms, along with a conference room and coffee shop. The simulation shows the river at a lower level compared to the previous year. The vegetation along the river is maturing, according to the image. The vegetation along Interstate Avenue is maturing as well.

The 1990 3D image shows no significant changes to the project area. However, the image shows that the railroad was expanded by one more line, which suggests that the lower geomorphological terrace was widened to accommodate this extension. The simulation also shows that the vegetation matured compared to the previous image.

The 2011 3D image shows a significant transformation of the project area. The Thunderbird Motel has been demolished and the site has been replaced with a parking lot. Interstate Avenue was expanded due to the construction of the MAX transit line. The Willamette River water level did not change significantly. The simulation shows more vegetation along Interstate Avenue.

The 2014, 2017, 2020, and 2023 3D images show little to no changes to the project area, as the site is still occupied by a parking lot. The river's edge stays the same as in the previous 3D image. However, the simulation shows vegetation growth over time.

The site-scale crest simulation (Figure 125) presents additional information on how historical crests affected the project site. The simulation creates an overlay of NOAA historic crests data (Table 3) onto the project site. The gauge simulation shows that seasonal and major flooding did not affect the project area due to its elevated position on a geomorphological terrace. The major floods of 1956, 1964, and 1996 covered the lower part of the geomorphological terrace, which included the flooding of railroad lines. (Lower Albina gauge historic crest simulations for each year can be found in Appendix B, Figure 289–Figure 300.)

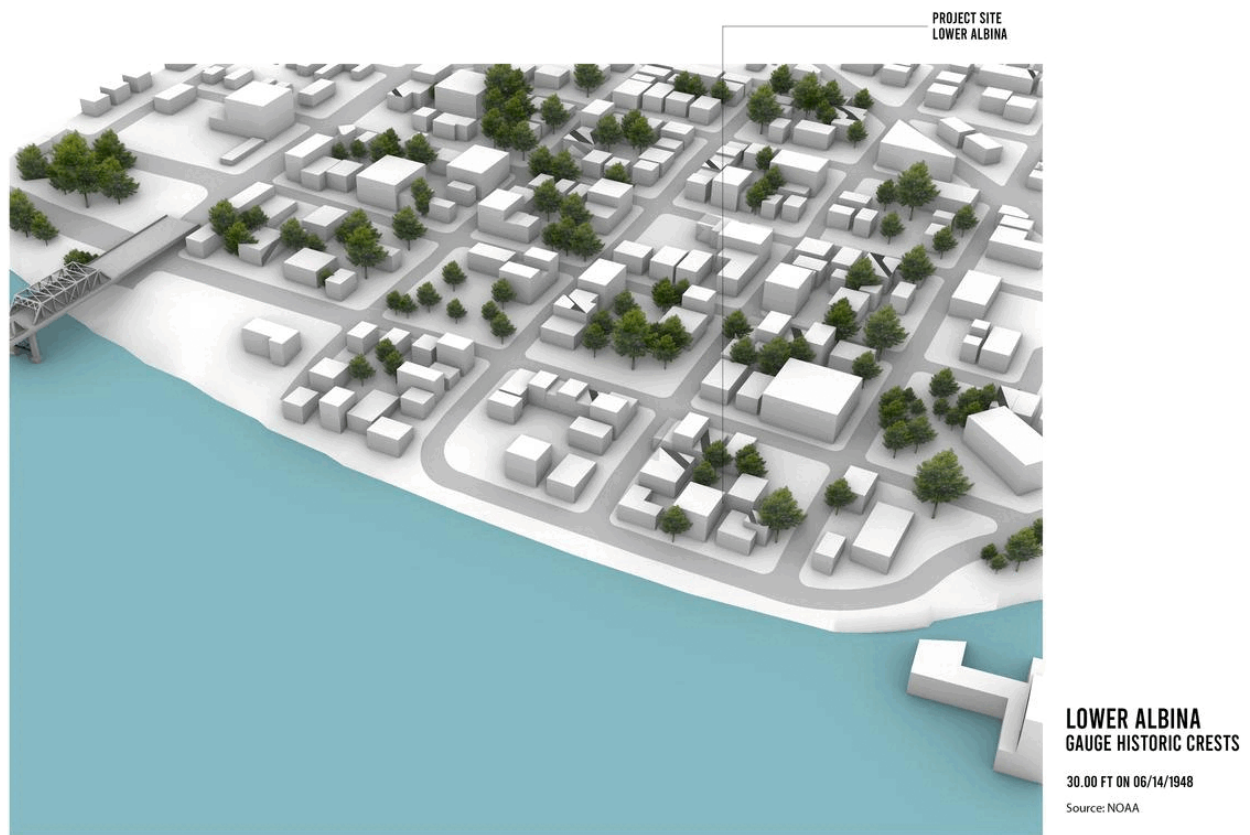


Figure 125. Lower Albina gauge historic crests simulation.

The site-scale simulation reveals how environmental and human processes have shaped the project site. The initial hypothesis that the fluvial processes on the smaller scale might reveal some patterns that were not visible on the larger scale was not confirmed. Even though the project site is located in close proximity to the river's edge, the simulation shows that fluvial processes had a small influence due to the site's topography. The simulation highlights the transformative impact of urbanization and changes in land use that contributed to the site's current configuration.

The site-scale simulation also reveals that vegetation patterns have been shaped by the urbanization process. Vegetation removal was a result of land-use changes: residential backyard vegetation was reintroduced along large infrastructure projects, such as Interstate Avenue and the MAX transit line. The presence of vegetation along the road suggests that human

intervention shaped the distribution and layout of trees. This suggests that vegetation on the site has been dependent on urbanization processes.

4.2 Summary

At the city scale, the comprehensive site analysis of geomorphological, hydrological, and vegetation processes provides an understanding of the dynamic evolution of the city, and especially the Albina neighborhood. The landform processes analysis gives an overview of environmental and human forces that have shaped the region over time and how geological formations have shaped the current topography of Portland. Fluvial processes highlight the historical significance of flooding events and the transformative effect of human activities. Vegetation processes show complex interactions between topography and climate, but also illustrate how urbanization changed vegetation patterns.

The geomorphological processes that have shaped Portland are divided into geological processes and artificial human activity. The geological foundation of the city is basalt bedrock formed by volcanic activity of the Columbia River Basalts. Another catastrophic event that shaped the city's geomorphology was the Missoula Floods. The Albina neighborhood is situated on the edge of the Missoula Flood depositional terrace. The changes influenced by artificial human activity are represented along the Willamette River. The artificial fill of wetlands and streams reflects the city's growth and development.

The hydrological processes along the Willamette River have also been influenced by environmental and human factors. The fluvial simulation illustrates shoreline extensions driven by industrial needs and city growth. The Willamette River changed its shape over time from a wide, braided river to a narrow, more controlled, urban waterway. Although the river narrows at the Lower Albina project site, where the river makes its natural bend, it surprisingly shows minimal changes over time at this location. This finding challenges the initial hypothesis that the river's bend would lead to erosion. Instead, this finding suggests that topographically higher sites like Lower Albina are less influenced by fluvial processes, while low-lying areas prone to flooding undergo significant transformations.

The site analysis and simulations also reveal that the transformative impact of human activity on the Willamette River was stronger than natural processes of flooding over time. Dredging played a significant role in shaping the Willamette River and adjacent areas. Such

human intervention has had a significant effect on economic development and the river's natural environment. The alterations to the river were made to facilitate navigation and infrastructural development. However, this process led to the artificial extension of river shorelines and the filling of wetlands and channels along the Willamette River. The low-lying areas along the river were significantly changed, while the higher elevation areas were left intact. This highlights the relationship between topography and the effects of dredging: low-lying areas were reshaped to accommodate industrial and infrastructural expansions, while elevated areas were less affected by such modifications.

Vegetation processes in Portland, including the Albina neighborhood, have been influenced by human activity and the region's climate and topography. While the climate, topography, and proximity to water bodies influences the types and distribution of vegetation, the simulation also reveal that urban processes have influenced vegetation distribution no less than natural processes. Over time, riparian vegetation was removed due to industrial growth. As the city was growing, urban projects left noticeable scars on the landscape.

At the neighborhood scale, analysis of geomorphological, hydrological, and vegetation processes show the main factors that influenced a tremendous transformation of Albina over time. The construction of major infrastructure projects, such as Interstate 5, the Veterans Memorial Coliseum, and the Moda Center, played a crucial role in reshaping the neighborhood. The simulation reveals the impact of urbanization on the entire neighborhood, such as displacement of residents, loss of connections inside the Albina neighborhood and to adjacent neighborhoods, loss of access to the river, and changes in vegetation cover. The findings support the initial hypothesis that on the neighborhood level, urbanization was the main factor of Albina's change and spatial segregation.

At the site scale, analysis of geomorphological, hydrological, and vegetation processes shows the transformation of the project site in response to natural and human influences. The project site went through significant transformations over time. Starting as a residential area, the site underwent changes due to construction of Interstate Avenue and the Veterans Memorial Coliseum and transformed into a motel area. Following the end of the motel era, the site underwent another transformation into a parking lot. The simulation shows the limited impact of fluvial processes on the smaller scale. It also shows that the main transformation forces to the

project site were urbanization and changes in land use. Additionally, on the site scale, the simulation illustrates the influence of urbanization on vegetation processes.

V. SIMULATION OF SITE-SPECIFIC PROCESSES

5.1 A Process-Based Landscape Approach to Landform Architecture

A process-based approach to landform architecture not only includes analysis of landscape-scale geological, cultural, and natural history, which were presented in Chapter 4, but also prioritizes in-depth understanding and integration of the dynamic processes that occur within the specific site. This approach explores how the relationship between the site's historical context and the dynamic processes that shape the current conditions can influence the shape of the landform building and adjacent landscape.

The proposed framework for a process-based approach to landform building includes a series of simulations that represent environmental processes similar to those that shape natural landforms. Each of these processes is reflective of the unique characteristics of the site and plays a critical role in shaping it. By understanding these processes, it is possible to design buildings that are not only contextually relevant but also sympathetic to their environment. This framework also acknowledges time and change as crucial factors in shaping the architecture and landscape.

In this chapter, the process-based landscape approach to landform architecture is focused on the detailed analysis of current processes on site and their simulations (Figure 126). This chapter documents a series of simulations in Grasshopper that test the interaction of various forms with environmental processes. The hypothesis is that the simulations will illustrate how site-specific processes can influence the building form and local microclimate. By simulating site-specific processes, this approach allows for a deep understanding of how a combination of site-specific conditions can inform architectural decisions.

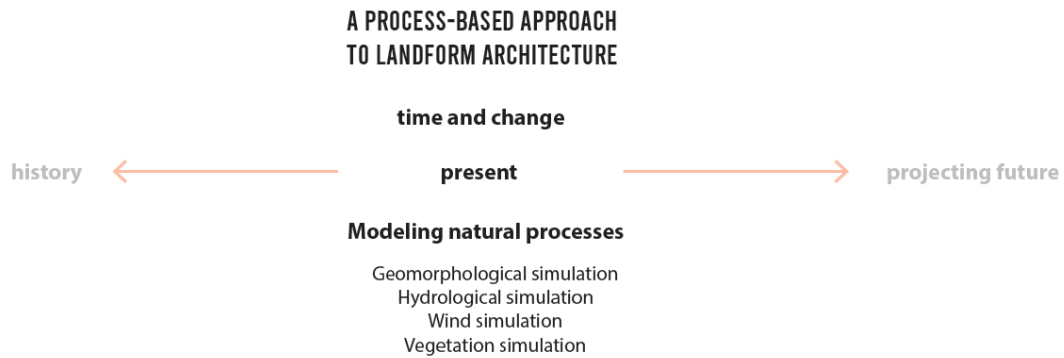


Figure 126. A process-based approach to landform architecture and analysis of a site’s current processes.

This phase of the design experiment recognizes that the site is not static but continuously evolving. By understanding these processes through 3D simulations, it becomes possible to design a landform building that is responsive to the context and adapts to future changes.

5.2 Current Processes on Site

Lower Albina in Portland is a dynamic urban neighborhood shaped by multiple processes. For the project site, specific attention is dedicated to geomorphological, hydrological, wind, and vegetation processes. These processes were selected because they actively shape the environmental conditions of the site and are similar to the processes that shape natural landforms. While the selected processes for this research are similar to exogenic processes, driven by external forces, such as wind and water, there are also endogenic processes that come from within the Earth and involve tectonic and volcanic activities. Processes selected for this study inform design decisions and shape not only the building but also the adjacent landscape. Analysis of these processes is pivotal for understanding the site’s topography, site interaction with water flow and river fluctuation, seasonal rainfall, wind influences on microclimate, and how vegetation evolves and shapes ecological systems.

Analysis of geomorphological processes includes analysis of current geological processes within the Lower Albina neighborhood. The historical overview in Chapter 4 did not reveal any active geomorphological processes at the landscape scale. The site is located on Missoula Flood coarse-grained deposits and is evidently resistant to erosion. Therefore, it is assumed that the

site's terrain is largely stable and there are little to no chances for future major geomorphological changes.

While there are no major geomorphological processes at the landscape scale, it is essential to analyze the current conditions, as they might influence design decisions. The geological history of the Lower Albina neighborhood includes both river and land geomorphology. The site is composed of geomorphological terraces that were shaped by deposition and erosion over a long period.

Analysis of the geomorphological processes began with a 3D model of the site in Rhino. The model was developed from 2024 GIS data that included 2-foot contour lines. In contrast to DEM data, the topographical model from 2-foot contour lines was more precise. The mesh was created using the Delaunay mesh triangulation method (Figure 127) in Grasshopper. This method constructs a mesh by connecting points into triangles.

The input data for this analysis consisted of the 2-foot contour lines, which were processed in Grasshopper to generate a point cloud. The Delaunay triangulation algorithm connected generated points to form a continuous mesh. The output was a 3D terrain model that illustrated the site's topography.

The resulting mesh model revealed that the project site is on the upper of two terraces (Figure 127). Each terrace slopes gently down toward the river. In addition to the terraces, the site model also revealed rounded edges dissected by erosion, likely caused by surface drainage across each terrace. The eroded forms indicate how water interacts with the land, shaping landform features over time.

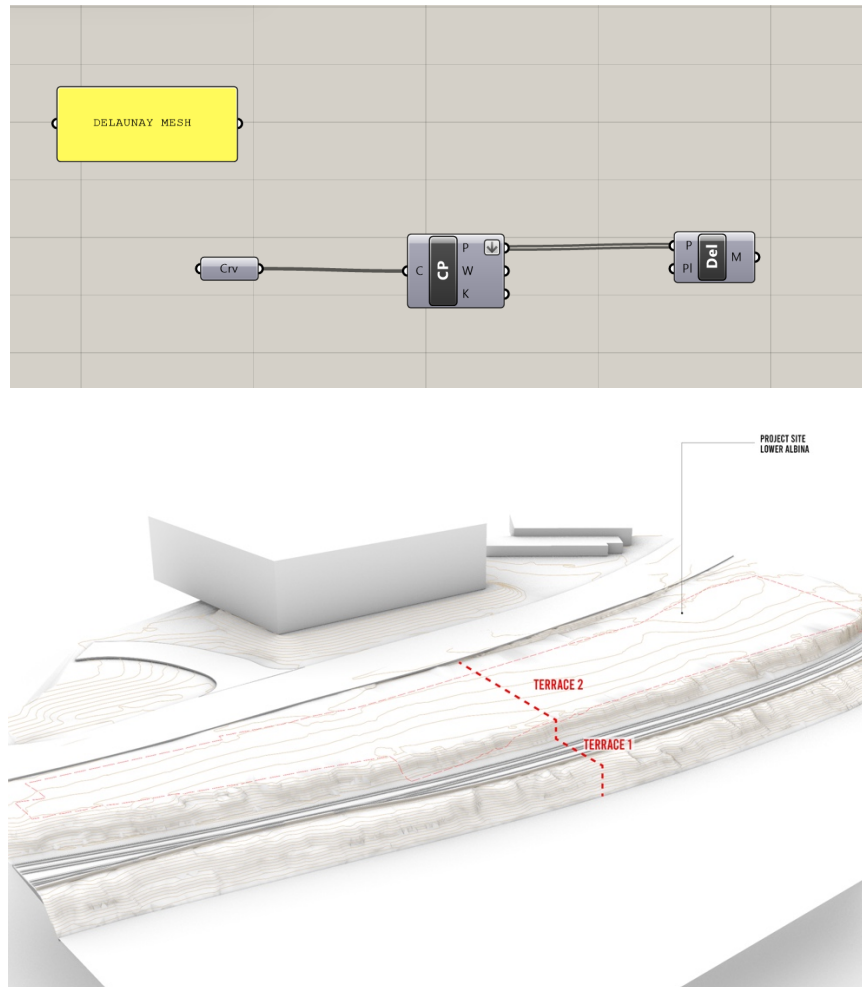


Figure 127. Top: Delaunay mesh definition in Grasshopper. Bottom: Site model with contour lines.

Analysis of hydrological processes includes analysis of the Willamette River's current processes and potential future changes, water runoff processes, and rainfall analysis. The historical overview in Chapter 4 revealed that there was little change in the Willamette River shoreline near the project site.

In 2012, FEMA mapped the flood plain for the Portland area, which was later digitized by the Portland Office of the Army Corps of Engineers. The outline of the flood area was collected from the GIS data and translated into a 2D AutoCAD drawing that was used for the 3D Rhino model and later converted into a 3D perspective image. The resulting 3D simulation (Figure 128) reveals that FEMA's 100-year flood does not reach the project site; it reaches only

the lower terrace and stops at the railroad. While the initial hypothesis was that river hydrological processes will be the main process that shapes the site and its landform architecture, the simulation reveals that due to the site's topography, the site would be unimpacted in a 100-year flood.

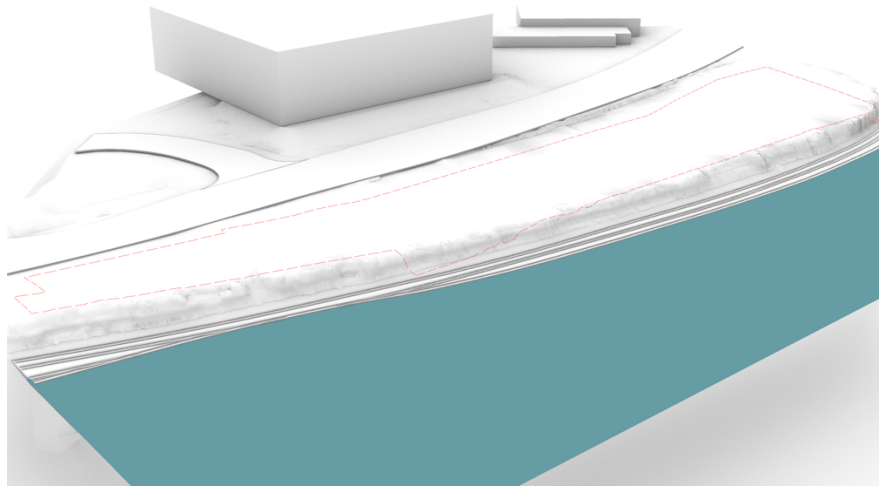


Figure 128. Simulation of FEMA's 100-year flood plain.

It is important to identify how hydrological processes currently shape the site and can change the site in the future. The surface water flow simulation (Figure 129) was performed in Rhino with the Groundhog plug-in for Grasshopper. Groundhog explores computational design in landscape architecture and offers tools for water analysis and terrain manipulations.

For the waterflow simulation, the input data was the mesh from the site's 3D model and GIS topographic information. The simulation focused on the project area, as N. Interstate Avenue and the MAX Light Rail line have storm drain grates along the road, which intercept and redirect a significant portion of surface runoff before it reaches the site. The simulation shows different scenarios of water volume flowing from the site to the Willamette River. These scenarios include a variety of rainfall intensities to examine how the changing patterns affect the surface runoff. The results showed that, generally, water flows evenly across the site; however, there are specific areas where runoff is concentrated. The areas where water flow is concentrated have higher potential for erosion. The concentrated flow paths appear where geomorphological terraces are dissected in the topographical model. This simulation insight suggests that surface drainage played a role in shaping the site's existing landform.

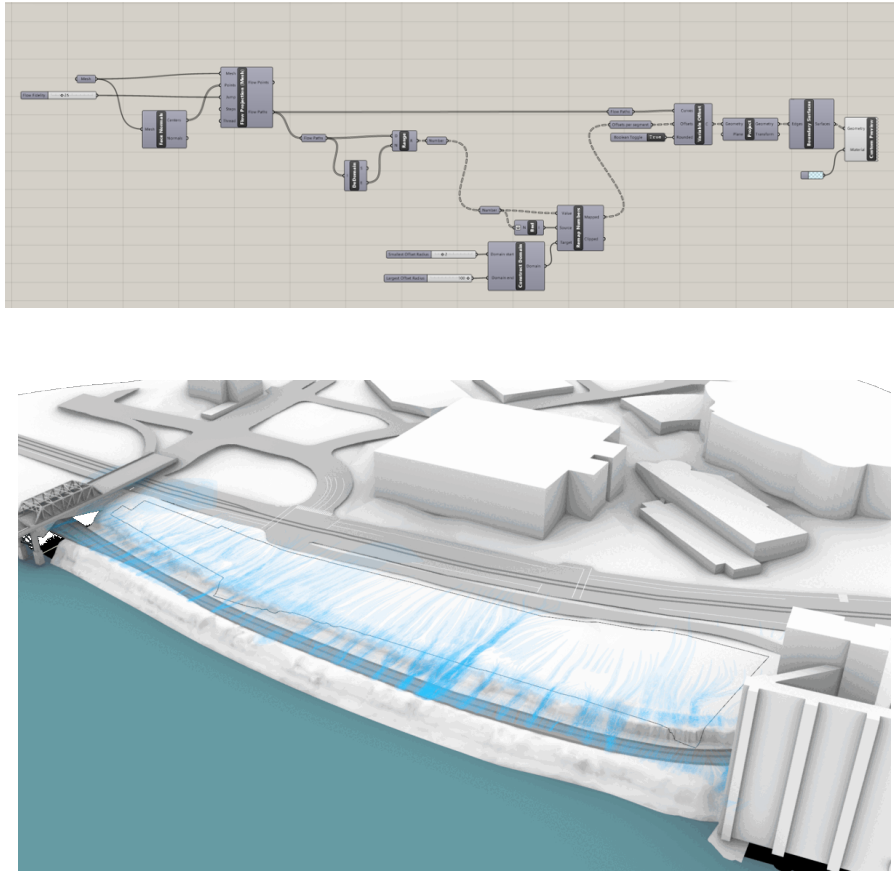


Figure 129. Top: Groundhog Grasshopper definition for surface water flow. Bottom: Surface water flow simulation (larger view in Appendix D, Figure 351).

The rainfall data was included in the analysis of hydrological processes. Climate in Lower Albina is characterized by wet winters and dry summers. On average, the rainfall data at Albina Rain Gage, located at 2920 N. Larrabee Avenue, receives about 36 to 43 inches of rainfall annually (City of Portland HYDRA Rainfall Network, 2023). Most of the rain falls between October and April, which is considered the wet season. While July and August are the driest months, November, December, and January are the wettest. The average rainfall for December is around 5.5 inches, while July and August receive 0.5 inches of rain. The wet season is characterized by frequent light rain, which contributes to the city’s lush landscape.

Analysis of wind processes on site includes wind rose analysis and wind simulation. Wind is influenced by the geographic location and surrounding topography. To simulate wind, a wind rose analysis using the Ladybug tool in Grasshopper was executed. The Ladybug tool is focused on environmental design and helps to analyze climate data, solar radiation, daylight, energy use, and environmental comfort.

The input data for the wind rose analysis with the Ladybug tool was the EPW data collected from the closest location—Portland International Airport. For the wind rose simulation with Ladybug, the input data was: (1) prevailing wind direction, (2) monthly wind patterns, and (3) wind speed (Figure 130).

The prevailing wind direction for the Lower Albina neighborhood is from the northwest with a wind speed of 10 meters per second (m/s) (Figure 131). In the summer and winter, the northwest wind from the coast is hot and dry, while the southeast wind is cold and dry (Figure 131–Figure 133). In January, the wind is from the southeast with a speed of 10 m/s. In February, the wind from the southeast is 10.5 m/s, while the northwest wind is 8 m/s. In March, the wind from the southeast is 10.5 m/s, while the northwest is 9.5 m/s. In April, wind from both directions reaches 9.5 m/s. In May and June, the southeast wind is 10 m/s, while the wind from the northwest is 9 m/s. In July, wind from the southeast is 10.5 m/s and 8 m/s from the northwest. In August, wind from the southeast decreases to 10 m/s and from the northwest to 7 m/s. In September and October, wind from the southeast is 9.8 m/s. In November and December, wind from the southeast decreases to 9.5 m/s.

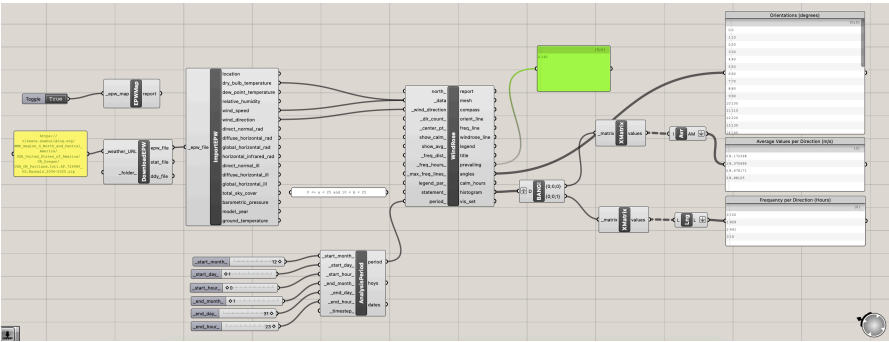
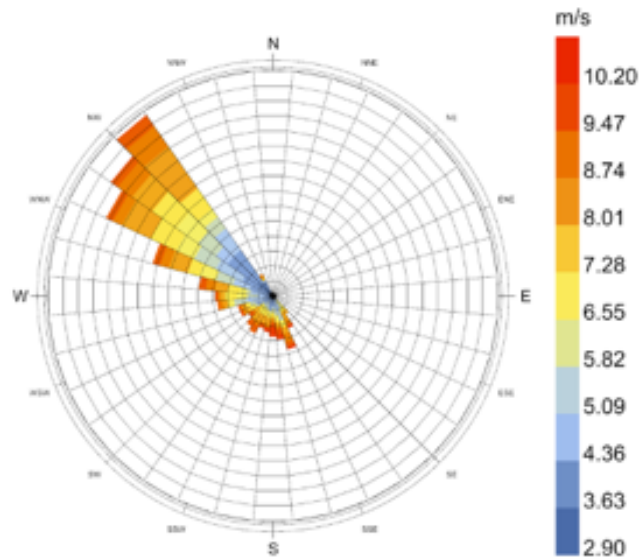
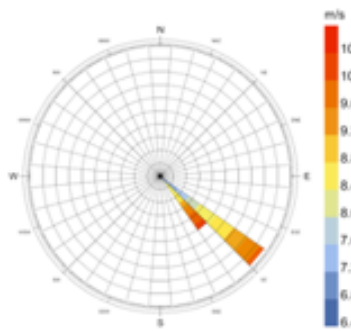


Figure 130. Ladybug + Grasshopper definition for wind rose analysis (larger view in Appendix D, Figure 352).



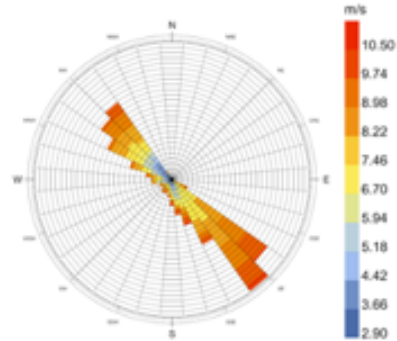
Wind Speed (m/s)
 time-zone: -8.0
 city: Portland.Intl.AP
 country: USA
 source: Climate-Normals
 period: 1/1 to 12/31 between 0 and 23 @1
 Calm for 0.0% of the time = 0 hours.
 Each closed polyline shows frequency of 1.1% = 50 hours.

Prevailing



Wind Speed (m/s)
 time-zone: -8.0
 city: Portland.Intl.AP
 country: USA
 source: Climate-Normals
 period: 1/1 to 1/31 between 0 and 23 @1
 Calm for 0.0% of the time = 0 hours.
 Each closed polyline shows frequency of 6.7% = 50 hours.

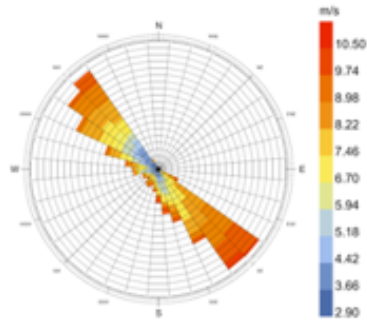
January



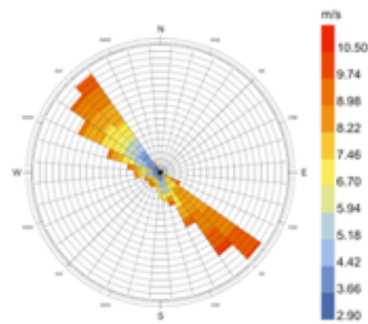
Wind Speed (m/s)
 time-zone: -8.0
 city: Portland.Intl.AP
 country: USA
 source: Climate-Normals
 period: 2/1 to 1/31 between 0 and 23 @1
 Calm for 0.0% of the time = 0 hours.
 Each closed polyline shows frequency of 0.6% = 50 hours.

February

Figure 131. Wind rose analysis for prevailing wind and monthly wind patterns from January to February.

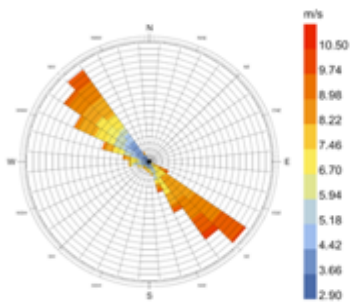


Wind Speed (m/s)
 time-zone: -8.0
 city: Portland Intl.AP
 country: USA
 source: Climate-Normals
 period: 3/1 to 1/31 between 0 and 23 @1
 Calm for 0.0% of the time = 0 hours.
 Each closed polyline shows frequency of 0.6% = 50 hours.



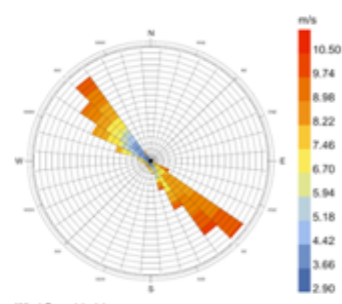
Wind Speed (m/s)
 time-zone: -8.0
 city: Portland Intl.AP
 country: USA
 source: Climate-Normals
 period: 4/1 to 1/31 between 0 and 23 @1
 Calm for 0.0% of the time = 0 hours.
 Each closed polyline shows frequency of 0.7% = 50 hours.

March



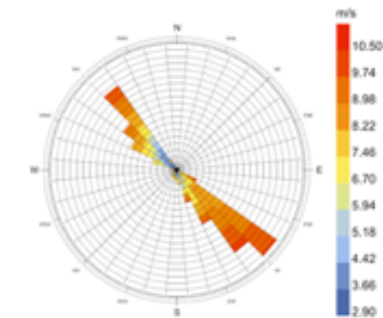
Wind Speed (m/s)
 time-zone: -8.0
 city: Portland Intl.AP
 country: USA
 source: Climate-Normals
 period: 5/1 to 1/31 between 0 and 23 @1
 Calm for 0.0% of the time = 0 hours.
 Each closed polyline shows frequency of 0.8% = 50 hours.

April



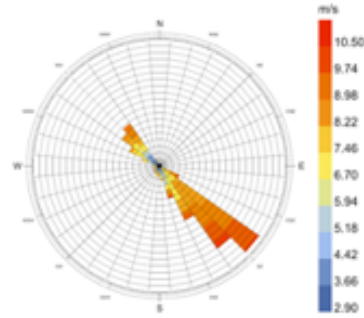
Wind Speed (m/s)
 time-zone: -8.0
 city: Portland Intl.AP
 country: USA
 source: Climate-Normals
 period: 6/1 to 1/31 between 0 and 23 @1
 Calm for 0.0% of the time = 0 hours.
 Each closed polyline shows frequency of 0.9% = 50 hours.

May



Wind Speed (m/s)
 time-zone: -8.0
 city: Portland Intl.AP
 country: USA
 source: Climate-Normals
 period: 7/1 to 1/31 between 0 and 23 @1
 Calm for 0.0% of the time = 0 hours.
 Each closed polyline shows frequency of 1.0% = 50 hours.

June



Wind Speed (m/s)
 time-zone: -8.0
 city: Portland Intl.AP
 country: USA
 source: Climate-Normals
 period: 8/1 to 1/31 between 0 and 23 @1
 Calm for 0.0% of the time = 0 hours.
 Each closed polyline shows frequency of 1.1% = 50 hours.

July

August

Figure 132. Wind rose analysis for prevailing wind and monthly wind patterns from March to August.

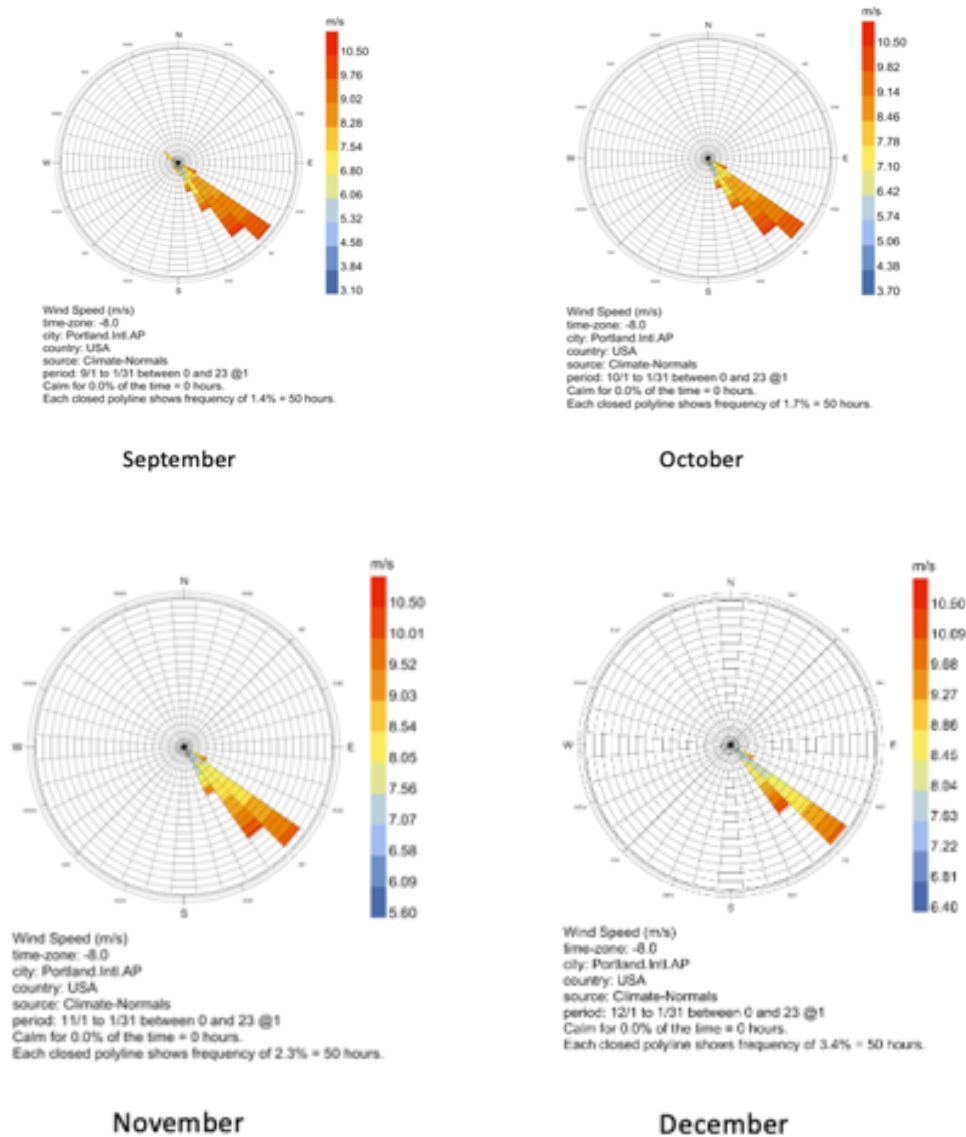


Figure 133. Wind rose analysis for monthly wind patterns from September to December.

The wind simulation for the project site and adjacent area represents the wind from two dominant directions: northwest and southeast. Both maximum and average wind conditions were simulated for each wind direction. The maximum wind condition was based on the maximum wind speed of 10.5 m/s from the northwest and southeast. An average condition was based on 6 m/s, which is considered a moderate wind speed for the Portland area. The wind simulation was performed with the use of the Butterfly plug-in in Grasshopper. The plug-in is used for CFD simulations within Rhino. It offers tools to simulate and visualize wind patterns around buildings, indoor air movement, and thermal comfort. Butterfly is designed to work with

OpenFOAM, an open-sourced CFD program, which enables detailed airflow analysis for architecture.

The input data for wind analysis with the Butterfly tool includes geometry from Rhino, wind speed, and wind direction information. The simulation of the current wind processes (Figure 134) includes analysis of wind from the northwest and southeast with 10.5 m/s and 6 m/s wind conditions. The input geometry was the site's neighboring buildings, the Veterans Memorial Coliseum and Annex Garage City Center Parking, and the site topography. Due to the geographical location of the project site, the two dominant wind directions from northwest and southeast are parallel to the longer edge of the site.

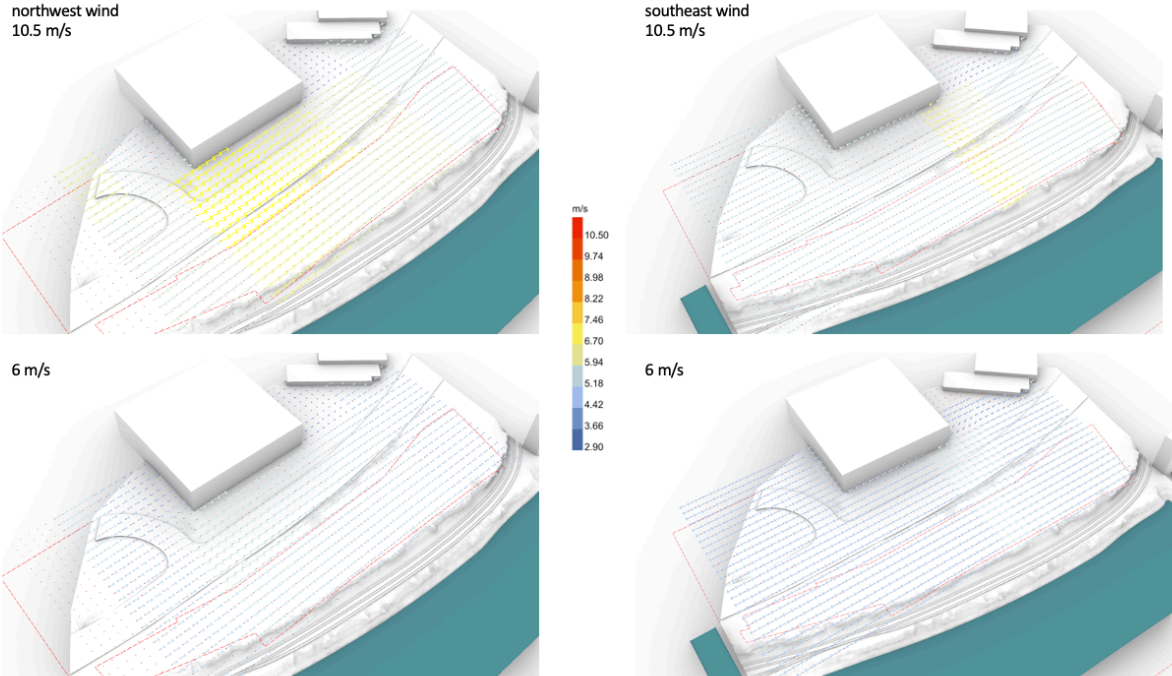


Figure 134. Current wind conditions for northwest and southeast winds.

The first wind condition was the northwest wind with windspeed 10.5 m/s. The simulation result illustrates that the wind speed changes from 5.5 m/s to 6 m/s, and back to 5.5 m/s along the project site. Moving toward the Veterans Memorial Coliseum, the wind speed increases from 5.5 m/s to 6.5 m/s, and back to 5.5 m/s. Perpendicular to the Veterans Memorial Coliseum facade, the wind speed changes from 5.9 m/s to 4.5 m/s. On the other side of the building, the wind speed decreases to 3.5 m/s and creates the wake effect. The wake effect usually happens behind a building, where the low-pressure zone is created. Such conditions often

create wind eddies—swirling air currents. At the end of the site, the wind speed returns to 5.5 m/s.

For the northwest 6 m/s wind condition, the wind speed is slower and reaches 4.5 m/s along the project site. When the wind faces the Veterans Memorial Coliseum, the speed changes from 4.5 m/s to 3.5 m/s. On the other side of the building, the wind creates a circular motion and reaches 3.5 m/s. At the end of the site, the wind speed returns to 5.5 m/s.

For the southeast 10.5 m/s wind condition on the project site area, the wind speed changes from 5 m/s to 6 m/s, and back to 5 m/s. While moving toward the Veterans Memorial Coliseum, the wind speed stays the same. Perpendicular to the Veterans Memorial Coliseum facade, the wind speed ranges between 3–3.5 m/s and does not create wind eddies. On the other side of the building, the wind ranges from 5.2 m/s to 5 m/s.

For the southeast 6 m/s wind condition, on the project site area, the wind speed changes from 3.5 m/s to 5 m/s, and back to 3.5 m/s. While moving toward the Veterans Memorial Coliseum, the wind speed also stays the same. Perpendicular to the Veterans Memorial Coliseum facade, the wind speed ranges between 3–3.5 m/s. On the other side of the building, the wind ranges from 4 m/s to 3.5 m/s.

The wind simulation results illustrate areas where wind speed changes due to building-induced effects, such as eddies or wake zones. These findings can inform the shape of the building and its orientation. In addition, areas with high wind speed might require a wind break before wind reaches the building. Such a wind break might be a landform feature or trees. Understanding where wind speed is stable and where it changes is also necessary for the site organization and optimal microclimate conditions.

It is also necessary to note that the Willamette River, similar to other major rivers, can influence the wind patterns in several ways. The open space along the river acts as a wind corridor, which allows wind to flow more freely and faster compared to landscapes with buildings, landforms, trees, and other obstacles. Additionally, the water surface is aerodynamically smoother than land and causes less friction.

Analysis of vegetation processes (Figure 135) is based on a 3D model in Rhino that represents the current condition of vegetation on site. The 3D model reveals that there are only a few deciduous trees on site. The majority of trees are located along two sides of N. Interstate Avenue and N. Larrabee Avenue. The character and amount of the vegetation are largely

influenced by urban processes described in Chapter 4. The current use of the site as an asphalt-covered parking lot makes the project area one of the hotter sites in Portland and prevents any vegetation from growing. The lack of vegetation on site contributes to higher temperatures and negatively affects local microclimate.

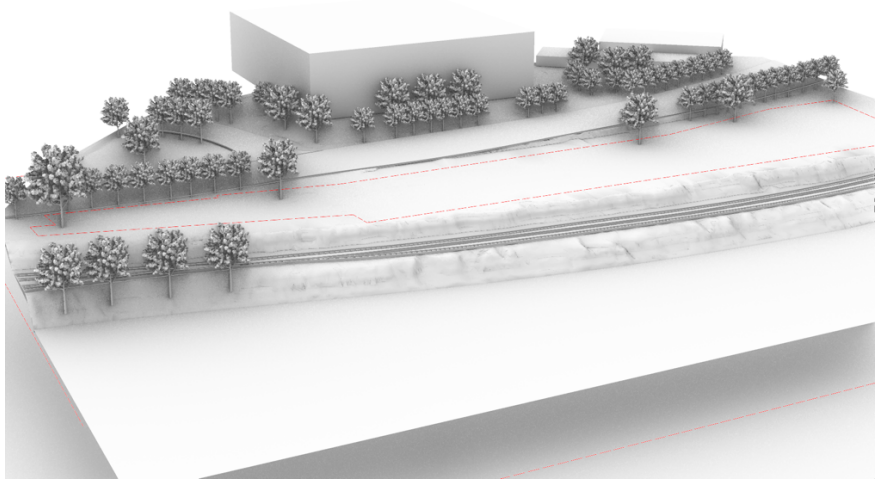


Figure 135. Simulation of vegetation process.

The following subchapter explores how findings from this analysis can inform the design process and how this approach can address site-specific challenges. A simulation that tests various factors was developed for each process.

5.3 Simulations

In the design process, analysis of existing conditions is followed by program development, site contextualization, and feasibility studies. These include understanding the needs and goals, environmental and socioeconomic factors, practical constraints, and regulatory requirements, which shape the early design stages. While being an essential part of the design process, these steps focus on static elements and ignore natural processes that continue to reshape the environment.

The proposed framework for landform design that is shaped by natural processes consists of geomorphological, hydrological, wind, and vegetation simulations. The process-based approach goes beyond static site analysis by introducing dynamic 3D simulations. These simulations help to explore how natural processes interact with architectural intervention. Such

an approach is relevant for landform architecture, as landform buildings are an integral part of the landscape.

The computational workflow (Figure 136) represents the simulation process of environmental processes that inform landform architecture design. The input for the series of simulations consists of a site model and localized climate data. The inputs are integrated into Rhino and Grasshopper, which serve as the main toolkit for running simulations. Within Grasshopper, the use of Anemone and Butterfly plug-ins allow for an iterative simulation process that includes running loops for geomorphological, hydrological, and vegetation simulations, and for simulating outdoor airflow. These simulations make it possible to identify the relationships between the proposed building design, landforms, and vegetation. The output data allows for visualizing how building form and placement affect environmental processes.

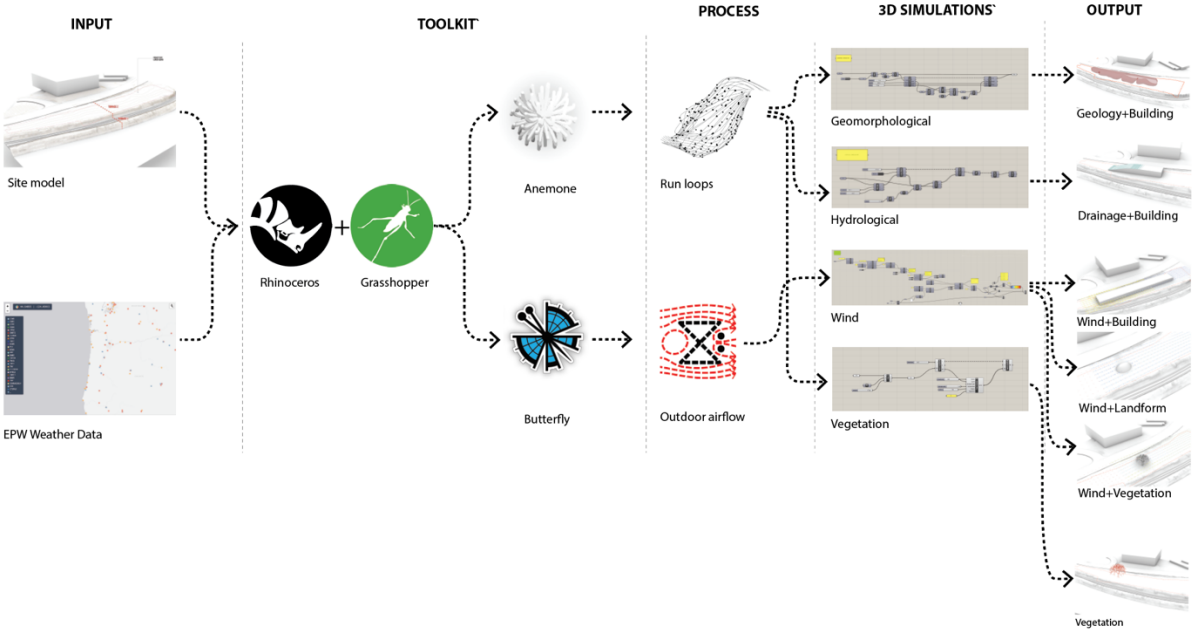


Figure 136. Computational workflow.

By incorporating 3D simulations into design, it is possible to explore the dynamic nature of the environment, anticipate future changes, and test design ideas with higher precision. The set of 3D simulations also helps to develop a deeper understanding of how design intervention might interact with natural processes. The process-based approach with 3D simulations

introduces iterative feedback loops and allows for quick adjustments of the design based on simulation results.

5.3.1 Geomorphological Simulation

Geomorphological simulation is the most foundational simulation in the process-based design, as it establishes the relationship between the proposed design and the ground surface. It constrains all subsequent processes and serves as a starting point from which all other simulations derive. The main purpose of this simulation is to understand how the site changes with design intervention. Such understanding is critical to understand how the proposed design might interact with natural forces, such as water, wind, and vegetation. The shape of the landform not only influences how these processes behave but also suggests how the landform building and surrounding landscape might respond to them over time.

While some landforms can be interpreted through contour lines. Contour lines help to develop a complex model that represents the natural history and geological features of the site. A similar idea lies behind geomorphological simulation, where the contour line can be simulated into a basic shape. Geomorphological simulation is the first step in form-finding in the process-based design.

The geomorphological simulation (Figure 137) visually represents the evolution of the landform. The geomorphological definition in Grasshopper is based on the Anemone plug-in. Such a plug-in creates loops and repeats the definition numerous times. The input data for this simulation was a curve line. Other components of the definition were number of iterations, height, and offset values. These parameters give the flexibility to generate a range of landform shapes to analyze the potential impact of each on the surrounding environment.

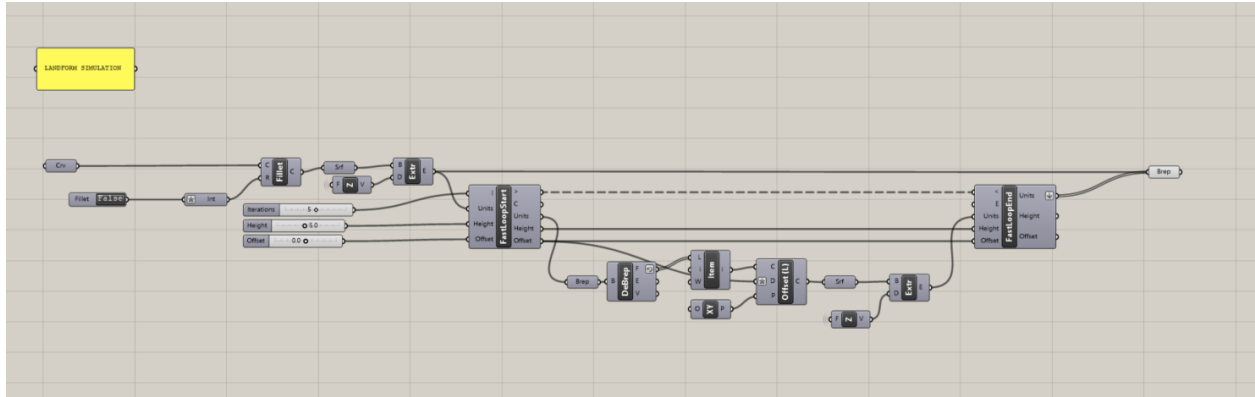


Figure 137. Geomorphological simulation. Definition in Grasshopper (larger view in Appendix D, Figure 353).

The simulation (Figure 138) starts from a closed curve derived from the site's existing contour lines and develops into a 3D polysurface set at a height of 2 feet, gradually growing by 2-foot increments into a 20-foot high polysurface. This shape was set as a basic polysurface for the following iterations.

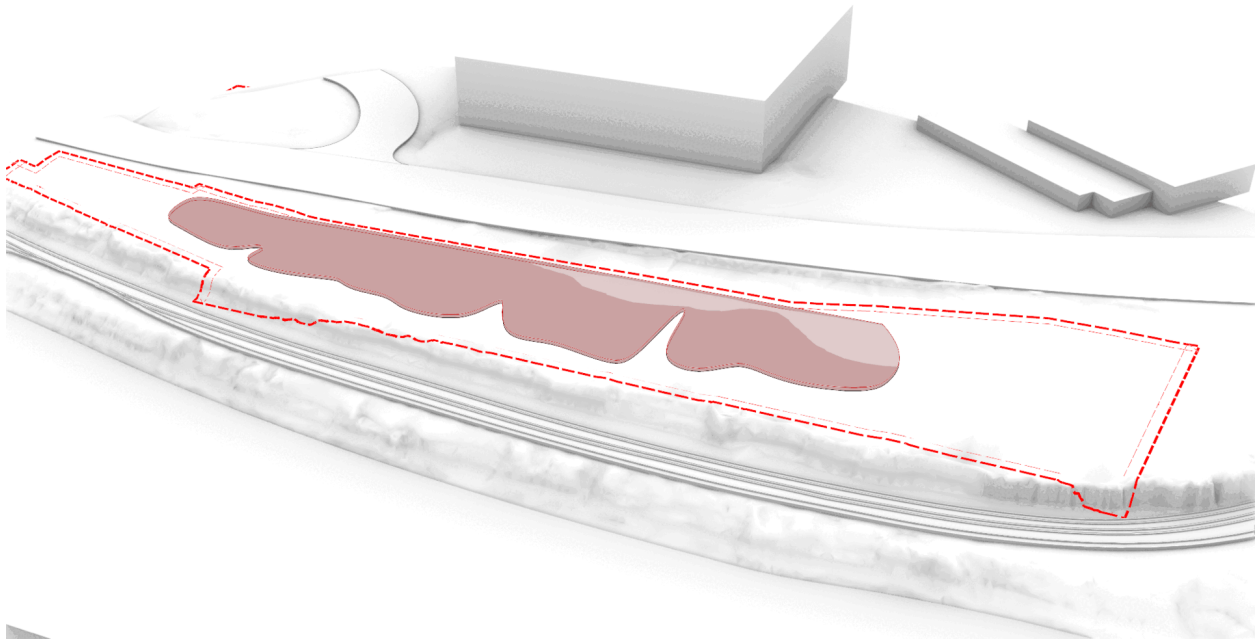


Figure 138. Geomorphological simulation.

Further simulation increased the growth value for the polysurface to 20 feet. When the polysurface reached a height of 120 feet (for comparison, Portland's Veterans Memorial Coliseum is 100 feet high), it became clear that at this height, the building was visually

disproportional for the area because it disrupted the surrounding waterfront context and conflicted with the idea of a horizontally extended landform.

The next version of the simulation used a number of iterations of the basic 3D polysurface rather than height to control growth. When the number of iterations reached three, it was clear that the building might have a maximum of three levels; otherwise, it would be disproportional to the context. A subsequent simulation used offset values to create separation between levels. The initial offset value between the two levels was 10 feet, iteratively increasing by 3 feet increments until reaching a 19-foot offset. The offset of 10 feet was applied to three levels; however, this result was also disproportional to the context.

Geomorphological simulations illustrate the interaction between potential landforms and the site. In this simulation study, the shapes of various heights, proportions, and offset forms were tested. The key findings reveal that extremely tall or layered forms conflict with the context. The simulation also revealed that the horizontally extended form is the most suitable for the project site.

Geomorphological simulation serves as a foundational step in process-based design that helps to test different forms. Later, those forms can be tested with the following simulations to understand the interaction with natural processes, such as water flows, wind flows, and vegetation growth. The landform growth simulation guides the following simulations.

5.3.2 Hydrological Simulation

Hydrological simulation is a part of the process-based framework that models water flow across an architectural surface. Since a landform building is a part of the landscape, water management practices used for landscape architecture become relevant for landform architecture. The main purpose of this simulation is to predict and analyze how rainfall and water runoff interact with the landform building. This knowledge is critical to determine potential water runoff challenges and water management needs.

Water runoff occurs when a large volume of water, rainfall or stormwater, exceeds the surface capacity to absorb it. This results in water flowing along slopes and landforms. While certain slopes and soil profiles shed water, others might retain water. A similar idea lies behind the landform building, as the amount and intensity of rainfall on a site and the presence of rainwater harvesting and stormwater drainage can impact the building's design and elements

such as the building envelope and roof. Heavy rainfall on a poorly draining roof can overwhelm it, causing a bathtub effect and damaging the building’s structural integrity. Hydrological simulation helps to simulate how water interacts with the building to mitigate extreme rainfall effects.

The Hydrological simulation (Figure 139) visually represents the water flow along the building surface and helps architects assess the runoff pattern and water distribution across an architectural form. The definition in Grasshopper is based on the Anemone plug-in, which allows for looping in order to repeat the definition results. The input data for this simulation is the surface geometry of a building. Other components of the definition are a number of points in u and v directions and repeat value. The u and v directions in Grasshopper refer to the parametric coordinate system, which is used to define the surface. In this simulation the number of points in the u and v directions define the resolution of the flow pattern and repeats the value sets to simulate the water flow. These parameters help to analyze different scenarios and intensities of water flow to identify areas that may need design adjustments.

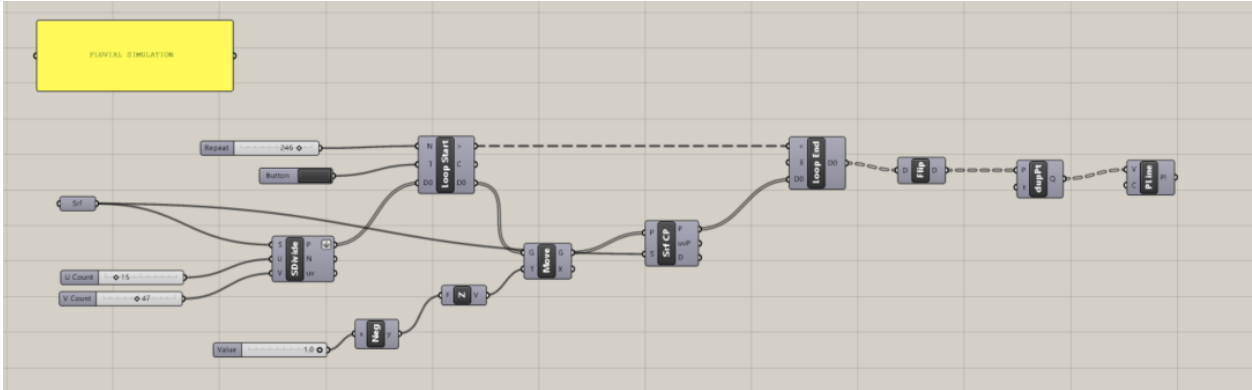


Figure 139. Hydrological simulation. Definition in Grasshopper
(larger view in Appendix D, Figure 354).

The hydrological simulation for Lower Albina (Figure 140–Figure 141 **Error! Reference source not found.**) starts with the exploration of the building and roof shapes and their ability to direct water. The input parameters for this simulation were the basic geometry modeled in Rhino. Other parameters were 15 points for u count and 45 points for v count. The number of points was chosen to ensure a balance between resolution to capture the water flow pattern without excessive processing time for the simulation. The number of iterations was set to 45 to allow for a sufficiently detailed simulation while maintaining computation time.

Multiple design options were explored to test how different architectural forms influence water flow. By comparing different geometries, the study identifies which configuration better controls runoff and prevents water accumulation.

For Option 1, the input geometry was a basic cuboid shape. The dimensions of such a shape (400 feet long, 90 feet wide, and 20 feet high) were selected to reflect a potential building footprint that fits within the site constraints while also maintaining appropriate proportions for the surrounding context. The output result of hydrological simulation for such geometry was not successful, as there was no single slope. For the following options, the geometry changes to create an angled surface.

For Option 2, the input geometry was a modified cuboid shape with a one-sloped landform. The simulation result shows no water flow on the part of the building that has a flat roof. The water flow increases toward the sloped part where the building connects to the ground. Such an option is similar to Option 2 and directs water to a small area.

For Option 3, the input geometry was a modified Option 3 with an elongated two-sloped landform. The building shape was aligned with the contours of the site's topography. The simulation shows water flowing toward the two short sides to the ground. While this option improved the water distribution compared to Option 3 by preventing excessive runoff into one side, it still directed water to two relatively small areas, which could pose a drainage challenge.

For Option 4, the input geometry was a modified Option 3 with a fold-like landform. The roof of the building is folded along its length. The output result of this hydrological simulation was a flow of water in both directions. While this option has wider short edges that connect to the ground, it has flatter areas that do not drain the water.

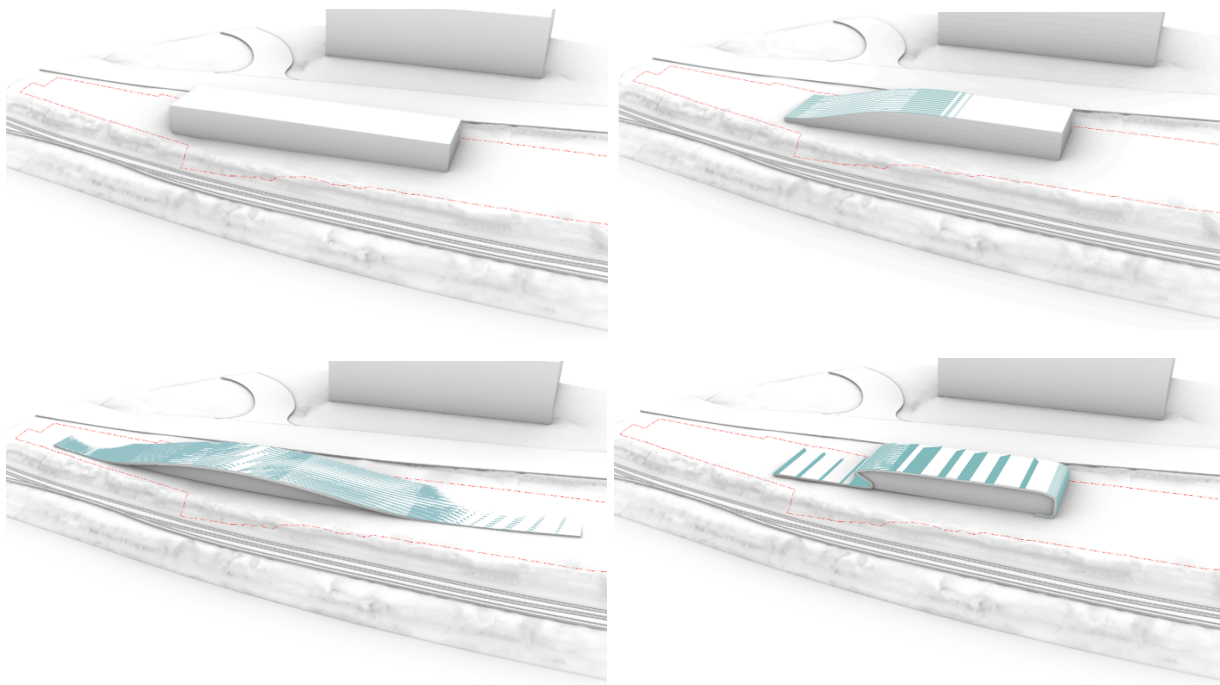


Figure 140. Hydrological simulation. Options 1–4.

For Option 5, the input geometry was a modified cuboid shape with rounded corners and a wave-like roof profile along the riverside facade, with a maximum overhang of 9 feet on each side. The output result of the hydrological simulation showed poor drainage performance on the flat part of the roof. On the other side of the roof, the simulation revealed bowl-like water movement. The flow of water on the other side of the roof was perpendicular to the main shape of the building, which was a better result than Option 2. While the shape of the roof concentrated water into two areas rather than in one area as with the single-sloped roof, the result still concentrated water.

For Option 6, the input geometry was a modified Option 3 with a wave-like roof profile along both long facades. The output result of hydrological simulation was more successful than Option 3, creating a flow of the water in two directions, perpendicular to the longer side of the building, concentrating water in four areas on the ground.

For Option 7, the input geometry was a modified Option 1. The main part of the building shape was a modified cuboid shape; however, the roof was solid with the building envelope, with no overhang. The roof was tilted to the street side by 3 degrees. The building had an angular and stepped shape. The output result of the hydrological simulation was a flow of water

perpendicular to the longer side of the building and toward the Veterans Memorial Coliseum. The direction of the flow perpendicular to the longer edge of the building is better, as it prevents water congestion in small areas. However, the direction of the flow toward the street creates a challenge for surface drainage, as it could potentially overwhelm existing drainage, lead to localized flooding, or require additional drainage solutions to manage runoff effectively.

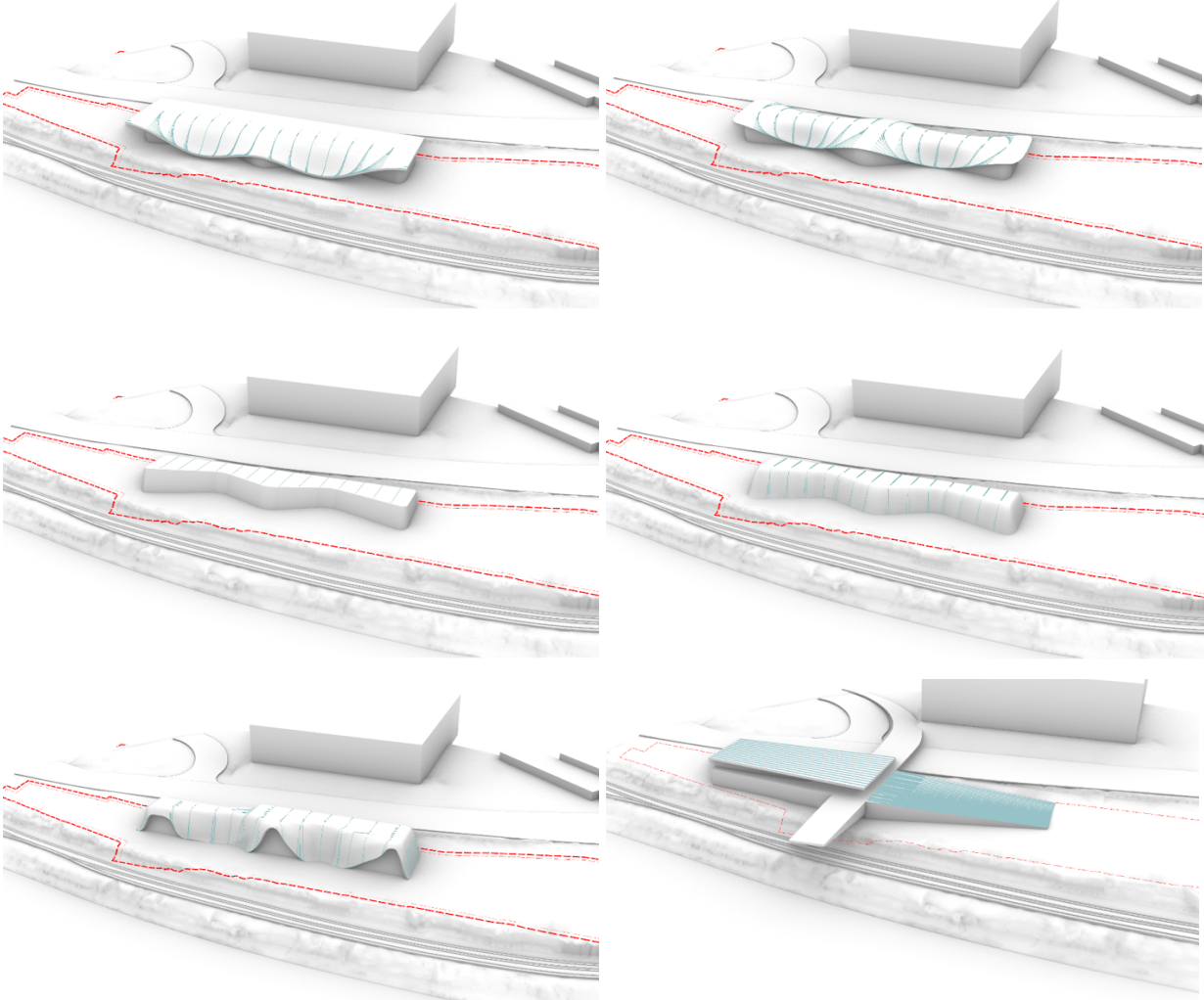


Figure 141. Hydrological simulation. Options 5–10.

For Option 8, the input geometry was a modified Option 8. The building walls were tilted inward along the z-axis by 5 degrees compared to the previous version. The output result of the hydrological simulation was an evenly distributed water flow along the roof and walls.

For Option 9, the input geometry was a combination of Option 7 and 9. The building envelope was more straightened, and the roof was in the form of a draped surface. The output

result of the hydrological simulation was less successful compared to Option 9, as some water flow is concentrated rather than being evenly distributed.

For Option 10, the input geometry was a proposal for the Arts Hub building for this site from El Dorado Architects, which serves as a comparison of how the proposed design differs from options presented in this research. While the dimensions of the building (500 feet long, 90 feet wide, and 20 feet high) are similar to Option 1, the simulation results were different due to the shape. The output result of the hydrological simulation showed that the water moved longer along the shallower angled portion of the roof, while it flowed rapidly along the steeper part of the roof connected to the ground. While the angled roof was an improvement compared to Option 1, as it facilitates water drainage more effectively, this design option was not ideal since it directed a large volume of water along the longer edge toward the narrow end of the building.

The key points that can be summarized as a result of the simulations are the following:

- (1) a single-sloped landform creates a large volume of water that is concentrated on one surface;
- (2) a landform that narrows where it meets the ground also creates a place for water accumulation;
- (3) a wave-like landform creates a bowl-like effect and accumulates water;
- (4) the water is dispersed better when it flows perpendicular to the long side of the facade;
- and (5) tilted walls and roof help guide water evenly across the surface and reduce water accumulation.

Based on the hydrological simulation, Option 9 shows the best simulation results as it disperses water without concentrating it in a single area at the ground level. The design also does not rely on roof gutters as they concentrate water flow. Instead, the combination of tilted roof and walls allows for even distribution and better drainage.

Each option tested how different roof geometries direct the water flow and helped to refine the initial design solutions. By integrating hydrological simulation into the design process, the final design can minimize water accumulation, prevent localized flooding, and reduce excessive moisture in specific areas. Such design decisions improve the microclimate of the site by promoting better drainage and lowering humidity levels around the building.

Hydrological simulations illustrate the interaction between rainfall and the landform building. In this simulation study, different geometry shapes were tested, such as cuboid, wave-like, and single-sloped forms. The key findings are that some forms, such as single-sloped or narrowing landforms, tend to focus on the accumulation of water. The wave-like forms create a bowl-like effect and also tend to accumulate water. The optimal configuration of the building

allows an even dispersal of water, such as when the water flows perpendicular to the longer face. The simulation also showed that tilted walls help to direct water away from the building more efficiently by reducing surface runoff concentration.

5.3.3 Wind Simulation

Wind simulation is an essential part of a process-based design and is one of the most site-specific simulations, as wind behavior is dependent on local topography, adjacent buildings, and site orientation relative to wind direction. The main purpose of wind simulation is to understand how landform building influences wind behavior and microclimate in order to understand how design impacts outdoor comfort at the pedestrian level. An understanding of proposed wind conditions early in the design process fosters effective wind management to create a comfortable environment.

The relationship between buildings and natural forces, such as wind, might not always be straightforward and visible, yet they affect each other. Buildings impact wind speed and can be used to create specific microclimatic conditions. Traditionally, buildings served a sheltering function, such as protection from rain, wind, and heat (Baniotopoulos, 2011; Kabošová et al., 2020; Krautheim et al., 2014). However, to address the current climate needs, buildings not only should be protected from natural forces but also are shaped by processes and reflect site-specific conditions related to these processes.

Wind speed is influenced by different built environments (Figure 142). Wind speed increases differently with height across urban and suburban environments. In dense urban environments, tall buildings create significant turbulence, reducing wind speed near the ground but increasing it at higher elevations. In suburban environments, where there is less building density, wind speed can be higher at ground level and increase gradually with height (Kobi et al., 2018; Kormaníková et al., 2018). In open land, without any vertical obstacles to block wind, wind speed is higher at the ground level. The wind also reaches its higher speed at lower elevations compared to the city core environment (Cochran & American Society, 2012; Krautheim et al., 2014; Figure 142). Environmental processes and architectural form are intertwined. This dissertation uncovers how local processes of wind shape the built environment and local microclimate through 3D simulations. Such simulations help to optimize building form and improve environmental performance.

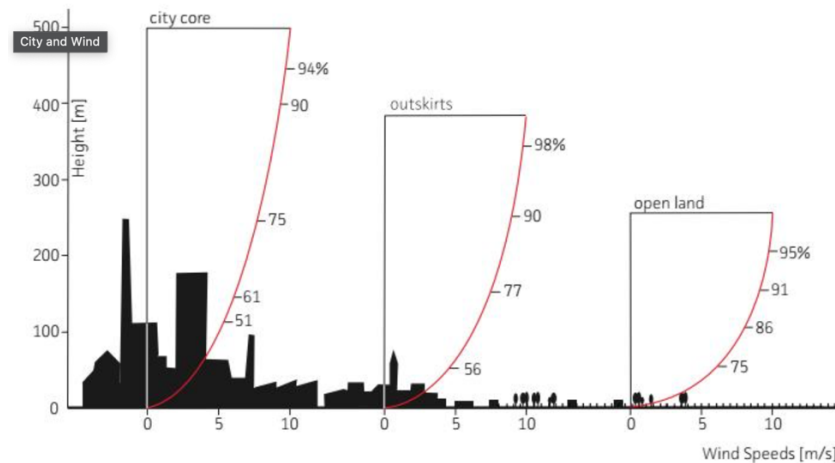


Figure 142. Diagram of wind speed in urban and non-urban environments. From Krautheim et al., 2014.

Current research strategies analyze existing software to incorporate microclimate analysis into the design process (Graham et al., 2020). Some authors explore how urban morphologies shape the microclimate (Zhu et al., 2023; Allegrini et al., 2015) and comfort level around the buildings (Jomehzadeh et al., 2020; Nagib & Corke, 1984; Bogdanović-Protić & Mitković, 2015) through case study analysis (Krautheim et al., 2014) and research through design experiments (Kabošová et al., 2020). Other studies focus on how building configuration might mitigate the wind's effect on high-rise buildings (Al-Najjar & Al-Azhari, 2021) and highlight the potential of parametric design (Kabošová et al., 2018; Yasa, 2016).

This research builds on the above studies about wind and investigates how architectural form and its position, landforms, and wind can shape the local microclimate. Landform buildings can have a significant effect on the wind as they merge with the surrounding landscape. Depending on the shape, the building can either increase or decrease the wind speed at a pedestrian level. Landform buildings can also disperse wind flow in such a way that prevents strong gusts or uncomfortable wind tunnels.

5.3.3.1 Building-Focused Wind Simulations on a Larger Scale

Wind simulation with the Butterfly tool in Grasshopper (Figure 143) represents the wind-flow patterns as they interact with the landform building, landscape, and vegetation. The wind simulation in Grasshopper is based on the Butterfly plug-in. Butterfly enables architects and

engineers to run CFD simulations using OpenFOAM, an open-source software for simulating fluid flow, heat transfer, and other physical processes. OpenFOAM facilitates wind analysis within Grasshopper and makes it easier to model how architectural form influences air movement. The input data for such simulation is building geometry, wind speed, and wind direction based on site-specific EPW data. Other components, such as point grids and vector fields, help to visualize how wind behaves when it meets obstacles like buildings or landforms. The main parameters of this simulation are wind speed and direction, which represent how design interventions affect the wind process.

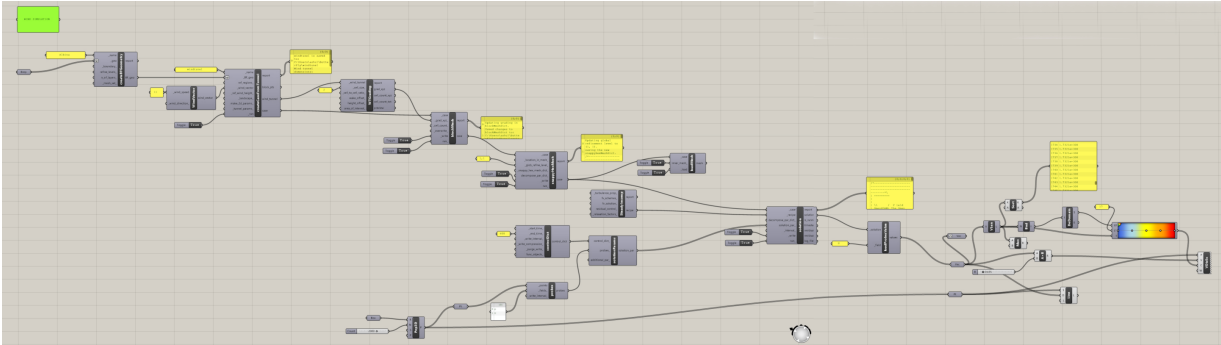


Figure 143. Wind simulation. Definition in Grasshopper (larger view in Appendix D, Figure 355).

Wind simulation for the site included multiple iterations of form for both the building and the landscape. The goal of these simulations is to find the form of the building and the adjacent environment that creates the most comfortable conditions with respect to wind. (For all wind simulations, see Appendix C, Figure 301–Figure 350.)

The input geometry for the first set of wind simulations were design options from the hydrological simulations. The simulations show how wind flows around the building at 60 feet high, which was chosen to show wind behavior from the ground level to above the roofline, where aerodynamic effects occur. The input parameters for this simulation were building geometry, north wind direction, 10 m/s wind speed, and bounding box for wind vectors. The north wind direction and 10 m/s wind speed were selected based on prevailing wind conditions at the site. The output result were 3D vectors that represent the wind flow.

The wind simulation for Option 1 (Figure 144) shows how the wind changes speed in the presence of a cuboid form. This option corresponds to the same geometry options used in the hydrological simulations; this helps to compare environmental processes for the developed

design. The plan view shows that along the site, most of the vectors stay the same speed of ~8.2 m/s. The perspective image shows that above the cuboid form, the wind speed increases to 8.9 m/s. The wind slows to 5.2 m/s behind the cuboid form. Side and front views show the increase of wind speed every 15 vertical feet: At 0–15 feet the wind reaches 5.2 m/s, at 15–30 feet the wind reaches 6.7 m/s, at 30–45 feet the wind reaches 7.5 m/s, and at 45–60 feet the wind reaches 8.2–8.9 m/s.

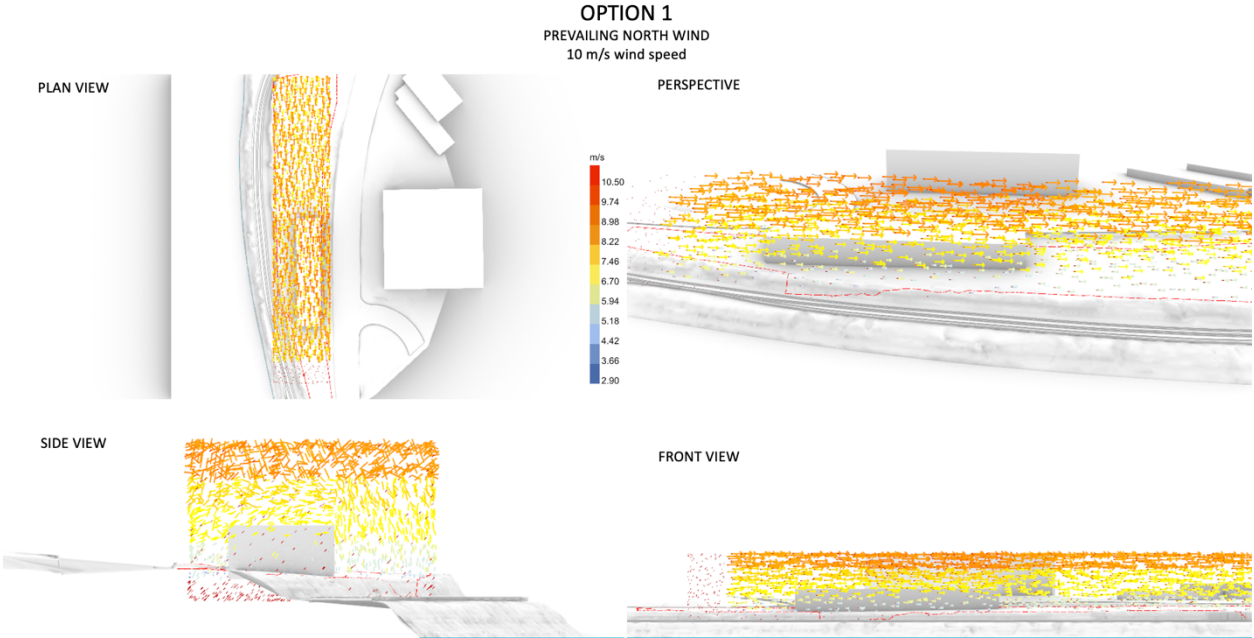


Figure 144. Wind simulation for prevailing wind 10 m/s for Option 1. Plan, perspective, side, and front views.

The wind simulation for Options 2–10 (Figure 145–Figure 146) shows that some design options, such as Options 5–10, increase wind speed to 10 m/s above the building, at the height of 45–60 feet. Other options, such as Options 3–5, show the increase of wind to 7.5–8.0 m/s at the height of 45–60 feet and a more comfortable position up to 20 feet, on a building level. While simulation results were useful for a general picture of how wind interacts with the design options at 15 feet and higher, they showed very little of how wind interacts with the building on the pedestrian level.

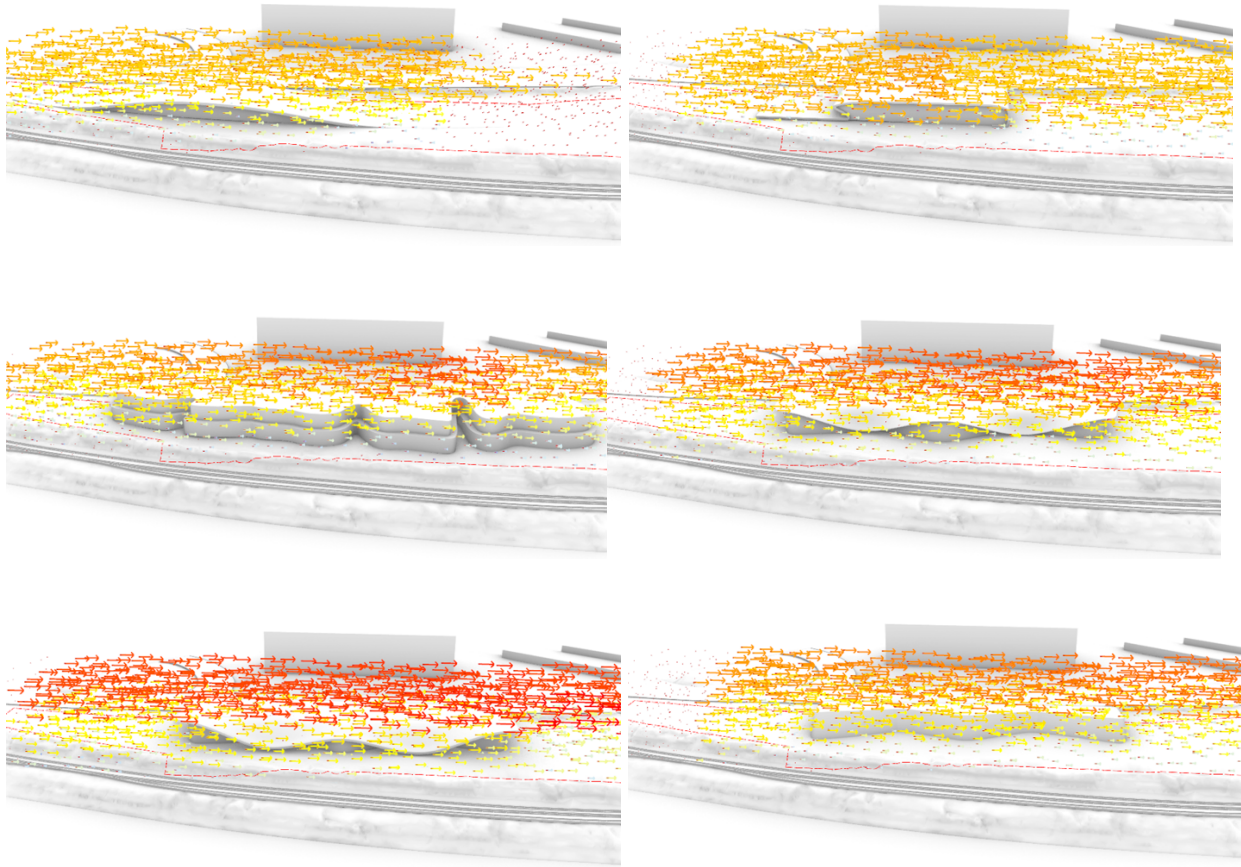


Figure 145. Wind simulation for prevailing wind 10 m/s for Options 2–7. Perspective views.

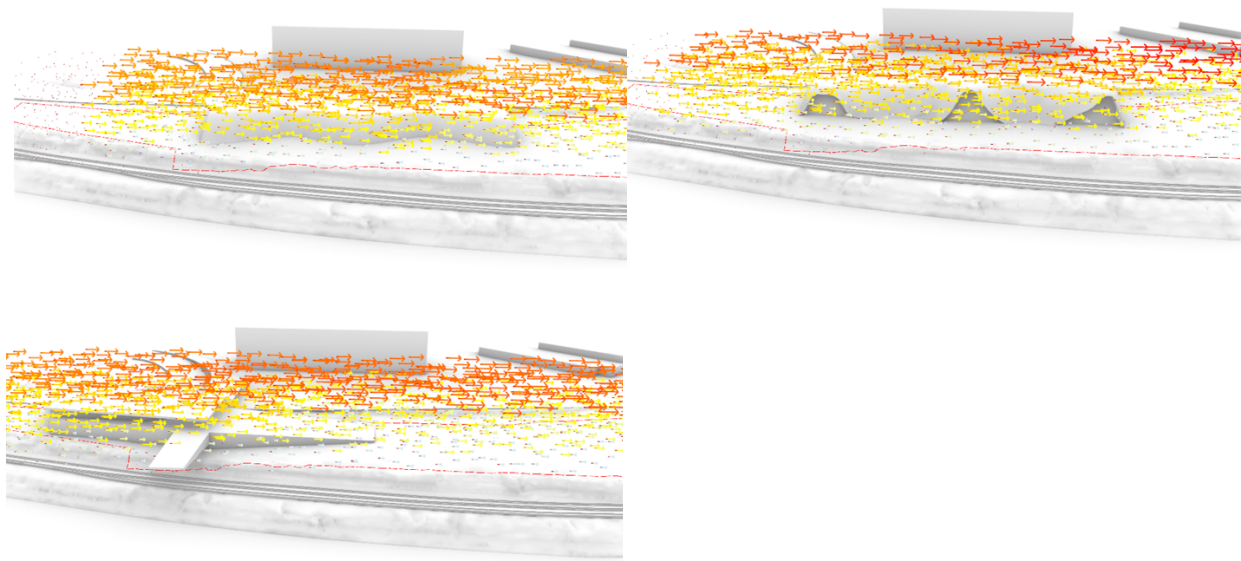


Figure 146. Wind simulation for prevailing wind 10 m/s for Options 8–10. Perspective views.

5.3.3.2 Building-Focused Wind Simulations on a Smaller Scale

The second set of simulations focused on how wind interacts with basic architectural forms at the pedestrian level. These forms were selected because they are basic architectural shapes commonly used in an urban context.

The inputs for this simulation were basic forms, north wind direction, 10 m/s wind speed as prevailing wind condition, and horizontal section plane at a height of approximately 6 feet. Since the site slopes toward the river, the height of the horizontal plane in relation to the ground varies. Throughout this section, the river-facing side is referred to as the “riverfront,” while the opposite side is referred to as “inland.” The “front” refers to the side of the building that faces the incoming wind from the north, while the opposite side is referred to as “behind the building” unless specified differently.

Figure 147 represents the wind simulation for the cuboid form. The simulation shows that the speed of the wind before it meets the building is 5.2 m/s. Once the wind hits one of the building facades, it changes to 4 m/s in front of the building and 6 m/s at the corners. The wind speed toward the riverfront is 5.2 m/s, while on the opposite side of the building the wind is 3.7 m/s. Behind the building, the wind reaches 5 m/s. The simulation represents the corner effect,

when wind increases around the corners of the building. Once the wind hits the building's facade, it changes direction and increases in speed around the corners.

Wind simulation for two cuboids (Figure 147), compared to one shape, illustrates a slower 4 m/s wind speed in front of the building's facade that faces the wind direction, similar values around the corner, near the riverfront, and behind the building. However, the space between the two shapes creates the channeling effect and increases wind speed to 6.7 m/s. This happens when wind is guided through a narrow space between two buildings, increasing the speed as it moves along such a corridor. This effect happens when buildings are closely spaced, have similar height, and create a continuous passage for wind flow. The narrower the gap relatively to the building height, the greater the wind acceleration.

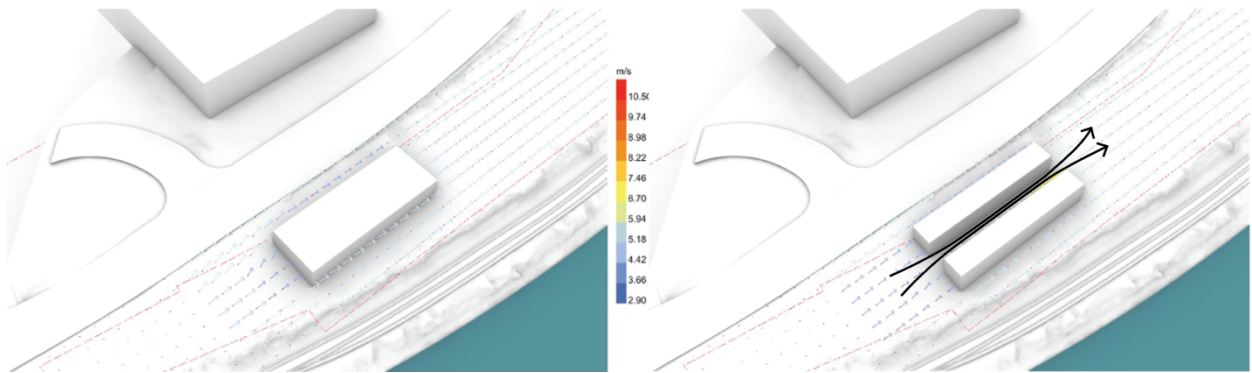


Figure 147. Left: Wind simulation for cuboid shape. Right: Wind simulation for two cuboids.

Once the front cuboid building is rotated 10 degrees toward the west, the wind speed increases around the building and reaches 6.5 m/s on the outer corners (Figure 148). The wind speed in between two buildings decreases to 4.4 m/s. When the building is rotated 10 degrees the opposite way, the wind speed decreases to 3.7 m/s in front of the building's facades (Figure 148). Compared to the previous simulation, the wind speed around the building decreases and ranges between 4–5 m/s. Between two buildings, the wind speed in the narrow part reaches 5.2 m/s, which creates the funneling effect. While a similar condition to the channeling effect, the funneling effect refers to wind being forced through a passage of buildings that meet sharply together, causing a bottleneck. The highest wind speed in such a situation is at the narrower space (or “neck”) as the opening decreases. The simulation shows that once the space between buildings increases, the wind speed decreases to 4.4 m/s toward the end.

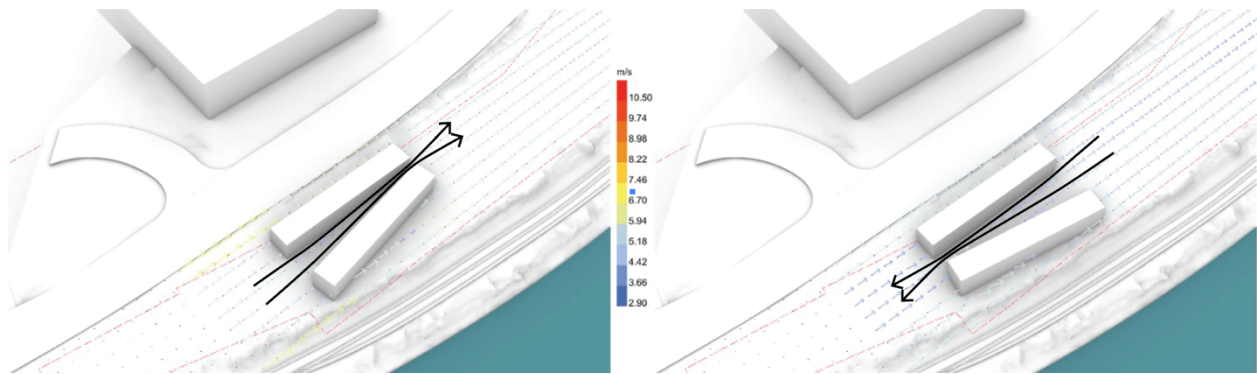


Figure 148. Wind simulation for two cuboid shapes rotated 10 degrees.

The following set of wind simulations illustrates one, two, and three cuboid buildings rotated 30 degrees (Figure 149). For a single building, the wind decreases from 6.4 m/s before it hits the building façade to 5.2 m/s once the wind hits the building. Around the corners, wind speed increases to 6.7 m/s. Behind the longer part of the building, the wind speed decreases to 3.6 m/s and creates a low-pressure zone. At the end of the building, wind speed returns to 6.4 m/s. For two buildings, wind speed in front of the building facade ranges between 3.6–4.4 m/s. Around the corner that is closer to the road, the wind speed reaches 6 m/s. Between two buildings that were positioned at a distance of 32 feet, there was no wind. Behind the second building, the wind reaches 6.7 m/s and creates the low-bar row effect. This condition happens when wind interacts with a series of low-rise buildings with wide, exposed windward facades. The wind increases as it flows over the rooftop and creates high speed zones with uncomfortable conditions. In contrast, when wind passes through gaps between building, the speed decreases. After the building ends, the wind speed decreases to 5.2–5.8 m/s. Three buildings create similar conditions to the set of two; however, compared to the simulation with two buildings, the wind speed behind the second building reached 6.7 m/s, while the presence of a third building decreases the wind to 5.0–5.5 m/s.

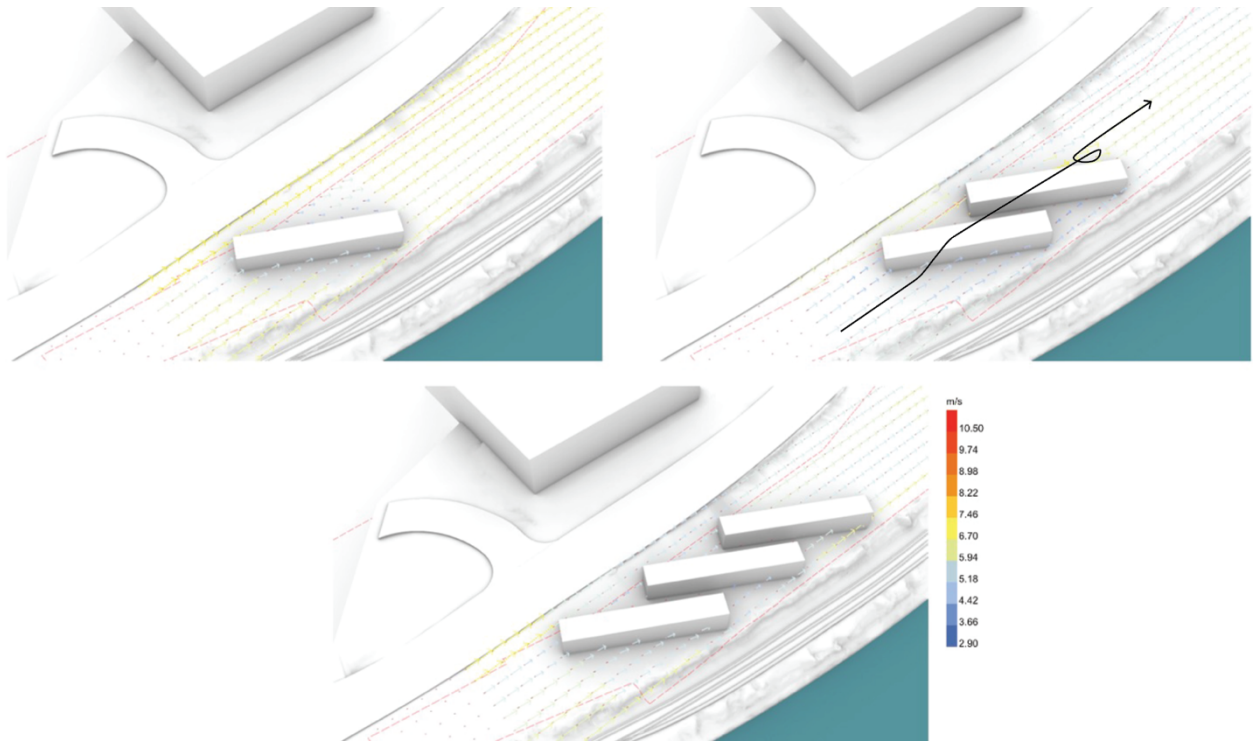


Figure 149. Wind simulation for one, two, and three cuboid shapes rotated 30 degrees.

Another set of wind simulations illustrates one, two, and three buildings (Figure 150) with wide facades exposed to the wind. For one building, the wind speed reaches 6.7 m/s before it hits the building facade and decreases to 5.2 m/s once the wind hits the building. Around the corners, the wind reaches 6.7 m/s. Behind the building, the wind decreases to 3.6 m/s and creates the low-bar row effect. After the zone of low speed, the wind returns to 5.7–6.5 m/s. For a set of two buildings, the wind conditions in front of the building are similar to the previous simulation. The wind speed decreases significantly between two buildings, and the low-speed zone behind the second building gets smaller. The wind returns to 5.7–6.5 m/s with shorter distance. For a set of three buildings, the space between the second and third building gets 5.2 m/s wind speed toward the corners. The wind speed behind the third building almost immediately increases to 6.0–6.5 m/s.

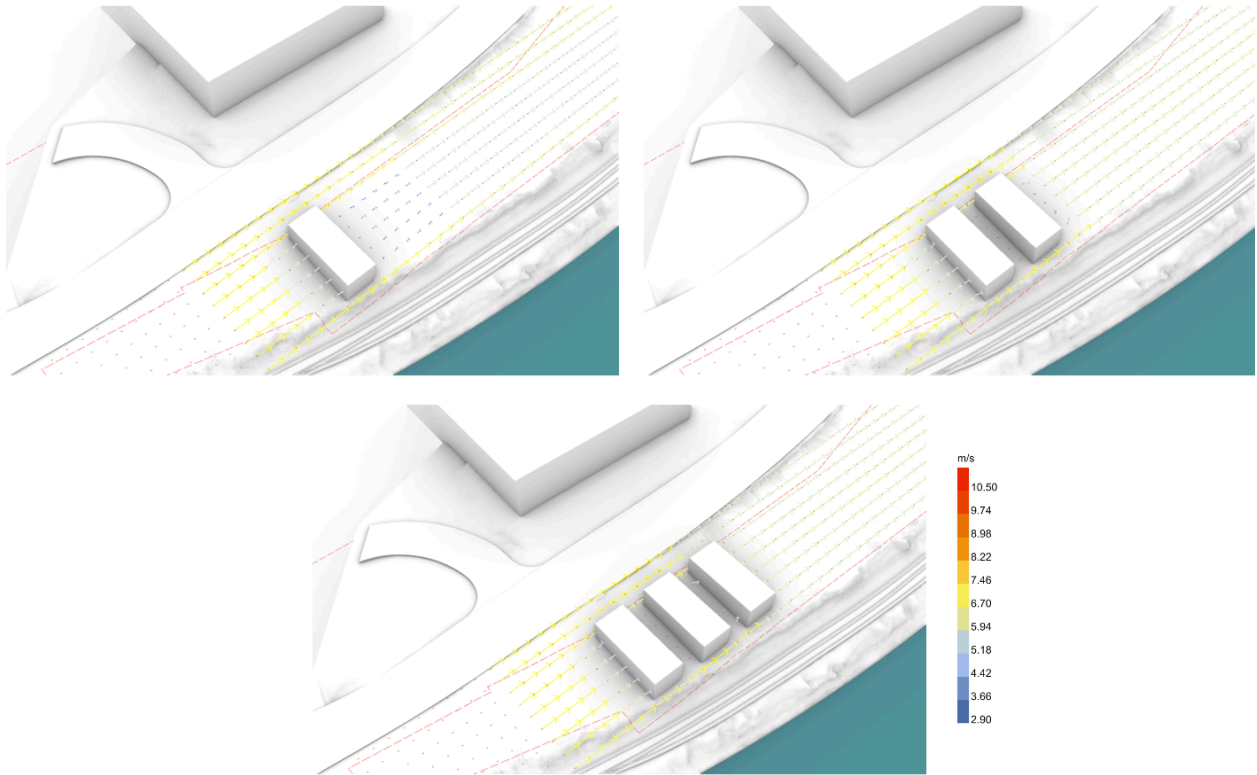


Figure 150. Wind simulation for one, two, and three cuboid shapes.

The following wind simulation is for building roofs with a single slope oriented against and along the wind (Figure 151). For the building with a slope oriented against the wind, the speed reaches 3.6 m/s before it hits the building facade and decreases to 3 m/s once the wind hits the building. Around the corners, the wind reaches 5 m/s. Toward the end of the sloped roof, the wind increases to 5.9 m/s. Further along the site, the wind decreases to 3.6 m/s, and 4.4 m/s by the riverfront. For the building with a slope oriented toward the wind, the speed reaches 3.6 m/s around the entire site. The wind increases 5 m/s along the slope.

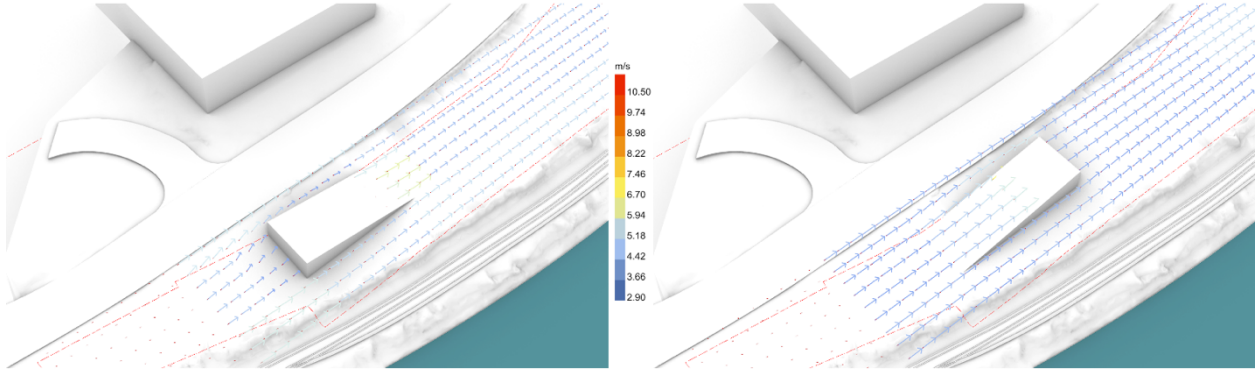


Figure 151. Wind simulation for one-sloped shapes.

Once the building form of a one-slope building is modified to a convex-like shape, the wind conditions change (Figure 152). For the building with a slope oriented along the wind, the speed reaches 5 m/s before it hits the building. Around the corners, the wind reaches 5.3 m/s. Behind the building, there is a windless zone. Further along the site, the wind decreases to 3.6 m/s. For the building with a slope oriented against the wind, the speed reaches 5 m/s before it hits the building facade and decreases to 3.6 m/s once the wind hits the building. Around the corners, the wind increases to 5.2 m/s and 5.9 m/s near the riverfront. Toward the end of the slope, the wind increases to 5.9 m/s. Further along the site, the wind decreases to 3.6 m/s.

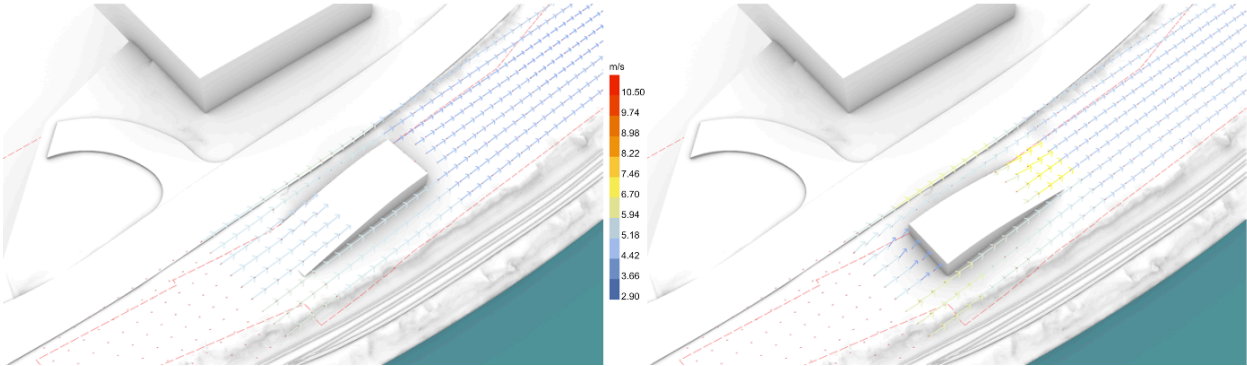


Figure 152. Wind simulation for convex-like shapes.

Another set of wind simulations were performed on concave-like shapes (Figure 153). For the building with a slope oriented toward the wind, the speed reaches 5 m/s before it hits the building. Around the corners, the wind reaches 5.3 m/s. Behind the building, there is a windless zone. Further along the site, the wind decreases to 3.6 m/s. For the building with a slope oriented against the wind, the speed reaches 5 m/s before it hits the building facade and decreases to 3.6 m/s once the wind hits the building. Around the corners, the wind increases to 5.2 m/s and 5.9 m/s near the riverfront. Toward the end of the slope, the wind increases to 5.9 m/s. Further along the site, the wind decreases to 3.6 m/s.

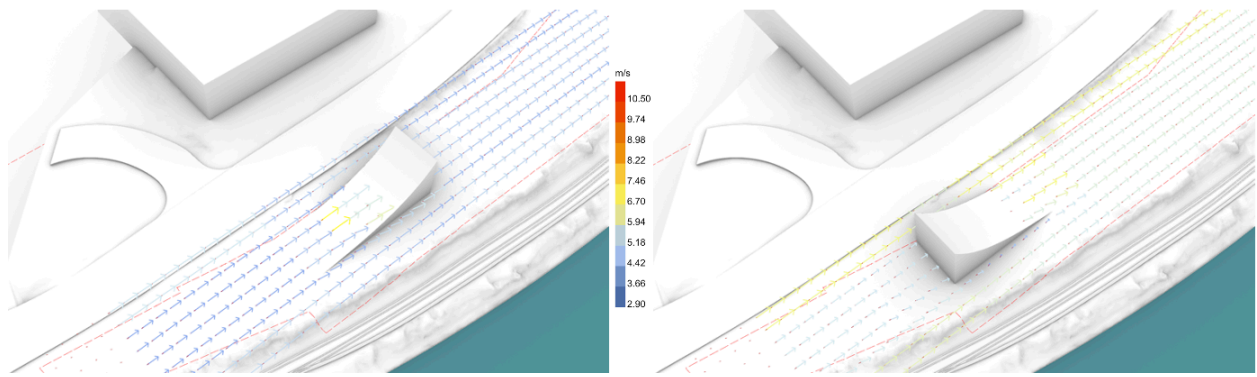


Figure 153. Wind simulation for a concave-like shapes.

The following set of wind simulations is for u-shaped buildings with right and fillet corners (Figure 154). For the u-shaped building with right angles, the speed reaches 6.5 m/s before it hits the building. Around the corners and along the long edges of the building, the wind reaches 5.3 m/s and 6.7 m/s by the riverfront. The u-shape creates a zone where wind decreases to 3.8–4.4 m/s. Behind the building, the wind decreases to 5.2 m/s. Compared to the previous simulation, the wind speed around the outer fillet edges increases to 5.9–6.7 m/s around the entire building. Fillet edges inside the u-shape also increase the wind speed to 5.2–6.5 m/s. The u-shape rotated in the opposite direction decreases the wind speed in front of the building facade and along the u-shape to 5.2 m/s.

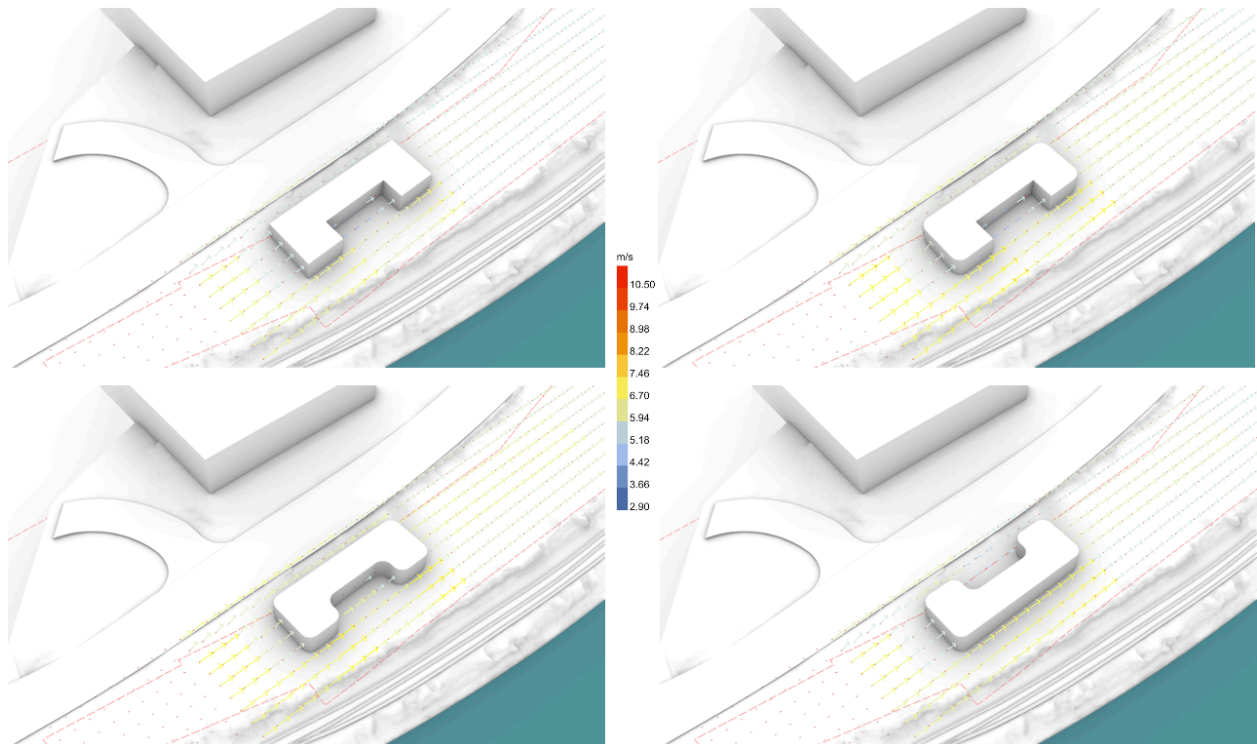


Figure 154. Wind simulation for u-shapes with right and fillet edges.

Another iteration of wind simulations was performed on a compressed u-shaped building with fillet edges, rotated every 45 degrees in relation to wind direction (Figure 155). Once the u-shape was positioned perpendicular to the wind toward the riverfront, the speed reached 6.5 m/s before it hit the building and decreased to 5.2 m/s once it hit the building. Around the corners and along the long edges of the building, the wind reached 5.3 m/s and 6.5 m/s by the riverfront. A smaller u-shaped courtyard compared to the previous set of simulations creates a windless zone. Behind the building, the wind decreases to 4.5 m/s. The option with a u-shape rotated 180 degrees toward the road does not change wind speed around the building and site. Once the u-shape is rotated toward the wind direction, the wind speed decreases to 5.2 m/s in front of the building and increases at the corners to 6.7 m/s. Behind the building appears a small wake zone with the wind speed of 3.6 m/s. Further along the site, the wind speed increases to 5.9 m/s. Once the u-shape is rotated 170 degrees against the wind direction and the longer facade is oriented toward the wind, it increases wind speed to 6.7 m/s before it hits the building and around the corners. Behind the building, the u-shaped courtyard creates a windless zone.

Once the building is rotated 45 degrees with a pointed angle toward the wind direction, the wind speed and conditions around the building change. The wind speed reaches 6.5 m/s

before it hits the building and around the corners. It decreases to 5.9 m/s only at some places before it hits the building. The u-shaped courtyard, rotated toward the riverfront, creates the low-bar row effect with 6.5 m/s wind speed, which decreases to 3.6–4.4 m/s. The wind speed behind the building reaches 5.9 m/s. Once the building gets rotated 180 degrees with a u-shaped courtyard facing the road, the wind conditions stay the same in relation to the courtyard shape. Once the u-shape courtyard is rotated toward the wind direction, the courtyard creates a zone with 5.2 m/s wind speed, compared to 6.5 m/s around the corners. Behind the building is a bigger wake zone compared to other simulations, with the wind speed of 3.6–4.4 m/s. Similar wind conditions are for the building rotated 180 degrees toward the riverfront.

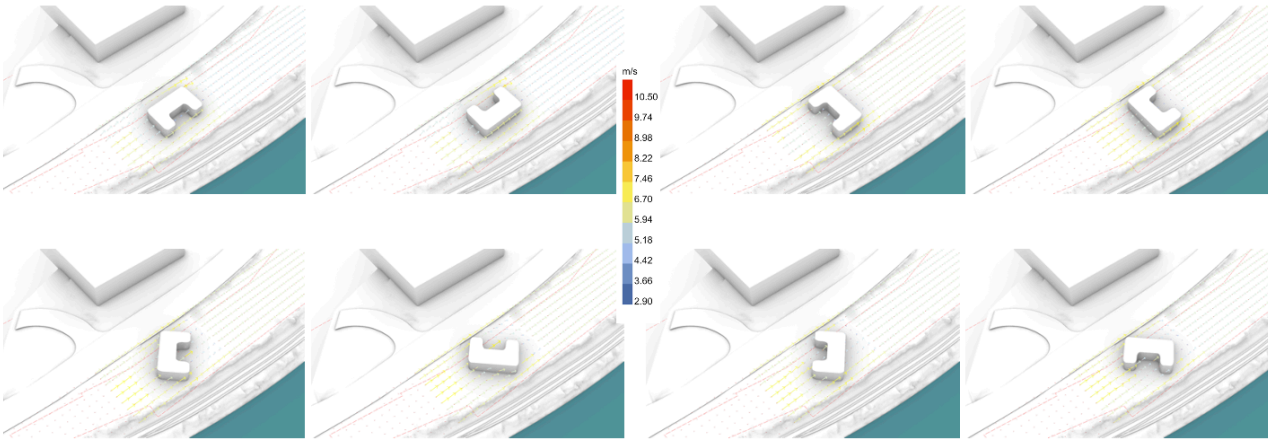


Figure 155. Wind simulation for u-shapes with fillet edges rotated every 45 degrees.

The following set of wind simulations is for u-shaped buildings with single-sloped roofs rotated every 90 degrees in relation to wind direction (Figure 156). For the u-shaped building with a slope toward the riverfront, the speed reaches 5 m/s before it hits the building. The wind speed decreases to 4.2 m/s around the taller building corner and stays 5 m/s by the corner that touches the ground. The wind speed by the u-shape increases a bit to 5.2 m/s and reaches 5.9 m/s behind the building edge. Around the opposite corner, the speed also increases to 5.9 m/s. Behind the building, the wind decreases to 3.6 m/s.

Once the building is rotated 90 degrees, with a longer and taller edge toward the wind direction, the wind speed increases to 6.5 m/s before it hits the building. Once the wind hits the building, the speed decreases to 5.2 m/s. Around the corners of the building, the wind reaches 5.9 m/s and 6.7 m/s by the riverfront. The sloped roof also creates a condition with 6.7 m/s wind speed. The u-shape creates a zone where the wind decreases to 3.0–3.6m/s. Behind the building,

the wind decreases to 5.2 m/s. Once the building is rotated with a sloped roof toward the wind direction, the wind speed increases to 7 m/s in front of the building, around the corners, and on the sloped roof. Behind the building is the small wake zone with the wind speed of 3 m/s. Further along the site, the wind speed reaches 5.9 m/s.

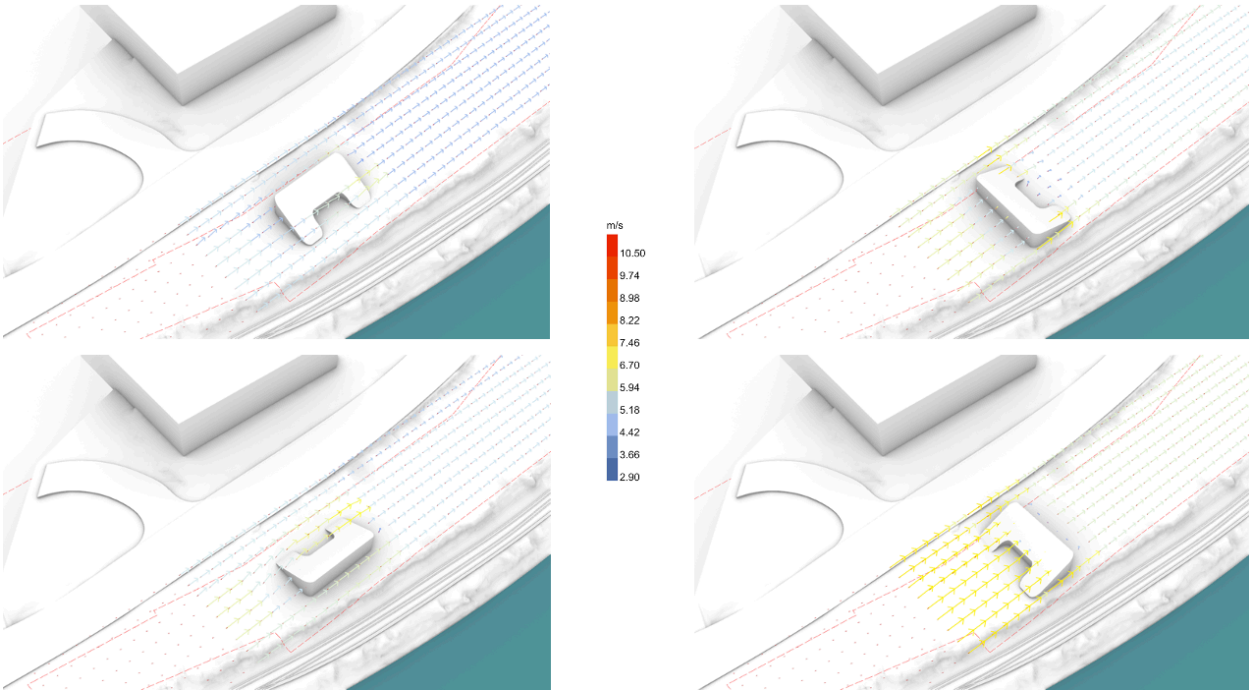


Figure 156. Wind simulation for one-sloped u-shapes with fillet edges.

The wind simulations illustrate that the interaction between the building and the wind creates specific wind effects. As the wind hits the building facade, it gets redirected and wind speed increases around corners (corner effect). The longer the face of the building toward the wind direction, the higher the speed around the corners. There are areas where wind decreases, such as in front of the building due to the impact of wind against the building facade. Behind the building, the wind speed decreases, too, and creates a wake zone.

Once the wind flows through a narrow gap between two buildings, oriented toward the wind direction, the wind speed increases and creates less comfortable conditions than around the single building (channeling effect). However, once one of the buildings is rotated, the wind conditions change. If the building is rotated in a way that creates a wider opening toward the wind direction, the speed between the two buildings increases. Once the building is rotated against the wind direction, the wind decreases inside the wider opening.

The position of the building on the site, such as rotating the building by 10, 30, 45, or 90 degrees, in relation to the wind direction can increase or decrease wind in specific conditions. Rotating a single-standing building by 10, 30, or 45 degrees at an angle to the wind increases the speed. In comparison, rotating the building by 90 degrees can either increase (the longer side of the building) or decrease (shorter side of the building) the wind speed. When there is a set of buildings rotated at an angle to the wind, the speed tends to decrease before it hits the building compared to a single building. The space between buildings creates more comfortable wind areas, where wind decreases and sometimes even disappears completely (depending on the size of the space). However, behind the set of buildings, the wind increases compared to the single building (low-bar row effect).

Different building shapes, such as single-sloped, convex, concave, and u-shaped buildings, can significantly influence wind conditions. Once a single-sloped building is rotated toward the wind direction, the wind speed does not change significantly, while rotation against the wind increases the wind speed on sloped edges. Convex buildings behave similarly to one-sloped buildings, while concave buildings increase the speed in both directions. Within u-shaped courtyards, wind tends to decrease as this area is sheltered; however, the courtyard's position in relation to the wind also matters. When the building courtyard is located 90 degrees toward the wind direction, there might be low wind speed or a windless zone (depending on the size of the courtyard). Once the building is rotated 45 degrees with a courtyard toward the wind, the speed increases.

Wind speed and conditions change around the right or fillet edges of the building due to the way the wind is redirected. The right or sharp corners redirect wind more abruptly, which causes higher wind speed on corners. The fillet corners change wind direction more smoothly, which can lower the wind speed around the corners and further along the building.

5.3.3.3 Landform Wind Simulations

The following set of wind simulations focused on hill-like landforms and their interaction with the wind. These forms were selected to explore how different curvatures and orientations influence wind behavior in contrast to the basic architectural forms examined earlier. For a single landform (Figure 157), the wind speed reaches 4.4 m/s before it hits the landform and decreases to 3.6 m/s once the wind hits the windward face. Because of the smooth and rounded

shape, there is little to no corner effect, and the wind returns to 4.4 m/s speed. Toward the end of the landform, the wind decreases to 3.6 m/s. Further along the site, the wind returns to 4.4 m/s. For an elongated landform, the wind decreases to 3.6 m/s before it hits the landform, while it stays the same around the corners and toward the end of the landform. The bigger difference happens once the landform is rotated 90 degrees with a longer edge perpendicular to the wind direction. In this simulation, the wind speed reaches 5.2 m/s before it hits the landform and decreases to 4.6 m/s once the wind hits it. Around the corners, there is a stronger corner effect, and the wind increases to 6.5 m/s speed. Behind the leeward face is a small wake zone with little to no speed, or 2.9 m/s. Further along the site, the wind returns to 5.2 m/s.

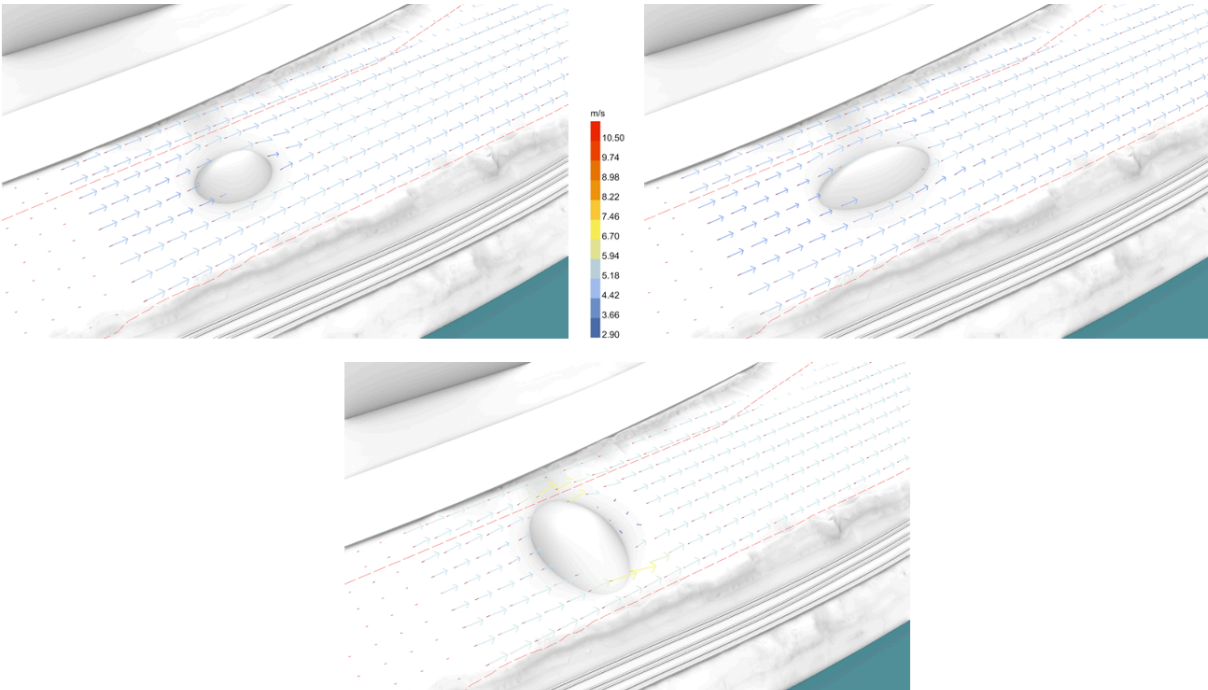


Figure 157. Wind simulations for single landforms.

For two landforms positioned perpendicular to wind direction (Figure 158), the wind speed reaches 5.2 m/s before it hits the landform and decreases to 5 m/s once the wind hits it. There is little to no corner effect around the outer edges of the landform; however, between landforms, the wind increases to 6.5 m/s. Behind the landform is a small wake zone with a wind speed of 3 m/s. Further along the site, the wind returns to 5.2 m/s. Once landforms are rotated 90 degrees and positioned parallel to the wind direction, the wind speed reaches 3.8 m/s before it hits the landform and decreases to 3.6 m/s once it hits it. Around the corners and between the

two landforms, the wind increases to 4.4 m/s. Behind the second landform, the wind speed increases to 6.5 m/s. Further along the site, the wind returns to 3.8 m/s.

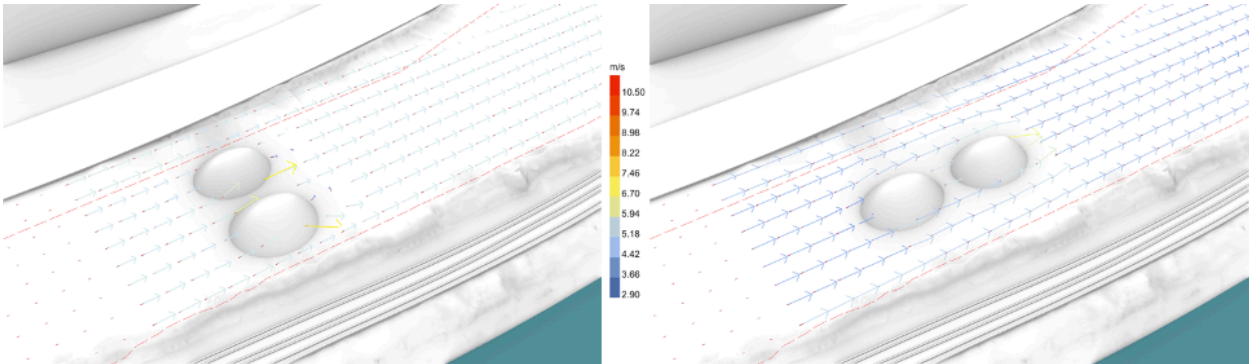


Figure 158. Wind simulations for two landforms.

For two landforms positioned 45 degrees toward the wind direction (Figure 159), the wind speed reaches 3.8 m/s before it hits the closest landform and decreases to 3.6 m/s once it hits it. For a landform that is positioned further, the wind speed reaches 4.4 m/s before it hits the landform and decreases to 3.6 m/s once it hits it. There is little corner effect around the outer edges of landforms where wind increases to 5 m/s. Behind the first landform, wind reaches 5.9 m/s and 6.2 m/s behind the second. Further along the site, the wind decreases to 3.6 m/s and later returns to 4.4 m/s. Once landforms are mirrored, the wind behind the landform close to the riverfront reaches 6.7 m/s.

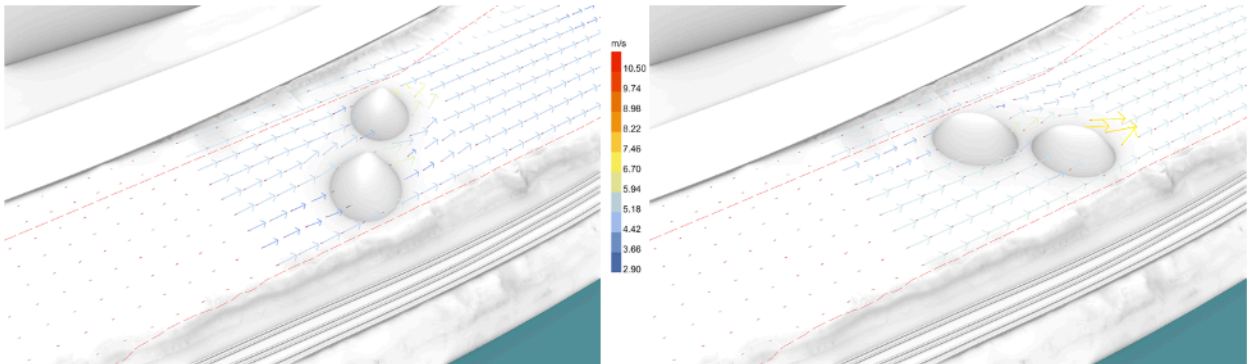


Figure 159. Wind simulations for two landforms rotated 45 degrees.

For three landforms located parallel to the wind direction (Figure 160), the wind speed reaches 5 m/s before it hits the closest landform. The corner effect around the first landforms shows the increase of wind to 5.2 m/s, and before the wind transitions to the second landform, the wind decreases to 3.8 m/s. However, when the wind transitions to the third landform, it

increases to 5.2 m/s and 5.6 m/s around the corners. Between the first and the second landform, there is no wind, while behind the second and third landforms the wind increases to 5.9 m/s. Behind the third landform, the wind reaches 5.9 m/s. Further along the site, the wind decreases to 4 m/s.

For three landforms rotated 15 degrees toward wind direction (Figure 160), the wind speed reaches 4.4 m/s before it hits landforms and decreases to 3.8 m/s once it hits them. The corner effect around the first landforms by the riverfront shows the increase of wind to 5.2 m/s, increases to 6 m/s around the second landform, and 6.7 m/s around the third landform. Along N. Thunderbird Way, the wind increases to 5.2 m/s around each landform. Between landforms and behind the third landform is a wake zone. Further along the site, the wind decreases to 4.4–5.2 m/s.

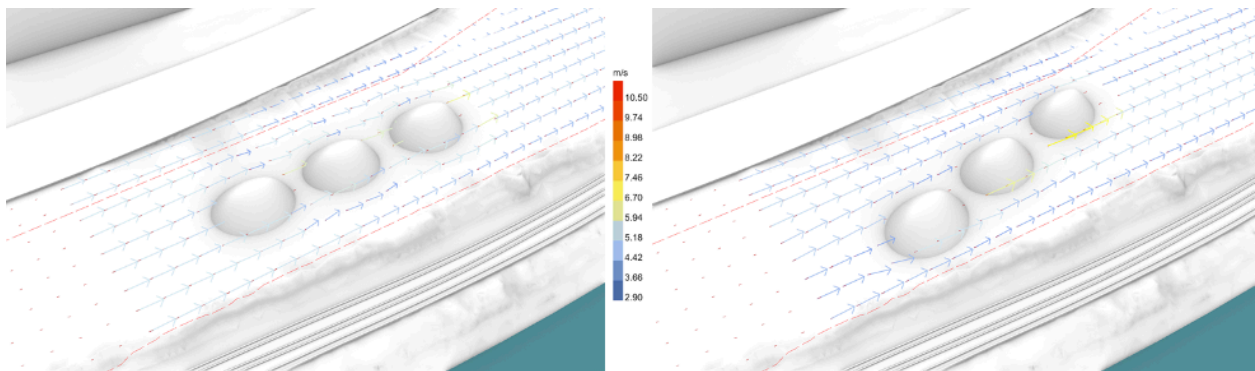


Figure 160. Wind simulations for three landforms.

Landforms interact with the wind similarly to buildings; the number of landforms, their orientation, and their positioning can either increase or decrease the wind speed. Single landforms decrease the wind speed if the longer side is parallel to the wind direction. If the landform is positioned perpendicular to the wind, it decreases the wind speed around the corners. When double landforms are placed perpendicular to the wind direction, they create a channeling effect and increase the speed in between them. However, when two landforms are parallel to the wind, they reduce the wind speed. When two landforms are rotated 45 degrees, the wind speed increases after each landform. When three landforms are positioned parallel to the wind direction, the simulation shows a slight increase in the wind after each landform. Once three landforms are rotated 15 degrees, the wind speed increases even more.

5.3.3.4 Vegetation Wind Simulation

The tree shape used in this simulation was created using a Grasshopper vegetation simulation. The simulation was used to create the tree structure. The resulting geometry was baked into Rhino, where the Pipe command was applied to assign thickness to the tree trunk and individual branches.

For a single tree (Figure 161) with the input wind speed 6 m/s, chosen to represent moderate wind conditions, the wind speed reaches 3.6–5.0 m/s before it meets the tree. The corner effect around the tree shows the increase of wind to 6 m/s. Behind the tree, the wind decreases to 3 m/s, and further along the site, the wind returns to 4.4 m/s. For the input wind of 10 m/s, the wind increases to 5.2– 5.9 m/s in front of the tree, 6.2 m/s around the tree crown, and 4.4 m/s behind the tree.

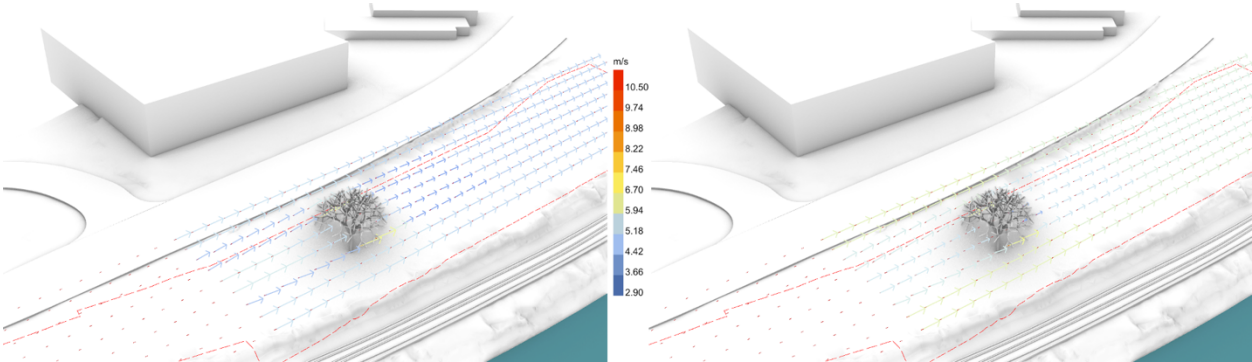


Figure 161. Wind simulation for single tree with 6 m/s and 10 m/s wind speed.

For two trees (Figure 162) with the distance of 9 feet between crowns, and an input wind speed of 10 m/s, the wind speed reaches 5.2 m/s before it meets the trees. The wind increases around the first tree crown to 6.2 m/s. Behind the first tree, the wind decreases to 4.8 m/s. Behind the second tree, the wind does not decrease and reaches 5.9 m/s, the same as further along the site. For two trees with no distance between the crowns, the wind speed behind the second tree slightly decreases to 3.6 m/s.

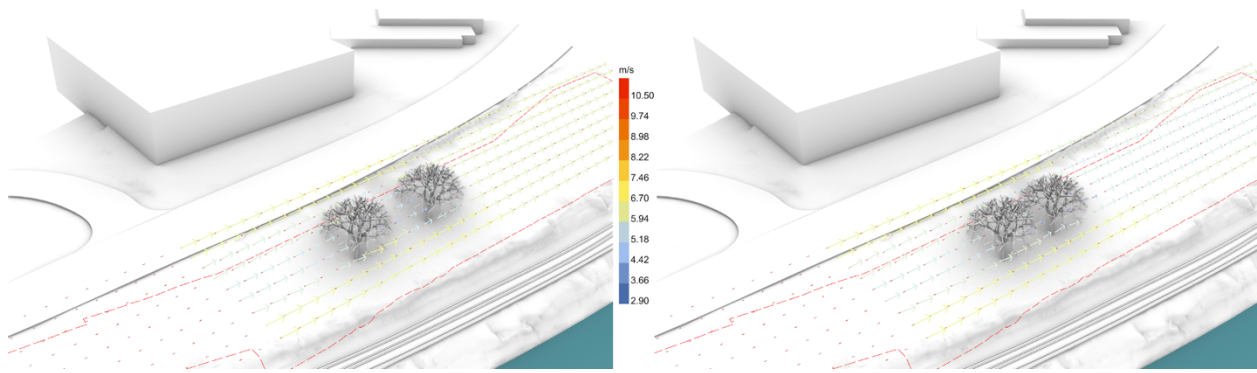


Figure 162. Wind simulation for two trees.

For three trees (Figure 163), the input wind speed reaches 5.2–6.2 m/s before it meets the trees. The wind increases around the tree crowns to 5.9 m/s and decreases to 3.6 m/s between the trees. Behind the third tree, the wind does not decrease and reaches 5.2 m/s. Further along the site, the wind decreases to 5.2–5.7 m/s. For trees rotated 15 degrees, the wind speed increases to 5.2–6.7 m/s before it meets the trees. The wind speed around the first crown decreases to 5.2 m/s, around the second crown to 4.4 m/s, and around the third to 3.6 m/s. Once the trees are rotated 30 degrees, the wind speed reaches 5.9–6.7 m/s before it meets the trees. In front of the first tree and around the tree crown, the wind decreases to 5.2 m/s. Around the second tree, the wind slightly decreases to 5 m/s, and 4.8 m/s around the third tree. Further along the site, the wind speed increases to 5.9–6.5 m/s. For trees rotated 45 degrees, the wind speed in front of the first tree reaches 5.2 m/s; the second, 5.9 m/s; and the third, 6.6 m/s. The wind decreases to 3.6 m/s behind the first tree, 4.4 m/s behind the second tree, and 5.2 m/s behind the third tree. Further along the site, the wind speed decreases to 5.2–5.9 m/s.

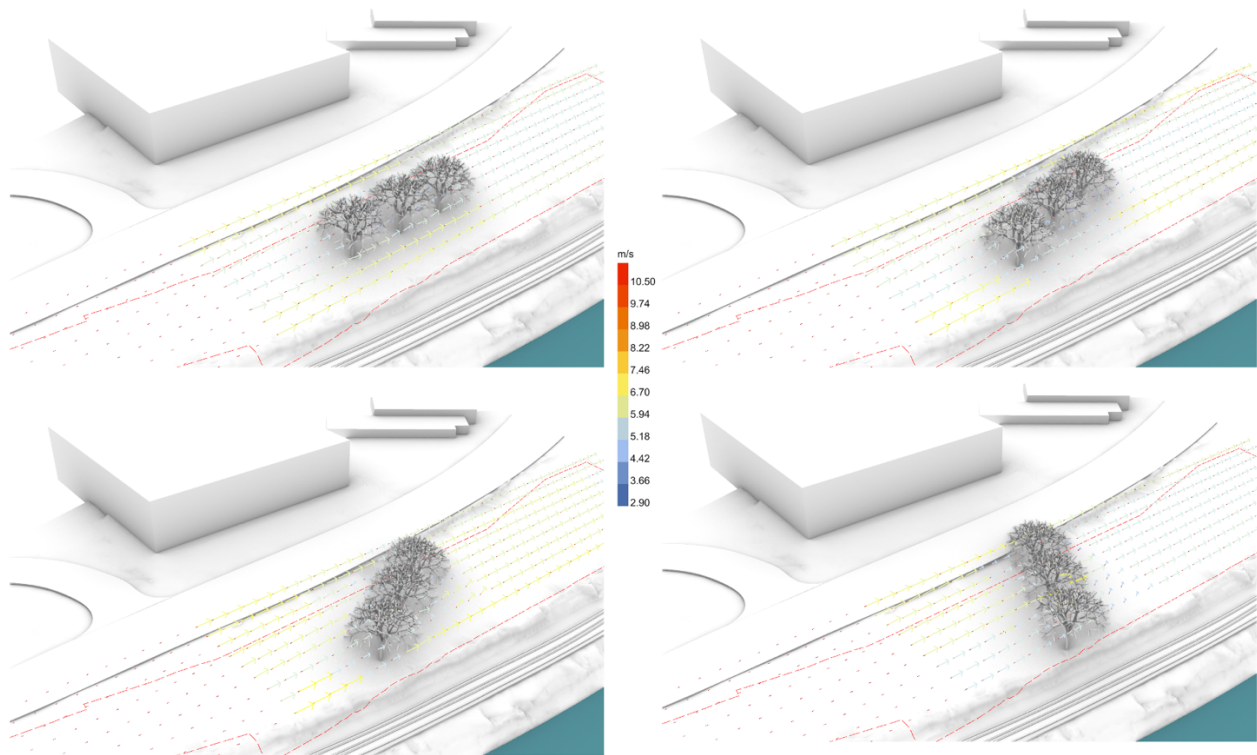


Figure 163. Wind simulation for three trees rotated 15, 30, and 45 degrees.

The wind simulation for trees shows that wind speed changes around the trees similarly to how it changes around the buildings. The wind speed increases around the crown due to the corner effect. Once the row of the trees is rotated, the wind speed increases. When the space between trees is bigger, the wind speed increases. Once the space between trees is smaller, the wind speed decreases. The wind speed also decreases behind trees, similarly to how it decreases behind buildings.

5.3.4 Vegetation Simulation

Vegetation simulation is the last simulation from the process-based set. The main purpose of this simulation is to visualize vegetation placement and growth to understand how the site changes with design intervention. The simulation helps to visually represent the growth of plants over time and test the interaction of plants with wind patterns. Such simulation complements previous simulations in terms of finding the most suitable design to create comfortable microclimate conditions.

In nature, the growth of a tree begins with the seed. Over time, the seed germinates, and the seedling grows and matures into a tree. The tree crown increases in size, as well as the number of branches under the influence of climate conditions. A similar idea lies behind vegetation simulation. The point or a group of points serve as “seeds” that initiate the growth of a tree in Grasshopper. By using an algorithm that mimics natural growth, it is possible not only to simulate tree growth but also to explore the spatial dynamic of the vegetation. The vegetation process is integrated into the design to address heat issues at the site.

The vegetation definition in Grasshopper is based on the Anemone plug-in, which creates tree growth cycles and repeats the growth process numerous times (Figure 164). The input data for such a simulation is a single point or group of points. Other components of the simulation are length, number of iterations, amplitude, radius, and number of segments. The length parameter defines the height of the tree trunk before the start of the branches. The amplitude parameter defines the maximum height of each iteration of branches. The radius parameter defines the radius of the tree crown. The number of segments defines the number of branches at the beginning of the definition. With each iteration, the number of branches is multiplied by three to mimic natural growth patterns where branches subdivide into smaller branches.

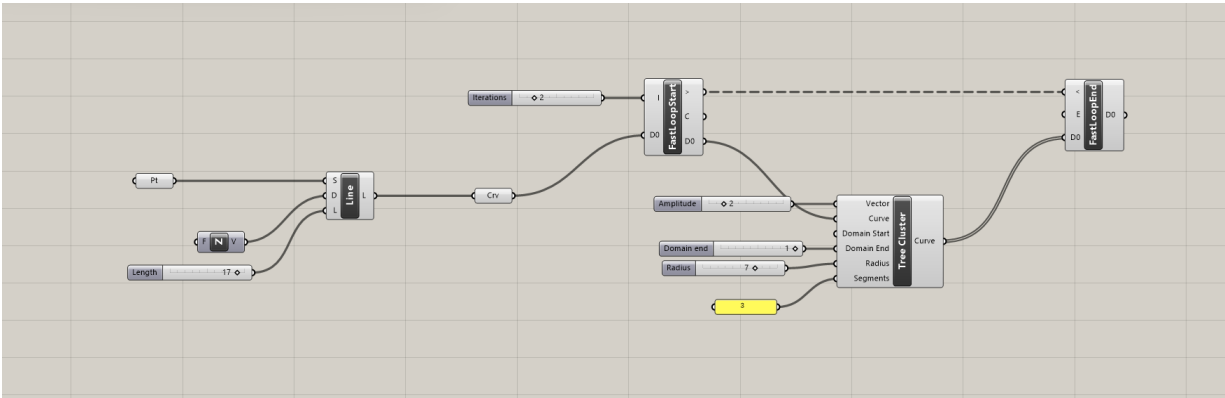


Figure 164. Vegetation simulation. Definition in Grasshopper (larger view in Appendix D, Figure 356).

Vegetation simulation for the site (Figure 165) started with a single point. The input parameters were the following: The length is 7 units, amplitude is 2, radius is 4, segments are 3, and the number of iterations is 5. The initial point grows into the tree trunk. The next step is a tree trunk with three segments of branches. The following iterations multiplied each branch segment by three.

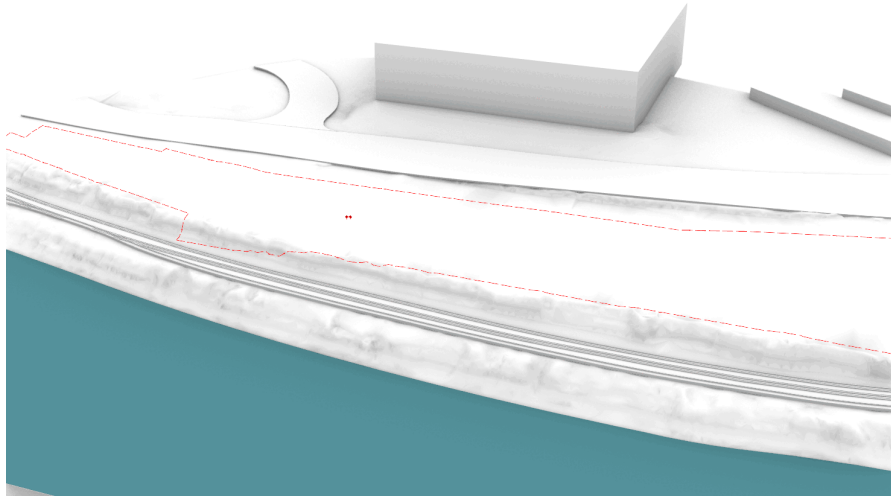


Figure 165. Vegetation simulation.

Once the tree was generated in Grasshopper, the geometry was “baked” and saved into Rhino. After that, the tree linework was transformed into pipes of different diameters, from 1.5 feet for a tree trunk that represents a mature tree, to 4 inches for branches that illustrate the average diameter for a mature tree. The linework was transformed to get surfaces for wind simulation. The resulting model was tested on how it interacts with the wind.

The vegetation simulation illustrates the growth of the tree. In this simulation study, the key findings are related to the visual appearance of trees over time and also seasonal changes. These models of trees were also tested on how they interact with the wind.

5.4 Integrated Simulation Framework

The set of design simulations in this chapter focused on the analysis of current processes on site and the interaction of architectural shapes with these processes. The visual summary of the simulation process (Figure 166) summarizes these investigations and represents an iterative design process.

Following the analysis of current site processes, the simulation process consisted of two different approaches to landform building design. The first approach was a form-finding approach that focused on massing of architectural shapes. The second approach was an exploration of basic forms within the project site and their interaction with environmental processes.

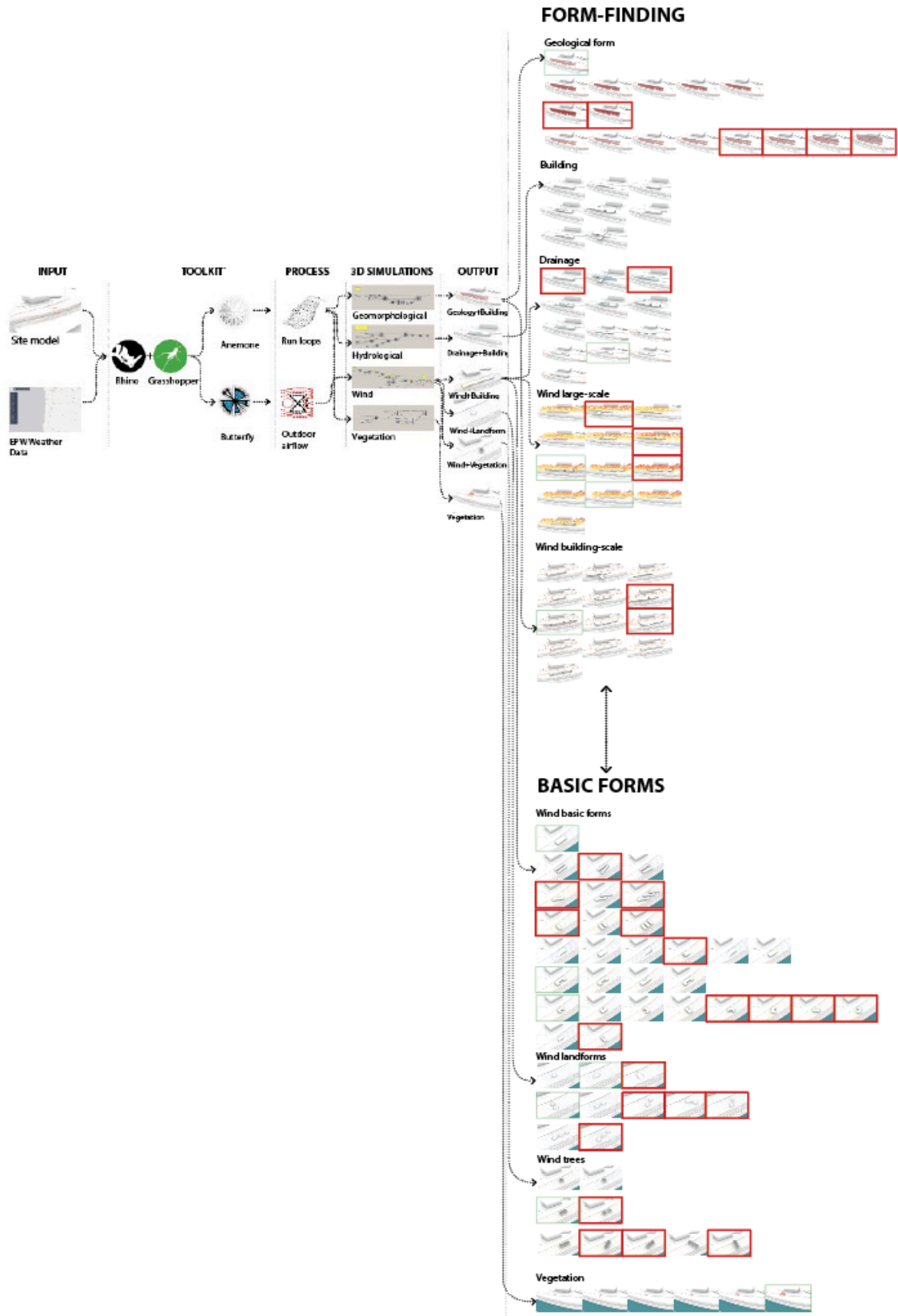


Figure 166. Visual summary of the simulation process.

The form-finding approach started with a process of finding an architectural form of the building right after analysis of the geological conditions of the site and geomorphological simulations (Figure 167). Based on this analysis, design options were generated from the site's contour lines. Each design was tested through hydrological and wind simulations to estimate which option was successful in terms of creating comfortable outdoor conditions and aligning with site processes.

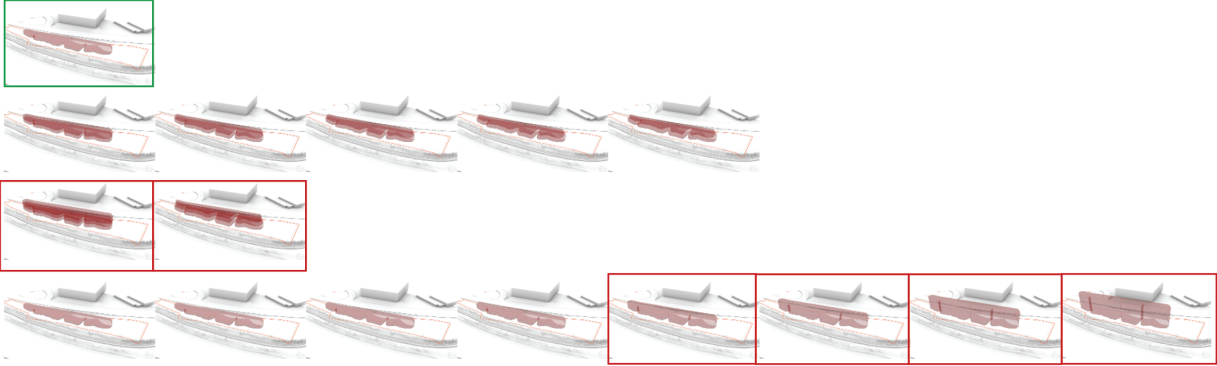


Figure 167. Visual summary of the geomorphological simulations.

The hydrological simulation revealed that Options 1 and 2 were not effective, as they did not drain water or they collected water into one concentrated area. However, Option 10 showed that angled roof and walls successfully drain the water (Figure 168).

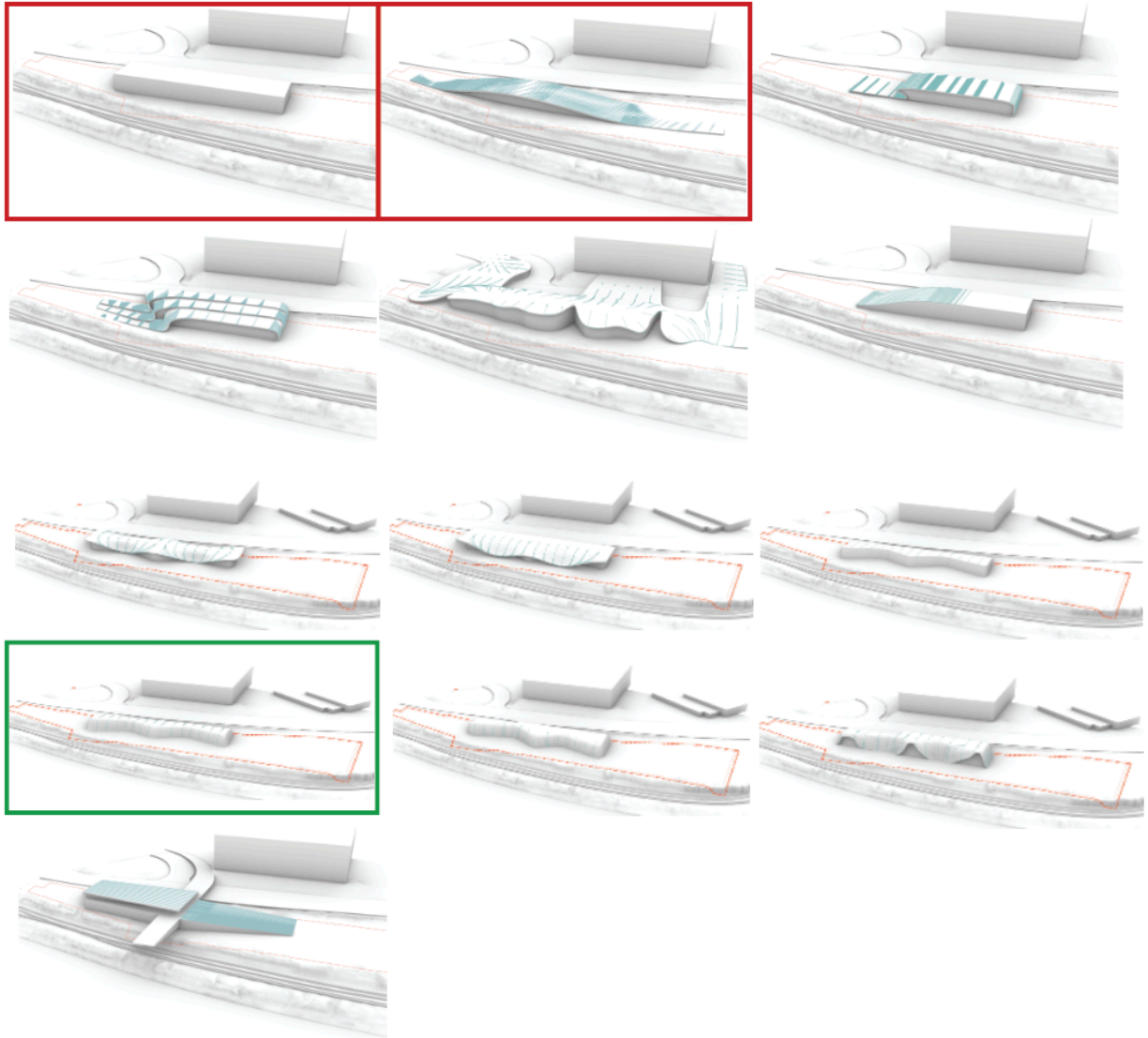


Figure 168. Visual summary of the hydrological simulations.

The wind simulation on a large scale revealed that Options 5, 8, and 13 create a rise in the wind speed up to 11 m/s above a height of 80 feet from the ground level. However, Options 6 and 10 showed a more comfortable wind speed of 8 m/s above the building height (Figure 169). The subsequent building-scale wind simulation confirmed that Option 6 shows comfortable wind conditions of 5–6 m/s on the pedestrian level (Figure 170).

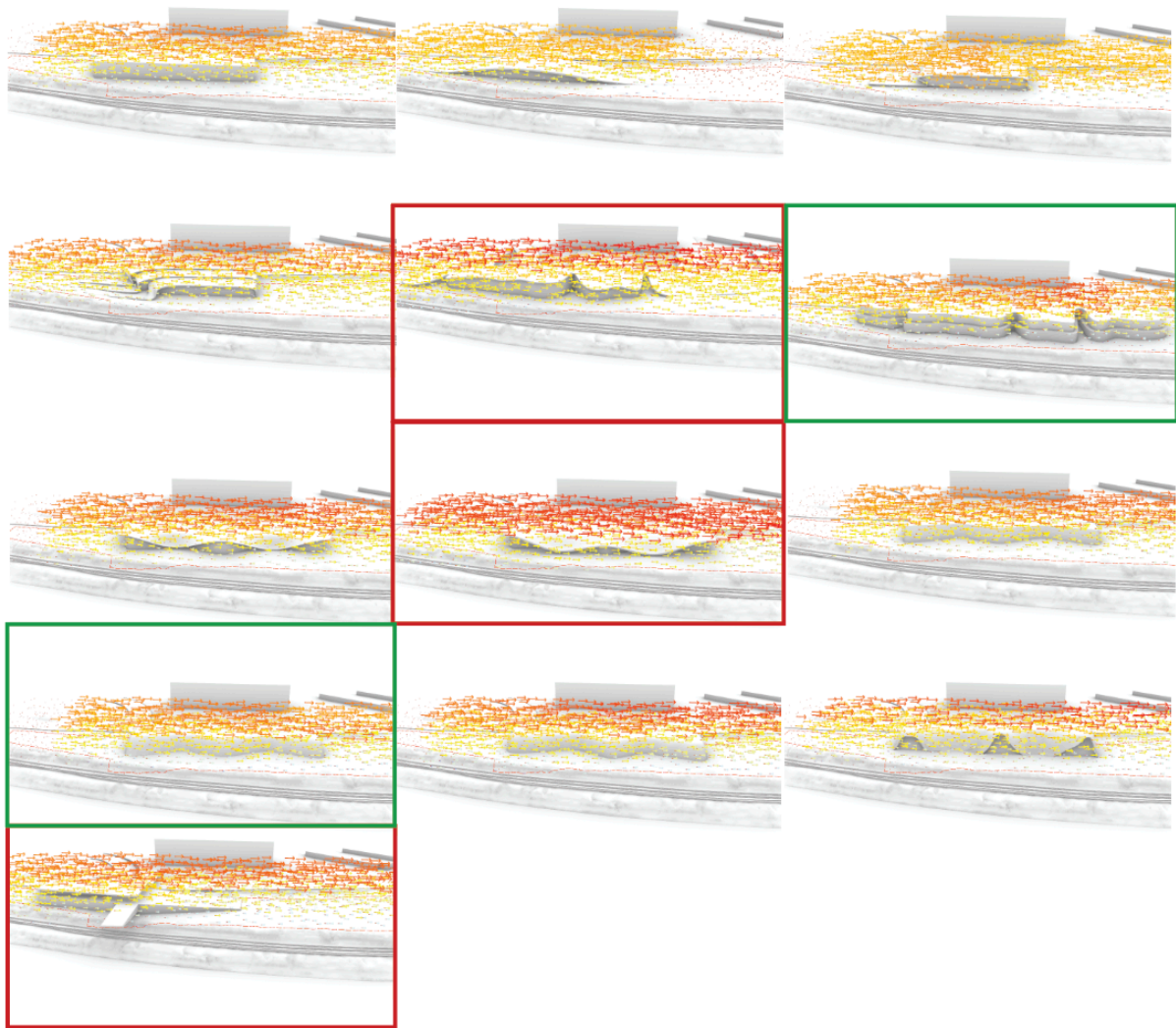


Figure 169. Visual summary of the large-scale wind simulations.

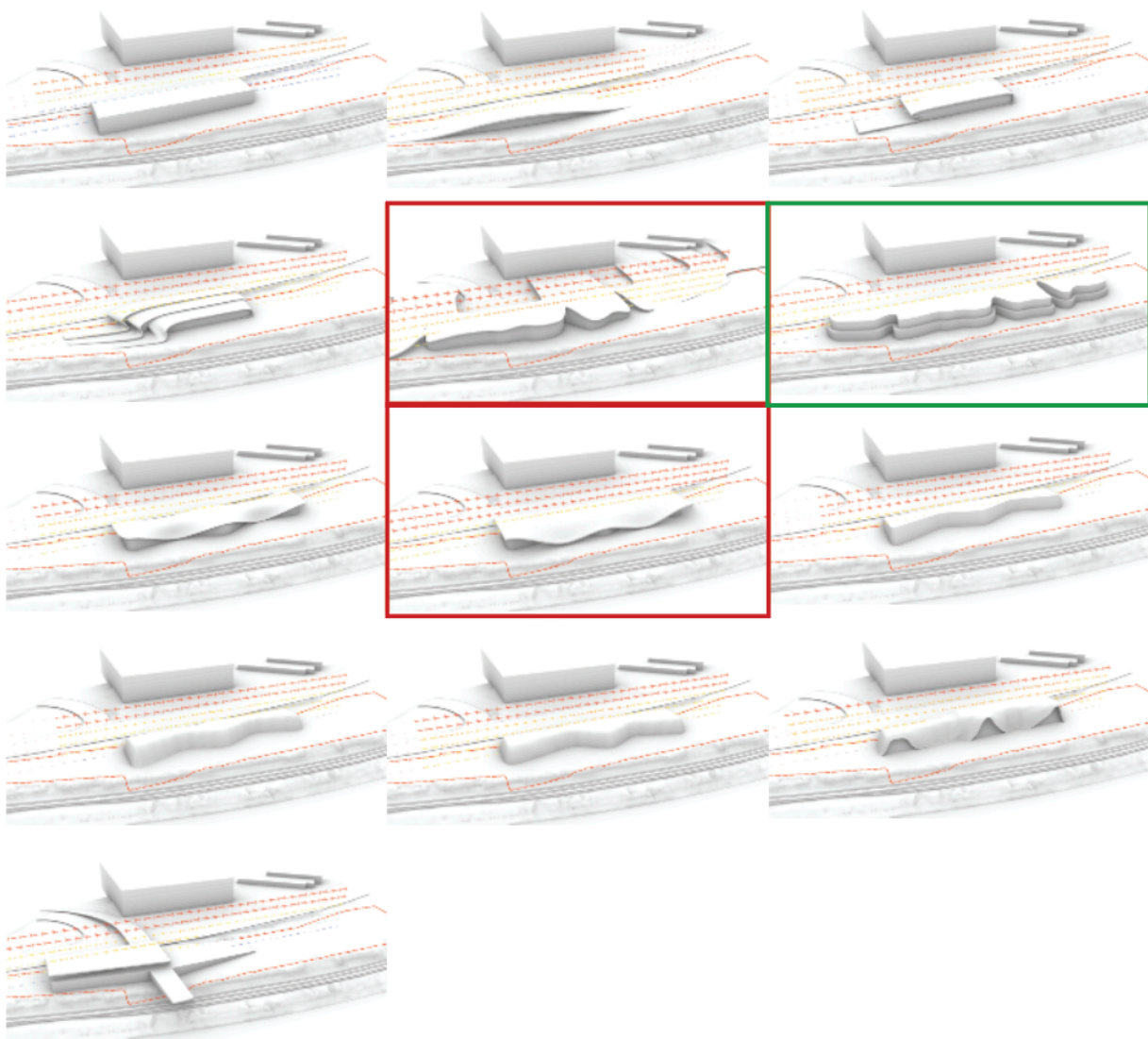


Figure 170. Visual summary of the building-scale wind simulations.

While these findings were useful, they did not produce a satisfactory result. After the form-finding process, the second approach of basic forms and their interaction with geomorphological, hydrological, wind, and vegetation processes was tested.

The second approach started with an integration of basic shapes, such as cuboid, two cuboids, three cuboids, sloped, and rotated shapes. The geomorphological simulations of basic forms revealed that the single-story building shape was the most suitable for the site compared to a two- or three-story building.

The wind simulations of basic forms (Figure 171) revealed that a simple cuboid-shaped building with pockets and a building with rounded corners showed 3–5 m/s wind speed on the pedestrian level. In other options, basic forms rotated 15–45 degrees showed an increase of wind speed up to 6.5 m/s, which would create uncomfortable conditions for visitors.



Figure 171. Visual summary of basic forms wind simulations.

Along with simulations of basic forms, simulations also tested the way the integration of landforms and trees will change the outdoor conditions. The simulation results showed that a single elongated landform or a set of two landforms minimizes wind speed to 4.4 m/s (Figure 172).

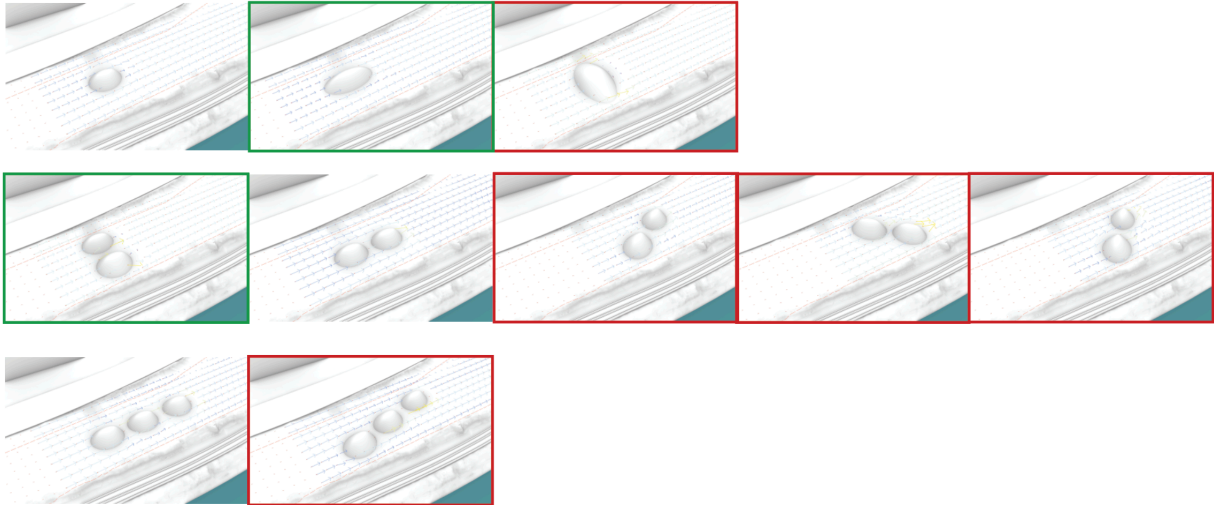


Figure 172. Visual summary of landform wind simulations.

Similarly to buildings and landforms, trees also minimize wind speed; however, their position on site plays a crucial role. Trees that merge together with their crown minimize wind speed, while those spaced at a distance apart maximize wind speed (Figure 173).

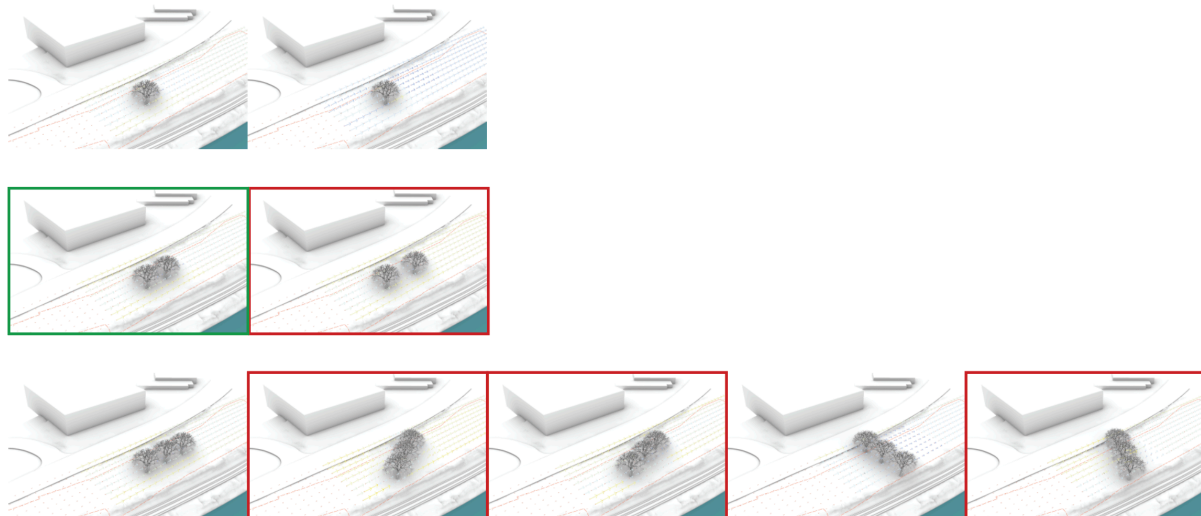


Figure 173. Visual summary of vegetation and wind simulation.

The visual summary of these two approaches synthesizes findings and highlights an iterative design process. The findings from this process contribute to the development of building design that responds to environmental processes within the project site.

5.5 Summary

The set of geomorphological, hydrological, wind, and vegetation simulations tested different interactions of various forms with natural processes. The simulations reveal how landform geometry impacts hydrological and wind processes. The outcomes illustrate that simulations effectively demonstrate known behaviors and validate their use for testing and developing new landform architecture strategies.

Wind simulations demonstrated that building shape, orientation, and spacing between a set of buildings influence wind speed and direction. Sharp corners increase wind speed, while rounded edges help mitigate extreme wind effects. Rotating buildings relative to prevailing wind conditions can either increase or decrease wind speed and influence pedestrian comfort.

Landforms interact with the wind similarly to buildings. Their orientation and number influences wind patterns. More site-specific conditions, such as topography and water features, influence the wind speed. Sloping terrain, similar to a one-sloped building, can increase or decrease wind speed depending on the orientation of the slope toward the wind direction. The wind tends to get stronger by the river and water features, as they create an open wind corridor without obstructions. In combination, these site-specific factors can significantly alter microclimate conditions. By adjusting building form and orientation, architects can create a more comfortable environment.

Vegetation simulations reinforce these findings by illustrating how trees influence wind conditions. Wind speed increases around tree crowns but decreases behind them. The arrangement and spacing of trees determine how effective the tree placement is in mitigating wind conditions.

The vegetation simulation complements earlier simulations and informs how the placement of the trees will influence microclimate conditions. The simulation illustrates tree growth over time, considering both visual changes and seasonal variations. The findings contribute to a broader understanding of how vegetation affects design strategies for integrating trees into a built environment.

The simulations illustrate that thoughtful placement of buildings, landforms, and vegetation can improve microclimate conditions. The key findings from each simulation will be applied into the design of the landform building in the following chapter.

VI. DESIGN EXPERIMENT

6.1 Introduction to the Design Experiment

The next stage of the process-based approach to landform architecture focuses on projecting the future (Figure 174). In this experiment, design becomes a tool to test a process-based landform architectural design approach that can help mitigate climate challenges and improve local microclimate. In such an iterative process, design is not the final goal, but rather the tool to explore options, and, by exploring the relationship between natural processes and building, align architectural design with landscape context.

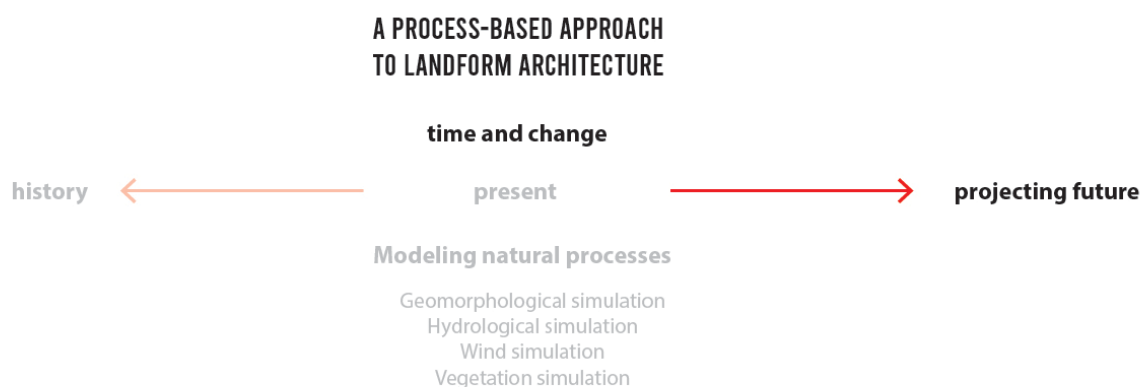


Figure 174. A process-based approach to landform architecture and an envisioned future.

This stage combines findings from previous chapters and tests how to use simulations to solve a design problem—how site-specific processes shape landform buildings and adjacent landscapes. This chapter illustrates how to use geomorphological, hydrological, wind, and vegetation simulations to reflect site-specific processes that shape landform architecture. This design experiment aims to test the proposed process-based framework.

By using computational design tools, this chapter not only shows how simulations can shape architecture that merges with the natural and cultural context but also illustrates how site-specific processes can shape the building and adjacent site at the early stages of the design process. This design experiment builds on the Albina Vision Trust’s commitment to environmental sustainability, equitable sustainability, and restorative justice that envisions redesigning the neighborhood (Albina Vision Trust, n.d.-a., n.d.-b). It highlights the potential

of landform architecture to address site challenges by integrating site-specific processes into the design process.

6.2 Design Experiment

The design experiment focuses on the transformation of the project site located along the Willamette River. The goal of the design project is to test how site-specific processes can shape a landform building and landscape and improve the environmental performance of such a design.

A landform building with an adjacent waterfront park should address site challenges. For the Lower Albina neighborhood, these challenges include strong winds from the northwest and southeast, an isolated riverfront due to historic urban redevelopment, and high temperatures during the summer. Strong winds from the northwest and southeast are exacerbated along the Willamette River, which increases discomfort and limits use of the space. An isolated riverfront limits local residents' access to the water. Dark, heat-absorbing surfaces such as asphalt increase the urban heat island effect and decrease users' comfort. These challenges create local microclimate conditions that require thoughtful design intervention.

This design experiment aims to mitigate these challenges by combining architectural and landscape architectural solutions. The design process starts with a series of geomorphological, hydrological, wind, and vegetation simulations that help to align architectural solutions with landscape processes. Geomorphological simulations inform the building geometry. Hydrological simulations optimize the building shape to address drainage and mitigate the risk of green roof erosion. Wind simulation refines architectural and landscape architectural form to decrease wind speed. Vegetation simulation explores how trees change over time.

6.2.1 Simulations

The decision-making process for the design experiment was based on the simulation results and the Integrated Simulation Framework from Chapter 5. The diagram of the simulation workflow for building design (Figure 175) illustrates two parallel, simulation-based approaches. These approaches, along with satisfactory results from the set of simulations, guided an iterative exploration of the landform building design. Each stage of the simulation process informed design development and subsequent design refinements. This integrative workflow allowed for the discovery of the most satisfactory building shape, landform configurations and design, and

tree placements that respond to geomorphological, hydrological, wind, and vegetation processes and create comfortable outdoor conditions.

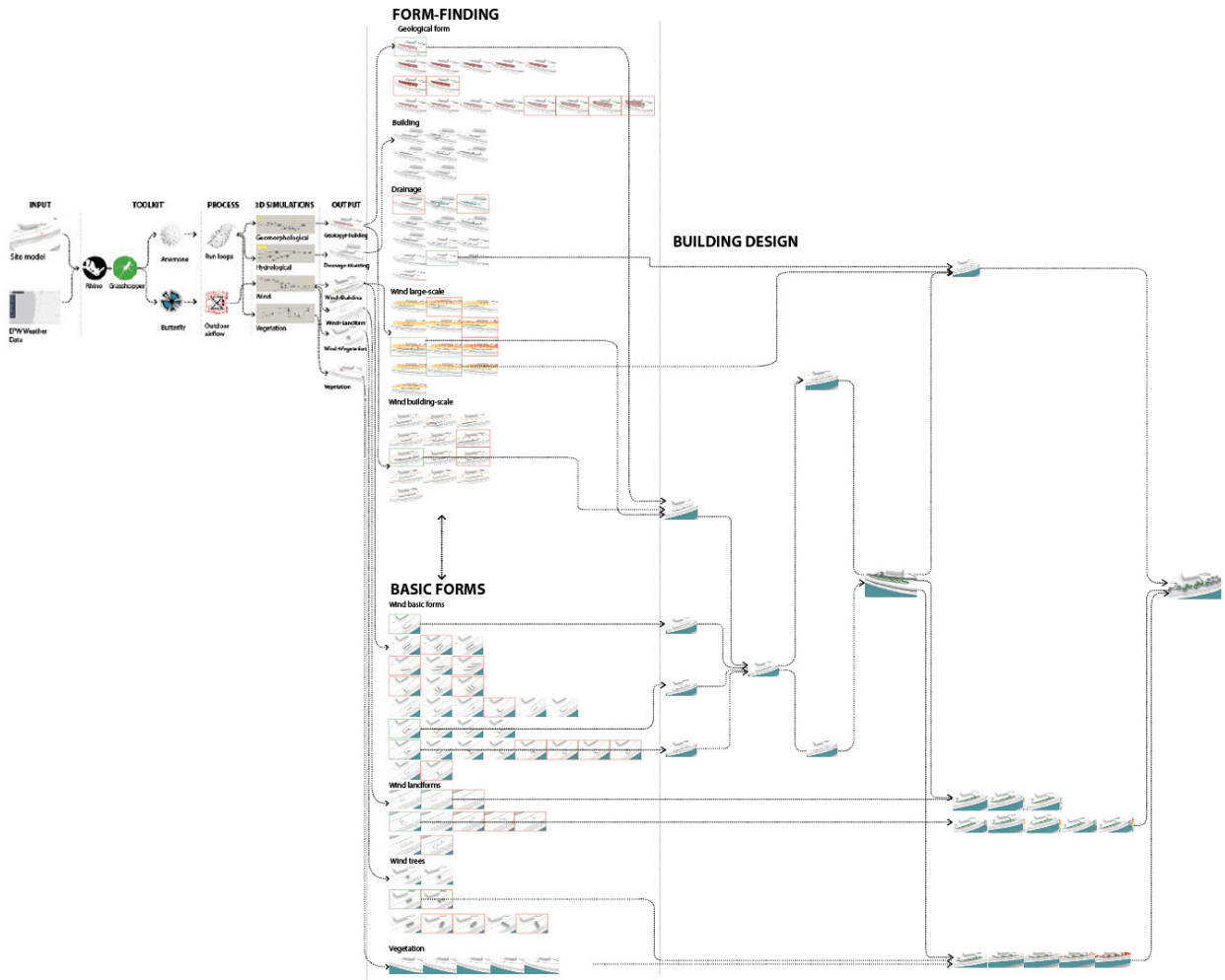


Figure 175. Simulation workflow diagram for building design.

The design experiment starts with a basic form that is slowly transformed by site-specific processes into a landform building (Figure 176). Through a series of 3D simulations, the initial form responds to geomorphological, hydrological, wind, and vegetation processes. Each simulation informs design adjustment and eventually shapes the building. The iterative design process helped to adjust the placement and shape of landforms along with the location of trees to optimize wind conditions and improve local microclimate (Figure 177).

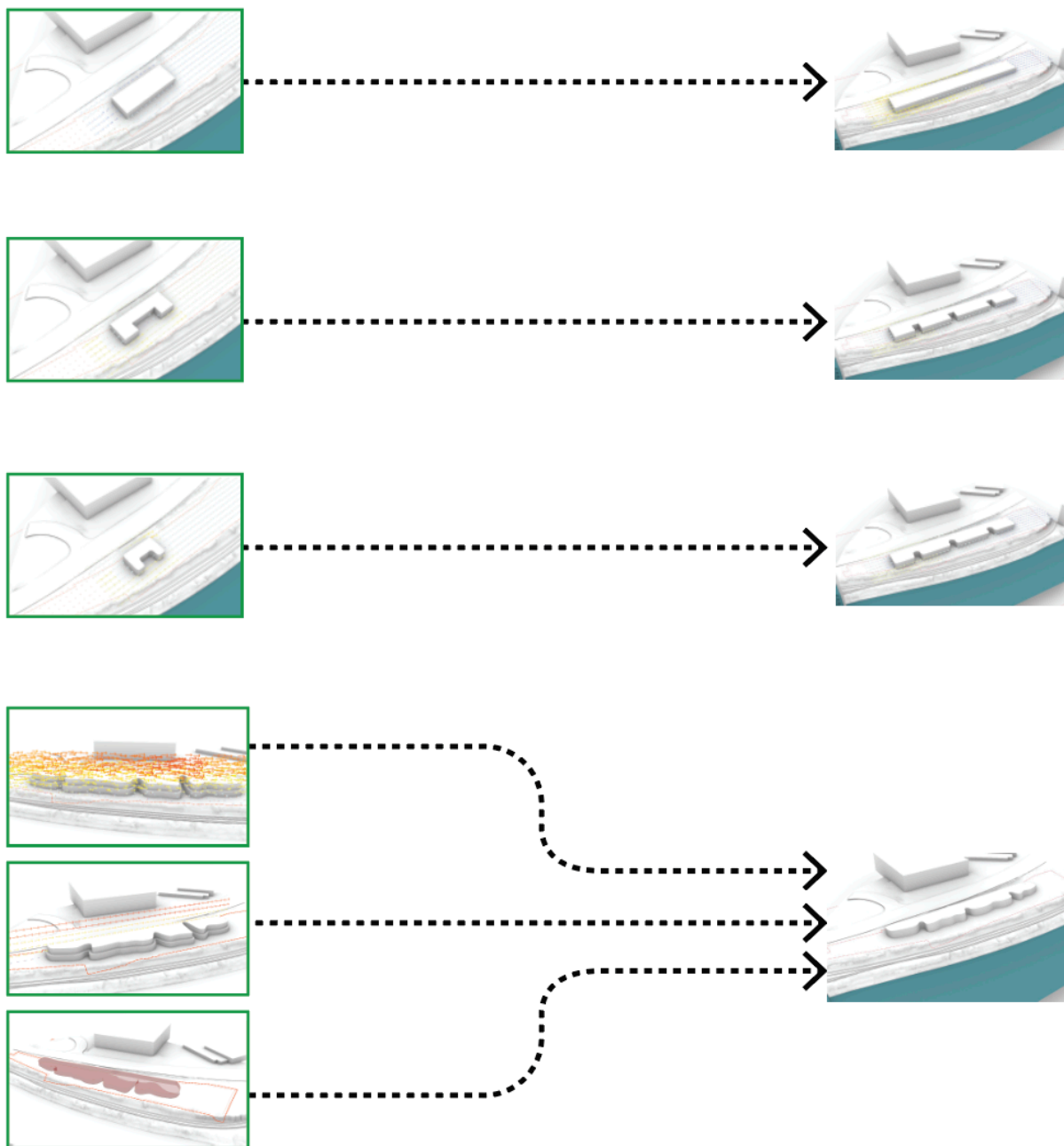


Figure 176. Visual summary of simulation process (building design).

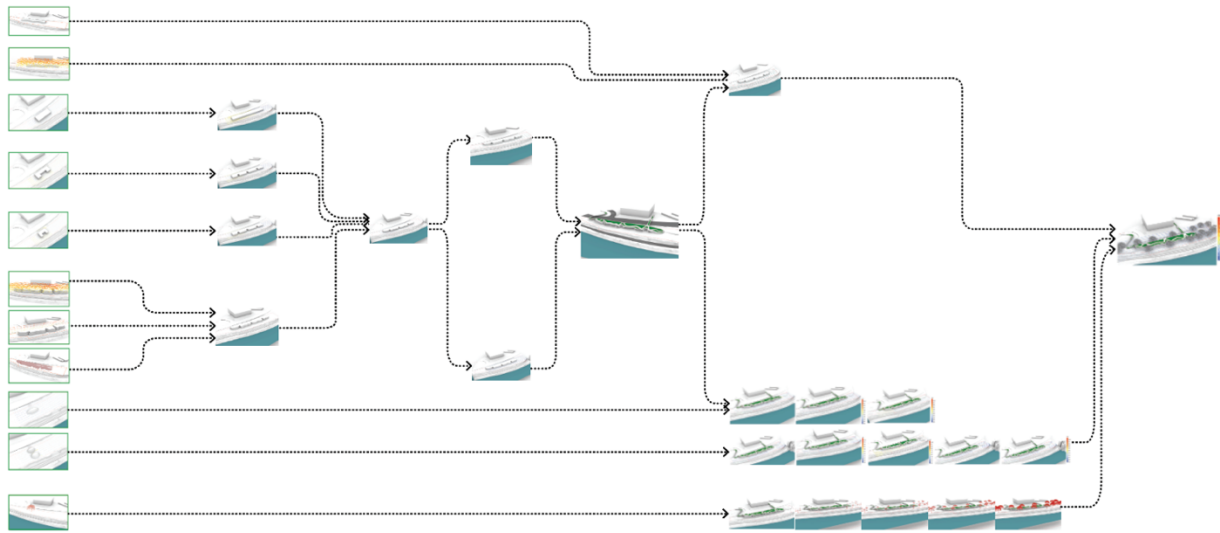


Figure 177. Visual summary of simulation process (building design, landforms, vegetation).

The design experiment begins with wind simulation, as wind is one of the most impactful processes along the Willamette River. Considering the site’s exposure to strong winds along the river, addressing wind processes early in the design process makes it possible for the building design to mitigate wind impacts and improve users’ comfort.

Wind simulation for the project site included multiple iterations based on findings from Chapter 5, such as how the position of the building in relation to the wind direction can either increase or decrease wind speed. The small u-shaped areas create windless zone, while larger u-shaped areas increase wind speed. Another important finding was that sharp corners increase wind speed, while rounded corners help mitigate extreme wind speed. Such simulations help to understand how buildings and wind interact and whether there are repeating principles that can be applied to design a landform building. The goal of these simulations is to refine the form of the building and the adjacent landscape in order to create the most comfortable conditions for pedestrians.

The wind simulation for the landform building starts with the basic form. The input parameters for the simulation were building geometry, predominant north wind direction, and 10 m/s wind speed that was selected based on prevailing wind conditions at the site. The output results were 3D vectors that represent wind flow. The vectors are located on the horizontal plane, at approximately the 6-foot level, which represents the pedestrian comfort level.

The first simulation used a cuboid shape (Figure 178), with dimensions 750 feet long, 100 wide, and 20 feet tall, the maximum allowed volume according to land use regulations. These dimensions were chosen to approximate the square footage of the El Dorado design for direct comparison. The wind speed reaches 5.9–6.5 m/s before it meets the building. Once the wind hits one of the building facades, it changes to 6.5 m/s in front of the building and 6.7 m/s around the corners. The wind speed of 6.7 m/s lasts along one-third of the building. The wind speed decreases after passing one-third of the building to 5.2–6 m/s, and again decreases even more after passing two-thirds of the building to 3.8–5.2 m/s. Behind the building, the wind speed decreases to 3.6–5.0 m/s. While the shape of the building was different in size from the cuboid shape in Chapter 5, the results supported the findings, such as that the wind decreases in front of the facade and increases around the corners. The wind also decreases behind the building, where the wind is blocked and creates a low-pressure wake zone. The simulation results for a cuboid shape show wind acceleration at corners and moderate wind speed along the riverfront. This building form does not create comfortable conditions on pedestrian level.

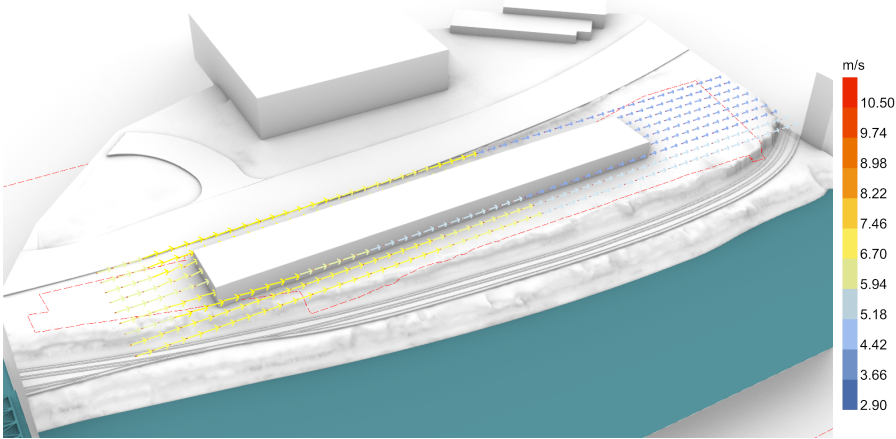


Figure 178. Wind simulation for cuboid building.

The following modification of the building shape was based on the finding that small pockets create a windless zone. The basic cuboid shape was modified to a building with three pockets (Figure 179) that also serve to separate program elements. The decision to use three pockets was based on spatial organization, as larger number of pockets might have fragmented the building program, while one large pocket would disrupt the airflow and create excessive

wind speed rather than providing a shelter. The location of the pockets was governed by the building program, with each pocket positioned to separate functional zones.

The dimensions of pockets that face the riverfront are 50 by 50 feet. The size of the pockets was determined through iterative testing, as documented in the previous chapter where basic forms were evaluated for their interaction with the wind. Once the size of the pocket is larger, it creates a reverse effect. This pocket size creates pedestrian comfort and semi-sheltered outdoor areas.

In this simulation, the wind speed reaches 5.2–6.0 m/s before it meets the building. Once the wind hits one of the building facades, it changes to 5 m/s in front of the building and 5.9 m/s around the corners. The wind pockets reduce wind speed and create a windless zone. Such a change in geometry also shows the decrease in the wind speed along the building. The wind speed decreases after passing one-third of the building to 5.2 m/s, and again decreases even more after passing two-thirds of the building, to 4 m/s. Behind the building, the wind speed decreases to 3.6–4.0 m/s. In this simulation, the introduction of pockets creates wind-sheltered areas and improves pedestrian comfort.

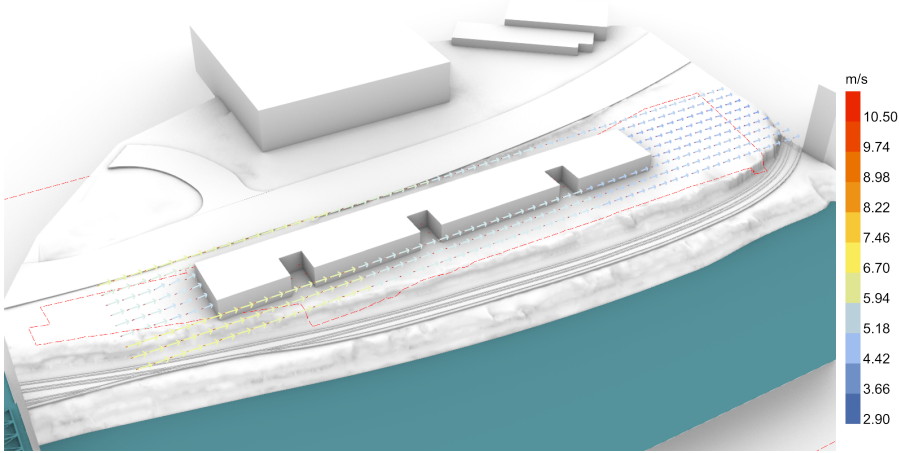


Figure 179. Wind simulation for cuboid building with three pockets.

The next modification of the building shape was also based on the findings from the previous chapter, which was related to the building corners. The wind tends to decrease around fillet corners, comparing to right angles, as they redirect wind more smoothly. The basic cuboid shape with wind pockets was modified and all corners were transformed to fillet (Figure 180). In this simulation, the wind speed reaches 5.0–5.9 m/s before it meets the building. Once the wind

hits one of the building facades, it decreases to 4.4 m/s in front of the building and 5.9 m/s around the corners. Along the building, the wind speed stays the same. Behind the building, the wind speed decreases to 3.2–3.8 m/s. In this simulation, fillet edges reduce wind speed at corners and improve pedestrian comfort along the riverfront.

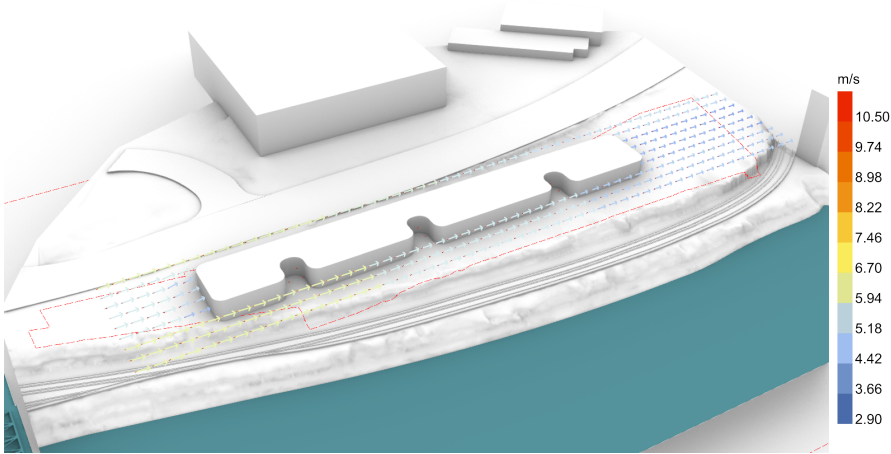


Figure 180. Wind simulation for cuboid building with fillet pockets.

The transition from wind to geomorphological simulation was driven by the need to refine the building’s form. While previous simulations helped to achieve progress in outdoor comfort on the pedestrian level, the form of the building remained detached from the site.

The geomorphological simulation for the project site started with a curved line as the input parameter, derived from the 1897 USGS topographical map of Portland (Figure 104). The map represents distinct contour lines of the geological terraces along the Albina neighborhood. The curve line for the simulation extends the geomorphological character of these terraces and guides the development of the design.

The geomorphological simulation for Lower Albina (Figure 182) derives from the 1897 USGS map of Portland (Figure 181), which provides a historical reference to the site’s geological conditions. This map was selected as the starting point for the simulation, as it captures the original topography before extensive urban development. Alternative approaches include contemporary data from LIDAR or GIS datasets instead of historical maps, geological surveys to understand erosion patterns, or parametric modeling of existing landforms.

The 1897 USGS map documents distinct contour lines representing the terraces along the river. As contour lines approach Lower Albina, their profile transitions to smoother and less

distinct, indicating the less distinct character of the terraces. This curve serves as a foundational element for the simulation. The footprint for the simulation was determined based on the site's constraints and parameters, including zoning regulations and access considerations. The chosen footprint represents the maximum possible building area for the site.

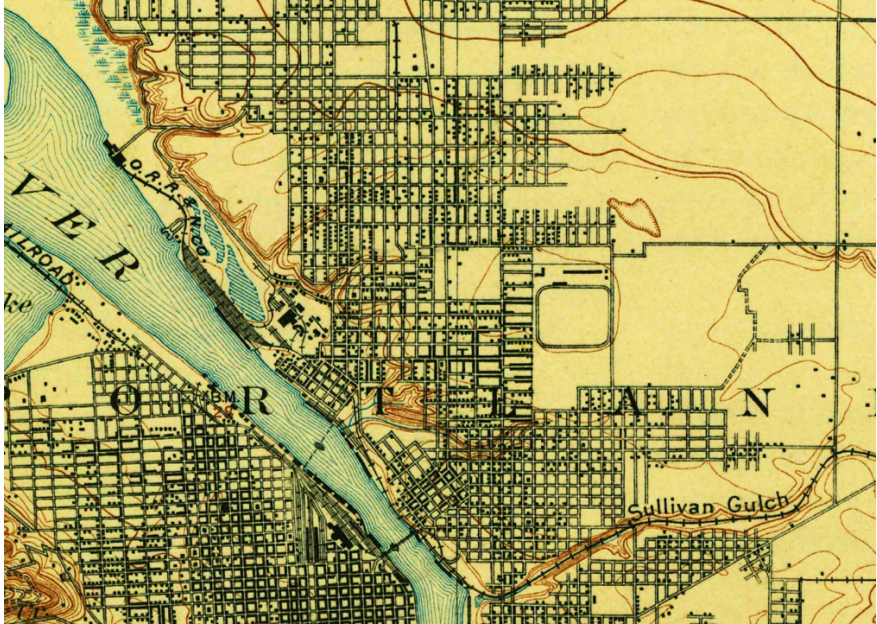


Figure 181. 1897 USGS map of Portland, fragment. From USGS, 2017.

The form generated by the simulation landform complements that of the existing geomorphological terraces. In relation to the existing urban context, the most appropriate shape was a horizontally stretched one-level landform building (Figure 182), as this form aligns with the site's topography, minimizes visual interruptions with the context, and integrates smoothly with existing landscape.

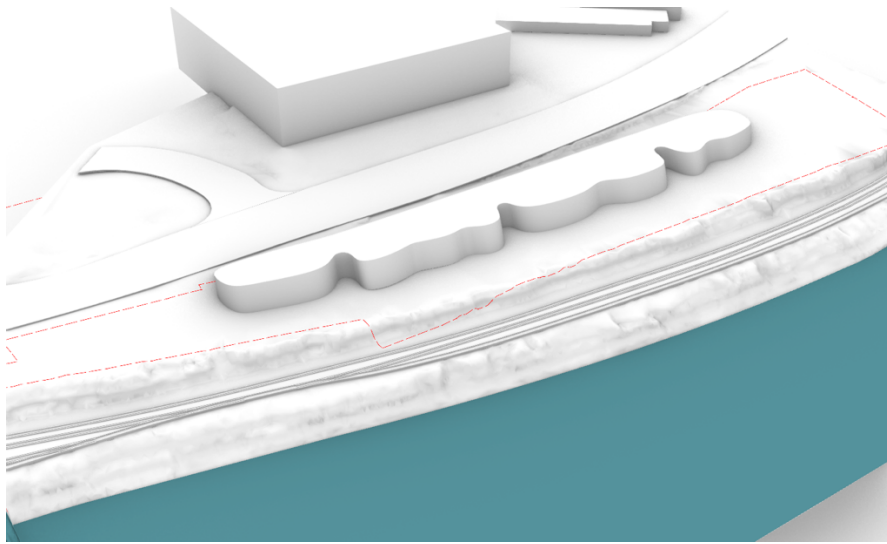


Figure 182. Geomorphological simulation.

The form of the building was adjusted based on the geomorphological simulation. This resulted in a building with more open pockets, a smaller width at the beginning and end of the building, and a wave-like facade along the longer edges. This change in geometry showed an even greater decrease of the wind speed (Figure 183). In this simulation, the wind speed reaches 4.4–5.0 m/s before it meets the building. There is no increase in the wind speed around the corners, where the wind speed stays at ~4.4 m/s. Further along the building, the wind speed slightly increases to 5 m/s. Even though the pockets in this simulation are more open, they remain a windless zone. After the wind passes two-thirds of the building, it gets redirected toward the riverfront. On the other side of the facade, toward the road, the wind decreases to 3.4 m/s. The wind disappears toward the end and behind the building. In this simulation, pedestrian comfort was further improved. The introduction of a wave-like facade and a smaller building width at the ends helped to prevent increased wind at the corners and disperse wind more evenly along the building facade. The adjustment in pocket shapes improved the outdoor comfort for visitors along the river, while maintaining these areas as windless zones. These building form refinements based on wind and geomorphological processes maintain a site-specific approach to landform architecture while also enhancing the pedestrian experience. The resulting shape was further tested for stormwater management.

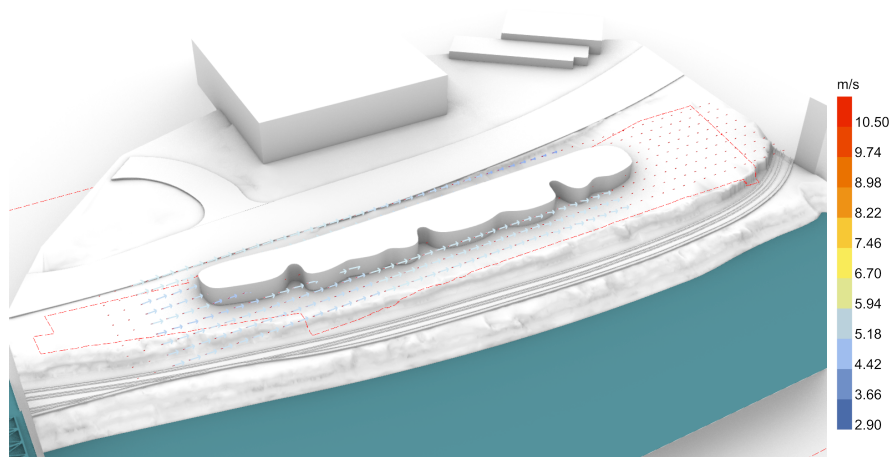


Figure 183. Wind simulation for cuboid building with wave-like facade.

For the hydrological simulation (Figure 184), the input geometry was a form that resulted from the landform simulation. The shape was further refined based on findings in Chapter 5, such as that the optimal configuration of the building, a horizontally stretched form, allows an even dispersal of the water. Another finding is to have a roof slope perpendicular to the longer face of the building. The roof of the landform building was tilted 5 degrees perpendicular to the longer edge of the building, to direct runoff away from the building and toward the riverfront. This building form helps control stormwater flow and reduce the risk of localized flooding and erosion, while also reinforcing the site's hydrological processes. The simulation results show that the gentle slope of the landform building's roof effectively drains stormwater off the building without concentrating flow onto the site. By directing runoff water toward the riverfront, this design integrates well into fluvial processes on site. Following the hydrological simulation, the next simulation will test how the shape interacts with the wind.

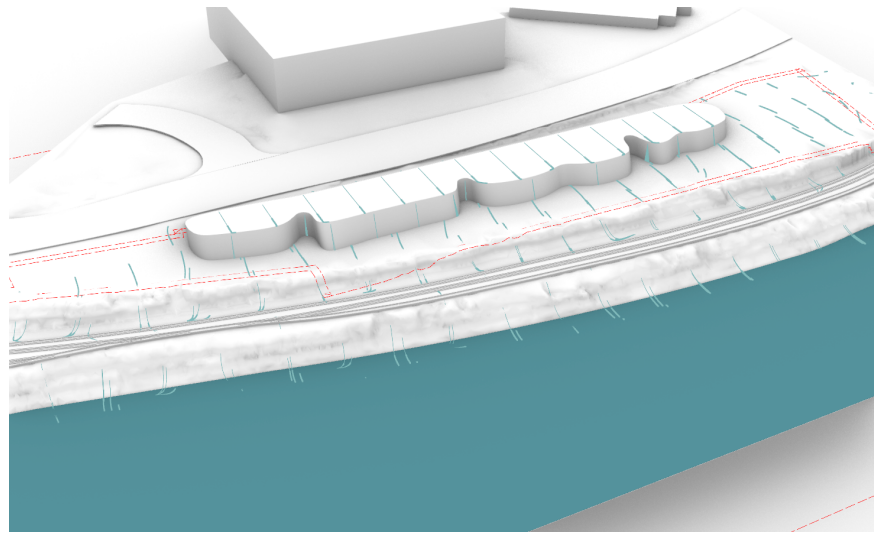


Figure 184. Hydrological simulation.

The following adjustment was based on findings from hydrological simulations. The roof of the building was tilted 5 degrees perpendicular to the longer edge as well as building walls. This change showed a decrease in the wind compared to previous results. In this simulation, the area in front of the building becomes a windless zone. The wind speed ranges between 3.6–4.4 m/s along the building and decreases to 3–4 m/s behind the building. This wind simulation (Figure 185) shows the most satisfactory result for the building shape. In this simulation, pedestrian comfort was further enhanced by changes in roof and wall geometry. The 5-degree tilt helps to direct wind more effectively, while preventing wind increase around the corners and making outdoor areas more comfortable.

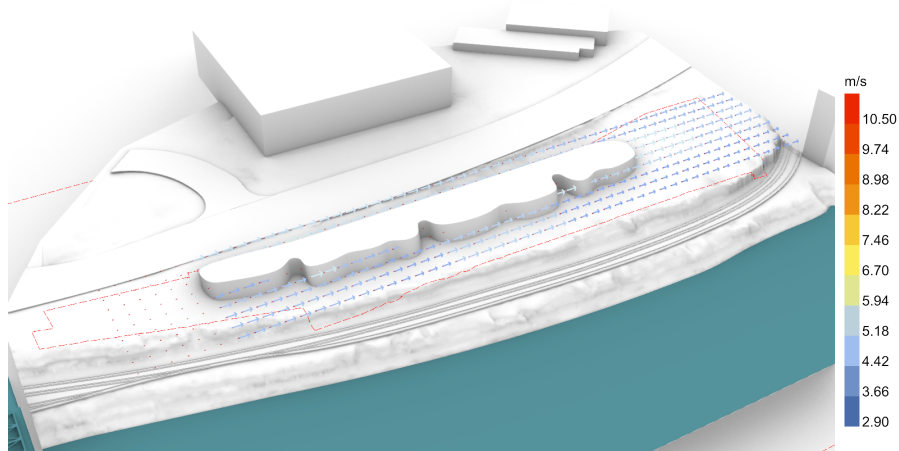


Figure 185. Wind simulation for building form.

The building shape with pedestrian bridges was tested on how it interacts with the wind. While the initial wind simulations informed the building form, the following simulations evaluate wind conditions after the additional design elements, such as pedestrian bridges, ramps, a glass facade, and a roof garden, were introduced. The pedestrian bridges connect the building to adjacent areas. The ramps improve accessibility on site. The glass facade is oriented to maximize the daylight. And the roof garden contributes to thermal regulation of the building and provides a public space on top of the building.

The input parameters for wind simulations were building shape, north and south wind directions, and 6 m/s, which is considered a moderate wind speed for the Portland area, and 10 m/s wind speed as the prevailing wind condition. The aim of the simulation is to identify the areas of increased wind speed around the building. Additional integration of landforms and vegetation helps to improve microclimatic conditions and identify the placement of public areas with the most comfortable exposure to the wind.

For the 6 m/s wind simulation (Figure 186) with north wind direction, the wind speed reaches 4.4 m/s before it meets the building. Once the wind hits one of the building facades, it changes to 3.8 m/s in front of the building and 5.2 m/s around the corners. Further along the building facade, the wind speed decreases to 3.6 m/s. Behind the sloping part of the building, the wind speed reaches 4.8 m/s. For the same wind speed with the south wind direction, the wind speed reaches 5.2 m/s before it meets the sloping part of the building. The wind speed around the corners does not increase. As the wind transitions along the building, it slowly decreases to 4.4 m/s and 3.6 m/s after passing one-half of the building. The wind speed increases around the last corner of the building to 5.2 m/s. However, behind the building, the wind conditions create a windless zone.

For the 10 m/s wind simulation (Figure 187) with north wind direction, the wind speed reaches 5.2–5.9 m/s before it meets the building. Once the wind hits one of the building facades, it changes to 3.8 m/s in front of the building and 5.9 m/s around the corners. The wind speed toward the riverfront reaches 6.5 m/s. Further along the building facade, the wind speed decreases to 4.4 m/s and increases again near the sloping part of the building to 5 m/s. Behind the sloping part of the building, the wind speed increases and reaches 5.2–6.5 m/s. For the same wind speed with the south wind direction, the wind speed reaches 6.5 m/s before it meets the sloping part of the building. The wind speed decreases once it meets the building to 5.2 m/s. As

the wind transitions along the wavy facade of the building, it slowly decreases to 3.6 m/s. Similarly to the previous simulation, there is a windless zone behind the building.

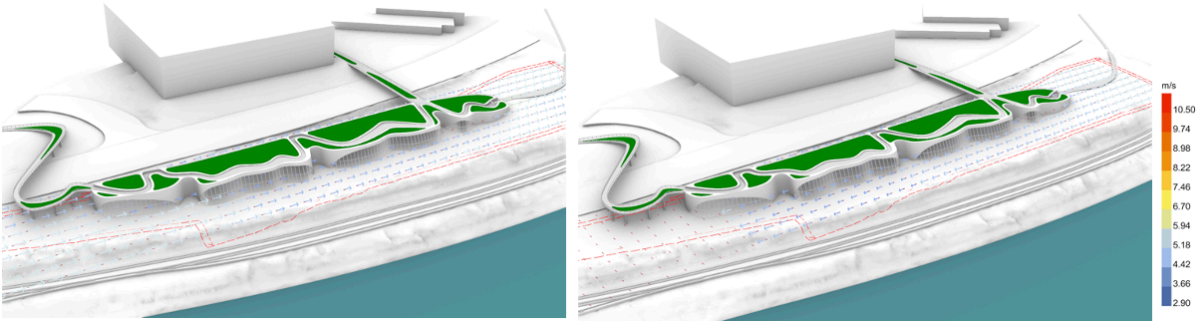


Figure 186. Wind simulation for a landform building, with wind speed of 6 m/s.

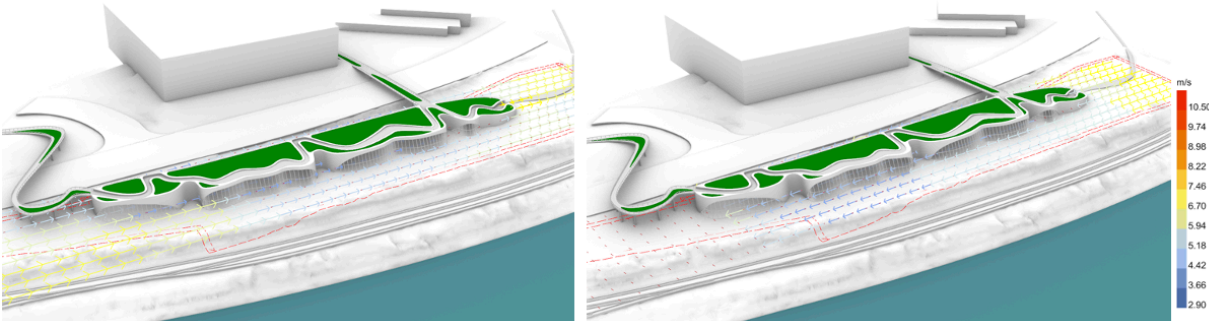


Figure 187. Wind simulation for a landform building, with wind speed of 10 m/s.

In this design experiment, the 3D simulations play a key role as they not only help shape the building but also help integrate the landform building and adjacent landscape to the context. The building integrates into historical, cultural, and natural contexts by combining architecture and landscape architecture strategies. The long and narrow shape of the building responds to the local processes and the site's geological history and zoning requirements. The location of historic streets influences the building design and pedestrian connection. Pedestrian bridges and a green walkable roof aim to reconnect the neighborhood to the Willamette River. The above adjustments create wind-sheltered zones in key pedestrian areas and improve outdoor comfort. The integration of pedestrian bridges keeps wind conditions comfortable around the building corners and along the riverfront facade. The gradual wind reduction along the wave-like facade

makes connection between the building, outdoor pocket spaces, and the riverfront more comfortable for visitors' use.

The next step was to test how an integration of landforms can improve wind conditions. The integration of landforms plays a critical role in mitigating wind conditions. The different iterations of landforms were tested through wind and hydrological simulations to improve the microclimate conditions.

The integration of landforms started from the north side with different landform variations. The input parameters for the north wind simulation (Figure 188) were the landform building, a landform of 50 by 80 by 6 feet, north wind direction, and 10 m/s wind speed. Compared to the building simulation without a landform, the wind speed does not change significantly due to the placement and size of the landform.

The next simulation (Figure 189) with an enlarged landform of 60 by 120 by 6 feet showed an improvement in wind conditions. Compared to the building simulation without a landform, the wind speed before it meets the building decreases to 5.2 m/s, and to 5.9 m/s near the riverfront. The wind speed along the building's wavy facade also decreases to 3.8 m/s. Behind the sloping part of the building, the wind speed decreases to 5.2–5.9 m/s.

The next iteration with an enlarged landform rotated 90 degrees showed an improvement compared to the previous simulation. The wind speed before it meets the building decreases to 5.2 m/s. The wind speed along the building's wavy facade also decreases to 3.6 m/s. Behind the sloping part of the building, the wind speed ranges between 3.6-4.4 m/s.

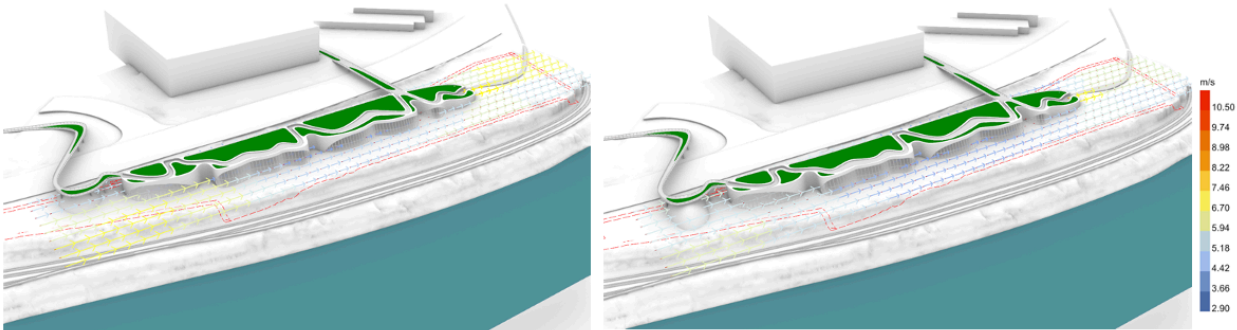


Figure 188. Wind simulation for north landform.

Once the landform was enlarged even more to 80 by 160 by 6 feet, the wind speed showed a further decrease (Figure 189). The wind speed before it meets the building decreases to

4.4 m/s. The wind speed along the building's wavy facade also decreases to 3.2 m/s. Behind the sloping part of the building, the wind speed decreases to 3.6 m/s.

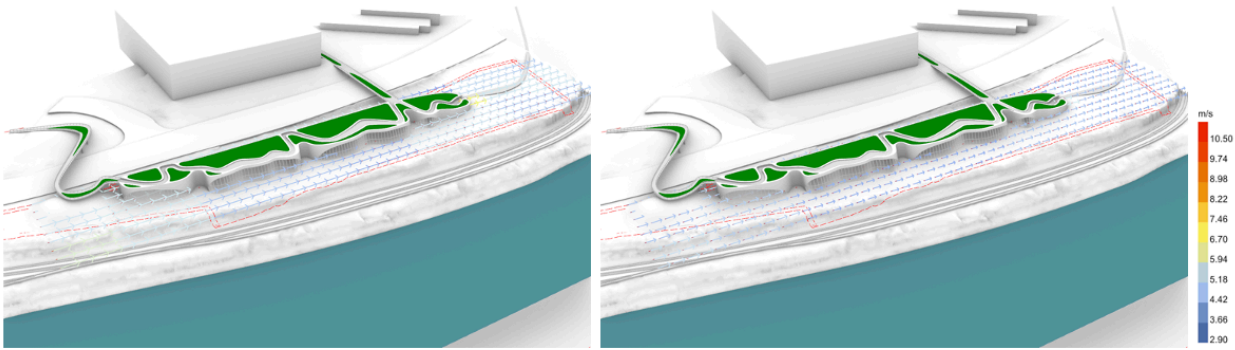


Figure 189. Wind simulation for enlarged north landform.

The next simulation (Figure 190) tested two landforms, each 80 by 160 by 6 feet, positioned one after another. Compared to the previous simulation, the wind speed before it meets the building increases to 5.9 m/s. The wind speed along the building's wavy facade also increases to 4.0–5.2 m/s. Behind the sloping part of the building, the wind speed increases to 4.4–5.2 m/s. Two landforms positioned one after another create a stronger wind on the site.

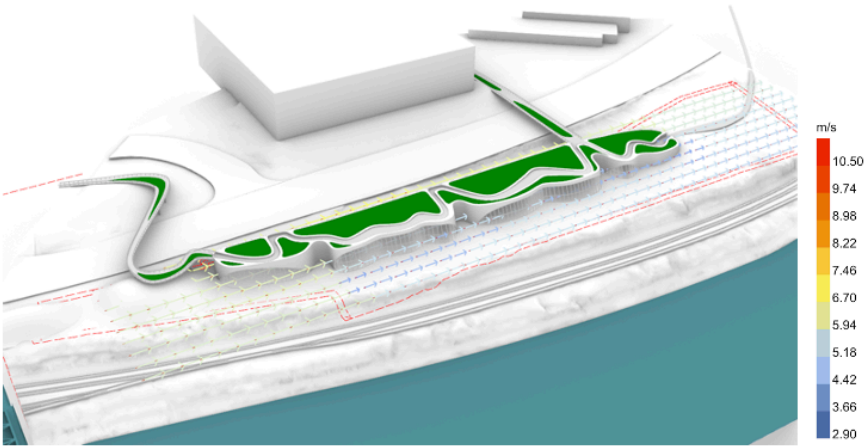


Figure 190. Wind simulation for two north landforms.

Another integration included the south landform and tested multiple variations to find how it changes wind conditions. The input parameters for wind simulation were the landform building, landform 60 by 120 by 6 feet, north wind direction, and 10 m/s wind speed. Once the south landform was added at the end of the building (Figure 191), the wind speed on the

opposite side of the building facade increased to 5 m/s. In front of the main wavy-like facade, the wind speed stays the same; however, at the end of the facade, the wind speed increases to 5.2 m/s. The position of the landform at the end of the building creates a windless zone. Behind the landform, the wind speed decreases to 3 m/s.

Another simulation tests how the wind speed changes when the landform is moved close to the roadway. The wind speed in front of the building and along the building facade stays the same. Such a change only shifts the low-speed zone toward the placement of the landform. Behind the building, the wind speed reaches 5.2 m/s, while near the landform and by the riverfront the wind speed decreases to 3 m/s.

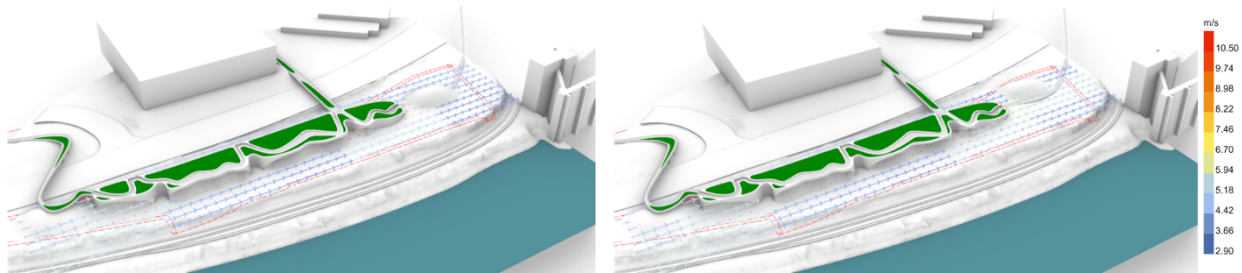


Figure 191. Wind simulation for south landform: Option 1.

Once the landform was pushed a bit further toward the road to create a more open area in front of the building, the wind condition in this area changed. The low-wind zone with a wind speed of 3 m/s moves with the landform and in front of the building, and the wind speed zone of 5.2 m/s grows in size.

To support the hypothesis about landform placement, in this simulation (Figure 192), the landform size was extended to 100 by 160 by 6 feet and moved to the previous location, close to the building. The dimensions of the landform were selected based on site and building dimensions to comfortably fit into the existing context. The area with the wind speed of 5.2 m/s gets smaller, which creates better conditions on site.

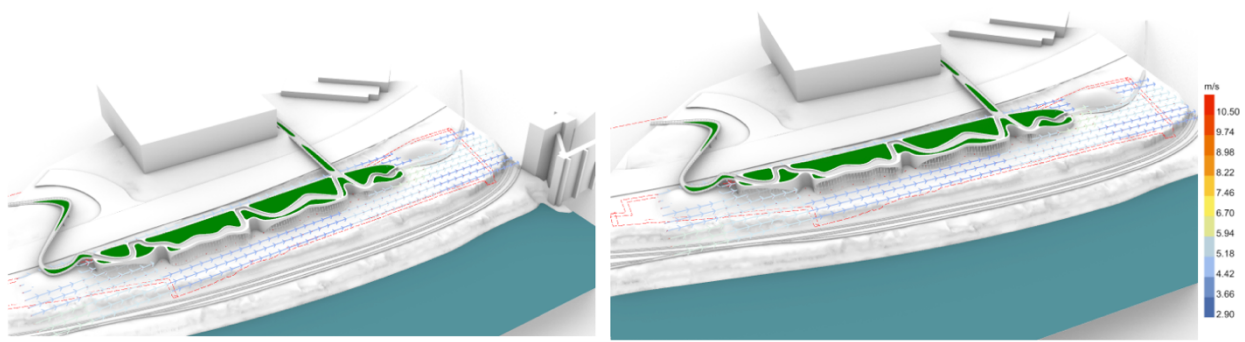


Figure 192. Wind simulation for south landform: Option 2.

The next simulation (Figure 193) tested how the integration of two landforms will change wind conditions. The placement of two landforms, each 100 by 160 by 6 feet, perpendicular to the road increased the wind speed around the entire site. The wind speed on the northern side of the site increased to 6.7 m/s. The wind speed along the wave-like facade increased to 5.9 m/s. In front of the landform, the wind speed decreased to 5.2 m/s. The small area between the building and landforms as well as between landforms becomes windless. Behind the landforms is a small windless zone. Further along, the landform did not create comfortable wind conditions on site and increased the wind speed to 6.5 m/s.

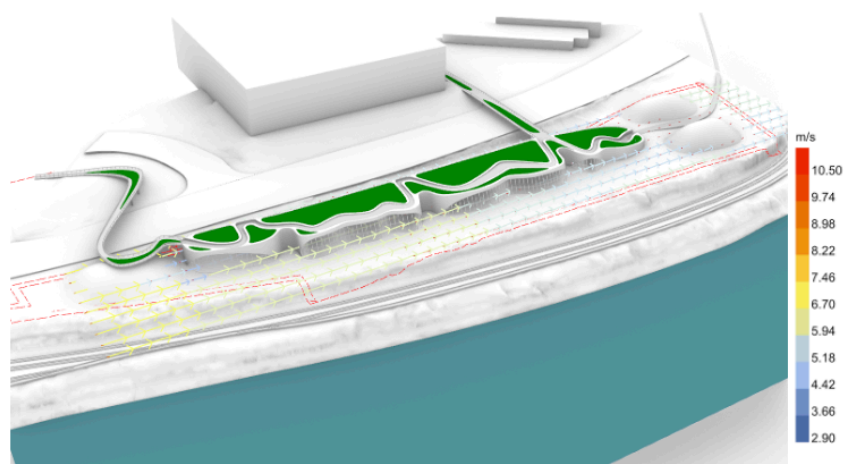


Figure 193. Wind simulation for two south landforms.

The wind simulations for the south wind with an integration of north and south landforms (Figure 194) illustrates how the wind improves with the change of landform size and place. While for the north wind conditions the chosen landform with the size 100 by 160 by 6 feet and

location close to the building showed the most satisfactory simulation result, with wind speed less than 5.2 m/s, it was important to test how the south wind would interact with the building and landforms. The input parameters for the south wind simulation were the landform building, north and south landforms, south wind direction, and 10 m/s wind speed.

The simulation shows that the wind speed before it meets the south landform reaches 5.2 m/s. In front of the building, the wind speed decreases to 5 m/s. Along the riverside facade, the wind speed changes from 5.2 m/s to 3.8 m/s. Behind the building and in front of the north landform, the wind speed decreases and creates a windless zone.

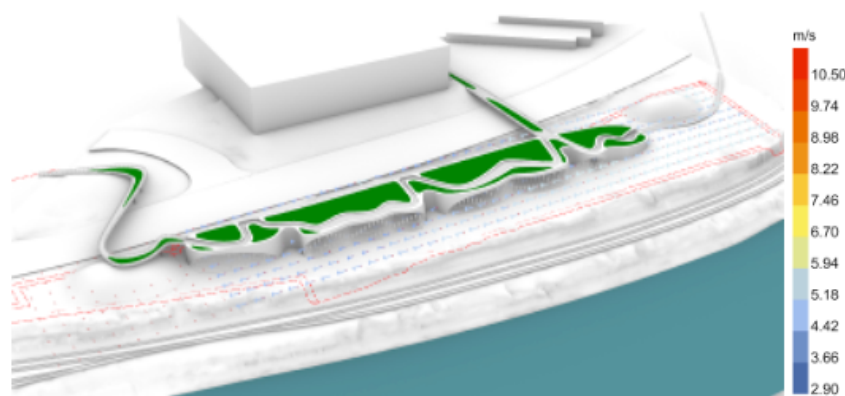


Figure 194. South wind simulation.

The above simulations illustrate that an integration of landforms influence wind conditions. The size, placement, and orientation of landforms affect wind speed and microclimate conditions, which supports the hypothesis that landform design can be used strategically to improve site conditions. The simulations demonstrate that thoughtfully positioned landforms can reduce wind speed in targeted areas, creating sheltered zones for pedestrians. The final placement of landforms includes one landform at the north side of the building and another landform at the south side of the building. Placing landforms on these sides helped to buffer incoming winds and create comfortable microclimates in adjacent public spaces.

Once the shape, size, and location of landforms were tested for their interaction with the wind process and the optimal shapes were selected, the next stage was to confirm that such design interacts well with other processes. For that purpose, the hydrological simulation was run to test how effectively the building and landscape design manages draining the water. The simulation results (Figure 195) show that the water from the building and adjacent landforms is

directed toward the river. A small amount of water is located behind landforms, toward N. Interstate Avenue; however, it will be easy to catch this volume with site drainage measures.

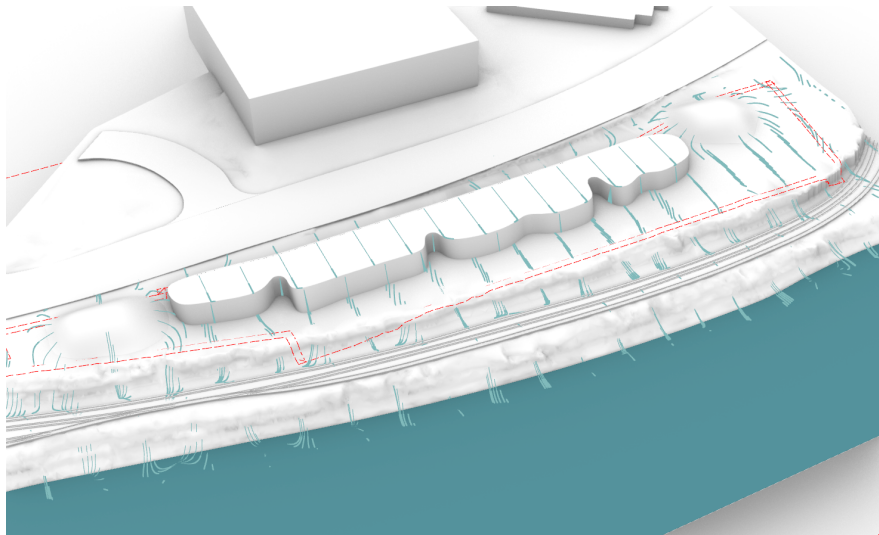


Figure 195. Hydrological simulation for the landform building and adjacent landforms.

Once the building form and the placement of landforms were confirmed, another step was to further improve pedestrian comfort and microclimate conditions by incorporating vegetation. The vegetation simulation begins after the landform building and adjacent landscape are designed. The input parameters for the simulation were a group of points. The placement of points is informed by previous simulations and the resulting microclimate conditions. The wind simulation shows that there are still areas in front of the building that have stronger wind based on the wind direction. The aim of the vegetation simulation is to illustrate how trees will change over time and influence the microclimate.

The simulation starts from a group of points located in the north and south parts of the site, in front of the building (Figure 196). While bigger groups of trees are toward the north and west, there are trees to the west and east, in locations where the wind was stronger compared to the rest of the site.

The vegetation simulation had five iterations. Additional parameters were the following: the length at 17 units; amplitude at 2; radius at 7, and segments at 3. The starting point grows into the tree trunk. The next step is a tree trunk with three segments of branches. The following iterations multiplied each branch segment by three.

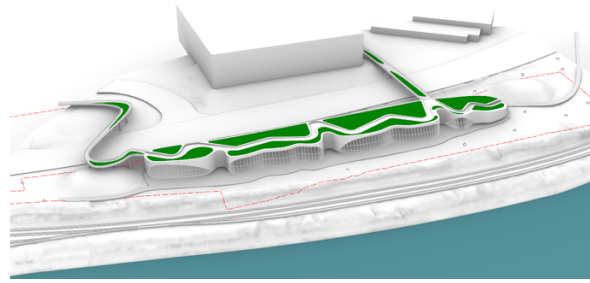


Figure 196. Vegetation simulation.

The next stage of tree simulations was a test of how seasonal changes might affect the appearance and overall aesthetic of the site. For this simulation, the color of the trees was changed to yellow (Figure 197, left) to represent the fall months and to green (Figure 197, right) to represent the spring months. The simulation shows how these changes might affect a visitor's experience and how the site's visual identity might change over one year.

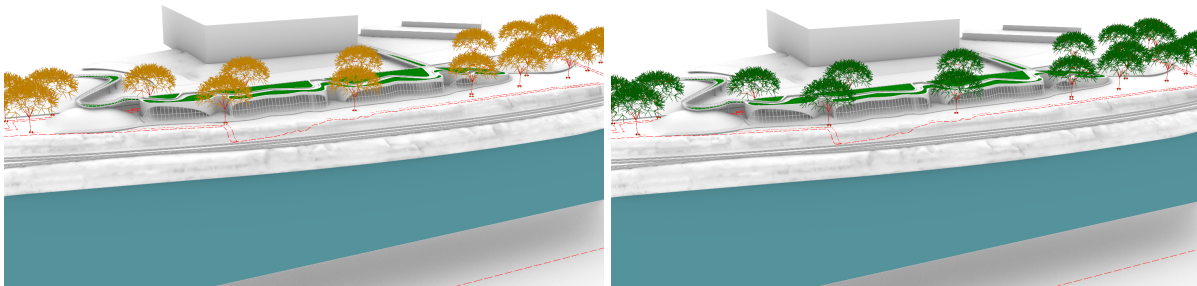


Figure 197. Seasonal vegetation simulation. Left: Fall months. Right: Spring months.

The results of the vegetation simulation inform the selection of vegetation species based on their shape, growth, seasonal changes, and ability to withstand wind conditions. The vegetation simulation complements previous simulations to develop the landform building and helps not only morphologically integrate the landform building and landscape, but also improve microclimatic conditions with design integration.

To test how effective the placement of trees is in terms of improvement of pedestrian comfort and shaping the microclimate of the site, the final set of wind simulations were performed. The input parameters for wind simulations were the landform building shape, north and south wind directions, and 10 m/s wind speeds. The aim of the simulation was to identify if

the placement of the trees is effective in improving the wind in areas that had the higher wind speed.

For the 10 m/s wind simulation with north wind direction (Figure 198), the wind speed reaches 4.4 m/s before it meets the building. For the rest of the site, the wind speed ranges between 3.6–4 m/s, which creates comfortable conditions around the building. The placement of the trees decreases the wind speed in areas with higher wind compared to the simulation with the building and adjacent landforms.

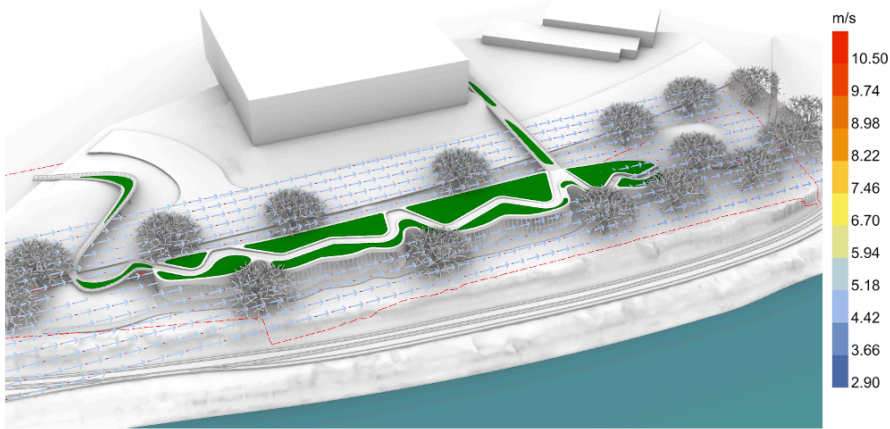


Figure 198. North wind simulation for building, landforms, and vegetation.

Another simulation was run to test whether the microclimate conditions stay comfortable when the wind changes direction to the south. For the 10 m/s wind simulation with south wind direction (Figure 199), the wind speed reaches 4.4 m/s before it meets the building. For the rest of the site, the wind speed ranges between 3.8–4 m/s, which is similar to the previous simulation with north wind direction. The placement of the trees decreases the wind speed from both north and south wind directions.

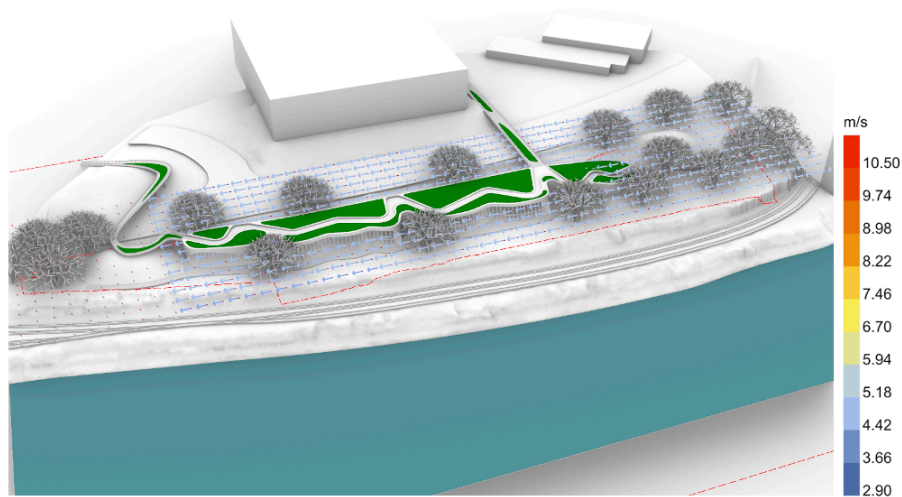


Figure 199. South wind simulation for building, landforms, and vegetation

The set of geomorphological, hydrological, wind, and vegetation simulations played a key role in shaping the building and landscape and analyzing their interaction with natural processes. Through an iterative design process, the design experiment investigated how the shape of the building, variation in landform sizes, and vegetation influence wind conditions, water drainage, and visitors' comfort at the site. This part of the research helped to explore how the combination of a landform architecture and landscape improved microclimatic conditions. The next stage explores the environmental performance of the developed design.

The geomorphological, hydrological, and wind simulations helped to find the most suitable form of the building and adjacent landscape to improve microclimate conditions. The further process requires input from a designer to shape the building by incorporating the program. This process highlights the guiding role of an architect in shaping the building and supplementing the role of the computational technologies.

6.2.2 Building Design

The building envelope was further refined in Rhino to respond to design challenges. The main idea behind the building design (Figure 200) is to integrate it well into the context. The long and narrow building form is influenced not only by the geological history of the site but also by the site's boundaries and Portland zoning requirements.

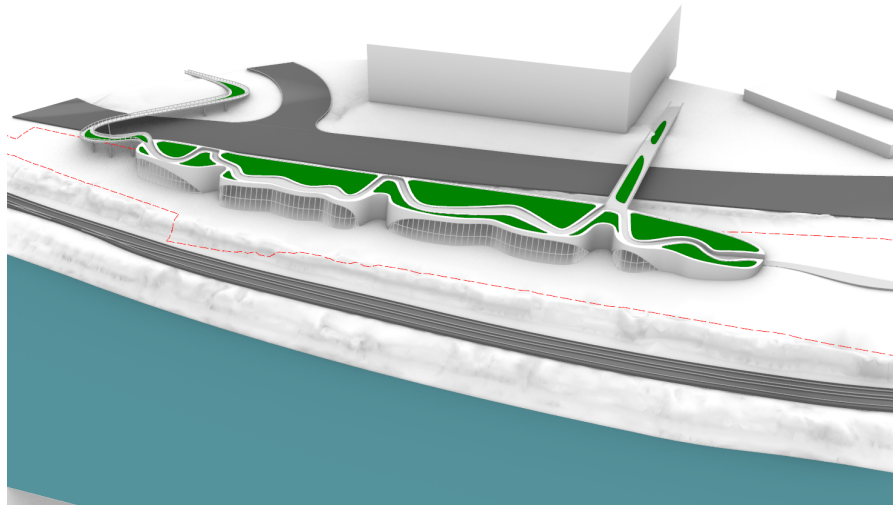


Figure 200. Bird's-eye view of the landform building from the Steel Bridge.

The project site's address is 1225 N. Thunderbird Way, a property that contains a Central Commercial (CX) designation base zone on a Comprehensive Plan Map (Figure 201). This zone is a high-density commercial area for urban development and allows for tall and large buildings with pedestrian-oriented streetscapes. The maximum height for the area is 75 feet or taller, or six or more stories. The Floor Area Ratio (FAR), which expresses the amount of floor area in relation to the site area, for this zone ranges from 4:1 to 15:1. The site dimensions are 1,270 by 230 feet, with an area of 198,200 square feet. The site's setbacks are 10 feet. For nonresidential uses, parking is not required in this area (Oregon Metro, Bureau of Land Management).



Figure 201. Zoning requirements for the site (outlined in white). From Oregon Metro, Bureau of Land Management, State of Oregon, State of Oregon DOT, State of Oregon GEO, Esri, HERE, Garmin, GeoTechnologies, Inc., USGS, EPA, and City of Portland, Oregon.

The project site also contains overlay zones, such as Design (d) and River (e, g, r) overlay zones. The Design overlay zone ensures that the city is developed in harmony with nature and for the use of residents. In this zone, the design builds on physical, natural, historic, and cultural characteristics of the location and promotes social interaction, as well as long-term resilience to changing climate conditions. The River overlay zone promotes the protection and restoration of the Willamette River area. The regulations within this area require a healthy river and watershed area, a riverfront with recreational and gathering spaces, and access to the river (Oregon Metro, Bureau of Land Management).

The project site is located 50 feet above the river level. The site is 25 feet lower than the Veterans Memorial Coliseum (Figure 202), which creates access challenges. The only existing connection to the site is at the N. Larrabee Avenue and N. Interstate Avenue intersection. Historically, there were four streets connecting the Albina neighborhood to the riverfront through the site.

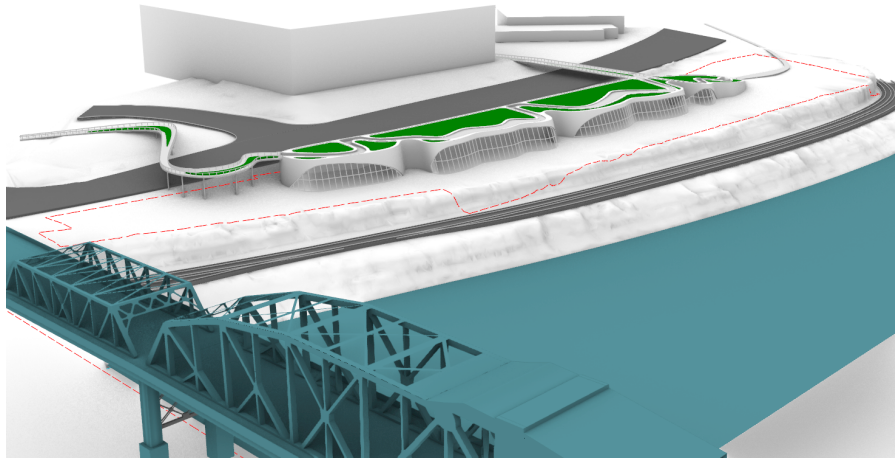


Figure 202. Bird's-eye view of the landform building from above the Broadway Bridge.

The pedestrian path in this design (Figure 203) improves the connectivity between the topographically higher area to the northeast and the walkable building roof. The path starts at the N. Broadway green plaza and crosses N. Interstate Avenue as a pedestrian bridge. The location of the bridge corresponds with the location of the historical Cherry Street (Figure 204) that used to connect the neighborhood to the riverfront (USGS map, 1948). The bridge brings people across N. Interstate Avenue to the roof. The roof becomes a park with its own paths and rest areas, with an overview of the Willamette River and Union Station across the river. As the path stretches along the building roof, it creates the second bridge south to the Veterans Memorial Coliseum. The location of the bridge corresponds with historical Halsey Street, which, according to a 1948 USGS map, connected the area to the riverfront. After reaching the Veterans Memorial Coliseum, the roof path slopes downward, transitions to the ground level, and merges into the surrounding landscape.

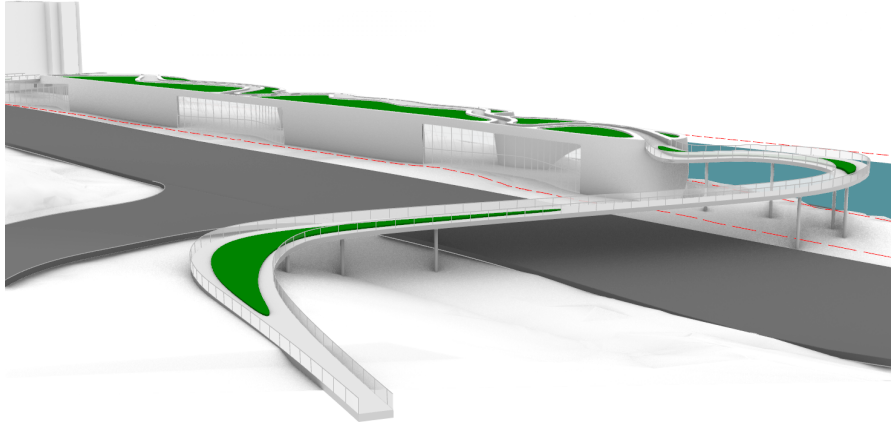


Figure 203. Pedestrian bridge from N. Broadway green plaza. Building glass sections.



Figure 204. Historic 1948 streets and the project site.

The building envelope along N. Interstate Avenue has four glass sections (Figure 205). The location of glass sections aligns with the historic locations of Cherry, McMillen, and Halsey Streets. The glass sections are slightly curved and create visual and physical access into the building. This geometry not only marks the location of historical streets but also helps to create a visual connection with the other side across the Willamette River.

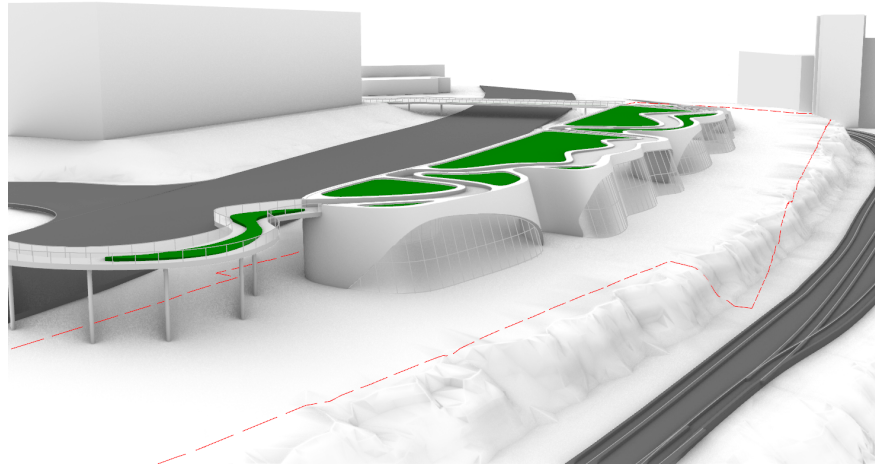


Figure 205. North side of the building.

The riverside of the building envelope is divided into four wave-like facades (Figure 206) separated by fillet pockets. The wave-like form and outdoor pockets help to mitigate wind effects and create comfortable microclimate conditions. The placement of the outdoor spaces between building programs makes an intentional connection to nature. Four parts of the building represent different planning needs and building program intentions. The program distribution responds to the site's relationship with the river. The areas inside and outside the building envelope range from public to private, which is influenced by the access to the site and circulation. At the north side of the building are located public spaces, such as a community meeting room, café/dining, and theater. This part of the building engages with the context and activates the riverfront. The transition from public to private areas happens toward the south end of the building, where the museum, makerspace, and reading rooms are located. At the very end of the building is a play area for kids that has a connection to the waterfront park. The waterfront park serves as an entry to the building and extension of the roof garden.

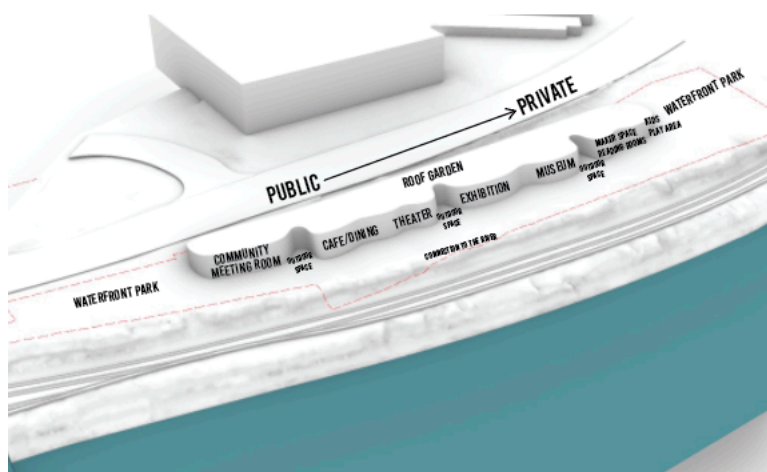


Figure 206. Building form and site program.

The aim of this design is not only to be aligned and shaped by local processes but also to reclaim the identity of the place and create a cultural community hub. As the south part of the building slopes down to the ground, the roof path joins the waterfront park (Figure 207). The building slowly merges with the rest of the site.

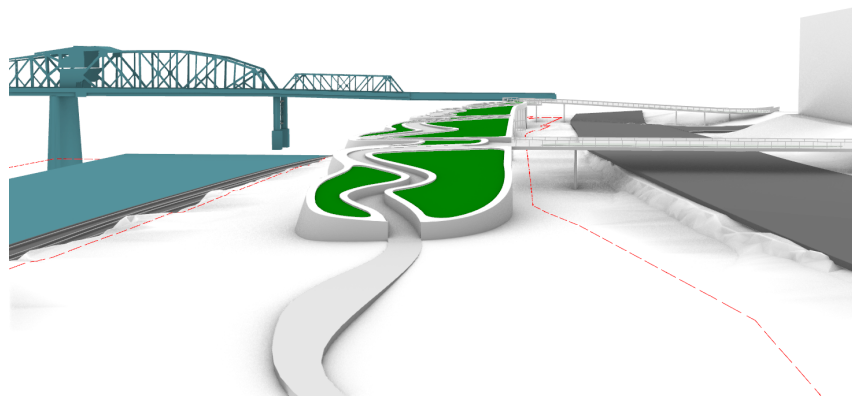


Figure 207. South side of the building.

6.2.3 Landscape Design

The landscape design is an extension of a landform building. The seamless transition of building into the landscape blurs the boundary between the building and the site. Such a combination of building and landscape creates a cohesive environment.

The pedestrian path along the green roof seamlessly continues to the site and wraps in front of the building and behind it. The path offers various experiences and connects different areas of the site. While the path by the road creates access to the building, the scenic path along the Willamette River creates an overview. The location of the path is similar to the historic location of the streets. The combination of a landform building, paths, landforms, and trees creates a waterfront park that highlights the site's connection to the river.

6.3 Environmental Performance of Landform Building

The next stage of the design experiment was focused on assessing the environmental performance of the building and adjacent landscape. By using 3D simulations, this stage is intended to analyze and understand how the proposed design might affect the local microclimate and lead to environmentally conscious decisions. To achieve this, a series of outdoor comfort UTCI microclimate maps were developed using Grasshopper simulations.

The UTCI is used to evaluate outdoor thermal comfort by calculating the effect of weather conditions in a specific environment on the human body (Jendritzky et al., 2012). The UTCI represents the thermal stress or comfort experienced by a person in specific conditions (Blazejczyk et al., 1993). The UTCI is a temperature value expressed in degrees Celsius (°C) and combines multiple environmental factors, such as air temperature, solar radiation, wind speed, and humidity. As UTCI indicates the levels of heat or cold stress that a human body experiences in different environments (Park et al., 2014), the built environment and material selection play a huge role in comfort level. These simulations aim to analyze how the combination of different architectural shapes along with landforms and different materials can improve the microclimate conditions and create a comfortable environment.

The series of 3D simulations was developed using the Honeybee Grasshopper plug-in. The Honeybee plug-in is one of the Ladybug tools that develops advanced environmental performance analysis. Honeybee develops daylight and radiation simulations by using the Radiance extension. The plug-in also creates energy models by using OpenFOAM and EnergyPlus (a building energy simulation program) which allows engineers, architects, and designers to optimize building performance throughout the design process. As a computation tool, Honeybee helps to explore design iterations to find an optimal solution more effectively than using other tools.

The input data for 3D simulations with Honeybee included the weather data (EPW), solar radiation and MRT, and wind speed data. To get these data it is necessary to run separate Ladybug simulations. The EPW data was collected via the Ladybug tool and collected from a Portland airport. The Ladybug tool also helped to calculate solar radiation exposure based on geometry and weather. The wind speed data was collected from previous Butterfly tool simulations.

The definition for the UTCI simulation in Grasshopper (Figure 208) requires additional data. Such data consists of a model, developed in Rhino, to which UTCI will be mapped, and a number between -360 and 360 degrees or a vector that indicates a north direction. To run the simulation it is also necessary to specify the run period, which consists of the start and end dates of the simulation. And, lastly, the simulation requires a schedule that specifies the relevant times during which UTCI will be evaluated.

The UTCI output data of the Honeybee simulations is a thermal comfort map that indicates areas of heat stress or comfort. The data is categorized into stress levels based on temperature results. On the extreme range, temperature above 46 °C is considered as extreme heat stress, between 38–46 °C as very strong heat stress, and 32–38 °C as strong heat stress. The moderate level of stress has subcategories: temperature between 26–32 °C is moderate heat stress, between 9–26 °C is no thermal stress, from 0–9 °C has slight cold stress, and between -13 °C and 0 °C has moderate cold stress. On the opposite extreme side, the temperature between -27 °C and -13 °C is strong cold stress, between -40 °C and -27 °C very strong cold stress, and below -40 °C is extreme cold stress.

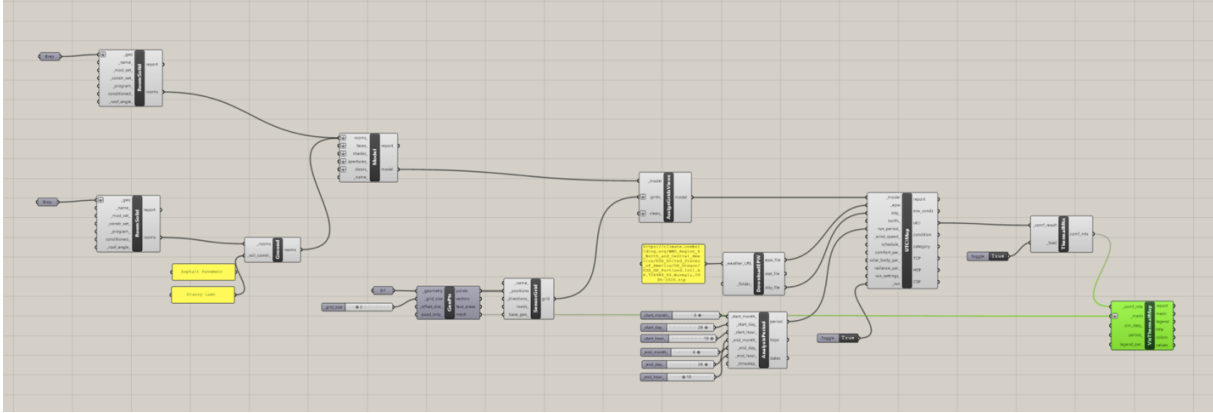


Figure 208. UTCI definition in Grasshopper (larger view in Appendix D, Figure 357).

The environmental performance analysis tested different design options. The initial simulation started with the existing conditions of the asphalt parking lot. The other design options included the basic cuboid shape, the design for a cultural space developed by El Dorado Architects, and the landform design developed in this dissertation.

The initial UTCI simulation was set to test current conditions on site (Figure 209). The input data consisted of the ground model of the existing site, north wind with 10 m/s wind speed, the run period at June 28, and time of 10:00 a.m. The ground material was selected as an asphalt pavement. The run period was selected for June 28 because in 2021 it was the hottest day on record in Portland, when the temperature reached a record 116 °F. The simulation result shows that the UTCI temperature reaches 24 °C, a moderate degree of heat stress.

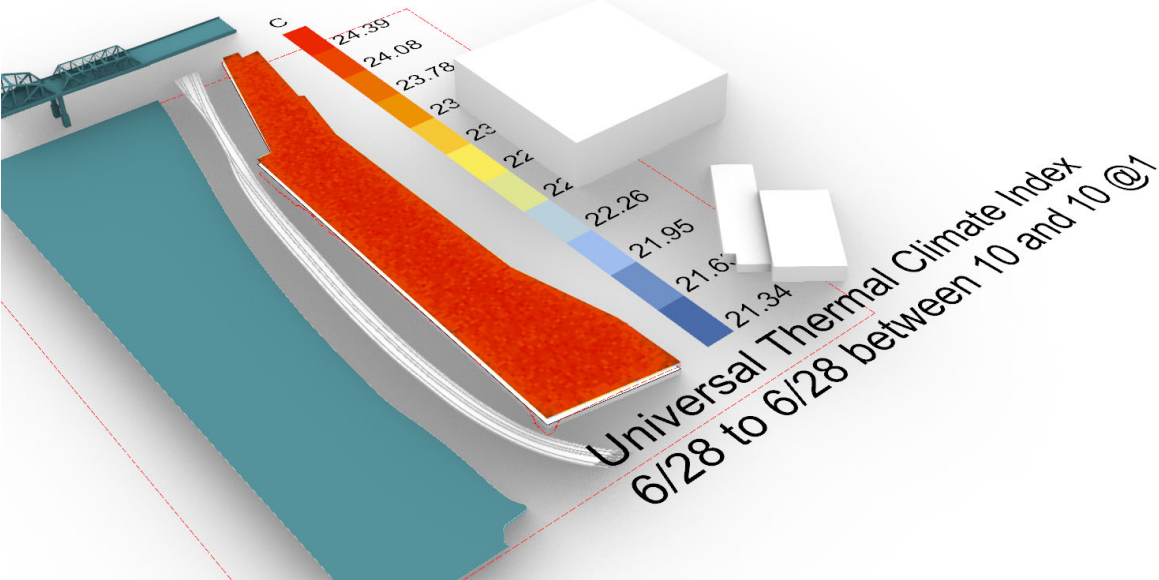


Figure 209. UTCI simulation for current site conditions.

The next simulation (Figure 210) tested how an integration of building geometry might change the output results. The building geometry was a simple cuboid shape. The simulation result shows that the UTCI temperature decreases to 22–23 °C compared to the previous simulation. Such data indicates no heat stress, which means a comfort zone. The north and east sides of the building have a small area with 14–15 °C, which indicates the building’s shadow.

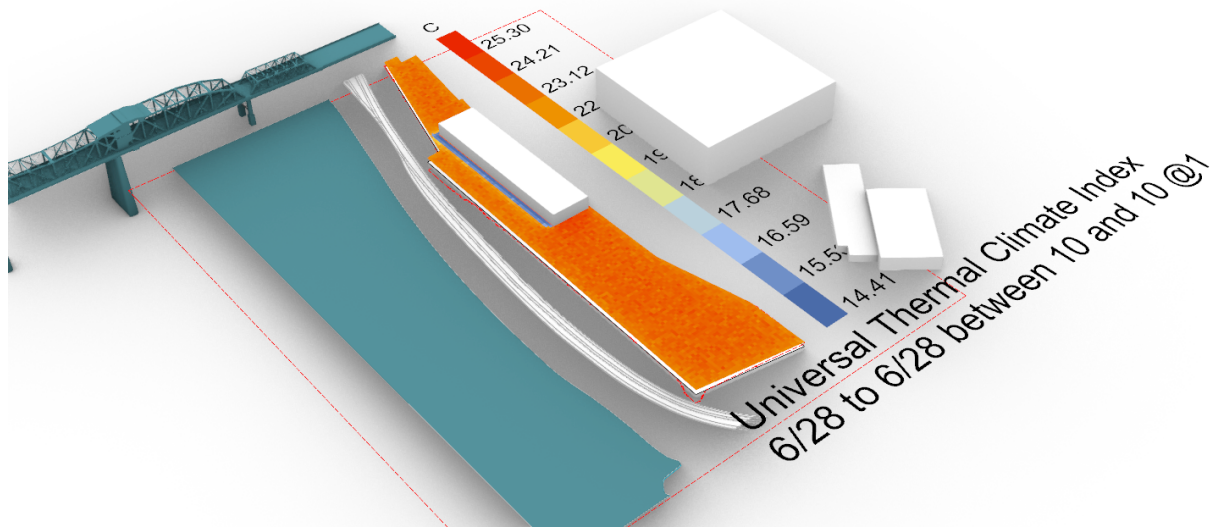


Figure 210. UTCI simulation for cuboid shape.

The next simulation (Figure 211) had the same input parameters, except for the building geometry. The building geometry used here was one of the design options for a community center, designed by El Dorado Architects. The simulation result shows that the UTCI temperature around the building decreases to 21–23 °C compared to the previous simulation. The east side of the building has a small area with a building shadow and a temperature of 14.5–16 °C. These UTCI results show no thermal stress and indicate a comfort zone. The sloping part of the roof that connects to the ground has a higher UTCI value of 27.7 °C, which indicates an area of moderate heat stress.

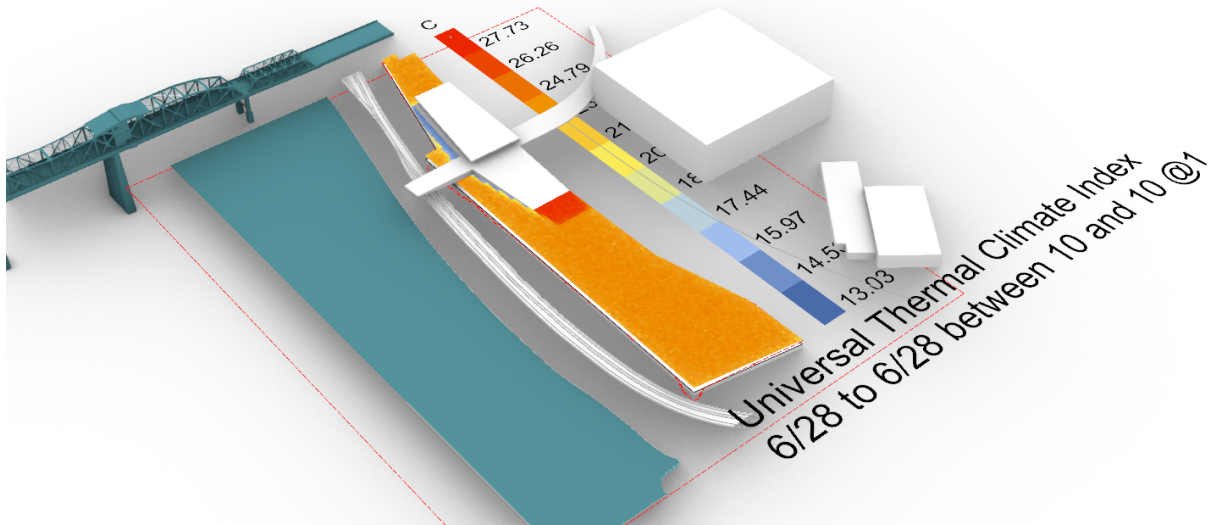


Figure 211. UTCI simulation for a community center building, developed by El Dorado Architects.

The next simulation (Figure 212) has two input parameters that change. One of them is the landform building geometry and park landforms. Another parameter is the ground material; this simulation uses a grassy lawn material. The simulation result shows that the UTCI temperature around the building decreases to 18–19 °C compared to the previous simulation. The area with landforms shows a temperature of around 14 °C. These UTCI results show no thermal stress and indicate a comfort zone.

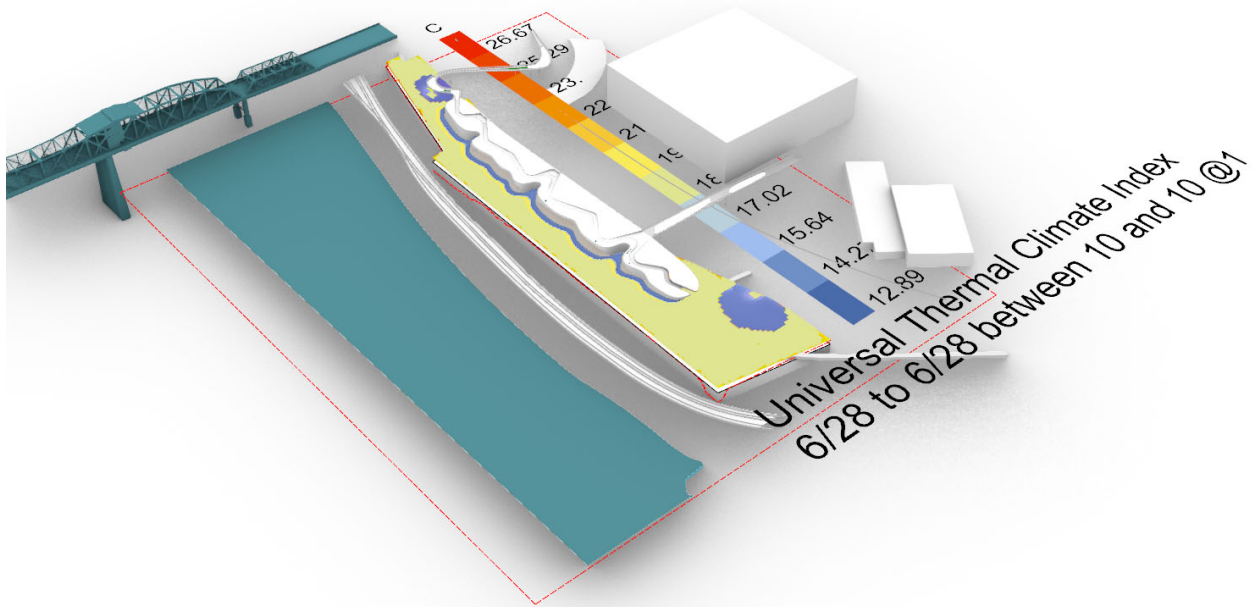


Figure 212. UTCI simulation for the landform building.

The last simulation (Figure 213) integrates a green roof into input geometry. The green roof design includes two types of materials: lawn for vegetated areas and concrete for the path. The simulation result shows that the UTCI temperature around the building and landscape does not change. The vegetated areas on the roof show 19 °C temperature and 21 °C for a walking path. These results stay within a comfort zone, and the simulation result shows no thermal stress.

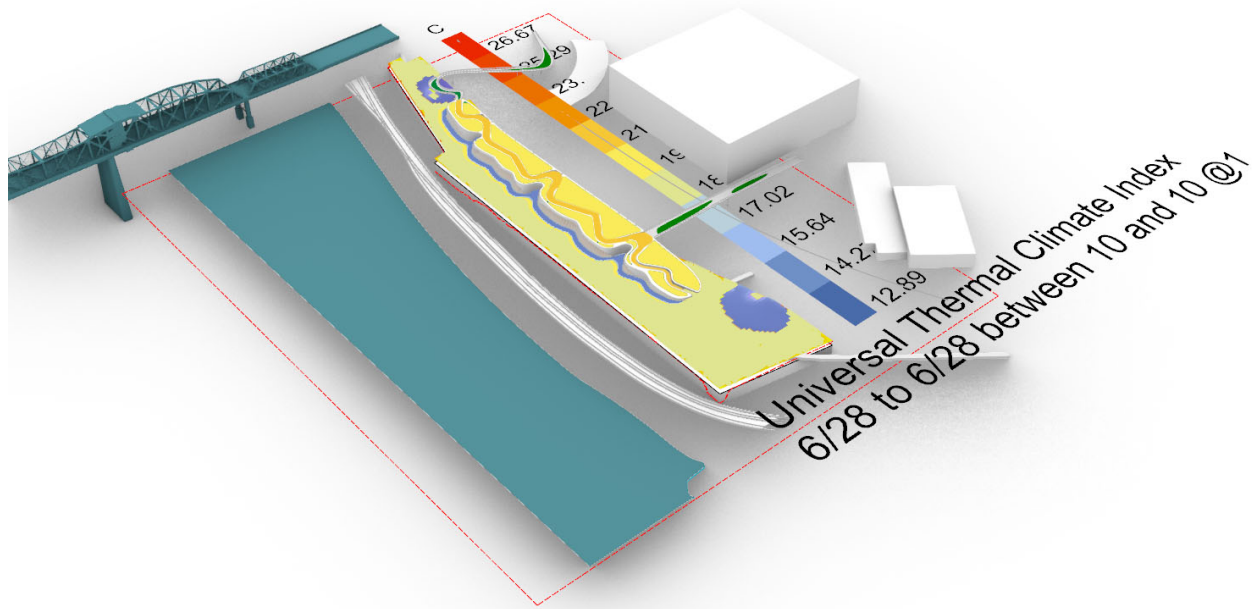


Figure 213. UTCI simulation for the landform building and green roof.

By using the UTCI index, the simulations illustrate how the selection of different materials and design scenarios influence the thermal stress level and overall comfort on site. The existing site's conditions and asphalt showed moderate heat stress and a temperature of 24 °C, while an integration of building geometry and a change to concrete material reduced the UTCI value and showed a decrease of temperature to 21–23 °C. The further change of building geometry to the landform building and the change to vegetation texture decrease the UTCI value to 18–19 °C. The simulation results show the potential of a landform building along with proper material selection to improve outdoor thermal conditions.

6.4 Summary

This chapter illustrates the final stages of a process-based approach to landform architecture that uses design as a tool for inquiry, using 3D simulations to address site-specific processes and design challenges and to improve the environmental performance of the landform

building and adjacent landscape. The geomorphological, hydrological, wind, and vegetation simulations help address site-specific challenges, such as strong winds, an isolated riverfront, and high temperatures.

The iterative design process along with the use of 3D simulations helped to transform a basic cuboid shape into a building with pockets and filleted edges, and finally to a wave-like form. Such transformations helped to minimize the effect of strong wind along the Willamette River and create windless zones. The landform building merges with the landscape to create a waterfront park. This part of the research shows the positive aspects of integrating 3D simulations into the design process and developing a landform building in harmony with natural processes.

The last stage of the design experiment was the evaluation of the environmental performance of the landform building and adjacent landscape through the use of UTCI thermal simulation to assess outdoor comfort. The simulation results showed that material selection, such as the replacement of asphalt with a grassy lawn, significantly reduces thermal stress and improves outdoor comfort. Among the key findings is that landform design achieved the best thermal performance. The design experiment shows the potential of process-based methodologies to develop landform buildings that enhance outdoor microclimate and improve the comfort level.

VII. CONCLUSIONS

This chapter synthesizes the key research findings of the dissertation in relation to research aims and questions. After summarizing theoretical, methodological, and evaluative contributions to knowledge, this chapter also presents the study's limitations and proposes a direction for future research. The conclusions presented in this chapter are valuable for academic and practical applications in landscape architecture and architecture.

This dissertation research highlights the limitation of the current form-based approach to landform architecture, which ignores landscape processes and fails to address climate-related challenges. The study contributes to knowledge by proposing a process-based approach that positions landform architecture as reflective of site-specific historical context and natural processes, and also addresses potential environmental challenges.

7.1. Contribution to Knowledge

The contributions of this dissertation span theory, method, and practice. The following sections review theoretical, methodological, and evaluative contributions to knowledge.

7.1.1 Theoretical Contribution

The theoretical contribution of this research is the traced evolution of landform design from ancient cultures to the integration of landforms in art, landscape architecture, and architecture. Ancient landforms were used for settlements, defense, and rituals. Analysis of ancient cultures showed how humans around the world designed landforms for protection, survival, and social needs. Ancient landforms had a significant influence on Land Art, where the dominant idea was to use natural materials to create large site-specific artworks in remote landscapes. This analysis helped to identify the limitations in existing approaches and develop the typology of landform architecture.

The proposed typology of landform architecture classifies projects into form-based and process-based categories. The form-based category includes a series of design directions represented via theoretical shifts and precedent study projects, where landform serves as a formal or metaphoric element. The process-based category introduces a theoretical shift toward dynamic, process-oriented design, where design interacts with site-specific processes.

The form-based category of landform architecture typology consists of the design approaches of cosmomorphism, hydromorphism, biomorphism, and geomorphism. Each of these directions was shaped by different metaphors and cultural, technological, economic, and industrial factors. Cosmomorphism used cosmic symbols and envisioned landforms as sculptures. Hydromorphism used hydrological metaphor to explore the relationships between water and earth to create site-specific designs. Biomorphism used biological metaphor to explore fluid forms and create nonlinear architecture. Geomorphism used geological metaphor to explore the use of digital programs and tools to imitate natural forms. Geomorphism included subcategories, such as topographical integration, geomorphological form, crystallographic form, and landscape integration. The topographical integration subcategory referred to how buildings or structures were integrated into the natural topography of a site. The geomorphological form subcategory used geological form as a metaphorical response to potential social, environmental, and urban changes. The crystallographic subcategory used geometric forms found in minerals

and crystals as inspiration for architectural form. The landscape integration category focused on the use of sustainable materials and solutions to integrate design into larger systems.

The study advances the field of landscape architecture and architecture by proposing a shift in paradigm from a form-oriented to a process-oriented approach to design. Compared to static approaches that prioritize aesthetic or metaphoric form, a process-based approach acknowledges the continuous transformation of landforms due to environmental, cultural, and technological influences. Through comparative analysis of process-based approaches in landscape architecture, the shift can be understood through the key stages, such as ecological process-based design, systems-derived process-based design, and phasing process-based design. The ecological stage considered seasonal and temporal changes in the landscape. The systems-derived stage focused on complex interactions between ecological and urban systems. The phasing stage focused on a framework for large-scale designs that sustain the development of the landscape over time. The advancement in digital technologies enables further development of process-based design that incorporates 3D modeling and simulations. The case study projects illustrated how advances in digital technologies and computational modeling can respond to site conditions.

The analysis of the evolution of process-based design and case study analysis of selected projects informed the development of a theoretical framework for a process-based approach in landform architecture that focuses on environmental and human processes that have shaped the site in the past and will continue to shape it in the future. This approach starts with a comprehensive analysis of geological history, hydrological processes, sedimentation patterns, and vegetation changes. In addition, this approach considers visible and invisible forces, such as processes of urbanization, economic changes, and environmental shifts. The process-based approach also embraces the idea of time, change, and history. The shift in paradigm influences the theory and practice of landscape architecture and architecture.

7.1.2 Methodological Contribution

The methodological contribution of this dissertation is the use of the Research through Design method that tests the proposed theoretical framework through a design experiment in Portland's Lower Albina neighborhood. Research through Design was suited for this study as it allowed for an iterative process, where analysis, 3D simulations, and design informed one

another. Another methodological contribution of this dissertation is to the case study analysis process in landscape architecture that includes 3D simulation as an integral part of the analysis.

A key methodological contribution of this research is a design framework to landform architecture that consists of 3D simulations for designers to shape a building and landscape based on local processes. Such a framework includes site-specific analysis of landform, fluvial, wind, and vegetation 3D simulations. Unlike the traditional case study method that relies on historical mapping and qualitative observations, this dissertation incorporates computational modeling to understand spatial transformation over time.

The study presents an in-depth analysis of the history of Portland, Oregon, and an analysis of processes that have shaped its current conditions at city, neighborhood, and site scales. The results of this analysis are presented in the form of 3D simulations that offer an enhanced understanding of the city's topography and relationships between the processes of urbanization and city development.

At the city scale, the comprehensive analysis of geomorphological, hydrological, and vegetation processes presented an understanding of the dynamic evolution of the city. The landform processes analysis gave an overview of environmental and human forces that have shaped the region over time and the way geological formations shaped the current topography of Portland. Fluvial processes highlighted the historical significance of flooding events and the transformative effect of human activities. Vegetation processes showed complex interaction between topography and climate, but also illustrated how urbanization changed vegetation patterns.

At the neighborhood scale, analysis of geomorphological, hydrological, and vegetation processes showed the main factors that influenced a tremendous transformation of the Albina neighborhood over time. The construction of major infrastructure projects, such as Interstate 5, the Veterans Memorial Coliseum, and the Moda Center, played a crucial role in reshaping the neighborhood. The simulation revealed the impact of urbanization on the entire neighborhood, such as displacement of residents, loss of connection inside the Albina neighborhood and to adjacent neighborhoods, loss of access to the river, and changes in vegetation cover. The findings supported the initial hypothesis that, on the neighborhood level, urbanization was the main factor of change and spatial segregation of Albina.

At the site scale, analysis of geomorphological, hydrological, and vegetation processes showed the transformation of the project site in response to natural and human influences. The project site went through significant transformations over time. Starting as a residential area, the site changed in the late 1950s to early 1960s due to the construction of N. Interstate Avenue and the Veterans Memorial Coliseum and transformed into a motel area. Following the end of the motel era in the 1990s, the site underwent another transformation into a parking lot. The simulation shows the limited impact of fluvial processes on the smaller scale. It also shows that the main transformation forces to the project site were urbanization and changes in land use.

This study also proposes landform building as a medium not only for environmental performance but also as a reparative design tool. Within Portland's Albina Vision community-driven efforts to address erasure and displacements, landform architecture is conceived as a tool for spatial and social repair. Historical inequities in tree canopy, loss of access to the river, and city fragmentation caused by infrastructural projects require site-specific interventions that consider the site's history, present conditions, and projected future along with site-specific processes. This research suggests that a strategically placed landform building with adjacent landscape offers a more holistic solution than tactical efforts. In this case, landform architecture becomes a platform for the city's investment—not only economic, but also ecological and cultural.

The study provided a comprehensive understanding of how environmental and human processes have shaped the city and Albina neighborhood, while also offering insights into the interplay between geological, hydrological, and vegetation processes.

7.1.3 Evaluative Contribution

The evaluative contribution of this dissertation is the use of a proposed framework for a process-based approach to landform architecture for a design experiment on a project site in the Lower Albina neighborhood. This framework included a series of 3D simulations, such as geomorphological, hydrological, wind, and vegetation, that represent natural processes.

The geomorphological simulation provided the foundational simulation in the process-based design that helped to understand how the site changes with design intervention. The hydrological simulation modeled the water flow across an architectural surface, revealing interactions between building geometry and drainage patterns. The wind simulation helped to

understand how design influenced wind behavior, microclimate, and outdoor comfort at the pedestrian level. The vegetation simulation helped to visualize vegetation placement and growth to understand how the site changes with design intervention.

The proposed framework was first tested on existing conditions within the project site. The set of simulations examined the interactions of various forms with environmental processes. The simulations revealed that the input geometry, such as building shape, landform configurations, and tree placement, impacts hydrological and wind processes. The hydrological simulation revealed how the input geometry interacts with the water flow. The wind simulations included a series of building, landform, and tree simulations. The building wind simulations demonstrated that building shape, orientation, and spacing between sets of buildings influence wind speed and direction. The landform wind simulations showed that landforms interact with the wind similarly to buildings: their orientation and number influence wind patterns. The vegetation wind simulation reinforced the findings about input geometry by illustrating how trees influenced wind conditions. The vegetation simulation complemented earlier simulations and illustrated how tree placement influenced microclimate conditions.

The set of 3D simulations illustrated that the placement of buildings, landforms, and vegetation can improve microclimate conditions by reducing wind exposure on the pedestrian level and controlling water runoff. The key findings from each simulation were applied to the design of the landform building, which enabled testing and refining a proposed framework for a process-based approach to landform architecture.

The findings from 3D simulations were applied in the design process. The proposed design framework with the set of 3D simulations was used to address site-specific processes and design challenges, and improve the environmental performance of the landform building and adjacent landscape. The iterative design process helped to transform a basic cuboid shape into a landform building that merges with the landscape to create a waterfront park.

The final stage of evaluative contribution to knowledge was the assessment of the environmental performance of selected design options. The resulting microclimate maps that use the UTCI to assess outdoor comfort illustrated how different design options and material selections can change human comfort levels. The set of 3D simulations showed the potential of landform buildings and adjacent landscapes to enhance the microclimate and improve the comfort level.

By integrating the concept of time, change, and history with theoretical, methodological, and evaluative contributions, this research advances the field of landscape architecture and architecture by proposing a new framework for landform architecture design.

7.2. Limitations of the Research

While this dissertation makes significant contributions to the theoretical understanding of landform architecture and the methodological approach to landform architectural design, it also has some limitations.

The research relies on digital tools, such as Rhino and Grasshopper, to create 3D simulations of site processes and environmental performance analysis. While the combination of such tools gives valuable insights, it reflects the current state of technology, which still has limitations in computational techniques, accuracy, and ease of use.

3D simulations that incorporate CFD require advanced knowledge of Grasshopper and OpenFOAM platforms and require significant computational resources. These simulations are time intensive, which makes the iterative design process more challenging. The complexity of setting simulations can limit accessibility for designers without specialized expertise.

Improvement in the current stage of technology and simulation techniques could enhance the simulation results by combining a set of 3D simulations into a simplified file, or possibly even one Grasshopper definition. Future advancements in technology, such as improved simulation techniques, AI-driven environmental analysis, and real-time feedback integration could significantly enhance the precision and use of these tools for simulation. While 3D simulations help to develop the concept stage of design, more advanced stages might require professional analysis from engineers, such as wind tunnel testing, to further refine performance assessment.

Another limitation is related to the availability of the data for 3D simulations. The accuracy of simulations depends on high-quality, site-specific input data. Environmental simulations mostly rely on EPW data, typically collected from the nearby airport. While the dataset provides useful information from airports around the world, not all project sites are located near the closest airport, which means that this data can impact the reliability of the simulation results. The limitation of the 3D simulation tools and the evaluation of environmental performance is that Honeybee and Ladybug present only selected materials for the UTCI

simulation. While higher-quality data may improve the accuracy of the simulation results, it is unlikely that better data over time might fundamentally alter the methodology or design approach.

7.3. Recommendations for Future Research

Building on the findings and limitations in this research, future research could explore the areas specified in this section.

This dissertation applies a process-based approach to a site in the Lower Albina neighborhood in Portland, Oregon, where the wind process played a key role in the design of a landform building with the adjacent landscape. The methodological framework introduced in this dissertation would benefit from its application in different climatic and geographic conditions, where other defining processes might shape the built environment. For coastal environments, hydrological simulations might play a key role in shaping the design and exploring how landform architecture can mitigate flooding and improve coastal resilience. For areas that require slope stability and erosion control, the geomorphological and hydrological simulations might guide a landform intervention. For dry areas, the framework could integrate solar radiation modeling, evaporative cooling strategies, and shade analysis. By testing the framework in different conditions, future research could refine site-specific strategies that respond to local conditions

In this dissertation, the design process was developed in response to the site-specific conditions of Lower Albina. The iterative design process combined two simulation-based approaches: a form-finding workflow that emerged from geomorphological site conditions; and a basic form-testing workflow that explored how basic geometries interact with site processes. The findings from these approaches were combined to develop a landform building design with adjacent landscape.

While the study illustrates an in-depth site analysis on the city, neighborhood, and site scale, along with extensive analysis of current site-specific processes, it is also essential to propose a generalized methodological framework. Such a framework can be adapted by other designers or researchers across different contexts in the following order:

- Historical analysis of the site. This step aims to trace changes and transformations, including environmental and human-induced, that occurred within the site. Such

analysis helps to understand the trajectory of change and identify what shaped the site to its current state.

- Analysis of current conditions and processes. This step requires determining specific environmental, human, and urban processes that continue to influence the site. This may also include environmental challenges that continue to persist within the site.
- Projection of potential future changes. After analysis of historical conditions and current processes is complete, this step determines what kind of environmental and urban changes might occur within the site.
- 3D simulations. This step requires a thoughtful contribution and a designer's guiding role. Depending on the project's goals and site-specific conditions, select a suitable workflow. This could involve a form-finding workflow, a basic-form-testing workflow, or a combination of both.
- Design development. Based on the findings from previous steps, this step envisions a development of the building and adjacent landscape. The iterative design process makes it possible to test and refine the design to ensure its alignment with environmental processes and project goals.

Future studies would also benefit from long-term investigations and data collection of changes in urban microclimates due to landform architecture integration. A longitudinal study that collects microclimatic data over a longer period of time would provide insights into how landform architecture impacts local conditions. Such a study might include collecting onsite temperature and wind speed data before and after the integration of landform design. In addition, it might be beneficial to track seasonal variations in environmental performance. Finally, investigating the long-term effects of vegetation growth on wind and microclimate regulations might inform future research.

Such investigations might lead to revising the proposed methodological framework and illustrate more specifically how landform architecture solutions can change the local microclimate and address environmental challenges.

APPENDICES

APPENDIX A. LANDFORMS SHAPED BY DIFFERENT PROCESSES

Landforms	Aeolian landforms Formed by wind erosion, weathering, and deposition (subprocesses)	Glacial landforms Formed by gravitational processes (active ice and snow processes, continental glaciation, frost action)	Igneous landforms Formed by volcanic eruption	Fluvial landforms Formed by erosion and sedimentation related to rivers and streams.	Coastal landforms Formed by marine processes (emergence and shoreline processes)
Processes	badlands dune (barchan, blowout, parabolic, parma, reversing self, shrub-coppice, star, transverse) foredune interdune flat ridge (barchanoid, hornoclimax, strike) bolsón burrhead butte caldon canyon cave cliff cuesta delta depression basin depression desert (desert pavement, desert vanish) dissected plateau diabazier dry lake eg entumed river channel flation gully gullch hoodoo hoodoo inverted relief limestone pavement loess deposit monadnock mesa paha pedestal pediment pediplain / peneplain pool potero ripple mark roche moutonnée sandhills, sand ramp, sand sea, sand sheet semi-bolson structural bench structural terrace sea table tepuai tupig tor truncated spur tundra valley ventifact water pocket weathering pit yardang trough	alias alpine glaciation arete bald baloon bluff burte cirque (floor, headwall) cliff col colliual hillslope corrie coulee crag and tail cuesta dala dalle dell dike drainage channel draw drumlin earth hummock escarpment esker faceted spur fjord flute flute fluvial terrace foothills fossa frost (boil, mound) gap giant ripples glacial horn glacier (cave, foreland, valley, quarry, uplands) glen gorge gully hollow hummock ice apron, margin sheet, wedge) interflute kame (moraine, terrace) kettle knob knoll ledge lowland mesa mima mound monadnock moraine (fluted ground, interlobate lateral, medial, recessional) moulin mound mountain (cove, pass, range, valley) net invitation (hollow, ridge) nose slope	lava flow air-fall tephra field block lava flow caldera central peak cinder cone collapse caldera complex crater complex volcano composite cone (stratovolcano) crater crater lake landscupe cryovolcano ejecta blanket fissure vent fumarole field exogenous dome expulsion caldera greyer high island impact crater intrusive dome lahar lava (blister, dome, field, flow, lake, plain, plateau, spine, tube) maar malpais mamelon mid-ocean ridge mud pot field mud volcano pit crater plug dome pressure ridge pseudocrater pumice cone pyroclastic cone (ash flow) shield volcano steptoe subglacial mound submarine volcano volcanic cone volcanic dam volcanic mountain lava plateau lava tube malpais mamelon mud volcano palisade flow pinnacle pleistocene simple crater spatter cone stratovolcano supervolcano trench tuya upheaved dome vent volcanic crater, dome, field, group, island volcanic plateau, plug volcano	at alluvial (fan, flat) anabranch anoyo badlands bajada bailena bank bar basin (floor, remnant) batolith bayou belta bolsón bottomland braided channel break burte cave channel cliff confluence crevasse spay cuesta cutbank channel delta stream dike dip slope drainage (area, basin, divide) draw erosional stream terrace fan flood plain fluvial island / fluvial terrace gligal gorge gravelbar marine terrace mid-ocean ridge mud flat hogback hoodoo inselberg lake levee mesa meander monadnock oxbow passage pediment playa pool ridge riffle rill river sandbank sandbar sand hills scablands scarp scarp slope shoal	abyssal (fan, plain) arch anabranch atoll ayre backshore / backbeach terrace (barrier) backwater barrier (bar, beach, flat, islands, reef) bay (gulf) beach (cusp, plain, ridge) biguit blowhole bolsón calanque channel chenier (plain) cliff coast channel coastal plain continental shelf coral (pinna-ck, reef) cove cusate foreland estuary faros firrh fjord ford geo reef (fringing) headland island inlet esker isthmus lagoon longshore bar machair marine terrace mid-ocean ridge mud flat oceanic (basin, atoll, plateau, trench) reef (organic patch, platform) peninsula pied (beach, ridge, estuary, mudflat, tidal flat) relict coastline ria river delta salt marsh sea (cove, cliff) seamount shelf atoll shoal shore slough split split stack submarine canyon surge channel tidal flat tombolo trench washover fan wave-built (terrace, platform) wetland

Figure 214. Different types of landforms and processes that shaped them.

APPENDIX B. HISTORICAL ANALYSIS OF PORTLAND

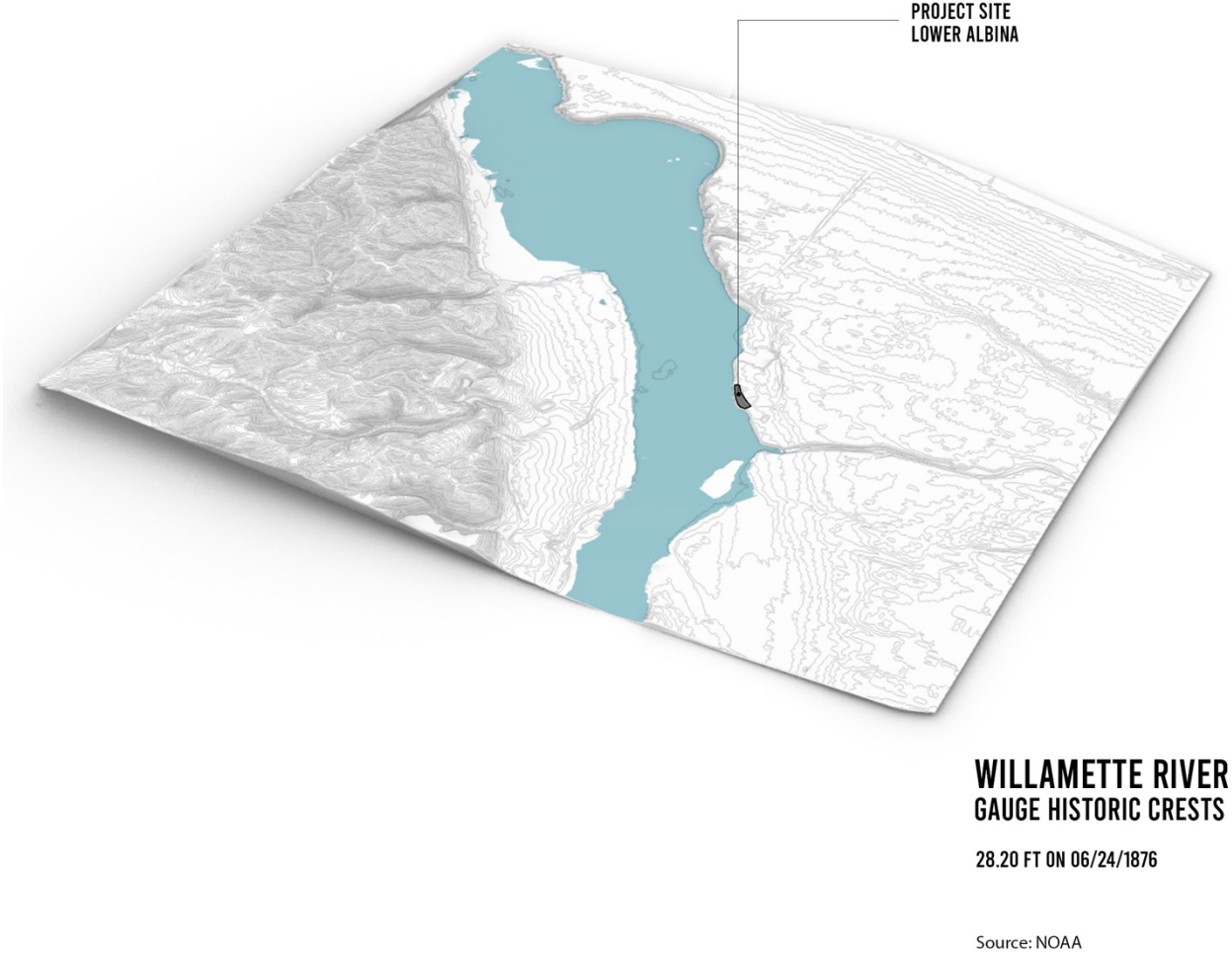


Figure 215. Willamette River gauge historic crest simulation on June 24, 1876.

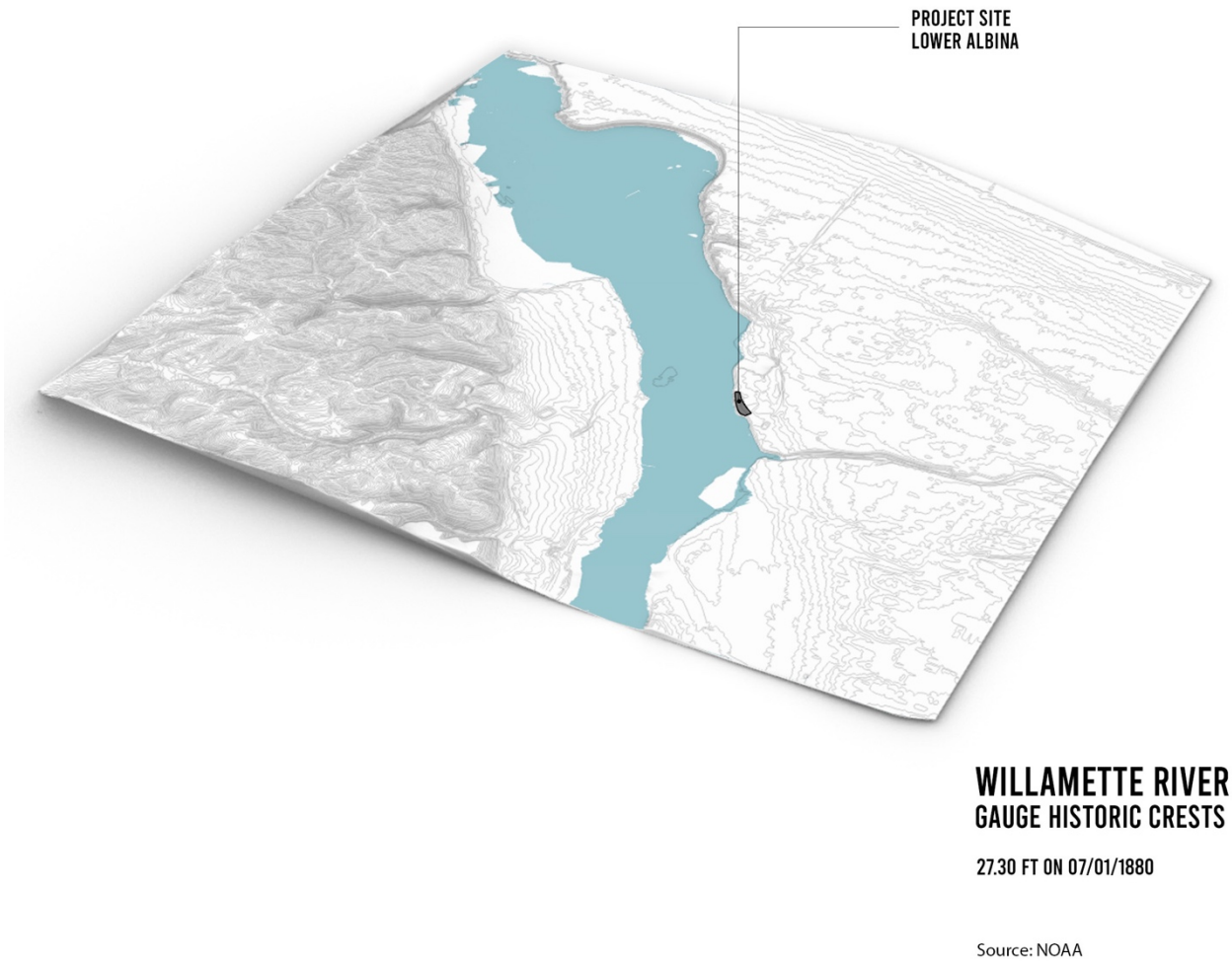


Figure 216. Willamette River gauge historic crest simulation on July 1, 1880.

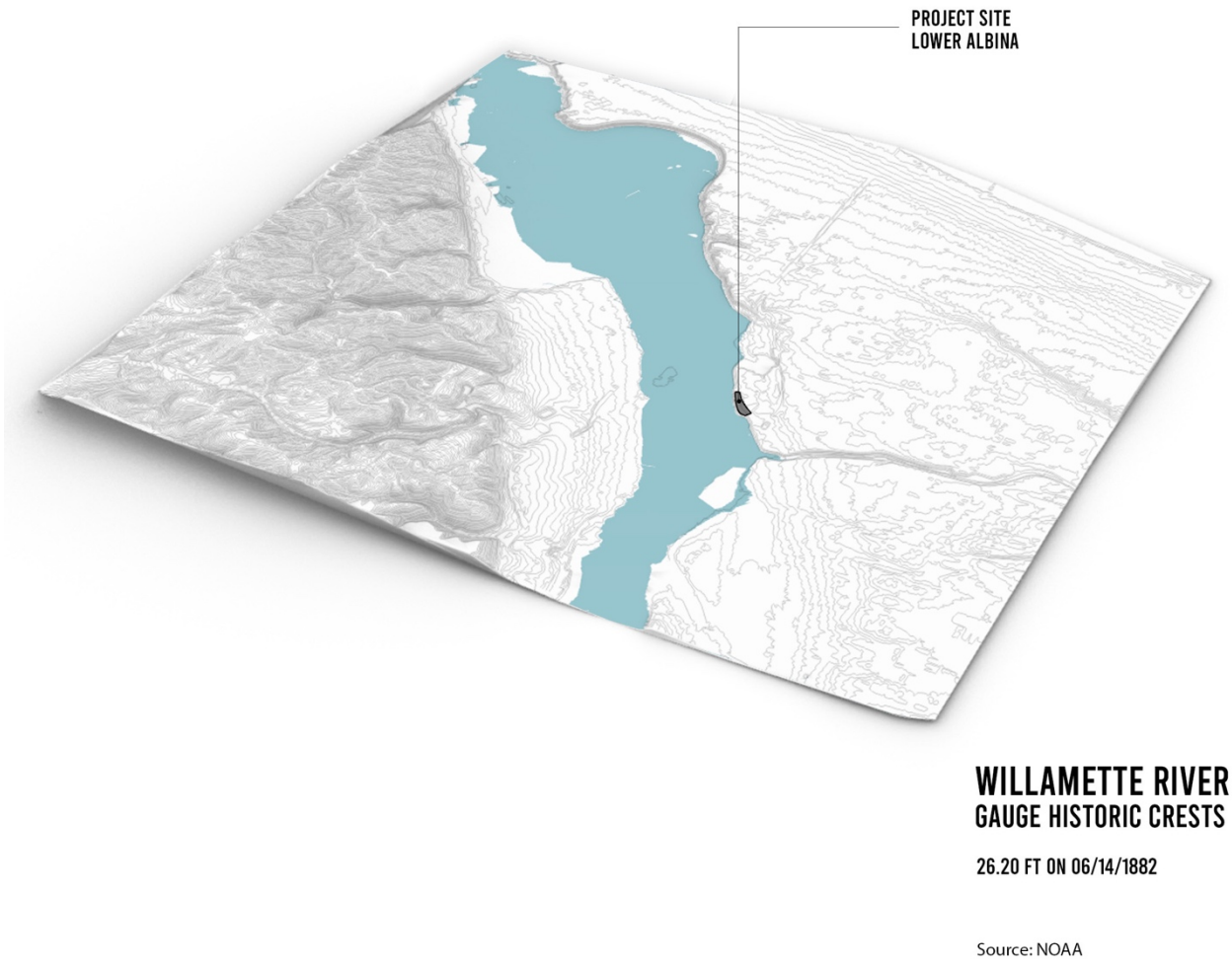


Figure 217. Willamette River gauge historic crest simulation on June 14, 1882.

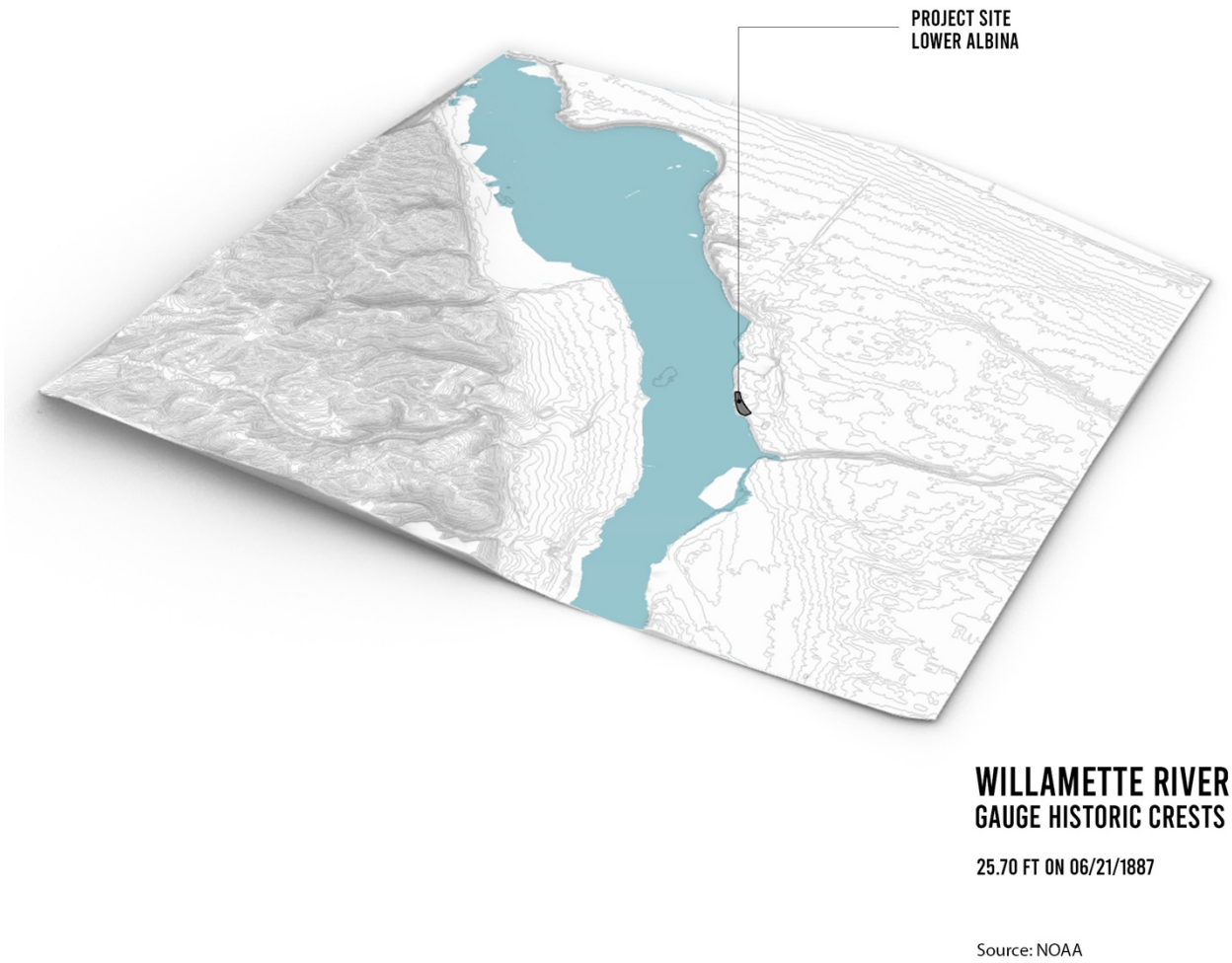


Figure 218. Willamette River gauge historic crest simulation on June 21, 1887.

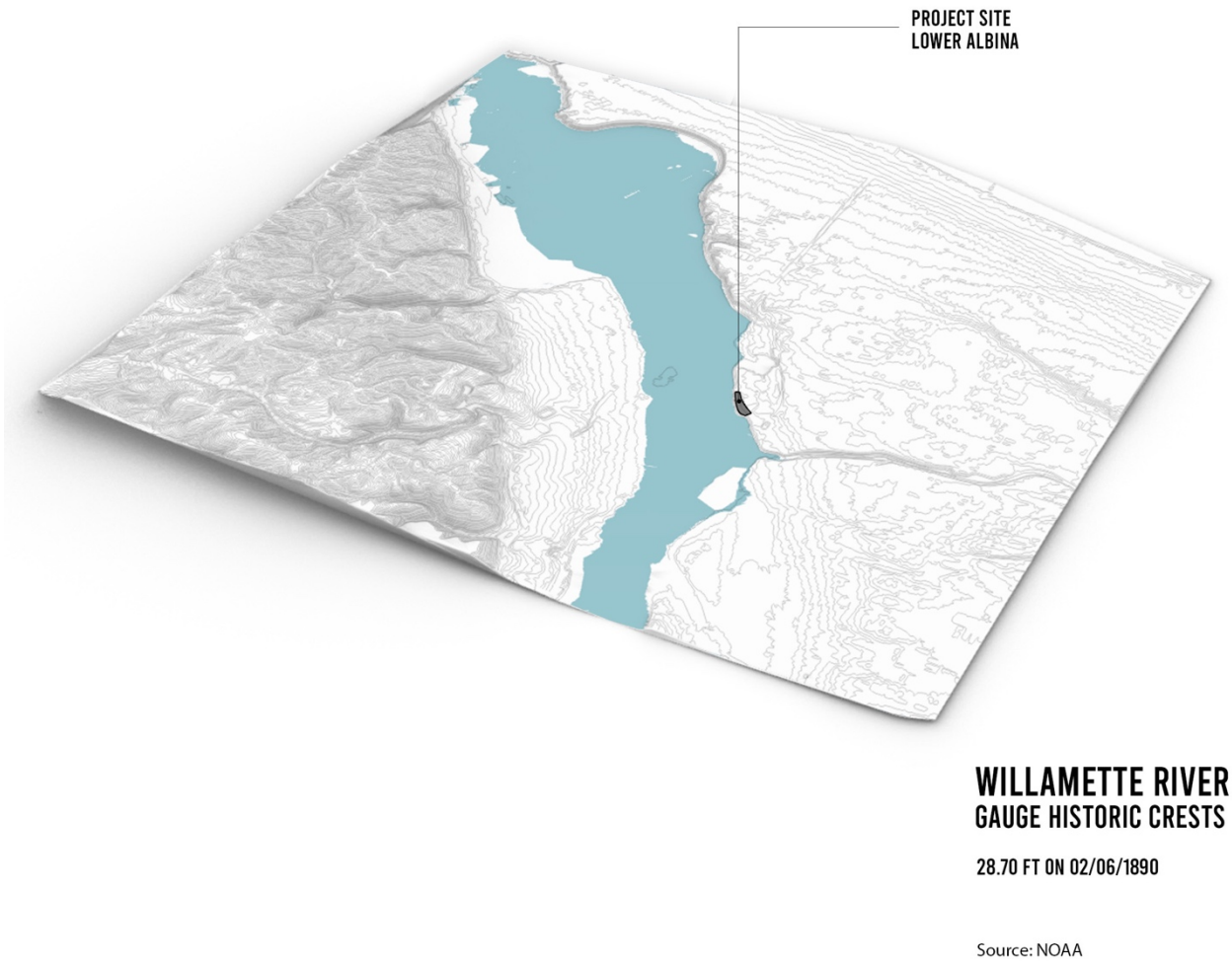


Figure 219. Willamette River gauge historic crest simulation on February 6, 1890.

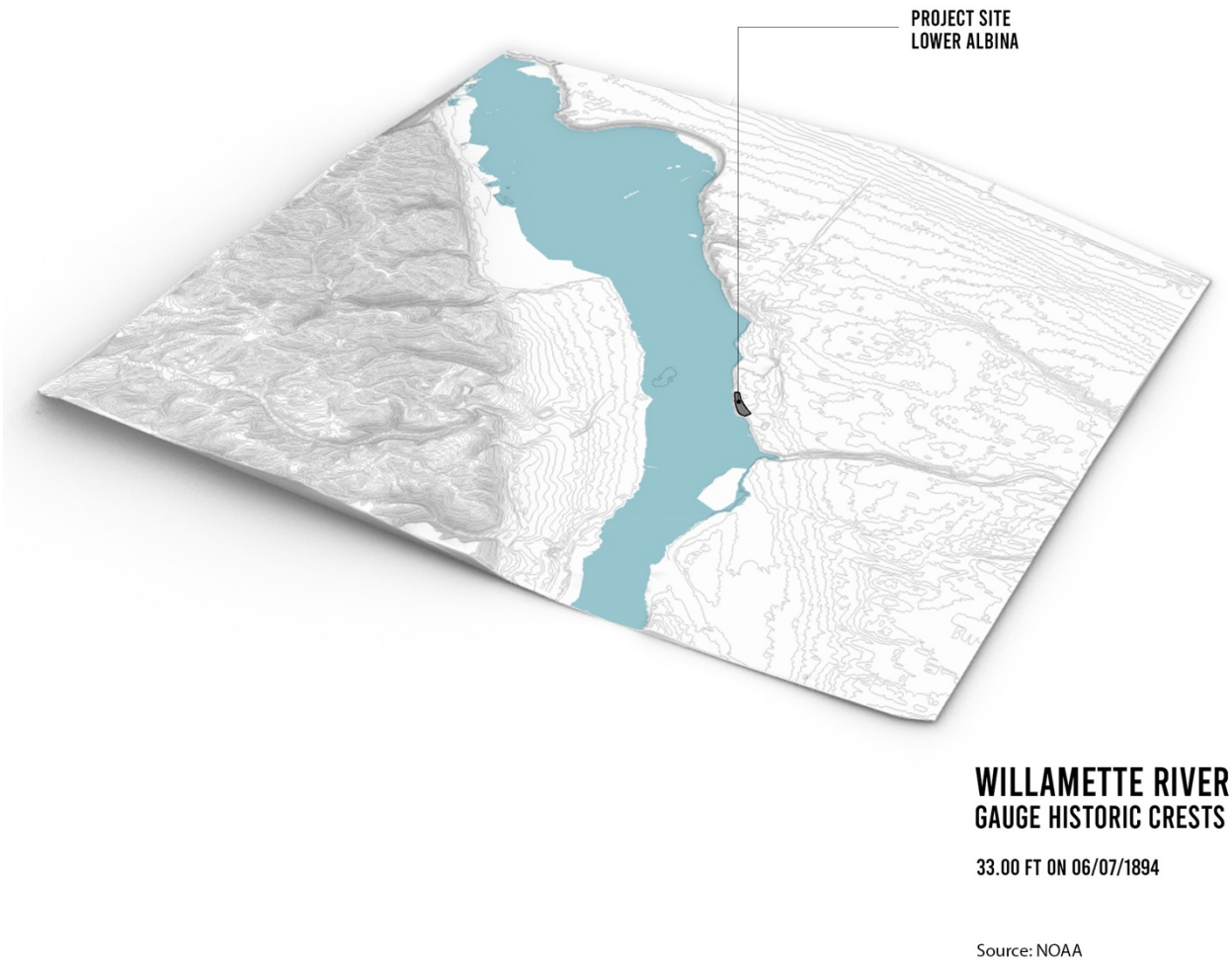


Figure 220. Willamette River gauge historic crest simulation on June 7, 1894.

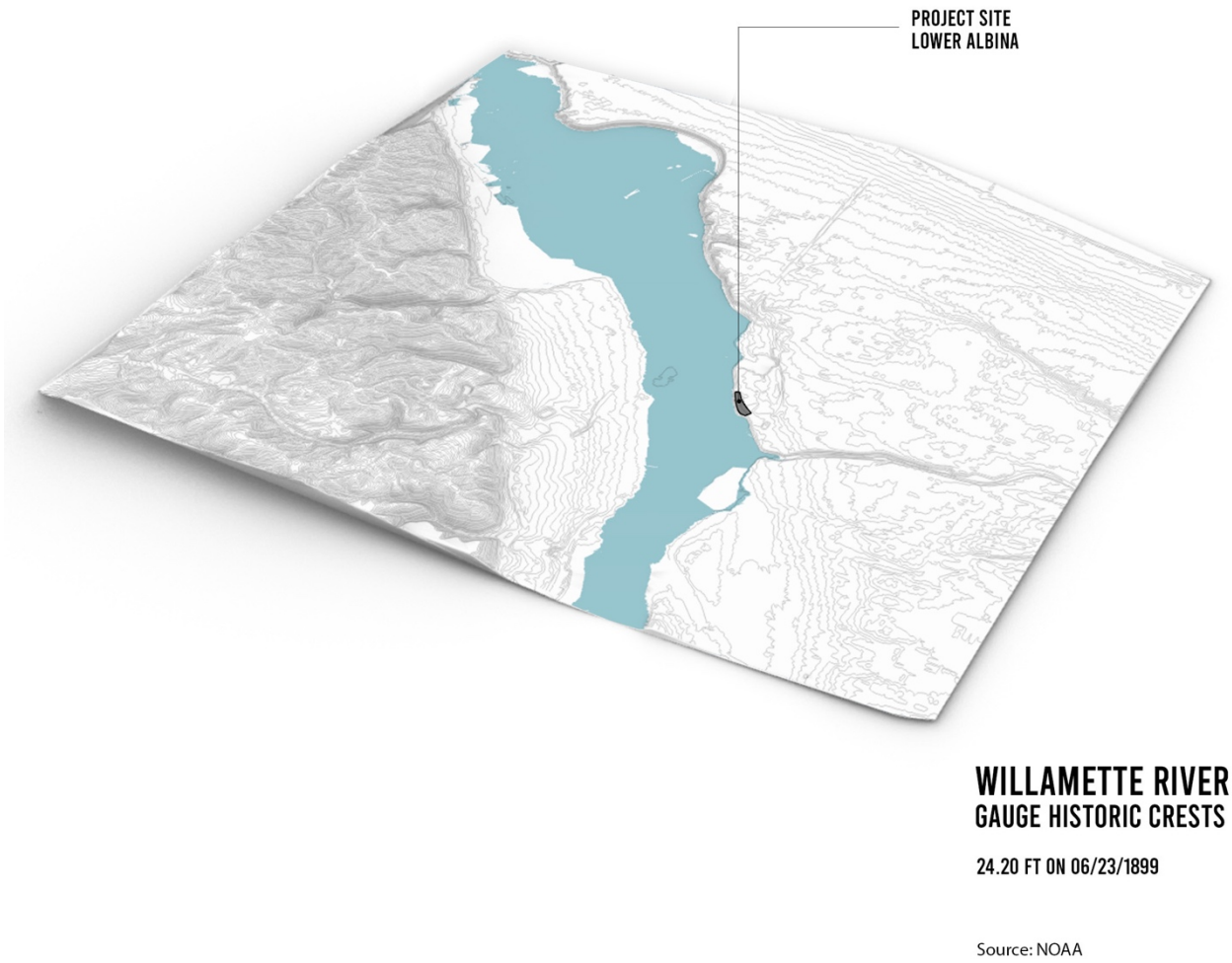


Figure 221. Willamette River gauge historic crest simulation on June 23, 1899.

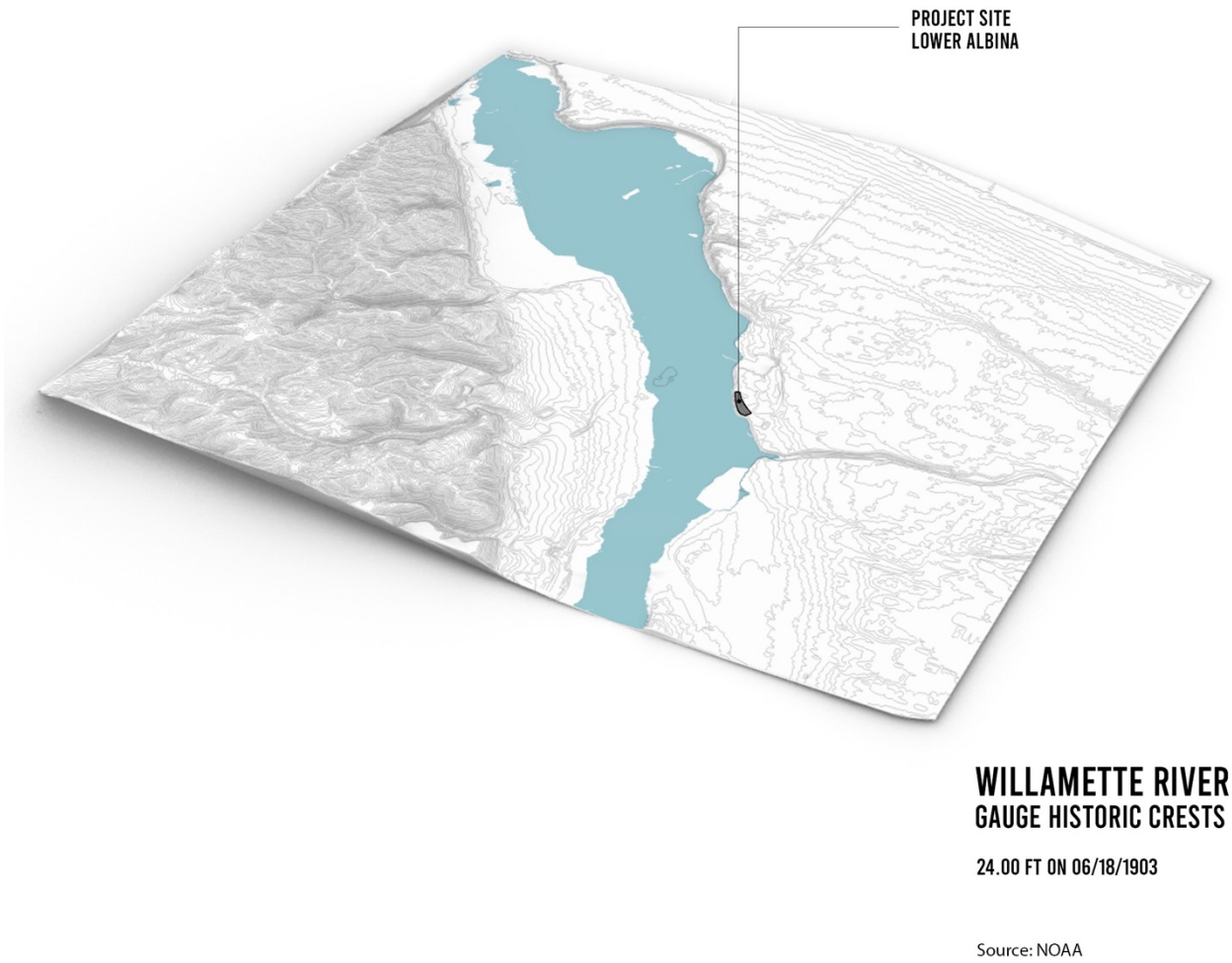


Figure 222. Willamette River gauge historic crest simulation on June 18, 1903.

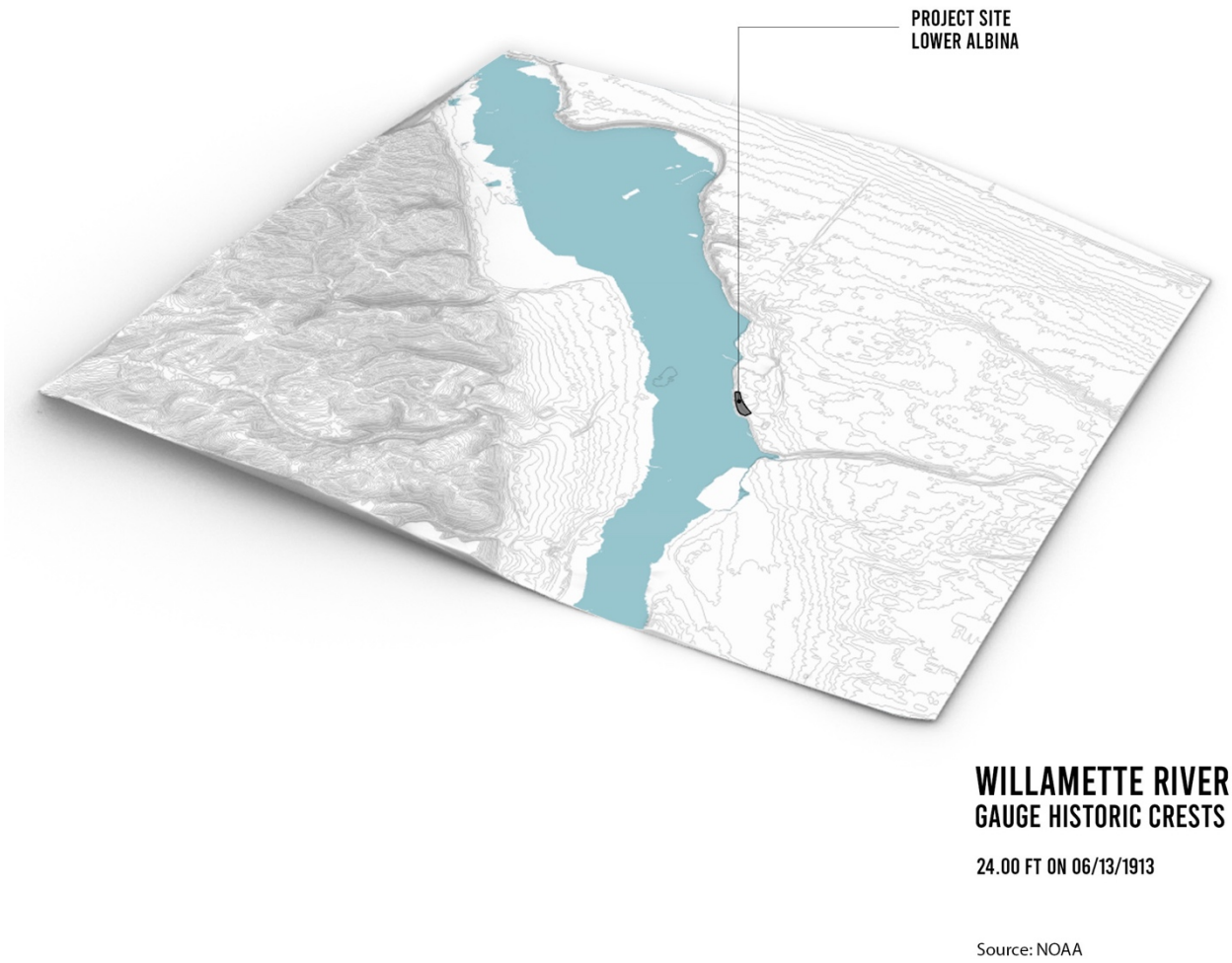


Figure 223. Willamette River gauge historic crest simulation on June 13, 1913.

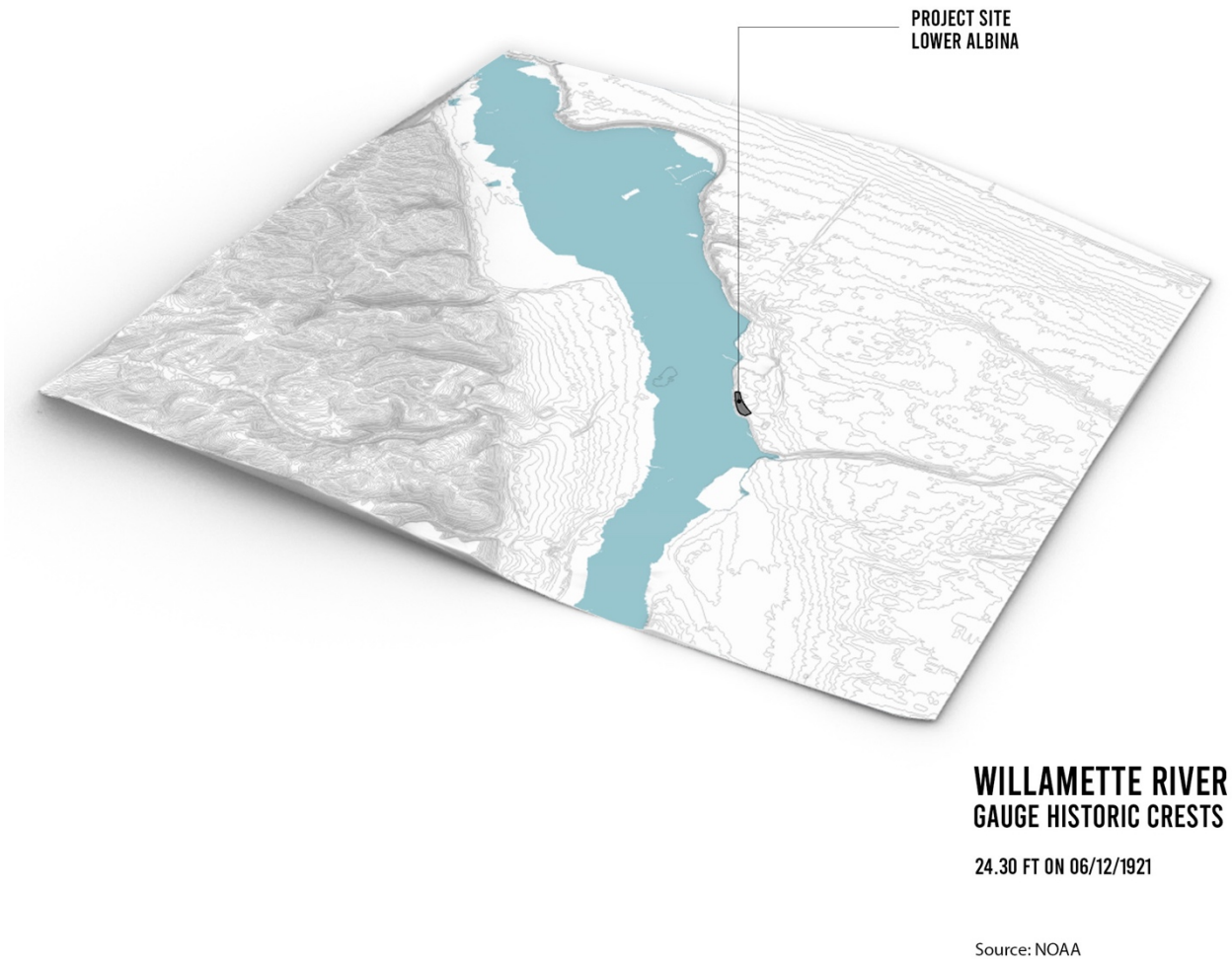


Figure 224. Willamette River gauge historic crest simulation on June 12, 1921.

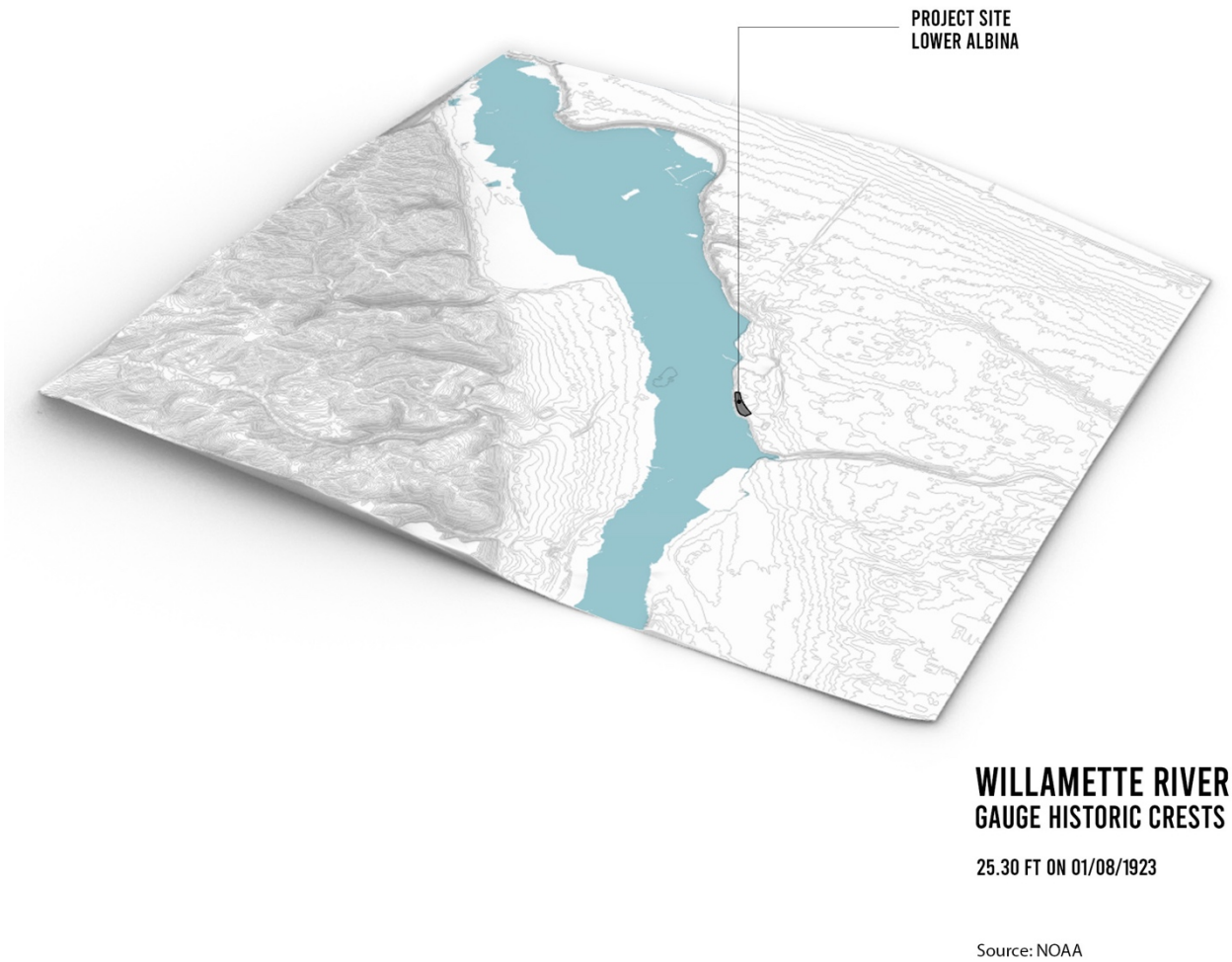


Figure 225. Willamette River gauge historic crest simulation on January 8, 1923.

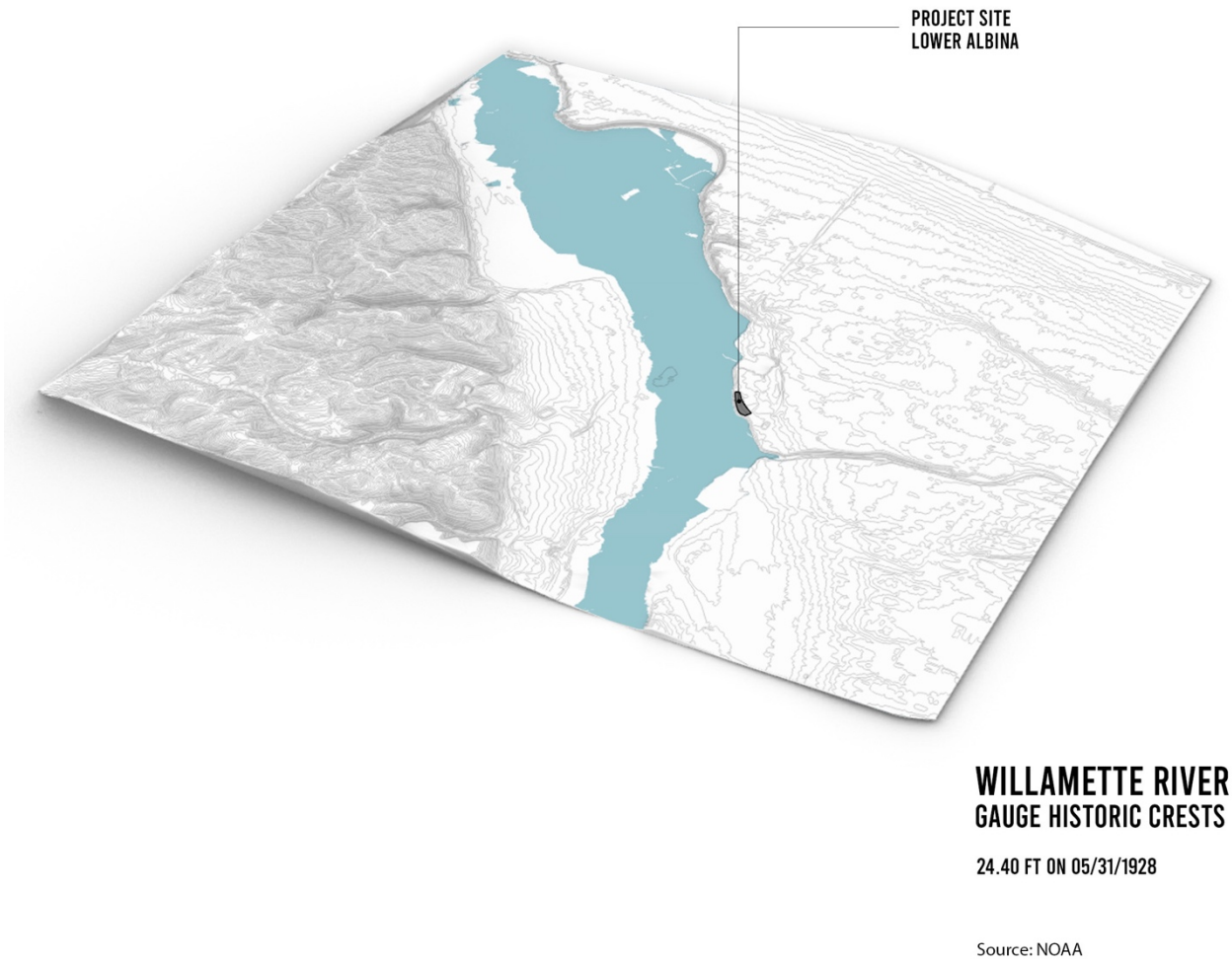
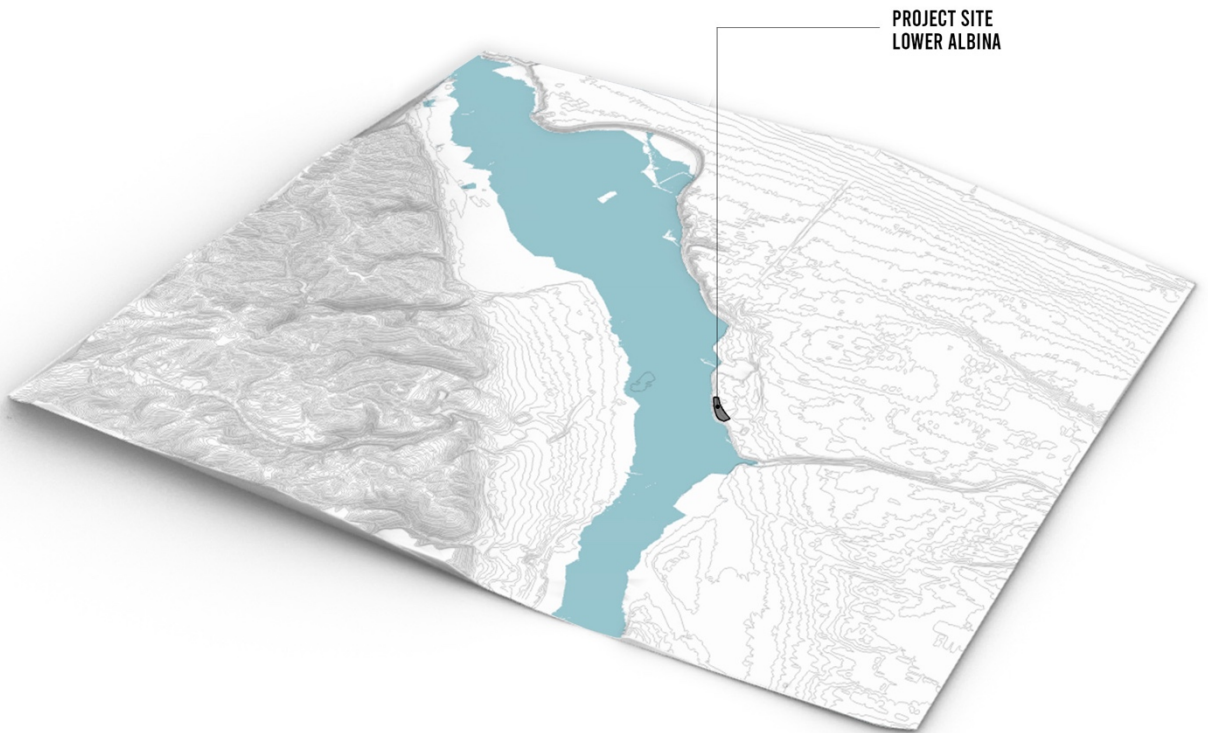


Figure 226. Willamette River gauge historic crest simulation on May 31, 1928.



**PROJECT SITE
LOWER ALBINA**

**WILLAMETTE RIVER
GAUGE HISTORIC CRESTS**

24.80 FT ON 06/13/1933

Source: NOAA

Figure 227. Willamette River gauge historic crest simulation on June 13, 1933.

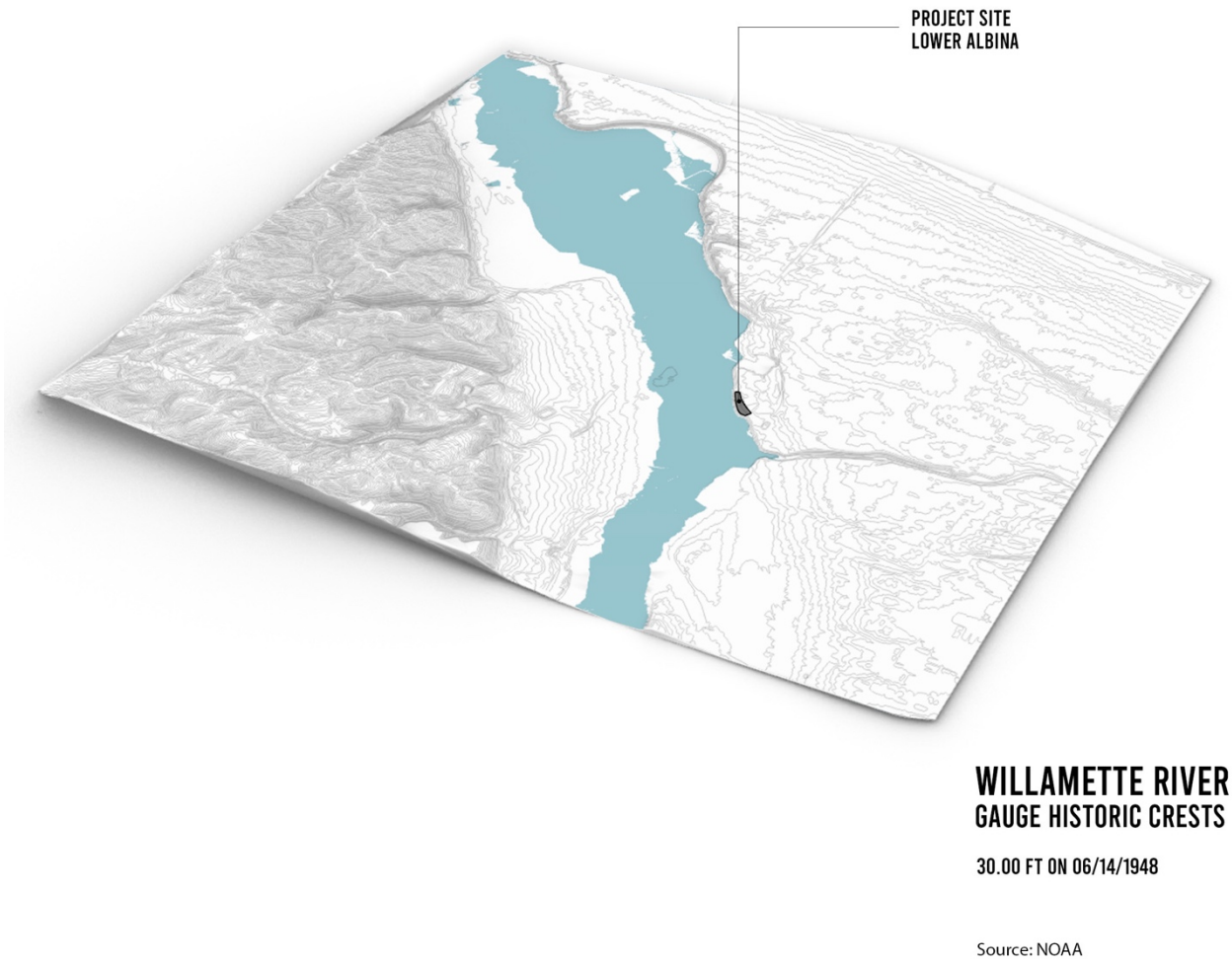


Figure 228. Willamette River gauge historic crest simulation on June 14, 1948.

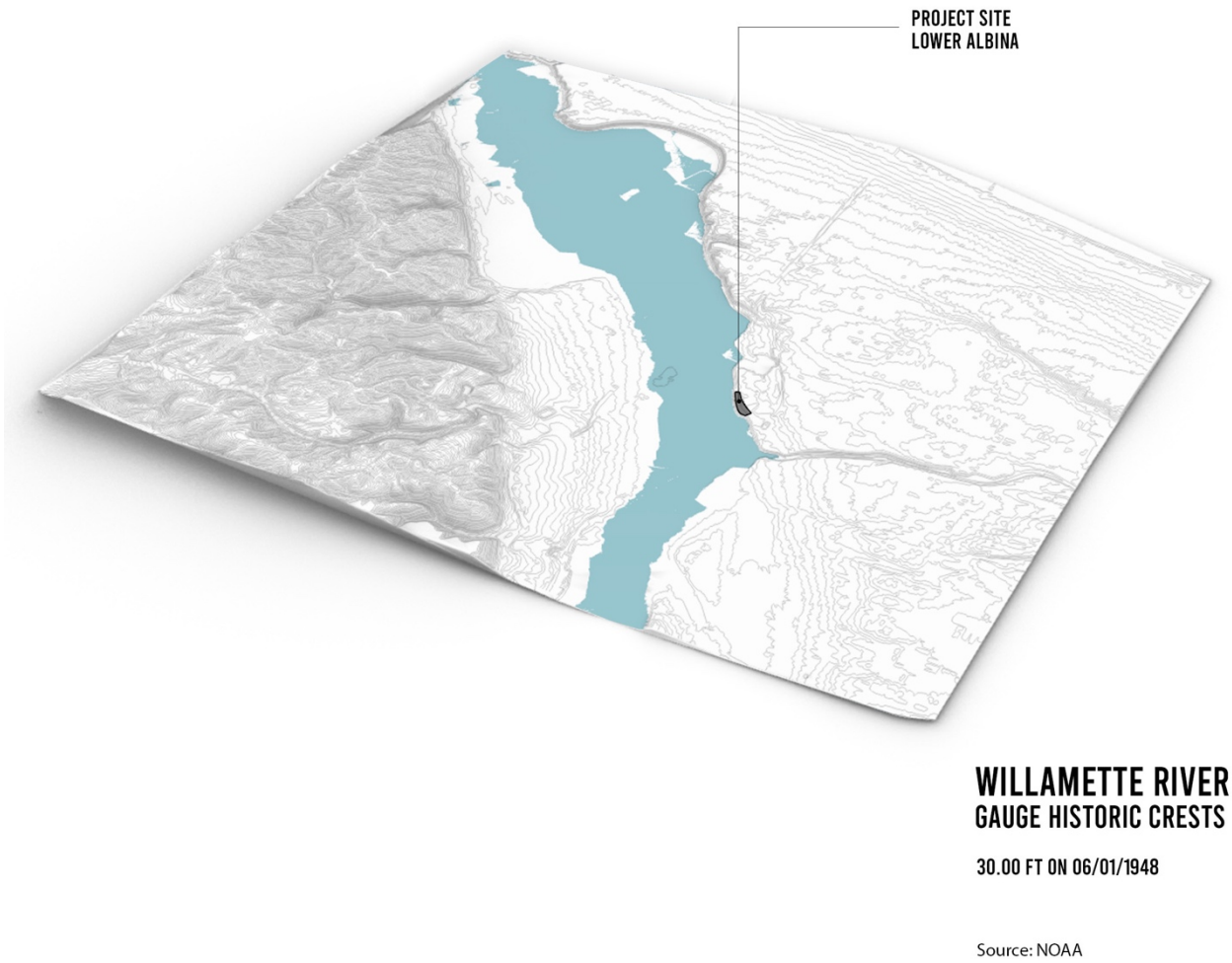


Figure 229. Willamette River gauge historic crest simulation on June 1, 1948.

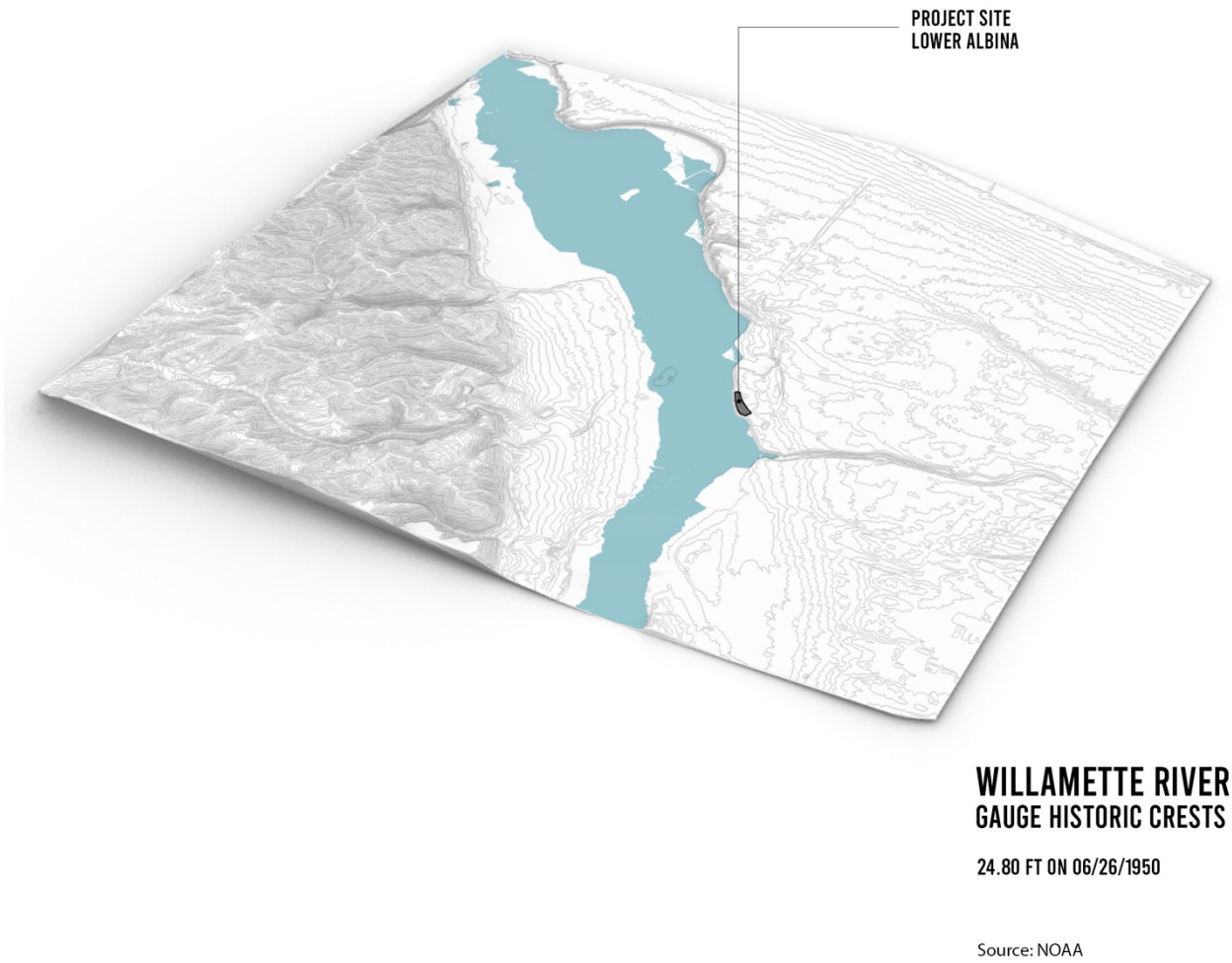


Figure 230. Willamette River gauge historic crest simulation on June 26, 1950.

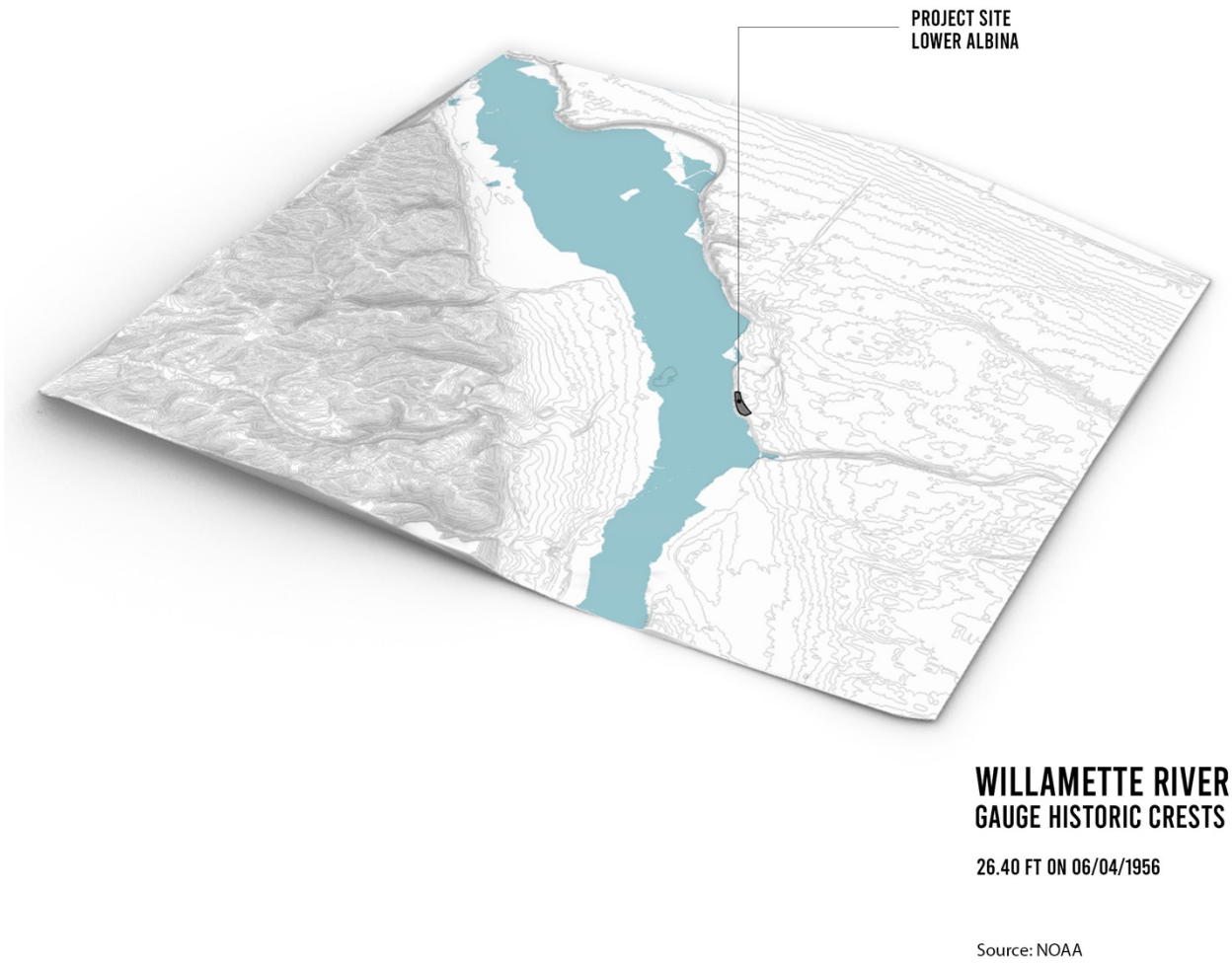


Figure 231. Willamette River gauge historic crest simulation on June 4, 1956.

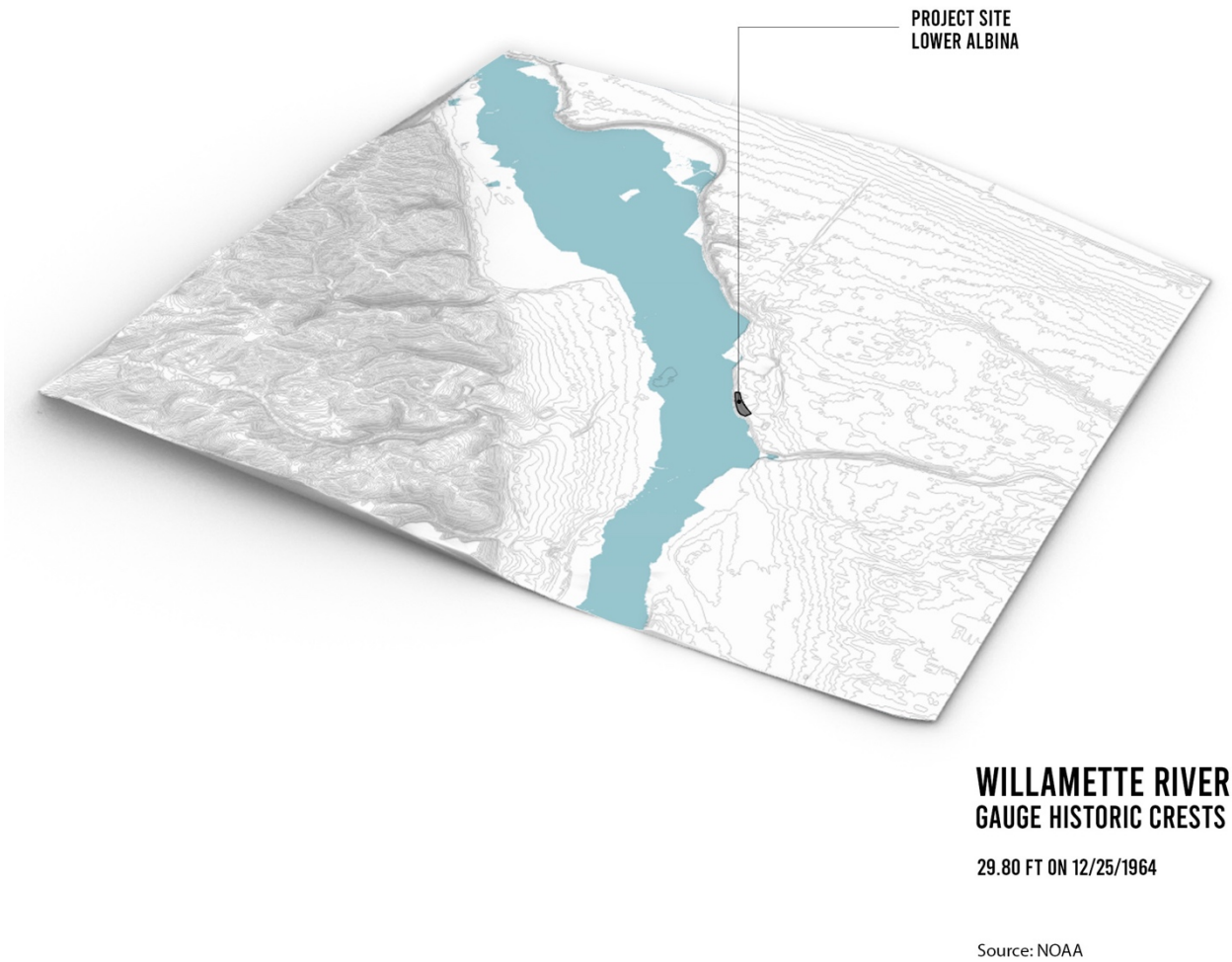


Figure 232. Willamette River gauge historic crest simulation on December 25, 1964.

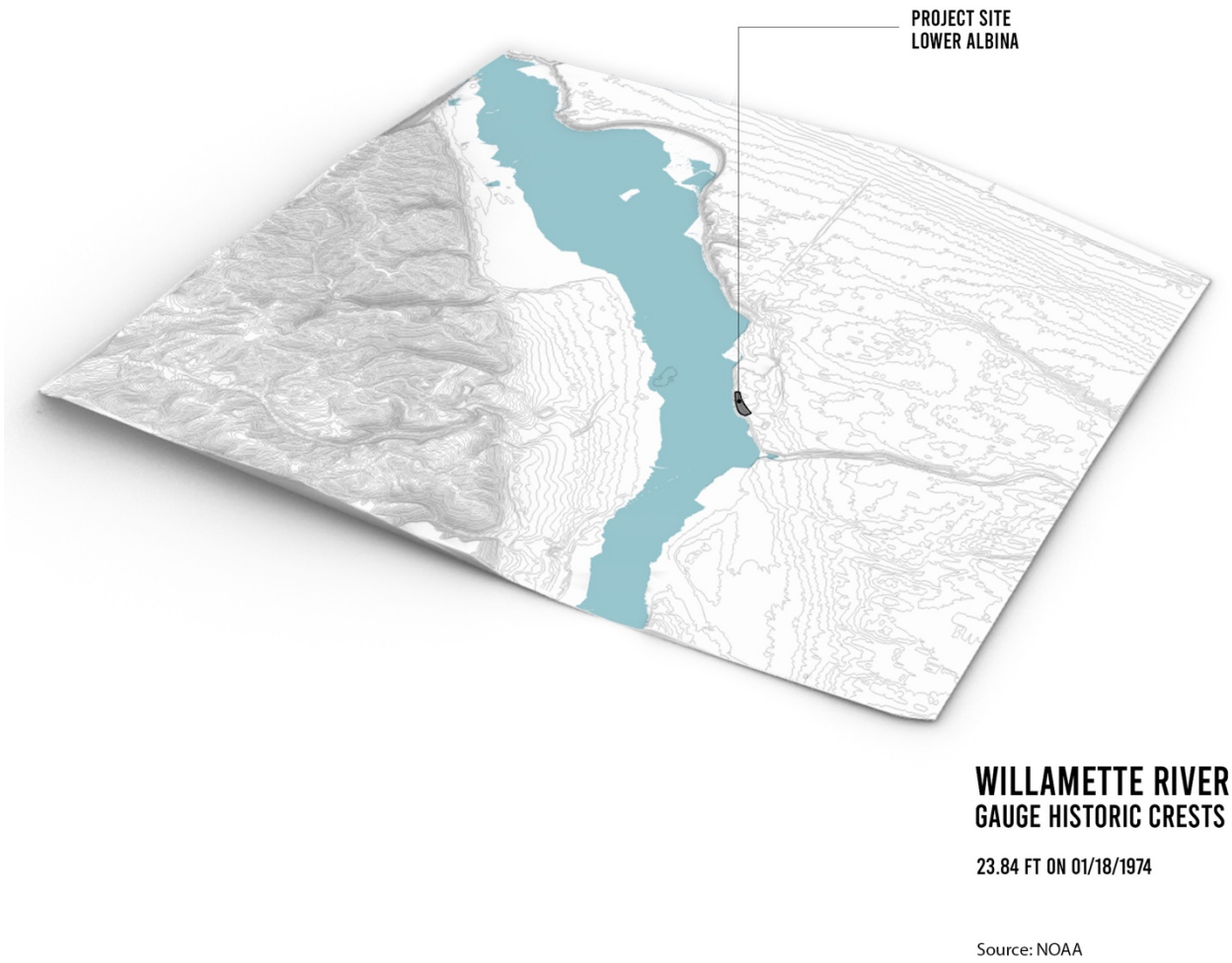


Figure 233. Willamette River gauge historic crest simulation on January 18, 1976.

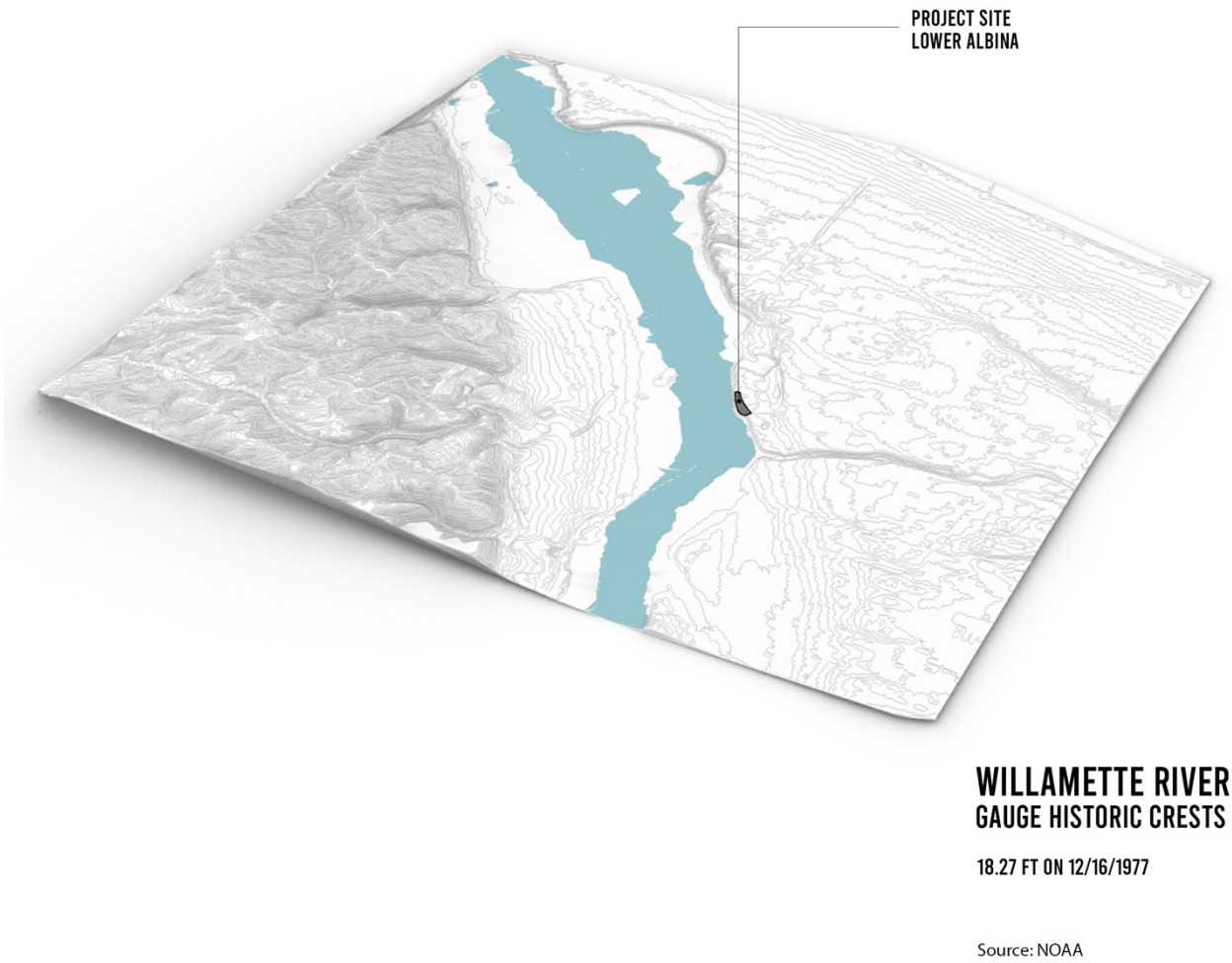


Figure 234. Willamette River gauge historic crest simulation on December 16, 1977.

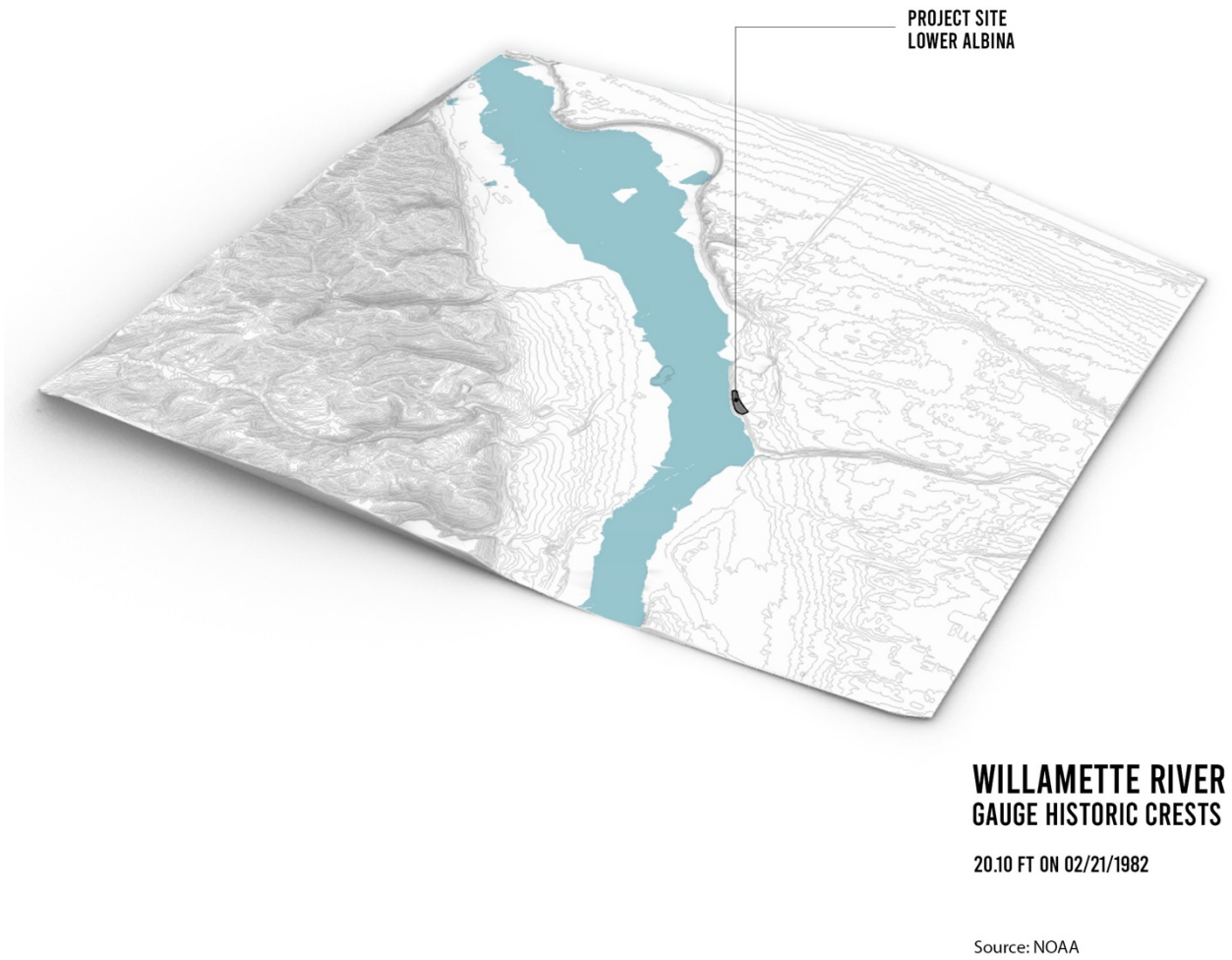


Figure 235. Willamette River gauge historic crest simulation on February 21, 1982.

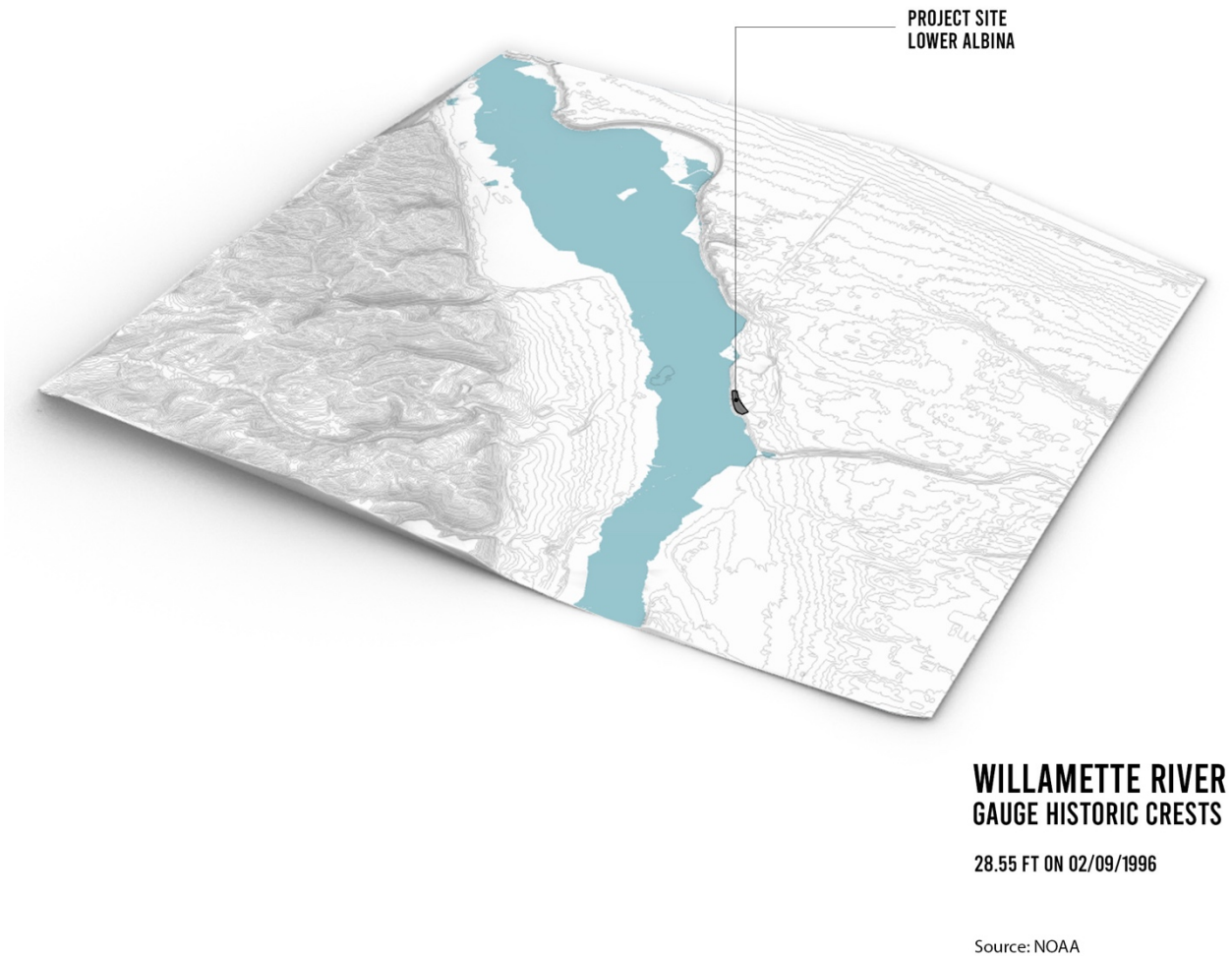


Figure 236. Willamette River gauge historic crest simulation on June 9, 1996.

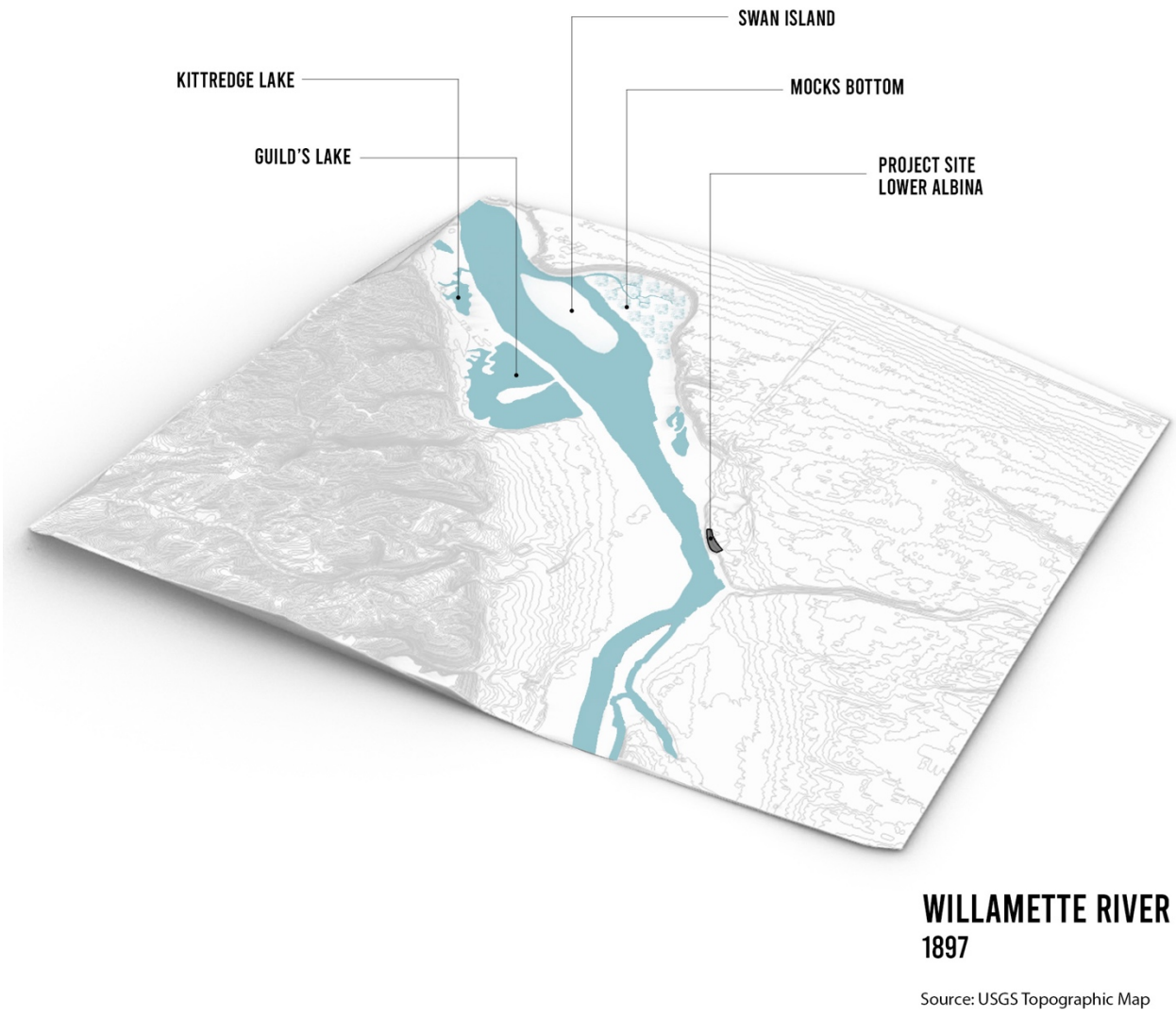


Figure 237. Simulation of the Willamette River in 1897.

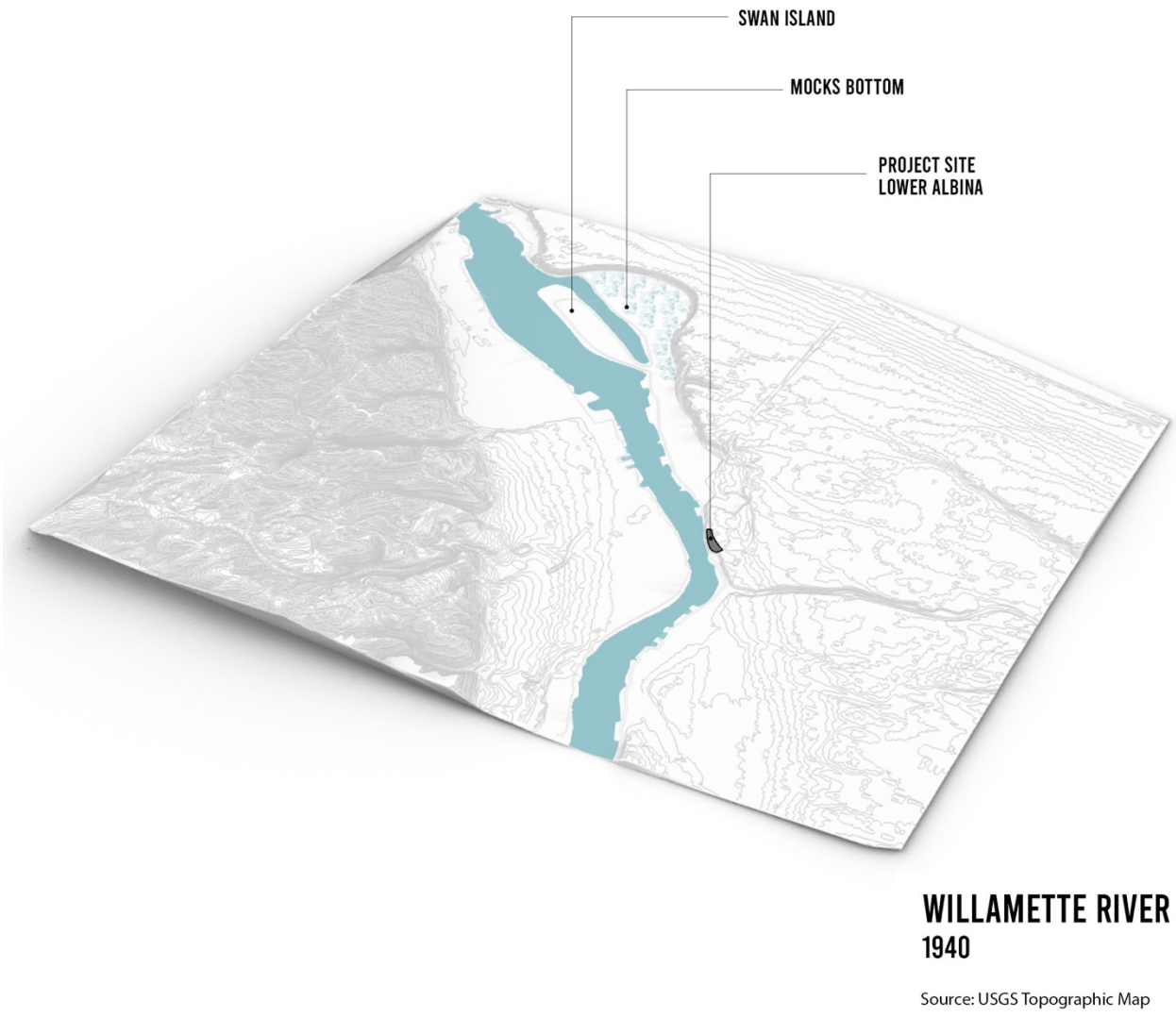


Figure 238. Simulation of the Willamette River in 1940.

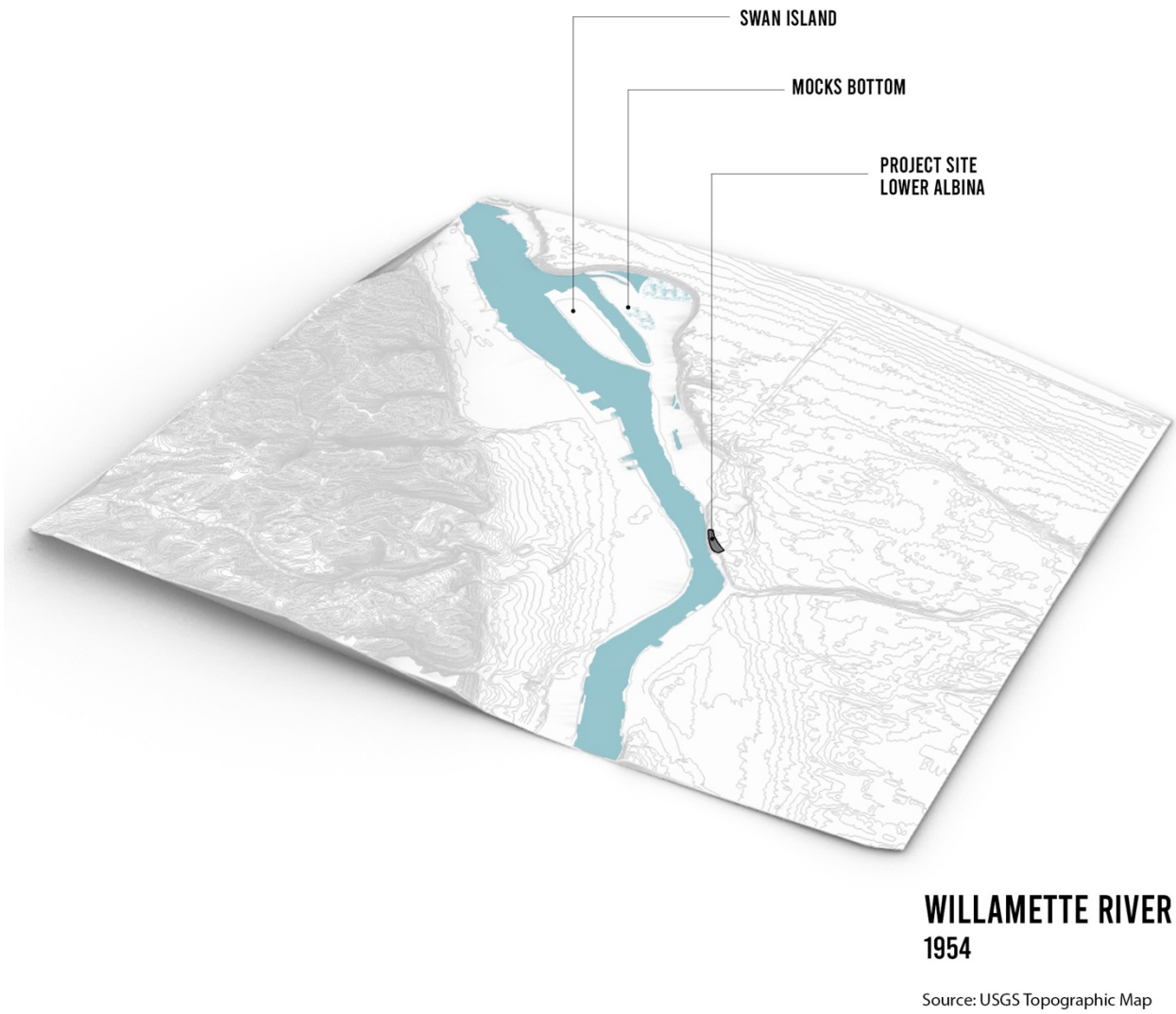


Figure 239. Simulation of the Willamette River in 1954.

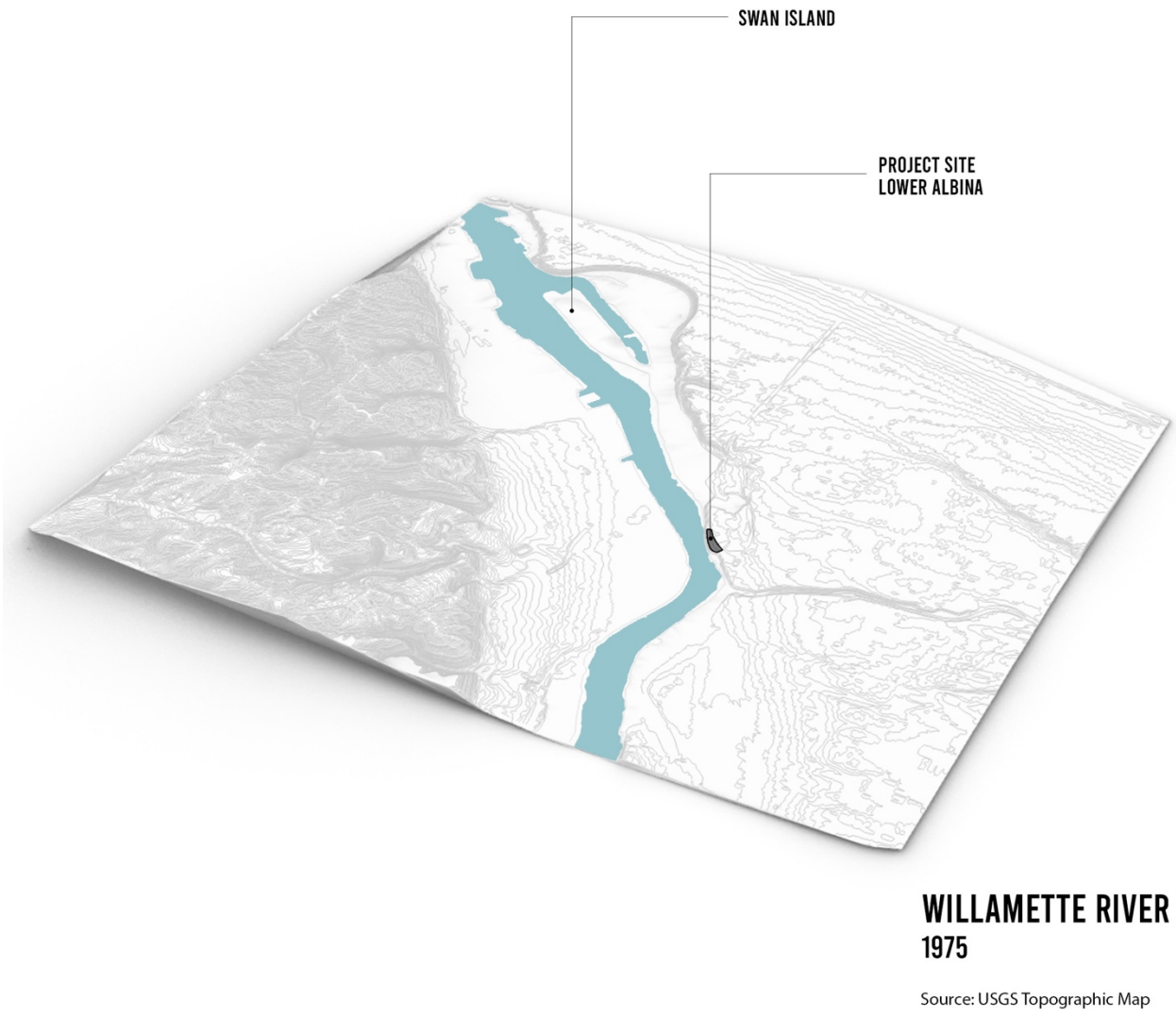


Figure 240. Simulation of the Willamette River in 1975.

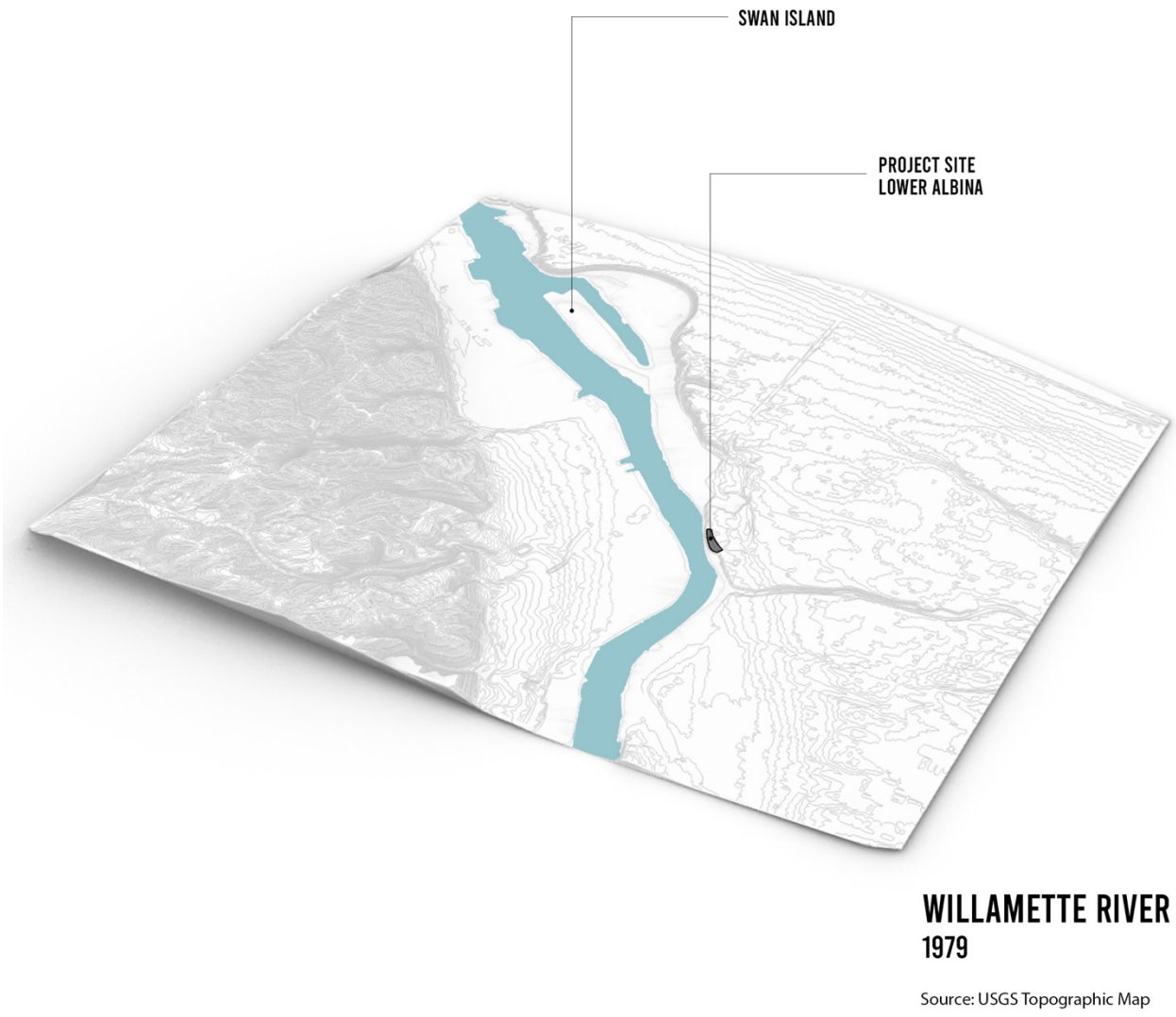


Figure 241. Simulation of the Willamette River in 1979.



Figure 242. Simulation of the Willamette River in 1990.

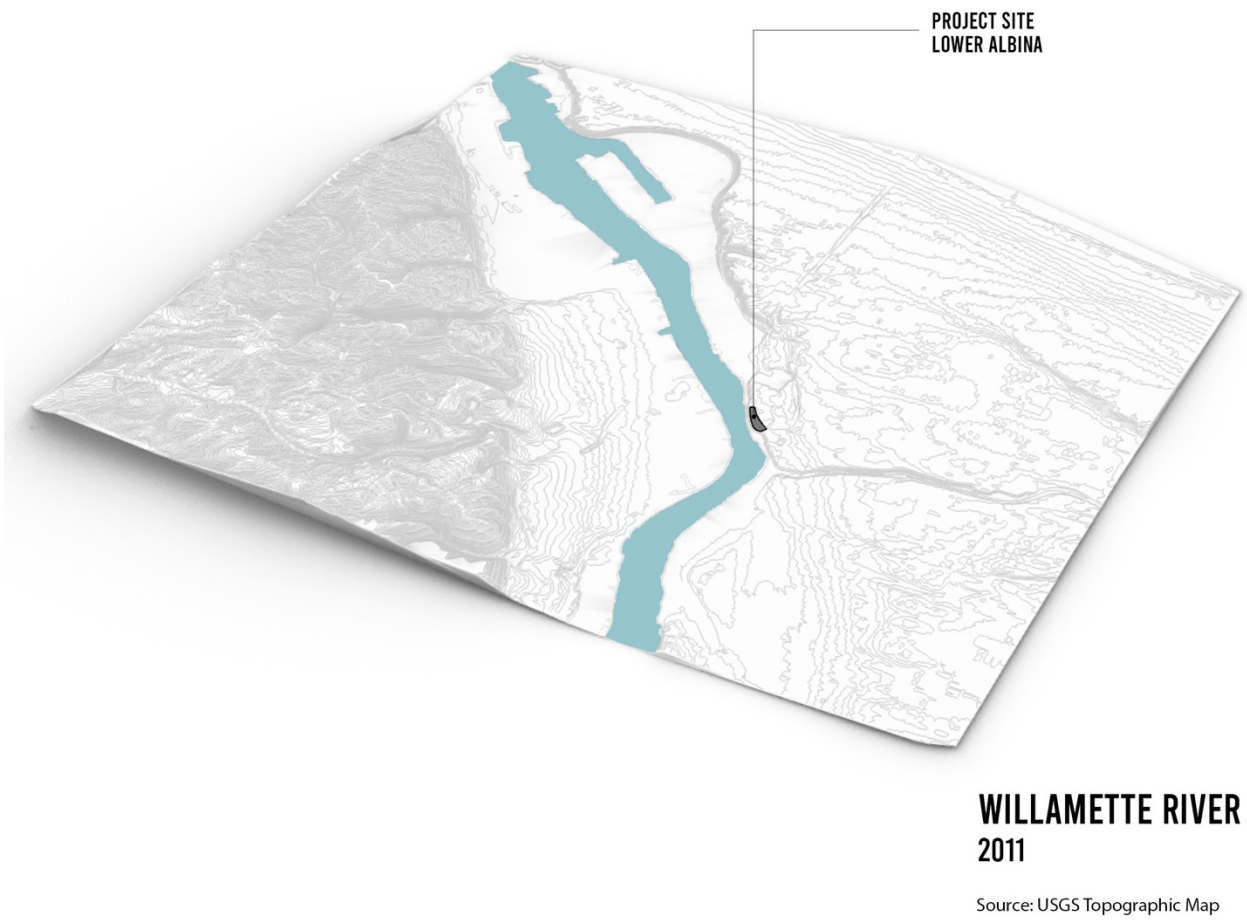


Figure 243. Simulation of the Willamette River in 2011.

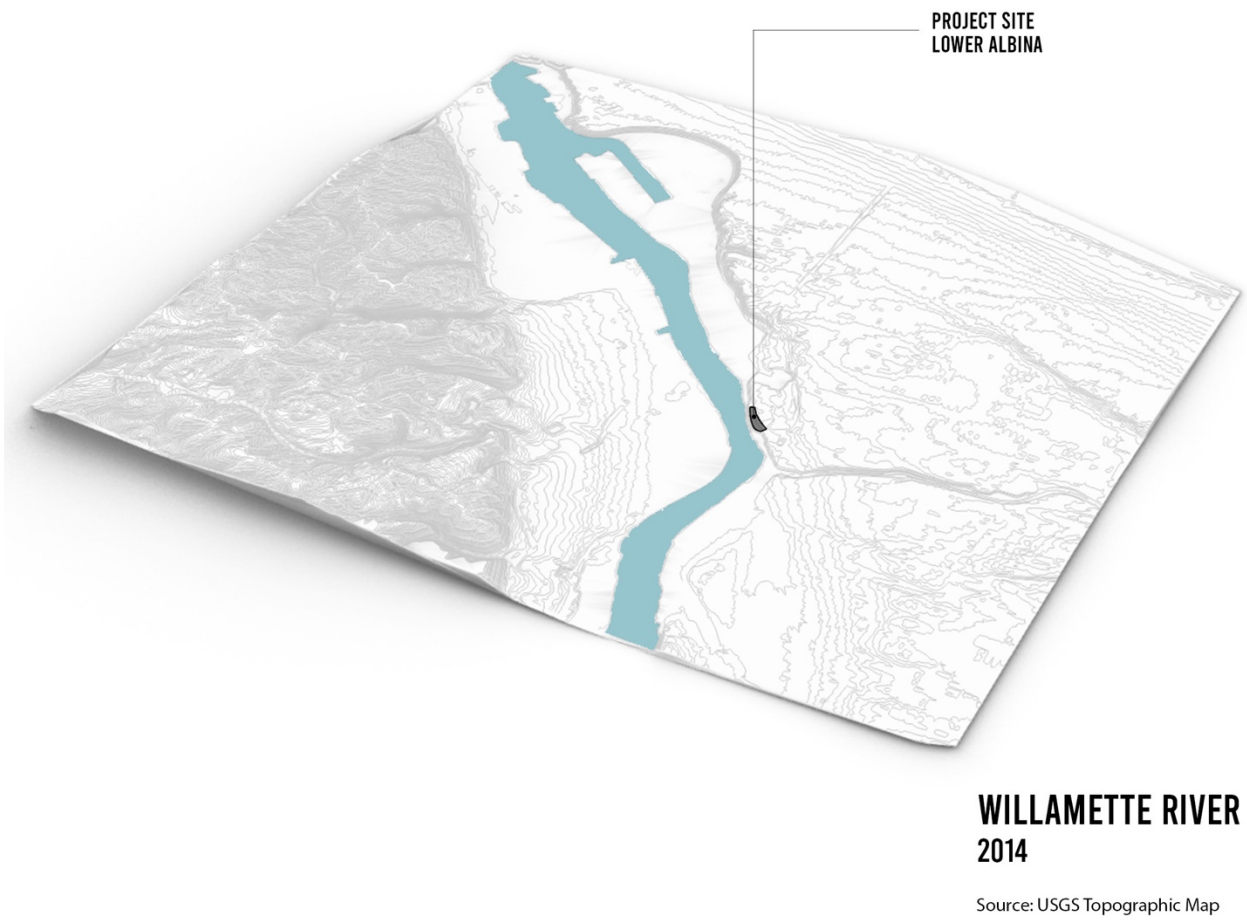


Figure 244. Simulation of the Willamette River in 2014.

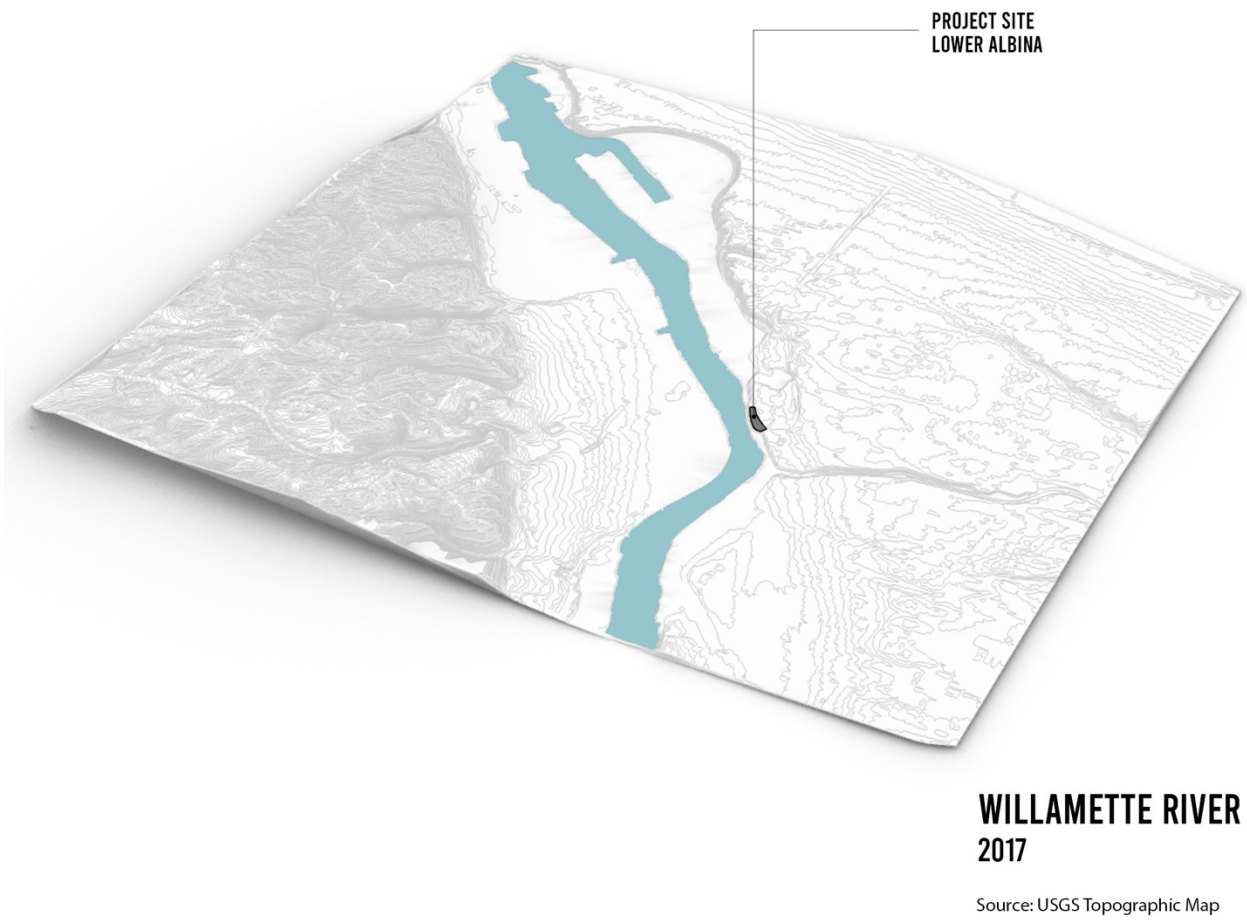


Figure 245. Simulation of the Willamette River in 2017.

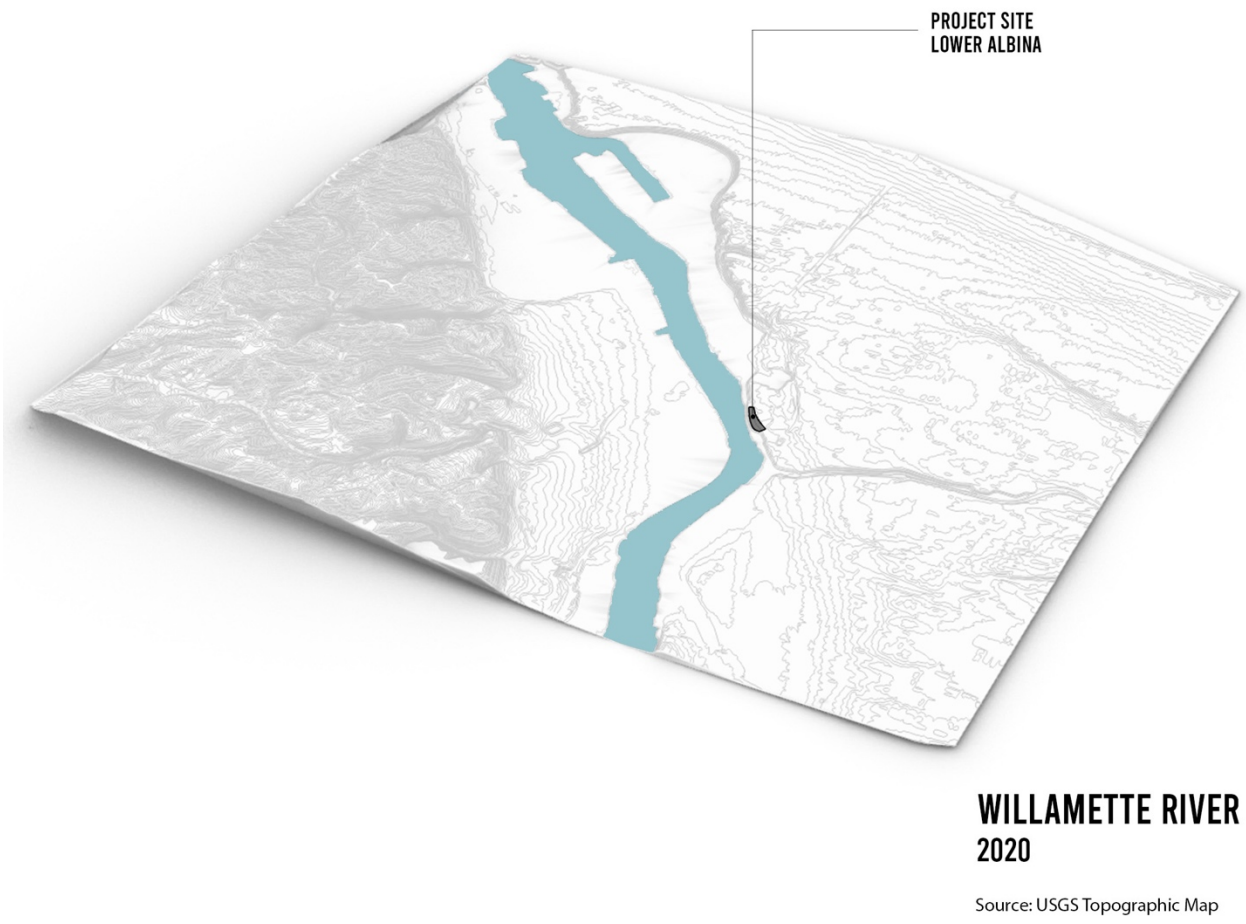


Figure 246. Simulation of the Willamette River in 2020.

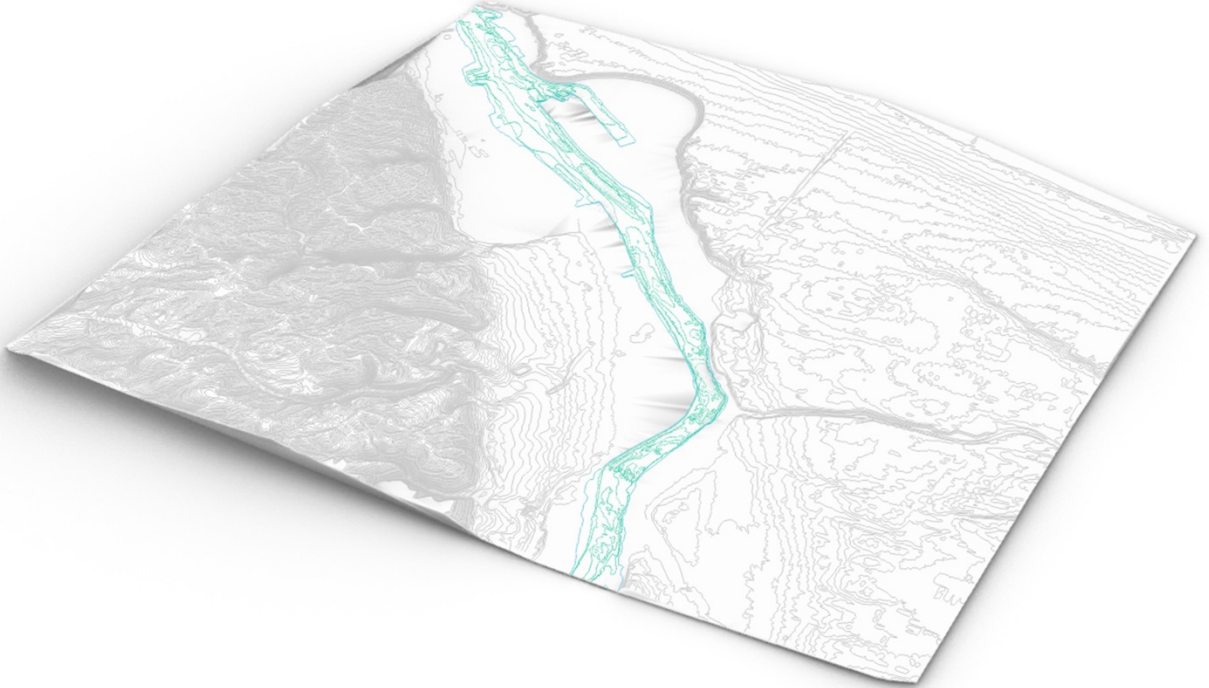


**WILLAMETTE RIVER
BATHYMETRY**

1888

Source: GIS

Figure 247. Willamette River bathymetry in 1888.



**WILLAMETTE RIVER
BATHYMETRY**

2005

Source: GIS

Figure 248. Willamette River bathymetry in 2005.



PROJECT SITE
LOWER ALBINA

VEGETATION
1951

Source: Google Earth
Oregon Statewide Aerial Imagery
Portland Maps Advanced

Figure 249. Portland vegetation simulation in 1951.



PROJECT SITE
LOWER ALBINA

VEGETATION
1970

Source: Google Earth
Oregon Statewide Aerial Imagery
Portland Maps Advanced

Figure 250. Portland vegetation simulation in 1970.



PROJECT SITE
LOWER ALBINA

VEGETATION
1975

Source: Google Earth
Oregon Statewide Aerial Imagery
Portland Maps Advanced

Figure 251. Portland vegetation simulation in 1975.



PROJECT SITE
LOWER ALBINA

VEGETATION
1990

Source: Google Earth
Oregon Statewide Aerial Imagery
Portland Maps Advanced

Figure 252. Portland vegetation simulation in 1990.



PROJECT SITE
LOWER ALBINA

VEGETATION
1994

Source: Google Earth
Oregon Statewide Aerial Imagery
Portland Maps Advanced

Figure 253. Portland vegetation simulation in 1994.



PROJECT SITE
LOWER ALBINA

**VEGETATION
2000**

Source: Google Earth
Oregon Statewide Aerial Imagery
Portland Maps Advanced

Figure 254. Portland vegetation simulation in 2000.



PROJECT SITE
LOWER ALBINA

**VEGETATION
2011**

Source: Google Earth
Oregon Statewide Aerial Imagery
Portland Maps Advanced

Figure 255. Portland vegetation simulation in 2011.



PROJECT SITE
LOWER ALBINA

VEGETATION 2014

Source: Google Earth
Oregon Statewide Aerial Imagery
Portland Maps Advanced

Figure 256. Portland vegetation simulation in 2014.



PROJECT SITE
LOWER ALBINA

**VEGETATION
2017**

Source: Google Earth
Oregon Statewide Aerial Imagery
Portland Maps Advanced

Figure 257. Portland vegetation simulation in 2017.

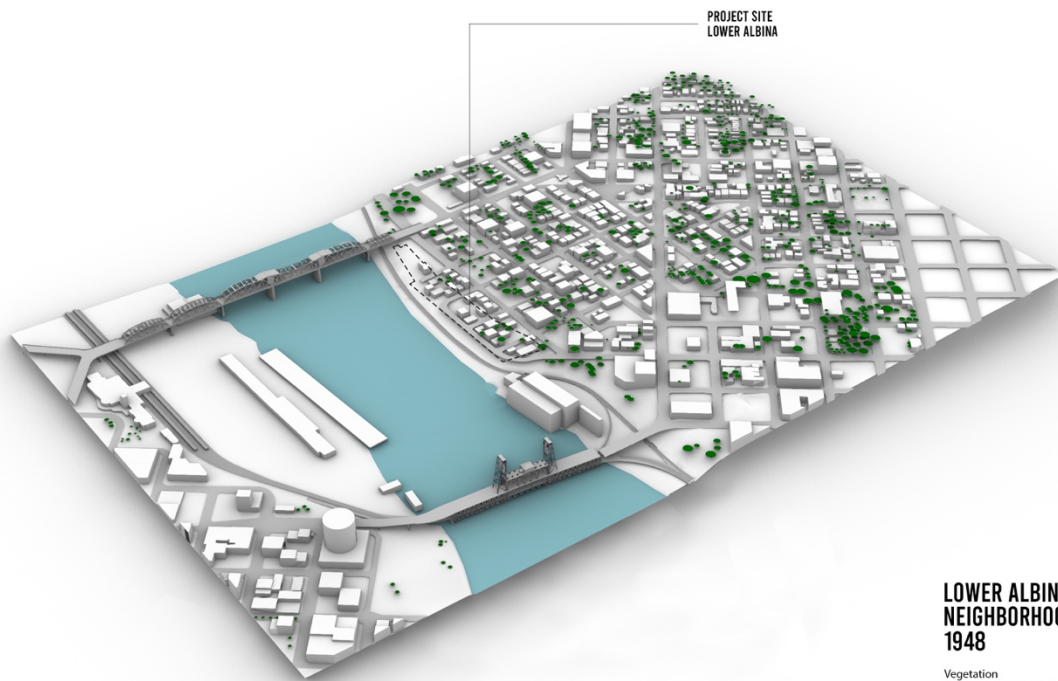


PROJECT SITE
LOWER ALBINA

VEGETATION 2020

Source: Google Earth
Oregon Statewide Aerial Imagery
Portland Maps Advanced

Figure 258. Portland vegetation simulation in 2020.



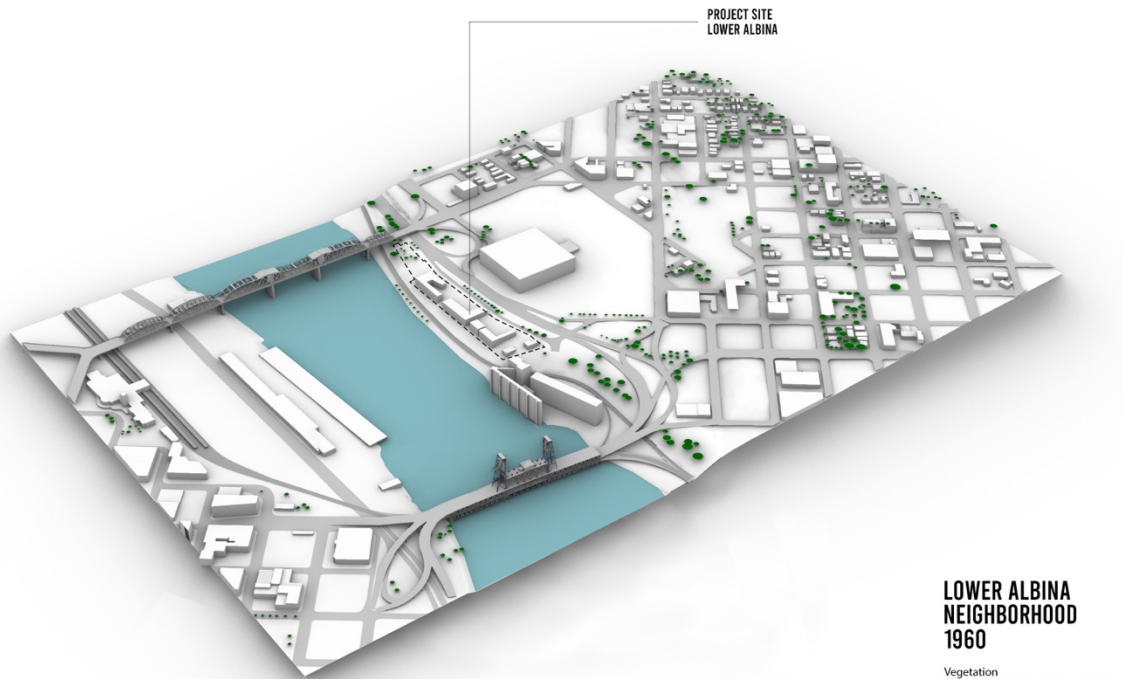
**LOWER ALBINA
NEIGHBORHOOD
1948**

Vegetation
Willamette river west side - 7 033 sq.f.
Willamette river east side - 361 282 sq.f.

Buildings footprint
Willamette river west side - 658 928 sq.f.
Willamette river east side - 1 587 572 sq.f.

Source: Google Earth
Oregon Statewide Aerial Imagery
Portland Maps Advanced

Figure 259. Lower Albina neighborhood simulation in 1948.



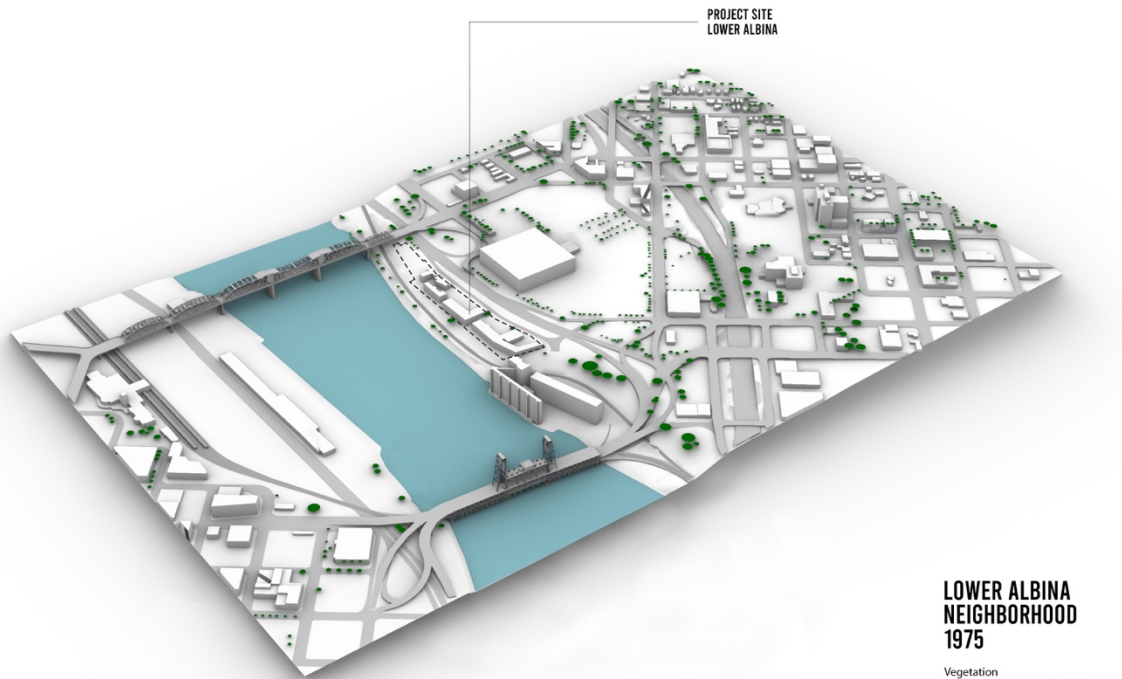
**LOWER ALBINA
NEIGHBORHOOD
1960**

Vegetation
Willamette river west side - 8 606 sq.f.
Willamette river east side - 193 279 sq.f.

Buildings footprint
Willamette river west side - 479 948 sq.f.
Willamette river east side - 1 034 532 sq.f.

Source: Google Earth
Oregon Statewide Aerial Imagery
Portland Maps Advanced

Figure 260. Lower Albina neighborhood simulation in 1960.



PROJECT SITE
LOWER ALBINA

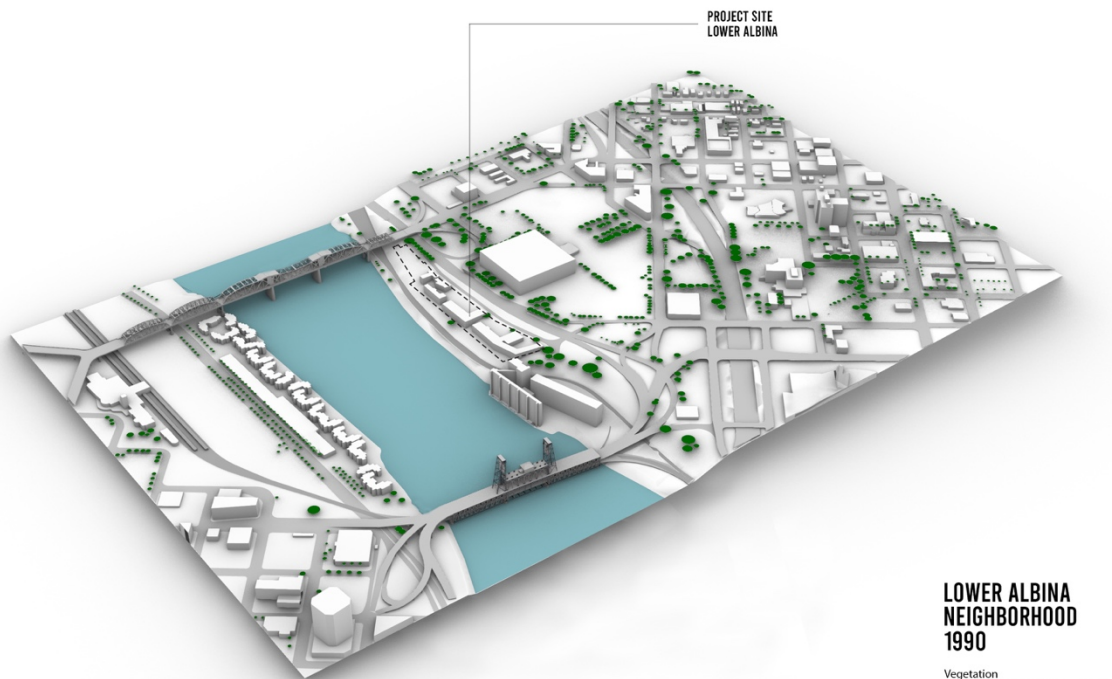
LOWER ALBINA NEIGHBORHOOD 1975

Vegetation
Willamette river west side - 21 567 sq.f.
Willamette river east side - 264 865 sq.f.

Buildings footprint
Willamette river west side - 398 552 sq.f.
Willamette river east side - 1 062 268 sq.f.

Source: Google Earth
Oregon Statewide Aerial Imagery
Portland Maps Advanced

Figure 261. Lower Albina neighborhood simulation in 1975.



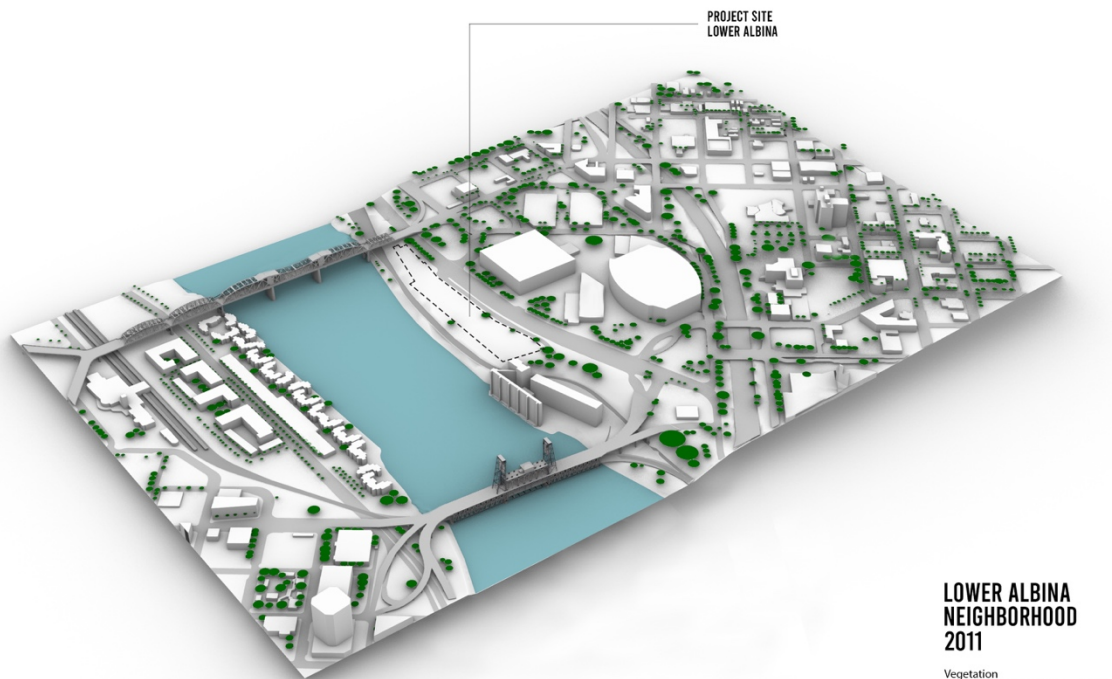
**LOWER ALBINA
NEIGHBORHOOD
1990**

Vegetation
Willamette river west side - 44 894 sq.f.
Willamette river east side - 434 746 sq.f.

Buildings footprint
Willamette river west side - 377 144 sq.f.
Willamette river east side - 1 110 470 sq.f.

Source: Google Earth
Oregon Statewide Aerial Imagery
Portland Maps Advanced

Figure 262. Lower Albina neighborhood simulation in 1990.



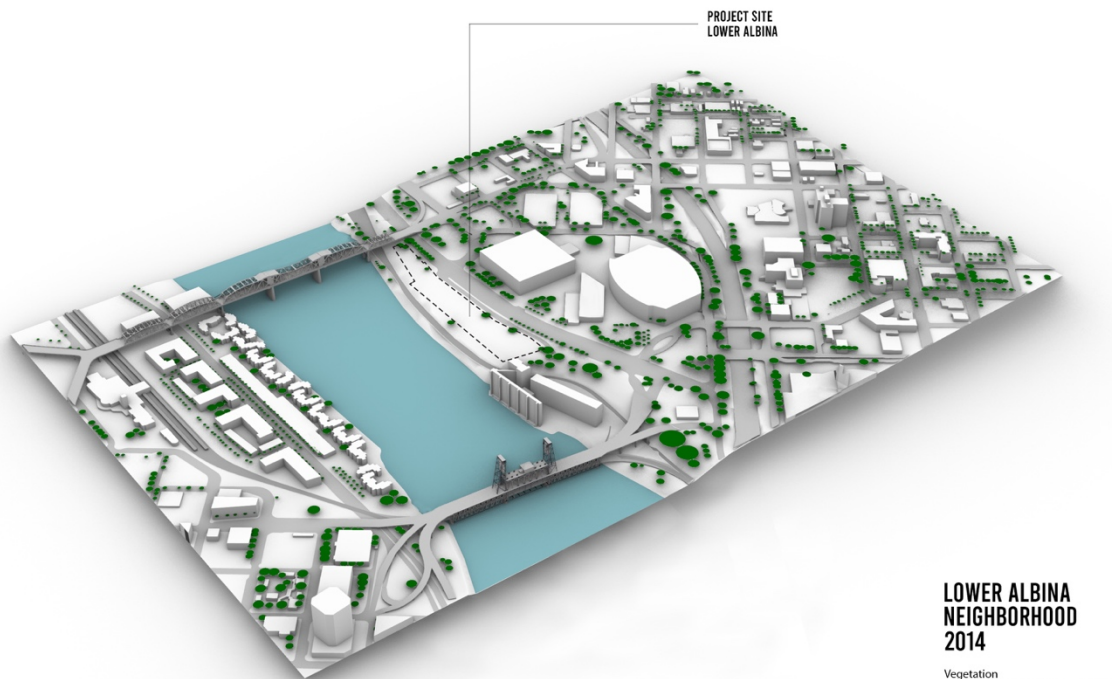
**LOWER ALBINA
NEIGHBORHOOD
2011**

Vegetation
Willamette river west side - 153 787 sq.f.
Willamette river east side - 658 684 sq.f.

Buildings footprint
Willamette river west side - 548 096 sq.f.
Willamette river east side - 1 481 062 sq.f.

Source: Google Earth
Oregon Statewide Aerial Imagery
Portland Maps Advanced

Figure 263. Lower Albina neighborhood simulation in 2011.



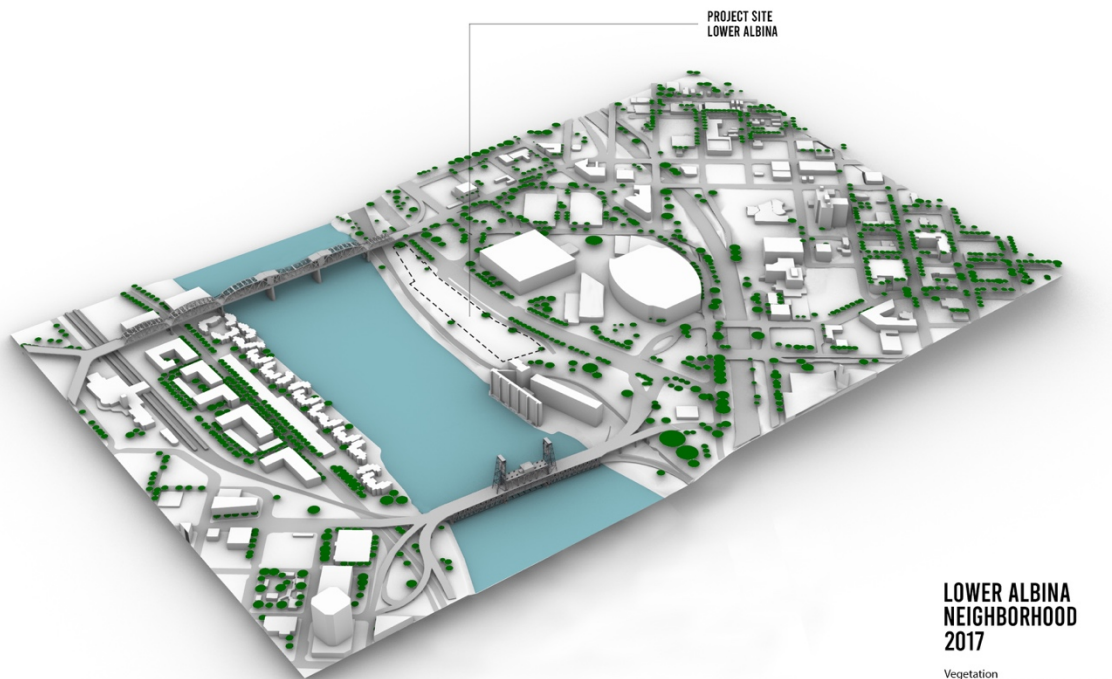
**LOWER ALBINA
NEIGHBORHOOD
2014**

Vegetation
Willamette river west side - 153 787 sq.f.
Willamette river east side - 676 752 sq.f.

Buildings footprint
Willamette river west side - 594 064 sq.f.
Willamette river east side - 1 483 062 sq.f.

Source: Google Earth
Oregon Statewide Aerial Imagery
Portland Maps Advanced

Figure 264. Lower Albina neighborhood simulation in 2014.



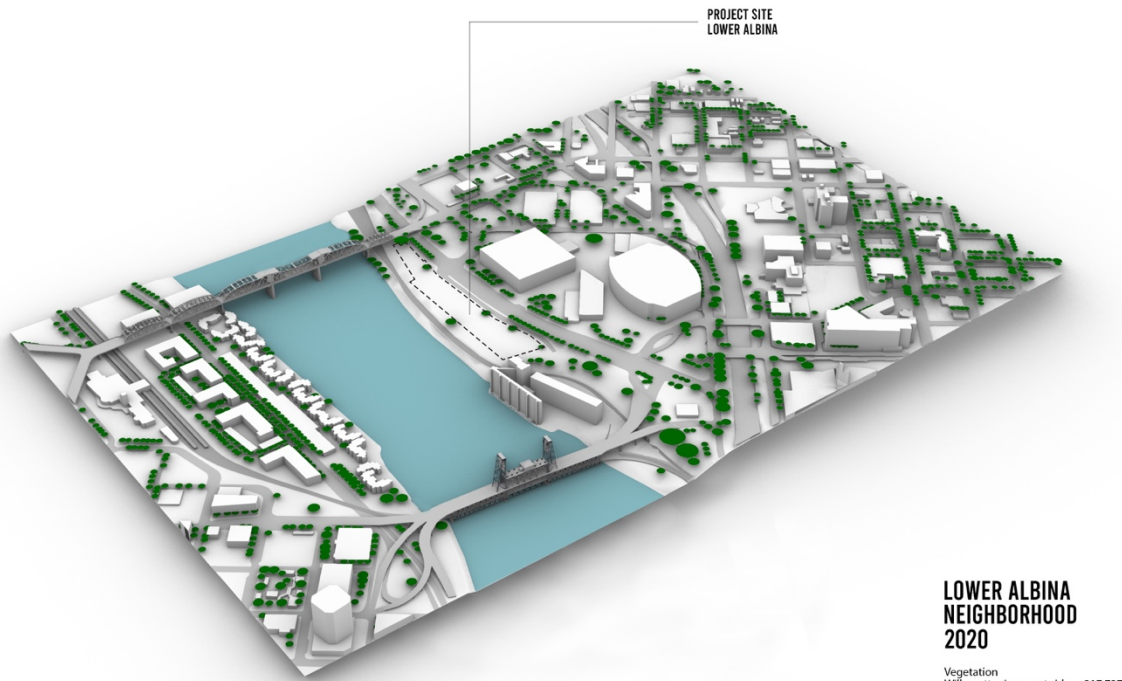
**LOWER ALBINA
NEIGHBORHOOD
2017**

Vegetation
Willamette river west side - 294 745 sq.f.
Willamette river east side - 790 962 sq.f.

Buildings footprint
Willamette river west side - 570 390 sq.f.
Willamette river east side - 1 512 121 sq.f.

Source: Google Earth
Oregon Statewide Aerial Imagery
Portland Maps Advanced

Figure 265. Lower Albina neighborhood simulation in 2017.



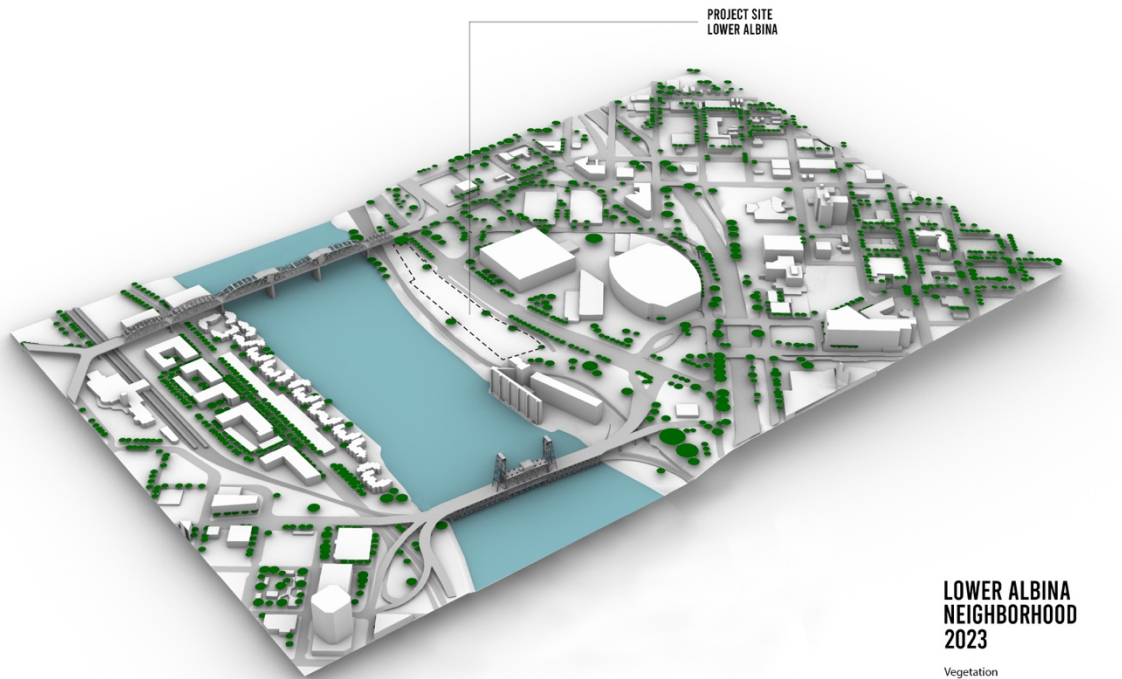
**LOWER ALBINA
NEIGHBORHOOD
2020**

Vegetation
Willamette river west side - 317 737 sq.f.
Willamette river east side - 843 106 sq.f.

Buildings footprint
Willamette river west side - 607 827 sq.f.
Willamette river east side - 1 512 121 sq.f.

Source: Google Earth
Oregon Statewide Aerial Imagery
Portland Maps Advanced

Figure 266. Lower Albina neighborhood simulation in 2020.



**LOWER ALBINA
NEIGHBORHOOD
2023**

Vegetation
Willamette river west side - 340 729 sq.f.
Willamette river east side - 881 062 sq.f.

Buildings footprint
Willamette river west side - 607 827 sq.f.
Willamette river east side - 1 512 121 sq.f.

Source: Google Earth
Oregon Statewide Aerial Imagery
Portland Maps Advanced

Figure 267. Lower Albina neighborhood simulation in 2023.

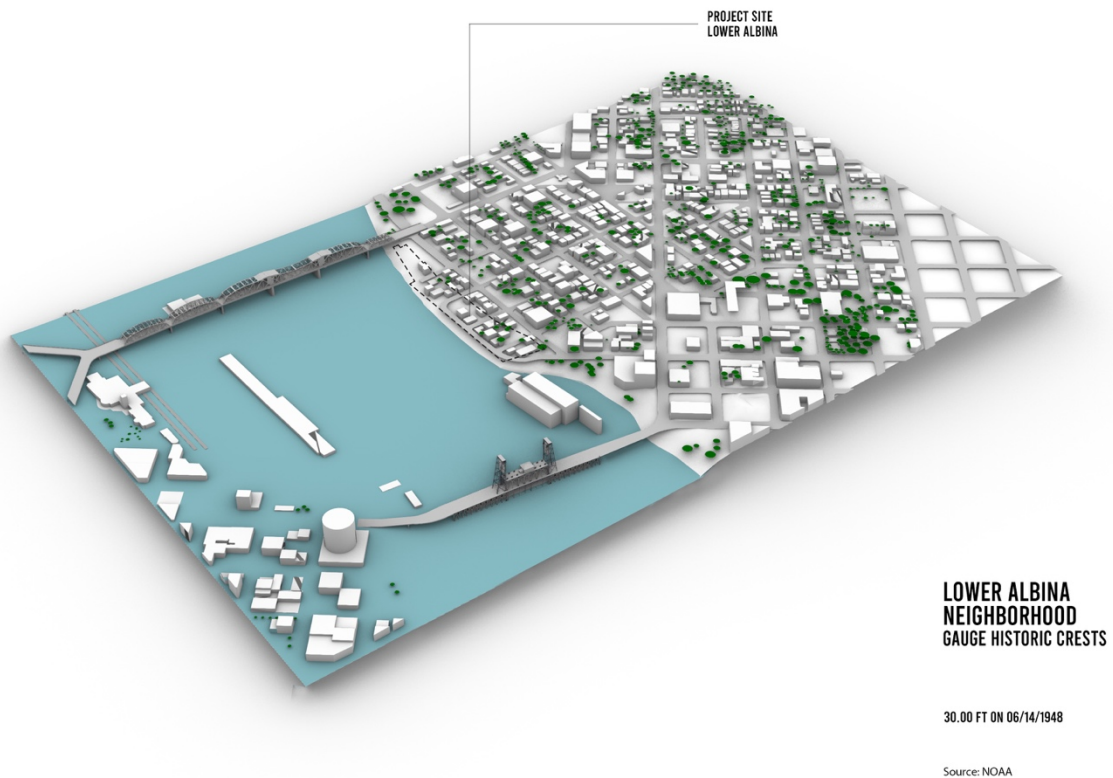


Figure 268. Lower Albina neighborhood gauge historic crest simulation on June 14, 1948.

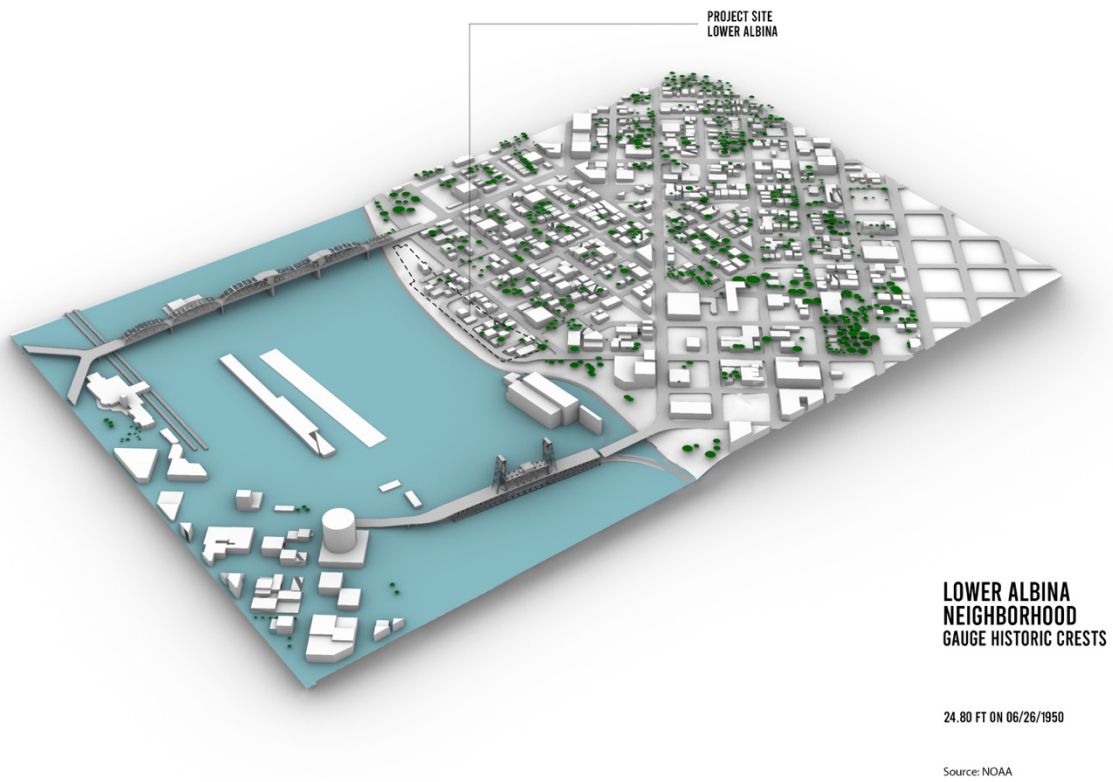


Figure 269. Lower Albina neighborhood gauge historic crest simulation on June 26, 1950.

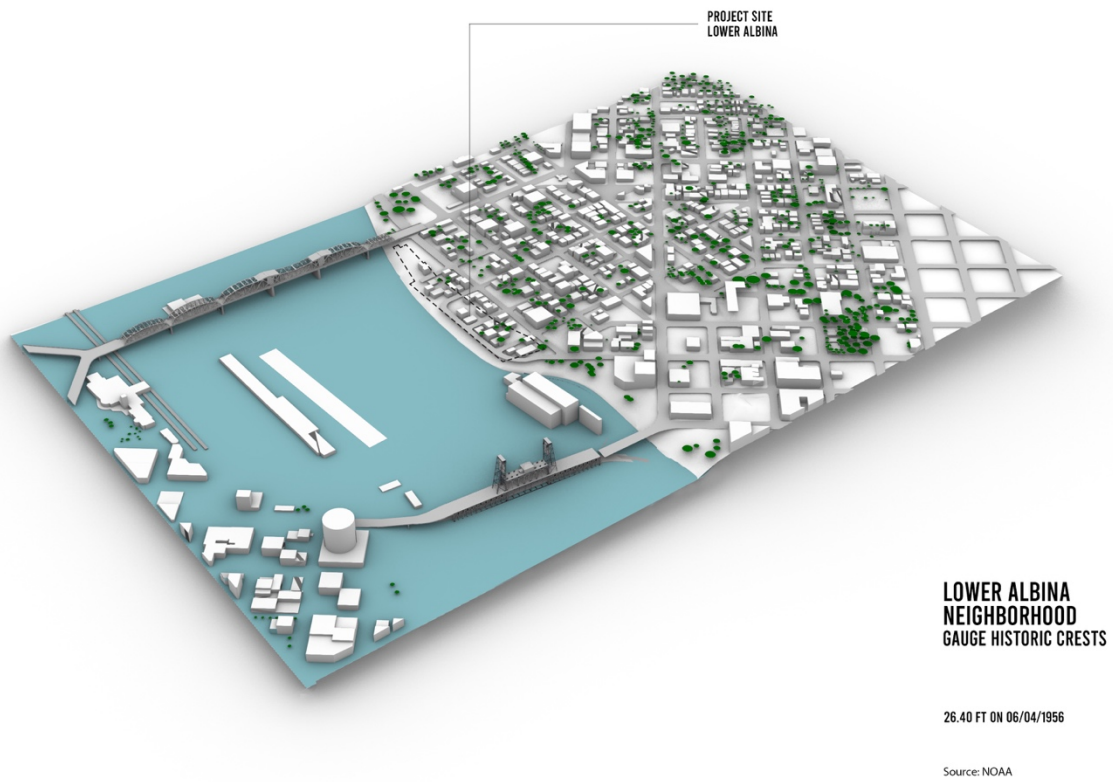


Figure 270. Lower Albina neighborhood gauge historic crest simulation on June 4, 1956.

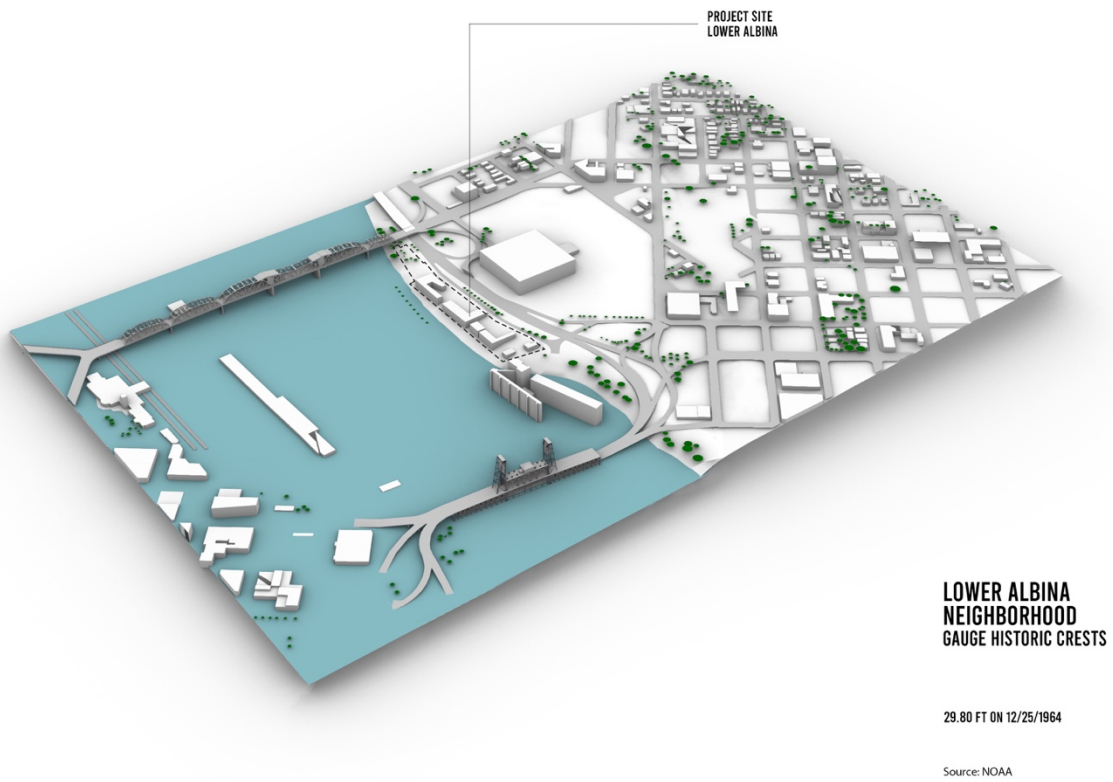


Figure 271. Lower Albina neighborhood gauge historic crest simulation on December 25, 1964.

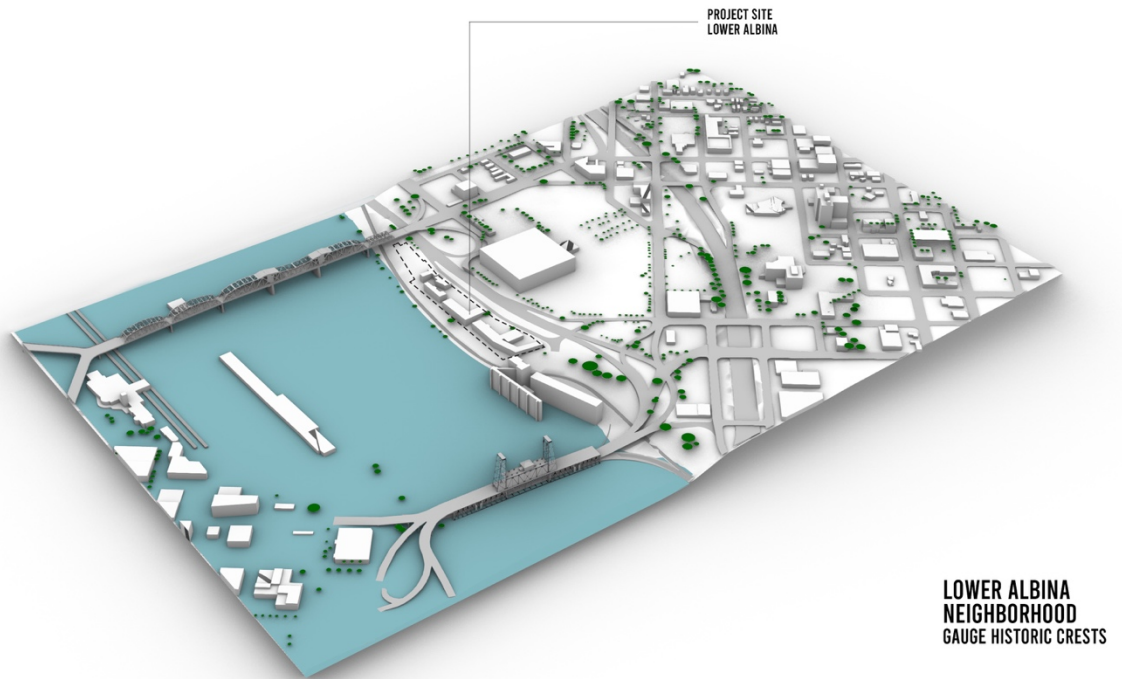


Figure 272. Lower Albina neighborhood gauge historic crest simulation on January 18, 1974.

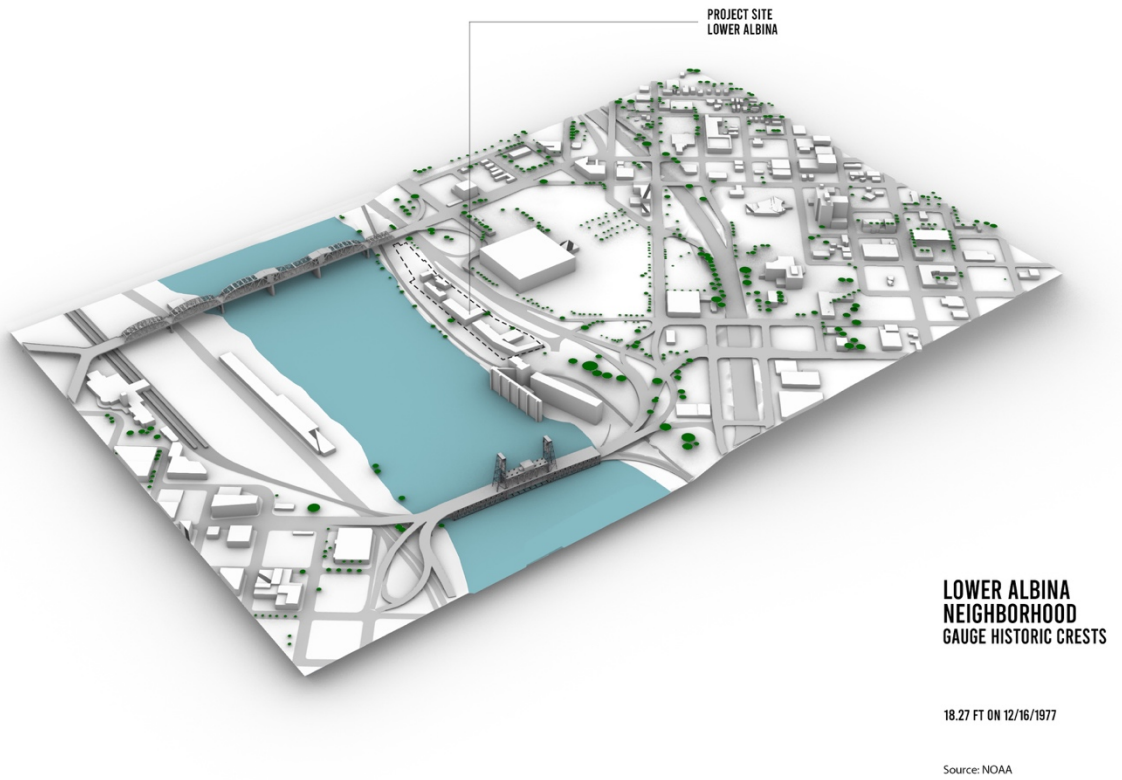


Figure 273. Lower Albina neighborhood gauge historic crest simulation on December 16, 1977.

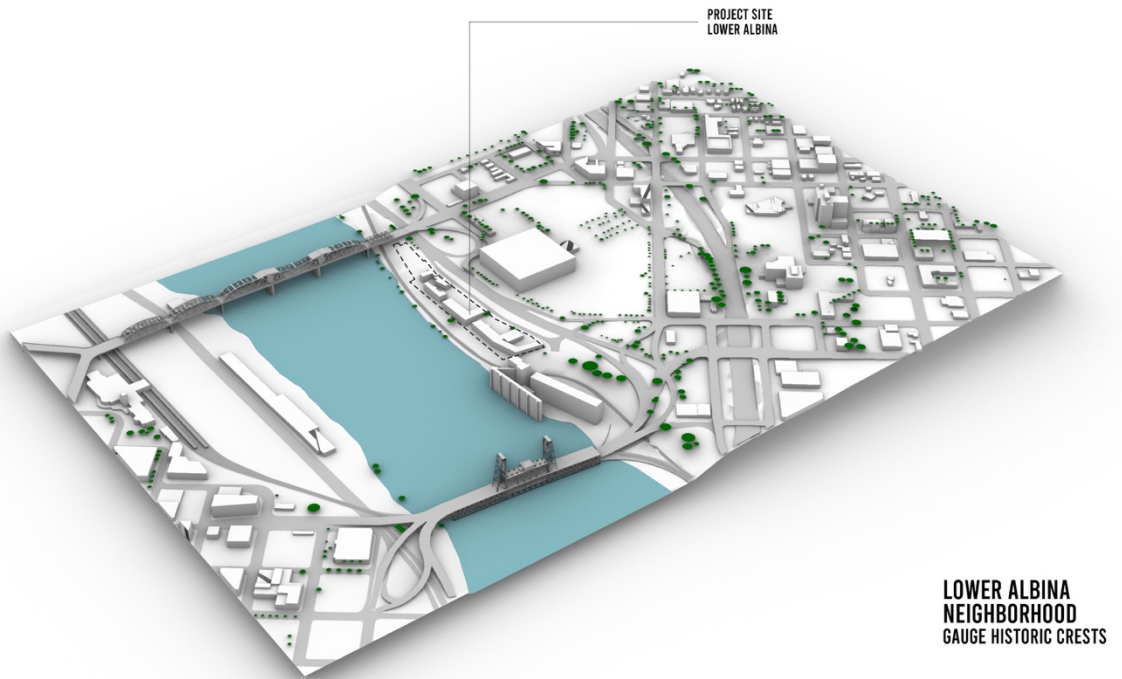


Figure 274. Lower Albina neighborhood gauge historic crest simulation on February 21, 1982.

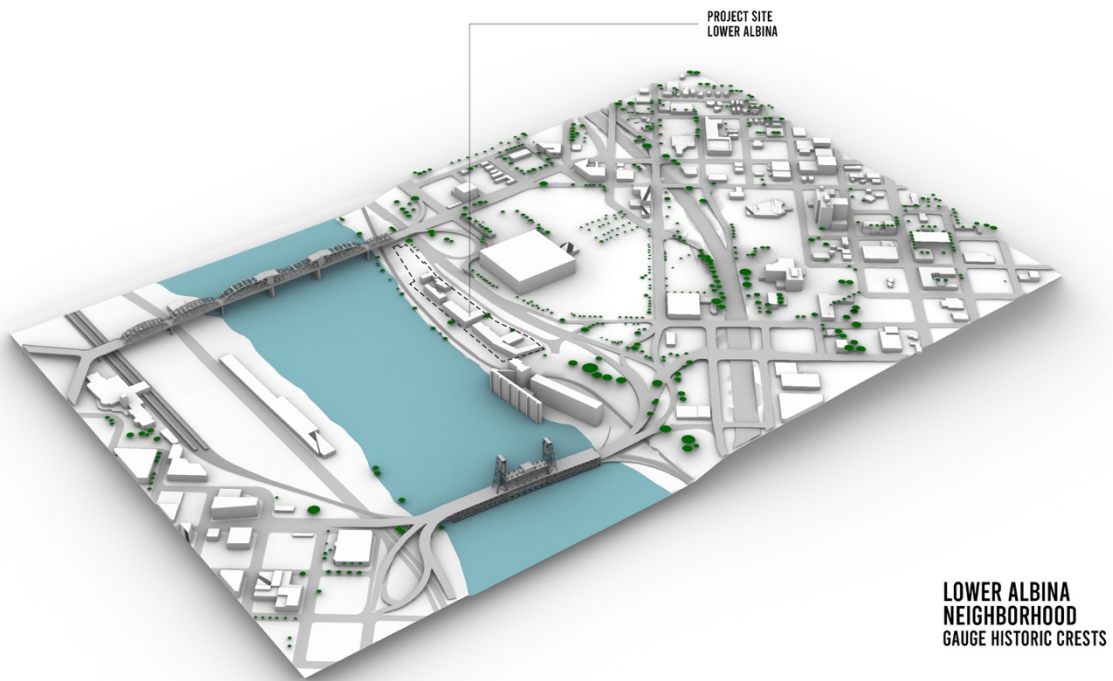


Figure 275. Lower Albina neighborhood gauge historic crest simulation on February 24, 1986.

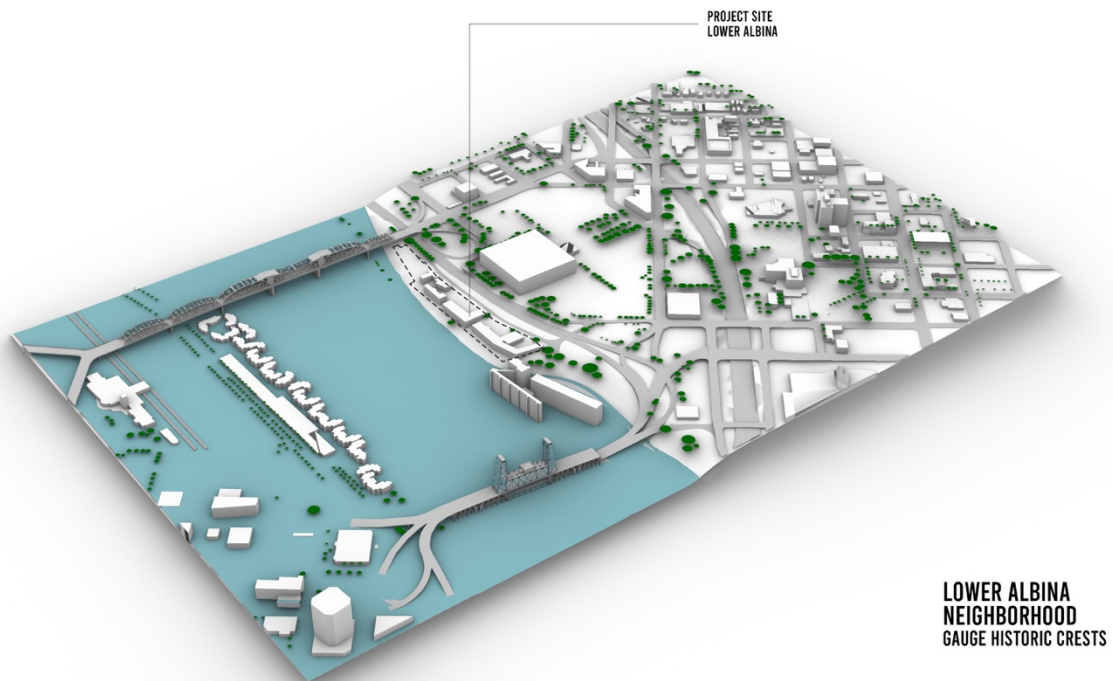


Figure 276. Lower Albina neighborhood gauge historic crest simulation on February 9, 1996.

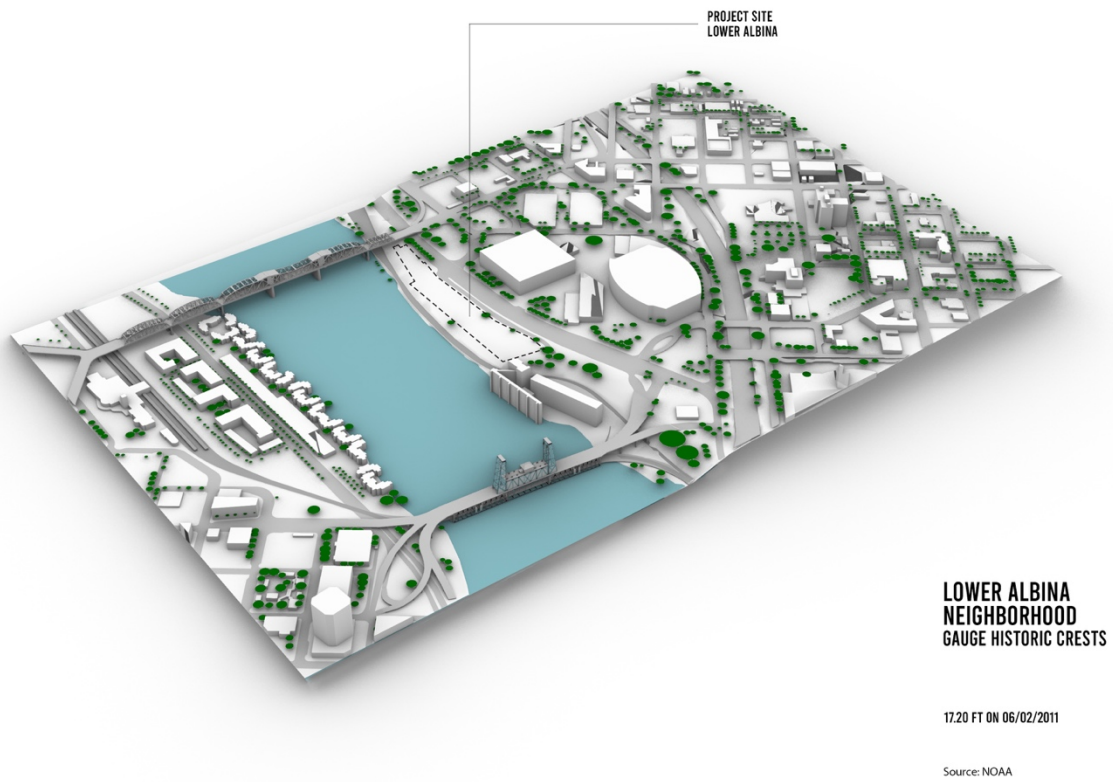


Figure 277. Lower Albina neighborhood gauge historic crest simulation on June 2, 2011.

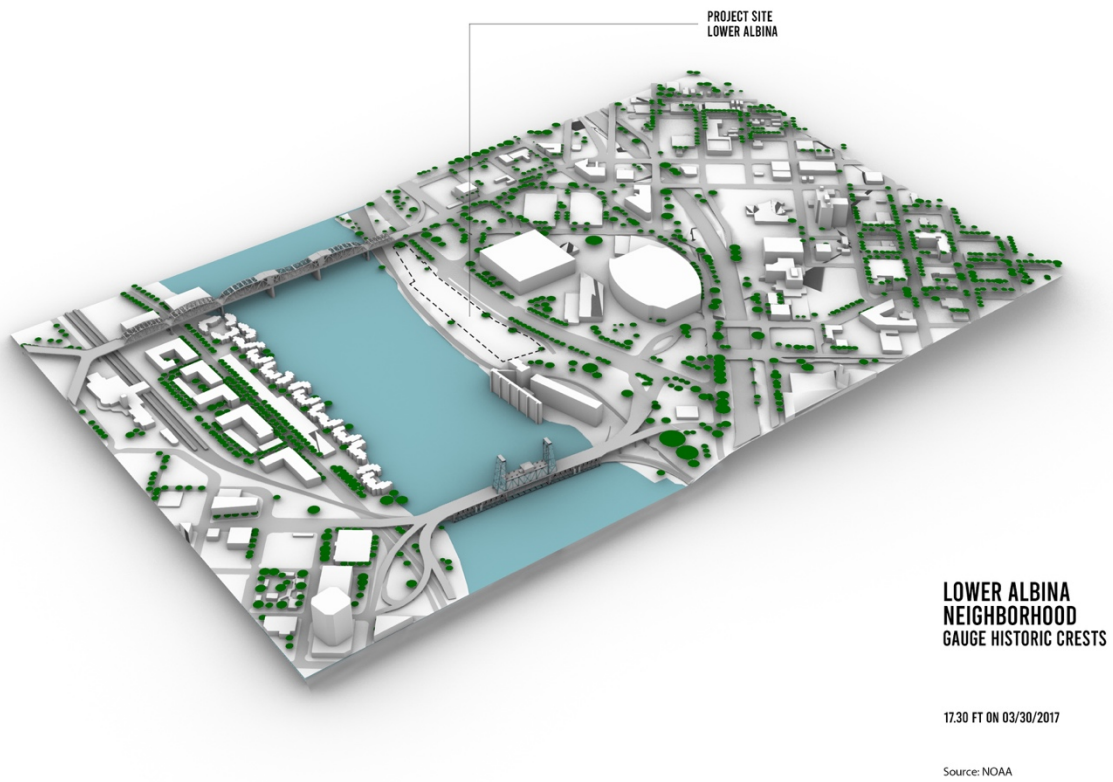


Figure 278. Lower Albina neighborhood gauge historic crest simulation on March 30, 2017.

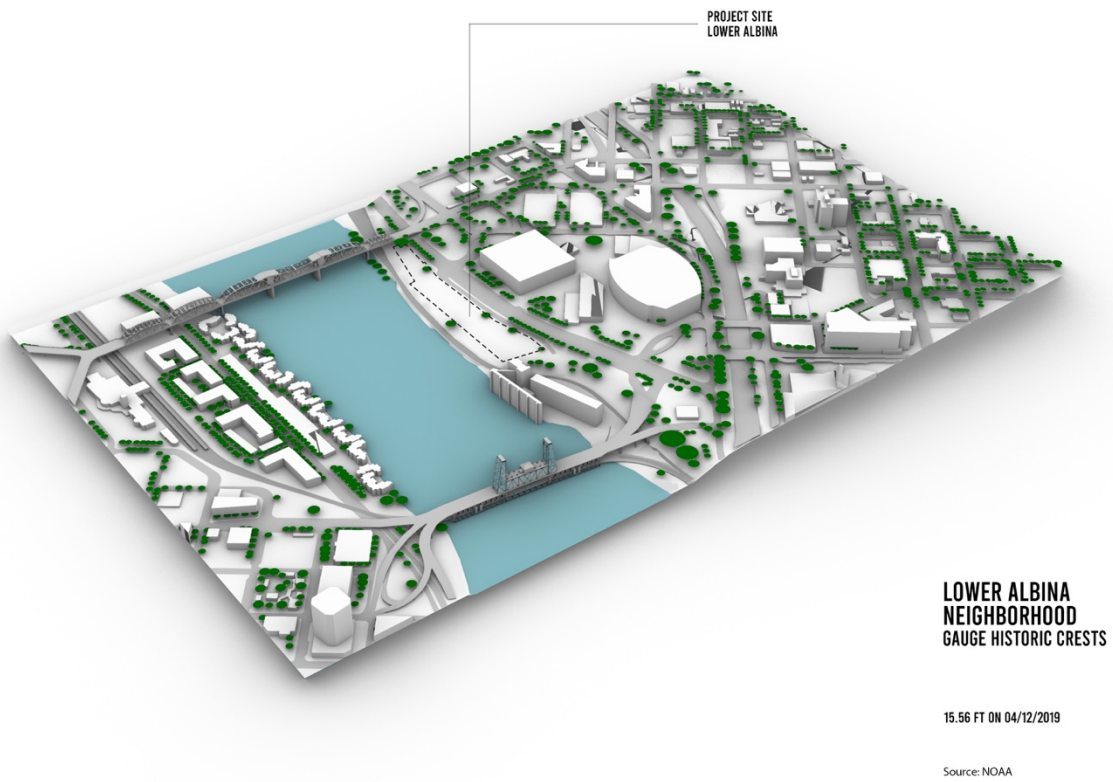


Figure 279. Lower Albina neighborhood gauge historic crest simulation on April 4, 2019.



Figure 280. Lower Albina in 1948, site scale simulation.

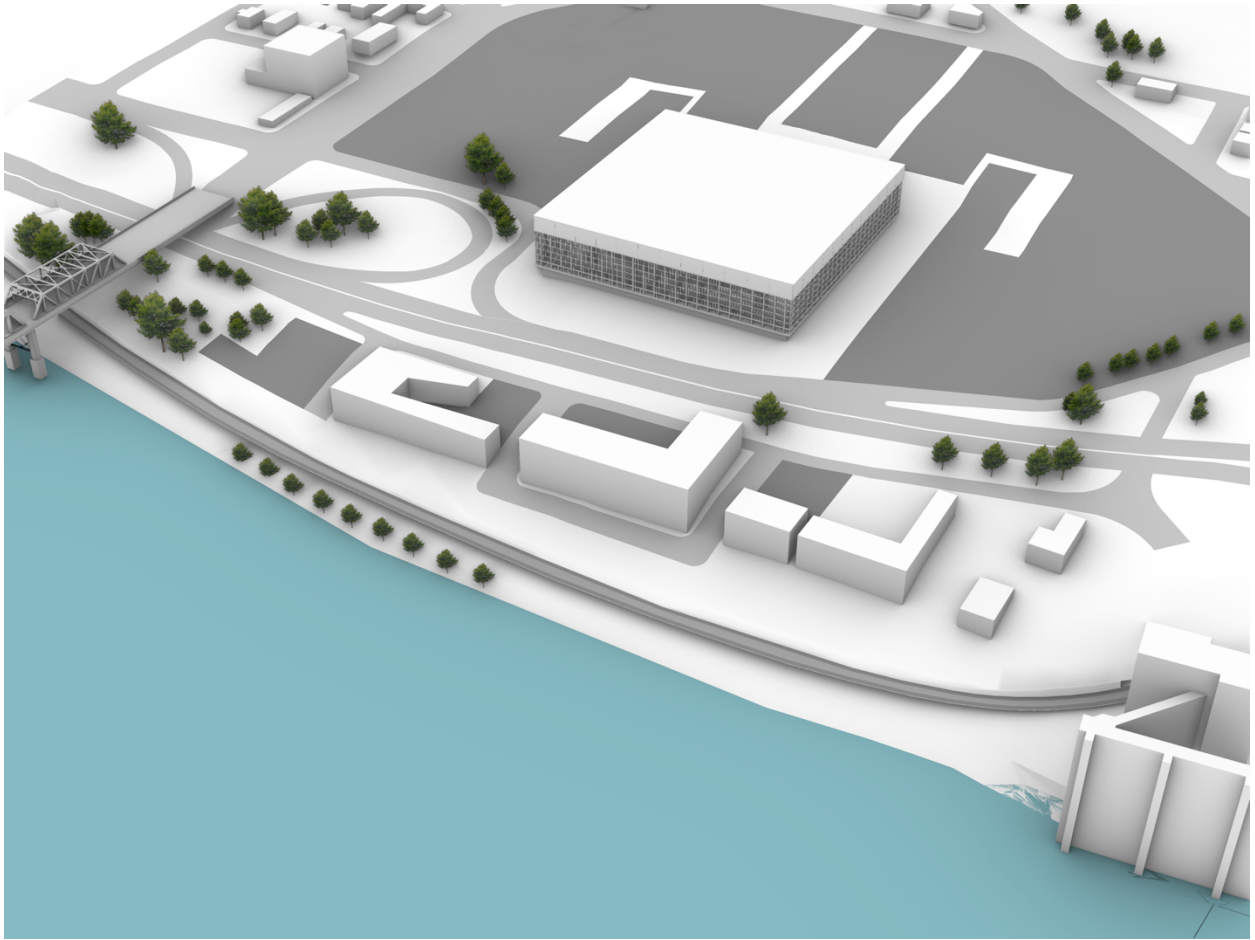


Figure 281. Lower Albina in 1960, site scale simulation.

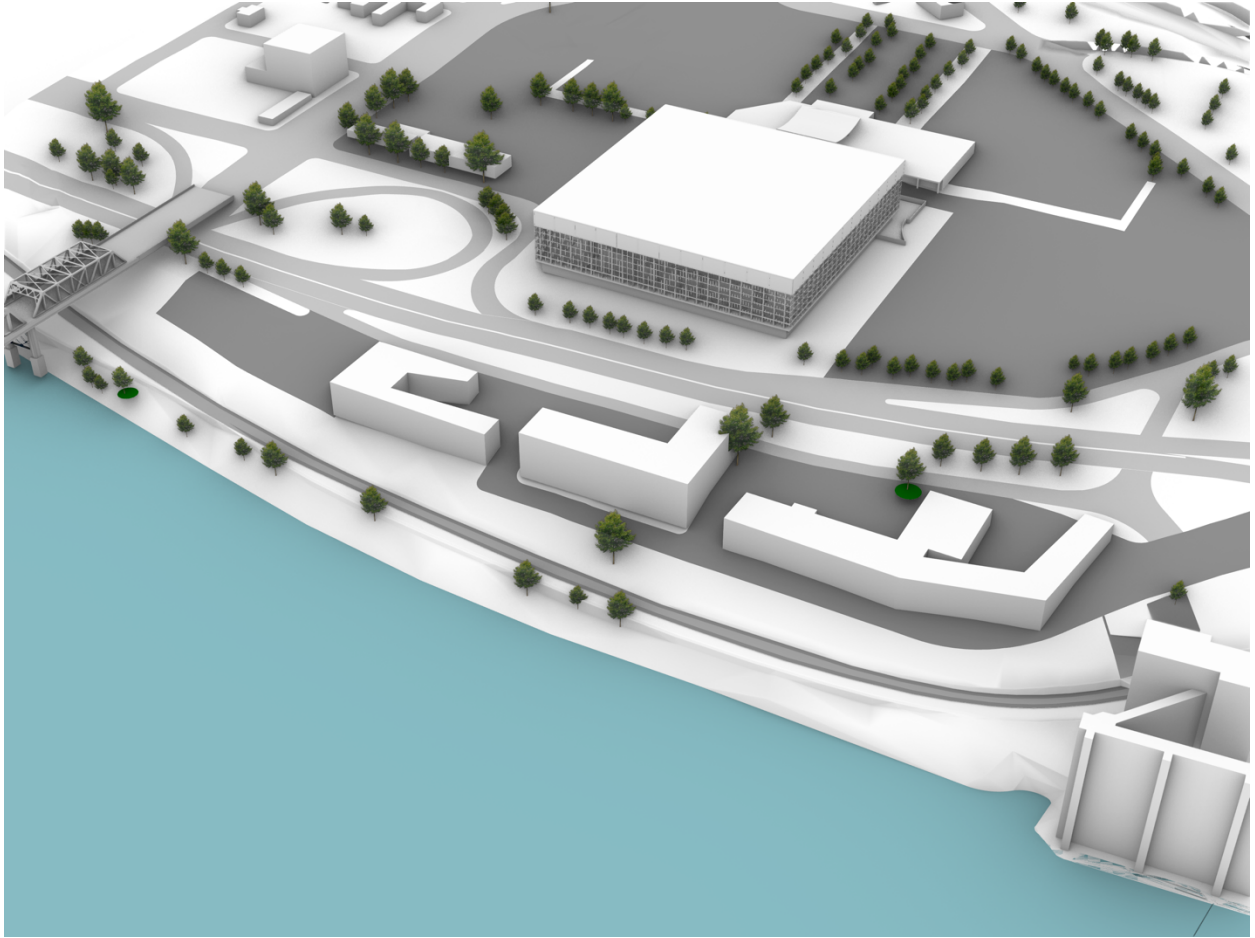


Figure 282. Lower Albina in 1975, site scale simulation.

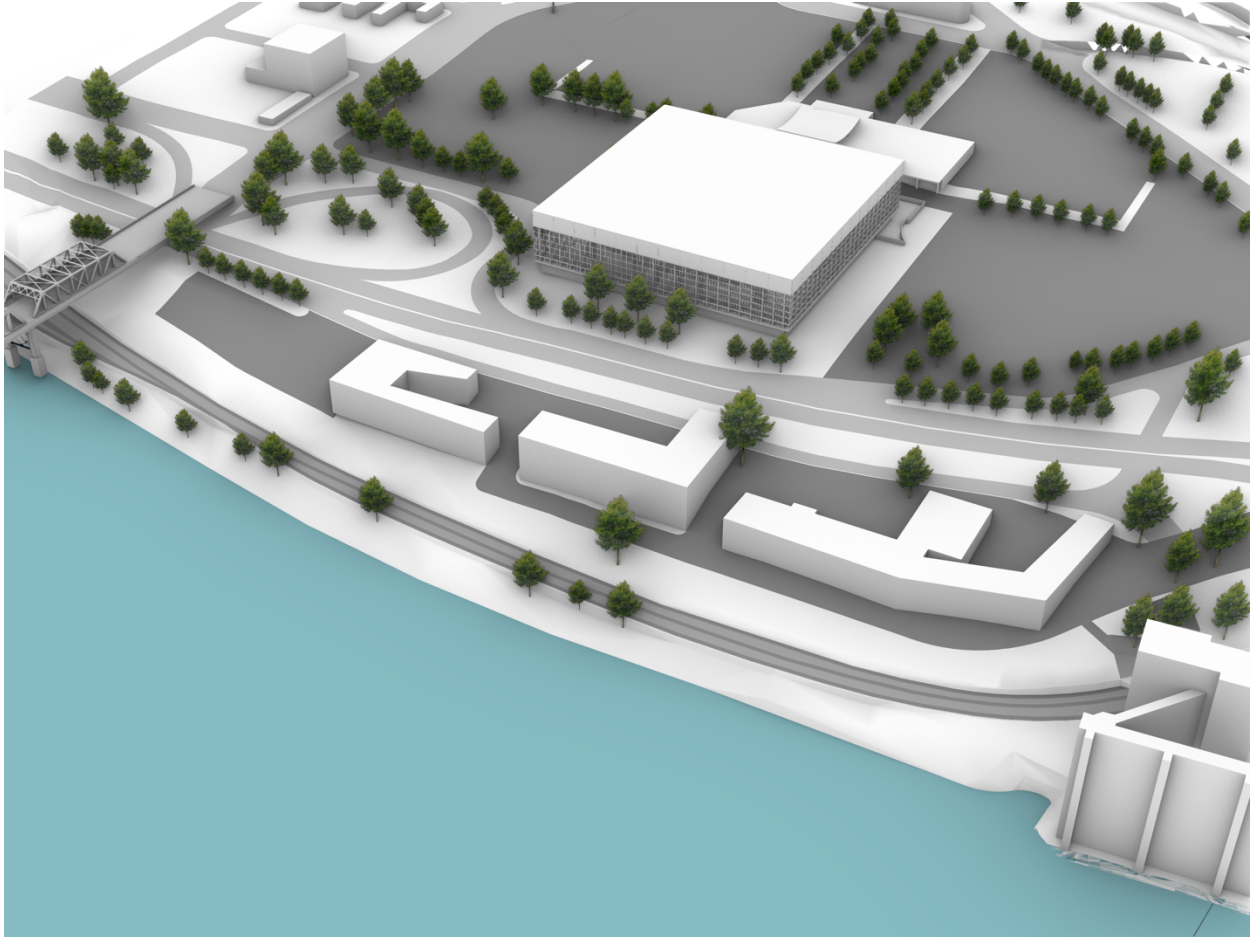


Figure 283. Lower Albina in 1990, site scale simulation.

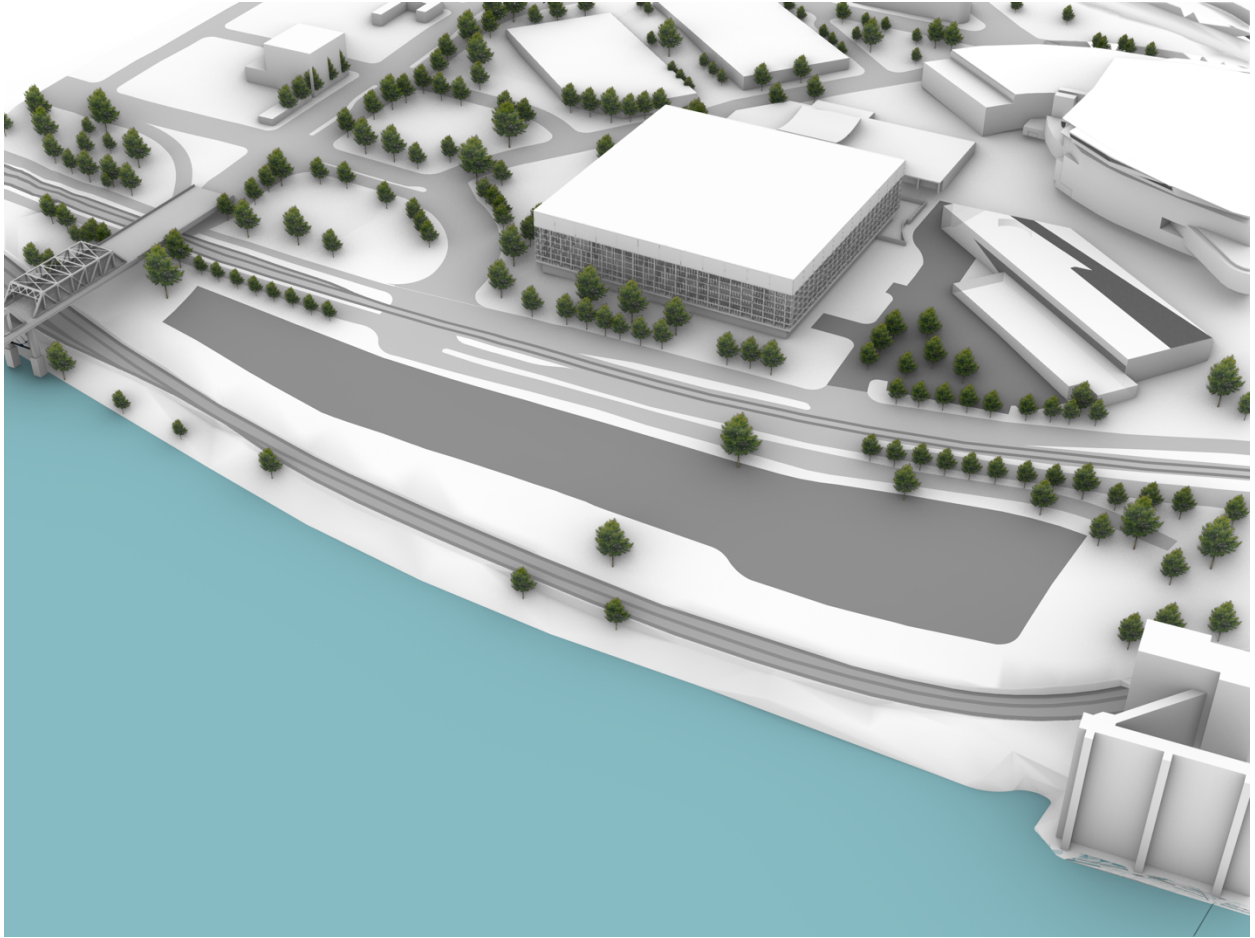


Figure 284. Lower Albina in 2011, site scale simulation.

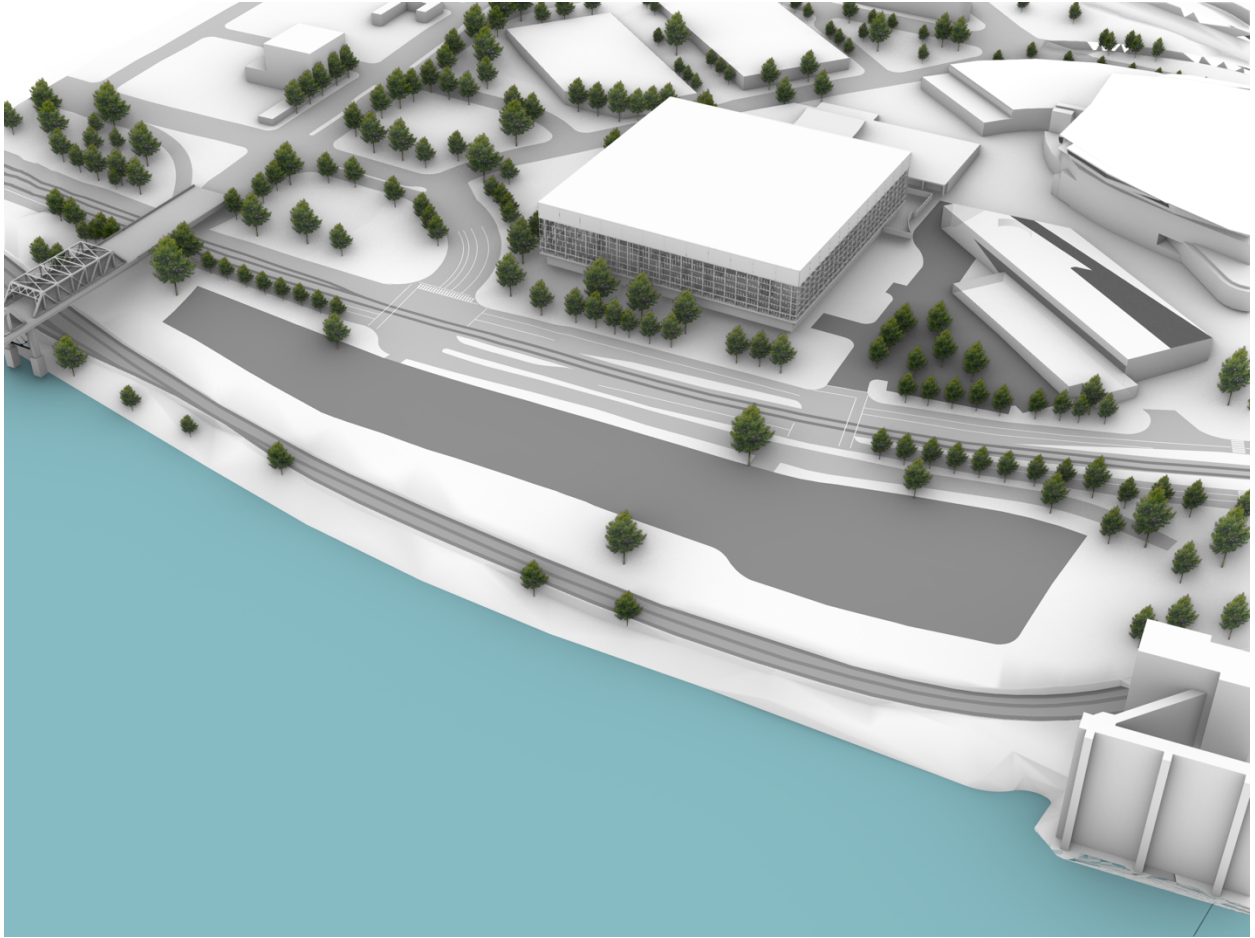


Figure 285. Lower Albina in 2014, site scale simulation.

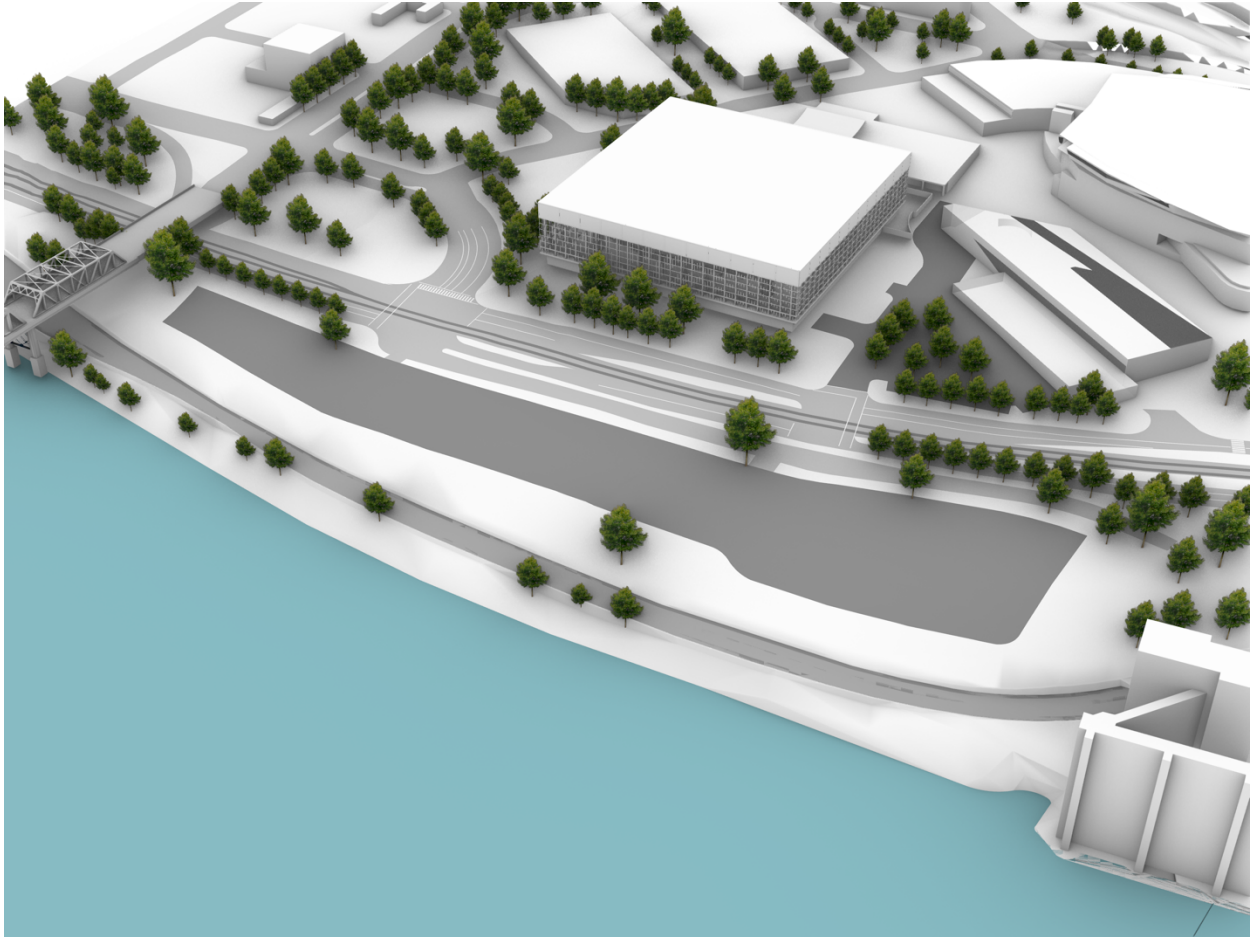


Figure 286. Lower Albina in 2017, site scale simulation.

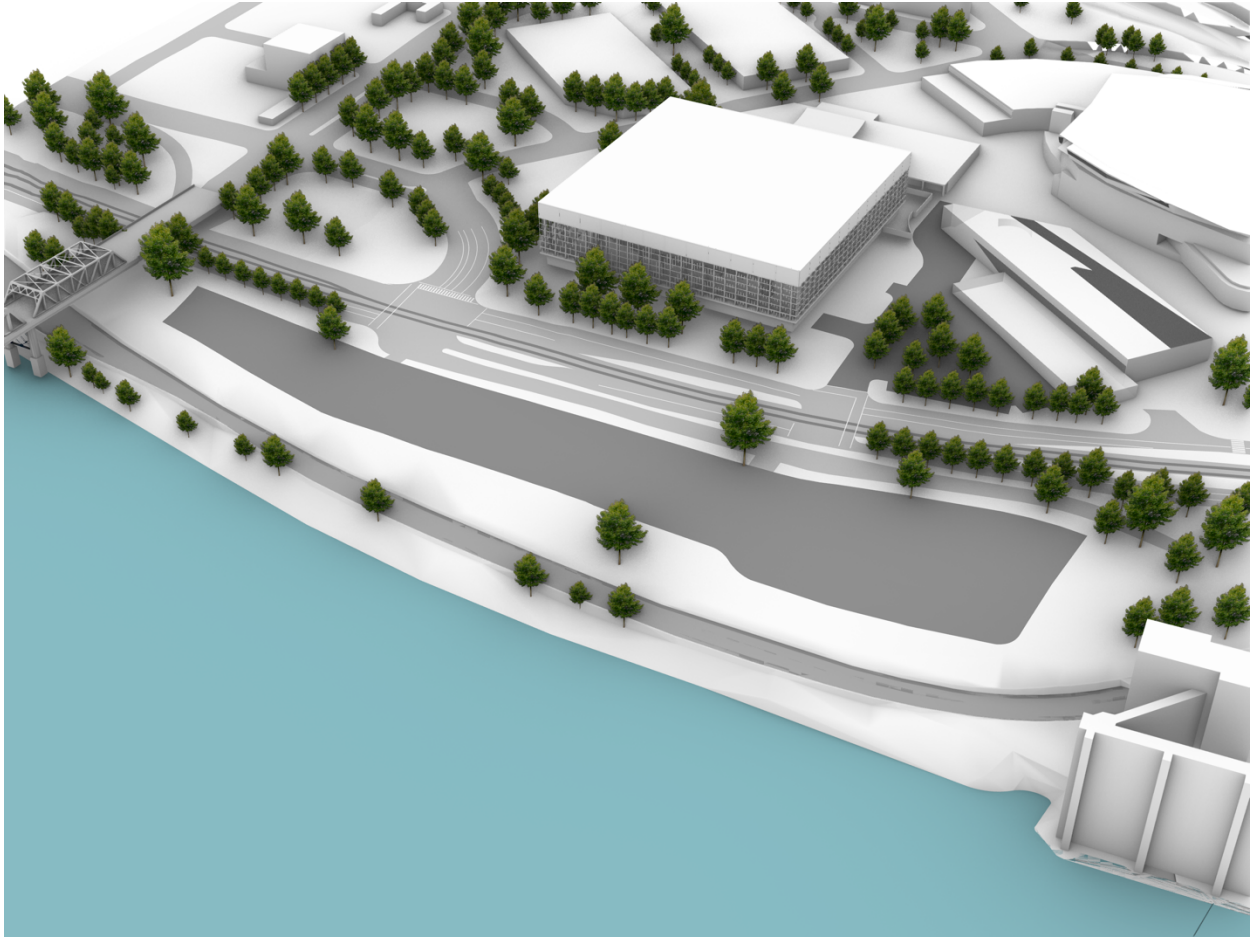


Figure 287. Lower Albina in 2020, site scale simulation.

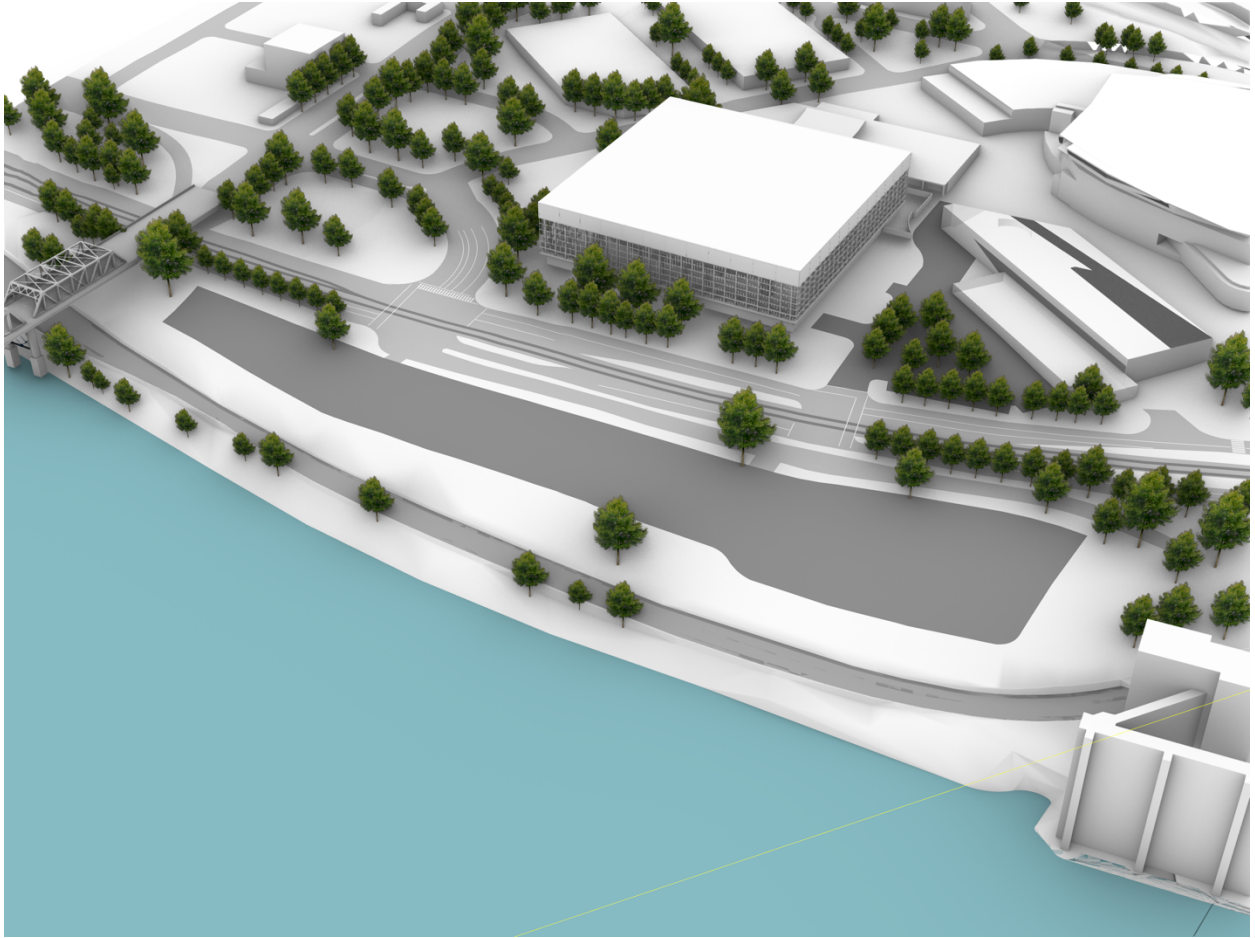


Figure 288. Lower Albina in 2023, site scale simulation.



Figure 289. Lower Albina gauge historic crest simulation on June 6, 1948.



Figure 290. Lower Albina gauge historic crest simulation on June 26, 1950.



Figure 291. Lower Albina gauge historic crest simulation on June 4, 1956.

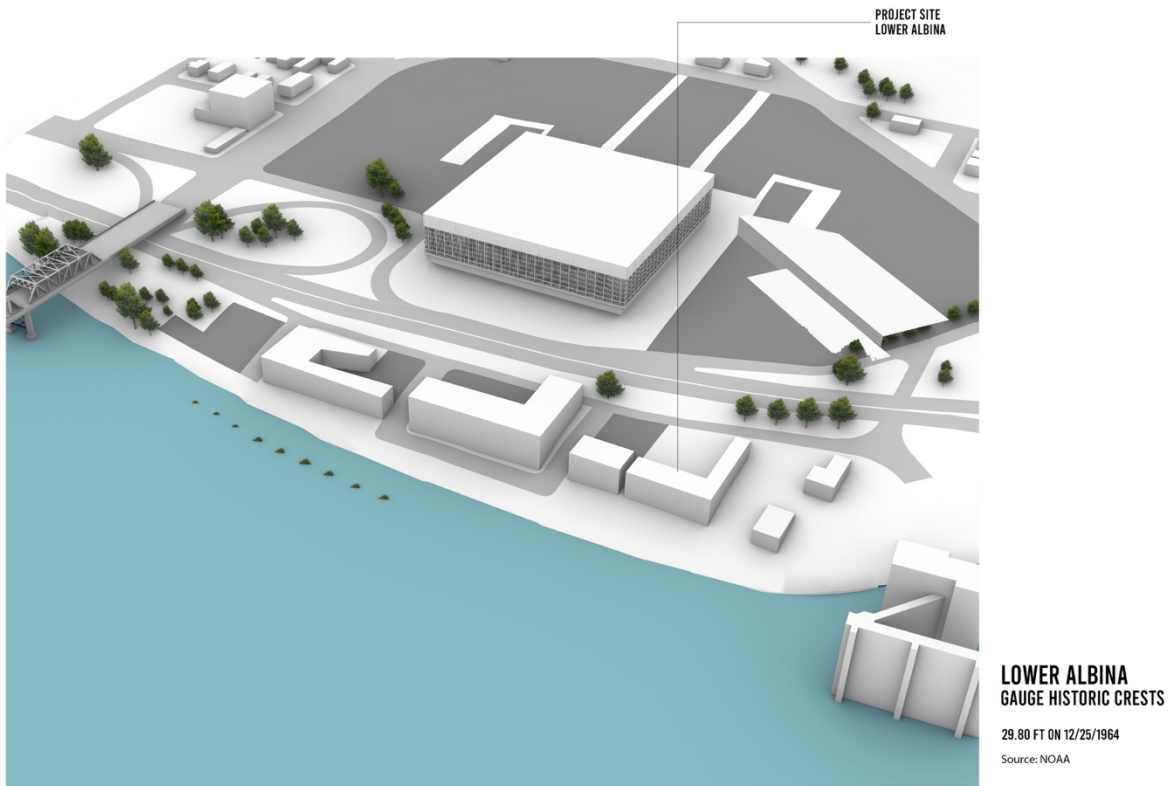


Figure 292. Lower Albina gauge historic crest simulation on December 25, 1964.

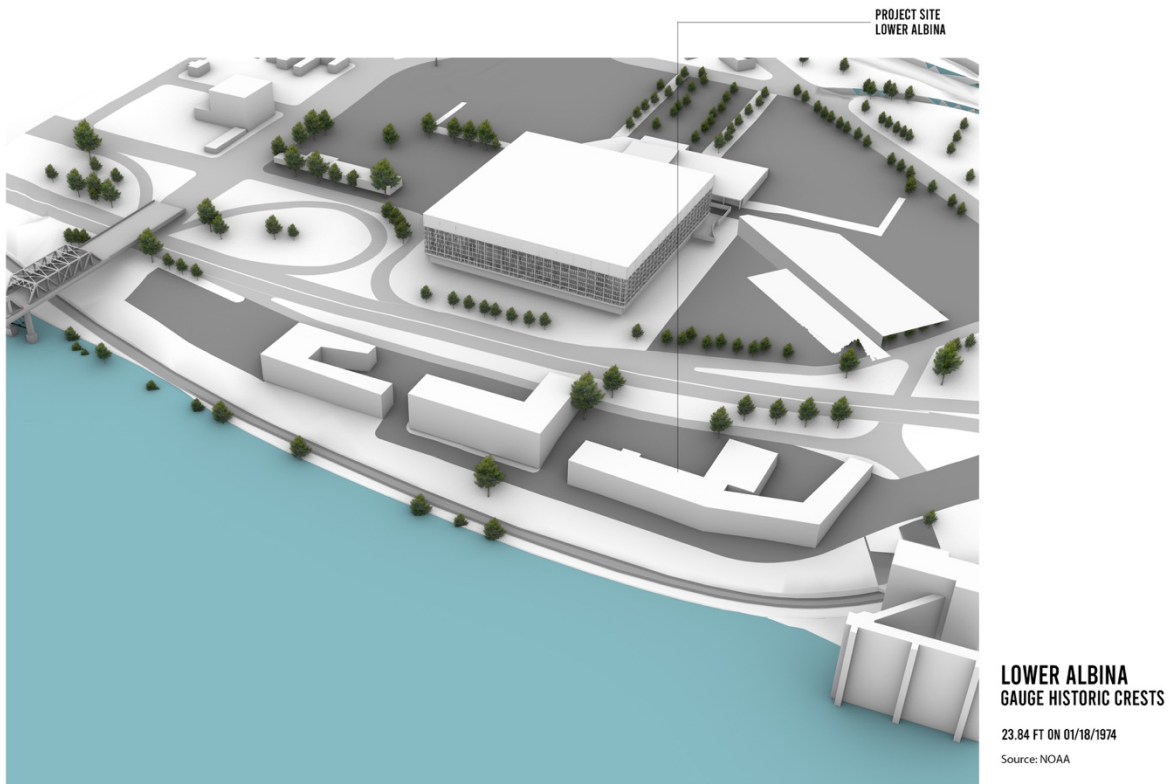


Figure 293. Lower Albina gauge historic crest simulation on January 18, 1974.

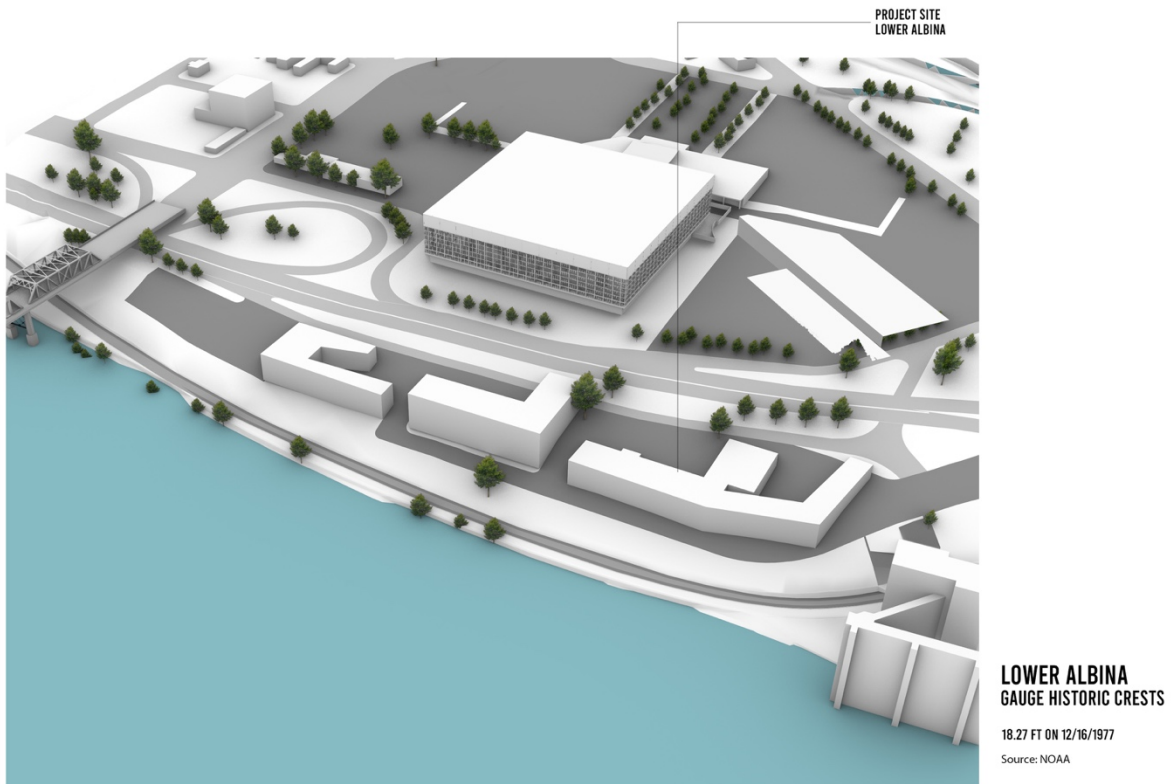


Figure 294. Lower Albina gauge historic crest simulation on December 16, 1977.



Figure 295. Lower Albina gauge historic crest simulation on February 21, 1982.

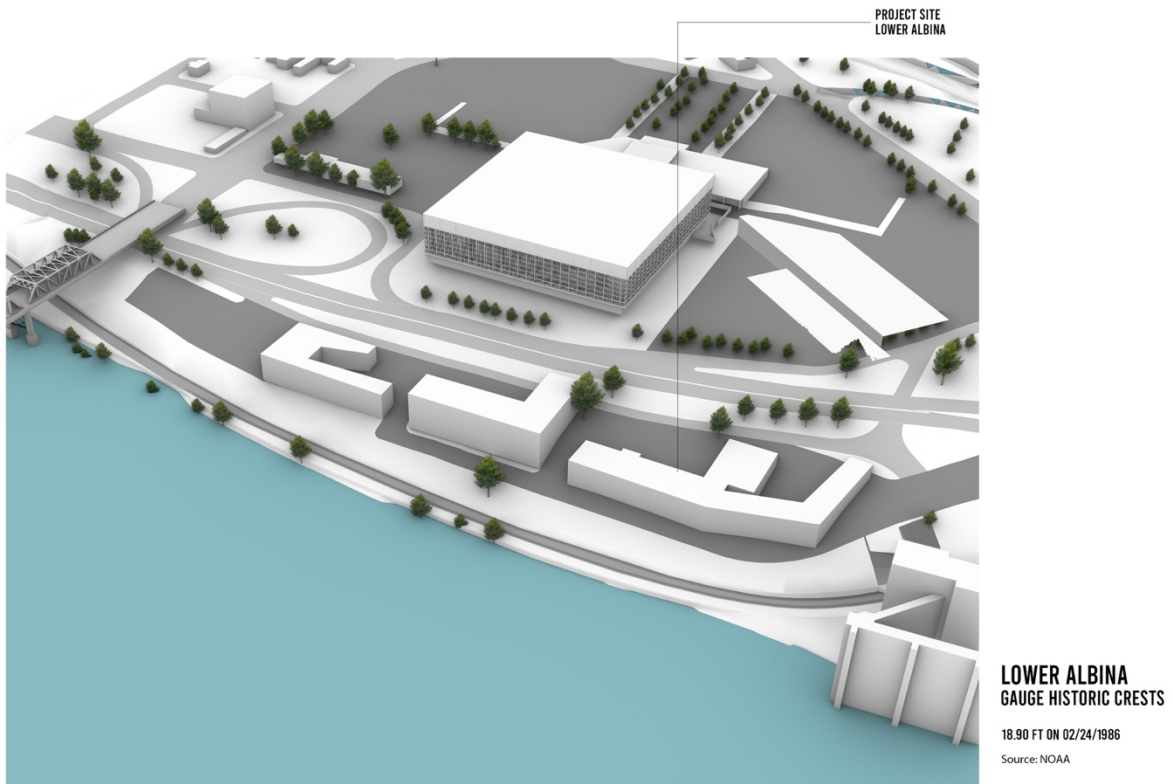


Figure 296. Lower Albina gauge historic crest simulation on February 24, 1986.



Figure 297. Lower Albina gauge historic crest simulation on February 9, 1996.

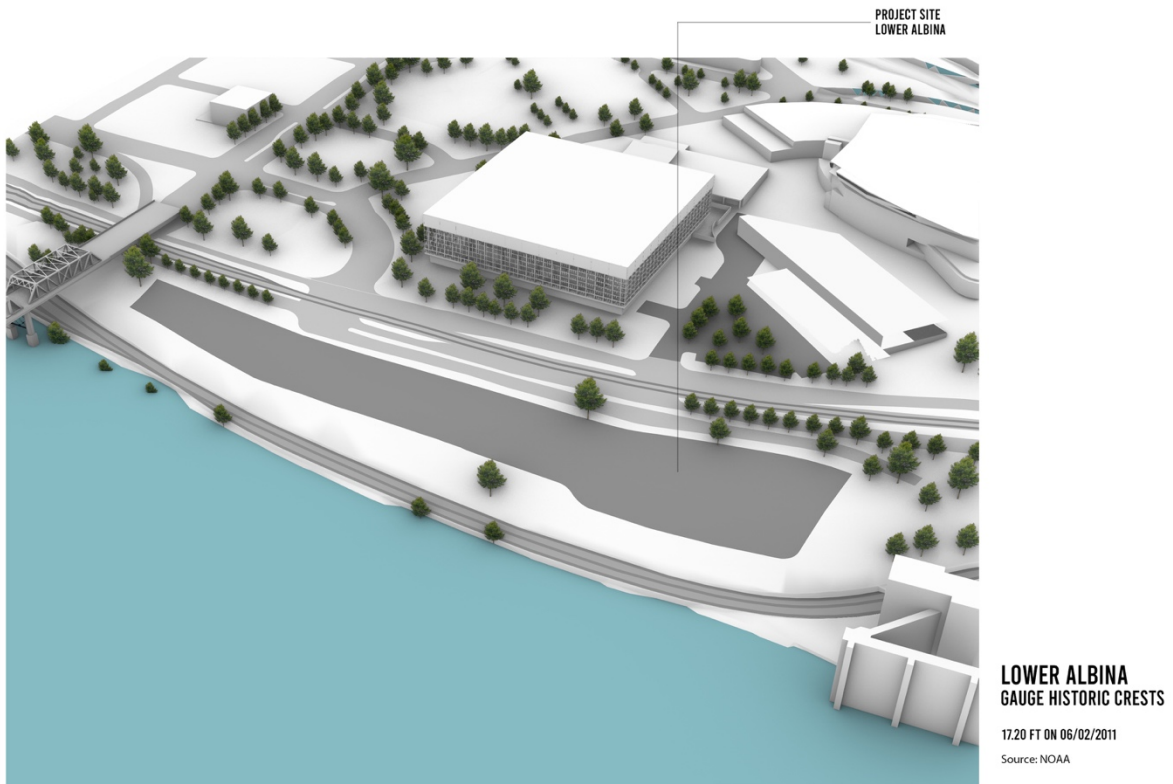


Figure 298. Lower Albina gauge historic crest simulation on June 2, 2011.

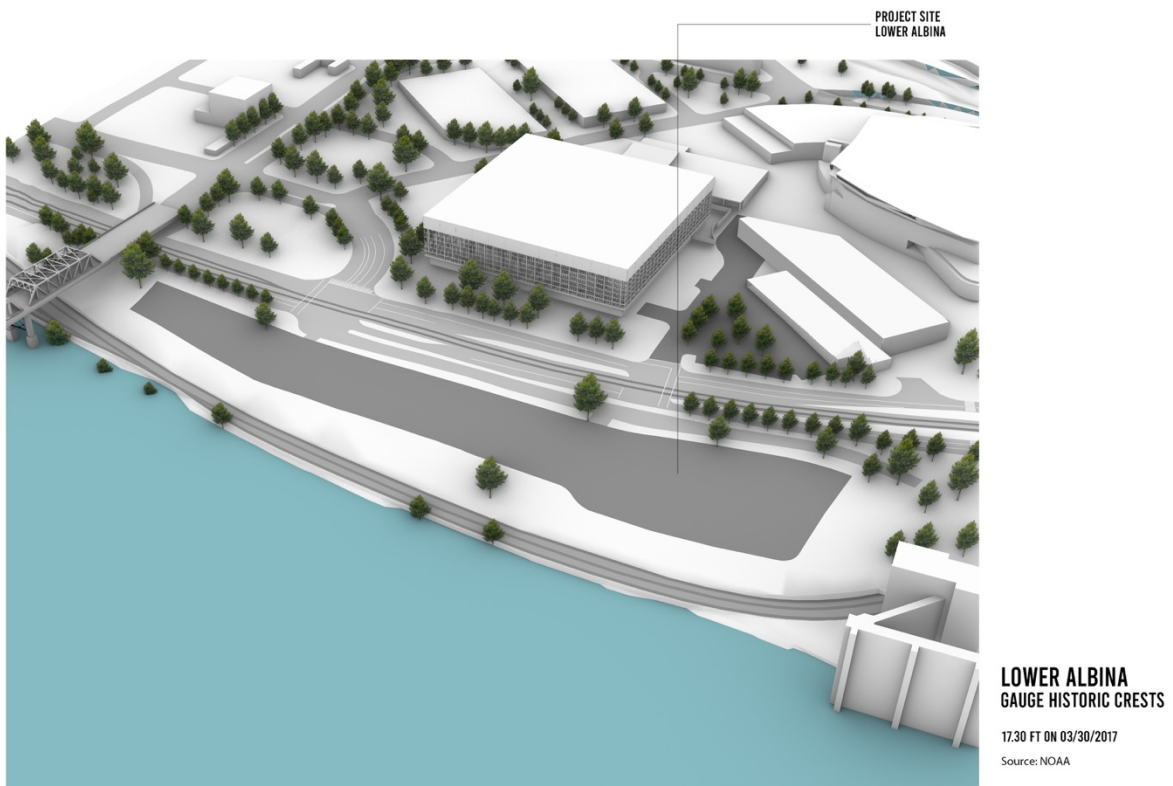


Figure 299. Lower Albina gauge historic crest simulation on March 30, 2017.

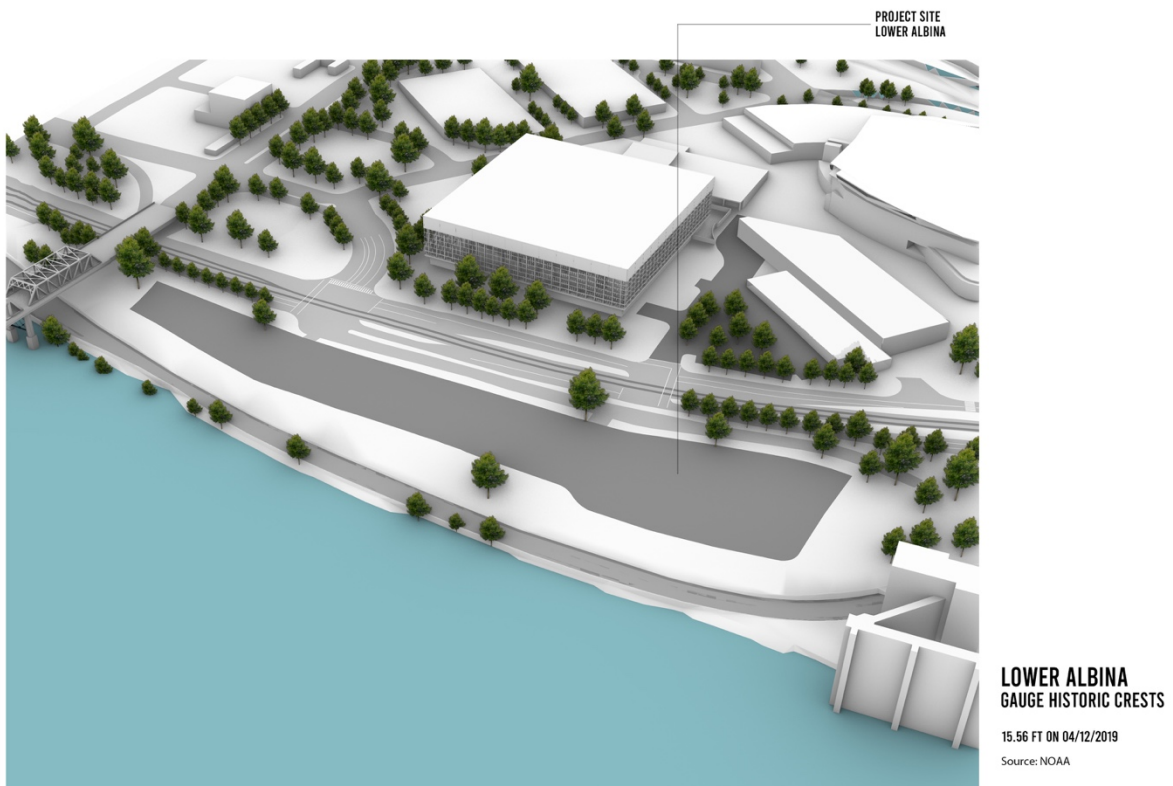


Figure 300. Lower Albina gauge historic crest simulation on April 12, 2019.

APPENDIX C. WIND SIMULATIONS

WIND SIMULATION
Scenario 1

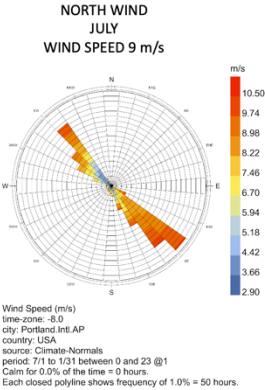


Figure 301. Wind simulation Scenario 1.

Wind rose for a north wind in July with wind speed of 9 m/s.

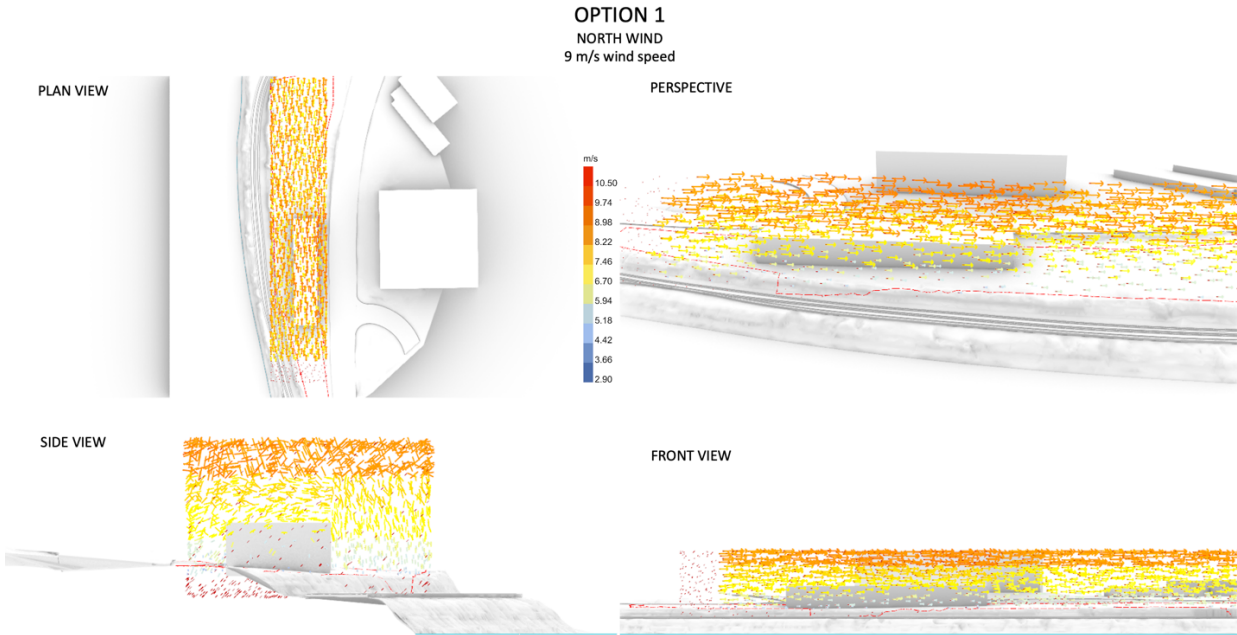


Figure 302. Wind simulation for Option 1. Plan view, perspective, side view, and front view.

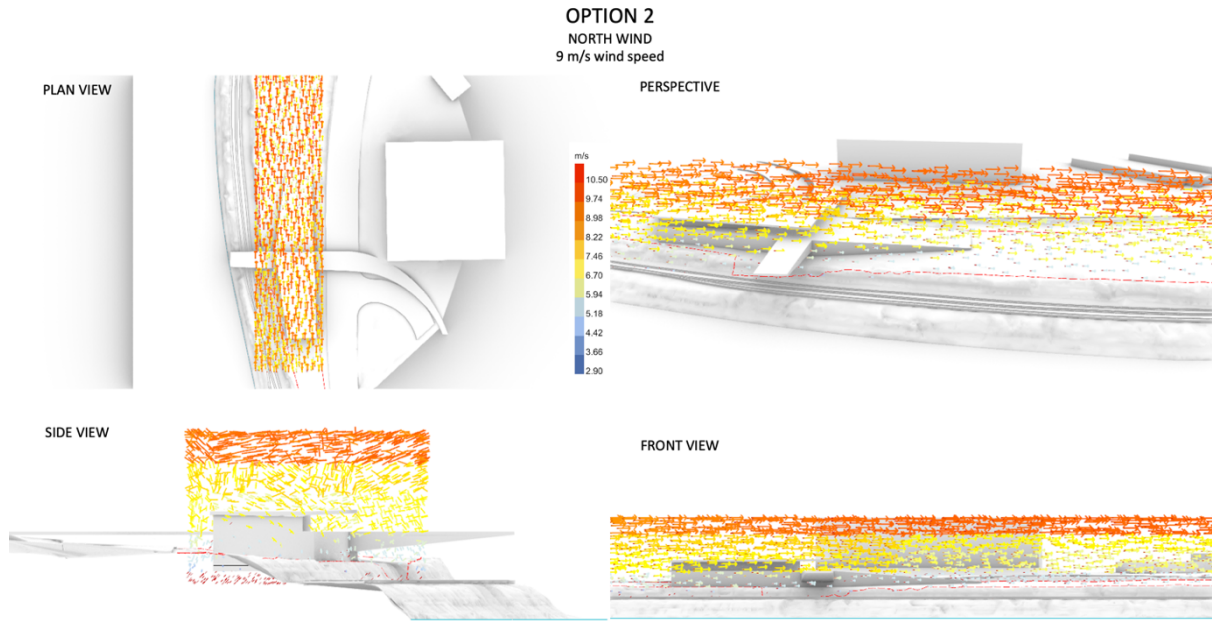


Figure 303. Wind simulation for Option 2. Plan view, perspective, side view, and front view

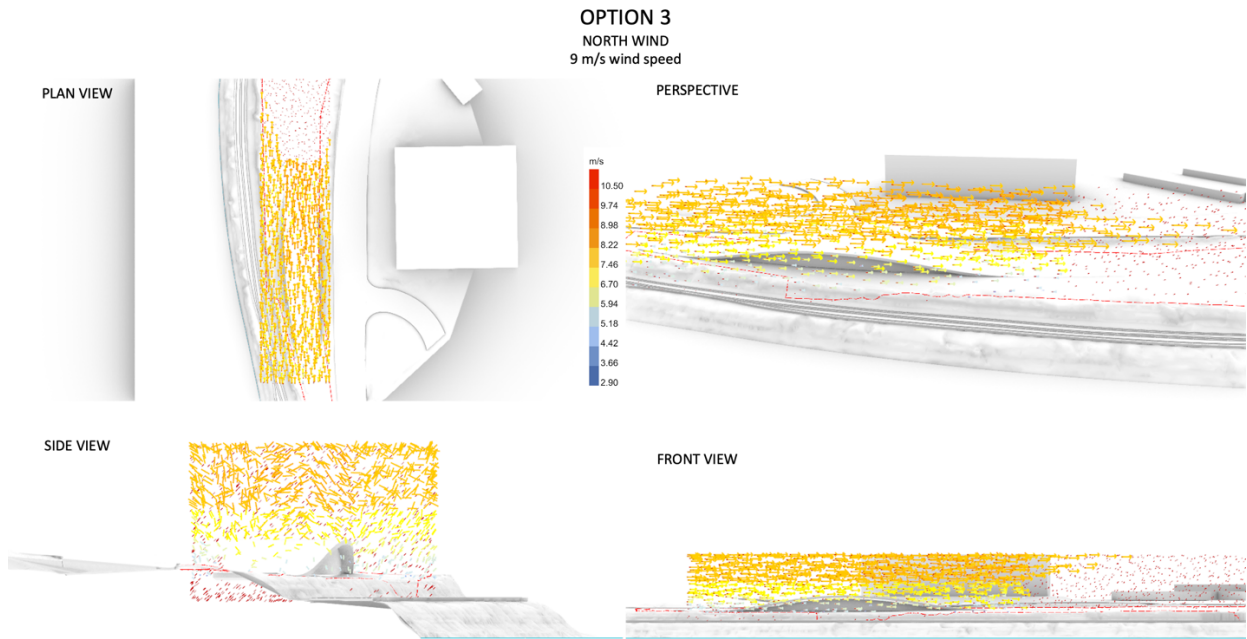


Figure 304. Wind simulation for Option 3. Plan view, perspective, side view, and front view.

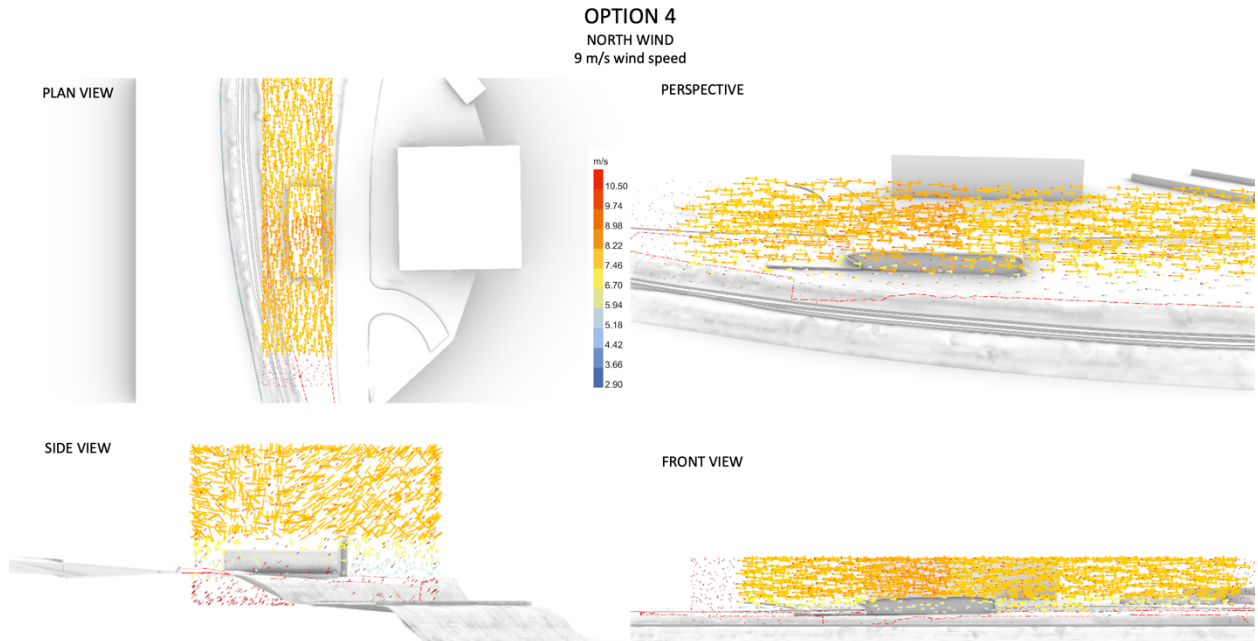


Figure 305. Wind simulation for Option 4. Plan view, perspective, side view, and front view.

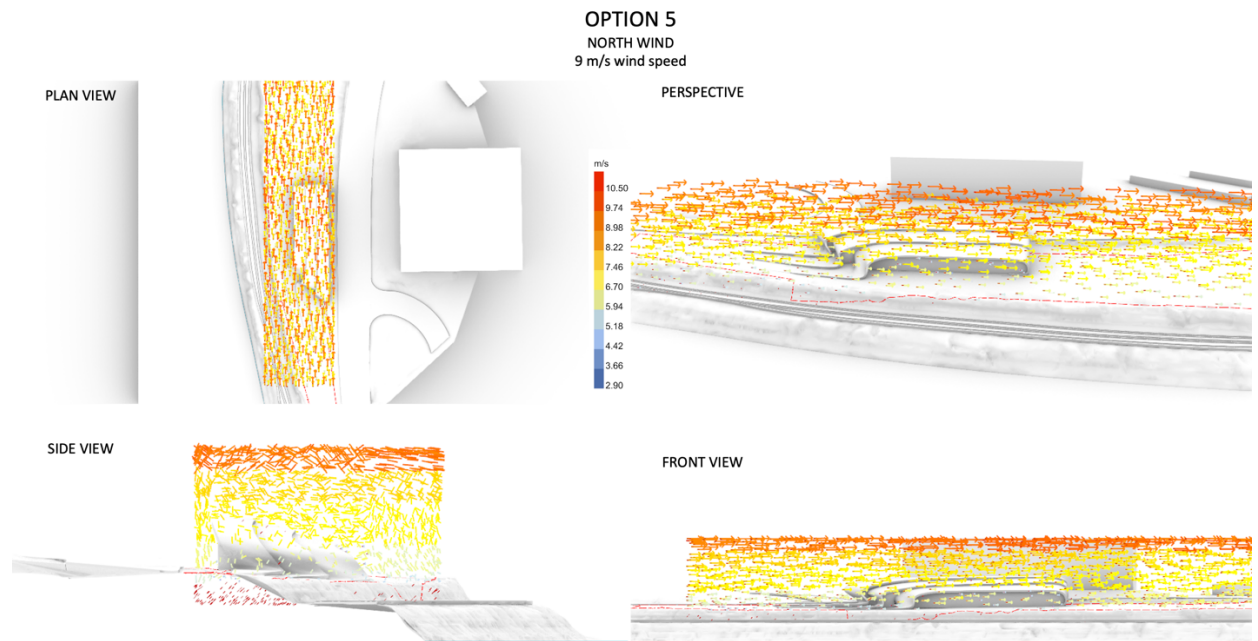


Figure 306. Wind simulation for Option 5. Plan view, perspective, side view, and front view.

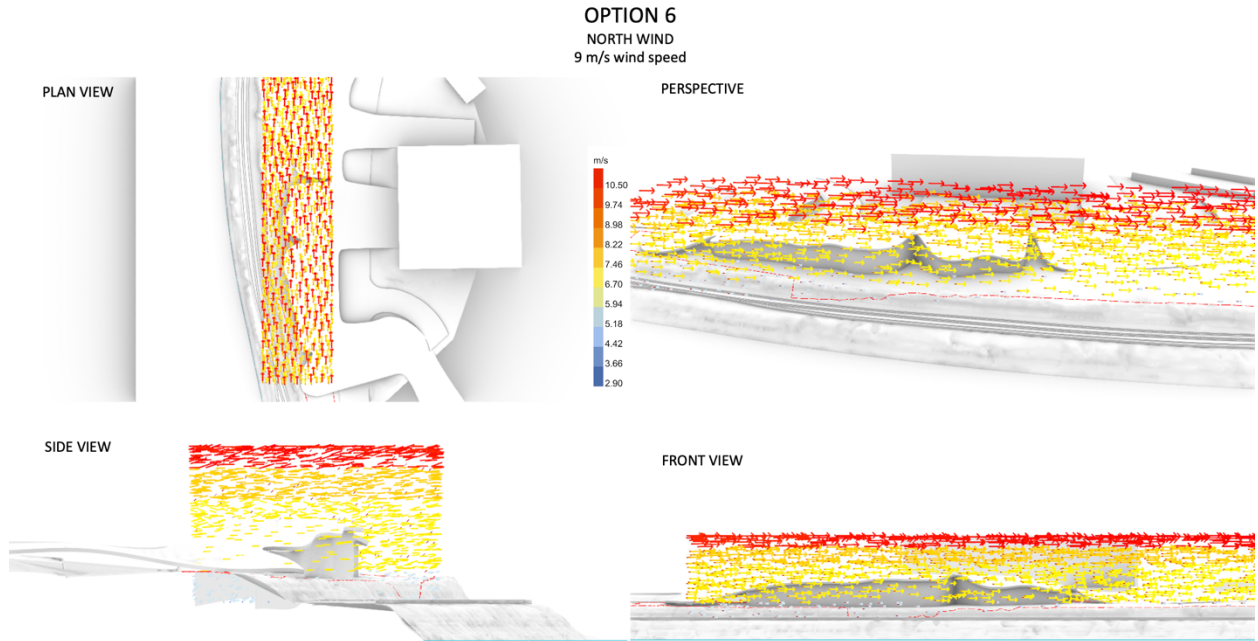


Figure 307. Wind simulation for Option 6. Plan view, perspective, side view, and front view.

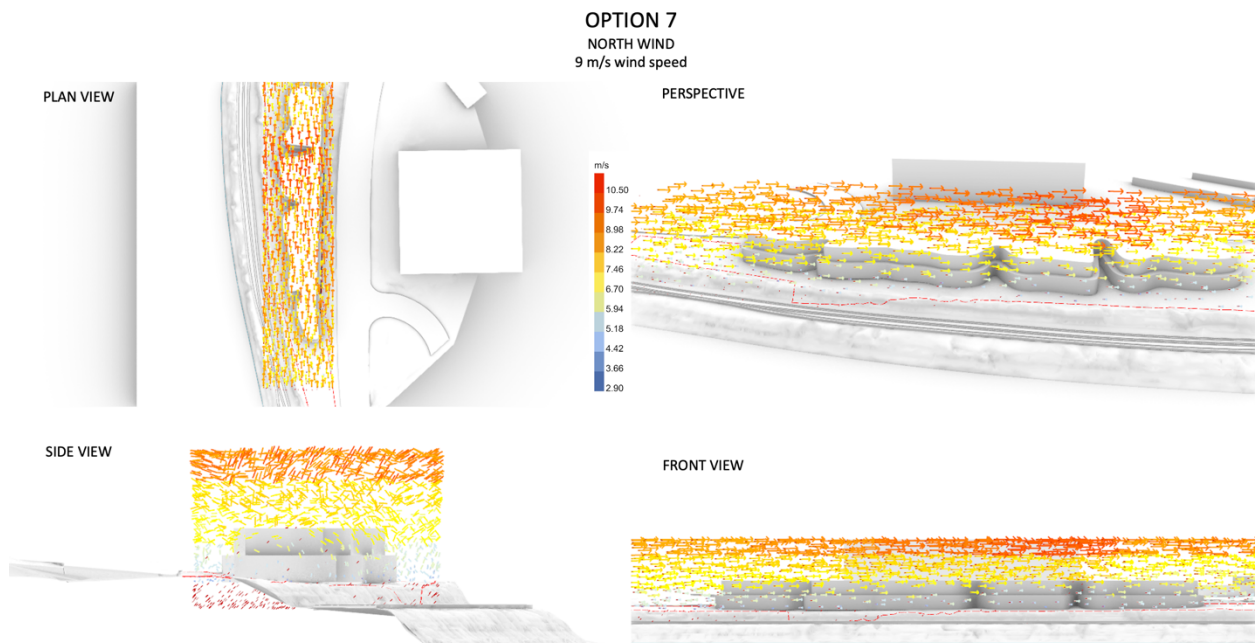


Figure 308. Wind simulation for Option 7. Plan view, perspective, side view, and front view.

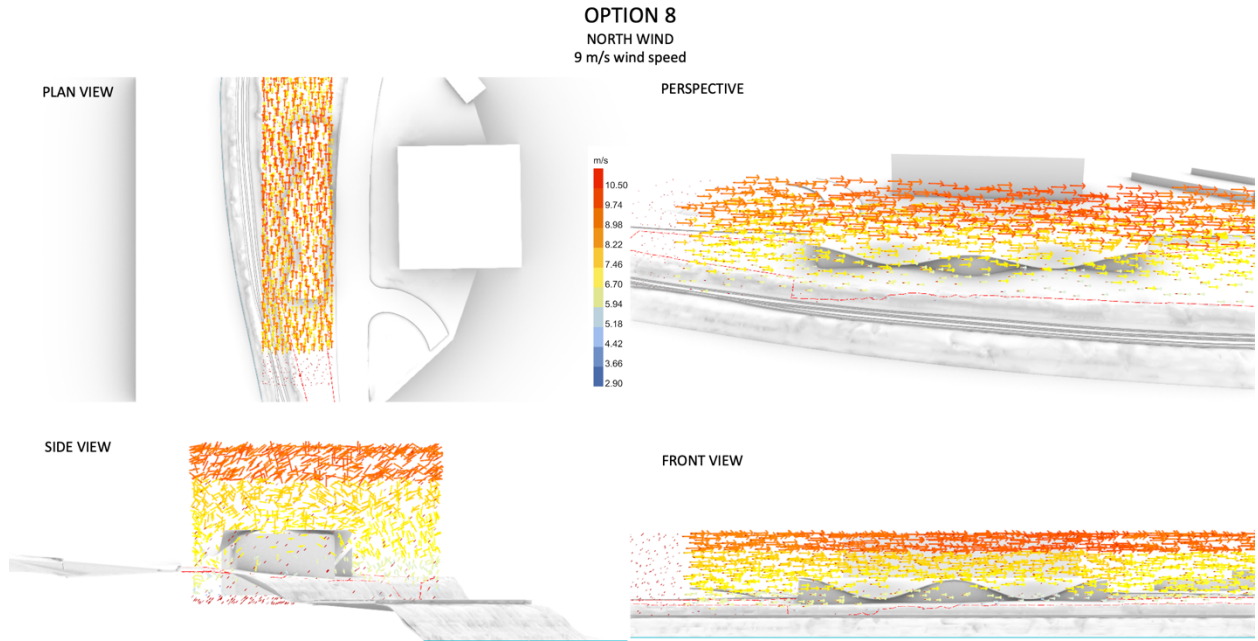


Figure 309. Wind simulation for Option 8. Plan view, perspective, side view, and front view.

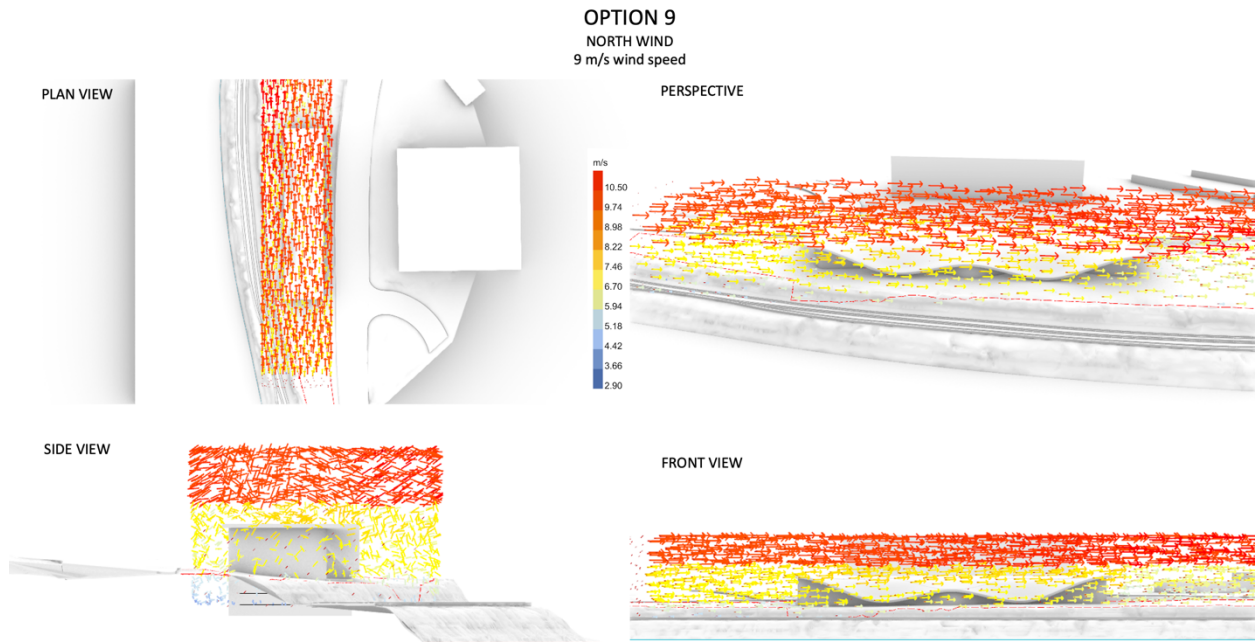


Figure 310. Wind simulation for Option 9. Plan view, perspective, side view, and front view.

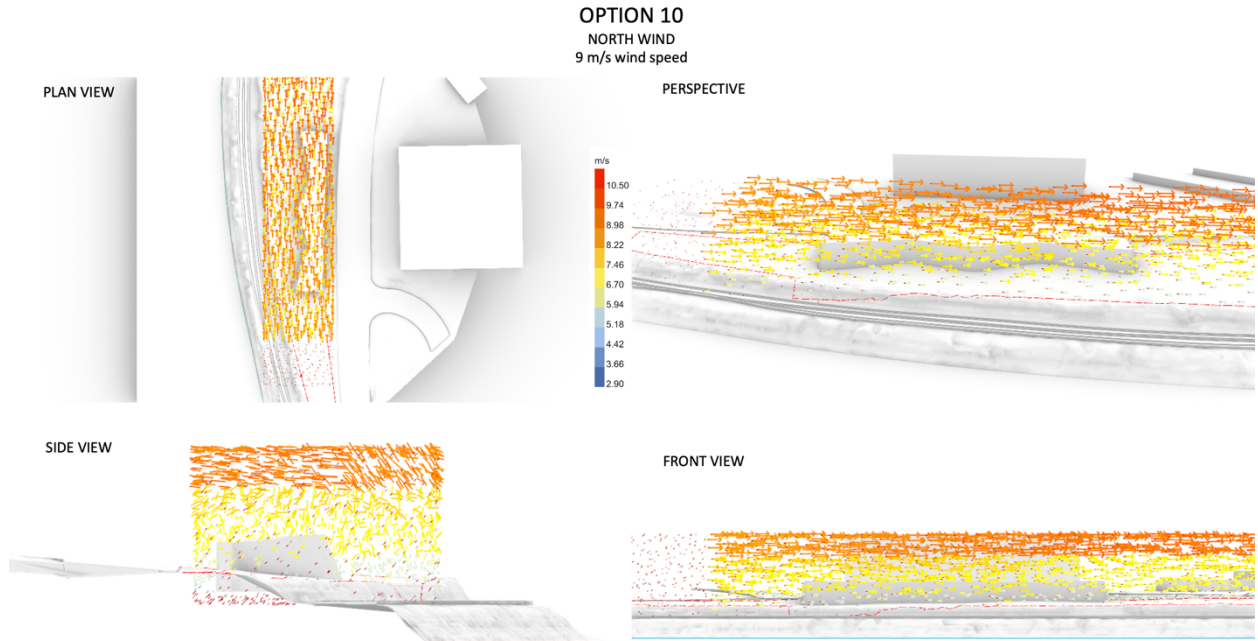


Figure 311. Wind simulation for Option 10. Plan view, perspective, side view, and front view.

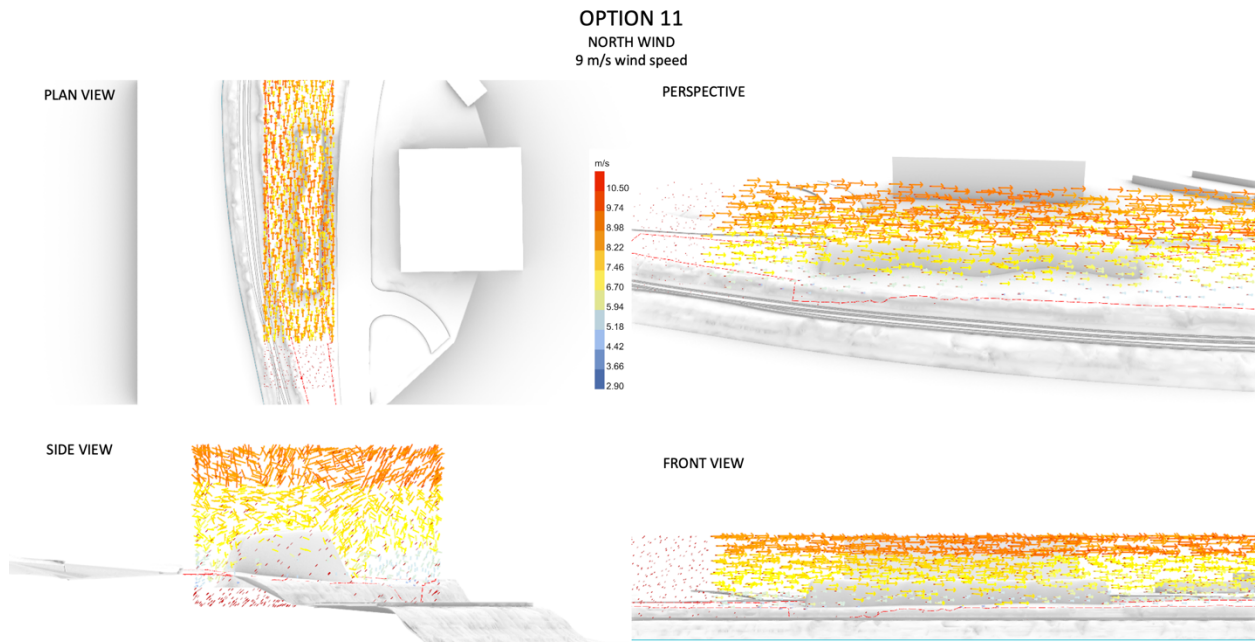


Figure 312. Wind simulation for Option 11. Plan view, perspective, side view, and front view.

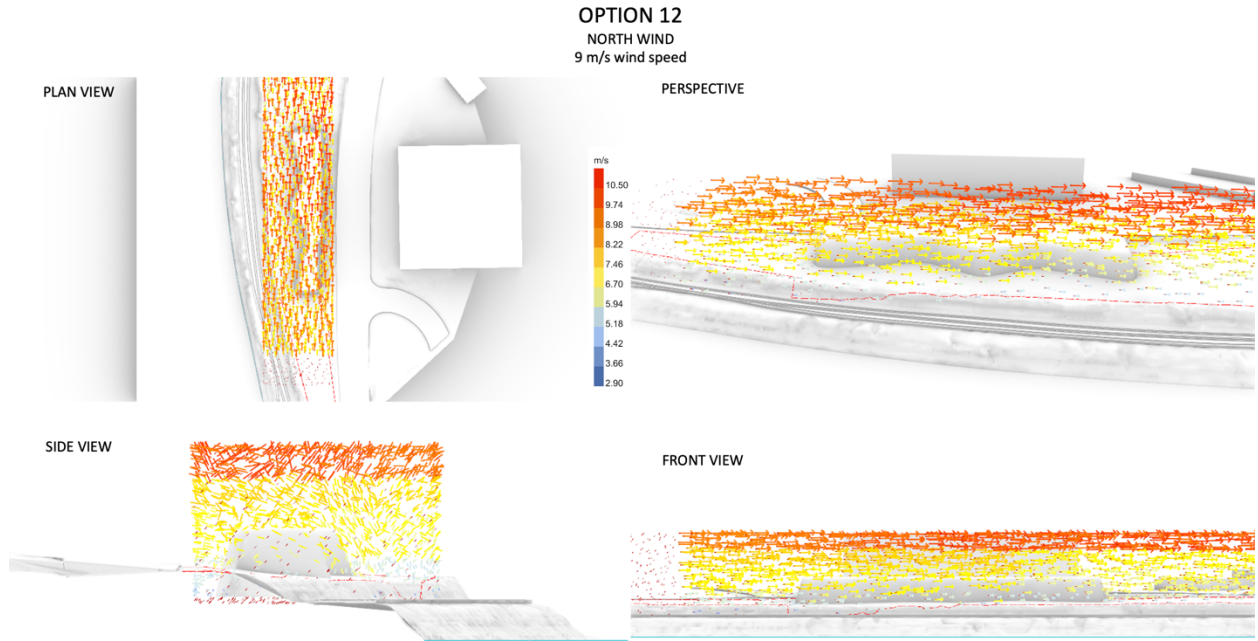


Figure 313. Wind simulation for Option 12. Plan view, perspective, side view, and front view.

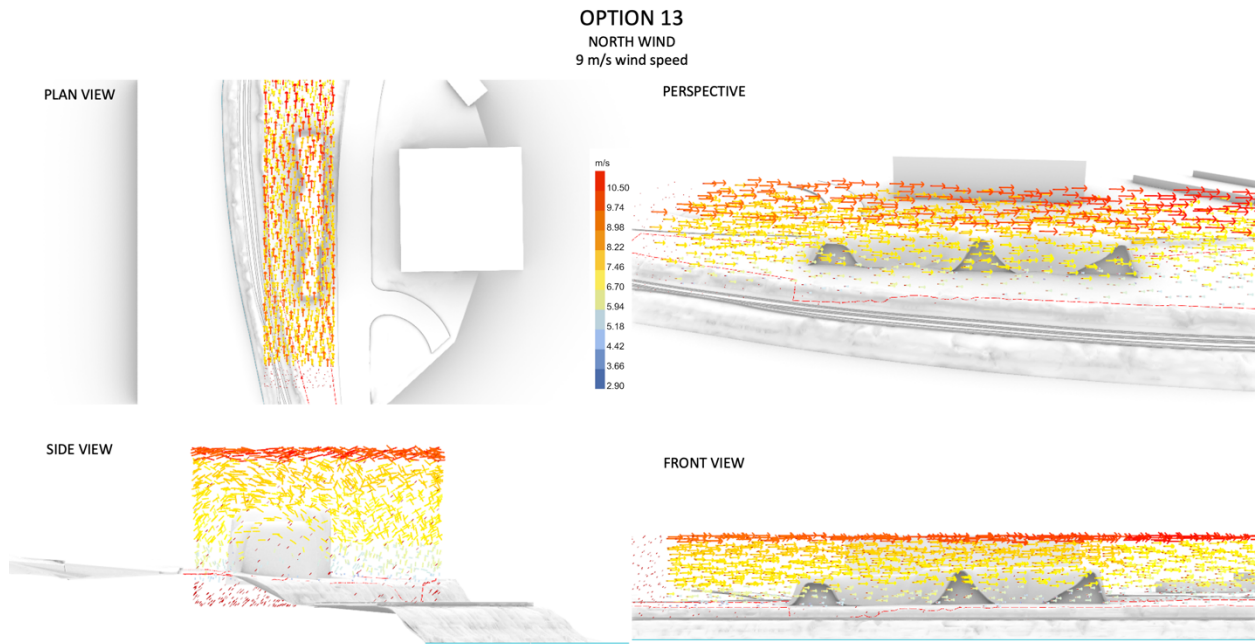


Figure 314. Wind simulation for Option 13. Plan view, perspective, side view, and front view.

WIND SIMULATION
Scenario 2

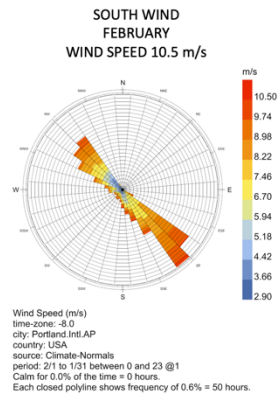


Figure 315. Wind simulation Scenario 2.

Wind rose for a south wind in February with wind speed of 10.5 m/s.

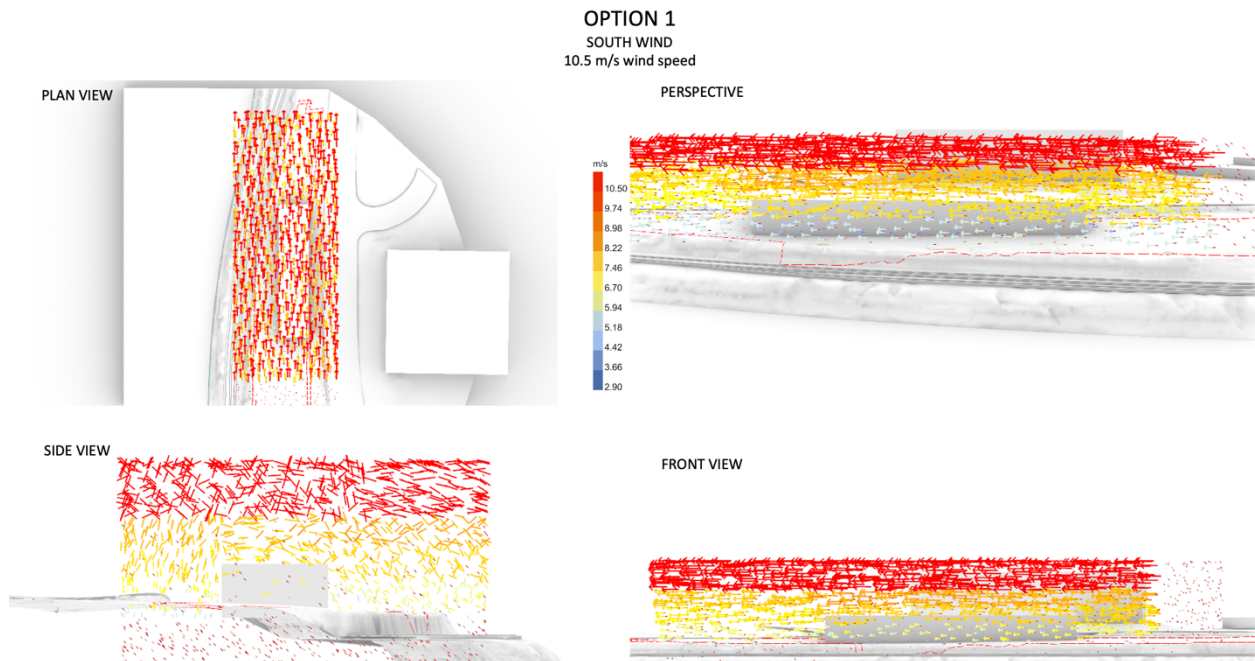


Figure 316. Wind simulation for Option 1. Plan view, perspective, side view, and front view.

OPTION 2
SOUTH WIND
10.5 m/s wind speed

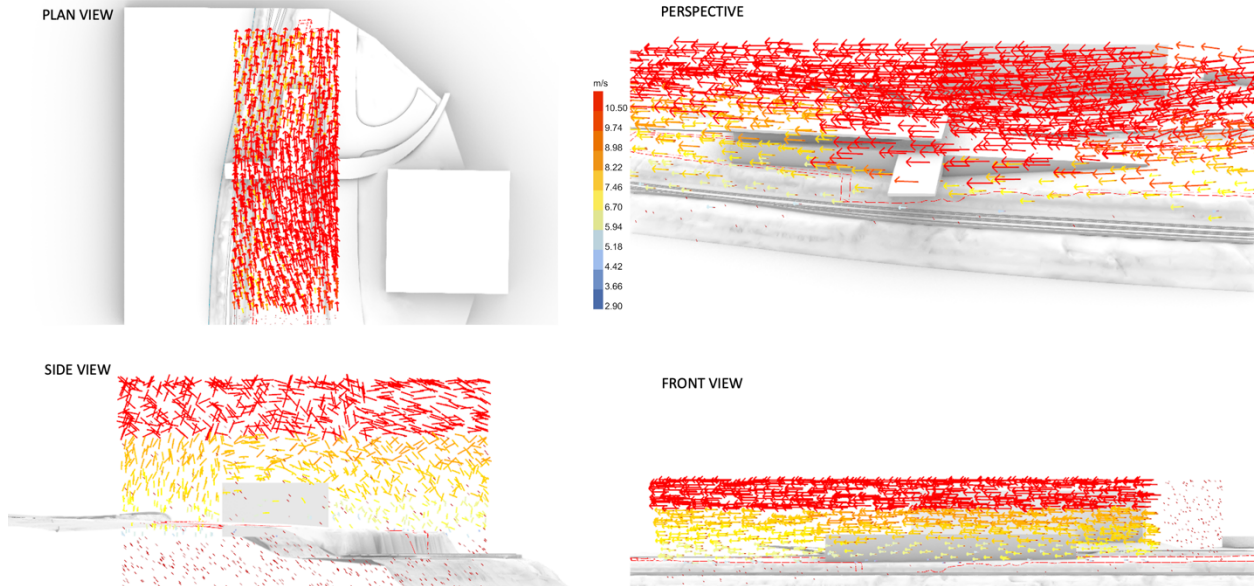


Figure 317. Wind simulation for Option 2. Plan view, perspective, side view, and front view.

OPTION 3
SOUTH WIND
10.5 m/s wind speed

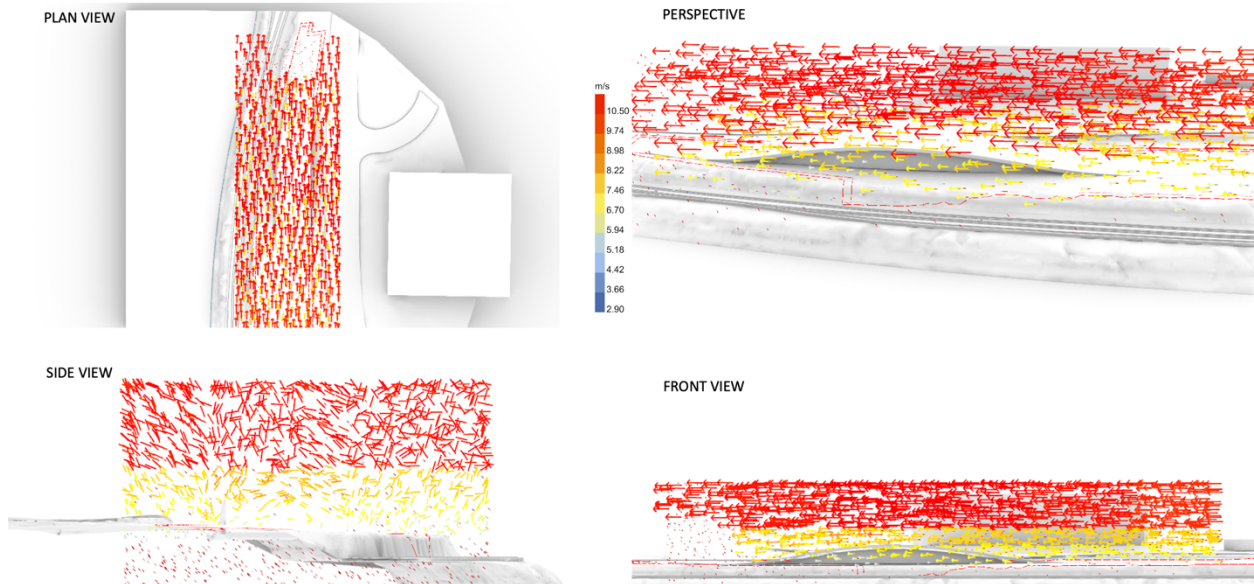


Figure 318. Wind simulation for Option 3. Plan view, perspective, side view, and front view.

OPTION 4
SOUTH WIND
10.5 m/s wind speed

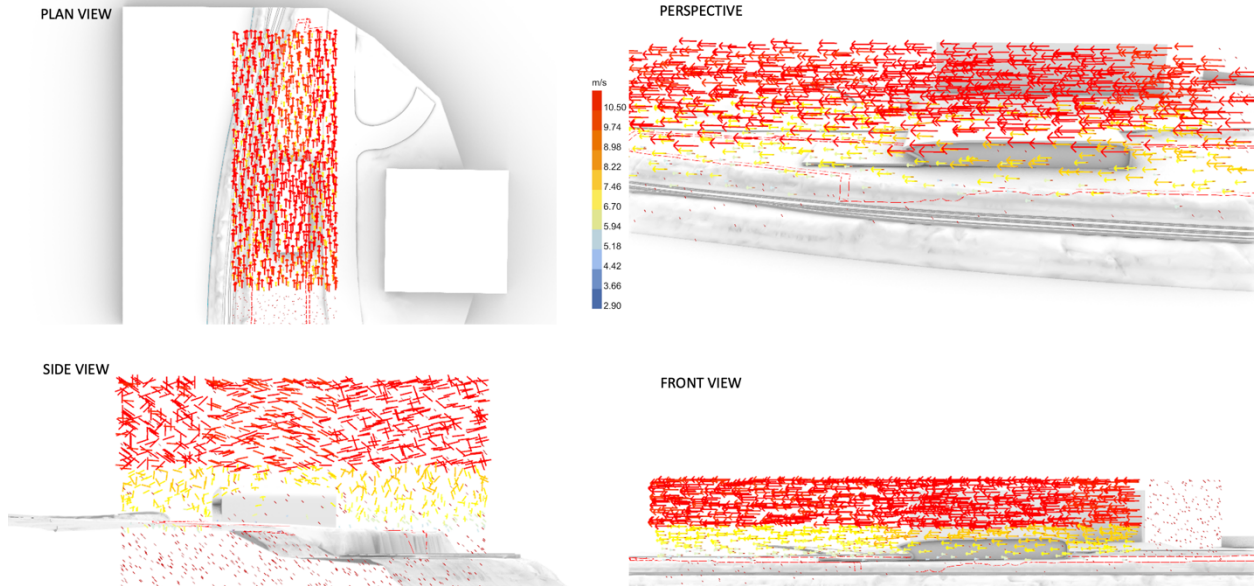


Figure 319. Wind simulation for Option 4. Plan view, perspective, side view, and front view.

OPTION 5
SOUTH WIND
10.5 m/s wind speed

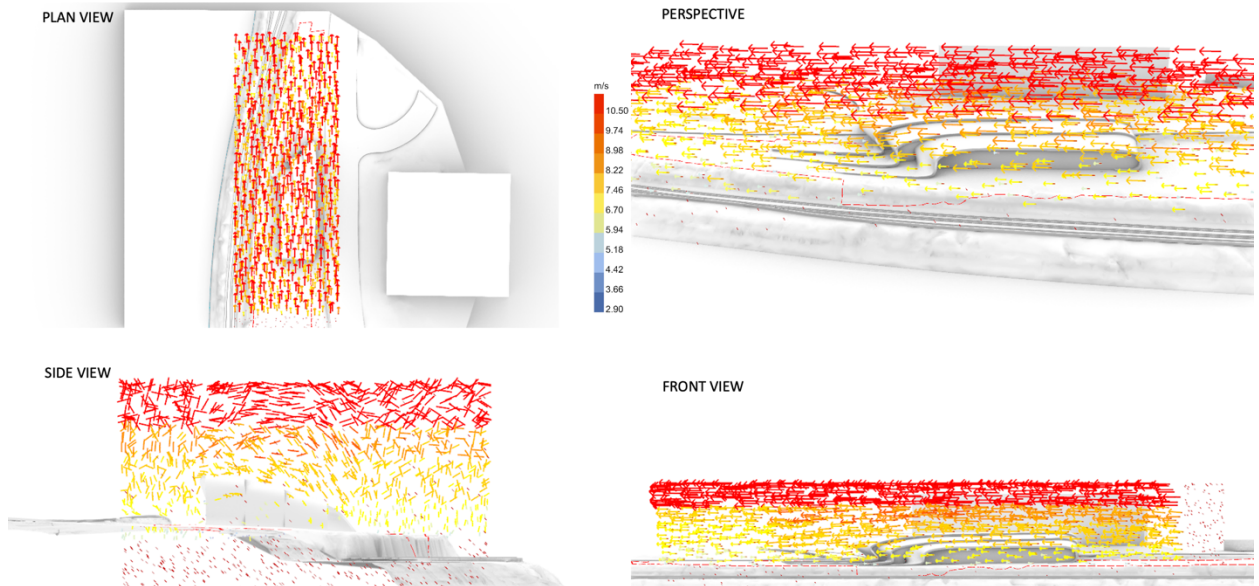


Figure 320. Wind simulation for Option 5. Plan view, perspective, side view, and front view.

OPTION 6
SOUTH WIND
10.5 m/s wind speed

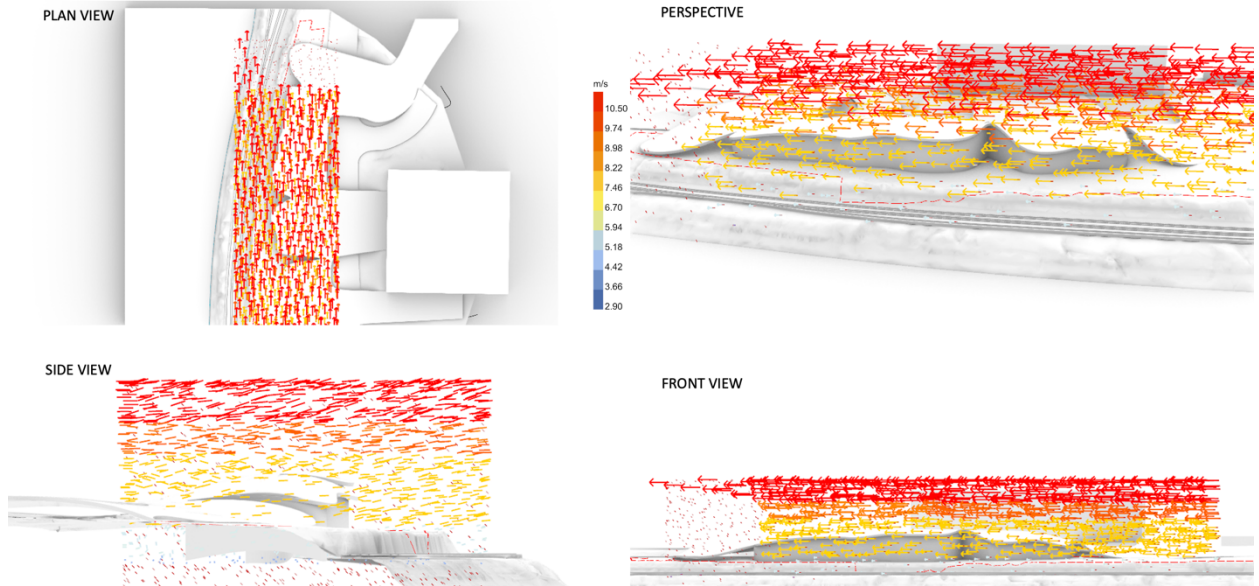


Figure 321. Wind simulation for Option 6. Plan view, perspective, side view, and front view.

OPTION 7
SOUTH WIND
10.5 m/s wind speed

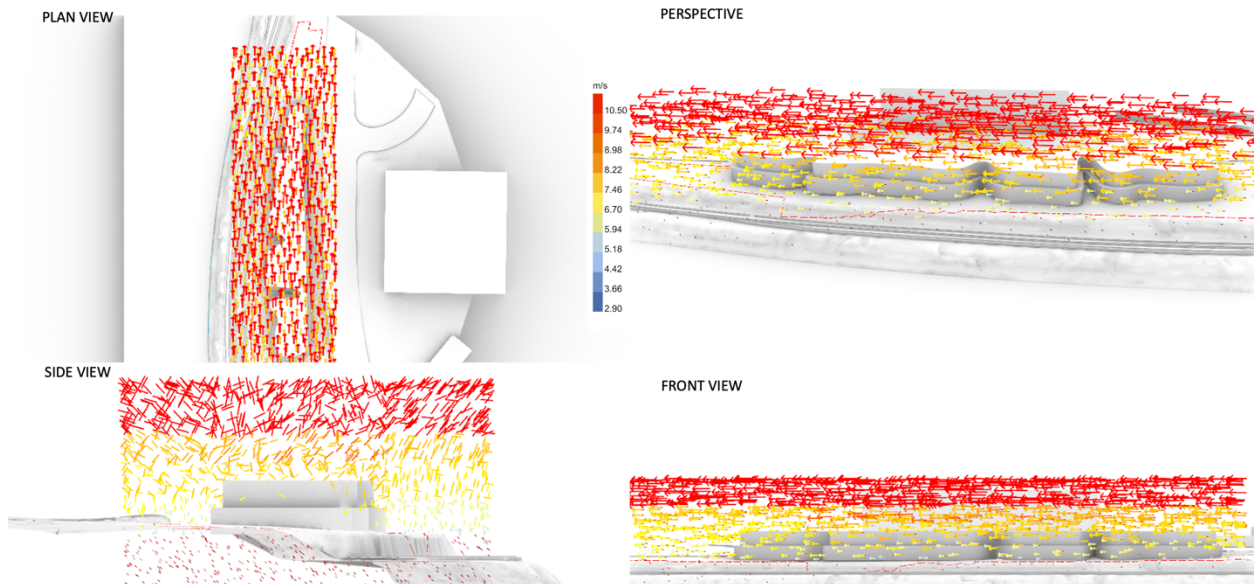


Figure 322. Wind simulation for Option 7. Plan view, perspective, side view, and front view.

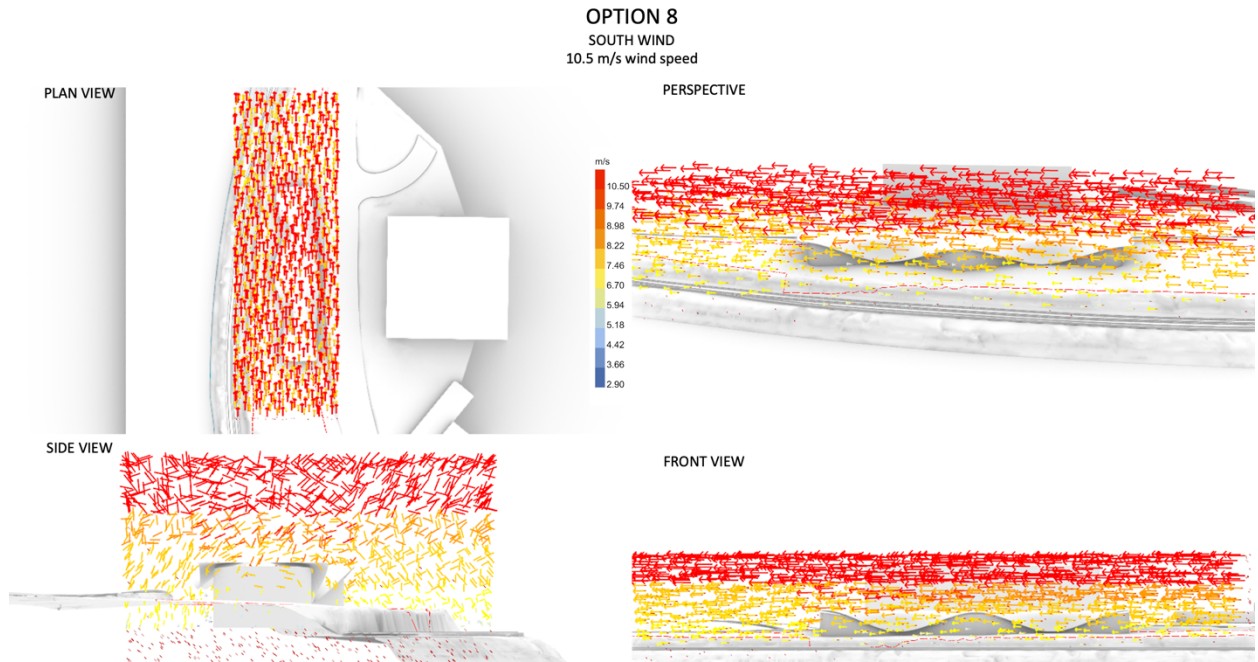


Figure 323. Wind simulation for Option 8. Plan view, perspective, side view, and front view.

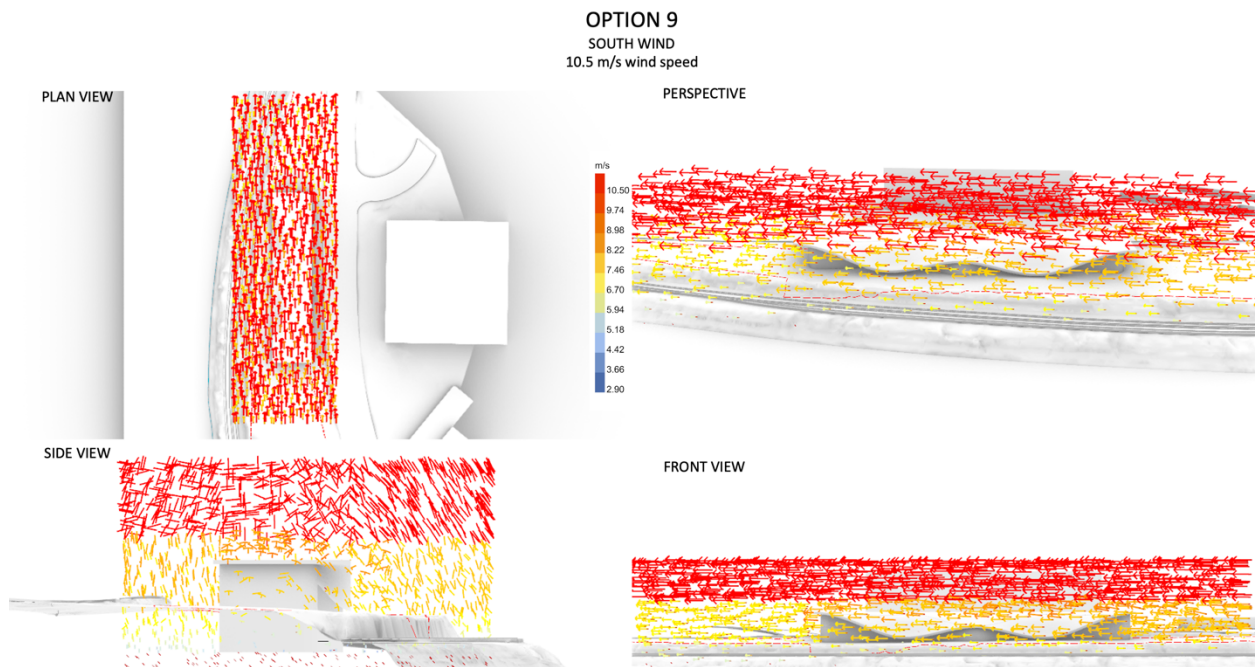


Figure 324. Wind simulation for Option 9. Plan view, perspective, side view, and front view.

OPTION 10
SOUTH WIND
10.5 m/s wind speed

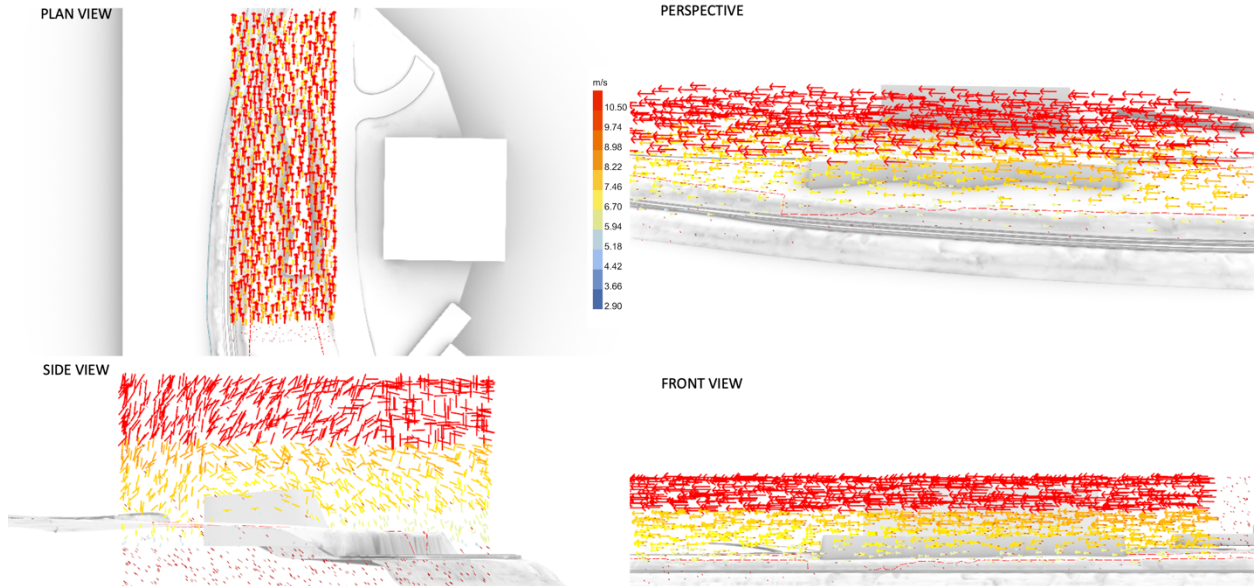


Figure 325. Wind simulation for Option 10. Plan view, perspective, side view, and front view.

OPTION 11
SOUTH WIND
10.5 m/s wind speed

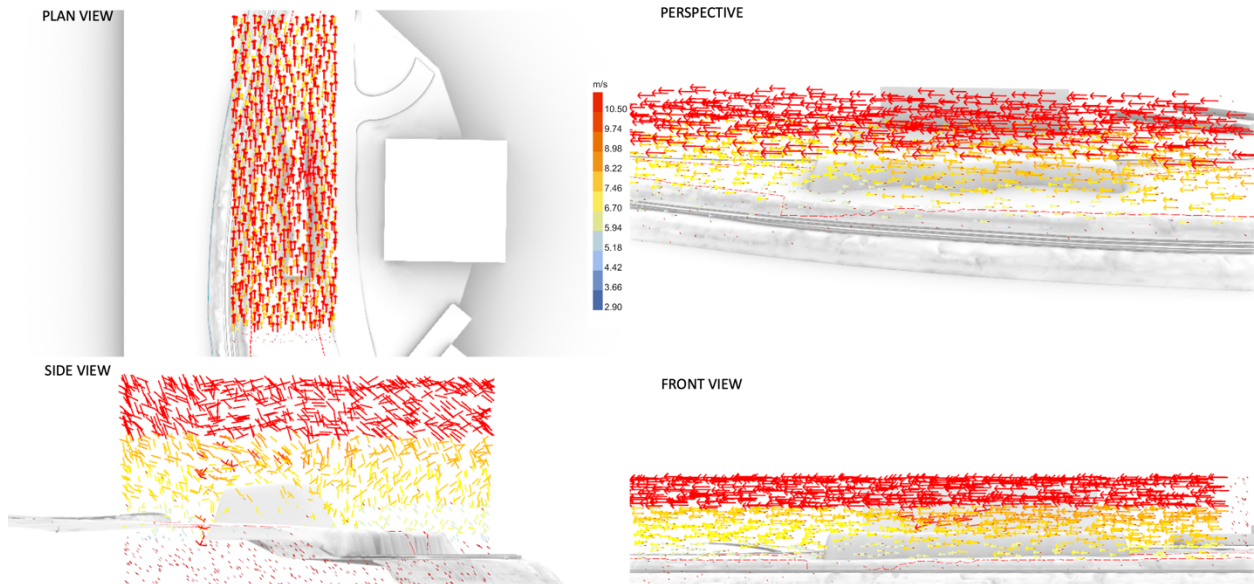


Figure 326. Wind simulation for Option 11. Plan view, perspective, side view, and front view.

OPTION 12
SOUTH WIND
10.5 m/s wind speed

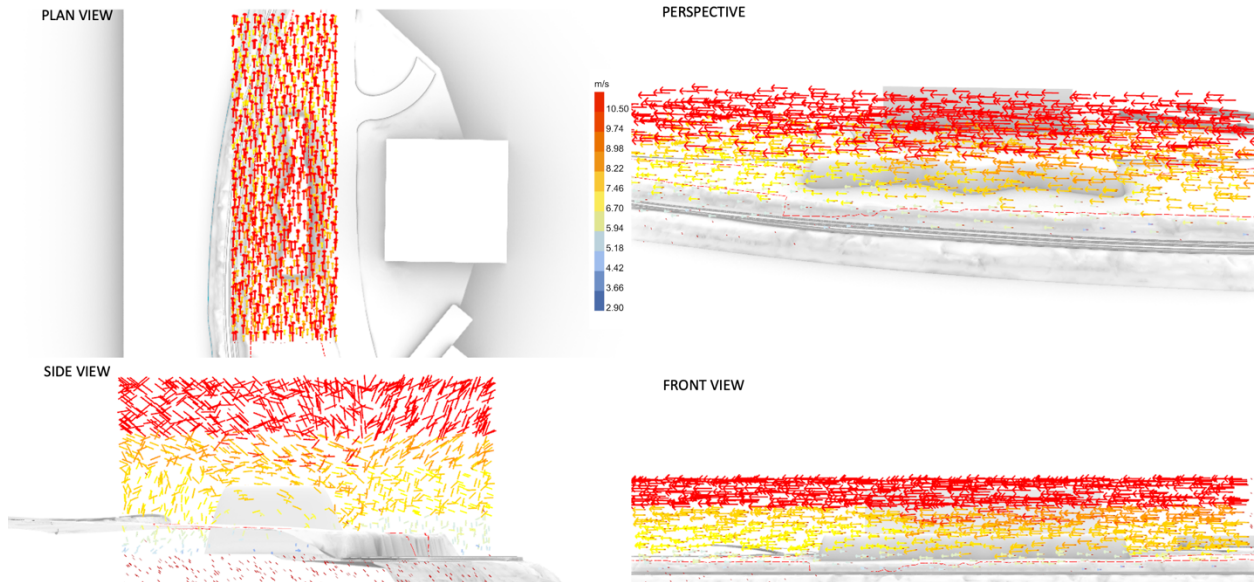


Figure 327. Wind simulation for Option 12. Plan view, perspective, side view, and front view.

OPTION 13
SOUTH WIND
10.5 m/s wind speed

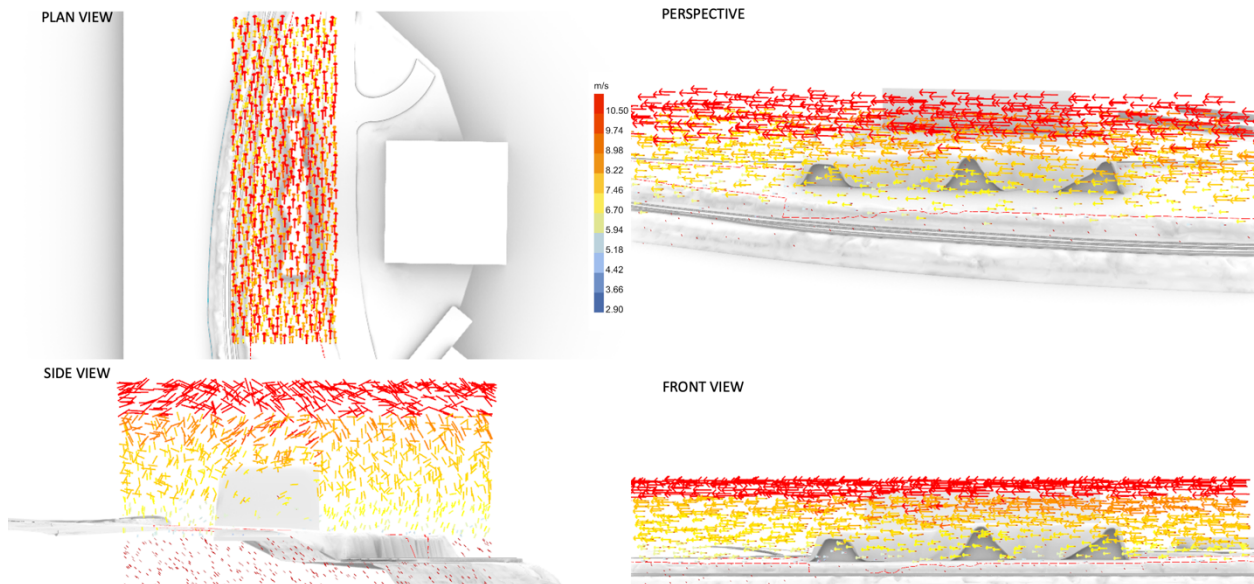


Figure 328. Wind simulation for Option 13. Plan view, perspective, side view, and front view.

WIND SIMULATION
Scenario 3

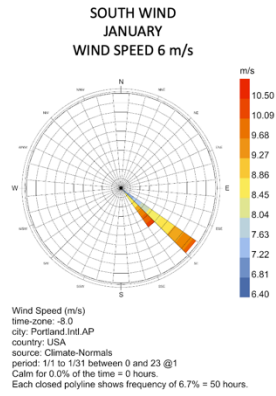


Figure 329. Wind simulation Scenario 3.

Wind rose for a south wind in January with wind speed of 6 m/s.

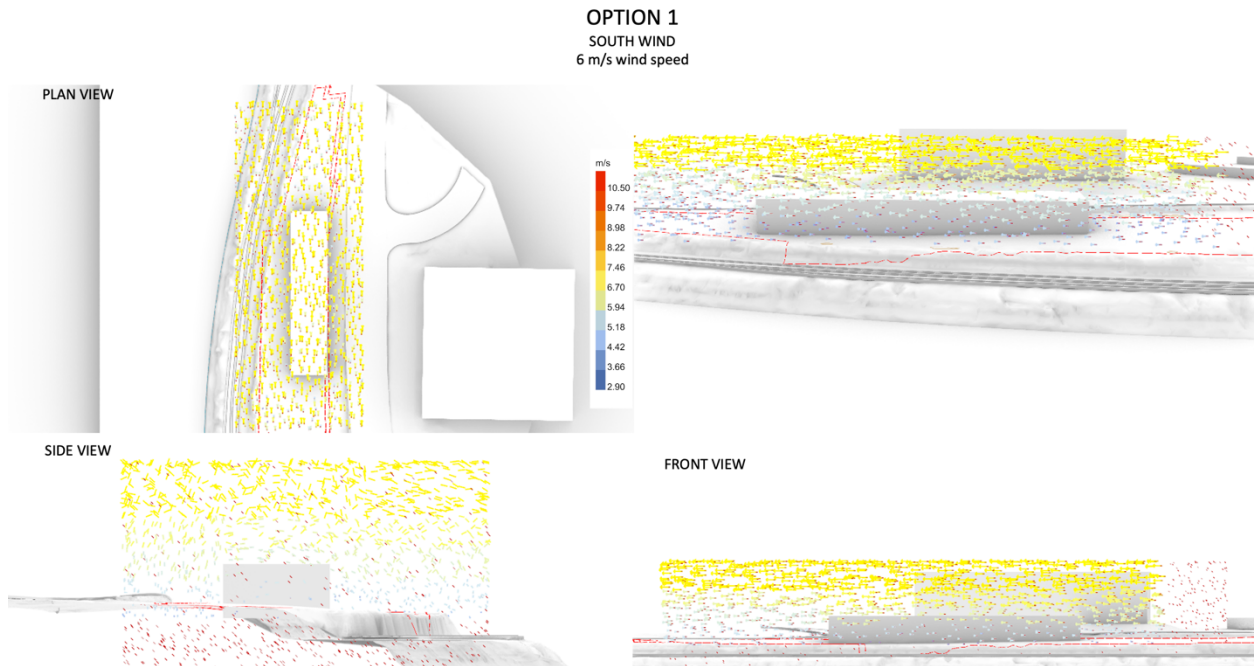


Figure 330. Wind simulation for Option 1. Plan view, perspective, side view, and front view.

OPTION 2
SOUTH WIND
6 m/s wind speed

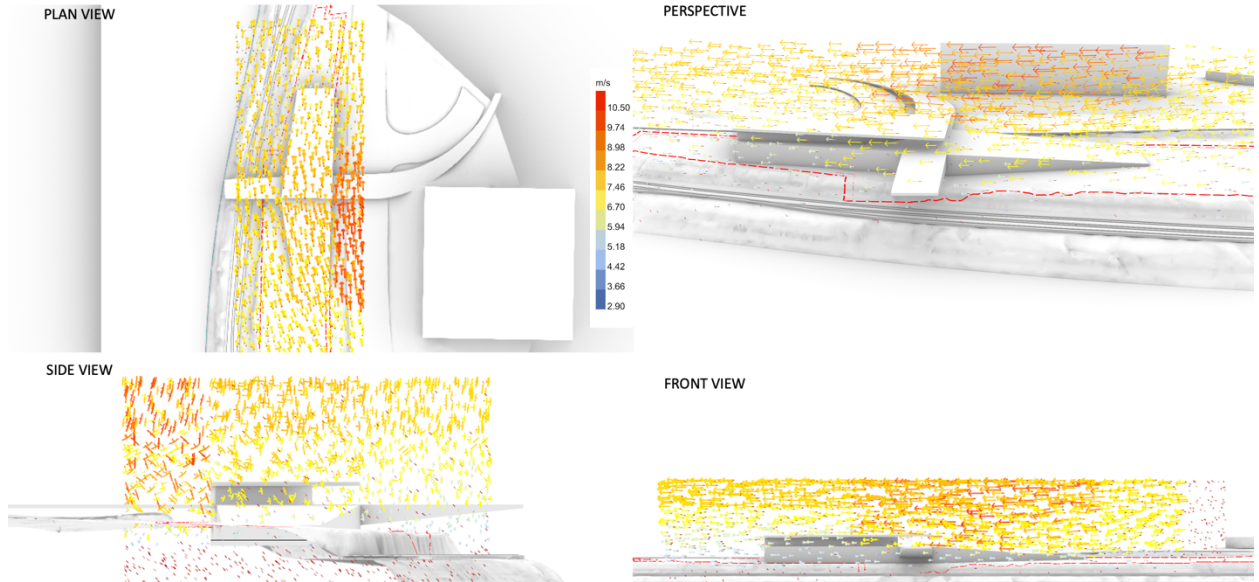


Figure 331. Wind simulation for Option 2. Plan view, perspective, side view, and front view.

OPTION 3
SOUTH WIND
6 m/s wind speed

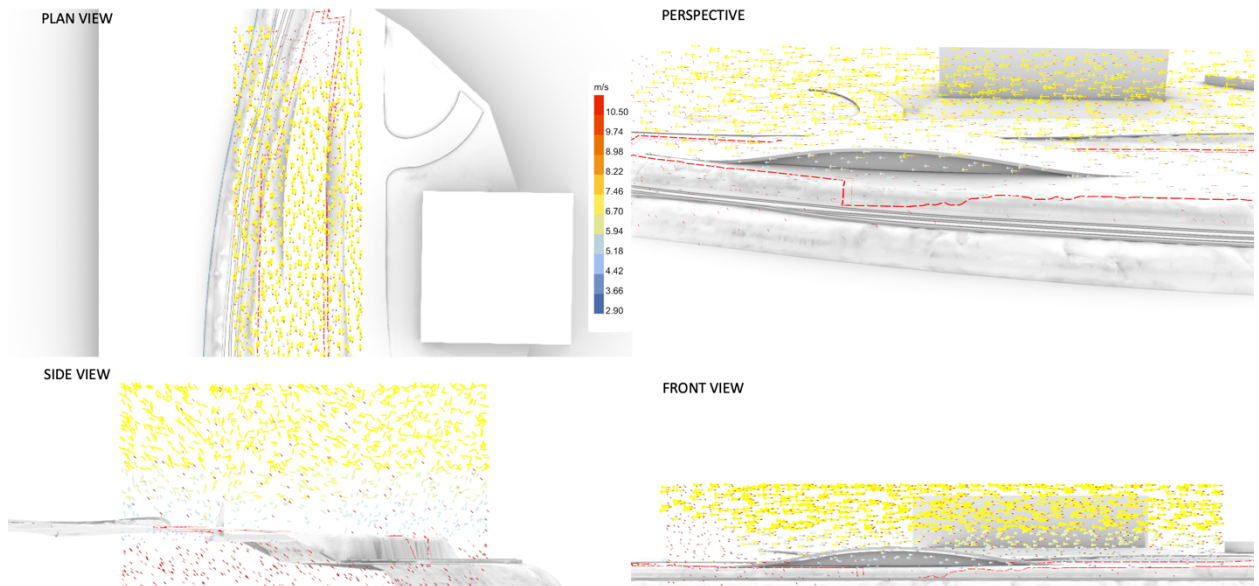


Figure 332. Wind simulation for Option 3. Plan view, perspective, side view, and front view.

OPTION 4
SOUTH WIND
6 m/s wind speed

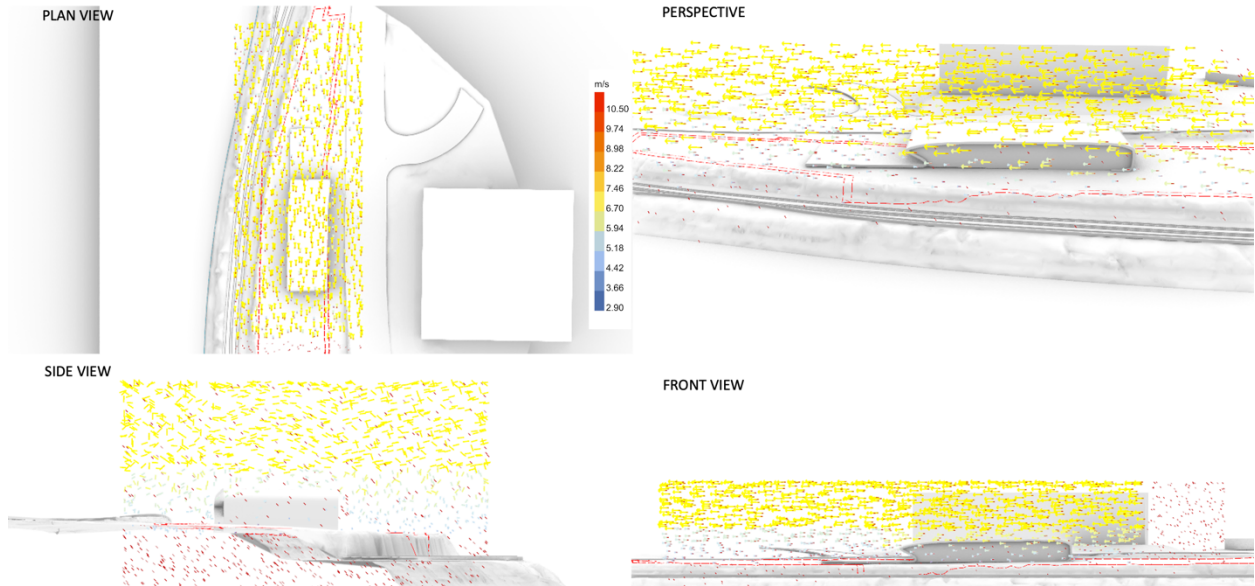


Figure 333. Wind simulation for Option 4. Plan view, perspective, side view, and front view.

OPTION 5
SOUTH WIND
6 m/s wind speed

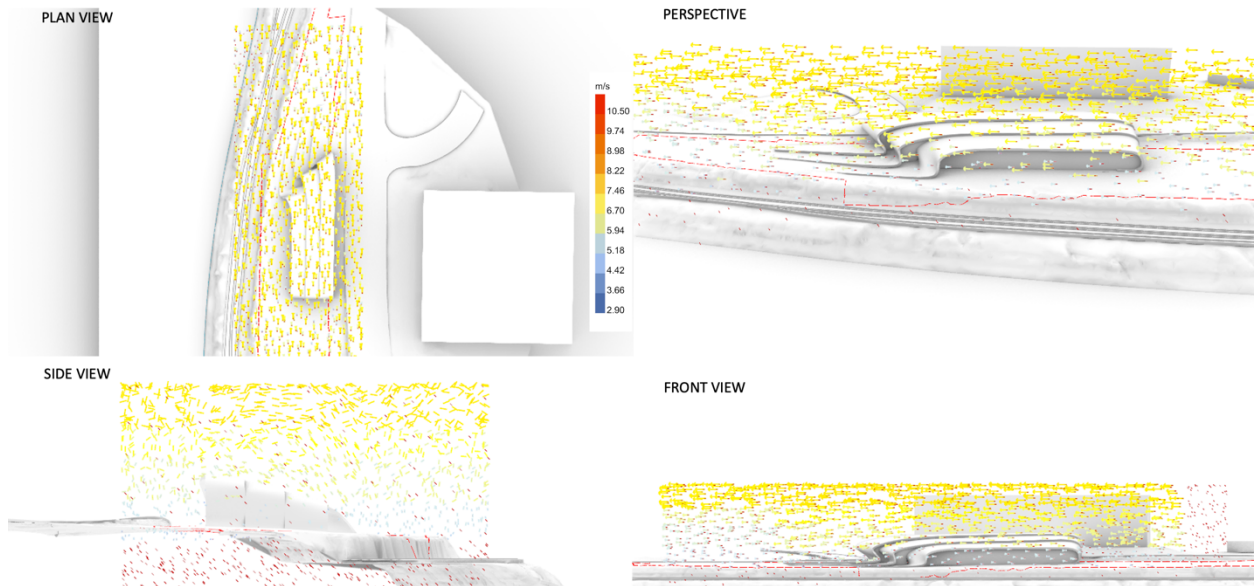


Figure 334. Wind simulation for Option 5. Plan view, perspective, side view, and front view.

OPTION 6
SOUTH WIND
6 m/s wind speed

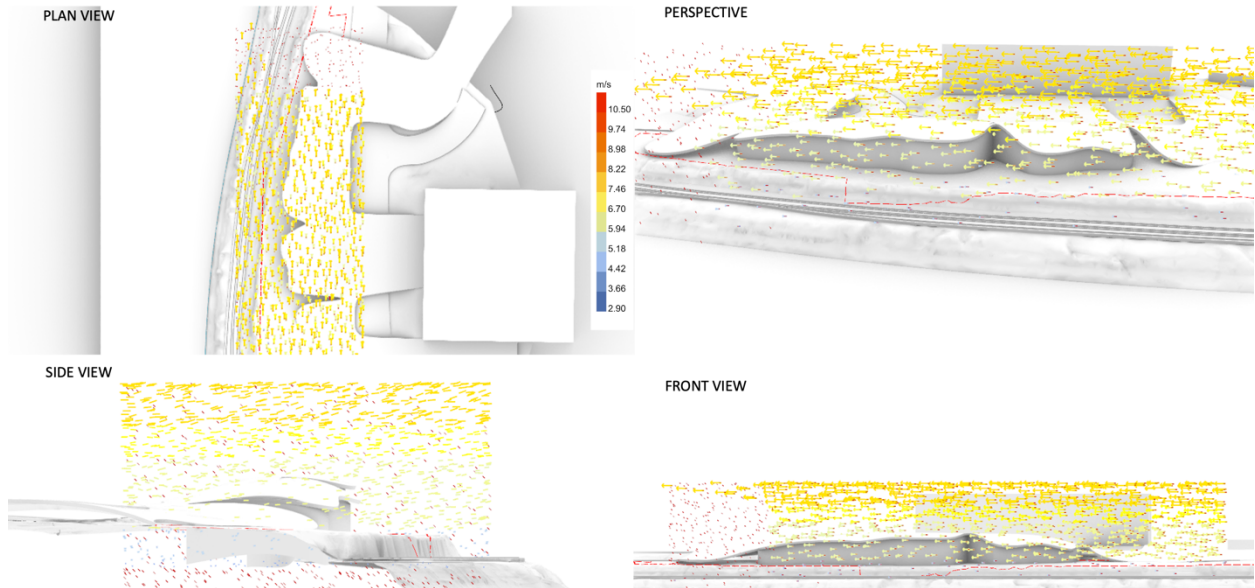


Figure 335. Wind simulation for Option 6. Plan view, perspective, side view, and front view.

OPTION 7
SOUTH WIND
6 m/s wind speed

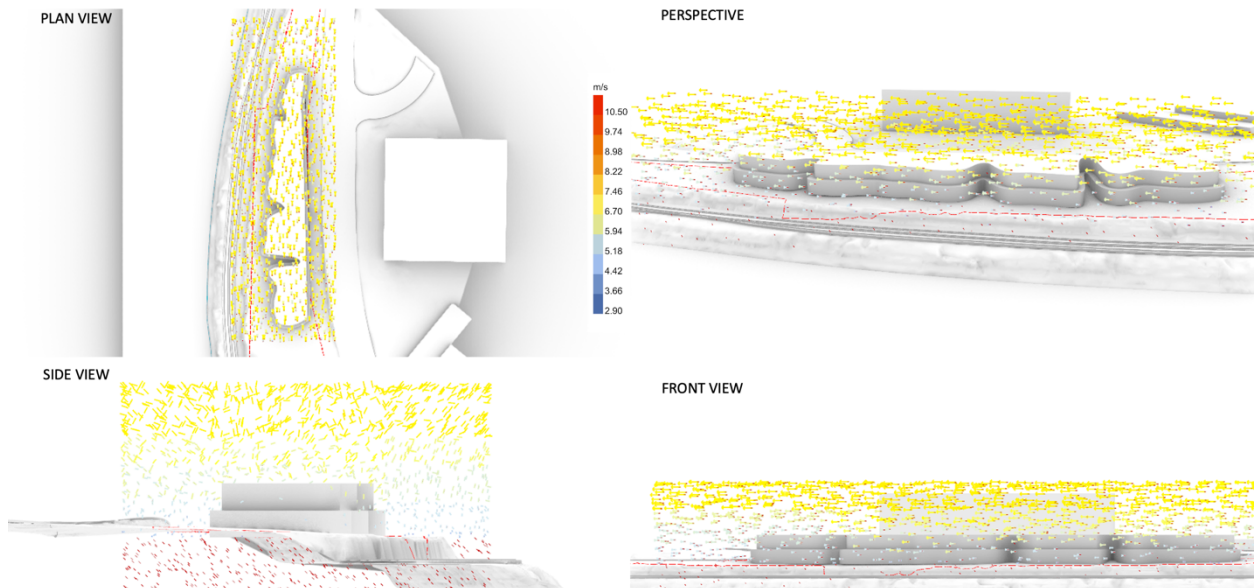


Figure 336. Wind simulation for Option 7. Plan view, perspective, side view, and front view.

OPTION 8
SOUTH WIND
6 m/s wind speed

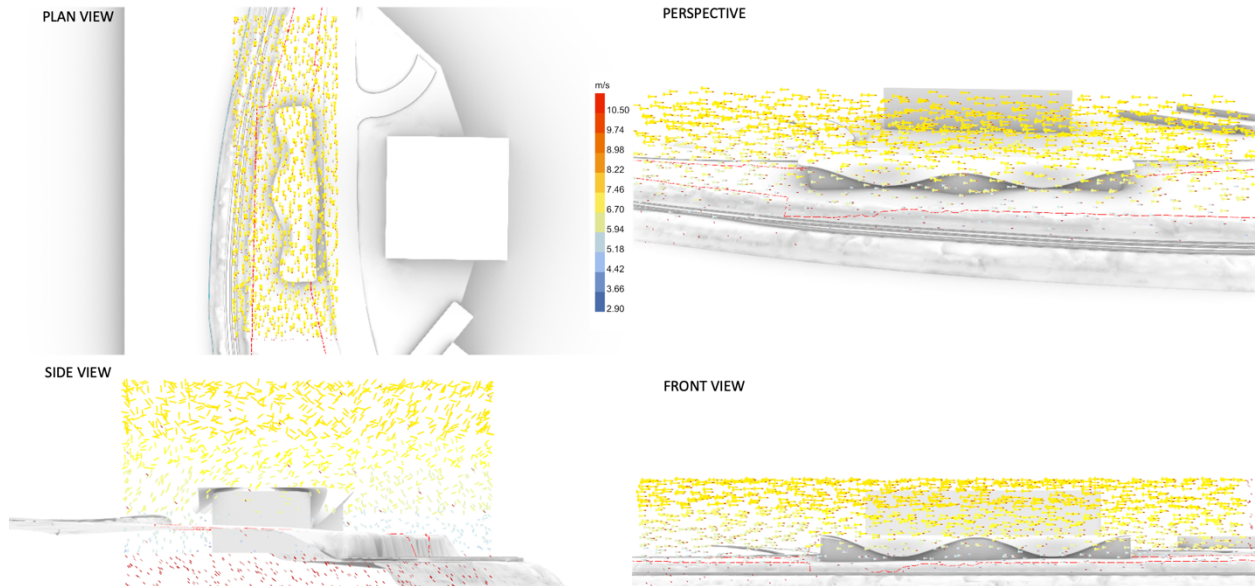


Figure 337. Wind simulation for Option 8. Plan view, perspective, side view, and front view.

OPTION 9
SOUTH WIND
6 m/s wind speed

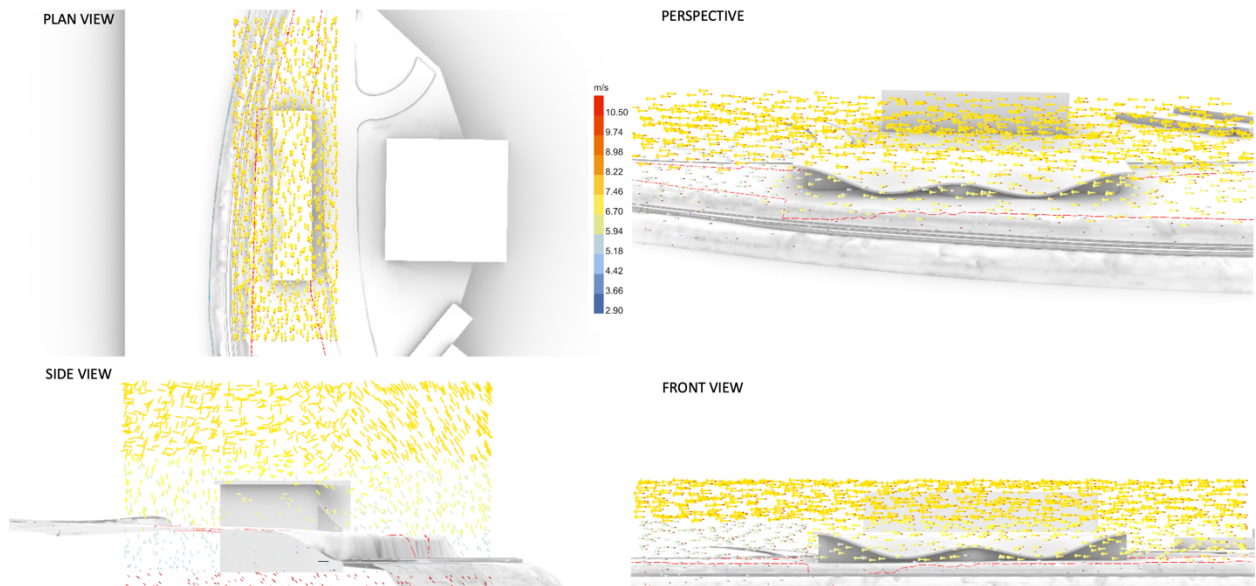


Figure 338. Wind simulation for Option 9. Plan view, perspective, side view, and front view.

OPTION 10
SOUTH WIND
6 m/s wind speed

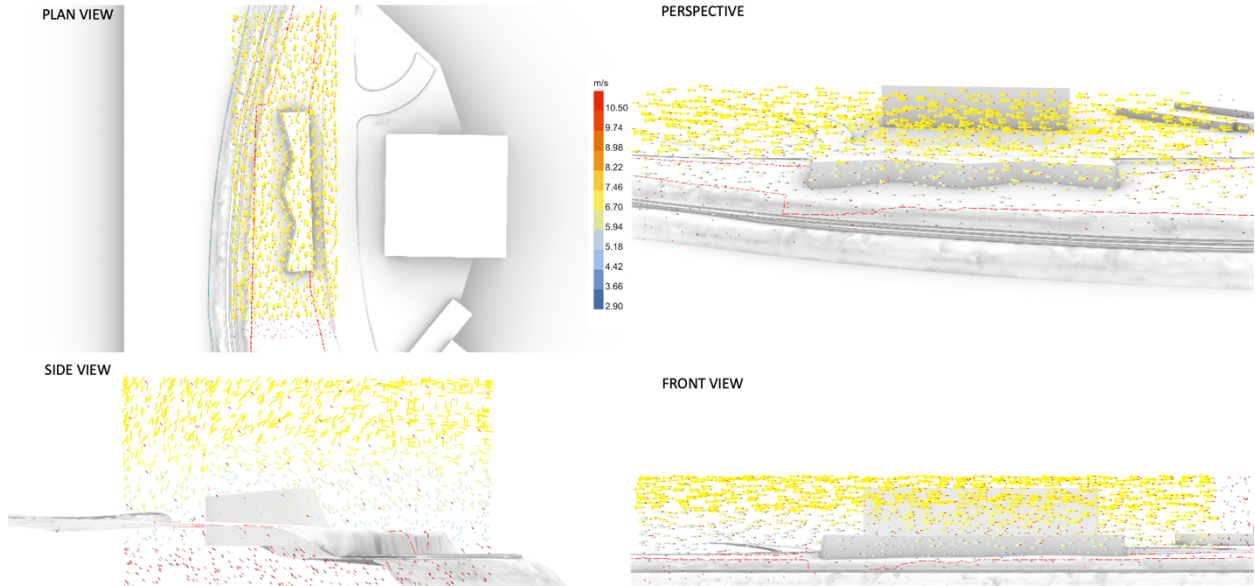


Figure 339. Wind simulation for Option 10. Plan view, perspective, side view, and front view.

OPTION 11
SOUTH WIND
6 m/s wind speed

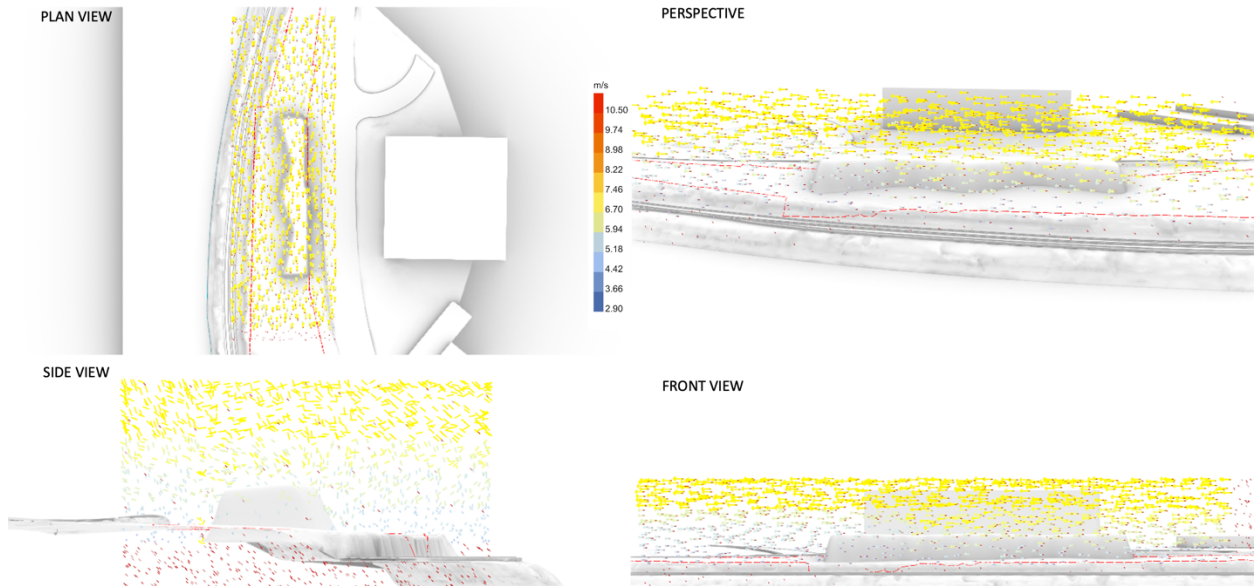


Figure 340. Wind simulation for Option 11. Plan view, perspective, side view, and front view.

OPTION 12
SOUTH WIND
6 m/s wind speed

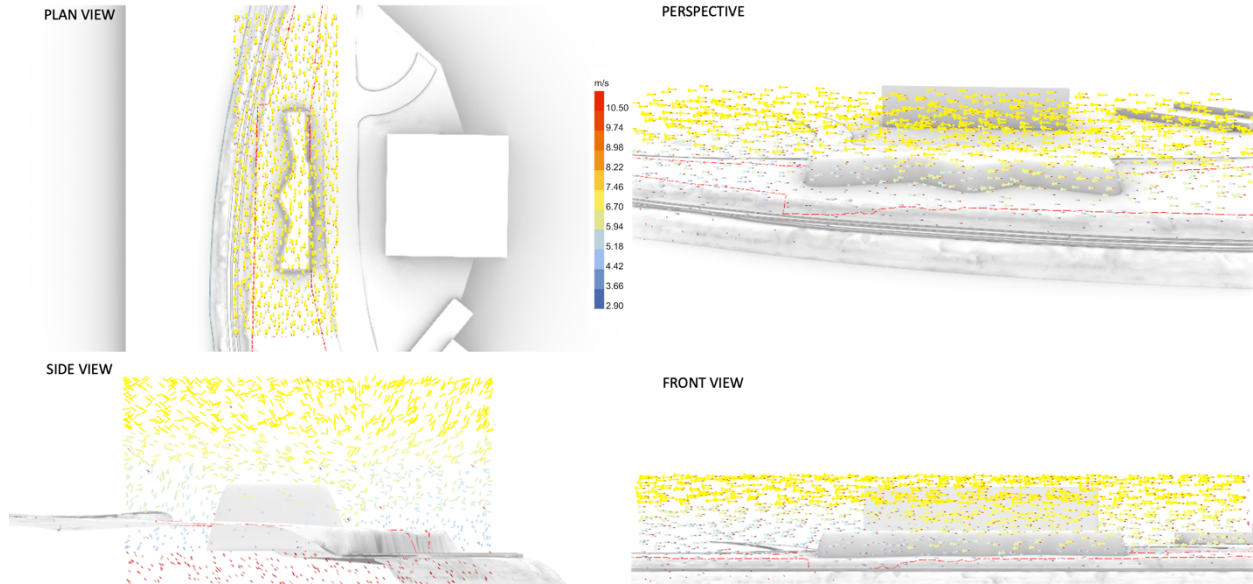


Figure 341. Wind simulation for Option 12. Plan view, perspective, side view, and front view.

OPTION 13
SOUTH WIND
6 m/s wind speed

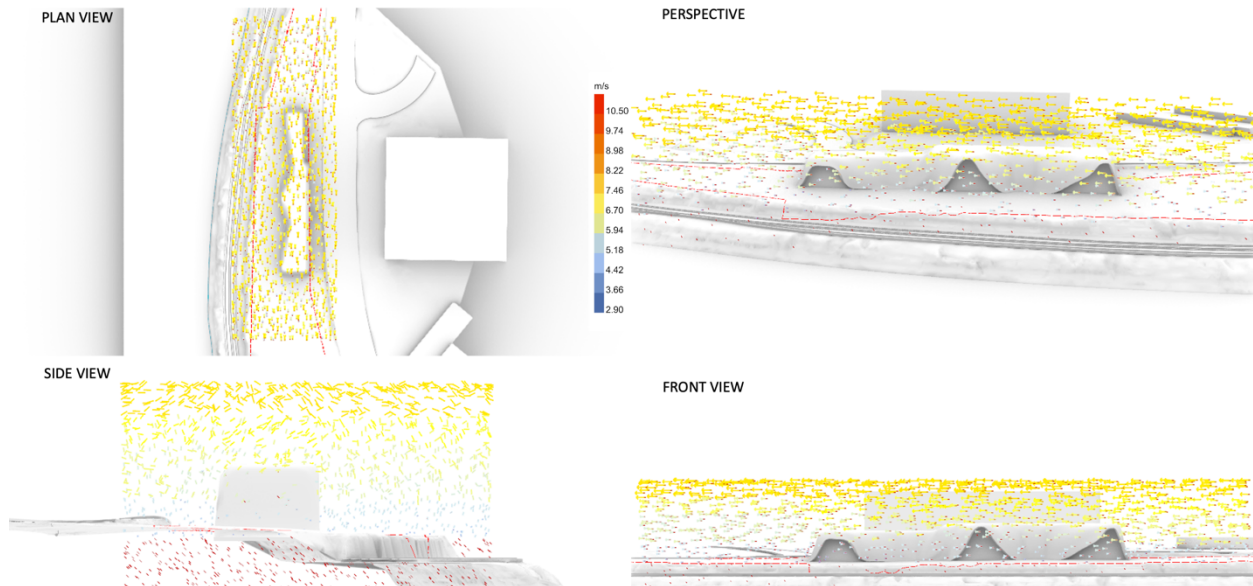
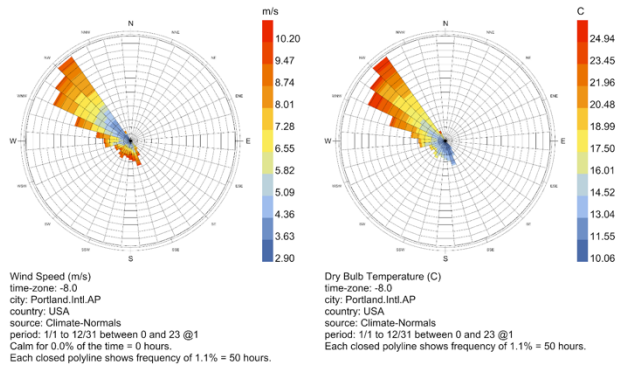


Figure 342. Wind simulation for Option 13. Plan view, perspective, side view, and front view.



Prevailing

Figure 343. Wind simulation Scenario 4.

Wind rose for a prevailing north wind with wind speed of 10 m/s.

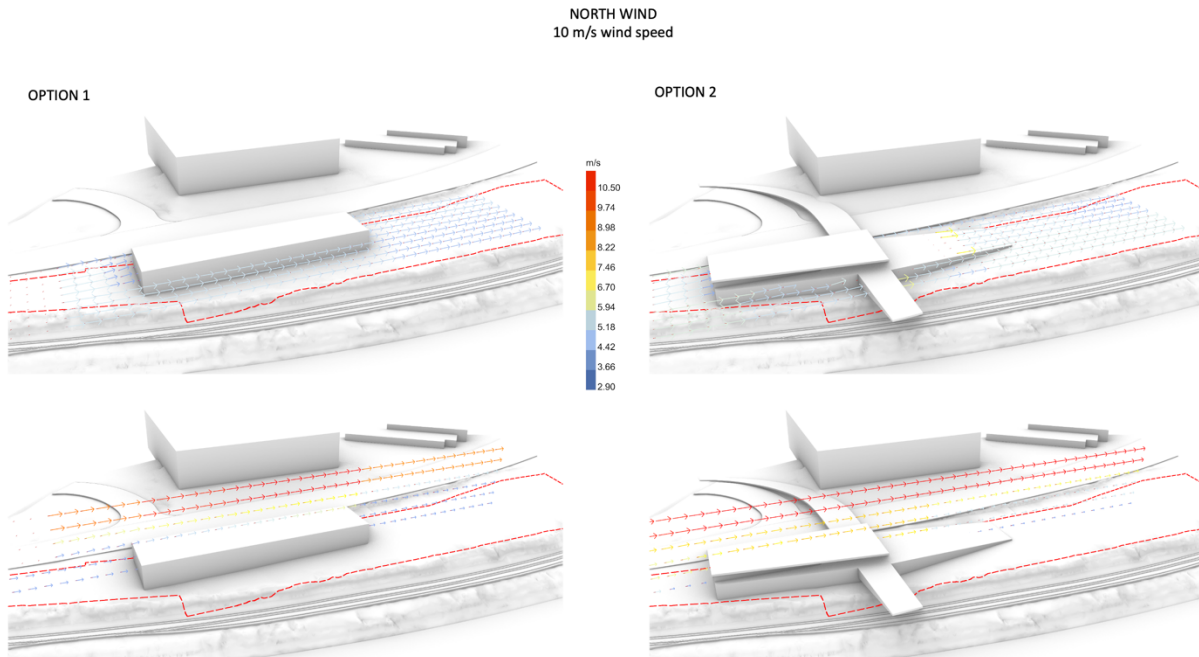


Figure 344. Wind simulation for Option 1 and 2. Perspective view with horizontal wind vectors and vertical wind vectors.

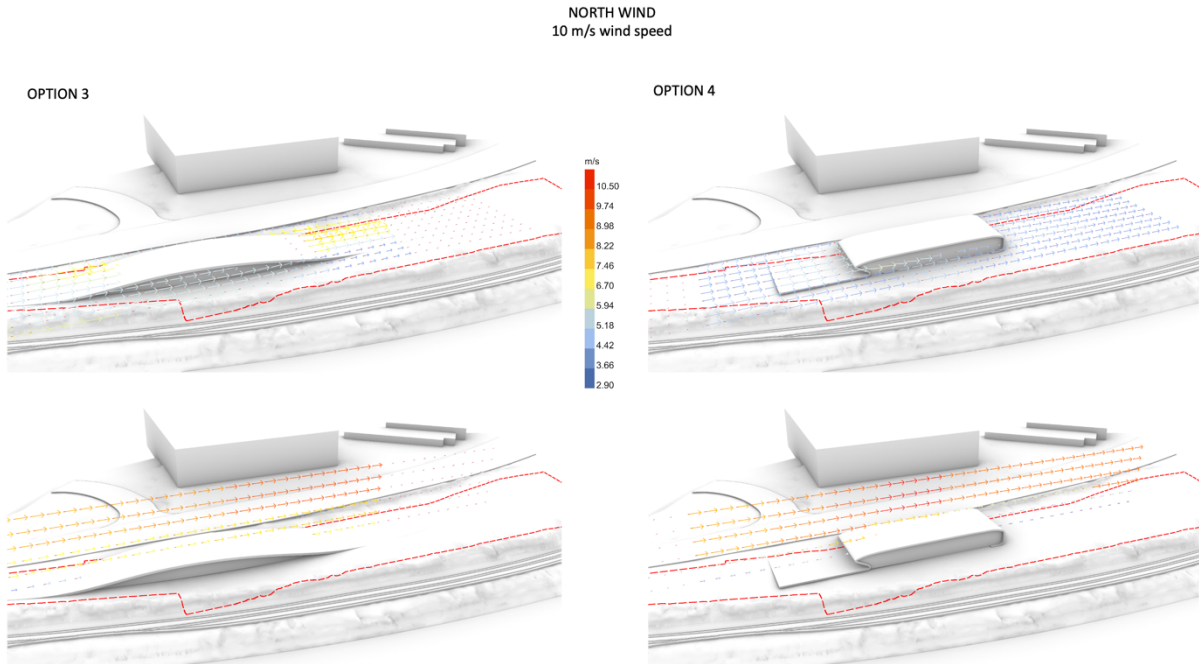


Figure 345. Wind simulation for Option 3 and 4. Perspective view with horizontal wind vectors and vertical wind vectors.

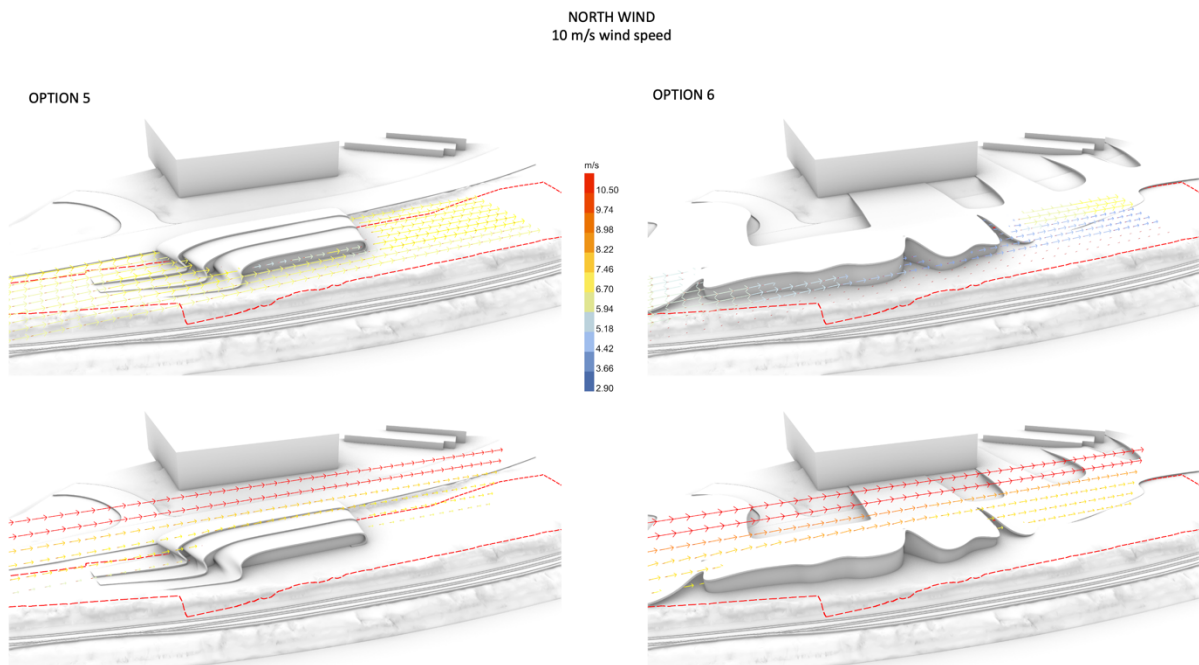


Figure 346. Wind simulation for Option 5 and 6. Perspective view with horizontal wind vectors and vertical wind vectors.

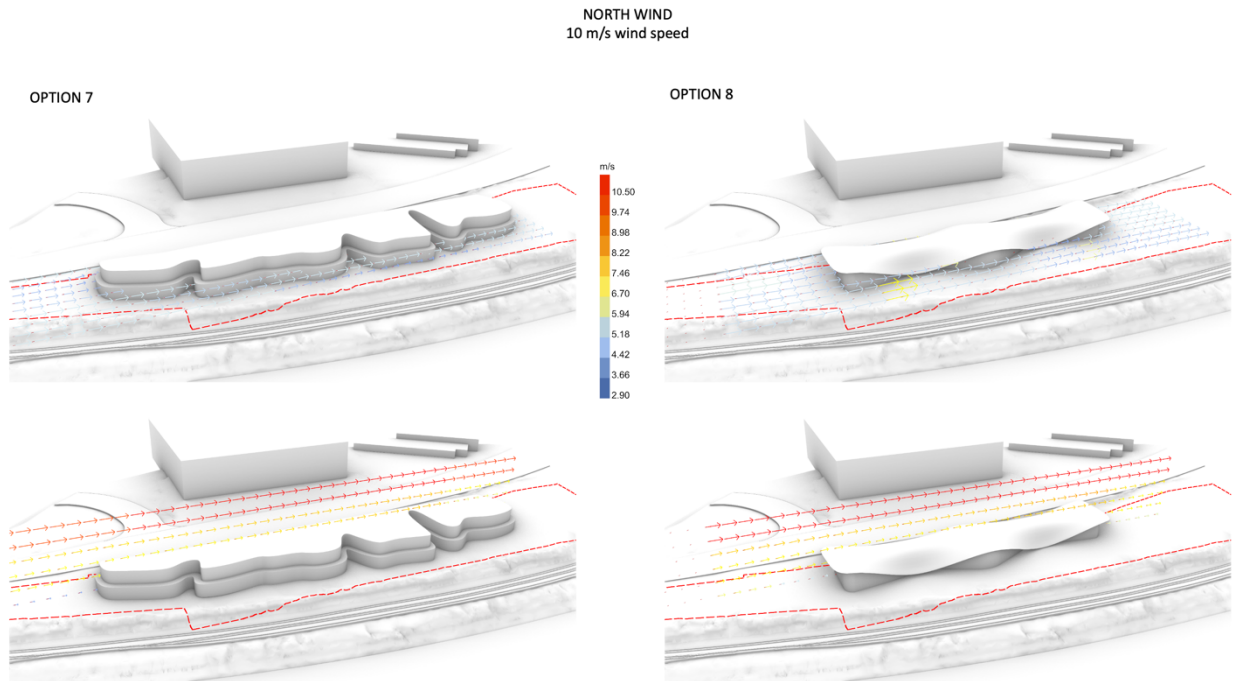


Figure 347. Wind simulation for Option 7 and 8. Perspective view with horizontal wind vectors and vertical wind vectors.

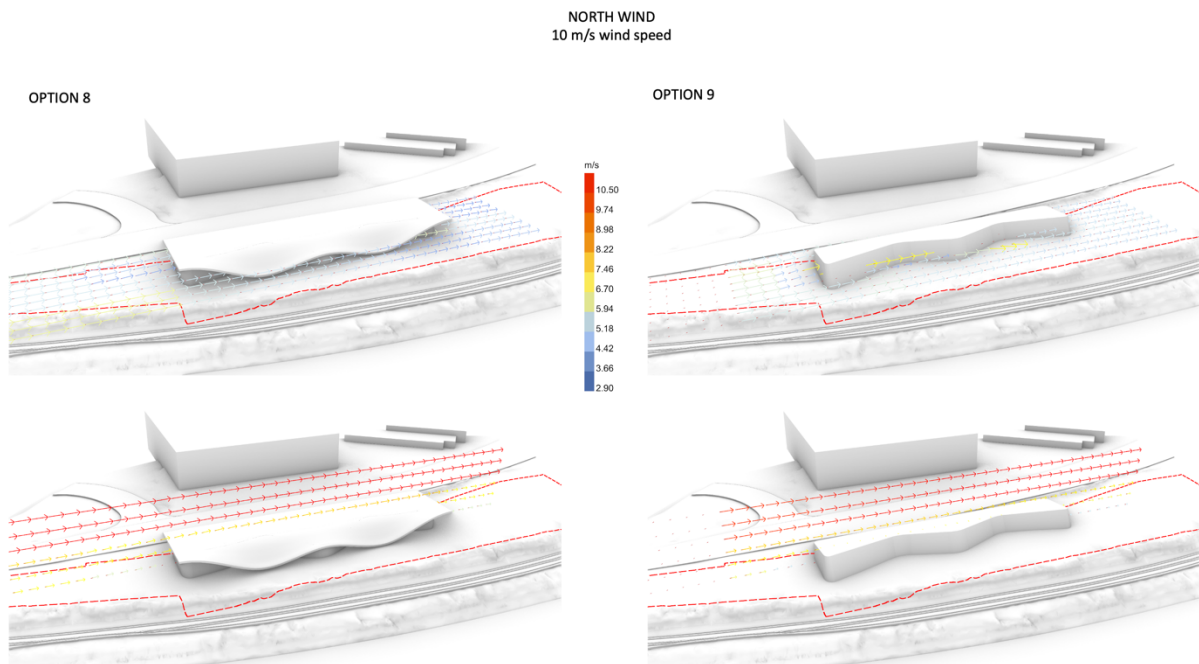


Figure 348. Wind simulation for Option 8 and 9. Perspective view with horizontal wind vectors and vertical wind vectors.

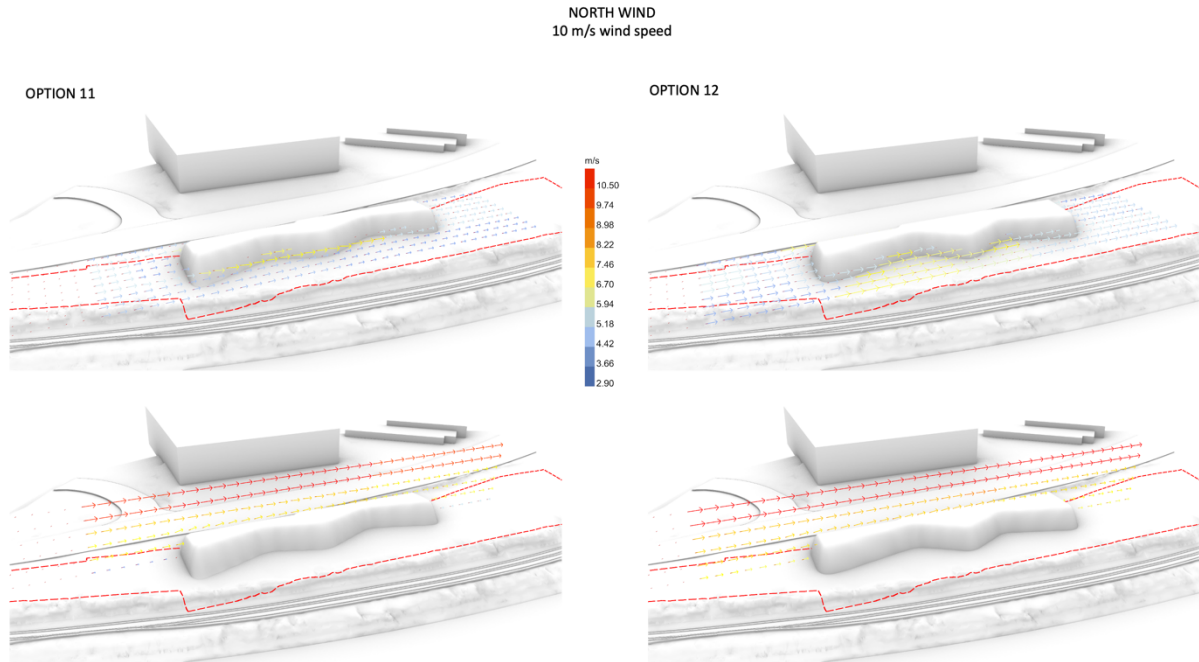


Figure 349. Wind simulation for Option 11 and 12. Perspective view with horizontal wind vectors and vertical wind vectors.

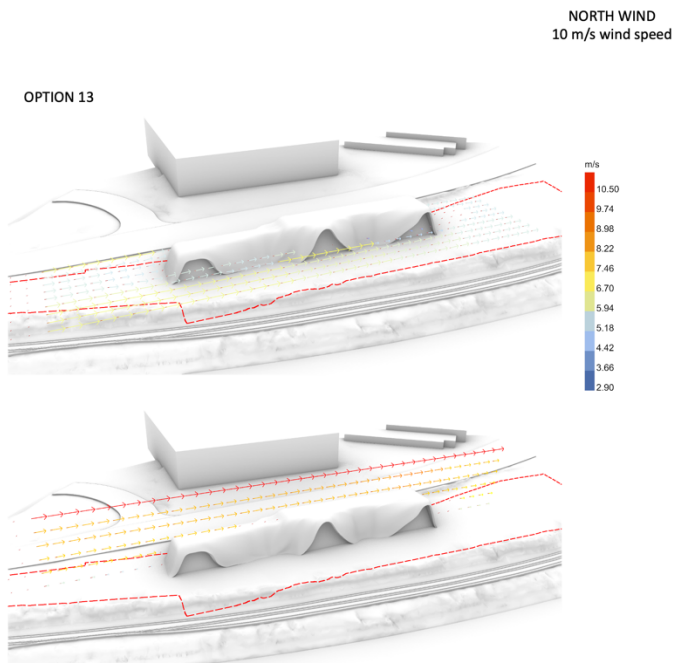


Figure 350. Wind simulation for Option 13. Perspective view with horizontal wind vectors and vertical wind vectors.

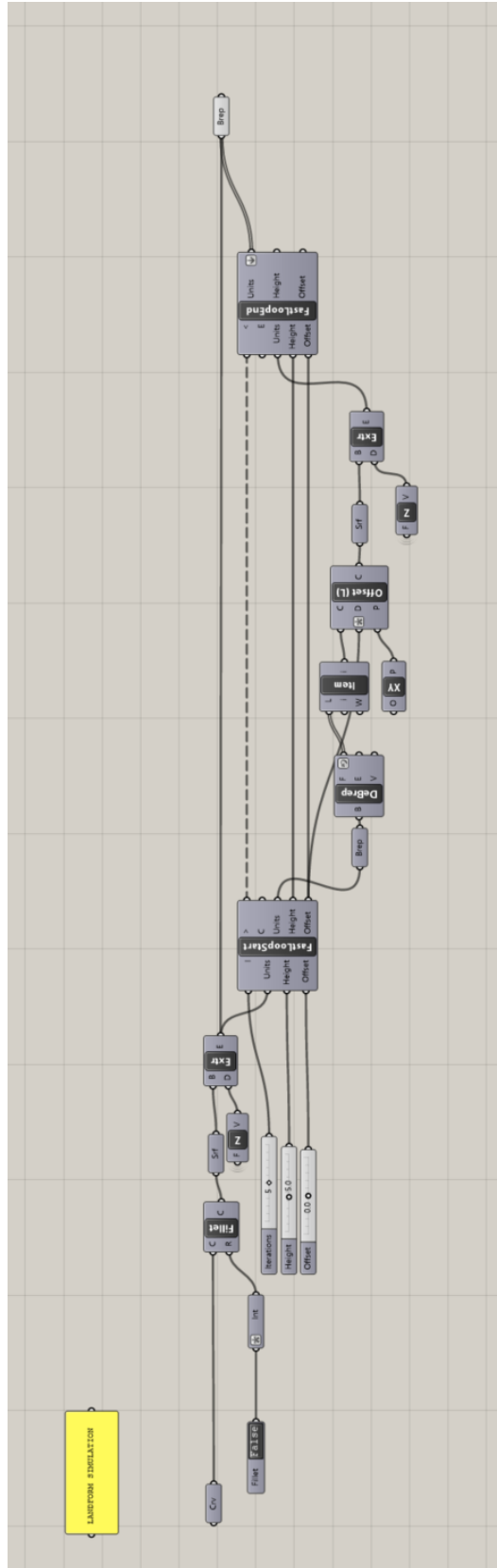


Figure 353. Definition for geomorphological simulation in Grasshopper.

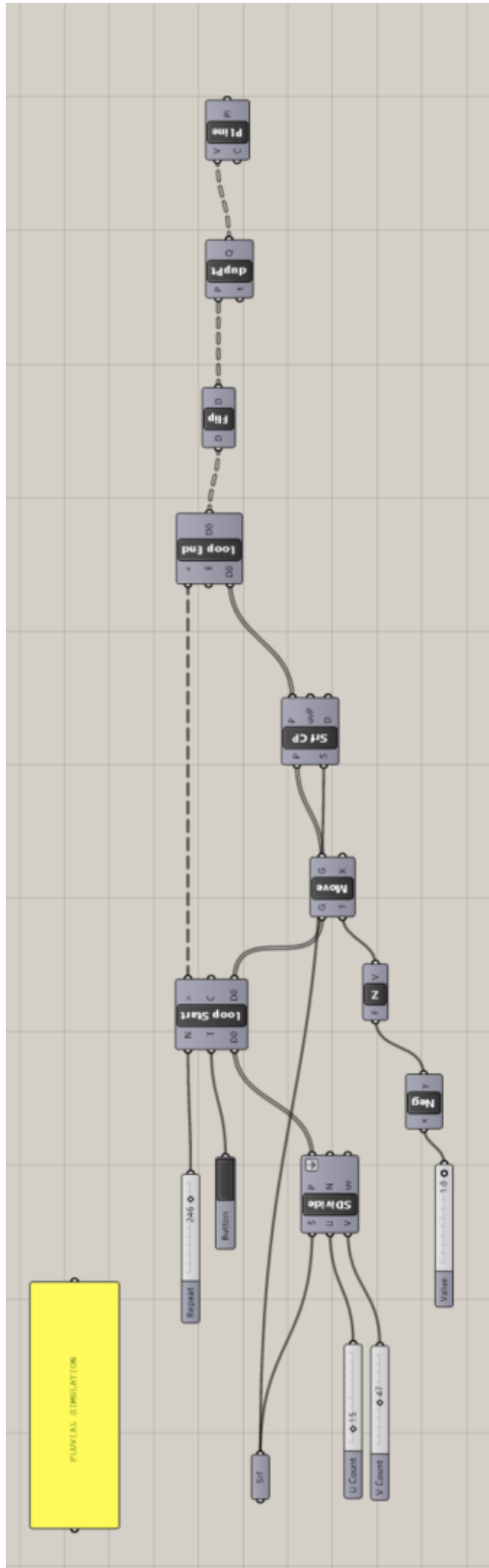


Figure 354. Definition for hydrological simulation in Grasshopper.

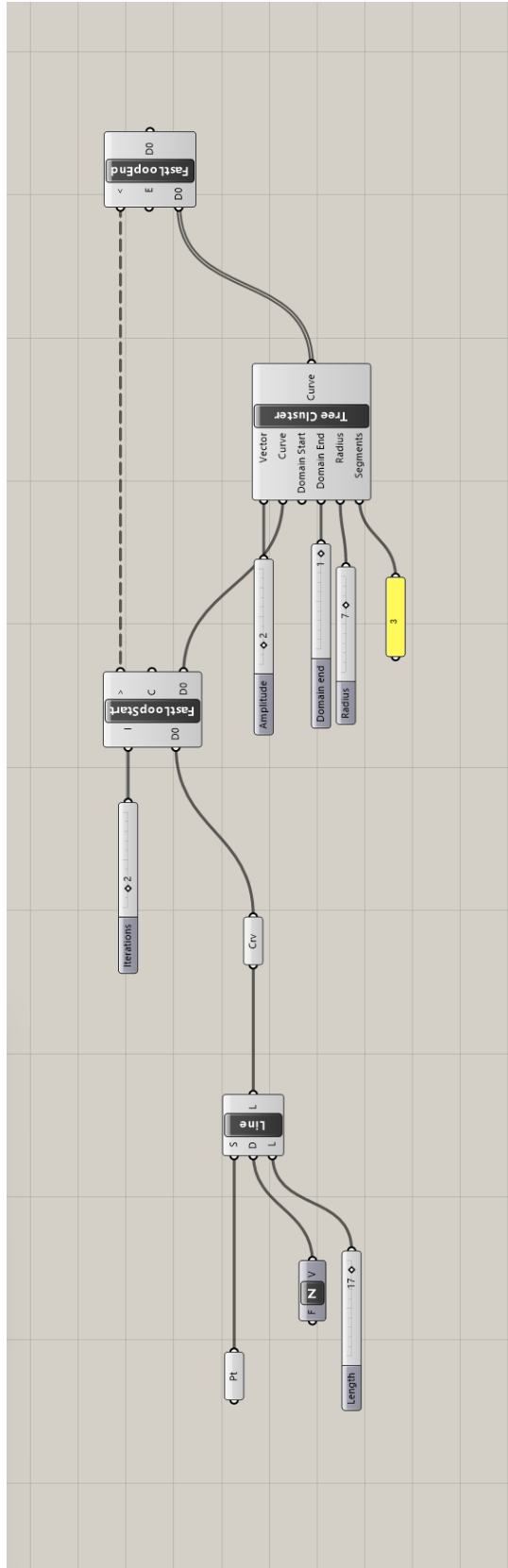


Figure 356. Definition for vegetation simulation in Grasshopper.

REFERENCES CITED

- Abbott, C. (2022). Port of Portland. *Oregon encyclopedia*. Retrieved December 5, 2023, from https://www.oregonencyclopedia.org/articles/port_of_portland/
- Aero Service Corp. *DFO*. 5D-76. [Aerial photograph]. 1:20,000. Philadelphia, PA: U.S. Department of Agriculture, Production and Marketing Administration, July 24, 1948. Retrieved from University of Oregon Libraries, Aerial Photography Collection. (n.d.).
- Ackley, B. (2016). Le Corbusier's Algerian fantasy: Blocking the casbah. *Bidoun*. Retrieved March 29, 2025, from <https://www.bidoun.org/articles/le-corbusier-s-algerian-fantasy>
- Albina Vision Trust. (n.d.-a). *Clean energy & environment*. <https://www.albinavisioninc.com/clean-energy-environmental-sustainability>
- Albina Vision Trust. (n.d.-b). *Restorative redevelopment*. <https://www.albinavisioninc.com/restorative-redevelopment>
- Allegrini, J., Dorer, V., & Carmeliet, J. (2015). Influence of morphologies on the microclimate in urban neighbourhoods. *Journal of Wind Engineering and Industrial Aerodynamics*, *144*, 108–117. <https://doi.org/10.1016/j.jweia.2015.03.024>
- Allen, S. & McQuade, M. (Eds.). (2011). *Landform building: Architecture's new terrain*. Lars Müller; Princeton University.
- Al-Najjar, S. F. & Al-Azhari, W. W. (2021). Review of aerodynamic design configurations for wind mitigation in high-rise buildings: Two cases from Amman. *Civil Engineering and Architecture*, *9*(3), 708–720. <https://doi.org/10.13189/cea.2021.090313>
- Amadeo, K. (2020, February 19). *President John F. Kennedy's economic policies. What were they, and how do they affect you today?*. (n.d.). The Balance. Retrieved May 25, 2022, from <https://www.thebalance.com/president-john-f-kennedy-s-economic-policies-3305560>
- Ancient Origins. (n.d.). *Discovering the majestic hillfort of Maiden Castle (Video)*. <https://www.ancient-origins.net/videos/maiden-castle-hillfort-0018857>
- Anderson, J. R. & Ortega, D. H. (Eds.). (2016). *Innovations in landscape architecture*. Routledge, Taylor & Francis Group.
- ArchDaily. (n.d.). *Underground Parking Katwijk aan Zee / Royal haskoningDHV*. Retrieved March 29, 2025, from <https://www.archdaily.com/791812/underground-parking-katwijk-aan-zee-royal-haskoningdhv>
- ArchDaily. (2013, March 3). *Landfill Reclamation: Fresh Kills Park develops as a natural coastal buffer and parkland for Staten Island*. <https://www.archdaily.com/339133/landfill-reclamation-fresh-kills-park-develops-as-a-natural-coastal-buffer-and-parkland-for-staten-island>
- Archer, B. (1995). The Nature of research. *CoDesign: International Journal of Cocreation in Design and the Arts*. <https://www.scribd.com/document/268010001/The-Nature-of-Research-Bruce-Archer-1995>

- Arifwidodo, S. D. & Tanaka, T. (2015). The characteristics of urban heat island in Bangkok, Thailand. *Procedia - Social and Behavioral Sciences*, 195, 423–428.
<https://doi.org/10.1016/j.sbspro.2015.06.484>
- Arquitectura Viva. (2022, February 7). *A critical story—Kenneth Frampton*.
<https://arquitecturaviva.com/articles/una-historia-critica>
- Baniotopoulos, C. (2011). *Environmental wind engineering and design of wind energy structures*. Springer Wien.
- Beardsley, J. (2006). *Earthworks and beyond: Contemporary art in the landscape* (4th ed). Abbeville Press.
- Belanger, P. (2016). *Landscape as infrastructure: A base primer* (0 ed.). Routledge.
<https://doi.org/10.4324/9781315629155>
- Belesky, P. (2018). *Testing terrain: Exploring the computational design of natural systems in landscape architecture* (PhD thesis). RMIT University.
- Berrizbeitia, A. (2007). Re-placing process. In J. Czerniak & G. Hargreaves (Eds.), *Large parks*. Princeton Architectural Press.
- Berrizbeitia, A. (2016). *On the limits of process: The case for precision in landscape [S07—29AB]*. *Scribd*. Retrieved February 25, 2023, from <https://ru.scribd.com/document/406065595/S07-29ABR-Berrizbeitia-On-the-Limits-of-Process-2016>
- Blazejczyk, K., Nilsson, H., & Holmér, I. (1993). Solar heat load on man: Review of different methods of estimation. *International Journal of Biometeorology*, 37(3), 125–132.
<https://doi.org/10.1007/BF01212621>
- Boettger, S. (2002). *Earthworks: Art and the landscape of the Sixties*. University of California Press.
- Bogdanović-Protić, I. & Mitković, M. (2015). Town planning parameters in the function of building energy efficiency. *Facta Universitatis - Series: Architecture and Civil Engineering*, 13(1), 1–9.
<https://doi.org/10.2298/FUACE1501001B>
- Booth, N. K. (1990). *Basic elements of landscape architectural design*. Waveland Press.
- Bourbon, F. (2007). *Petra: An archaeological guide: History, civilization and monuments*. Magnus.
- Brinkhuijsen, M. (2008). *Landscape 1:1: A study of designs for leisure in the Dutch countryside* [Doctoral dissertation, Wageningen University]. <https://library.wur.nl/webquery/wurpubs/375552>
- Brubaker Aerial Surveys. [BRU]. 89. [Aerial photograph]. [1:8,400]. Portland, OR: Brubaker Aerial Surveys, [1940]. Retrieved from University of Oregon Libraries, Aerial Photography Collection.
- Brunt, J. (2023). *Land art: Creating artworks in and with the landscape*. Schiffer Publishing.
- Butler, G. (2018, June 1). *Never-seen photos show how historic 1948 flood swamped Portland*. Oregonlive.com. https://www.oregonlive.com/news/erry-2018/06/4790f951283141/neverseen_photos_show_how_1948.html

- Candy, L. & Edmonds, E. (2018). Practice-based research in the creative arts: Foundations and futures from the front line. *Leonardo*, 51(1), Art. 1. https://doi.org/10.1162/LEON_a_01471
- Cantrell, B. & Holzman, J. (2016). *Responsive landscapes: Strategies for responsive technologies in landscape architecture* (First edition). Routledge.
- Cantrell, B. & Mekies, A. (Eds.). (2018). *Codify: Parametric and computational design in landscape architecture*. Routledge, Taylor & Francis Group.
- Carmo, M. (Ed.). (2013). *The digital turn in architecture 1992–2012*. Wiley.
- Carmo, M. (Ed.). (2015). Introduction: Twenty years of digital design. In *The digital turn in architecture 1992–2012* (pp. 8–14). John Wiley & Sons, Inc. <https://doi.org/10.1002/9781118795811.ch0>
- Carson, R. (1962). *Silent spring* (40th anniversary ed., 1st Mariner Books ed.). Houghton Mifflin.
- Carson, R., Steingraber, S., & Darling, L., (2018). *Silent spring & other writings on the environment*. The Library of America.
- Christy, J. A. & Alverson, E. R. (2011). Historical vegetation of the Willamette Valley, Oregon, circa 1850. *Northwest Science*, 85(2), 93–107. <https://doi.org/10.3955/046.085.0202>
- The City of Portland, Oregon. (n.d.). *Willamette River history: About the watershed*. <https://www.portlandoregon.gov/bes/article/231478>
- Climate-ADAPT. (n.d.-a). *Thermal comfort indices—Mean radiant temperature, 1979–2020*. Retrieved January 18, 2025, from <https://climate-adapt.eea.europa.eu/en/metadata/indicators/thermal-comfort-indices-mean-radiant-temperature-1979-2019>
- Climate-ADAPT. (n.d.-b). *Thermal comfort indices—Universal thermal climate index, 1979–2020*. Retrieved December 12, 2024, from <https://climate-adapt.eea.europa.eu/en/metadata/indicators/thermal-comfort-indices-universal-thermal-climate-index-1979-2019>
- Cochran, L. & American Society of Civil Engineers (Eds.). (2012). *Wind issues in the design of buildings*. American Society of Civil Engineers.
- Collins, H. (2019). *Creative research: The theory and practice of research for the creative industries* (2nd edition). Bloomsbury Visual Arts.
- Columbia Slough Watershed Council. (2020, August 27). *Urban heat islands: A peek into Portland's shady history*. <https://www.columbiaslough.org/blog/portland-urban-heat-islands>
- Commandeur, I. & Riemsdijk-Zandee, T. Van. (2012). *Robert Smithson, art in continual movement*. Alauda Publications.
- Corbo, S. (2020). *From formalism to weak form: The architecture and philosophy of Peter Eisenman*. Routledge.
- Corner, J. (Ed.). (1999). *Recovering landscape: Essays in contemporary landscape architecture*. Princeton Architectural Press.

- Corner, J. (2006). Terra Fluxus. In C. Waldheim (Ed.), *The Landscape Urbanism Reader*. Princeton Architectural Press.
- Corner, J. (2007). Foreword. In J. Czerniak & G. Hargreaves (Eds.), *Large parks*. Princeton Architectural Press.
- Courtright, J. (2021, March 22). *How ODOT destroyed Albina: The untold story*. City Observatory. <https://cityobservatory.org/how-odot-destroyed-albina-the-untold-story/>
- Cross, N. (2006). *Designerly ways of knowing*. Springer.
- Czerniak, J. (Ed.). (2001). *CASE: Downsview Park Toronto*. Prestel; Harvard University, Graduate School of Design.
- Czerniak, J., Hargreaves, G. & Harvard University (Eds.). (2007). *Large parks*. Princeton Architectural Press, in association with the Harvard University Graduate School of Design.
- Darke, J. (1979). The primary generator and the design process. *Design Studies*, 1(1), Art. 1. [https://doi.org/10.1016/0142-694X\(79\)90027-9](https://doi.org/10.1016/0142-694X(79)90027-9)
- Davis, D. (2013). *Modelled on software engineering: Flexible parametric models in the practice of architecture* [Unpublished doctoral dissertation]. RMIT University. https://www.danieldavis.com/papers/danieldavis_thesis.pdf
- Deitz, P. (2009). Machine in the garden: Charles Jencks's Garden of Scottish Worthies. *Architectural Record*. <https://www.architecturalrecord.com/articles/5704-machine-in-the-garden-charles-jencks-s-garden-of-scottish-worthies>
- Delano Aerial Surveys. *CM*. 10-54. [Aerial photograph]. 1:12,000. Portland, OR: Delano Aerial Surveys, June 22, 1961. Retrieved from University of Oregon Libraries, Aerial Photography Collection. (n.d.).
- Delano Aerial Surveys. *MET*. 12-49. [Aerial photograph]. 1:13,000. Portland, OR: Delano Aerial Surveys, September 23, 1964. Retrieved from University of Oregon Libraries, Aerial Photography Collection. (n.d.).
- Delano Aerial Surveys. *MET-71*. 1-6. [Aerial photograph]. 1:8,400. Portland, OR: Delano Aerial Surveys, February 16, 1971. Retrieved from University of Oregon Libraries, Aerial Photography Collection. (n.d.).
- Delano Aerial Surveys. *OHP*. 22-17. [Aerial photograph]. 1:9,600. Portland, OR: Delano Aerial Surveys, 1956. Retrieved from University of Oregon Libraries, Aerial Photography Collection. (n.d.).
- Delano Aerial Surveys. *C&GS*. W9572. [Aerial photograph]. 1:12,000. Portland, OR: Delano Aerial Surveys, September 2, 1963. Retrieved from University of Oregon Libraries, Aerial Photography Collection. (n.d.).
- Delano Photographics, Inc. *MET 75*. 12-13. [Aerial photograph]. 1:12,000. Portland, OR: Delano Photographics, Inc., September 18, 1975. Retrieved from University of Oregon Libraries, Aerial Photography Collection. (n.d.).

- Delano Photographics, Inc. *PO-80*. 10-29. [Aerial photograph]. 1:24,000. Portland, OR: Delano Photographics, Inc., April 26, 1980. Retrieved from University of Oregon Libraries, Aerial Photography Collection. (n.d.).
- Delano Photographics, Inc. *PO-86*. 10-15. [Aerial photograph]. 1:24,000. Portland, OR: Delano Photographics, Inc., June 13, 1986. Retrieved from University of Oregon Libraries, Aerial Photography Collection. (n.d.).
- Delano Photographics, Inc. *SBG-PORT-SI*. A-1. [Aerial photograph]. 1:8,400. Portland, OR: Delano Photographics, Inc., August 21, 1983. Retrieved from University of Oregon Libraries, Aerial Photography Collection. (n.d.).
- Deming, M. E. & Swaffield, S. R. (2011). *Landscape architecture research: Inquiry, strategy, design*. Wiley.
- Desvigne, M. & Imbert, D. (2019). *A Landscape Inventory: Michel Desvigne Paysagiste*. ORO editions.
- Dibling, K., Martin, J. K., Olson, M. S., & Webb, G. (2006). Photo essay: Guild's Lake industrial district: The process of change over time. *Oregon Historical Quarterly*, 107(1), 88–105.
- Downton, P. (2005). *Design research* (Reprinted). RMIT University Press.
- 1852 public land survey of Portland, Oregon [Map]. (n.d.). Data Basin. Retrieved March 29, 2025, from <https://databasin.org/datasets/2d7f52c2d6e147639d70b938368c38f1/>
- Eisenman Architects. (n.d.). *City of Culture of Galicia 2011*. <https://eisenmanarchitects.com/City-of-Culture-of-Galicia-2011>
- El Dorado. (n.d.). *Albina vision community investment plan*. Retrieved December 1, 2024, from <https://eldo.us/albina-vision-community-investment-plan>
- ElMalvaney. (2010, February 10). Before and after: Mississippi River Basin model. *Preservation in Mississippi*. <https://misspreservation.com/2010/02/10/before-and-after-mississippi-river-basin-model/>
- Encyclopædia Britannica. (n.d.-a). Petra. In *Britannica.com*. Retrieved March 29, 2025, from <https://www.britannica.com/place/Petra-ancient-city-Jordan>
- Encyclopædia Britannica. (n.d.-b). Stonehenge. In *Britannica.com*. Retrieved March 29, 2025, from <https://www.britannica.com/topic/Stonehenge>
- Fahy, B., Brenneman, E., Chang, H., & Shandas, V. (2019). Spatial analysis of urban flooding and extreme heat hazard potential in Portland, OR. *International Journal of Disaster Risk Reduction*, 39, 101117. <https://doi.org/10.1016/j.ijdr.2019.101117>
- Federal Emergency Management Agency (FEMA). (2013). *Local Mitigation Planning Handbook*. (n.d.). https://www.fema.gov/sites/default/files/2020-06/fema-local-mitigation-planning-handbook_03-2013.pdf

- Fondation Le Corbusier. (n.d.). *Projects > Urban planning, projects A,B,C,H, Algiers, Algeria, 1930*. Retrieved May 1, 2025, from <https://www.fondationlecorbusier.fr/en/work-architecture/projects-urban-planning-projects-abch-algiers-algeria-1930/>
- Fractal Foundation. (n.d.). *What is chaos theory?* <https://fractalfoundation.org/resources/what-is-chaos-theory/>
- Frampton, K. (1999). *Megaform as urban landscape / The 1999 Raoul Wallenberg Lecture*. University of Michigan College.
- Frampton, K. (2021). Megaform as urban landscape. *Journal of Delta Urbanism*, 2, Art. 2.
- Frayling, C. (1993). *Royal College of Art Research Papers. Volume 1, Number 1, 1993/4: Research in art and design*. Royal College of Art.
- Gayne, M. K. (2003). Japanese Americans at the Portland YWCA. *Journal of Women's History*, 15(3), 197–203. <https://doi.org/10.1353/jowh.2003.0067>
- Gibson, K. J. (2007). Bleeding Albina: A history of community disinvestment, 1940–2000. *Transforming Anthropology*, 15(1), 3–25. <https://doi.org/10.1525/tran.2007.15.1.03>
- Giroto, C. (2016). *The course of landscape architecture*. Thames & Hudson.
- Glanville, R. (2014). The sometimes uncomfortable marriages of design and research. In P. A. Rodgers & J. Yee (Eds.), *The Routledge Companion to Design Research* (1st ed., pp. 9–22). Routledge. <https://doi.org/10.4324/9781315758466-3>
- Glossary of Meteorology. (n.d.). *Stokes wave*. Retrieved May 2, 2025, from https://glossary.ametsoc.org/wiki/Stokes_wave
- Goldman Sachs. (2022, February 20). *Insights—Taking the heat: Making cities resilient to climate change*. <https://www.goldmansachs.com/insights/pages/taking-the-heat.html>
- Google Arts & Culture. (n.d.). *The Gold Pectoral of the Scythian Ruler*. Retrieved May 2, 2025, from <https://artsandculture.google.com/story/the-gold-pectoral-of-the-scythian-ruler/pwXRxnYztYpqiA>
- Gothein, M. L. S. (2014). *A history of garden art: From the earliest times to the present day. Volume 1* (W. P. Wright, Ed.; L. Archer-Hind, Trans.). Cambridge University Press.
- Graham, J., Berardi, U., Turnbull, G., & McKaye, R. (2020). Microclimate analysis as a design driver of architecture. *Climate*, 8(6), 72. <https://doi.org/10.3390/cli8060072>
- Grebogi, C., Ott, E., & Yorke, J. A. (1987). Chaos, strange attractors, and fractal basin boundaries in nonlinear dynamics. *Science*, 238(4827), 632–638. <https://doi.org/10.1126/science.238.4827.632>
- Greg Lynn Form. (n.d.). *Stranded Sears Tower*. <https://glform.com/buildings/stranded-sears-tower/>
- Guallart Architects. (n.d.). *Denia Mountain*. <https://www.guallart.com/projects/denia-mountain>
- Guallart, V. (2009). *Geologics: Geography, information, architecture*. Actar.

- Gustafson Porter + Bowman. (n.d.-a). *Cultuurpark Westergasfabriek*. <https://www.gp-b.com/cultuurpark-westergasfabriek>
- Gustafson Porter + Bowman. (n.d.-b). *Diana, Princess of Wales Memorial*. <https://www.gp-b.com/diana-princess-of-wales-memorial>
- Gustafson Porter + Bowman (n.d.-c). *Landform*. Retrieved August 15, 2022, from <https://heyzine.com/flip-book/0500653f84.html#page/1>
- Haddad, E. (2009). Charles Jencks and the historiography of post-modernism. *The Journal of Architecture*, 14(4), Art. 4. <https://doi.org/10.1080/13602360902867434>
- Hargreaves, G., Czerniak, J., Berrizbeitia, A., & Kelly, L. C. (2009). *Hargreaves: The alchemy of landscape architecture*. Thames & Hudson.
- Hargreaves Jones. (n.d.-a). *Byxbee Park* <https://www.hargreaves.com/work/byxbee-park/>
- Hargreaves Jones. (n.d.-b). *Guadalupe River Park*. <https://www.hargreaves.com/work/guadalupe-river-park/>
- Hargreaves Jones. (n.d.-c). *Landscape architect Vol. 2*. Retrieved March 29, 2025, from <https://www.hargreaves.com/ideas/landscape-architect-vol-2/>
- Hart, M. A. & Sailor, D. J. (2009). Quantifying the influence of land-use and surface characteristics on spatial variability in the urban heat island. *Theoretical and Applied Climatology*, 95(3–4), 397–406. <https://doi.org/10.1007/s00704-008-0017-5>
- Harvard GSD. (2016, April 19). *Anita Berrizbeitia, “On the limits of process: the case for precision in landscape”* [Video recording]. <https://www.youtube.com/watch?V=xbxd1iznh7i>
- Harvard Old Maps Online. (n.d.-a). *Portland-Vancouver and vicinity*. Old Maps Online. Retrieved March 29, 2025, from <https://www.oldmapsonline.org/en/maps/56e39759-44c1-4db4-a183-1b0c12103a9a?Year=1964&gid=41ee6874-2c07-4975-b3a8-94168d1d00b7#position=11.214/0/0>
- Harvard Old Maps Online. (n.d.-b). *Portland-Vancouver and vicinity by Geological Survey (U.S.)*. Retrieved May 2, 2025, from https://www.oldmapsonline.org/images/omo_share_img.jpg
- Harvey, J. W. & Phumiruk, D. (2017). *Maya Lin: Artist-architect of light and lines* (First Edition). Henry Holt and Company.
- Hedberg, D.-P. B. (2020). *Environmental history of Albina Neighborhood Improvement Committee’s tree program*. <https://static1.squarespace.com/static/5a403646f9a61e1bb326be98/t/5ef3867537c56873d6e43958/1593017982745/2020.01.3-OHC-Env.Hist.AlbinaTrees.pdf>
- Heritage Ireland. (n.d.). *Dún Aonghasa – Ancient Stone Fort*. <https://heritageireland.ie/places-to-visit/dun-aonghasa/>
- Hidden Architecture. (n.d.) *HtwoOexpo*. <https://hiddenarchitecture.net/htwoexpo/>
- Hobhouse, P. & Edwards, A. (2020). *The story of gardening*. Princeton Architectural Press.

- Holt/Smithson Foundation. (n.d.-a). *Amarillo Ramp*. <https://holtsmithsonfoundation.org/amarillo-ramp>
- Holt/Smithson Foundation. (n.d.-b). *Asphalt rundown*. Retrieved March 29, 2025, from <https://holtsmithsonfoundation.org/asphalt-rundown>
- Holt/Smithson Foundation. (n.d.-c). *Breaking Ground: Broken Circle/Spiral Hill* [Film]. <https://holtsmithsonfoundation.org/breaking-ground-broken-circlespiral-hill>
- Holt/Smithson Foundation. (n.d.-d). *Broken Circle/Spiral Hill*. <https://holtsmithsonfoundation.org/broken-circle-spiral-hill>
- Howett, C. (1977). New directions in environmental art. *Landscape Architecture*, 67(1), 38–46. JSTOR.
- Jacob, S. (2013). Faster, but slower. *Log*, 29, Art. 29. JSTOR.
- Jenkes, C. (n.d.). *The Scottish World*. Charles Jenks. Retrieved March 29, 2025, from <https://www.charlesjenks.com/projects-the-scottish-world>
- Jencks, C. (1973). *Modern movements in architecture*. Penguin.
- Jencks, C. (1987). Postmodern and late modern: The essential definitions. *Chicago Review*, 35(4), Art. 4. <https://doi.org/10.2307/25305377>
- Jencks, C. (Ed.). (1991). *The language of post-modern architecture* (6th, rev.enl. Ed). Academy Editions.
- Jencks, C. (2000, July 12). Jencks' theory of evolution, an overview of 20th century architecture. *Architectural Review*. <https://www.architectural-review.com/archive/jencks-theory-of-evolution-an-overview-of-20th-century-architecture>
- Jencks, C. (Ed.). (2002). *The new paradigm in architecture: The language of post-modernism* (7th ed.). Yale University Press.
- Jencks, C. (Ed.). (2005). *The garden of cosmic speculation—Charles Jencks* (1. Paperback ed.). Lincoln.
- Jencks, C. (2007). *Critical modernism: Where is post-modernism going?* Wiley.
- Jencks, C. (2011). *The universe in the landscape: Landforms*. Frances Lincoln.
- Jencks, C. (2015a). Nonlinear Architecture (1997). In M. Carpo (Ed.), *The Digital Turn in Architecture 1992–2012* (pp. 80–107). John Wiley & Sons, Inc. <https://doi.org/10.1002/9781118795811.ch6>
- Jencks, C. (2015b, March 12). In what style shall we build? *Architectural Review*. <https://www.architectural-review.com/essays/postmodernism/in-what-style-shall-we-build>
- Jencks, C., & Kropf, K. (Eds.). (2006). *Theories and manifestoes of contemporary architecture* (2nd ed). Wiley-Academy.
- Jendritzky, G., de Dear, R., & Havenith, G. (2012). UTCI—Why another thermal index? *International Journal of Biometeorology*, 56(3), 421–428. <https://doi.org/10.1007/s00484-011-0513-7>

- Jomehzadeh, F., Hussen, H. M., Calautit, J. K., Nejat, P., & Ferwati, M. S. (2020). Natural ventilation by windcatcher (Badgir): A review on the impacts of geometry, microclimate and macroclimate. *Energy and Buildings*, 226, 110396. <https://doi.org/10.1016/j.enbuild.2020.110396>
- Kabošová, L., Katunský, D., & Kmet, S. (2020). Wind-based parametric design in the changing climate. *Applied Sciences*, 10(23), 8603. <https://doi.org/10.3390/app10238603>
- Kaiser, P., Kwon, M., & Museum of Contemporary Art (Los Angeles, Calif.) (Eds.). (2012). *Ends of the earth: Land art to 1974*. The Museum of Contemporary Art, Los Angeles; Distributed by Prestel.
- Kastner, J. & Wallis, B. (Eds.). (2005). *Land and environmental art*. Phaidon Press.
- Kilroy-Ewbank, L. (n.d.). *Mesa Verde*. Smarthistory. Retrieved May 9, 2025, from <https://smarthistory.org/mesa-verde-cliff-dwellings/>
- Kim, M. & Lee, H. (2008). *Landscape architect*. Archiworld.
- King, G. K. (2017, June 12). Building with heat, humidity and light: Jade Eco Park in Taichung by Philippe Rahm. *Architectural Review*. <https://www.architectural-review.com/buildings/building-with-heat-humidity-and-light-jade-eco-park-in-taichung-by-philippe-rahm>
- Kline, T. & Bahus, K. (1999). *Willamette Basin reservoirs*. The Willamette Basin Reservoir Study. https://www.oregon.gov/OWRD/wrdpublications1/1998_04_Willamette_Brochure.pdf
- Knowles, R. L. (1980). *Energy and form: An ecological approach to urban growth*. MIT Press.
- Kobi, M. & Roesler, S. (Eds.). (2018). *The urban microclimate as artifact: Towards an architectural theory of thermal diversity*. Birkhäuser.
- Kolarevic, B. (Ed.). (2009). *Architecture in the digital age: Design and manufacturing* (Reprint). Taylor & Francis.
- Kormaníková, L., Achten, H., Kopřiva, M., & Kmet, S. (2018). Parametric wind design. *Frontiers of Architectural Research*, 7(3), 383–394. <https://doi.org/10.1016/j.foar.2018.06.005>
- Krautheim, M., Pasel, R., Pfeiffer, S., & Schultz-Granberg, J. (Eds.). (2014). *City and wind: Climate as an architectural instrument*. DOM publ.
- Kubo, M. (2012). Landform building: Architecture's new terrain. Stan Allen and Marc McQuade, eds. *Journal of Architectural Education*, 66(1), Art. 1. <https://doi.org/10.1080/10464883.2012.714915>
- LaGro, J. A. (2009). *Site analysis: Informing context-sensitive and sustainable site planning and design* (Third Edition). Wiley.
- Lailach, M. (2007). *Land art* (U. Grosenick, Ed.). Taschen.
- Landezine. (n.d.). *Chulalongkorn University Centenary Park by Landprocess*. Landezine International Landscape Award. Retrieved March 29, 2025, from <https://landezine-award.com/chulalongkorn-university-centenary-park/>
- Landscape Architecture Foundation. (2019, August 4). *Landscape Performance Series: Crissy Field*. <https://www.landscapeperformance.org/case-study-briefs/crissy-field>

- Landscape Theory. (2010, January 1). *Kathryn Gustafson*.
<https://landscapetheory1.wordpress.com/tag/kathryn-gustafson/>
- Langdon, D. (n.d.). AD Classics: Yokohama International Passenger Terminal / Foreign Office Architects (FOA). *ArchDaily*. <https://www.archdaily.com/554132/ad-classics-yokohama-international-passenger-terminal-foreign-office-architects-foa>
- Lawson, B. (2006). *How designers think: The design process demystified* (4. Ed). Elsevier/Architectural Press.
- Lenzholzer, S., Duchhart, I., & Koh, J. (2013). "Research through designing" in landscape architecture. *Landscape and Urban Planning*, 113, 120–127.
<https://doi.org/10.1016/j.landurbplan.2013.02.003>
- Lenzholzer, S., Nijhuis, S., & Cortesão, J. (2018, June 26). *Research through design in landscape architecture: A first State of the Art*. <https://doi.org/10.21606/dma.2017.293>
- Levy, L. & Gustafson, K. (1998). *Kathryn Gustafson: Sculpting the land*. Spacemaker Press.
- Lin, M. Y., Andrews, R., & Beardsley, J. (2006). *Maya Lin: Systematic landscapes*. Henry Art Gallery, University of Washington; Yale University Press.
- Lin, M. Y., Brenson, M., Fox, W. L., Goldberger, P., Jodidio, P., Phillips, L., Sobel, D., McPhee, J., & Lin, T. (2015). *Maya Lin: Topologies*. Rizzoli.
- Lin, Z. (2016). Metabolist utopias and their global influence: Three paradigms of urbanism. *Journal of Urban History*, 42(3), Art. 3. <https://doi.org/10.1177/0096144216635169>
- Lintott, S. (2007). Ethically evaluating land art: Is it worth it? *Ethics, Place & Environment*, 10(3), 263–277. <https://doi.org/10.1080/13668790701567002>
- Loughner, C. P., Allen, D. J., Zhang, D.-L., Pickering, K. E., Dickerson, R. R., & Landry, L. (2012). Roles of urban tree canopy and buildings in urban heat island effects: Parameterization and preliminary results. *Journal of Applied Meteorology and Climatology*, 51(10), 1775–1793.
<https://doi.org/10.1175/JAMC-D-11-0228.1>
- Lynes, A. (2018, August 15). Albina Vision aims to restore Portland's historically African American neighborhood. *The Oregonian*.
https://www.oregonlive.com/portland/2018/08/albina_vision_aims_to_restore.html
- MacColl, E. K. (1979). *The growth of a city: Power and politics in Portland, Oregon, 1915–1950*. Georgian Press.
- MacKenzie, G. (2013). The universe in the landscape: Landforms: by Charles Jencks. *Green Letters*, 17(1), 89–89. <https://doi.org/10.1080/14688417.2012.753332>
- Makido, Y., Hellman, D., & Shandas, V. (2019). Nature-based designs to mitigate urban heat: The efficacy of green infrastructure treatments in Portland, Oregon. *Atmosphere*, 10(5), Art. 5.
<https://doi.org/10.3390/atmos10050282>
- Manfredi, M. A. & Weiss, M. (2008). *Weiss/Manfredi: Surface/subsurface*. Princeton Architectural Press.

- Manfredi, M. A. & Weiss, M. (Eds.). (2015). *Public natures: Evolutionary infrastructures* (First edition). Princeton Architectural Press.
- March, T. (2010). *Guild's Lake Courts: An impermanent housing project* [Doctoral dissertation]. Portland State University. <https://doi.org/10.15760/etd.2806>
- Marwick, A. (1998). *The Sixties: Cultural revolution in Britain, France, Italy, and the United States, c. 1958–c. 1974*. Oxford University Press.
- Maya Lin Studio. (n.d.-a). *Flutter*. <https://www.mayalinstudio.com/art/flutter>
- Maya Lin Studio. (n.d.-b). *The Wave Field*. <https://www.mayalinstudio.com/art/the-wave-field>
- Maya Lin Studio. (n.d.-c). *Storm King Wavefield*. <https://www.mayalinstudio.com/art/storm-king-wavefield>
- McArthur, L. A., & McArthur, L. L. (2003). *Oregon geographic names* (7th ed., rev. enl). Oregon Historical Society Press; Distributed by University of Washington Press.
- McHarg, I. L. (1992). *Design with nature* (25th anniversary ed). John Wiley & Sons, Inc.
- M'Closkey, K. (2013). *Unearthed: The landscapes of Hargreaves Associates* (1st ed). University of Pennsylvania Press.
- M'Closkey, K. & VanDerSys, K. (2017). *Dynamic patterns: Visualizing landscapes in a digital age*. Routledge, Taylor & Francis Group.
- MDP Michel Desvigne Paysagiste. (n.d.). *Jarden elementaires: Villa Medici 1986–1989*. <https://micheldesvignepaysagiste.com/fr/jardins-elementaires-3>
- Mecanoo. (n.d.). *Library Delft University of Technology*. Retrieved March 29, 2025, from <https://www.mecanoo.nl/projects/project/27/library-delft-university-of-technology>
- Meir, I. A., Garb, Y., Jiao, D., & Cicelsky, A. (2009). Post-occupancy evaluation: An inevitable step toward sustainability. *Advances in Building Energy Research*, 3(1), Art. 1. <https://doi.org/10.3763/aber.2009.0307>
- Michael Van Valkenburgh Associates Inc. (n.d.). Retrieved March 29, 2025, from <https://mrvainc.com>
- Milburn, L.-A. S. & Brown, R. D. (2003). The relationship between research and design in landscape architecture. *Landscape and Urban Planning*, 64(1–2), Art. 1–2. [https://doi.org/10.1016/S0169-2046\(02\)00200-1](https://doi.org/10.1016/S0169-2046(02)00200-1)
- Mostafavi, M., Doherty, G., & Harvard University (Eds.). (2013). *Ecological urbanism: Ecological urbanism conference in spring 2009 at the Harvard Graduate School of Design*. L. Müller.
- Museum of Modern Art (New York, N.Y.) (Ed.). (1999). *MOMA highlights: 325 works from the Museum of Modern Art*. Museum of Modern Art : Distributed by H.N. Abrams.
- MVRDV (n.d.-a). *NTR Headquarters*. <https://www.mvrdv.com/projects/166/ntr-headquarters>
- MVRDV (n.d.-b). *Villa VPRO*. <https://www.mvrdv.com/projects/172/villa-vpro>

- Nagib, H. M. & Corke, T. C. (1984). Wind microclimate around buildings: Characteristics and control. *Journal of Wind Engineering and Industrial Aerodynamics*, 16(1), 1–15.
[https://doi.org/10.1016/0167-6105\(84\)90046-1](https://doi.org/10.1016/0167-6105(84)90046-1)
- National Geographic. (2025, March 30). *Top 10 Machu Picchu secrets*.
<https://www.nationalgeographic.com/travel/article/secrets>
- National Trust. (n.d.). *Dorset: Hambledon Hill*. <https://www.nationaltrust.org.uk/visit/dorset/hambledon-hill>
- Nijhuis, S. (2013). *Principles of landscape architecture*. In Farina, E. and Nijhuis, S. (Eds.), *Flowscales: Exploring landscape infrastructures* (pp. 52–61). Mairia Libros Publishers.
<https://doi.org/10.13140/RG.2.1.1446.3126>
- Nijhuis, S. & Bobbink, I. (2012). Design-related research in landscape architecture. *Journal of Design Research*, 10(4), Art. 4. <https://doi.org/10.1504/JDR.2012.051172>
- Nijhuis, S. & de Vries, J. (2019). Design as research in landscape architecture. *Landscape Journal*, 38(1–2), Art. 1–2. <https://doi.org/10.3368/lj.38.1-2.87>
- Northern Light Studio, Inc. *PO90*. 10-16. [Aerial photograph]. 1:24,000. Portland, OR: Northern Light Studio, Inc., July 15, 1990. Retrieved from University of Oregon Libraries, Aerial Photography Collection.
- Northern Light Studio, Inc. *PO96*. 10-16. [Aerial photograph]. 1:24,000. Portland, OR: Northern Light Studio, Inc., July 6, 1996. Retrieved from University of Oregon Libraries, Aerial Photography Collection.
- Norwood, L. (n.d.). Urban renewal. *Prosper Portland*. Retrieved February 26, 2023, from <https://prosperportland.us/what-we-do/urban-renewal/>
- O’Doherty, Brian. (1974). *Public art and the government: A progress report*. [Art in America]; worldcat.org.
- O’Donnell, J. (2022). *Where villages are built into cliffs*. BBC.
<https://www.bbc.com/travel/article/20160602-mesa-verdes-surprising-story>
- OMA. (n.d.-a). *Downsview Park*. <https://www.oma.com/projects/downsview-park>
- OMA. (n.d.-b). *Parc de la Villette*. <https://www.oma.com/projects/parc-de-la-villette>
- Oregon Department of Geology and Mineral Industries (DOGAMI) (2012). *Portland Metro Missoula Floods Inundation Extent and Primary Flood Features* [Interactive Map Series IMS-36]. Retrieved from <https://pubs.oregon.gov/dogami/ims/p-ims-036.htm>
- Oregon Department of Transportation (ODOT). (n.d.) *History of Albina*. I-5 Rose Quarter Improvement Project. <https://www.i5rosequarter.org/history-of-albina/>
- Oregon History Project. n.d. *Albina, Portland, 1909*. Retrieved December 14, 2023, from <https://www.oregonhistoryproject.org/articles/historical-records/albina-portland-1909/>

- Oxford University Press. (n.d.-a). Microclimate. In *Oxford Advanced Learner's Dictionary*. Retrieved March 29, 2025, from <https://www.oxfordlearnersdictionaries.com/us/definition/english/microclimate?Q=microclimate>
- Oxford University Press. (n.d.-b). Simulation. *Oxford Advanced Learner's Dictionary*. Retrieved March 29, 2025, from <https://www.oxfordlearnersdictionaries.com/us/definition/english/simulation>
- Park, S., Tuller, S. E., & Jo, M. (2014). Application of Universal Thermal Climate Index (UTCI) for microclimatic analysis in urban thermal environments. *Landscape and Urban Planning*, 125, 146–155. <https://doi.org/10.1016/j.landurbplan.2014.02.014>
- PARKKIM. (n.d.). *Yanghwa Riverfront: Mud-Infrastructure*. <http://parkkim.net/projects/1016/>
- Philippe Rahm architectes. (n.d.-a). *Jade Eco Park*. <http://www.philipperahm.com/data/projects/taiwan/index.html>
- Phillips, L. (2015). Introduction. In M. Lin, *Maya Lin: Topologies*. Skira Rizzoli.
- Pollak, L. (2007). Matrix landscape: Construction of identity in the large park. In J. Czerniak & G. Hargreaves (Eds.), *Large parks*. Princeton Architectural Press.
- Port of Portland. (n.d.). *Navigation*. Retrieved December 4, 2023, from <https://www.portofportland.com/Navigation>
- Portland.gov. (2024, November 12). *Reconnecting Albina Planning Project (RAPP)*. <https://www.portland.gov/bps/planning/reconnecting-albina>
- Portland Maps Advanced. (n.d.-a). *Portland Zoning*. Retrieved December 2, 2024, from <https://www.portlandmaps.com/bps/zoning/#/map/R215941>
- Portland Maps Advanced. (n.d.-b). *Portland Zoning*. Retrieved March 29, 2025, from <https://www.portlandmaps.com/bps/zoning/#/map/>
- Prigann, H., Strelow, H., & David, V. (Eds.). (2004). *Ecological aesthetics: Art in environmental design: theory and practice*. Birkhäuser.
- Prominski, M., & Koutroufinis, S. (2009). Folded Landscapes: Deleuze's concept of the fold and its potential for contemporary landscape architecture. *Landscape Journal*, 28(2), 151–165. <https://doi.org/10.3368/lj.28.2.151>
- Report of the Park Board 1904*. (n.d.). Portland City Archive, AD/116. Retrieved February 8, 2025, from <https://efiles.portlandoregon.gov/Record/2776561/>
- Ricardo, R. (n.d.). Material thinking. *Landscape Australia*. Retrieved March 29, 2025, from https://landscapeaustralia.com/articles/063-la157_part3_parkkim/
- Robbins, W. (2023). Willamette River. *Oregon encyclopedia*. https://www.oregonencyclopedia.org/articles/willamette_river/
- Rockefeller Foundation. (1967). *President's Review and Annual Report, 1967*. Rockefeller Foundation. <https://www.rockefellerfoundation.org/wp-content/uploads/Annual-Report-1967-1.pdf>

- Rodgers, P. A. & Yee, J. (Eds.). (2015). *The Routledge companion to design research*. Routledge, Taylor & Francis Group.
- Rogers, E. B. (2001). *Landscape design: A cultural and architectural history*. Harry N. Abrams.
- Roos, R.E. (1997). *The history and development of Portland's Irvington neighborhood*. Roy E. Roos.
- Roos, R. (2022). Albina area (Portland). *Oregon encyclopedia*. Retrieved December 22, 2023, from https://www.oregonencyclopedia.org/articles/albina_area_portland/
- Rose, B. (1975). *American art since 1900* (Rev. and expanded ed). Praeger.
- RTD Conference Series. (2015, June 4). *RTD 2015 provocation by Sir Christopher Frayling part 1: research through design evolution* [Video]. Vimeo. <https://vimeo.com/129775325>
- Ruthen, S. (2019, March 6). Book Review - Public Natures: Evolutionary Infrastructures. *Spacing National*, 47. <http://spacing.ca/national/2019/03/06/book-review-public-natures-evolutionary-infrastructures/>
- Sailor, D. J. (2007). Mitigation of urban heat islands—Recent progress and future prospects. *Environmental Modelling & Software*, 22(10), 1529–1541.
- Schön, D. A. (1983). *The reflective practitioner: How professionals think in action*. Basic Books.
- Shapiro, G. (1995). *Earthwards: Robert Smithson and art after Babel*. University of California Press.
- Sherman, S. A., Varni, J. W., Ulrich, R. S., & Malcarne, V. L. (2005). Post-occupancy evaluation of healing gardens in a pediatric cancer center. *Landscape and Urban Planning*, 73(2–3), Art. 2–3. <https://doi.org/10.1016/j.landurbplan.2004.11.013>
- Simon, H. A. (1974). *The sciences of the artificial* (4th print.). MIT Press.
- Simon, K., & Steinemann, A. (2000). Soil bioengineering: Challenges for planning and engineering. *Journal of Urban Planning and Development*, 126(2), 89–102. [https://doi.org/10.1061/\(ASCE\)07339488\(2000\)126:2\(89\)](https://doi.org/10.1061/(ASCE)07339488(2000)126:2(89))
- Skovgaard, D. (2007). Oregon voices: Memories of the 1948 Vanport flood. *Oregon Historical Quarterly*, 108(1), 88–106.
- Smith, H. (Ed.). (2009). *Practice-led research, research-led practice in the creative arts*. Edinburgh University Press.
- Smithson, R. & Flam, J. D. (1996). *Robert Smithson, the collected writings*. University of California Press.
- Smithson, R., Tsai, E., Butler, C. H., Crow, T. E., Alberro, A., & Roth, M. (2004). *Robert Smithson*. University of California Press.
- Snøhetta. (n.d.). *MAX IV Laboratory Landscape*. <https://www.snohetta.com/projects/max-iv-laboratory-landscape-2>

- Sprott, J. C., Wang, X., & Chen, G. (2013). Coexistence of point, periodic and strange attractors. *International Journal of Bifurcation and Chaos*, 23(05), 1350093. <https://doi.org/10.1142/S0218127413500934>
- Stan Allen Architect. (n.d.). *New Maribor Art Gallery*. <https://www.stanallenarchitect.com/work/new-maribor-art-gallery/>
- Steenbergen, C. M., Meeks, S., & Nijhuis, S. (2008). *Composing landscapes: Analysis, typology and experiments for design*. Birkhäuser.
- Steinitz, C. (1995). Design is a verb; Design is a noun. *Landscape Journal*, 14(2), Art. 2. <https://doi.org/10.3368/lj.14.2.188>
- Strickland, E. (1993). *Minimalism—Origins*. Indiana University Press.
- Takenaka, T. & Okabe, A. (2011). Development of the seed scattering system for computational landscape design. *International Journal of Architectural Computing*, 9(4), 421–436. <https://doi.org/10.1260/1478-0771.9.4.421>
- Tiberghien, G. A. (1995). *Land art*. Princeton Architectural Press.
- Tiberghien, G. A. (2018). *Land art travelling*. Fage éditions.
- Tovsta Mohyla. (2024). In *Wikipedia*. https://en.wikipedia.org/w/index.php?Title=Tovsta_Mohyla&oldid=1266131129
- Treib, M. & Gillette, J. B. (Eds.). (2011). *Meaning in landscape architecture & gardens: Four essays, four commentaries*. Routledge.
- Trimble, D. E. (1963). *Geology of Portland, Oregon and adjacent areas*. U.S. Geological Survey.
- Tuchman, M. (1967). *American sculpture of the Sixties*. Los Angeles County Museum of Art.
- Tucker, K. (2024). Guild's Lake. *Oregon encyclopedia*. Retrieved February 27, 2023, from https://www.oregonencyclopedia.org/articles/guild_s_lake/
- UNstudio. (n.d.). *Möbius House*. <http://www.unstudio.com/en/page/12105/m%C3%b6bius-house>
- U.S. Army Air Force. *2M-1`6. 4A*. [aerial photograph]. 1:4,750. U.S. Army Air Force, August 1942. Retrieved from University of Oregon Libraries, Aerial Photography Collection. (n.d.).
- U.S. Army Air Force, 16th Domestic Photographic Unit. *4m726 N. W. River Survey, Portland, Oregon*. 103v-61. [Aerial photograph]. 1:9,400. [Bolling Field, District of Columbia]: U.S. Army Air Force, 16th Domestic Photographic Unit, September 26, 1944. Retrieved from University of Oregon Libraries, Aerial Photography Collection.
- U.S. Army. *Willamette, R.B., Portland*. 4599. [Aerial photograph]. 1:10,200. [Portland, OR]: U.S. Army, May 14, 1939. Retrieved from University of Oregon Libraries, Aerial Photography Collection.
- U.S. Army Corps of Engineers. (n.d.). *Portland district and a history of floods: 1964 flood*. Retrieved December 7, 2023, from <https://www.nwp.usace.army.mil/Missions/Flood-Risk-Management/1964-Flood/>

- U.S. Census Bureau. (n.d.). *QuickFacts: Portland city, Oregon*. Retrieved May 2, 2025, from <https://www.census.gov/quickfacts/portlandcityoregon>
- U.S. Department of Commerce, N. (n.d.). *Flooding in Oregon*. NOAA's National Weather Service. Retrieved December 12, 2023, from <https://www.weather.gov/safety/flood-states-or>
- U.S. Environmental Protection Agency (EPA). (2014, February 28). *Heat island effect* [Collections and Lists]. <https://www.epa.gov/heatislands>
- U.S. Environmental Protection Agency (EPA). (2022, February 20). *Heat Island Effect*. <https://www.epa.gov/heatislands>
- U.S. Geological Survey. (2017, March 9). *1897 topographic map of Portland, OR* [Map]. <https://www.usgs.gov/media/images/1897-topographic-map-portland-or>
- U.S. Geological Survey. (2021, March 30). *Geologic map of the greater Portland metropolitan area and surrounding region, Oregon and Washington*. <https://www.usgs.gov/maps/geologic-map-greater-portland-metropolitan-area-and-surrounding-region-oregon-and-washington>
- U.S. Geological Survey. (n.d.-a). *1940 Historical Topographic Map*. (n.d.). <https://www.usgs.gov/programs/national-geospatial-program/historical-topographic-maps-preserving-past>
- U.S. Geological Survey. (n.d.-b). *1954 Historical Topographic Map*. (n.d.). <https://www.usgs.gov/programs/national-geospatial-program/historical-topographic-maps-preserving-past>
- U.S. Geological Survey. (n.d.-c). *1916 Historical Topographic Map*. (n.d.). <https://www.usgs.gov/programs/national-geospatial-program/historical-topographic-maps-preserving-past>
- U.S. Geological Survey. (n.d.-d). *1975 Historical Topographic Map*. (n.d.). <https://www.usgs.gov/programs/national-geospatial-program/historical-topographic-maps-preserving-past>
- U.S. Geological Survey. (n.d.-e). *1990 Historical Topographic Map*. (n.d.). <https://www.usgs.gov/programs/national-geospatial-program/historical-topographic-maps-preserving-past>
- U.S. Geological Survey. (n.d.-f). *2011 Topographic Map*. (n.d.). <https://www.usgs.gov/programs/national-geospatial-program/historical-topographic-maps-preserving-past>
- U.S. Geological Survey. (n.d.-g). *2014 Historical Topographic Map*. (n.d.). <https://www.usgs.gov/programs/national-geospatial-program/historical-topographic-maps-preserving-past>
- U.S. Geological Survey. (n.d.-h). *2017 Historical Topographic Map*. (n.d.). <https://www.usgs.gov/programs/national-geospatial-program/historical-topographic-maps-preserving-past>

- U.S. Geological Survey. (n.d.-i). *2020 Historical Topographic Map*. (n.d.).
<https://www.usgs.gov/programs/national-geospatial-program/historical-topographic-maps-preserving-past>
- van den Brink, A. (Ed.). (2017). *Research in landscape architecture: Methods and methodology*. Routledge/Taylor & Francis Group.
- Vaughan, L. (Ed.). (2017). *Practice based design research*. Bloomsbury Academic.
- Voelkel, J., Hellman, D., Sakuma, R., & Shandas, V. (2018). Assessing vulnerability to urban heat: A study of disproportionate heat exposure and access to refuge by socio-demographic status in Portland, Oregon. *International Journal of Environmental Research and Public Health*, 15(4), 640. <https://doi.org/10.3390/ijerph15040640>
- Voelkel, J. & Shandas, V. (2017). Towards systematic prediction of urban heat islands: Grounding measurements, assessing modeling techniques. *Climate*. <https://doi.org/10.3390/cli5020041>
- Voelkel, J., Shandas, V., & Haggerty, B. (2016). Developing high-resolution descriptions of urban heat islands: A public health imperative. *Preventing Chronic Disease*, 13, 160099. <https://doi.org/10.5888/pcd13.160099>
- The Volga Germans in Portland. (n.d.). *A Short history of Albina*.
<https://www.volgagermansportland.info/a-short-history-of-albina.html>
- WAC, Corp. *WAC-00-WV*. 9-38. [Aerial photograph]. 1:24,000. Eugene, OR: WAC, Corp., June 26, 2000. Retrieved from University of Oregon Libraries, Aerial Photography Collection. (n.d.).
- Waite, R. B., Atwater, B. F., Lehnigk, K., Larsen, I. J., Bjornstad, B. N., Hanson, M. A., & O'Connor, J. E. (2021). Upper Grand Coulee: New views of a channeled scabland megafloods enigma. In A. M. Booth & A. L. Grunder (Eds.), *From Terranes to Terrains: Geologic Field Guides on the Construction and Destruction of the Pacific Northwest* (pp. 245–300). Geological Society of America. [https://doi.org/10.1130/2021.0062\(07\)](https://doi.org/10.1130/2021.0062(07))
- Waldheim, C. (Ed.). (2006). *The landscape urbanism reader* (1st. ed.). Princeton Architectural Press.
- Waldheim, C. (2016). *Landscape as urbanism: A general theory*. Princeton University Press.
- Walliss, J. & Rahmann, H. (2016). *Landscape architecture and digital technologies: Re-conceptualising design and making*. (0 ed.). Routledge. <https://doi.org/10.4324/9781315713526>
- Wang, D. & Groat, L. N. (2013). *Architectural research methods: David Wang, Linda N. Groat* (2nd Edition). Wiley.
- War Department, U.S. Corps of Engineers, *Willamette Valley Project, Portland*. 5966. [Aerial photograph]. 1:15,000. Portland, OR: U.S. Department of Agriculture, Agriculture Adjustment Administration, May 12, 1936. Retrieved from University of Oregon Libraries, Aerial Photography Collection.
- Way, T. (2018). *GGN: Landscapes 1999–2018*. Timber Press.
- Weilacher, U. (1996). *Between landscape architecture and land art*. Birkhäuser.

- Weiss, M. & Manfredi, M. A. (2000). *Site specific: The work of Weiss/Manfredi Architects*. Princeton Architectural Press.
- Western Aerial Contractors, Inc. *VWAC MCE-NPP*. 61-3758. [Aerial photograph]. 1:20,400. Portland, OR: U.S. Army Corps of Engineers, November 6, 1961. Retrieved from University of Oregon Libraries, Aerial Photography Collection.
- Willingham, W. (2023) Willamette River flood of 1894. *Oregon encyclopedia*.
https://www.oregonencyclopedia.org/articles/willamette_flood_1894_/
- Willingham, W. (2024). Swan Island. *Oregon encyclopedia*. Retrieved December 5, 2023, from
https://www.oregonencyclopedia.org/articles/swan_island/
- Yasa, E. (2016). Computational evaluation of building physics: The effect of building form and settled area, microclimate on pedestrian level comfort around buildings. *Building Simulation*, 9(4), 489–499. <https://doi.org/10.1007/s12273-016-0277-4>
- Zeisel, J. (2006). *Inquiry by design: Environment/behavior/neuroscience in architecture, interiors, landscape, and planning* (Rev. Ed). W.W. Norton & Company.
- Zhu, J., Feng, J., Lu, J., Chen, Y., Li, W., Lian, P., & Zhao, X. (2023). A review of the influence of courtyard geometry and orientation on microclimate. *Building and Environment*, 236, 110269. <https://doi.org/10.1016/j.buildenv.2023.110269>
- Zimmerman, J., Forlizzi, J., & Evenson, S. (2007). Research through design as a method for interaction design research in HCI. *Proceedings of the SIGCHI Conference on Human Factors in Computing Systems - CHI '07*, 493–502. <https://doi.org/10.1145/1240624.1240704>
- Zimmerman, J., Stolterman, E., & Forlizzi, J. (2010). An analysis and critique of *Research through Design*: Towards a formalization of a research approach. *Proceedings of the 8th ACM Conference on Designing Interactive Systems - DIS '10*, 310. <https://doi.org/10.1145/1858171.1858228>